Université de Montréal

Analyse spectro-photométrique des naines blanches froides dans l'échantillon Gaia

par

Alexandre Caron

Département de physique
Faculté des arts et des sciences

Mémoire présenté en vue de l'obtention du grade de
Maître ès sciences (M.Sc.)
en Astrophysique

10 février 2023

© Alexandre Caron, 2022

Université de Montréal

Faculté des arts et des sciences

Ce mémoire intitulé

Analyse spectro-photométrique des naines blanches froides dans l'échantillon Gaia

présenté par

Alexandre Caron

a été évalué par un jury composé des personnes suivantes :

Patrick Dufour
(président-rapporteur)

Pierre Bergeron
(directeur de recherche)

Nicole St-Louis
(membre du jury)

Résumé

Ce mémoire présente une analyse spectro-photométrique de 2880 naines blanches situées dans un rayon de 100 pc du Soleil, plus froides que $T_{\rm eff} \sim 10{,}000$ K, et possédant de la photométrie *grizy* de Pan-STARRS et une mesure de parallaxe trigonométrique de Gaia. Les données photométriques JHK dans le proche infrarouge sont également incluses, lorsque disponibles, et s'avèrent essentielles pour l'interprétation des naines blanches les plus froides de l'échantillon. Une analyse détaillée de chaque objet individuel est effectuée en utilisant des modèles d'atmosphère de pointe appropriés pour chaque type spectral, y compris les DA, DC, DQ, DZ, les DA riches en hélium, et les naines blanches dites faibles dans l'infrarouge (IR-faint). Les distributions en température et en masse de chaque sous-échantillon sont discutées, ainsi que l'évolution spectrale des naines blanches froides. L'échantillon présente peu d'évidence quant à la transformation des étoiles DA en naines blanches avec une atmosphère riche en hélium par le processus de mélange convectif entre $T_{\rm eff} = 10{,}000$ K et $\sim$6500 K. Cependant, cette tendance change radicalement dans les environs de $T_{\rm eff} = 6500$–5500 K où la fraction de naines blanches avec une atmosphère riche en hélium atteint $\sim$45%. Pour les étoiles plus froides ($T_{\rm eff} \lesssim 5200$ K), les résultats indiquent que la majorité des DC ont une atmosphère dominée par l'hydrogène. Un mécanisme possible impliquant la cristallisation et le magnétisme est proposé afin d'expliquer cette transformation soudaine d'une atmosphère riche en hélium en une atmosphère riche en hydrogène. Finalement, cette analyse montre que les naines blanches de type DQ, DZ et DC pourraient former une population plus homogène qu'on ne le pensait auparavant.

Mots clefs : étoiles : paramètres fondamentaux – étoiles : évolution – étoiles : fonction de masse – étoiles : abondances – naines blanches

Abstract

This work presents a spectro-photometric analysis of 2880 cool white dwarfs within 100 pc of the Sun and cooler than $T_{\rm eff} \sim$ 10,000 K, with *grizy* Pan-STARRS photometry and Gaia trigonometric parallaxes available. The data sets are also supplemented with near-infrared *JHK* photometry, when available, which is shown to be essential for interpreting the coolest white dwarfs in the sample. A detailed analysis of each individual object is performed using state-of-the-art model atmospheres appropriate for each spectral type including DA, DC, DQ, DZ, He-rich DA, and the so-called IR-faint white dwarfs. The temperature and mass distributions of each subsample are discussed, as well as the spectral evolution of cool white dwarfs. The sample shows little evidence for the transformation of a significant fraction of DA stars into He-atmosphere white dwarfs through the process of convective mixing between $T_{\rm eff}$ = 10,000 K and ∼6500 K, although the situation changes drastically in the range $T_{\rm eff}$ = 6500–5500 K where the fraction of He-atmosphere white dwarfs reaches ∼45%. However, there is strong evidence that at even cooler temperatures ($T_{\rm eff} \lesssim$ 5200 K), most DC white dwarfs have H atmospheres. A possible mechanism to account for this sudden transformation from He- to H-atmosphere white dwarfs involving the onset of crystallization and the occurrence of magnetism is presented. Finally, the results drawn from this work have shown that DQ, DZ, and DC white dwarfs may form a more homogeneous population than previously believed.

Keywords : stars : fundamental parameters – stars : evolution – stars : mass function – stars : abundances – white dwarfs

Table des matières

Liste des tableaux

Table des figures

Liste des sigles et des abréviations

CIA ..... Collision Induced Absorption

DEC ..... Declination

DPAC ..... International Gaia Data Processing and Analysis Consortium

DR(X) ..... Data Release X

ESA ..... European Space Agency

HR ..... Hertzsprung-Russell

ICRF ..... International Celestial Reference Frame

MKO ..... Mauna Kea Observatory

MWDD ..... Montreal White Dwarf Database

NASA ..... National Aeronautics and Space Administration

NEOO ..... Near-Earth Object Observations Program

Pan-STARRS ..... Panoramic Survey Telescope and Rapid Response System

PMRA ..... Proper Motion Right Ascension

PMDEC ..... Proper Motion Declination

RA ..... Right Ascension

SDSS ..... Sloan Digital Sky Survey

2MASS ..... Two Micron All-Sky Survey

UKIDSS ..... UKIRT Infrared Deep Sky Survey

VISTA ..... Visible and Infrared Survey Telescope for Astronomy

Remerciements

Je tiens d'abord à remercier mon directeur de recherche, Pierre Bergeron, sans qui la réalisation de ce projet n'aurait pas été possible. Grâce à ses conseils et son expérience dans le domaine, j'ai eu la confiance et la liberté d'avancer dans ce projet sachant que si je commettais une erreur, il allait me remettre dans le droit chemin. La quantité de travail qu'il effectue afin d'aider ses étudiants à réussir va au-delà de ce qui est nécessaire et j'en serai toujours reconnaissant. Je souhaite aussi remercier mes amis et collègues de travail qui m'ont soutenu chacun à leur façon durant cette aventure. Merci à Antoine pour avoir trouvé les erreurs dans mes codes fortran. Merci à Olivier pour m'avoir introduit à comment aller chercher la photométrie avec python. Merci à Patrick pour m'avoir donné des conseils lors de la rédaction de mon mémoire. Merci à Simon pour avoir mis à jour le MWDD une centaine de fois lors de mon projet. Merci à François (et son père) pour m'avoir sorti du pétrin à Barcelone. Enfin, merci à mes parents qui m'ont encouragé durant la totalité de mon parcours scolaire.

Chapitre 1

Introduction

1.1. Formation d'une naine blanche

Les naines blanches représentent le stade final de l'évolution des étoiles de masse faible à intermédiaire ($M < 7 - 8\ M_{\odot}$), soit environ 97% des étoiles de la Galaxie (Fontaine et al., 2001). La vie d'une telle étoile se résume en différentes phases. Initialement, une proto-étoile se forme à l'intérieur d'un nuage géant d'hydrogène et de poussière par effondrement gravitationnel. La contraction de celui-ci due à sa propre gravité lui permet d'avoir, en son centre, une température assez élevée pour fusionner l'hydrogène en hélium. C'est le début de la vie de l'étoile. Les réactions de fusion libèrent de l'énergie, qui se propage du coeur vers la surface de l'étoile. Le gradient de pression thermique vient équilibrer la force de gravité et permet une existence stable de l'étoile. Cette première phase de la vie d'une étoile est appelée séquence principale, et il s'agit de la période durant laquelle l'hydrogène en son centre devient de l'hélium. Le parcours de l'étoile sur la séquence principale se termine lorsque l'hydrogène en son centre est épuisé. À ce moment, l'étoile est composée d'un noyau d'hélium inerte entouré par une couche d'hydrogène. Situé entre le noyau et l'enveloppe se trouve une zone de combustion d'hydrogène, qui en se déplaçant vers la surface, laisse derrière elle un noyau d'hélium grandissant. Puisque le noyau est inerte et que sa masse augmente, celui-ci se contracte et libère de l'énergie gravitationnelle. Afin que l'équilibre thermique de l'étoile soit maintenue, l'enveloppe gazeuse prend de l'expansion. L'étoile devient alors une géante rouge. Durant cette phase, l'étoile perd une partie importante de sa masse sous forme de vent stellaire, soit la partie externe de son enveloppe qui s'évapore. La température au centre de l'étoile continue à augmenter avec la contraction du noyau provoquant, éventuellement, la fusion de l'hélium en carbone et en oxygène. L'étoile entre alors dans sa prochaine phase appelée, branche horizontale. Cette étape est caractérisée par la fusion de l'hélium au centre accompagnée par le brûlage d'une couche d'hydrogène située plus haut. De façon similaire aux étapes précédentes, un noyau de carbone et d'oxygène inerte est créé et des zones de

combustions d'hélium et d'hydrogène se propagent vers l'extérieur. La masse du noyau augmente et sa contraction cause une expansion de l'enveloppe. Il s'agit de la deuxième phase de géante rouge. Cette fois-ci, la contraction du noyau n'est pas suffisante pour déclencher une nouvelle combustion nucléaire. L'enveloppe stellaire devient donc instable et la majorité de sa masse est éjectée via un événement appelé nébuleuse planétaire. Au centre de cet éclat de matière se trouve l'ancien noyau de l'étoile, qui est maintenant une naine blanche.

1.2. Structure d'une naine blanche

Les naines blanches sont des objets ayant des propriétés physiques extrêmes. Elles ont généralement une masse de 0.6 $M_\odot$ concentrée à l'intérieur d'un rayon similaire à celui de la Terre, menant ainsi à une gravité de surface de l'ordre de $\log g = 8$. L'intérieur d'une naine blanche est typiquement composé de carbone et d'oxygène à parts égales en masse, soit $X_{\rm C} = X_{\rm O} = 0.5$. Le noyau est entouré d'une enveloppe d'hélium $q({\rm He}) \equiv M_{\rm He}/M_* = 10^{-2}$ ainsi qu'une couche d'hydrogène mince $q({\rm H}) = 10^{-10}$ ou épaisse $q({\rm H}) = 10^{-4}$, résidus de l'étoile parente. Dans le cas des étoiles naines blanches, ce qui empêche l'étoile de s'effondrer davantage malgré son immense gravité est la pression de dégénérescence des électrons qui agit à ces densités extrêmement élevées. La physique quantique dicte, via le principe d'exclusion de Pauli, que 2 électrons ne peuvent pas occuper le même état quantique. Lorsque la densité augmente, les électrons se rapprochent, les forçant à augmenter leur énergie cinétique afin de satisfaire ce principe. L'équilibre gravitationnel de la naine blanche est donc dû à la pression causée par les mouvements des électrons dégénérés. Il existe une limite théorique quant à la pression possible que peut exercer les électrons dégénérés, soit quand ceux-ci se déplacent à la vitesse de la lumière. Cette pression correspond à une masse maximale, appelée masse de Chandrasekhar, qui est d'environ 1.4 $M_\odot$. Au-delà de cette masse limite, la naine blanche s'effondre sous la force de gravité et explose en supernova. Par exemple, les supernovae de type Ia sont provoquées par des conditions physiques identiques, soit une naine blanche qui accrète de la matière jusqu'à franchir la limite de Chandrasekhar. Dans ce cas particulier, la luminosité de ces explosions est identique. Ceci permet de déduire les distances des sources de ces explosions, et donc de cartographier l'Univers.

Un autre avantage du fait qu'une naine blanche ne produit pas de fusion nucléaire est la cosmochronologie. Effectivement, d'un point de vue thermique, l'évolution d'une naine blanche se résume uniquement par un refroidissement continu en fonction du temps. En connaissant la température initiale, le taux de refroidissement et la température présente, on peut déduire l'âge de la naine blanche. La seule manière dont l'énergie interne peut s'échapper est par radiation. L'enveloppe stellaire d'une naine blanche agit alors comme une couverture isolante, car la présence de certains éléments peut augmenter son opacité. Il est

donc important de bien connaître la composition des couches externes, et en particulier leurs atmosphères, afin d'estimer leur âge correctement.

1.3. Atmosphères et évolution spectrale

Il est important de bien faire la distinction entre la composition atmosphérique et le type spectral d'une naine blanche. D'abord, l'atmosphère n'est constituée que d'une infime partie de l'enveloppe gazeuse de l'étoile. L'intense champ gravitationnel du noyau compacte l'enveloppe en une couche si dense et opaque que seule une mince partie à la surface de l'étoile est observable. De plus, de telles conditions permettent un tri gravitationnel très efficace, de telle sorte que les éléments lourds coulent vers le fond alors que les éléments légers flottent à la surface. Les éléments visibles dans le spectre de l'étoile sont donc ce qui détermine son type spectral. Les principaux type spectraux sont : DA pour l'hydrogène, DB pour l'hélium neutre, DO pour l'hélium ionisé, DQ pour le carbone et DZ pour le calcium (et autres métaux). Si le spectre est dépourvu de raies, celui-ci est classé DC. Cependant, la présence ou l'absence de traces d'éléments dans le spectre d'une naine blanche ne permet pas toujours de décrire la composition de l'atmosphère. Effectivement, une étoile classée DC peut avoir une atmosphère riche en hydrogène, mais avoir une température trop faible pour que des raies de Balmer soient visibles.

De plus, la composition de l'atmosphère peut changer au cours de l'évolution d'une naine blanche suite à l'effet de différents mécanismes de transport des éléments. Le premier mécanisme agit à l'échelle microscopique et se nomme diffusion. Il s'agit du mouvement net de particules causé par un gradient spatial associé à une caractéristique du système physique. Il existe trois principaux types de diffusion dans un plasma stellaire. D'abord, le tri gravitationnel, mentionné précédemment, est en fait une forme de diffusion créée par le gradient de pression. Celui-ci va donc stratifier les constituants de l'atmosphère selon la densité de masse. Ensuite, la diffusion survient lorsque deux espèces de particules sont présentes dans un système. Dans ce cas, le déplacement est causé par un gradient de concentration et est appelé diffusion chimique. Enfin, un gradient de température va causer la diffusion thermique. De façon similaire au tri gravitationnel, cette diffusion cherche à faire couler les particules lourdes vers le centre de l'étoile. Le deuxième mécanisme est la convection, qui dans ce cas, effectue un transport macroscopique de la matière. Les couches de plasma d'hélium et d'hydrogène de la naine blanche agissent comme une couverture limitant la quantité de radiation émergente à la surface, soit la quantité d'énergie qui peut s'échapper de l'étoile. Lorsque la quantité d'énergie provenant d'une couche sous-jacente est plus grande que ce que le mécanisme de transfert radiatif permet d'accommoder, des cellules de plasma chaudes sont transportées vers la surface et des cellules froides se dirigent

vers le centre. Une telle situation survient lorsque le critère de Schwarzschild est satisfait :

$$|\frac{\partial T}{\partial r}| > |\frac{\partial T}{\partial r}|_{\text{ad}} \tag{1.3.1}$$

où r est la coordonnée radiale, T la température et ad signifie adiabatique. En d'autres termes, la convection s'amorce lorsque le gradient de température dans l'étoile dépasse celui associé à une cellule de plasma faisant une ascension adiabatique. Les régions convectives d'une étoile voient donc leurs composants chimiques mélangés de façon homogène. Ensuite, le troisième mécanisme de transport est le vent stellaire. Celui-ci est le résultat d'un transfert de quantité de mouvement entre des photons provenant de l'intérieur et les atomes à la surface de l'étoile. Dans le cas des naines blanches les plus chaudes, l'intensité lumineuse à la surface est si forte que la force engendrée par le mouvement des photons parvient à contrer la force gravitationnelle. Ceci crée donc une perte de matière à la surface de l'étoile. Le dernier mécanisme de transport pertinent à l'étude des naines blanches est appelé accrétion et celui-ci a l'effet contraire au vent solaire. C'est le processus par lequel une étoile acquiert de la matière en provenance de son environnement. Dans le cas des naines blanches, il s'agit habituellement de nuages d'hydrogène et d'hélium. Il est aussi évident, vu la présence d'éléments lourds dans les spectres de certaines naines blanches, que des résidus planétaires sont aussi victimes d'accrétion par ces corps célestes. Ce mécanisme change la composition chimique de l'atmosphère de l'étoile.

L'ensemble de ces mécanismes se manifeste à différents stades de la vie des naines blanches et sont la source de leur évolution spectrale. Bédard et al. (2022b) explore en détail l'évolution spectrale des naines blanches chaudes d'un point de vue théorique et observationnel. Le travail présenté dans ce mémoire se penche sur les naines blanches froides dans le but de compléter les morceaux manquants du casse-tête.

1.4. L'étude des naines blanches

La détermination des paramètres physiques des naines blanches (masse, température effective, rayon, gravité de surface, composition atmosphérique, âge) dans le but d'étudier les propriétés globales de ces étoiles a été explorée sous une multitude d'angles durant les deux dernières décennies. Avec les constantes avancées scientifiques et technologiques, la quantité ainsi que la qualité des données augmentent et les modèles sont améliorés afin de reproduire les nouvelles observations. Il y a deux principales méthodes permettant de déterminer ces paramètres. La première est la méthode spectroscopique, où des spectres observés sont comparés aux prédictions de modèles afin de mesurer T_{eff} et $\log g$, qui sont

ensuite converties en masse à l'aide de modèles d'évolution stellaire. La deuxième est la méthode photométrique, où des magnitudes mesurées à travers divers bandes passantes sont converties en flux moyens puis comparés, eux-aussi, aux prédictions de modèles. Dans ce cas-ci, $T_{\rm eff}$ et l'angle solide $\pi(R/D)^2$ sont ajustés de façon à mieux reproduire la distribution d'énergie de l'étoile. Les autres paramètres sont alors déduits à l'aide des modèles évolutifs.

La méthode photométrique a été utilisée pour la première fois par Bergeron et al. (1997a) afin d'obtenir des valeurs de $T_{\rm eff}$ ainsi que la composition atmosphérique de 110 naines blanches froides à partir de photométrie dans le domaine visible $BVRI$ et infrarouge JHK, et de spectres à Hα. Dans cette étude, la masse n'a pu être déterminée que pour 60 étoiles ayant une mesure de parallaxe connue. Dans le but de produire une analyse plus complète d'un échantillon de naine blanches froides, Bergeron et al. (2001a) se sont basés sur le *Yale Parallax Catalog* afin de sécuriser une mesure de parallaxe pour les 152 étoiles de leur échantillon. Ces études ont mis en lumière l'évolution des naines blanches sous l'angle de la composition atmosphérique, plus particulièrement en ce qui concerne la présence ou non d'hydrogène, car elles étaient basées sur des modèles H-pur, He-pur et mixte H/He pour tous les types de naines blanches. Cependant, ceci n'est pas adéquat pour l'analyse des étoiles de type DQ et DZ, qui montrent respectivement des traces de carbone et de métaux dans leurs spectres. Des modèles d'atmosphères incluant des abondances de carbone ont été utilisés pour la première fois avec la méthode photométrique afin de déterminer les paramètres physiques de 56 étoiles DQ dans Dufour et al. (2005a). De façon similaire dans Dufour et al. (2007a), des modèles incluant des traces de métaux ont permis l'analyse d'un échantillon de 157 DZ avec la méthode photométrique. Avec ces nouveaux modèles, les masses des DQ et DZ obtenues étaient de $< M > = 0.62\ M_{\odot}$ et $< M > = 0.63\ M_{\odot}$, respectivement. Les valeurs obtenues en utilisant les modèles He-pur étaient significativement plus élevées avec $< M > = 0.73\ M_{\odot}$ et $< M > = 0.78\ M_{\odot}$, respectivement. Puisque les naines blanches ont une masse d'environ, $M \approx 0.6\ M_{\odot}$, ces nouvelles masses étaient donc une amélioration prometteuse. Suivant l'amélioration apportée par ces nouveaux modèles, Giammichele et al. (2012a) ont effectué l'analyse d'un volume complet à l'intérieur de 20 pc de naines blanches ayant un type spectral connu. La méthode spectroscopique ainsi que la méthode photométrique ont été utilisées, en fonction de la disponibilité des données, afin de déterminer les paramètres de 168 étoiles.

Jusqu'à maintenant, les études à l'intérieur de volumes complets ne comprenaient que quelques centaines d'étoiles tout au plus. L'arrivée de missions de collecte de données par balayage du ciel telles que Gaia DR2 (Gentile Fusillo et al., 2019a), SDSS (Kepler et al., 2019a) et Pan-STARRS (Chambers et al., 2016a) allait révolutionner le domaine. Étant donné la multiplication du nombre de données astronomiques disponibles, les analyses qui ont suivi cette période sont certainement davantage significatives d'un point de vue statistique. Trois principales études de volume complet à l'intérieur de 100 pc faisant l'usage de parallaxes

trigonométriques tirées de Gaia DR2 ont été effectuées avant le travail présenté dans ce mémoire. D'abord, Bergeron et al. (2019b) ont effectué une analyse axée sur les effets apportés par l'utilisation de photométrie Pan-STARRS *grizy* ou SDSS *ugriz* sur la détermination des paramètres physiques de 1827 DA et 843 non-DA. Cette expérience a démontré l'existence d'incertitudes reliées à la méthode photométrique, qui sont probablement causées par des erreurs de calibration photométrique. Les différences de $T_{\rm eff}$ obtenues suggèrent que Pan-STARRS et SDSS ne se situent pas exactement sur le système de magnitudes AB. Celui-ci est défini comme étant le logarithme de la densité spectrale de flux avec comme point zéro 3631 janskys. L'application de ce système est discutée dans la section 3.1. L'utilisation simultanée de la photométrie SDSS u avec Pan-STARRS *grizy* semble produire les valeurs de $T_{\rm eff}$ les plus exactes. Ensuite, Blouin et al. (2019b) a étudié un échantillon plus restreint de 501 naines blanches froides à l'aide de la photométrie Pan-STARRS *grizy* accompagnée de 2MASS JHK. Cette analyse fait l'usage des plus récents modèles d'atmosphère afin de modéliser les DQ et DZ correctement, ainsi que des modèles H-pur, He-pur et mixtes pour les DA et DC. Les résultats de ce travail montrent qu'il est important, lors de l'étude de naines blanches froides, d'inclure de la photométrie infrarouge afin d'inférer la présence d'hydrogène dans l'atmosphère. Subséquemment, Kilic et al. (2020a), faisant aussi l'usage des plus récents modèles d'atmosphère, analysèrent un échantillon de 2361 naines blanches ayant un type spectral connu en utilisant la photométrie Pan-STARRS *grizy* et SDSS u disponibles. Cette étude est importante car tous les types de naines blanches sont analysées avec les modèles d'atmosphère appropriés, ce qui a permis d'obtenir un meilleur portrait global des paramètres physiques, notamment en ce qui concerne les distributions de masses.

Dans tous les cas, ces échantillons sont incomplets selon un ou plusieurs des critères suivants : ils sont non représentatifs de ce que l'on retrouve dans le ciel (ne contiennent pas tous les types spectraux), ils n'utilisent pas les meilleurs modèles d'atmosphère, et/ou ils n'utilisent qu'une partie de la photométrie disponible. Il y avait donc un besoin pour un projet rassemblant toutes les naines blanches à l'intérieur de 100 pc avec l'ensemble de la photométrie importante et les modèles d'atmosphère les plus récents.

1.5. Ce projet

Les études précédentes ont permis de tracer la voie afin de produire l'échantillon de naines blanches le plus complet et le moins biaisé possible. Ce projet fait donc usage des meilleurs modèles d'atmosphère pour tous les types de naines blanches froides connues à ce jour (DA, DC, DQ, DZ, HeDA, IR-Faint) en plus de photométrie SDSS u, Pan-STARRS *grizy* et l'ensemble de la photométrie infrarouge JHK disponible à l'intérieur de 100 pc. Les paramètres physiques des étoiles sont déterminés à l'aide de la méthode spectro-photométrique, utilisant la parallaxe trigonométrique de Gaia DR2/EDR3 et les données spectrales disponibles dans

le Montreal White Dwarf Database (MWDD). Le MWDD (Dufour et al., 2017a) a comme objectif de rassembler l'ensemble des données de toutes les naines blanches ayant un type spectral connu précédemment et dont l'analyse est présentée dans un article. Jusqu'à ce jour, la base de données contient 38,836 étoiles ayant un spectre disponible et 29,334 ayant soit un type spectral connu ou étant une candidate. Le MWDD fait référence à plus de 120 articles représentant des travaux de toutes tailles, allant de relevés de plusieurs milliers d'étoiles à de simples échantillons de quelques dizaines d'objets. L'échantillon de ce projet comprend 2880 étoiles ayant un type spectral connu et 5358 candidates. Ceci représente donc le plus grand échantillon de naines blanches étudié avec ce type d'analyse.

Ce mémoire est présenté en 5 chapitres. Le présent chapitre avait comme objectif d'expliquer au lecteur comment une naine blanche se forme, comment elle est structurée, quels sont les différents types de naines blanches, et par quels mécanismes ceux-ci peuvent changer au cours de leur évolution. Le deuxième chapitre discute de l'ensemble des données d'observations utilisées dans le cadre de ce travail. L'origine, la validité et l'utilité des différents types de données sont discutés dans les sous-sections pour Gaia, Pan-STARRS, SDSS, la photométrie infrarouge et les données spectrales. Le troisième chapitre explique comment les données d'observations sont utilisées pour calculer les paramètres physiques des naines blanches de l'échantillon. La méthode spectro-photométrique est expliquée en détail pour chaque type de naine blanche. Les difficultés rencontrées lors de l'adoption des paramètres physiques et les solutions permettant de les surmonter sont discutées pour chaque type d'étoile. De plus, des exemples d'objets problématiques sont présentés. Le quatrième chapitre est l'article rédigé dans le cadre de ce projet. Celui-ci contient une analyse détaillée des résultats et une discussion des différentes implications de ces résultats sur l'évolution spectrale des naines blanches froides. Le dernier chapitre est la conclusion, qui résume les principaux résultats de ce travail.

Chapitre 2

Observations

2.1. Définition de l'échantillon

Pour mener à bien cette analyse, il était nécessaire d'étudier un volume complet de naines blanches autour de la Terre. Les critères de sélection ont donc été choisis dans le but de construire un échantillon homogène de naines blanches froides. Pour qu'une naine blanche soit incluse dans l'échantillon, elle doit respecter les critères suivants :

- Avoir une mesure de parallaxe provenant du catalogue Gaia DR2. Afin d'éviter les mesures erronées et de définir un standard de précision minimal pour l'échantillon, seul les objets ayant une mesure satisfaisant $\sigma_\pi/\pi < 0.1$ sont retenus.
- Avoir les points photométriques *grizy* de Pan-STARRS. Dans le but d'utiliser la technique photométrique, le système Pan-STARRS est préférable à Gaia, car les bandes utilisées représentent la distribution d'énergie plus adéquatement et permettent d'obtenir des paramètres physiques plus exacts. L'utilisation de données de Pan-STARRS contraint le volume étudié à une déclinaison au nord de $-30°$.
- Respecter la condition $T_{\rm eff} < 10{,}000$ K basée sur l'analyse. Cette borne supérieure permet d'assurer que l'évolution spectrale des naines blanches froides soit incluse en son entièreté.
- Être située à une distance moindre de 100 parsec. En deçà de cette distance, l'extinction de la lumière causée par la matière interstellaire est négligeable. De plus, la fine précision de Gaia permet d'avoir une probabilité de détection de presque 100% à l'intérieur de 100 parsec. Ceci assure que l'échantillon est complet dans ce volume.
- Le type spectral de l'étoile doit être identifié. Avoir le type spectral de l'étoile est essentiel pour nous aider à spécifier l'abondance atmosphérique des étoiles ayant $T_{\rm eff} > 6000$ K.

Pour construire l'échantillon en se basant sur les critères précédents, les objets ont été sélectionnés dans la base de données du MWDD, où s'y retrouvent les naines blanches du catalogue Gaia DR2 tel que décrit dans Bergeron et al. (2019b). Les spectres contenus dans le

MWDD proviennent majoritairement du SDSS DR14. Le reste des spectres utilisés dans cette analyse proviennent de différentes études précédentes tel que mentionné dans la section 2.6. Afin de produire une analyse photométrique plus complète, deux systèmes photométriques additionnels ont été utilisés, soit le point u-(SDSS) et les points J, H et K. La photométrie infrarouge acquise provient de différents catalogues, soit MKO, VISTA, 2MASS et UKIDSS et est présentée en détail dans le tableau 2.5.1. Ces données additionnelles n'étaient pas disponibles pour toutes les étoiles de l'échantillon, mais dans un cas idéal, l'analyse photométrique d'un objet serait basée sur les points u-(SDSS), $grizy$-(Pan-STARRS) et JHK. L'échantillon final comprend 8238 objets, soit 2880 étoiles de type spectral connu et 5358 candidates. L'échantillon d'étoiles connues est donc très volatile, car à tout moment, un nouveau catalogue de spectres peut émerger, réduisant le nombre de candidates et augmentant le nombre de naines blanches avec un type spectral confirmé. Les mesures de parallaxe et de photométrie des étoiles connues de l'échantillon sont présentées dans le tableau A.1 (Annexe A).

2.2. Gaia

La mission Gaia est la plus grande collecte de données astronomiques jamais réalisée. L'objectif principal de la mission est de construire une carte tridimensionnelle des positions et vitesses des étoiles de notre galaxie afin de déterminer leurs propriétés astrophysiques (Gaia Collaboration 2016a). Afin de compléter cette tâche colossale, l'ESA a conçu le télescope satellitaire Gaia contenant les instruments nécessaires à l'obtention de données astrométriques et photométriques d'étoiles. De plus, le centre de traitement de données DPAC a été sélectionné pour transformer les données brutes de Gaia et les publier. Le satellite est situé au point de Lagrange L2 du système gravitationnel Soleil-Terre-Lune. Orbiter le Soleil à cette position lui demande une quantité minimale de carburant permettant à la mission d'avoir une durée de vie de 5 ans. Cette longue durée de vie est nécessaire afin d'observer le ciel entier et de mesurer les variations en position et magnitude des objets. La mission est divisée en plusieurs stades de collectes et traitements de données. Environ 1000 jours après le lancement en 2013, le satellite Gaia avait mesuré la position d'environ 1 milliard d'objets ayant une magnitude $G < 20.7$. Ces données sont présentées dans le catalogue Gaia DR1 (Gaia Collaboration 2016b). Cependant, puisqu'il s'agit de la première prise de données de la mission, les mesures astrométriques variables [1] ne pouvaient pas être déterminées pour les objets jamais enregistrés précédemment. Il a donc fallu attendre la fin du deuxième stade de traitement de données, soit la sortie du catalogue Gaia DR2 (Gaia Collaboration 2018b), afin d'avoir une base de données plus complète. Ce catalogue contient la position de 1.7 milliards d'objets et pour 1.3 milliards d'entre eux, une mesure de parallaxe et du mouvement propre

1. Demandant des mesures à différentes époques.

sont aussi disponibles. Les données utilisées dans ce projet proviennent de Gaia DR2 et sont présentées dans les sections 2.2.1 et 2.2.2.

2.2.1. Données astrométriques

La capacité de mesurer la position d'une étoile avec précision est à la base de l'astrométrie de Gaia. Le référentiel utilisé dans Gaia DR2 est le Repère de Référence Céleste International (ICRF) à l'époque J2015.5. Les coordonnées sont donc mesurées selon l'ascension de droite (RA ; degrés) et la déclinaison (DEC ; degrés) de l'ICRS à cette époque.

Afin de construire une carte en trois dimensions, il faut à la fois la position et la distance des objets. Une façon fiable de mesurer la distance d'une étoile par rapport à la Terre, est la parallaxe trigonométrique. Cela consiste à utiliser l'orbite de la Terre autour du Soleil pour mesurer la position apparente d'une étoile à deux moments différents de l'année, soit lorsque la Terre est située à deux côtés opposés du Soleil. En utilisant l'angle résultant de ces deux mesures et la distance Terre-Soleil, il est possible de déduire la distance de l'étoile. Cependant, il est difficile d'effectuer ce genre de mesure en utilisant un télescope au sol, car l'atmosphère terrestre, étant turbulente, cause des aberrations. Ceci a limité le nombre d'étoiles ayant une mesure de parallaxe à environ 8000 avant la fin des années 1990 (van Altena et al., 1995). En 1997, l'ESA a révolutionné l'astronomie en lançant le satellite Hipparcos, qui a mesuré la parallaxe de 117,955 objets (ESA ; 1997). Le succès de cette mission fut le catalyste permettant la création de Gaia, qui a tout autant révolutionné l'astrophysique en multipliant le nombre d'objets ayant une mesure de parallaxe par 10,000.

En plus de la parallaxe, mesurer la position d'un objet à différents instants permet de calculer son mouvement propre. Celui-ci est mesuré selon les coordonnées des positions, soit le mouvement propre selon l'ascension droite (PMRA ; mas/année) et selon la déclinaison (PMDEC ; mas/année). Une des utilités de connaître le mouvement propre d'un objet est de pouvoir calculer sa position à une époque passée ou future, facilitant ainsi l'identification de l'objet correspondant dans un catalogue différent.

Il est important de mentionner que le satellite Gaia a aussi mesuré la vitesse radiale pour plus de 1 milliard d'objets. Cependant, ce projet n'en fait pas l'usage. Les données astrométriques utilisées sont donc les coordonnées, la parallaxe et les mouvements propres.

2.2.2. Données photométriques

L'instrument photométrique de Gaia est hautement intégré dans l'instrument astrométrique, ce qui lui permet de mesurer la photométrie d'objets en utilisant le même télescope et plan focal. Ceci assure que les mesures astrométriques soient cohérentes avec les mesures photométriques. L'instrument opère dans le domaine visible et dans l'infrarouge proche. Les bandes photométriques utilisées sont montrées à la figure 2.1. Ce sont des bandes larges soit,

G (330-1050 nm), $G_{\rm BP}$ (330-680 nm) et $G_{\rm RP}$ (640-1050 nm) et ne sont donc pas optimales pour bien modéliser la distribution d'énergie d'une étoile.

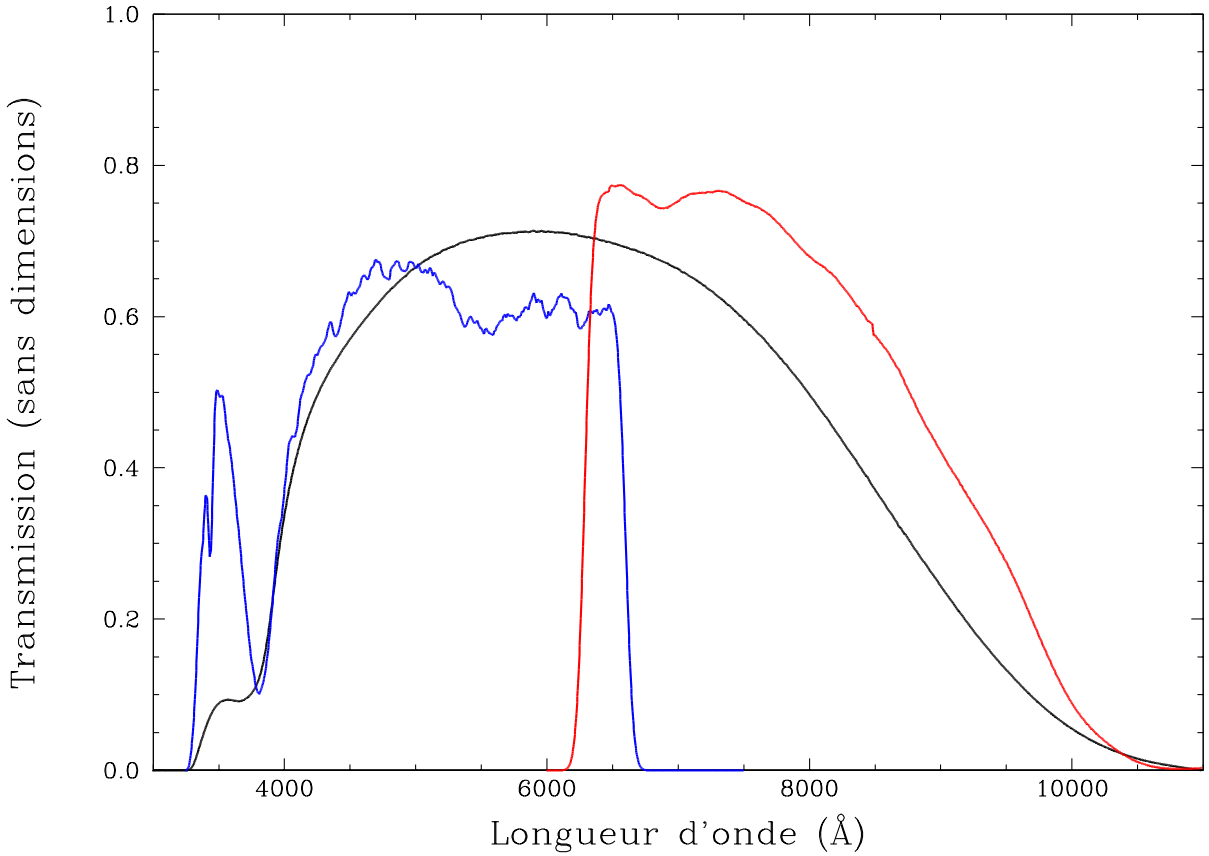

FIGURE 2.1 Bandes passantes des filtres G (noir), $G_{\rm BP}$ (bleu) et $G_{\rm RP}$ (rouge) de Gaia. L'axe vertical illustre la réponse des filtres selon la longueur d'onde d'un photon incident.

Le catalogue Gaia DR2 contient des mesures de photométrie multi-bandes pour plus de 1 milliards d'objets. La tâche d'extraire les naines blanches de cet échantillon a été effectuée en premier par Gentile Fusillo et al. (2019a). Ils ont montré l'échantillon Gaia DR2 sous forme d'un diagramme HR, soit M_G vs. $G_{\rm BP} - G_{\rm RP}$ (voir Figure 2.2 tiré de Gentile Fusillo et al. 2019a) résultant en la classification d'environ 260,000 candidates avec un haut niveau de confiance ($P_{\rm WD} > 0.75$). Dans un tel graphique, les naines blanches peuvent être identifiées comme faisant partie d'un groupe distinct des autres étoiles, car elles sont plus petites et chaudes, ce qui se traduit comme moins lumineuses et davantage bleutées. Ils ont alors utilisé différentes coupures pour séparer la zone contenant les naines blanches du reste de l'échantillon (voir leur Section 2.1). Les données de Gaia DR2 incluses dans le MWDD sont obtenues de deux façons, soit pour les naines blanches connues et les candidates. Pour les naines blanches connues, les données proviennent de différents articles et travaux de

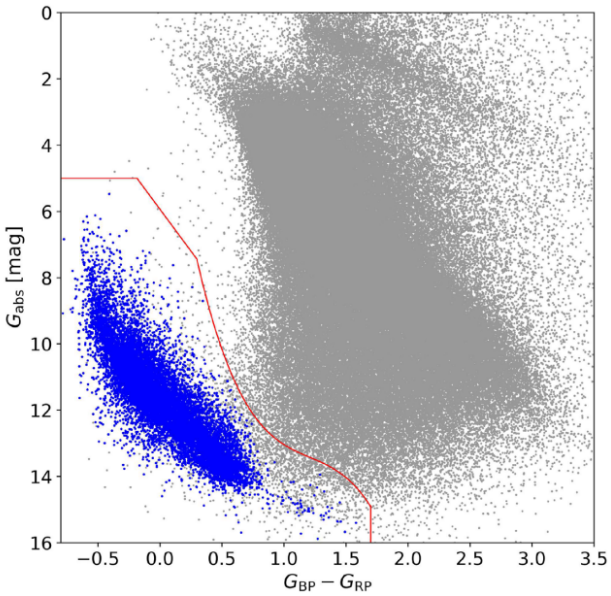

FIGURE 2.2 Diagramme HR tiré de Gentile Fusillo et al. (2019a) montrant un échantillon représentatif des objets inclus dans Gaia DR2. Les points gris sont des objets ayant $\pi/\sigma_\pi > 1$ et les points bleus sont des naines blanches avec un type spectral connu. Les traits rouges sont les coupes utilisées afin de sélectionner les candidates.

recherche incluant celui mentionné précédemment. Dans le cas des candidates, les étoiles sont sélectionnées selon certains critères [2], incluant la coupure suivante dans le diagramme HR de Gaia DR2 : $G + 5\log\pi > 3.333(G_{\rm BP} - G_{\rm RP}) + 8.333$. L'échantillon de ce projet, étant basé sur les étoiles contenues dans le MWDD, est donc dérivé de ces mêmes contraintes de sélection que pour les données de Gaia.

Celui-ci est présenté dans la Figure 2.3, soit les étoiles contenues dans le MWDD ayant une mesure de parallaxe plus précise que 10%, situées à une distance inférieure à 100 parsecs, ayant $T_{\rm eff} < 10{,}000$ K, basée sur l'analyse effectuée dans ce projet et pour lesquelles les données photométriques *grizy* de Pan-STARRS sont disponibles. De plus, les séquences de couleurs théoriques sont présentées pour des naines blanches de 0.6 $M_\odot$ ayant une atmosphère riche en hydrogène et riche en hélium, ainsi que 0.7 $M_\odot$ ayant une atmosphère riche en hélium. On remarque, dans ce diagramme couleur-magnitude, une bifurcation entre les étoiles DA et non-DA dans la région $0.0 < (G_{\rm BP} - G_{\rm RP}) < 0.8$. On peut voir que les étoiles de type DA suivent assez bien les modèles d'atmosphère riches en hydrogène. Par contre, les étoiles non-DA semblent être décalées par rapport aux modèles à 0.6 $M_\odot$ avec une atmosphère riche en hélium dans la région $0.1 < (G_{\rm BP} - G_{\rm RP}) < 0.8$, puis suivent mieux les modèles riches en hydrogène pour $(G_{\rm BP} - G_{\rm RP}) > 0.8$. Deux hypothèses ont été proposées pour expliquer ce phénomène. La première concerne la composition atmosphérique. Il est évident dans ce cas-ci, que les modèles d'atmosphère riches en hélium échouent à reproduire le comportement des

2. https ://www.montrealwhitedwarfdatabase.org/faq.html

étoiles non-DA à 0.6 $M_{\odot}$. La deuxième souligne le fait qu'une différence de masse des étoiles causerait une différence de leurs rayons et donc de leurs magnitudes absolues, résultant en un décalage dans un tel graphique. Effectivement, comme le montre la figure 2.3, la population de naines blanches non-DA suit assez bien la courbe de 0.7 $M_{\odot}$ avec une atmosphère riche en hélium. La littérature récente vient mettre en lumière laquelle de ces explications est la plus appropriée afin d'expliquer ce phénomène. Une nouvelle séquence évolutive DO-DA-DC calculée dans Bédard et al. (2021) montre que des étoiles DA deviennent des DC composées d'une atmosphère riche en hélium avec une trace d'hydrogène $\log \mathrm{H/He} = -5$. Cette nouvelle séquence à 0.6 $M_{\odot}$ suit bien la branche d'étoiles non-DA, montrant que l'ajout d'une trace d'hydrogène dans l'atmosphère de ces étoiles riches en hélium est nécessaire afin de correctement les représenter, confirmant ainsi la première hypothèse mentionné par Bergeron et al. (2019b). Cette séquence est montrée dans la figure 2.5, qui présente les données photométriques de Pan-STARRS de façon similaire à la figure 2.3. Une remarque additionnelle sur la figure 2.3 est qu'aucune des séquences de couleurs théoriques n'arrive à reproduire la distribution des étoiles non-DA à basse température. Ce phénomène est exploré plus en détail dans l'article au chapitre 4.

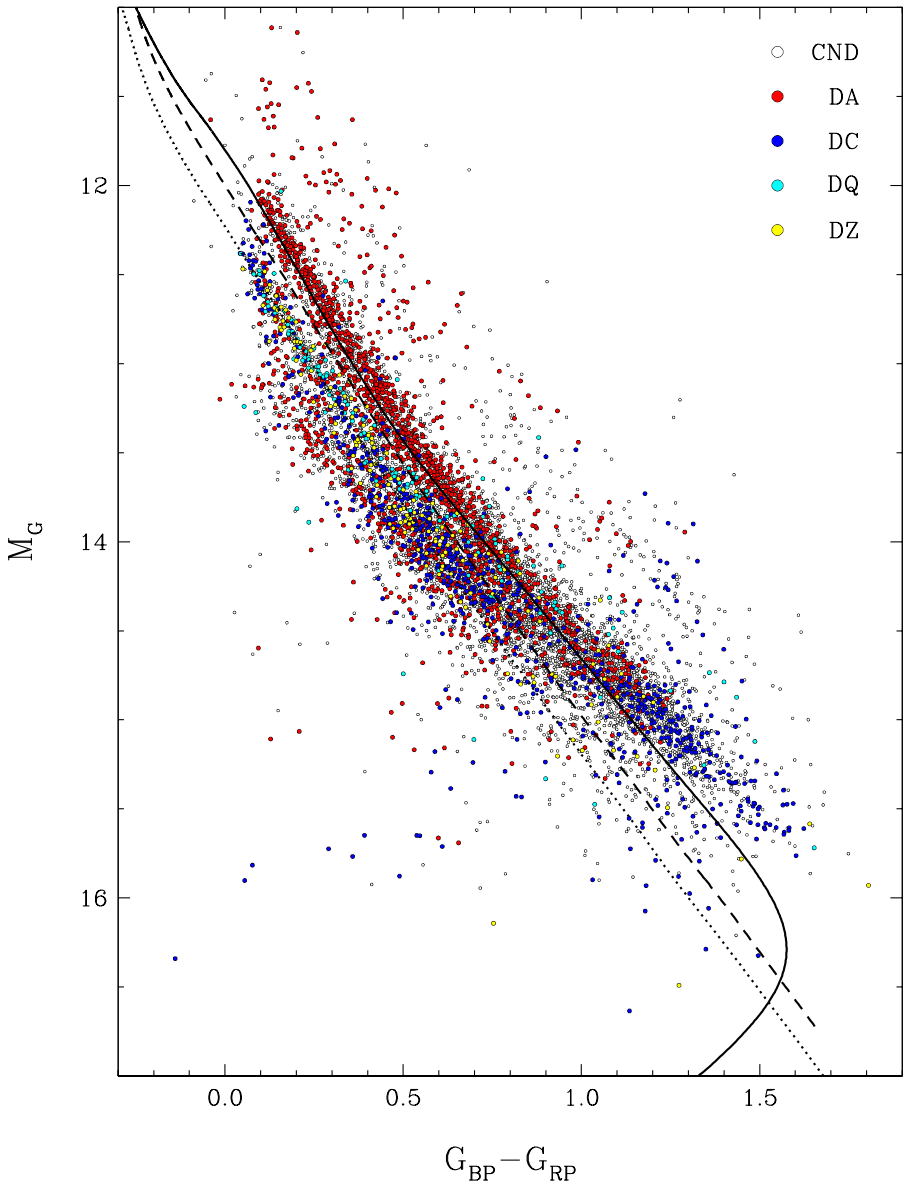

FIGURE 2.3 Diagramme couleur-magnitude M_G vs. $G_{\rm BP}-G_{\rm RP}$ pour les naines blanches dans le MWDD ayant une mesure de parallaxe plus précise que 10%, une distance inférieure à 100 parsecs, $T_{\rm eff} < 10{,}000$ K, basée sur l'analyse effectuée dans ce projet et pour lesquelles les données photométriques *grizy* de Pan-STARRS sont disponibles. La figure comprend 1764 étoiles de type DA (rouge), 810 DC (bleu), 145 DQ (cyan), 158 DZ (jaune) et 5358 candidates (blanc). Les séquences de couleurs théoriques sont montrées avec masses constantes pour 0.6 $M_\odot$ avec atmosphère riche en hydrogène (trait plein) et riche en hélium (tirets), et 0.7 $M_\odot$ avec atmosphère riche en hélium (trait pointillé).

2.3. Pan-STARRS

Le *Panoramic Survey Telescope and Rapid Response System* (Pan-STARRS) est un centre de récolte et traitement de données astronomiques situé au sommet du mont Haleakala à Hawaii dédié à faire de l'imagerie rapide du ciel. Il est composé de 2 télescopes identiques, soit PS1 et PS2 permettant de produire de l'imagerie du ciel selon 6 filtres photométriques g, r, i, z, y et w. Aujourd'hui, ses activités sont en majeure partie financées par le programme NEOO de la NASA, qui a comme objectif d'identifier les objets proches de la Terre. Le centre travaille actuellement de concert avec ATLAS (Tonry et al., 2018) afin de détecter les astéroïdes et comètes potentiellement dangereux visibles depuis Hawaii. Cependant, les objectifs scientifiques qui ont motivé le développement de Pan-STARRS n'étaient pas seulement limités à l'observation d'objets dangereux. Au début de ses opérations, durant les 4 années suivant 2010, le télescope Pan-STARRS1 (PS1) a effectué plusieurs sondages répondant à différents objectifs scientifiques (Chambers et al., 2016a). Ces relevés sont accessibles publiquement depuis 2016 et une multitude de projets de recherche en ont fait l'utilisation. Parmi ceux-ci, le plus ambitieux était le 3π *Steradian Survey*, qui consistait en une observation détaillée de tout le ciel au nord de $\delta > -30°$ à travers les 5 filtres photométriques *grizy* (Flewelling et al., 2020). Les données de Pan-STARRS1 utilisées dans ce projet proviennent en grande partie de ce relevé.

Le télescope Pan-STARRS1 couvre le domaine du visible et de l'infrarouge proche. Ce projet fait l'usage de 5 de ces filtres, soit g (400-550 nm), r (550-700 nm), i (700-850 nm), z (800-950 nm) et y (900-1100 nm), illustrés à la figure 2.4. La figure montre aussi les bandes de Gaia et permet donc de comparer les deux systèmes. On remarque que les filtres de Pan-STARRS sont beaucoup moins larges que ceux de Gaia, mais couvrent essentiellement le même domaine du spectre. Ceci permet d'échantillonner la distribution d'énergie d'une étoile de façon plus précise et offre une meilleure sensibilité à des variations de flux.

Les bases de données du MWDD ont fourni la photométrie *grizy* pour la majorité des naines blanches connues de cet échantillon et une partie des candidates. La photométrie manquante a été obtenue via un code Python qui fait l'utilisation du module astroquery de numpy. Ce module permet de faire des recherches dans VizieR pour divers catalogues en utilisant les coordonnées de position de l'ICRS à l'époque J2000. La recherche de photométrie pour une étoile s'effectue de la manière suivante :

- Les coordonnées J2015.5 de Gaia DR2 sont converties en J2000 à l'aide du mouvement propre.
- Une requête est effectuée dans le catalogue PS1 de VizieR. Ceci retourne tous les objets inclus dans un certain rayon autour de la position de l'étoile.
- La photométrie correspondant le mieux à l'étoile est sélectionnée.

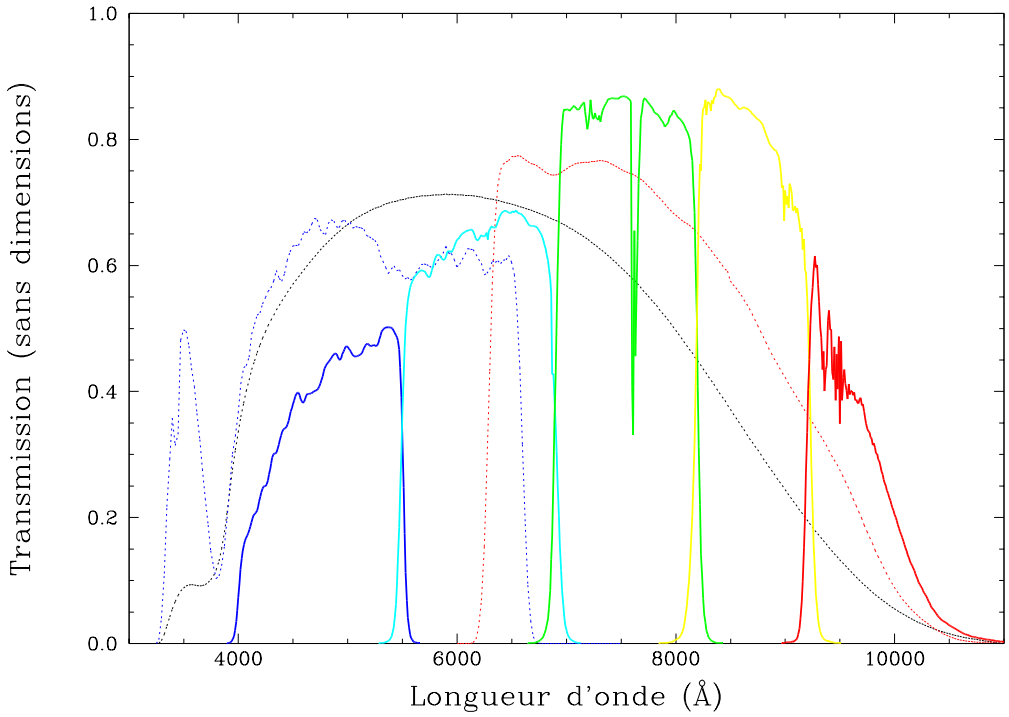

FIGURE 2.4 Bandes passantes des filtres *grizy* de Pan-STARRS sur lesquels sont superposées les bandes G, $G_{\rm BP}$ et $G_{\rm RP}$ de Gaia. L'axe verticale illustre la réponse des filtres selon la longueur d'onde d'un photon incident. Les courbes en traits pleins représentent les filtres g (bleu), r (cyan), i (vert), z (jaune) et y (rouge). Les courbes en pointillés représentent les filtres G (noir), $G_{\rm BP}$ (bleu) et $G_{\rm RP}$ (rouge).

Effectuer une requête dans un rayon, parfois aussi petit que 0.5 arcsec, peut retourner plus d'une vingtaine d'objets. Il faut alors sélectionner la photométrie correspondante à l'étoile en question. Le moyen utilisé ici est de comparer la photométrie Pan-STARRS des objets résultant de la requête avec la photométrie SDSS de l'étoile si elle est disponible. Seuls les points g, r et z sont comparés, car ils couvrent environ les mêmes régions du spectre. L'objet Pan-STARRS ayant une différence moyenne minimale de ces points est choisi. En pratique, cette approximation est assez bonne, car la majorité des objets sortant de ces requêtes n'ont pas un ensemble de magnitudes qui correspond à une naine blanche. Afin d'augmenter les chances de sélectionner un ensemble de photométrie qui correspond à l'étoile, la différence maximale que peut avoir chaque point a été posée arbitrairement à 0.3. Si aucun objet résultant de la requête n'est accepté, la requête est effectuée à nouveau en augmentant le rayon, pour aller jusqu'à un rayon de 2 arcsecs. Si la photométrie SDSS n'est pas disponible pour un objet, la photométrie de Gaia est convertie en g et r de SDSS à l'aide des équations suivantes :

Posons BR $= G_{\rm BP} - G_{\rm RP}$

$$g_{\rm SDSS} \approx G - 0.13518 + 0.46245(BR) + 0.25171(BR)^2 - 0.021349(BR)^3 \tag{2.3.1}$$

$$r_{\rm SDSS} \approx G - 0.12879 + 0.24662(BR) - 0.027464(BR)^2 - 0.049465(BR)^3 \tag{2.3.2}$$

Les équations 2.3.1 et 2.3.2 sont tirées de Evans et al. (2018) et sont aussi disponibles dans la documentation de Gaia [3]. Le processus de sélection est alors effectué en comparant seulement les valeurs de g et r. Comme un des objectifs de ce projet est de produire une analyse statistique, il était important d'obtenir la photométrie du plus grand nombre d'étoiles possible. Entre autres, dans le cas des candidates, si de nouveaux types spectraux deviennent disponibles durant l'analyse, il sera alors facile d'ajouter ces étoiles à l'échantillon. Les données Pan-STARRS de cet échantillon sont présentées à la figure 2.5. Celle-ci montre M_g vs. $g - z$ pour toutes les étoiles de l'échantillon. Superposés aux données sont des courbes de couleurs théoriques toutes pour des masses de 0.6 $M_\odot$, soit H-pur, He-pur, $\log {\rm H/He} = -5$ et $\log {\rm H/He} = -2$.

De façon générale, les étoiles DA et non-DA sont bien représentées par les courbes H-pur et $\log {\rm H/He} = -5$ respectivement. Cependant, deux populations d'étoiles DA se situent à l'extérieur de la séquence à 0.6 $M_\odot$ habituelle. La population à luminosité plus élevée peut être expliquée par des systèmes binaires de naines blanches contenant au moins une DA. Dans le cas de la population moins lumineuse, il s'agit d'étoiles DA massives dont l'origine n'est pas encore tout à fait connue. Celles-ci sont moins lumineuses, car plus une naine blanche est massive, plus son rayon est petit. Une partie de cette population provient d'anciens systèmes binaires contenant deux étoiles qui ont fusionné. Il existe plusieurs types de systèmes binaires permettant la création d'une seule naine blanche massive : MS + MS, post-MS + MS, MS + WD et WD + WD avec MS pour séquence principale et WD pour naine blanche. Selon Temmink et al. (2020), la fusion de deux étoiles est le mécanisme qui est progéniteur de $10-30\%$ des naines blanches et qui compte pour $30-50\%$ des naines blanches massives. Cependant, Kilic et al. (2020a) trouvent que les naines blanches issues de systèmes binaires ne permettent pas d'expliquer à elles seules l'existence de la population de DA massives. Puisque ce type de figure ne donne qu'un avant goût de la masse des étoiles, cette population sera traitée avec plus grande précision dans la section 4. La courbe de couleur avec $\log {\rm H/He} = -2$ permet de représenter, en partie, une séquence de DC qui se dirige vers le bleu. Il s'agit en fait des fameuses étoiles IR-faint discutées en détail dans Bergeron et al. (2022a). Lorsque l'atmosphère d'une naine blanche refroidit et devient plus dense, l'hydrogène moléculaire peut alors entrer en collision avec l'hélium ($\rm H_2 - He$), ce qui résulte

3. https ://gea.esac.esa.int/archive/documentation/GDR2/

en une absorption de flux dans l'infrarouge appelée *collision−induced absorption* (CIA) par l'hydrogène moléculaire. Ce déficit de flux infrarouge est visible dans la distribution d'énergie de ces objets. Dans ce diagramme, cela se traduit par une excursion du côté bleu car le flux est redistribué dans ces régions.

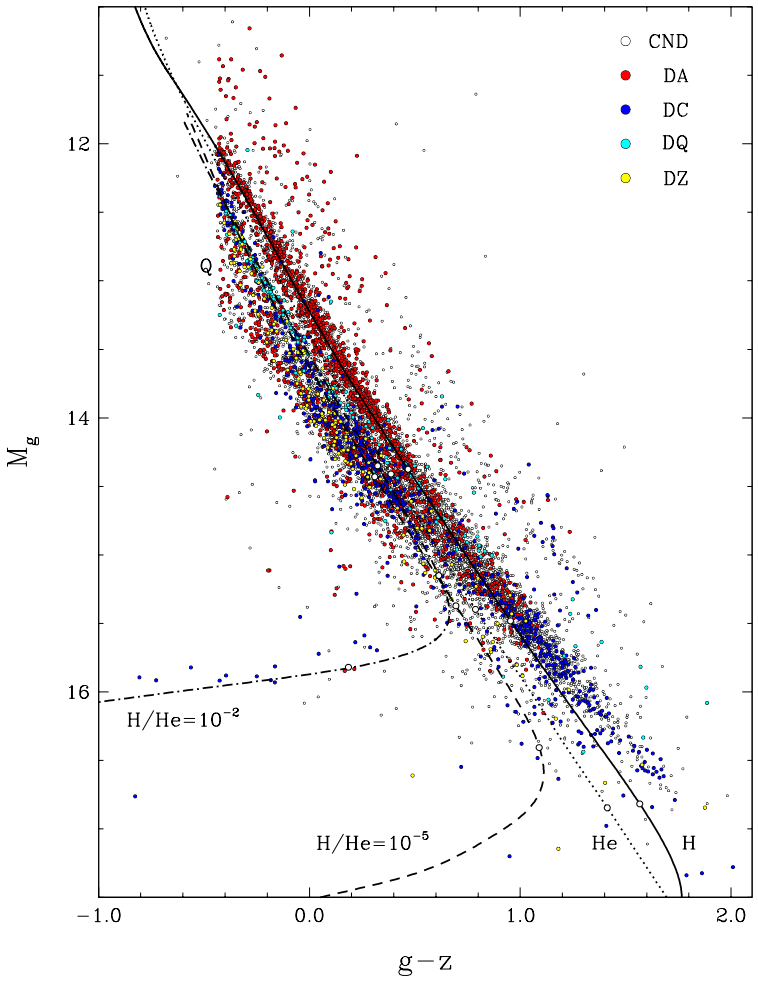

FIGURE 2.5 Diagramme couleur-magnitude M_g vs. $g-r$ de Pan-STARRS pour les étoiles de l'échantillon tiré du MWDD. Les étoiles connues ainsi que les candidates sont montrées avec différentes couleurs indiquées dans la légende. Les séquences de couleurs théoriques sont montrées avec masses constantes pour 0.6 $M_\odot$ avec atmosphère H-pur (trait plein), He-pur (pointillé), mixte avec trace d'hydrogène $\log \mathrm{H/He} = -5$ (tirets) et $\log \mathrm{H/He} = -2$ (point-tirets). Les cercles blancs sur chaque courbe indiquent l'emplacement de $T_{\mathrm{eff}} = 6000$ K, 5000 K, and 4000 K.

En regardant de plus près la région $(g-z) > 0.4$, on voit que les DQ subissent une bifurcation plus importante et à plus haute température que celle des DC, de façon à créer une branche distincte du reste des étoiles. Dans le cas des DZ, la bifurcation semble être plus faible, car ces étoiles se retrouvent en partie en dessous de la courbe à 0.6 $M_\odot$ riche

en hydrogène, contrairement aux DC. Étant donné la proximité des différentes populations d'étoiles dans cette figure, il est difficile de présenter clairement les courbes de couleurs théoriques de façon à contraindre les abondances atmosphériques des DQ et DZ. La section 2.4 analyse ces populations plus en détail à l'aide de la photométrie SDSS.

L'échantillon comporte 7 objets plus brillants que la limite de saturation de Pan-STARRS soit g=13.5. Pour ces objets, nous avons donc utilisé de la photométrie $BVRI$, qui a une limite de saturation plus élevée, au lieu de $grizy$. Les différents points sont donnés dans le tableau 2.1.

Tableau 2.1 – Photométrie BVRI utilisée.

Nom J	B	V	R	I
J0049+0522	12.09	12.38	12.15	11.89
J0138−0459	13.19	12.86	12.63	12.38
J0431+5858	12.73	12.43	12.17	11.86
J0740−1724	13.36	13.06	12.89	12.70
J1205−2333	13.04	12.90	12.66	12.52
J1634+1736	13.36	13.14	13.34	...
J2142+2059	13.37	13.24	13.10	12.98

2.4. Sloan Digital Sky Survey

Le Sloan Digital Sky Survey (SDSS) est un des plus anciens programmes d'observation d'objets célestes encore opérationnel aujourd'hui. Depuis le début de ses opérations en 2000, il a produit une multitude de relevés touchant une grande variété d'objets célestes. Le télescope de SDSS est situé à l'observatoire d'Apache Point au Nouveau-Mexique. Il permet d'observer le ciel à travers 5 filtres photométriques u, g, r, i et z et d'effectuer de la spectroscopie dans le domaine du visible et de l'infrarouge. Les relevés SDSS sont cumulatifs et divisés en différentes phases dont 4 qui sont actuellement complétées. Les deux premières phases, SDSS-I et SDSS-II, ont été complétées en 2008 avec la publication de SDSS DR7 (Abazajian et al., 2009), SDSS-III en 2014 avec SDSS DR12 (Alam et al., 2015) et SDSS-IV en 2020 avec SDSS DR17 (Abdurro'uf et al., 2021). Les relevés totalisent aujourd'hui plus d'un demi milliard d'objets ayant de la photométrie $ugriz$ et 4 millions de spectres dans le domaine du visible. Grâce à ces relevés, la quantité de naines blanches ayant un type spectral connu a grandement augmenté (Eisenstein et al., 2006; Kleinman et al., 2013a; Kepler et al., 2019a). Ce catalogue est limité à un volume bien défini du ciel, ceci permet de produire un échantillon d'étoiles non-biaisées et d'obtenir une meilleure estimation des fonctions de luminosité et de masses

des naines blanches (Kilic et al., 2020a). Les données utilisées dans ce projet proviennent du SDSS DR16 (Ahumada et al., 2020).

Le système photométrique utilisé par SDSS comprend une région du spectre allant du proche ultraviolet jusqu'au proche infrarouge. Il comprend 5 filtres, soit u (300-400 nm), g (400-550 nm), r (550-700 nm), i (700-850 nm) et z (800-1100 nm), illustrés à la figure 2.6. Pour la majorité des objets de ce projet, l'analyse photométrique fait seulement l'usage du point u de SDSS. Cette bande est située dans la région du saut de Balmer et permet donc de prédire s'il y a présence d'hydrogène dans l'atmosphère de la naine blanche. Pour certains objets où la photométrie Pan-STARRS $grizy$ est de mauvaise qualité, il peut être préférable d'utiliser l'ensemble de la photométrie SDSS. La figure 2.6 permet de comparer les systèmes photométriques de Pan-STARRS et SDSS. La réponse des filtres dans le proche infrarouge est bien meilleure pour Pan-STARRS, c'est pourquoi il est préférable d'utiliser ce système conjointement à la bande u de SDSS afin de mieux échantillonner la distribution d'énergie des étoiles.

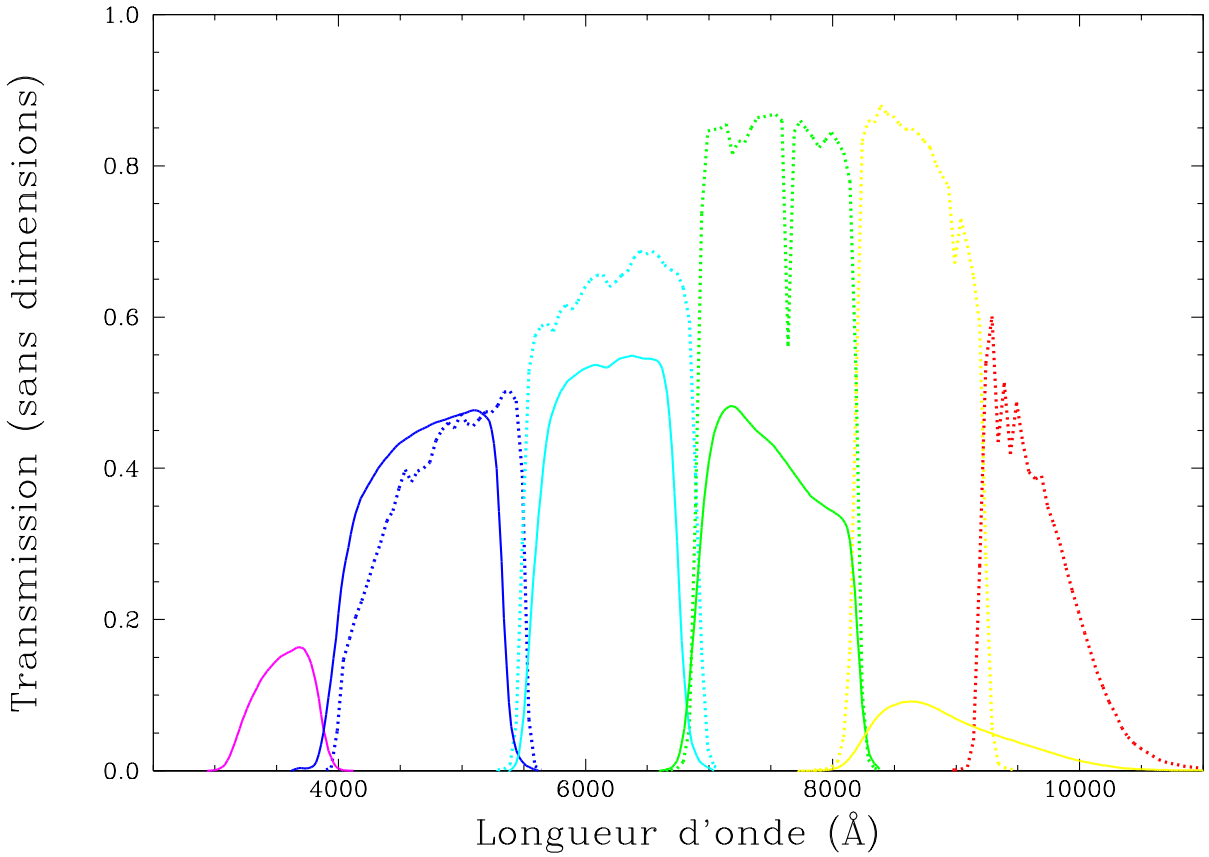

FIGURE 2.6 Bandes passantes des filtres *ugriz* de SDSS (traits pleins) sur lesquelles sont superposées les bandes *grizy* de Pan-STARRS (pointillés). Les courbes représentent les filtres *ugrizy* de gauche à droite respectivement. L'axe verticale illustre la réponse des filtres selon la longueur d'onde d'un photon incident.

La photométrie *ugriz* utilisée dans ce projet provient majoritairement de SDSS DR16. Les données ont été récupérées en utilisant une méthode similaire à celle expliquée dans la section 2.3. Afin de sélectionner l'ensemble de photométrie SDSS correspondant à l'étoile, les valeurs de g et r sont estimées en utilisant les équations 2.3.1 et 2.3.2, puis comparées aux résultats de la recherche. Si la photométrie Pan-STARRS est connue pour cet objet, la valeur de z est utilisée pour affiner la recherche davantage. Ceci offre une meilleure représentation de la distribution d'énergie et permet d'isoler le bon ensemble de données. La photométrie *ugriz* a été obtenue pour 4284 objets de l'échantillon, soit 82% des étoiles connues et 36% des candidates. Les étoiles ayant au moins un point u, g et r sont présentées dans la figure 2.7. Celle-ci montre M_g vs $u-g$ ainsi que les mêmes séquences de couleurs théoriques à 0.6 $M_\odot$ utilisées dans la figure 2.5.

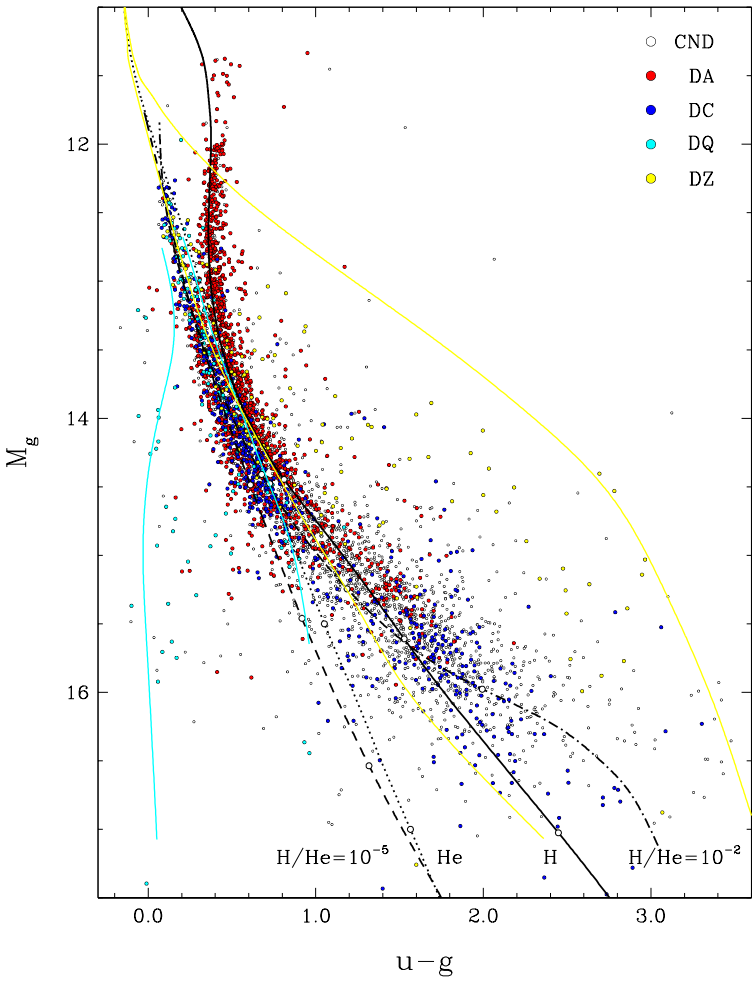

FIGURE 2.7 Même figure que 2.5, mais pour M_g vs. $u-g$ de SDSS. Des courbes de couleurs théoriques à 0.6 $M_\odot$ sont montrées pour les étoiles DQ (cyan) avec $\log \mathrm{C/He} = -5$ (gauche) et $\log \mathrm{C/He} = -7.5$ (droite) et pour les étoiles DZ (jaune) avec trace d'hydrogène $\log \mathrm{H/He} = -5$ et calcium $\log \mathrm{Ca/He} = -11.5$ (gauche) et $\log \mathrm{Ca/He} = -7$ (droite).

L'élément le plus frappant de la figure 2.7 est la bifurcation entre les DA et non-DA à $u-g < 0.4$ qui s'explique facilement par le saut de Balmer. La présence d'hydrogène dans une atmosphère d'étoile vient étouffer son flux dans l'ultraviolet, résultant en une différence marquée avec la couleur des étoiles dépourvues d'hydrogène. Dans cette figure apparaissent deux branches distinctes pour les étoiles DQ et DZ, qui n'étaient pas visibles précédemment avec la photométrie Gaia et Pan-STARRS. Des séquences de couleurs théoriques à 0.6 $M_\odot$ ont été sélectionnées avec différentes abondances de C et Ca afin de contraindre les régions définies par ces branches. La majorité des étoiles DQ sont incluses à l'intérieur des séquences $\log \mathrm{C/He} = -5$ et $\log \mathrm{C/He} = -7.5$. Dans le cas des DZ, la presque totalité des étoiles sont situées à l'intérieur des séquences $\log \mathrm{Ca/He} = -11.5$ et $\log \mathrm{Ca/He} = -7$ avec toutes

deux une trace d'hydrogène $\log \mathrm{H/He} = -5$. Bien qu'il aurait été possible de contraindre ces populations d'étoiles en utilisant des modèles avec différentes masses et abondances, les courbes choisies ici semblent être les plus appropriées.

2.5. Photométrie infrarouge

Dans les deux dernières décennies, il y a eu trois principaux programmes d'imagerie dans le domaine du proche infrarouge. Le premier fut le Two Micron All-Sky Survey (2MASS), qui a cartographié la sphère céleste entière dans les bandes J (1.25 µm), H (1.65 µm) et K_S (2.16 µm) (Skrutskie et al., 2006). Celui-ci a été un précurseur pour les deux autres programmes, soit le UKIRT Infrared Deep Sky Survey (UKIDSS) et le Visible and Infrared Survey Telescope for Astronomy (VISTA). UKIDSS a cartographié l'hémisphère nord du ciel dans les bandes Z (0.88 µm), Y (1.03 µm), J (1.25 µm), H (1.63 µm) et K (2.20 µm) (Hewett et al., 2006) alors que le télescope VISTA a observé l'hémisphère sud du ciel dans les bandes Z (0.88 µm), Y (1.02 µm), J (1.25 µm), H (1.65 µm) et K_S (2.20 µm) (Emerson et al., 2006; Dalton et al., 2006). Ce projet fait l'usage de photométrie JHK provenant de ces trois systèmes. Ajouter des données dans l'infrarouge à notre ensemble de points photométriques permet d'échantillonner une plus grande partie de la distribution d'énergie des étoiles et donc d'obtenir des valeurs plus précises de leurs paramètres physiques. De plus, la photométrie infrarouge permet d'identifier la présence d'hydrogène dans une atmosphère de naine blanche froide via le mécanisme de CIA. Ceci permet donc d'identifier la composition atmosphérique des naines blanches avec $T_{\mathrm{eff}} < 5200$ K malgré le fait que les raies d'hydrogène ne soient plus visibles à ces températures. Les données proviennent d'une multitude de relevés dans chacun des systèmes, mais MKO (UKIDSS) et VISTA, étant de meilleure qualité, sont priorisées par rapport à 2MASS pour les étoiles moins brillantes. Des données JHK du système Bessel ont aussi été incluses pour 20 étoiles.

Tableau 2.2 – Photométrie JHK

Système	J	H	K ou Ks
MKO	1665	758	714
VISTA	542	169	400
2MASS	404	685	488
BESSEL	20	20	20

Les données photométriques acquises pour l'échantillon de ce projet sont présentées dans le tableau 2.2. Ce dernier montre le nombre d'étoiles ayant un point J, H ou K en provenance

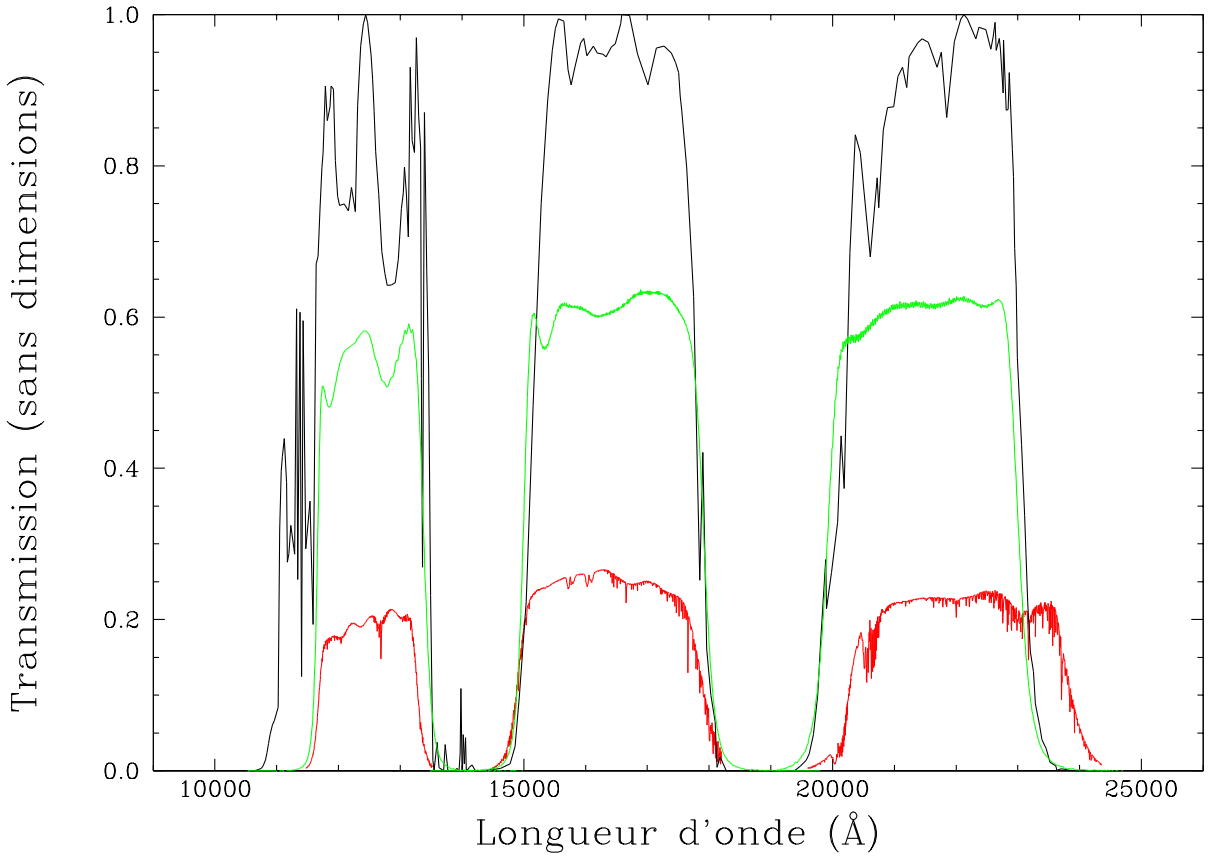

FIGURE 2.8 Bandes passantes des filtres J (gauche), H (milieu) et K (droite) des systèmes MKO (rouge), VISTA (vert) et 2MASS (noir). L'axe verticale illustre la réponse des filtres selon la longueur d'onde d'un photon incident. Les systèmes sont normalisés à des maximums différents.

d'un certain système photométrique. Seules les étoiles ayant un type spectral connu en font partie. Un total de 2644 étoiles ont de la photométrie dans au moins une des trois bandes, incluant 1473 ayant l'ensemble JHK complet. Ceci représente respectivement 92% et 51% de l'échantillon d'étoiles connues. Ces données proviennent en majeure partie du travail de Sandy Leggett, qui a cherché les différents relevés de photométrie infrarouge afin de récolter les plus récentes mesures associées à nos étoiles ayant un type spectral connu. Les bandes JHK du système MKO, ainsi que celles de VISTA et 2MASS sont illustrées à la figure 2.8. On remarque que les bandes J et K de 2MASS sont moins bien définies et sont donc de qualité inférieure à celles des deux autres systèmes. Par contre ces trois systèmes couvrent un domaine spectral similaire, ce qui permet d'inclure ces données dans l'échantillon et de préserver son homogénéité.

2.6. Données spectroscopiques

Avec sa vaste couverture du ciel, le Sloan Digital Sky Survey a certainement permis la classification spectrale de la majorité des naines blanches connues aujourd'hui. Dans la dernière décennie, il y a eu deux principaux travaux menés afin d'étudier les spectres de naines blanches parmi les relevés de SDSS. Le premier travail a été effectué par Kleinman et al. (2013a), qui a permis de classifier 20,407 spectres de naine blanche à partir du SDSS DR7. Le deuxième travail, Kepler et al. (2019a), a identifié le type spectral de 20,088 naines blanches dans le SDSS DR14. Puisque les relevés du SDSS sont cumulatifs, cela implique que la qualité de certaines données augmente avec le temps. Différentes sections du ciel sont observées à plusieurs reprises, permettant de combiner les spectres de certaines étoiles pour obtenir un meilleur rapport signal sur bruit. Ce projet fait usage des spectres de SDSS inclus dans les bases de données du MWDD, qui ont été extraits directement de SDSS DR14. Les spectres couvrent un domaine de longueur d'onde s'étalant de 3800 à 9200 Å. Parmi les étoiles ayant un type spectral connu dans cet échantillon, 42% ont un spectre du SDSS, représentant 1036 étoiles. Des exemples de spectres inclus dans le MWDD provenant de SDSS sont présentés aux figures 2.9 et 2.10, identifiés par un astérisque.

L'échantillon de ce projet est basé sur les étoiles incluses dans le MWDD et fait l'utilisation de ses spectres. Cela implique des spectres provenant directement de SDSS, mais aussi des spectres de Kilic et al. (2020a), Tremblay et al. (2020a), Bergeron et al. (2001a), Limoges et al. (2015a) et autres. L'échantillon contient un total de 1227 spectres provenant de SDSS et 2754 provenant d'autres sources. Le nombre de naines blanches ayant au moins un spectre, toutes sources confondues, est 2678. Idéalement, le type spectral associé à un objet du MWDD provient directement des bases de données de SIMBAD. Ceci permet donc de relier une étoile à la source de sa classification spectrale. Cependant, il est possible qu'un objet affiche plusieurs types spectraux, car il a été étudié dans différents articles. Ceci peut être dû au fait qu'avec les avancées technologiques, certaines étoiles sont observées à nouveau avec des appareils plus précis, permettant d'obtenir un meilleur rapport signal sur bruit. Certaines raies spectrales faibles qui étaient cachées par le bruit sont révélées, permettant de corriger les classifications fautives de certaines DC.

Le travail effectué dans ce projet a permis de corriger des erreurs de classification pour 88 naines blanches connues et d'identifier le type spectral de 26 candidates. Le tableau 2.3 montre le type spectral affiché dans le MWDD pour les 114 étoiles ainsi que leur nouvelle classification suite à nos corrections. Certaines étoiles ont été reclassifiées comme candidates dû au manque de données spectrales fiables disponibles. De plus, la classification DQpec a été remplacée par DQ.

Des exemples de spectres provenant du MWDD sont présentés dans les figures 2.9 et 2.10 pour différents type spectraux de naines blanches incluses dans cet échantillon. Les spectres

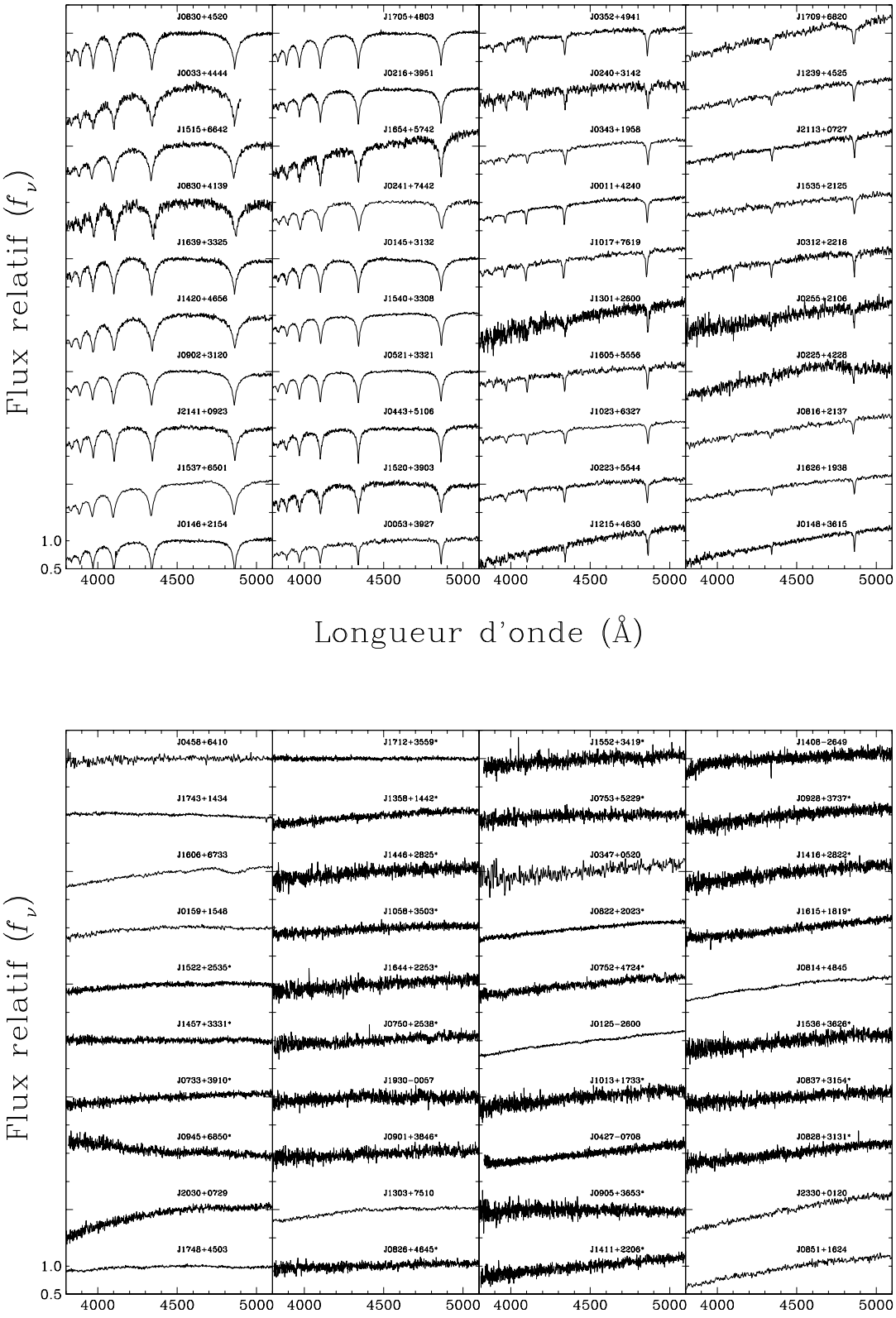

FIGURE 2.9 Exemples de spectres d'étoiles de type DA (haut) et de type DC (bas).

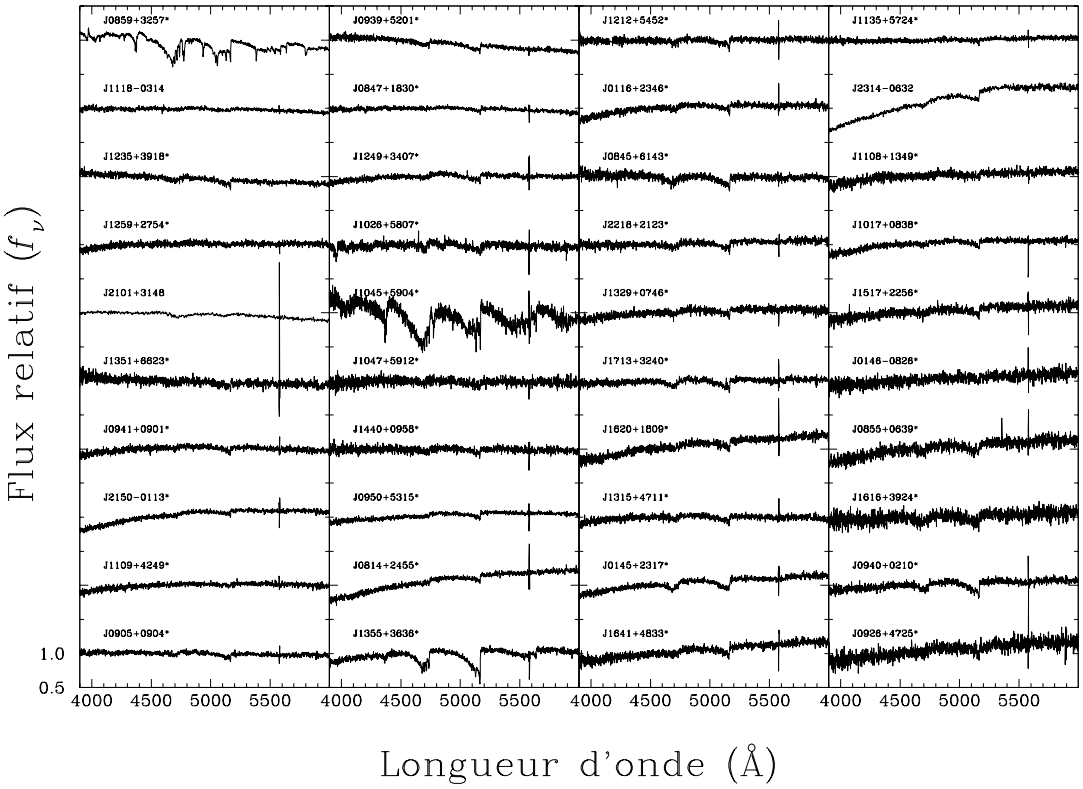

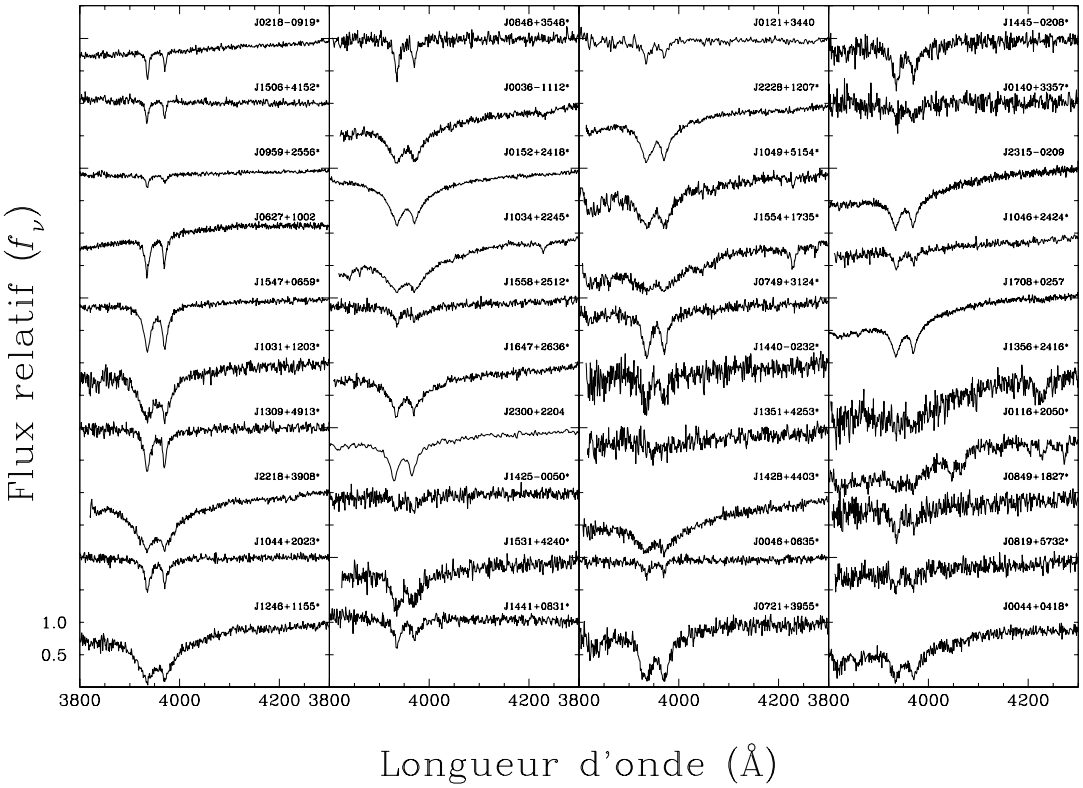

FIGURE 2.10 Exemples de spectres d'étoiles de type DQ (haut) et de type DZ (bas).

sont disposés selon la température calculée via la méthode photométrique avec l'étoile la plus chaude située en haut à gauche et la plus froide en bas à droite. Les spectres notés par un astérisque proviennent de SDSS. Le panneau du haut de la figure 2.9 montre des étoiles de type DA. Ces spectres sont caractérisés par les raies d'absorption Hβ (4861.32 Å), Hγ (4340.46 Å), Hδ (4101.73 Å), Hε (3970.07 Å) et H8 (3889.02 Å) de la série de Balmer causées par la présence d'hydrogène dans l'atmosphère de ces étoiles. Les raies sont beaucoup plus fortes lorsque $T_{\rm eff}$ est élevée. La raie Hα (6562.80 Å) n'est pas montrée ici, car certains des spectres ne l'incluaient pas. Le panneau du bas montre des spectres d'étoiles de type DC qui ne montre aucune raie d'absorption. Ces naines blanches ont généralement une atmosphère constituée d'hélium si la température est suffisamment élevée ($T_{\rm eff} > 5000$ K). Dans le cas des étoiles DC plus froides, la température est trop faible pour que les raies d'hydrogène soient visibles dans leur spectre. Les données spectroscopiques ne sont donc pas suffisantes pour déterminer les compositions atmosphériques de ces étoiles. Une méthode permettant de résoudre ce problème est discutée dans la section 3.1.1.

Le panneau du haut de la figure 2.10 montre des étoiles de type DQ. Ces naines blanches ont des atmosphères composées majoritairement d'hélium avec des traces de carbone moléculaire C_2. La présence de C_2 dans l'atmosphère est reflétée par les bandes de Swan visibles dans le spectre. Le panneau du bas montre les étoiles de type DZ. Ces naines blanches ont aussi des atmosphères riches en hélium, mais avec des traces de métaux et parfois aussi des traces d'hydrogène. La présence de métaux est principalement visible par les raies d'absorption H (3933 Å) et K (3969 Å) du Ca II. Habituellement les traces d'hydrogène contenues dans ces étoiles sont faibles et sont plus facilement visibles dans la région de Hα. Des exemples de ces étoiles sont présentés dans la section 3.1.3. L'origine de ces différents types spectraux et les mécanismes permettant la création de ces étoiles sont présentés plus en détail dans les sections 3.1.1 pour les DA et DC, 3.1.2 pour les DQ et 3.1.3 pour les DZ.

Tableau 2.3 – Correction des erreurs de classifications spectrales du MWDD.

Gaia DR2	MWDD	Reclassification
1057653804222121600	DB :	DC :
2337472660210623488	DB	CND
2387595031633735168	DB	CND
2425650847058388224	CND	DC
2780434524599787136	CND	DC
2815415285174565248	CND	DC
3079642326059886208	CND	DA
3427482725113315200	CND	DC

Tableau 2.3 *suite sur la page suivante*

Tableau 2.3 *(suite)*

Gaia DR2	MWDD	Reclassification
3651747667992161920	DA+DC ?	DA
3656509794586217984	CND	DA
3684741301817503872	CND	DA
3725570772761744384	DA+DC ?	DAZ
3767515389014753152	DA	DAH
4013717723468865152	DB :	DC
4073522222505044224	CND	DA
4361621688038664064	CND	DA
447166581862730752	DB	CND
4487104135457345920	DB ?	CND
4881098119928195456	DB	DC
675590693439332096	DA	DAH
719266799987963392	DC+M	DC
814576110016081920	CND	DC
2768190500551905408	DC+M	DC
915672081021495552	DH :	DH
740483560857296768	DQpecP	DQ
551153263105246208	DAe	DAH :
290531967521897856	DC :DA	DC
1602197696772907648	DC	DA
5034187758131178880	A5	CND
1118460924703171584	DC/DZ	CND
4450425359563998848	DQ	CND
709051168734737024	DA+DC ?	DA :
1545014807135001088	DA+dM	DC
2675091174536113792	DC+M	DC
4227915744043939584	DA+DC	DA
4420124124769394176	DC-DQ	DA
1290050262657404544	DC/DQ	DC
131978710009614336	B	CND
134083729316431872	B	CND
3300838845520683008	B	CND
3896315612771069184	DC/DQ	DC
1265985590961480192	DC/DQ	DC

Tableau 2.3 *suite sur la page suivante*

Tableau 2.3 *(suite)*

Gaia DR2	MWDD	Reclassification
603155765049434752	DC/DQ	DC
2702527013306504064	DC/DQ	DC
624090737025312000	DC/DQ	DC
2687584757658775424	DAB	CND
1809844934461976832	DAepv	CND
780275504757613568	CND	DA
3884899559633556224	DQ	DC
1527940564084210816	DA	DAH
2792315366213367296	DA	DAP
4027510375284724608	DQ	DC
1643544689800386176	DQ	DC
2524879812959998592	DAH :	DA
960039814744267520	DA	DAH
3933386712453327360	DAweak	DA+DC
1498271406743008640	DA	DAH :
4518917168694695168	DA	DA+DC
2681243457490130304	DA	DC
1999615350008375552	DA	DA+DC
618571635330439040	DZ	DC
2528728726428345216	DA	DC
5070533180139377792	DB	CND
55103056018558592	DA :	DC
291186211300158592	DAZ	DZA
6246049446837287680	DA	DAH :
127366331745660288	DA	DC
902414964384353408	CND	DC
3691095100341397632	CND	DC
1394479501945576064	CND	DC
4449818459207085696	CND	DC
1253770497813126144	DC	DA
3911460633824772224	DC	DQA
3654870693331906304	CND	DC
4600426645699105664	CND	DA
4508113436149576960	CND	DQ

Tableau 2.3 *suite sur la page suivante*

Tableau 2.3 *(suite)*

Gaia DR2	MWDD	Reclassification
4228576550540445184	CND	DC
4463261431966304768	CND	DC
688818750329816192	CND	DC
925003537421986304	CND	DC
2564945432560219008	DAZ :	DZA
2877080497170502144	CND	DC
3303137301563100544	CND	DC
1582663189077609088	DC	DA
3146523896095375744	DC	DA
1540371883066128768	DC	DA
1315371255234720896	DZA	DA
915672081021495552	DH	DAH :
2979519903882838528	sdB	DA :
1928174375826595072	sdOD	DA :
6310405202436481024	sdB	DA :
2839397832801325952	sdB	DA :
4019734594693512704	No	DC :
1767957488499891968	DZ	DZA
3694399755554510720	DZP	DZH
306779618349361920	DZ	DZH
921642532239821440	DZ	DZH
1471788161655374080	DZ	DZH
1356633384004567168	DZ	DZH
1764481588648685440	DZ	DZA
2808103391115590016	DC	DA
4891567154251463680	DC	DA
3326650224581677312	DC	DAH
900399039877540096	DC	DA
3791951961927535616	DC	DA
1670992421335403904	DC	DA
1232045934759720192	DC	DA
6907079269131974912	DC	DA
1666074615061406336	DZ	DC
634839219101579136	DZ	DC

Tableau 2.3 *suite sur la page suivante*

Tableau 2.3 *(suite)*

Gaia DR2	MWDD	Reclassification
2377643661128402048	DA	DAH
3418741367154043648	DA	DAH :
3746179365877952256	DA	DAH
3688402091422432128	DAO	DA :
2776464325551066880	DZA	DZAH :

Chapitre 3

Détermination des paramètres physiques

3.1. Méthode spectro-photométrique

La méthode spectro-photométrique permet de déterminer les paramètres physiques et la composition atmosphérique d'une naine blanche en utilisant les données spectrales de façon complémentaire à la méthode photométrique. La partie spectroscopique de cette technique sera expliquée dans les sous-sections suivantes, car celle-ci varie selon le type spectral de l'étoile. Cependant, la partie photométrique est essentiellement la même peu importe le type de naine blanche étudié et sera donc expliquée une seule fois. Cette méthode a été développée par Bergeron et al. (1997a) et fait l'usage de la photométrie, la parallaxe ainsi que des modèles d'évolution stellaire afin de calculer les paramètres physiques d'une naine blanche. D'abord, les magnitudes obtenues par photométrie sont converties en flux observés afin d'être comparés aux flux prédits par des modèles d'atmosphère. Les équations nécessaires à la conversion varient selon le système de magnitude. Les systèmes de magnitude SDSS et Pan-STARRS sont définis en termes de magnitudes AB_ν à la fréquence ν en hertz (Holberg & Bergeron, 2006a). Les magnitudes m_ν sont converties en flux moyens f_ν^m à l'aide de l'équation suivante :

$$m_\nu = -2.5 \log f_\nu^m + c_m \tag{3.1.1}$$

où

$$f_\nu^m = \frac{\int_0^\infty f_\nu S_m(\nu) d[\log \nu]}{\int_0^\infty S_m(\nu) d[\log \nu]} \tag{3.1.2}$$

et où $S_m(\nu)$ est la fonction de transmission de la bande passante correspondante, f_ν est le flux de l'étoile reçu sur Terre et c_m est une constante, qui dans le cas du système AB_ν, est égale à -48.60. Afin de transformer correctement les bandes u, i et z de SDSS dans le

système AB_ν, il est nécessaire d'appliquer les corrections suivantes tirées de Eisenstein et al. (2006) :

$$\begin{aligned} u &= u_{\rm SDSS} - 0.040 \\ i &= i_{\rm SDSS} + 0.015 \\ z &= z_{\rm SDSS} + 0.030 \end{aligned} \tag{3.1.3}$$

Pour la photométrie JHK, le système de magnitude utilisé est basé sur Véga. Dans ce système, les magnitudes m_λ sont converties en flux moyens f_λ^m à l'aide de l'équation suivante :

$$m_\lambda = -2.5 \log f_\lambda^m + c_m \tag{3.1.4}$$

où

$$f_\lambda^m = \frac{\int_0^\infty f_\lambda S_m(\lambda) \lambda d\lambda}{\int_0^\infty S_m(\lambda) \lambda d\lambda} \tag{3.1.5}$$

et où f_λ est le flux de l'étoile reçu sur Terre et $S_m(\lambda)$ est la fonction de transmission de la bande passante correspondante. La valeur de c_m est isolée dans l'équation 3.1.4 en utilisant le flux tabulé de Véga. Les constantes sont présentées dans le tableau 3.1 pour les différents systèmes de photométrie infrarouge.

Tableau 3.1 – Points zéros des systèmes de photométrie infrarouge.

Système	J	H	K
MKO	−23.81417	−24.83432	−26.00342
VISTA	−23.83721	−24.87465	−25.91724
2MASS	−23.76771	−24.86404	−25.92455
Bessel	−23.75551	−24.84898	−25.99941

Puisque toutes les étoiles de l'échantillon se situent à une distance moindre que 100 parsecs, la correction due au rougissement est ignorée. Les fonctions de transmissions des filtres utilisés sont montrées dans le chapitre 2 et sont tirées de Doi et al. (2010) pour $ugriz$, Tonry et al. (2012a) pour $grizy$ et Hewett et al. (2006) pour JHK. Les flux moyens observés sont alors comparés au flux théoriques. Bien entendu, les modèles d'atmosphère prédisent le flux monochromatique de l'étoile, alors que les mesures représentent un échantillonage de flux moyens dans certaines bandes de la distribution d'énergie. Le flux théorique est donc converti

en flux moyens H_λ^m pour chaque bande en substituant f_ν par H_ν dans l'équation 3.1.2 et f_λ par H_λ dans l'équation 3.1.5 où H_ν et H_λ sont le flux monochromatique d'Eddington par unité de fréquence ν et de longueur d'onde λ, respectivement. En pratique, un facteur de c/λ^2 est appliqué à f_ν^m et H_ν^m afin d'obtenir f_λ^m et H_λ^m, permettant ainsi une homogénéité dans les calculs de flux. Selon la loi du carré inverse, on peut déduire la relation suivante entre le flux théorique de l'étoile et celui mesuré sur Terre :

$$f_\lambda^m = 4\pi(R/D)^2 H_\lambda^m \tag{3.1.6}$$

où R/D est le ratio du rayon de l'étoile sur sa distance à la Terre. Des grilles contenant les valeurs de H_λ^m en fonction de $T_{\rm eff}$ et $\log g$ sont produites pour différentes abondances N(He), N(H) et N(Z) selon le type spectral de naine blanche étudié (voir sections suivantes). L'équation 3.1.6 contient 2 paramètres libres, soit $T_{\rm eff}$ et l'angle solide $\pi(R/D)^2$. Cependant, la distance peut être déduite de la parallaxe, laissant R comme seul inconnu. Le rayon est converti en masse à l'aide des séquences évolutives de Bédard et al. (2021), basées sur des modèles de naines blanches ayant un coeur à part égale en C et O, une enveloppe d'hélium $q(\mathrm{He}) \equiv M_{\rm He}/M_* = 10^{-2}$ et une couche d'hydrogène mince $q(\mathrm{H}) = 10^{-10}$ pour les solutions He-pur ou mixte, ou une couche épaisse de 10^{-4} pour les solutions H-pur. La gravité de surface peut alors être calculée avec l'équation suivante :

$$g = \frac{GM}{R^2} \tag{3.1.7}$$

où G est la constante gravitationnelle. L'objectif est de déterminer la valeur de $T_{\rm eff}$ et de l'angle solide de sorte que les équations 3.1.6 et 3.1.7 soient cohérentes. Pour déterminer ces paramètres, on utilise une méthode de minimisation par les moindres carrées de Levenberg-Marquardt (Press et al., 1986a). Une valeur de χ^2 est calculée à l'aide de l'équation suivante :

$$\chi^2 = \sum_{i=1}^{N} \frac{(f_\lambda^i - 4\pi(R/D)^2 H_\lambda^i)^2}{\sigma_i} \tag{3.1.8}$$

où N est le nombre de points photométriques utilisés et σ_i leur incertitude. Obtenir la solution qui correspond le mieux à la photométrie de l'étoile revient donc à minimiser une fonction en deux dimensions, soit en suivant la direction du gradient sur la grille de flux synthétiques. Ce procédé itératif débute en posant comme valeurs initiales $T_{\rm eff} = 8000$ K et $\log g = 8.0$, qui est un point de départ assez général sur la grille. Ces valeurs sont utilisées afin d'obtenir une première estimation de $T_{\rm eff}$ et de l'angle solide. La mesure de parallaxe permet de déduire le rayon R de l'angle solide, qui est ensuite converti en masse à l'aide des séquences évolutives. La gravité est alors calculée avec l'équation 3.1.7 et le résultat obtenu est généralement

différent de la valeur initiale de $\log g = 8.0$. Ce processus est répété jusqu'à ce qu'il y ait cohérence entre le minimum atteint sur la grille et les séquences évolutives. Les incertitudes sur les paramètres sont calculées en propageant l'erreur de la parallaxe trigonométrique lors des itérations et peuvent être obtenues à l'aide de la matrice de covariance. Puisque la somme dans l'équation 3.1.8 est pondérée par l'incertitude des points photométriques, la solution adoptée sera davantage dépendante des mesures les plus précises. L'utilisation de mesures photométriques modernes est donc problématique dans ce genre de calculs, car les barres d'erreurs, étant minuscules, contraignent la solution à passer par certains points. Afin de contrer ce problème, une valeur minimale de $\sigma_i = 0.03$ est utilisée dans le calcul du χ^2, mais les incertitudes sur les paramètres physiques sont basées sur les valeurs réelles de σ_i. Les quantités physiques résultant de la méthode de minimisation peuvent être utilisées pour calculer la luminosité de l'étoile avec :

$$L = 4\pi R^2 \sigma T_{\rm eff}^4 \tag{3.1.9}$$

où σ est la constante de Stefan- Boltzmann. On peut ensuite calculer la magnitude bolométrique avec la relation suivante :

$$M_{\rm bol} = -2.5 \log L/L_{\odot} \tag{3.1.10}$$

où $L_{\odot}$ est la luminosité solaire. L'ensemble des paramètres physiques calculés par la méthode photométrique est fourni au tableau A.2 (Annexe A) et toutes les sorties des objets de l'échantillon sont disponible en ligne comme matériel supplémentaire [1].

3.1.1. DA et DC

Parmi les naines blanches de cet échantillon ayant un type spectral connu, 89.4% sont classées comme une variante de DA (DA, DAZ, DAH, DAP, DA :, DAH :) ou DC (DC, DCP, DC :). Calculer les paramètres physiques de ces étoiles demande simplement l'utilisation de la méthode photométrique expliquée précédemment en supposant différentes compositions atmosphériques. Il y a trois compositions possibles qui permettent de modéliser la distribution d'énergie de ces étoiles : H-pur, He-pur et mixte H/He. Les grilles de valeurs H_λ^m utilisées sont calculées en supposant des abondances atmosphériques de $N(\mathrm{He})/\mathrm{N(H)} = 0$ pour H-pur, $N(\mathrm{H})/\mathrm{N(He)} = 0$ pour He-pur et $\log \mathrm{H/He} \in [-5.0, -1.5]$ par incréments de 0.5 dex pour mixte H/He. La conversion du rayon en masse est effectuée en utilisant les séquences évolutives mentionnées précédemment, soit une naine blanche ayant une enveloppe d'hydrogène épaisse $q(\mathrm{H}) = 10^{-4}$ pour la solution H-pur et une enveloppe d'hydrogène mince

1. http ://www.astro.umontreal.ca/~bergeron/MNRAS

$q(\mathrm{H}) = 10^{-10}$ pour les solutions He-pur et mixte H/He. Dans le cas des étoiles DC froides, on ne connait pas, à priori, la composition atmosphérique. Nous calculons alors trois solutions, soit une pour chaque type de grille de modèles. Le procédé permettant de choisir la meilleure solution parmi ces trois est discuté dans la section 3.2.2. Pour les DA et DC, les données spectrales ne sont pas utilisées dans le calcul des paramètres. Des exemples de solutions typiques d'étoiles de type DA et DC sont montrés à la figure 3.1.

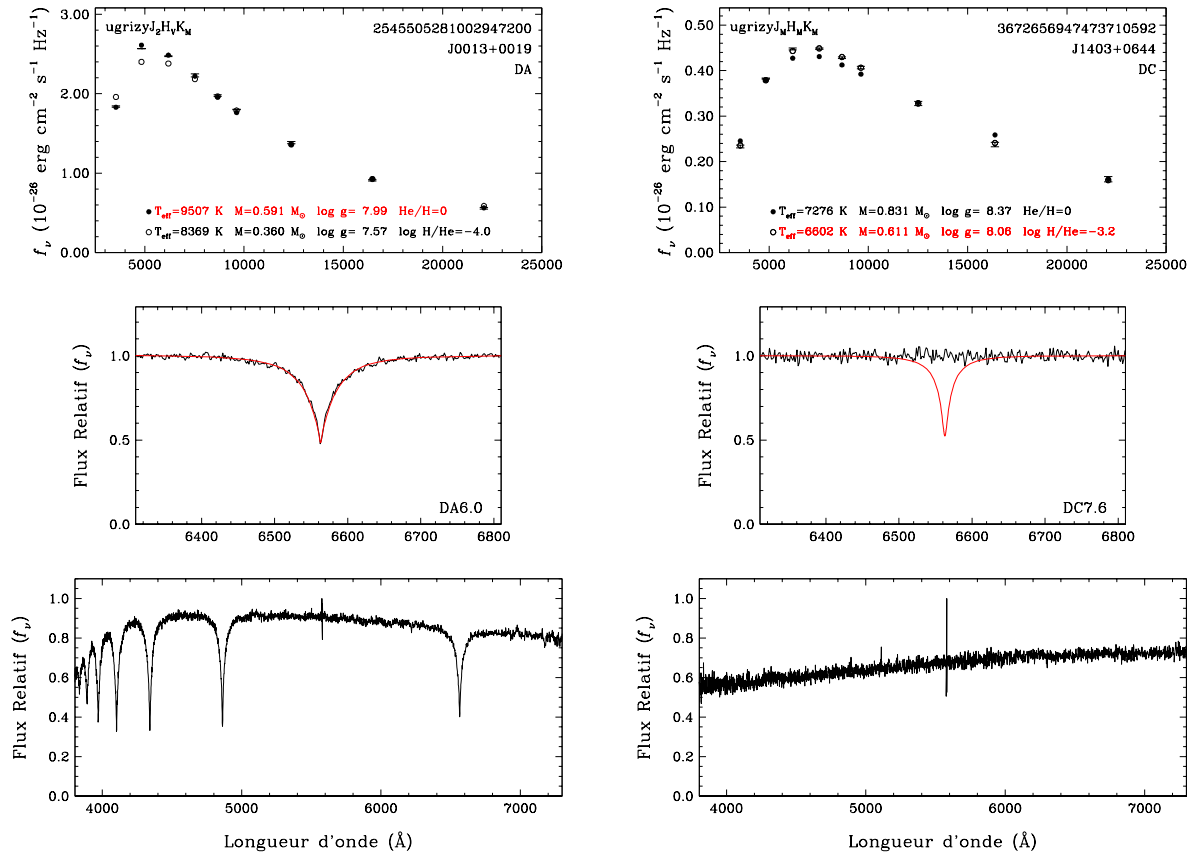

(a) Étoile DA typique.

(b) Étoile DC typique.

FIGURE 3.1 Exemples de naines blanches de type DA (gauche) et DC (droite) traitées via la méthode spectro-photométrique. Le panneau du haut montre la distribution d'énergie de l'étoile ainsi que l'ajustement aux solutions d'atmosphères H-pur (cercles pleins) et mixte H/He (cercles vides). Le panneau du milieu montre le spectre observé dans la raie Hα (noir) superposé au spectre théorique (rouge) interpolé aux valeurs de T_{eff} et $\log g$ de la solution H-pur. Le panneau du bas montre le spectre observé en entier.

Le formalisme utilisé afin de présenter une analyse d'objets via la méthode spectro-photométrique est similaire pour tous les types spectraux. La structure générale sera expliquée une seule fois ici et les subtilités seront indiquées dans les sections appropriées. Le panneau du haut montre la distribution d'énergie de l'étoile. Les identifiants de l'objet, soit le nom J basé sur les coordonnées de Gaia DR2, l'identifiant Gaia DR2 et le type spectral

sont situés dans le coin supérieur droit du panneau. La photométrie observée est représentée par des barres d'erreurs et les bandes utilisées sont indiquées dans le coin supérieur gauche. De plus, des indices sont ajoutés aux points JHK afin d'identifier le système photométrique utilisé pour ceux-ci : M (MKO), V (VISTA), B (Bessel) et 2 (2MASS). Le meilleur ajustement fourni par les modèles d'atmosphère est montré par des cercles pleins ou vides et les paramètres correspondants sont présentés dans le bas du panneau. Dans le cas où 2 solutions sont affichées sur un même panneau, la solution adoptée est alors montrée en rouge. Le panneau du centre montre le spectre observé (noir) normalisé à l'unité, comparé au spectre théorique (rouge) interpolé aux paramètres obtenus de la méthode photométrique et convolué à la résolution appropriée. De plus, le type spectral sous forme d'indice en température $50{,}400/T_{\rm eff}$ est indiqué dans le coin inférieur droit. Le panneau du bas montre le spectre utilisé dans son ensemble.

En ce qui concerne les étoiles DA et DC, la région spectrale montrée dans le panneau du centre est préférablement celle appartenant à Hα, car il s'agit de la raie la plus forte. Si le spectre de l'objet n'inclut pas la région de Hα, la région de Hβ est alors utilisée, l'objectif ici étant de s'assurer que les étoiles DA montrent des raies d'hydrogène dans leur spectre et que les DC n'en montrent pas. Pour les étoiles DA et DC, deux solutions photométriques sont présentées, soit en supposant une atmosphère H-pur (cercles pleins) et He-pur ou mixte (cercles vides). La figure 3.1a présente J0013+0019, qui est une solution quasi-parfaite d'étoile de type DA. Toutes les bandes de la distribution d'énergie sont en accord avec la solution H-pur. La figure 3.1b montre J1403+0644, une étoile DC typique dont la distribution d'énergie est en meilleur accord avec la solution mixte. Les données spectrales ne sont pas utilisées dans la méthode de calculs des paramètres physiques.

3.1.2. DQ

Parmi les naines blanches de cet échantillon ayant un type spectral connu, 5% sont classées comme une variante de DQ (DQ, DQZ, DQP, DQA). L'approche permettant de déterminer les paramètres physiques de ces étoiles est identique à celle décrite dans Dufour et al. (2005a, 2007a), mais en utilisant les modèles d'atmosphère améliorés de Blouin et al. (2018a, 2018c). En bref, la méthode photométrique est utilisée afin de calculer $T_{\rm eff}$ et $\log g$, puis l'abondance de C dans l'atmosphère est modifiée de façon à ajuster le spectre théorique au spectre observé de l'étoile. La région spectrale $\lambda \in [4400\ \text{Å}, 6200\ \text{Å}]$, appartenant aux bandes de Swan du C_2, est requise afin de contraindre l'abondance de C dans l'atmosphère. Les nouveaux modèles d'atmosphère de DQ décrivent l'opacité des bandes de Swan du C_2 à l'aide d'une liste de raies complètes contrairement à la méthode de raies plus approximative utilisée dans Dufour et al. (2005a). Habituellement, l'abondance initiale de C utilisée dans la solution photométrique est différente de celle obtenue de l'ajustement spectroscopique. Ce processus est donc répété

jusqu'à cohérence entre les deux. Les étoiles DQ ont des atmosphères dominées par l'hélium et la conversion du rayon en masse est donc effectuée à l'aide de la séquence évolutive d'une naine blanche ayant une couche d'hydrogène mince $q(\mathrm{H}) = 10^{-10}$. De façon générale, puisque les observations ne montrent pas de DQ froides avec de fortes abondances de C et pas de DQ chaudes avec faibles abondances de C, deux grilles de valeurs de H_λ^m différentes sont utilisées en fonction de la température des étoiles (Coutu et al., 2019a). La première grille est générée avec $T_{\mathrm{eff}} \in [5000\ \mathrm{K}, 9000\ \mathrm{K}]$, $\log g \in [7{,}9]$ et $\log \mathrm{C/He} \in [-8.0, -4.0]$ et la deuxième avec $T_{\mathrm{eff}} \in [8000\ \mathrm{K}, 16{,}000\ \mathrm{K}]$, $\log g \in [7{,}9]$ et $\log \mathrm{C/He} \in [-5.0, -1.0]$. De plus, deux autres grilles de modèles sont utilisées dans le cas de certains objets ne pouvant pas être traités par les deux précédentes. La première contient une trace d'hydrogène et est définie comme : $\log \mathrm{H/He} = -4$, $T_{\mathrm{eff}} \in [7000\ \mathrm{K}, 10{,}000\ \mathrm{K}]$, $\log g \in [7{,}9]$ et $\log \mathrm{C/He} \in [-4.0, -7.0]$. La deuxième est plus froide et est définie comme : $T_{\mathrm{eff}} \in [4000\ \mathrm{K}, 5500\ \mathrm{K}]$, $\log g \in [7.5, 8.5]$ et $\log \mathrm{C/He} \in [-6.0, -8.0]$. L'ensemble des grilles est illustré plus loin à la figure 3.8.

Des exemples de solutions typiques d'étoiles DQ chaudes et froides sont montrés à la figure 3.2. Les spectres d'étoiles DQ sont caractérisés par la présence de raies atomiques de carbone pour $T_{\mathrm{eff}} > 10{,}000$ K et de bandes de C_2 moléculaires à plus basses températures avec une transition continue entre les deux régimes. La forme des bandes est influencée par la pression atmosphérique ainsi que l'abondance de C_2. En termes d'exemple, J1355+3636 (3.2a) et J1028+3512 (3.2b) illustrent bien les deux formes de bandes typiques retrouvées dans les DQ chaudes et froides, respectivement. La pression plus élevée dans l'atmosphère de J1028+3512 cause une déformation des bandes de Swan, ce qui est assez différent de l'allure de dents de scies retrouvée dans le spectre de J1355+3636. Dans les deux cas, les modèles d'atmosphère chauds et froids arrivent à bien reproduire les spectres observés.

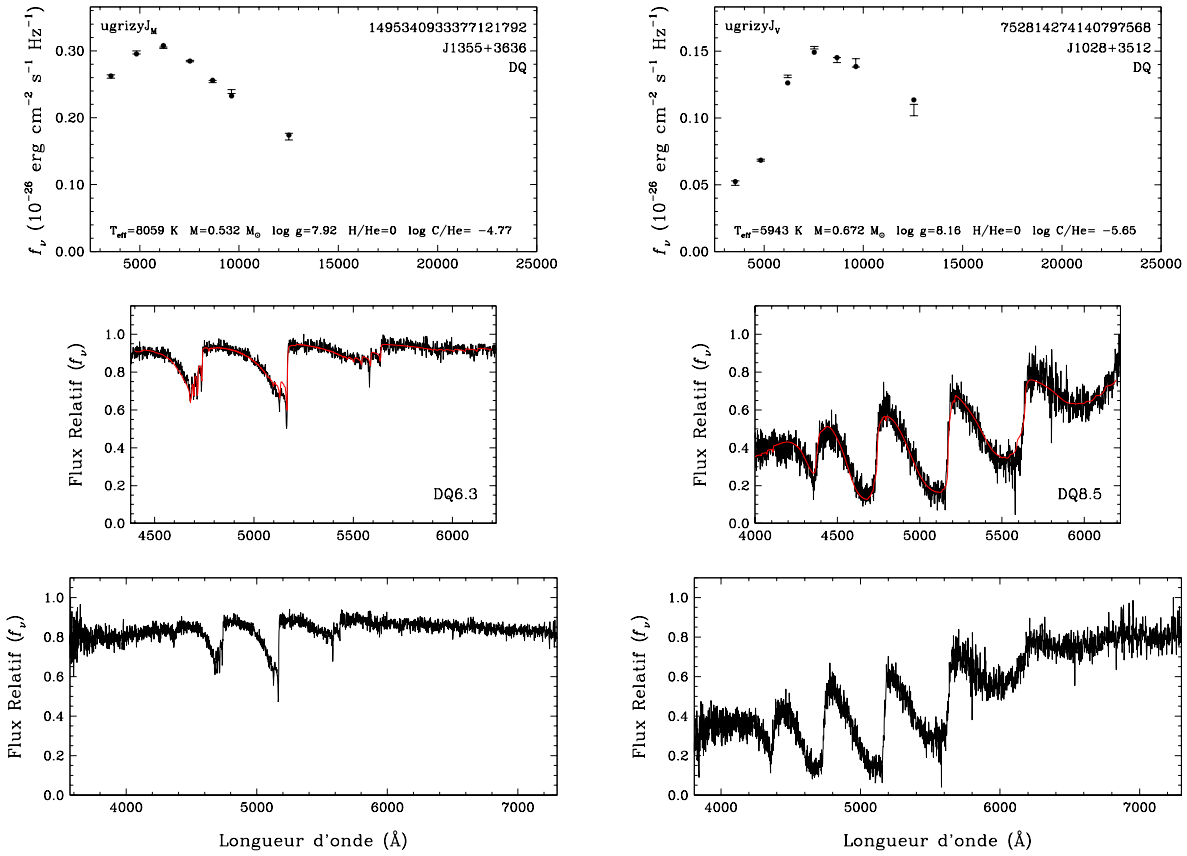

(a) Étoile DQ chaude typique.

(b) Étoile DQ froide typique.

FIGURE 3.2 Exemples de naines blanches de type DQ chaude (gauche) et DQ froide (droite) traitées via la méthode spectro-photométrique. La solution cohérente avec la distribution d'énergie de l'étoile et son spectre observé est donnée dans le panneau du haut. Le panneau du centre montre le spectre théorique (rouge) ajusté au spectre observé (noir) et celui du bas montre le spectre observé dans son ensemble.

3.1.3. DZ

Parmi les naines blanches de cet échantillon ayant un type spectral connu, 5.5% sont classées comme une variante de DZ (DZ, DZA, DZP, DZ :). Les paramètres physiques de ces étoiles, ainsi que certaines DAZ, sont obtenus de façon similaire aux DQ et font aussi l'utilisation de modèles d'atmosphère améliorés de Blouin et al. (2018a, 2018c). Suite à l'obtention d'une solution photométrique, l'abondance atmosphérique de Ca est modifiée de façon à ajuster le spectre théorique au spectre observé. Les régions spectrales appartenant au doublet H (λ = 3933 Å) et K (λ = 3969 Å) du Ca II ainsi qu'à la raie de résonance du Ca I (λ = 4226 Å) sont utilisées afin de contraindre l'abondance de Ca/He. Pour les autres métaux, les abondances Fe/He, Mg/He et Na/He sont fixées en fonction du calcium selon des rapports d'abondance solaire. La principale amélioration apportée aux modèles

d'atmosphère de DZ est l'utilisation de la théorie des profils de raies unifiées (unified line theory) de Allard et al. (1999) afin de calculer l'opacité des transitions les plus fortes, et l'utilisation de profil de Lorentz ou van der Waals pour les transitions moins importantes. Les naines blanches de type DZ ont une atmosphère riche en He. La conversion du rayon en masse est donc aussi effectuée à l'aide de la séquence évolutive d'une naine blanche ayant une couche d'hydrogène mince $q(\mathrm{H}) = 10^{-10}$. Cependant, ces étoiles ont habituellement une trace d'hydrogène dans leur atmosphère, ceci amène un paramètre additionnel dont il faut tenir compte dans les grilles de modèles. Dans le calcul, l'abondance atmosphérique d'hydrogène est constante et dépend de la grille de valeurs H_λ^m utilisées. Ce projet fait l'usage des abondances $\log \mathrm{H/He} \in [-1, -2, -3, -4, -5]$ et $N(\mathrm{H})/\mathrm{N(He)} = 0$. Toutes ces grilles sont générées avec $T_{\mathrm{eff}} \in [4000\ \mathrm{K}, 16{,}000\ \mathrm{K}]$, $\log g \in [7{,}9]$ et $\log \mathrm{Ca/He} \in [-12.0, -7.0]$. De plus, une nouvelle grille de modèles H-pur avec traces de Ca a été utilisée afin de traiter certaines étoiles DZ et DAZ. Ses dimensions sont $T_{\mathrm{eff}} \in [4500\ \mathrm{K}, 9000\ \mathrm{K}]$, $\log g \in [7{,}9]$ et $\log \mathrm{Ca/H} \in [-5.5, -10.5]$. L'ensemble des grilles est illustré plus loin à la figure 3.10. Des exemples de solutions d'étoiles DZ avec différentes abondances d'hydrogène sont montrés dans la figure 3.3. La figure 3.3a présente J1708+0257, qui est un exemple d'étoile DZ typique qui ne montre que des raies H et K du Ca. Dans le cas de J1833+3217, présenté dans la figure 3.3b, la raie Hα est aussi visible, ce qui permet de la classifier comme une DZA. Une atmosphère ayant une abondance d'hydrogène de $\log \mathrm{H/He} = -3$ a été choisie afin de reproduire la raie Hα observée. De plus, le spectre théorique obtenu de la méthode de minimisation permet de bien représenter les raies du Ca II et du Ca I.

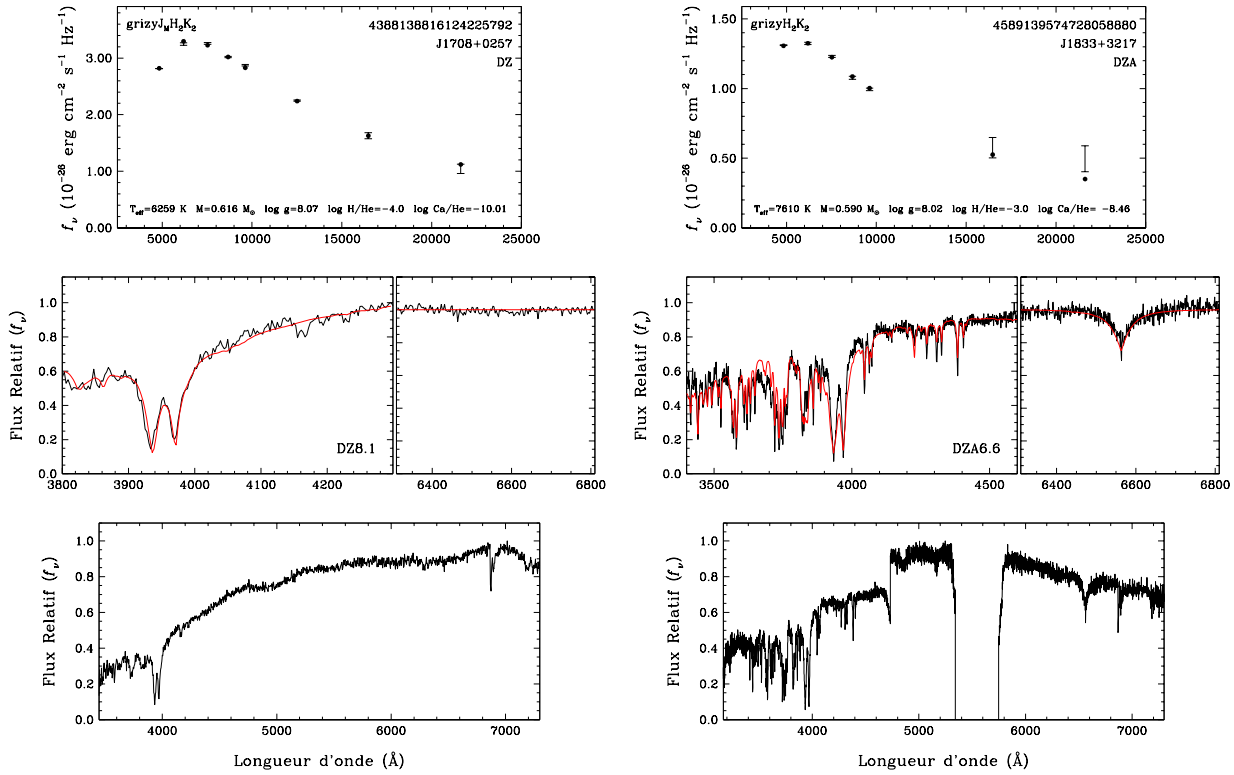

(a) Étoile DZ typique.

(b) Étoile DZA typique.

FIGURE 3.3 Exemples de naines blanches de type DZ (gauche) et DZA (droite) traitées via la méthode spectro-photométrique. La solution cohérente avec la distribution d'énergie de l'étoile et son spectre observé est donnée dans le panneau du haut. Le panneau du centre gauche montre le spectre théorique (rouge) ajusté au spectre observé (noir). Celui de droite montre le spectre théorique (rouge) interpolé aux valeurs des paramètres atmosphériques de la solution superposée à la région de Hα observée (noir). Le panneau du bas montre l'ensemble du spectre observé.

3.1.4. HeDA

Parmi les naines blanches classifiées DA, certaines ont une atmosphère dominée par l'hélium. Ces étoiles montrent des raies d'hydrogène élargies par les interactions de van der Waals et leurs distributions d'énergie sont mieux représentées par une solution d'atmosphère riche en hélium (Giammichele et al., 2012a; Rolland et al., 2018a). Cet échantillon contient 17 de ces étoiles, notées HeDA. Les paramètres physiques de ces étoiles sont déterminés en utilisant la méthode photométrique ainsi que le spectre observé de l'étoile dans la région de Hα. Pour une étoile donnée, le ratio H/He est sélectionné manuellement, contraignant l'utilisation d'une grille de valeurs H_λ^m et de spectres synthétiques correspondant à cette abondance d'hydrogène. Suite au calcul de la solution photométrique, un spectre synthétique interpolé aux valeurs de $T_{\rm eff}$ et $\log g$ est superposé au spectre observé de l'étoile. Les grilles de valeurs

H_λ^m utilisées sont générées pour des valeurs de $T_{\rm eff} \in [6000\ {\rm K}, 12{,}000\ {\rm K}]$, $\log g \in [7.0, 9.0]$ et des abondances atmosphériques $\log {\rm H/He} \in [-5.0, -1.0]$ par incréments de 0.5. À titre indicatif, une solution photométrique supposant une atmosphère H-pur ainsi que la raie Hα théorique correspondante sont aussi montrées. La figure 3.4 montre deux exemples d'étoiles de type HeDA, soit J0851+5426 et J1159+0007. Dans les deux cas, la raie correspondant à la solution H-pur est trop profonde, d'où le besoin de sélectionner manuellement l'abondance la plus appropriée.

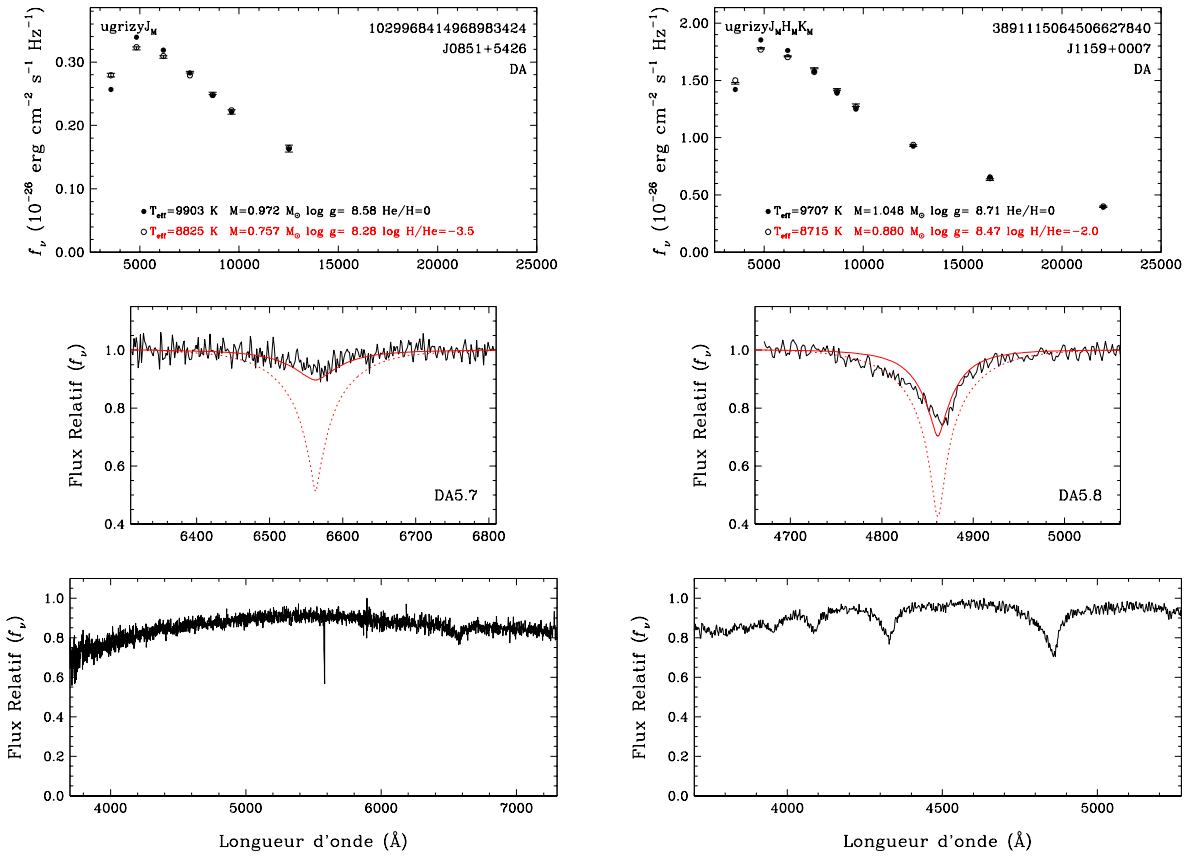

FIGURE 3.4 Exemples de naines blanches de type HeDA traitées via la méthode spectrophotométrique. Le panneau du haut montre la distribution d'énergie de l'étoile ainsi que l'ajustement aux solutions d'atmosphères H-pur (cercles pleins) et mixte H/He (cercles vides). Les spectres théoriques interpolés aux solutions H-pur (rouge, pointillé) et mixte (rouge, trait plein) sont superposés au spectre observé. Le panneau du bas montre le spectre observé dans son ensemble.

3.1.5. IR-Faint

Certaines naines blanches montrent une très grande absorption de flux dans le domaine du visible et du proche infra-rouge. Ce déficit de flux est causé par le *collision – induced absorption* (CIA) par l'hydrogène moléculaire qui entre en collision avec l'hélium

($H_2 - He$ CIA). Ce phénomène devient apparent lorsque l'atmosphère d'une naine blanche refroidit et devient plus dense. Dans une atmosphère H-pur, le CIA causé par les collisions $H_2 - H_2$ apparaît à $T_{\rm eff} < 4000$ K, ce qui fait qu'auparavant, les naines blanches montrant un grand déficit de flux dans le proche infrarouge étaient appelées *ultracool*. Cependant, les naines blanches froides riches en hélium ont une opacité plus faible et une pression atmosphérique plus grande, ce qui force le CIA $H_2 - He$ à apparaître à des températures effectives plus élevées. La classification *ultracool* n'est donc pas appropriée et ce type de naine blanche a été récemment renommé infrared-faint (Bergeron et al., 2022a). Cet échantillon contient 47 étoiles IR-faint, soit 42 DC, 4 DZ et 1 DQ. À l'exception de J0041−2221 qui est traitée comme une étoile DQ froide (voir section 3.2.3), les paramètres physiques de ces étoiles sont déterminés en utilisant la méthode photométrique habituelle, mais en ajustant aussi le ratio H/He. La grille de modèles utilisée s'étend sur $T_{\rm eff} \in [2500\ {\rm K}, 12{,}000\ {\rm K}]$, $\log g \in [7.0,9.0]$ et comprend des abondances allant de $\log {\rm H/He} \in [-5,2]$. Des exemples de solutions typiques d'étoiles IR-faint sont montrés dans la figure 3.5.

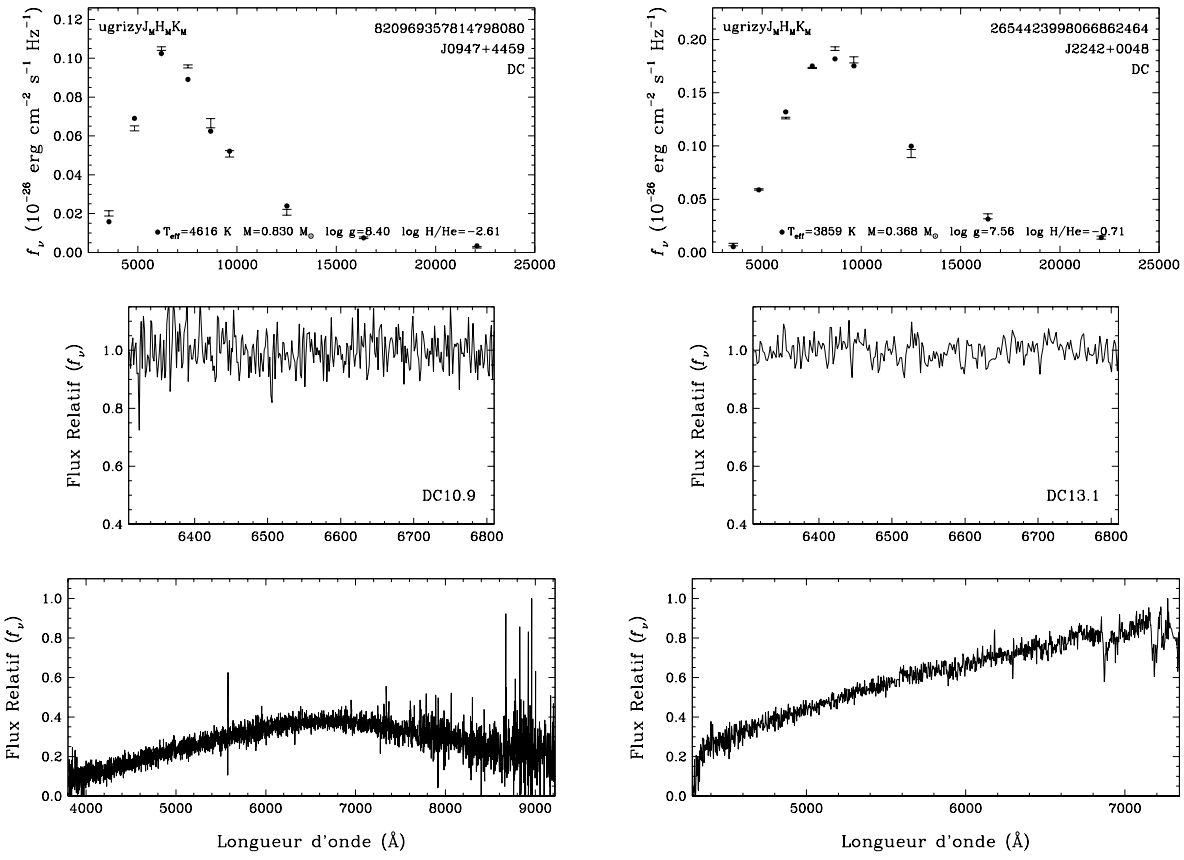

FIGURE 3.5 Exemples de naines blanches de type IR-Faint traitées via la méthode spectrophotométrique. Le panneau du haut montre la solution photométrique ajustée à la distribution d'énergie observée. Le panneau du centre et du bas montrent la région de Hα et l'ensemble du spectre observé respectivement.

Déterminer les paramètres physiques des étoiles IR-faint ne demande que l'utilisation des données observationnelles de la méthode photométrique. C'est pourquoi, dans ce cas-ci, le spectre théorique extrapolé n'est pas montré. Le spectre observé de chaque objet est tout de même affiché par cohérence avec les autres type de naines blanche dans l'échantillon. Dans le cas de J0947+4459, il est assez évident, à première vue, qu'il s'agit d'une IR-faint, car de l'absorption de flux est visible à partir des bandes izy. Cependant, dans le cas de J2242+0048, l'absorption est présente, mais elle commence à plus grandes longueurs d'onde. Excluant la photométrie JHK, sa distribution d'énergie est semblable à une naine blanche typique. Il est donc possible que certaines étoiles dans l'échantillon soient des IR-faint cachées en simple DC froides dû au fait que nous n'avons pas de photométrie infrarouge pour ces objets. Il est donc important d'obtenir des mesures de photométrie infrarouge afin de déterminer correctement les paramètres physiques de ce type d'objet. Parmi les objets plus froids que 5000 K dans cet échantillon, seul 39 (11%), dont 9 étant déjà identifiés comme IR-faint, n'ont aucune mesure dans les bandes JHK. Malgré le fait que le nombre d'objets concernés soit assez faible, il serait tout de même rassurant d'avoir à notre disposition l'information permettant de rejeter la possibilité que ces objets soient des IR-faint.

3.2. Paramètres adoptés

3.2.1. DA et HeDA

Dans le cas des naines blanches de type spectral DA qui ne montrent pas de signes de présence d'hélium dans leur atmosphère, les paramètres adoptés sont ceux dérivés de la solution H-pur. Ceci est le cas pour 1712 DA. En général, le spectre théorique est en très bon accord avec la région observée à Hα. Ceci est impressionnant, car le spectre n'est pas utilisé dans la méthode de détermination des paramètres. L'ensemble des paramètres adoptés de toutes les étoiles de type DA de l'échantillon sont présentées dans le tableau A.2 (Annexe A). Pour les étoiles HeDA, trouver la bonne solution revient à du essai-erreur. Il faut supposer une abondance d'hydrogène de façon à représenter le spectre observé le mieux possible. Les paramètres physiques adoptés des 17 étoiles HeDA de cet échantillon sont aussi présentés dans le tableau A.2 (Annexe A).

Pour certains types d'objets, la méthode spectro-photométrique n'arrive pas à bien reproduire les observations. La figure 3.6 montre J1714+3918, une DAH et J2229+3024, une DA dans un système binaire. Dans le cas des DAHs, soit des DA magnétiques, la région Hα observée montre une séparation en trois raies due à l'effet Zeeman. Comme on le voit pour J1714+3918, nos modèles n'arrivent pas à reproduire les raies d'hydrogène observées. Ceci n'est pas une surprise, car ceux-ci ne tiennent simplement pas compte de l'effet d'un champ magnétique sur les raies. La méthode photométrique arrive toutefois à trouver une solution

satisfaisante quant à la distribution d'énergie de ces étoiles pour la majorité des cas. Pour le deuxième cas, les signes apparents qu'une naine blanche fait partie d'un système binaire sont la masse et le flux dans l'infrarouge. Effectivement, la présence de deux étoiles est perçue comme une seule étoile ayant une grande luminosité. Afin de compenser cet excès, la méthode photométrique doit prédire un plus grand rayon, et étant donné la relation masse-rayon des naines blanches, une masse plus faible. Il faut cependant être prudent, une masse inférieure à 0.5 $M_{\odot}$ n'est pas un argument suffisant afin de qualifier un objet comme étant un système binaire. Ensuite, si une naine blanche est accompagnée d'une étoile de type dM, ceci se traduira par un excès de flux dans l'infrarouge. Ceci est visible pour J2229+3024. Les bandes $yJHK$ ont été exclues de la procédure de détermination des paramètres afin d'éviter une contamination de flux en provenance du compagnon. Cet objet fait donc définitivement partie d'un système binaire. Un mauvais ajustement à la photométrie et/ou au spectre observé sont aussi des signes de la présence d'un compagnon, car l'information des deux objets contenue dans la lumière est alors mélangée. Il est aussi possible d'obtenir un bon ajustement à la photométrie et au spectre pour un objet donné, mais qu'il s'agisse quand même d'un système binaire. Par exemple, il peut être difficile de différencier deux DA ayant des températures semblables à une seule DA. Dans un tel cas, le seul indice disponible serait la faible masse.

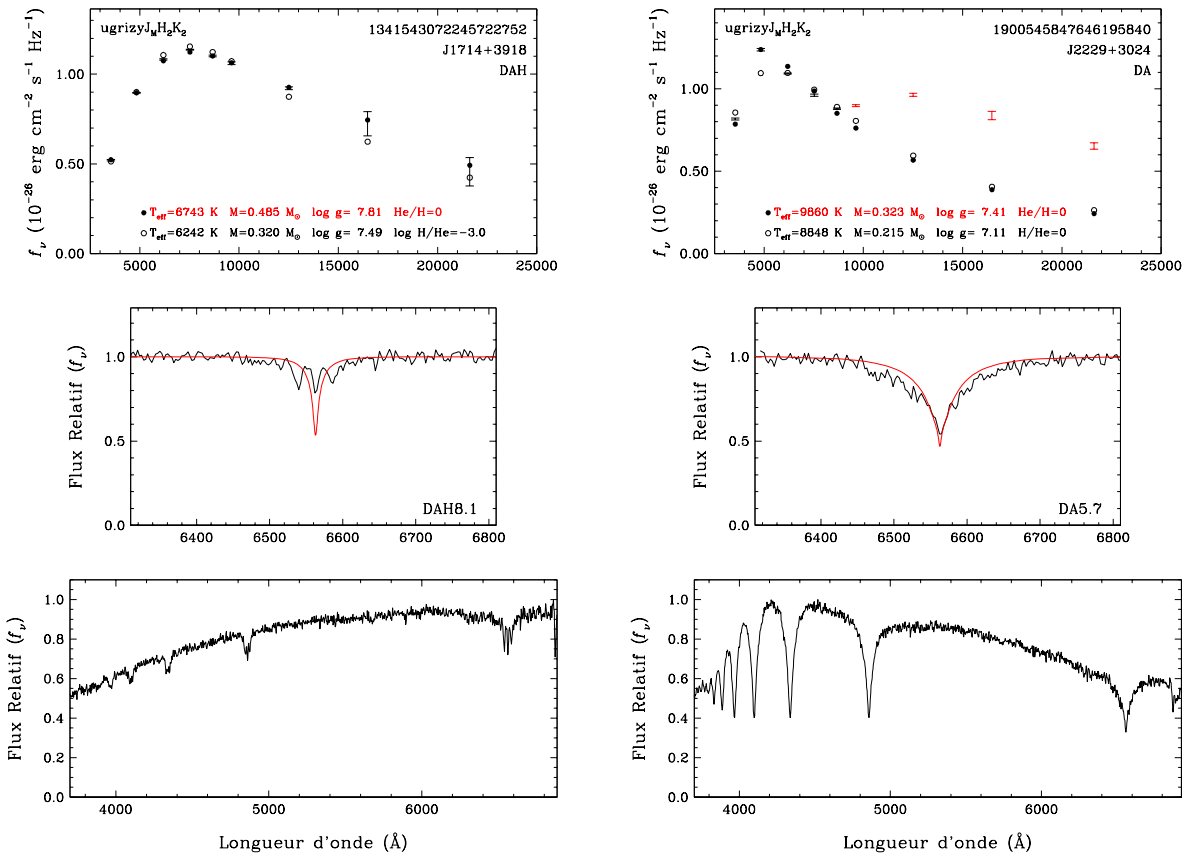

FIGURE 3.6 Exemples de naines blanches de type DAH et DA+M traitées via la méthode spectro-photométrique. Le panneau du haut montre la distribution d'énergie de l'étoile ainsi que l'ajustement aux solutions d'atmosphères H-pur (cercles pleins) et mixte H/He (cercles vides). La photométrie en rouge n'est pas incluse dans le calcul des paramètres. Le panneau du milieu montre le spectre observé (noir) superposé au spectre théorique (rouge) interpolé aux valeurs de $T_{\rm eff}$ et $\log g$ de la solution H-pur. Le panneau du bas montre le spectre observé en entier.

3.2.2. DC et IR-Faint

Pour les naines blanches de type DC, la détermination des paramètres est plus complexe. Le fait que trois compositions atmosphériques soient possibles afin de modéliser ce type d'étoile nous force à faire des choix de nature physique et statistique afin d'adopter la meilleure solution pour un objet donné. La méthode utilisée afin d'adopter les paramètres physiques de ces naines blanches dépend, entre autres, de $T_{\rm eff}$ et de notre meilleure compréhension de la physique des modèles évolutifs. D'abord, si la température effective est assez élevée ($T_{\rm eff} > 5200$ K), de sorte que des raies de Balmer devraient être visibles s'il y avait de l'hydrogène dans l'atmosphère, la solution H-pur est exclue. Il suffit alors de choisir entre la solution He-pur ou mixte. L'accord entre la population d'étoiles non-DA et la courbe de couleur théorique d'abondance $\log {\rm H/He} = -5$, discuté dans la section 2.2.2, nous pousse à

croire qu'il y a toujours une certaine quantité d'hydrogène présente dans l'atmosphère de ces étoiles. C'est pourquoi la solution retenue pour les DC est mixte H/He si $T_{\rm eff} > 6500$ K, là où les non-DA suivent bien la courbe. Pour les DC situées dans l'intervalle 6500 K $< T_{\rm eff} <$ 5200 K, la solution ayant le plus faible χ^2 est retenue. Dans le cas des DC froides ($T_{\rm eff} < 5200$ K), les trois types de solutions sont possibles. Jusqu'à tout récemment, la façon de traiter les DC à ces températures était de choisir le meilleur χ^2. Cependant, une méthode statistique robuste a été développée et utilisée par Blouin et al. (2019a). Ceux-ci ont argumenté que la solution mixte comporte un paramètre libre additionnel, soit l'abondance d'hydrogène, ce qui a comme conséquence de diminuer le χ^2 davantage. Ils utilisent donc la méthode du critère de l'information d'Akaike (AIC), qui pénalise un modèle en fonction du nombre de paramètres libres qu'il contient (Akaike, 1974; Anderson & Burnham, 2002). Malgré le fait que cette méthode soit beaucoup plus robuste que ce qui était fait précédemment, nous ne l'utilisons pas pour deux raisons. La première raison est qu'effectuer des statistiques à partir des différences de structure retrouvées dans les modèles avec et sans la présence d'hydrogène demande de la photométrie extrêmement précise et une conversion des magnitudes en flux exacte. Or ceci n'est pas toujours le cas même pour Pan-STARRS et SDSS tel que discuté dans la section 4. La deuxième raison est que la population d'étoiles DC froides dans la figure 2.5 est en meilleur accord avec la séquence de couleur H-pur que mixte, suggérant que toutes ces étoiles ont des atmosphères dominées par l'hydrogène. La solution retenue pour les DC ayant $T_{\rm eff} < 5200$ K est donc H-pur. Les solutions sélectionnées pour les 768 étoiles DC de l'échantillon qui ne sont pas des IR-faint sont illustrées dans la figure 3.7. Une observation frappante de cette figure est qu'il existe une transition graduelle entre une population de DC ayant une atmosphère mixte et une autre ayant une atmosphère He-pur alors que la méthode de sélection dans cette région dépend du χ^2. La raison est que le CIA commence à être apparent à partir de $T_{\rm eff} < 6000$ K, ce qui fait en sorte qu'une solution ayant une trace d'hydrogène à cette température sera très différente et donc il est plus facile de choisir la solution He-pur. Il est important de souligner que la visibilité des raies d'hydrogène dans un spectre ne dépend pas simplement de $T_{\rm eff}$, mais aussi de la gravité de surface ainsi que du rapport signal sur bruit. Les modèles de raies à notre disposition tiennent seulement compte de certaines valeurs de $T_{\rm eff}$ et $\log g$, nous forçant à faire un choix arbitraire, mais qui représente quand même bien le comportement de la majorité des naines blanches. Choisir 5200 K comme valeur n'est donc pas hors de l'ordinaire. Les paramètres physiques calculés des étoiles DC sont disponibles dans le tableau A.2 (Annexe A).

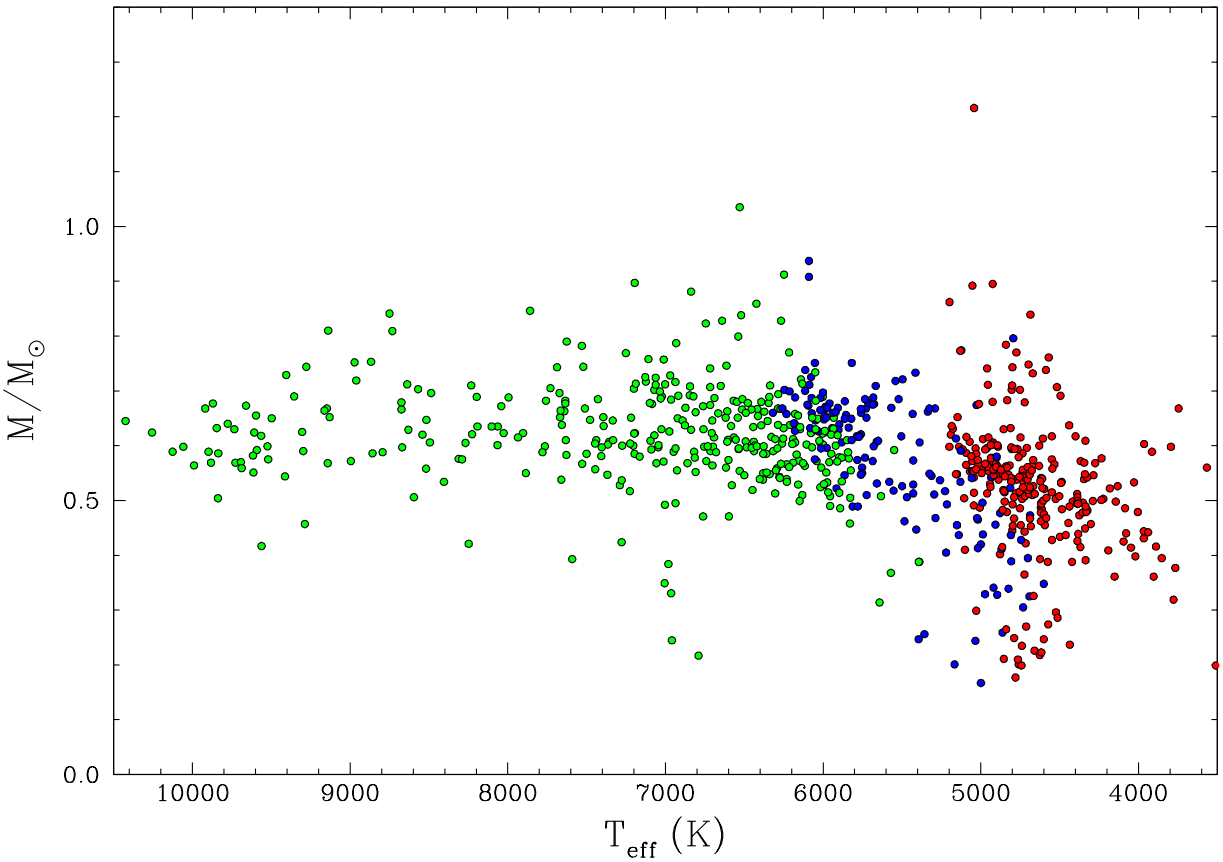

FIGURE 3.7 Diagramme M vs $T_{\rm eff}$ en fonction de la composition atmosphérique pour les DC de l'échantillon. Les étoiles ayant une atmosphère H-pur sont montrées en rouge, He-pur en bleu et mixte en vert.

Pour les étoiles de type IR-faint, les paramètres adoptés sont ceux tirés de la solution d'atmosphère mixte. En général, le meilleur ajustement à la photométrie est satisfaisant, mais on est loin du niveau de précision que peut atteindre les méthodes des autres types spectraux. À l'exception des 4 DZ et 1 DQ, toutes les IR-faint sont des DC. Les trouver demande donc de chercher parmi les DC dont l'ajustement photométrique est problématique dû au déficit de flux dans l'infrarouge. Les paramètres adoptés des IR-faint de l'échantillon sont présentés dans le tableau A.2 (Annexe A).

3.2.3. DQ et DZ

La sélection des paramètres physiques des étoiles DQ et DZ demandent une intervention manuelle pour chaque étoile, soit en modifiant certaines conditions initiales dans le calcul numérique. Dans le cas des DQ, il faut choisir la meilleure solution entre celle supposant une atmosphère chaude ou froide. Pour les DZ, il faut choisir la meilleure solution en supposant différentes abondances d'hydrogène. Dans tous les cas, cela revient à calculer une solution en utilisant différentes grilles de modèles. Les paramètres adoptés pour les étoiles DQ et DZ

sont présentés dans le tableau A.2 (Annexe A). Parmi celles analysées ici, 5 n'avaient pas de spectre disponible, mais avaient tout de même des abondances de métaux publiées.

Pour ces deux types d'étoiles, une des étapes essentielles de la méthode spectrophotométrique est la mesure de l'abondance de métaux dans l'atmosphère à l'aide du spectre. Or, pour certains objets, le spectre n'était pas disponible. Ceci est le cas pour 5 DZ (J1442+0635, J0153+0911, J0733+2315, J2147−2910 et J1551+1439) et une DQ (J0018+0233), où les paramètres physiques ont été déterminés via la méthode photométrique en supposant une atmosphère mixte H/He. Pour 5 étoiles DZ (J0124−2229, J0512−0505, J0823+0546, J1738−0826 et J2343−1659), les abondances atmosphériques de C et H publiées dans la littérature ont été utilisées afin de déterminer les paramètres physiques.

Une des difficultés survenue en traitant les étoiles DQ et DZ via la méthode spectrophotométrique est que la méthode de minimisation pouvait extrapoler des solutions en dehors des grilles de modèles. Pour éviter cela, les figures 3.8 et 3.10 ont permis de visualiser les résultats afin de se convaincre qu'elles étaient incluses à l'intérieur de nos grilles. La figure 3.8 montre les paramètres adoptés des DQ de l'échantillon ayant un spectre disponible.

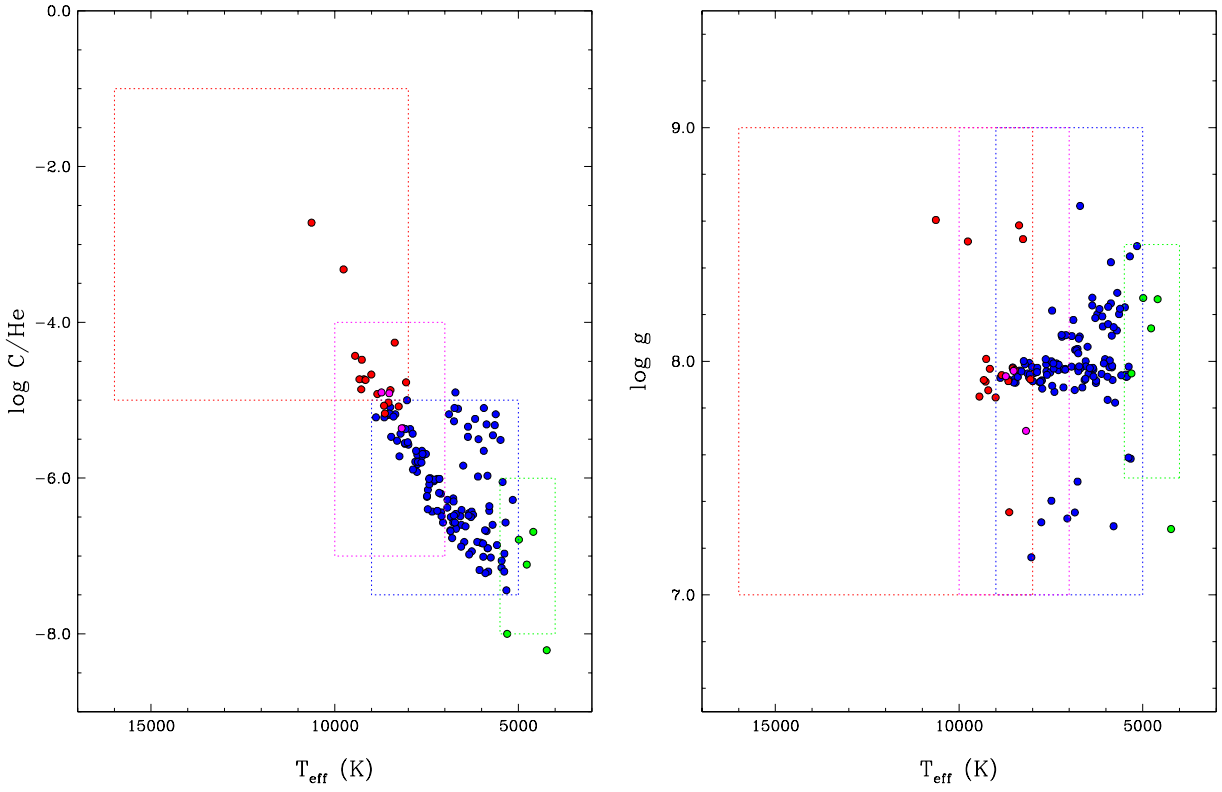

FIGURE 3.8 Paramètres adoptés des étoiles DQ de l'échantillon. L'abondance de C (gauche) ainsi que $\log g$ (droite) sont montrés en fonction de $T_{\rm eff}$. Les limites des grilles de modèles sont illustrées par des boîtes pointillées et les paramètres des étoiles sont montrés par des cercles pleins de couleur correspondant à la grille utilisée. La grille chaude est montrée en rouge, les deux grilles froides en bleu et vert et la grille avec trace d'hydrogène en magenta.

On remarque que pour certaines DQ, utiliser la grille d'atmosphère chaude (rouge) produit une solution en bon accord avec la photométrie et le spectre observé, mais qui est en fait une extrapolation. Ceci est visible dans le panneau de gauche, où 4 DQ chaudes (J1618+0611, J2101+3148, J0941+0901 et J0118+1610) ont une solution qui converge du côté froid de la frontière entre la grille chaude et froide (bleue). Pour 3 de ces objets, l'accord entre le spectre théorique et observé est moins bon en utilisant la grille froide. Dans le cas de J1618+0611, les solutions obtenues à l'aide de la grille chaude et froide sont pratiquement identiques. Puisque dans tous les cas, les extrapolations ne sont pas extrêmes, les solutions basées sur la grille chaude ont été retenues. Deux autres grilles de modèles sont montrées dans la figure 3.8 afin de traiter de cas spéciaux. La première, montrée ici en vert, va jusqu'à $T_{\rm eff} = 4000$ K et a permis de déterminer les paramètres de 5 objets plus froids

(J0041−2221, J1247+0646, J1113+0146, J1011+2845 et J1803+2320). Il est tout de même difficile d'obtenir des solutions satisfaisantes pour deux d'entre eux (voir figure 3.9).

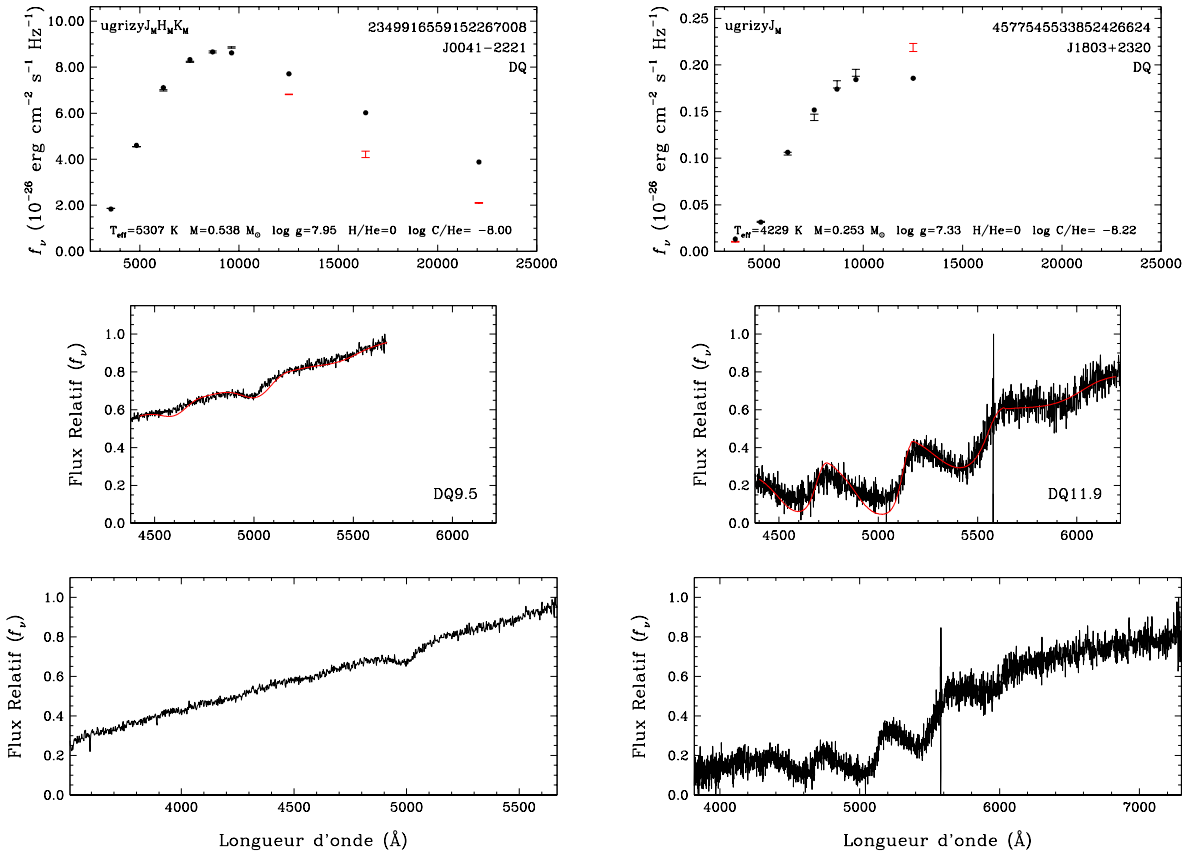

FIGURE 3.9 Solutions adoptées pour deux objets de type DQ problématiques. La solution ajustée à la distribution d'énergie de l'étoile ainsi qu'à son spectre observé est présentée dans le panneau du haut. La photométrie montrée en rouge n'est pas considérée lors du calcul des paramètres. Le panneau du centre montre le spectre théorique (rouge) ajusté au spectre observé (noir) et celui du bas montre le spectre observé dans son ensemble.

Pour J0041−2221, la solution converge en dehors de la grille, mais il est possible d'obtenir un bon ajustement au spectre observé en forçant l'abondance à $\log \mathrm{C/He} = -8.0$. Cependant, il faut exclure la photométrie JHK de la méthode de minimisation, car celle-ci montre des signes de CIA. Tel que discuté précédemment, cet objet est une IR-faint, cependant les modèles disponibles dans cette catégorie d'étoiles ne contiennent pas de carbone. Un modèle d'atmosphère de DQ incluant des traces d'hydrogène à basse température serait peut-être nécessaire afin de modéliser cet objet correctement. Dans le cas de J1803+2320, il n'est pas possible d'obtenir un meilleur ajustement à la photométrie et au spectre observé en augmentant l'abondance de C. Tel que discuté dans l'article au chapitre 4, il s'agit fort probablement d'un système binaire avec une autre naine blanche.

De façon similaire aux DQ, la figure 3.10 montre les paramètres adoptés des étoiles DZ de l'échantillon ayant un spectre disponible.

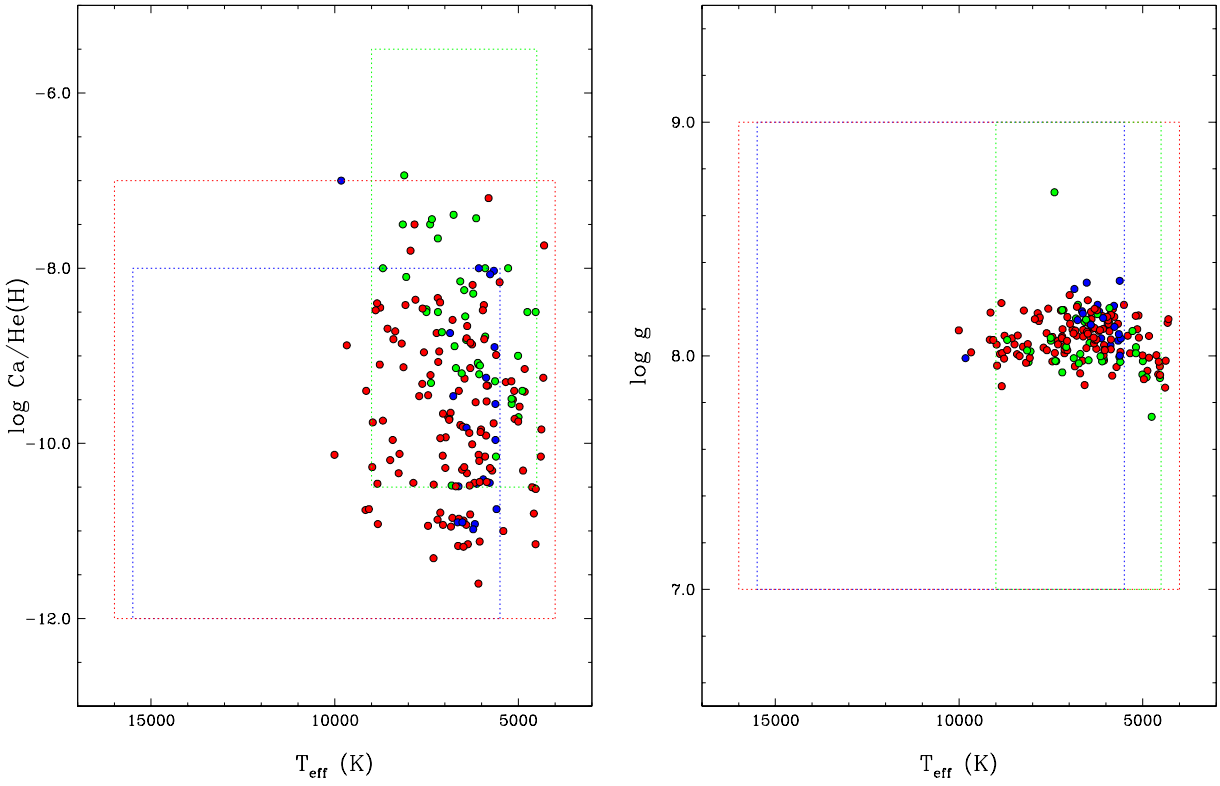

FIGURE 3.10 Paramètres adoptés des étoiles DZ de l'échantillon. L'abondance de Ca (gauche) ainsi que $\log g$ (droite) sont montrés en fonction de $T_{\rm eff}$. Les limites des grilles de modèles sont illustrées par des boîtes pointillées et les paramètres des étoiles sont montrés par des cercles pleins de couleur correspondant à la grille utilisée. Les modèles d'abondances $\log {\rm H/He} = [-1.0, -1.5, -2.0]$ ont les mêmes dimensions et sont montrés en bleu. Les modèles d'abondances $\log {\rm H/He} = [-3.0, -4.0, -5.0]$ et He-pur ont les mêmes dimensions et sont montrés en rouge. La grille H-pur avec trace de métaux est montrée en vert.

On remarque dans le panneau de gauche qu'il n'y a qu'une seule étoile DZ extrapolée. Il s'agit de J1731+3705, dont la solution est présentée dans la figure 3.12a. La principale source de difficulté lors de la détermination des paramètres des DZ n'était pas les extrapolations. Dans certains cas, la méthode de minimisation ne parvenait pas à converger sur une solution qui était en accord avec le spectre observé. Il a donc été nécessaire de forcer l'abondance de Ca, soit par essai-erreur ou en utilisant les valeurs disponibles dans la littérature. Ceci est probablement causé par le fait que la méthode de minimisation utilisée ici comporte un paramètre libre additionnel, soit l'abondance individuelle des métaux. Ceci ajoute donc

des minima locaux dans les grilles de modèle dans lesquels ces solutions sont destinées à converger.

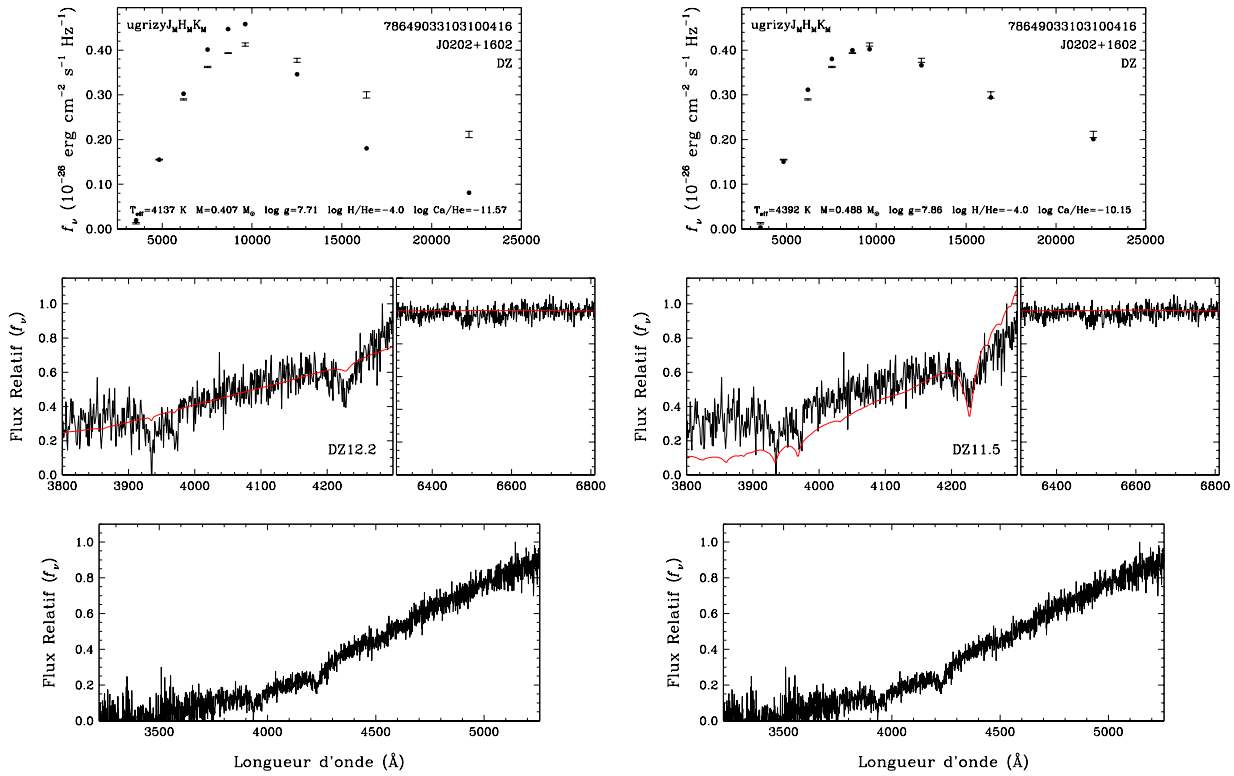

FIGURE 3.11 Comparaison entre deux solutions pour l'objet J0202+1602. La figure de gauche montre une solution où l'abondance de Ca/He est dérivée de la méthode de minimisation alors que celle de droite une solution où l'abondance est forcée à la valeur indiqué. L'ajustement à la distribution d'énergie de l'étoile ainsi qu'à son spectre observé est présentée dans le panneau du haut. Le panneau du centre gauche montre le spectre théorique (rouge) ajusté au spectre observé (noir). Celui de droite montre le spectre théorique (rouge) interpolé aux valeurs des paramètres physiques de la solution superposé à la région de Hα observée (noir). Le panneau du bas montre l'ensemble du spectre observé.

Un exemple est montré dans la figure 3.11 avec l'objet J0202+1602. À gauche, la solution est dérivée de la méthode de minimisation habituelle et à droite l'abondance de Ca a été forcée de façon à reproduire le mieux possible le spectre observé. Il s'agit ici d'un cas où rien ne fonctionne. La solution photométrique n'arrive pas à s'ajuster sur la distribution d'énergie dans le visible et l'infrarouge et l'ajustement sur le spectre observé ne reproduit pas les raies visibles. La meilleure solution que nous puissions obtenir pour cet objet est montrée à droite. La distribution d'énergie théorique est, dans l'ensemble, en accord avec la photométrie mesurée. Le spectre synthétique quant à lui, n'est pas parfait, mais arrive tout de même à reproduire, en partie, les raies observées.

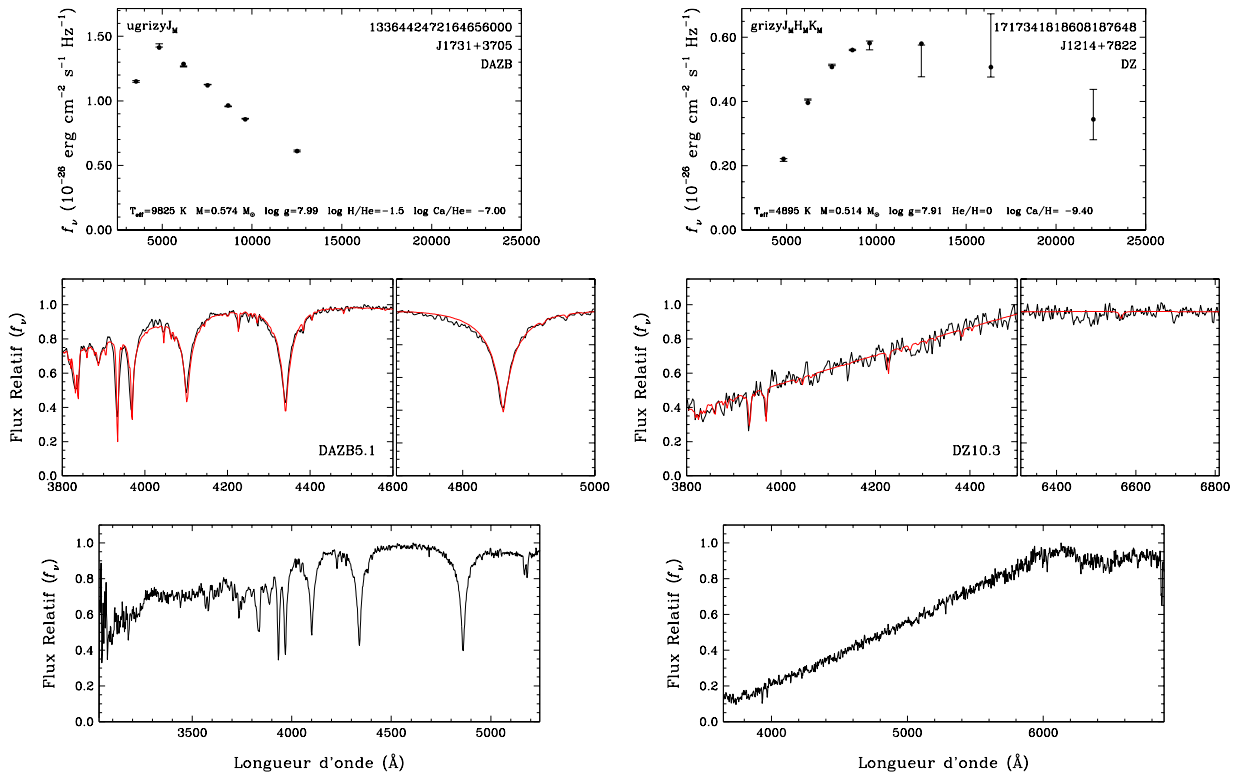

FIGURE 3.12 Solution adoptée pour J1731+3705 une DAZB connue et J1214+7822 une DZ avec atmosphère H-pur. L'ajustement à la distribution d'énergie de l'étoile ainsi qu'à son spectre observé est présentée dans le panneau du haut. Le panneau du centre gauche montre le spectre théorique (rouge) ajusté au spectre observé (noir). Celui de droite montre le spectre théorique (rouge) interpolé aux valeurs des paramètres physiques de la solution superposé à la région de Hα observée (noir). Le panneau du bas montre l'ensemble du spectre observé.

La figure 3.12 présente 2 objets d'intérêt particulier. D'abord J1731+3705, aussi connue sous le nom de GD 362, est une DAZB précédemment étudiée dans Gianninas et al. (2004) et Zuckerman et al. (2007). L'ajustement à la photométrie et au spectre observé est excellent. Malgré cette solution quasi-parfaite, l'intérêt pour cet objet provient du fait qu'il s'agit ici d'une extrapolation et l'abondance de calcium a été forcée à $\log \mathrm{Ca/He} = -7.0$. Notre solution spectro-photométrique ($T_{\mathrm{eff}} = 9825$ K, $\log g = 7.99$, $\log \mathrm{H/He} = -1.5$) est plus froide, moins massive et plus riche en hélium que la solution obtenue dans Zuckerman et al. (2007, $T_{\mathrm{eff}} = 10{,}540$ K, $\log g = 8.24$, $\log \mathrm{H/He} = -1.14$), mais a tout de même été conservée, car elle est en meilleur accord avec le spectre observé. Il est possible que la solution plus chaude et massive de Zuckerman et al. souffre d'effets hydrodynamiques 3D discutés dans Tremblay et al. (2013). Un argument pourrait être fait quant au choix de modèle utilisé afin de modéliser J1731+3705, car la figure 3.10a montre que l'objet est situé sur la limite des grilles rouges. Cependant ces modèles ne contiennent pas assez d'hydrogène pour bien représenter la

raie observée à Hα. Enfin, J1214+7822 est un autre objet intéressant, car il s'agit de la seule étoile de type spectral DZ (et non pas DZA) de l'échantillon ayant une atmosphère dominée par l'hydrogène. Effectivement, parmi toutes les grilles de modèles disponibles, seule la grille H-pur permet de reproduire la distribution d'énergie dans l'infrarouge pour cet objet et il n'y a pas de raie visible à Hα.

Chapitre 4

A Spectro-photometric Analysis of Cool White Dwarfs in the Gaia and Pan-STARRS Footprint

Accepté pour publication dans Monthly Notices of the Royal Astronomical Society.

Alexandre Caron[1], P. Bergeron[1], Simon Blouin[2], and S. K. Leggett[3]
[1]Département de Physique, Université de Montréal, C.P. 6128, Succ. Centre-Ville, Montréal, QC H3C 3J7, Canada
[2]Department of Physics and Astronomy, University of Victoria, Victoria, BC V8W 2Y2, Canada
[3]Gemini Observatory/NSF's NOIRLab, 670 N. A'ohoku Place, Hilo, HI 96720, USA

Abstract

We present a spectro-photometric analysis of 2880 cool white dwarfs within 100 pc of the Sun and cooler than $T_{\rm eff} \sim$ 10,000 K, with *grizy* Pan-STARRS photometry and Gaia trigonometric parallaxes available. We also supplement our data sets with near-infrared *JHK* photometry, when available, which is shown to be essential for interpreting the coolest white dwarfs in our sample. We perform a detailed analysis of each individual object using state-of-the-art model atmospheres appropriate for each spectral type including DA, DC, DQ, DZ, He-rich DA, and the so-called IR-faint white dwarfs. We discuss the temperature and mass distributions of each subsample, as well as revisit the spectral evolution of cool white dwarfs. We find little evidence in our sample for the transformation of a significant fraction of DA stars into He-atmosphere white dwarfs through the process of convective mixing

between $T_{\rm eff}$ = 10,000 K and ∼6500 K, although the situation changes drastically in the range $T_{\rm eff}$ = 6500–5500 K where the fraction of He-atmosphere white dwarfs reaches ∼45%. However, we also provide strong evidence that at even cooler temperatures ($T_{\rm eff} \lesssim 5200$ K), most DC white dwarfs have H atmospheres. We discuss a possible mechanism to account for this sudden transformation from He- to H-atmosphere white dwarfs involving the onset of crystallization and the occurrence of magnetism. Finally, we also argue that DQ, DZ, and DC white dwarfs may form a more homogeneous population than previously believed.

Keywords stars : abundances – stars : evolution – stars : fundamental parameters – stars : luminosity function, mass function – white dwarfs

4.1. Introduction

The determination of the fundamental parameters of white dwarfs – effective temperature, radius, mass, surface gravity, chemical composition, and cooling age – is of utmost importance for our understanding of their global properties such as their temperature and mass distributions, and their spectral evolution as well. The use of white dwarfs as cosmochronometers, whether it is through the study of their luminosity function or just by finding the oldest members of a given population, also requires precise and accurate stellar parameters. There are basically two main techniques that have been applied to large samples of white dwarfs. The first one is the spectroscopic technique (Bergeron et al., 1992; Liebert et al., 2005; Koester et al., 2009; Gianninas et al., 2011; Tremblay et al., 2011), where optical spectra are compared to the predictions of detailed synthetic spectra to measure both the effective temperature, $T_{\rm eff}$, and surface gravity, $\log g$ (and in some instances the abundance of trace elements), which are then converted into stellar mass using evolutionary models. The second technique is the photometric technique (Bergeron et al., 1997b; Hollands et al., 2018; Tremblay et al., 2019a), where magnitudes are converted into average fluxes in several bandpasses, and compared to the prediction of model atmospheres, synthetic photometry in this case (Holberg & Bergeron, 2006b). Here, $T_{\rm eff}$ and the solid angle $\pi(R/D)^2$ are the fitted parameters, where R is the stellar radius and D is the distance from Earth, which can be obtained from trigonometric parallax measurements.

Over the years, we have observed a constant evolution of observational data and theoretical models, with sometimes one aspect being ahead of the other. For instance, Bergeron et al. (1992) applied the spectroscopic technique to a sample of only 129 DA stars using model spectra that included the Hummer-Mihalas occupation probability formalism (Hummer & Mihalas, 1988), which allowed for the first time realistic quantitative measurements of the atmospheric parameters. All observed spectra in those days were secured individually using single-slit spectroscopy. In more recent years, the Sloan Digital Sky Survey (SDSS), with its very efficient multi-fiber spectrograph, has revolutionized the field by providing tens of

thousands white dwarf spectra, and uncovered several new spectral classes (Kleinman et al., 2013b; Kepler et al., 2019b). But detailed analyses of such large white dwarf samples has also revealed problems with the microphysics of model spectra (see, e.g., Genest-Beaulieu & Bergeron 2019a).

Similarly, Bergeron et al. (1997b, 2001b) applied the photometric technique to over 200 white dwarfs by measuring optical *BVRI* and near-infrared *JHK* photometry of individual stars, with only 152 with trigonometric parallax measurements available. Their model atmospheres relied on pure hydrogen, pure helium, or mixed H/He compositions, which could lead to large uncertainties when applied to DQ and DZ white dwarfs. Dufour et al. (2005b, 2007b) analysed only years later the same DQ and DZ stars using detailed model atmospheres including traces of carbon and heavier elements. Now the amount of photometric and astrometric data required to apply the photometric technique has sky rocketed, thanks to large photometric surveys such as the SDSS and Pan-STARRS (Panoramic Survey Telescope And Rapid Response System ; Chambers et al. 2016b, Tonry et al. 2012b), and most importantly the Gaia astrometric mission, which provided precise astrometric and photometric data for ∼260,000 high-confidence white dwarf candidates (Gentile Fusillo et al., 2019b, 2021). Such large data sets have recently been equally matched by improvements with model atmospheres, in particular at the cool end of the white dwarf sequence where high atmospheric densities are reached (Kowalski & Saumon, 2006; Kowalski et al., 2007; Blouin et al., 2017, 2018b,d; Blouin & Dufour, 2019). In parallel, similar efforts have been put forward to secure spectroscopic observations of white dwarf candidates in the Gaia survey (Kilic et al., 2020b; Tremblay et al., 2020b; O'Brien et al., 2022).

Given these large amounts of data, it is common to attack the problem by plowing through the photometric data sets and use the photometric technique by making sound assumptions regarding the atmospheric composition of each white dwarf in the sample (see, e.g., Bergeron et al. 2019a, López-Sanjuan et al. 2022). However, there are some limitations to this approach since ideally, one should perform a tailored model atmosphere analysis of each individual object in the sample, including also spectroscopic data. This is particularly important for DQ and DZ stars since the presence of heavy elements in the photospheric regions is known to affect the global atmospheric structure and thus the derived atmospheric parameters (Dufour et al., 2005b, 2007b).

In this paper, we present such a detailed spectro-photometric analysis of all spectroscopically identified white dwarfs within 100 pc from the Sun, based on Gaia distances. We restrict our analysis to objects below $T_{\rm eff} \sim 10{,}000$ K and use a homogeneous set of model atmospheres to study the DA, DC, DQ, DZ, He-rich DA, and the so-called IR-faint white dwarfs present in our sample. Our secondary goal is to improve our global effort to provide

the best physical parameters of each white dwarf in the Montreal White Dwarf Database [1] (MWDD ; Dufour et al. 2017b).

We present in Section 4.2 the selection of our white dwarf sample and observational data sets, which are then analysed in Section 4.3 using model atmospheres and fitting techniques appropriate for each spectral type. We present selected results in Section 4.4 including a discussion of the spectral evolution of white dwarfs. Our conclusions follow in Section 4.5.

4.2. Observational Data

4.2.1. Sample Selection

We first selected all white dwarfs – spectroscopically confirmed as well as candidates – found in the MWDD within 100 pc from the Sun. We chose this distance limit to avoid problems related to interstellar reddening. As specified in the MWDD, the white dwarf candidates in the 100 pc sample are selected from the Gaia Data Release 2 (DR2, Gaia Collaboration et al., 2018a), allowing for the error on the parallax measurement ; we also included 27 objects for which the parallax measurements became available only in the Gaia Early Data Release 3 (EDR3 ; Gaia Collaboration et al. 2022) [2]. The recommendations described in Lindegren et al. (2018) were used to remove non-Gaussian outliers in colours and absolute magnitudes, and the sample was limited to objects with $> 10\sigma$ significant parallax (Bergeron et al. 2019a, Kilic et al. 2020b, MWDD). A cut in the $(G_{\rm BP} - G_{\rm RP}) - M_G$ plane was then performed to select the white dwarf candidates (see also Kilic et al. 2020b). Finally, we retained only objects with Pan-STARRS *grizy* photometry measured in at least 3 photometric bands, and restricted our analysis to white dwarfs cooler than $T_{\rm eff} \sim 10{,}000$ K based on the photometric analyses described below.

Considering all the selection criteria, we end up with 8238 objects in our sample, including 2880 spectroscopically confirmed white dwarfs and 5358 white dwarf candidates.

4.2.2. Photometric and Spectroscopic Data

As mentioned above, we make use of the Pan-STARRS *grizy* photometry available in the MWDD, although in the course of our analysis, we discovered several erroneous, or simply missing, photometric data sets in the MWDD, which have been corrected since. We also supplement our *grizy* data sets with SDSS u magnitudes, which represent a powerful diagnostic for the study of cool white dwarfs, as demonstrated in Kilic et al. (2020b). When the Pan-STARRS photometry appeared in error, we rely instead on the SDSS *griz* photometry. Finally, 7 white dwarfs in our sample are brighter than $g = 13.5$ (e.g., WD 0135-052 = EG

1. http ://montrealwhitedwarfdatabase.org/
2. We estimated that the parallax zero-point corrections proposed by Lindegren et al. (2021) are of the order of 0.010 mas for our sample and were thus not applied.

11 = L870-2 with $g = 12.95$) and the magnitudes are obviously saturated, in agreement with the limits provided in Magnier et al. (2013). For these objects we adopt instead the optical *BVRI* photometry available in the MWDD.

Bergeron et al. (1997b, 2001b) discussed at length the importance of using near-infrared *JHK* photometry for the analysis of cool white dwarfs. Blouin et al. (2019c), for instance, revisited the spectral evolution of cool white dwarfs by restricting their sample only to objects with infrared photometry available in the Two Micron Sky Survey (2MASS). Here we go further by including all *JHK* photometry published in the literature, and also matched the spectroscopically confirmed white dwarf sample to the near-infrared photometric catalogs provided by 2MASS, the Tenth Data Release of the UKIRT Infrared Deep Sky Survey (UKIDSS), the UKIRT Hemisphere Survey (UHS) JBand Data Release, and the Visible and Infrared Survey Telescope for Astronomy (VISTA) public survey (see also Leggett et al. 2018). We end up with about 92% of the objects in our sample having *JHK* photometry in at least one band (usually *J*), 61% in at least two bands, and 51% in all three.

Optical spectra are also used in our model atmosphere analysis to constrain the atmospheric composition of the objects in our sample in the case of DA and DC stars, or to measure the carbon and metal abundances in the case of DQ and DZ stars, respectively. We rely here on the spectra available in the MWDD, which have been secured from various sources, but mostly from the SDSS. For some objects without spectra, we rely on the spectral types provided in the MWDD, which come essentially from Simbad. Some of these spectral types can be confirmed from the spectra published in the literature (see, e.g., Kawka et al. 2007), while others have published spectral types without any actual spectra being displayed, and these should be considered more uncertain. Also, in the course of our analysis, we revised some of the published spectral types, and these are indicated in the results presented below.

We summarize in Table 1 the observational data used in our analysis, where we provide for each object the given J name based on Gaia coordinates, Gaia ID (DR2 ; if not available the EDR3 is given and marked by a star symbol in Table 1), spectral type, trigonometric parallax measurement (ϖ), SDSS *u* photometry, Pan-STARRS *grizy* photometry, and near-infrared *JHK* photometry. The spectral types followed by an asterisk symbol correspond to newly assigned types based on our analysis.

4.2.3. Colour-Magnitude Diagrams

Before proceeding with a detailed model atmosphere analysis of the observational material described above, it is worth examining a few colour-magnitude diagrams. Figure 4.1 shows the M_g versus $(g-z)$ colour-magnitude diagram built from Pan-STARRS photometry. White dwarfs of various spectral types are identified by different colours. Also superposed are cooling sequences for 0.6 $M_\odot$ CO-core models with pure H and pure He compositions, as well as

TABLEAU 4.1 Observational Data. The spectral types followed by an asterisk symbol correspond to newly assigned types based on our analysis. This table, including uncertainties, is available in its entirety in machine-readable form as well as a pdf file.

Name	Gaia ID (DR2/EDR3*)	Sp Type	ϖ (mas)	u	g	r	i	z	y	J	H	K
J0000+0132	2738626591386423424	DA	14.95	16.65	16.23	16.34	16.48	16.64	16.75	16.23	16.14	16.24
J0000+1906	2774195552027050880	DC	9.800	23.29	20.32	19.73	19.52	19.43	19.34	18.65	···	···
J0001+3237	2874216647336589568	DC	10.15	20.42	19.49	19.16	19.06	19.04	19.01	18.32	···	···
J0001+3559	2877080497170502144	DC*	11.66	20.04	19.03	18.85	18.83	18.58	18.45	17.81	···	···
J0001−1111	2422442334689173376	DC	13.51	19.09	18.48	18.28	18.28	18.31	18.35	17.72	···	17.75
J0002+0733	2745919102257342976	DA	11.85	18.31	17.84	17.76	17.78	17.83	17.87	17.23	17.07	17.06
J0002+0733	2745919106553695616	DAH	12.19	18.52	18.05	17.98	18.01	18.09	18.15	17.59	17.44	17.51
J0002+1610	2772241822943618176	DA	9.817	19.55	18.93	18.71	18.64	18.67	18.72	17.98	17.66	17.54
J0002+6357	431635455820288128	DC	38.07	···	17.64	16.99	16.72	16.65	16.59	15.8	15.58	15.51
J0003+6512	432177373309335424	DC	10.66	···	17.59	17.61	17.73	17.84	17.94	···	···	···

mixed compositions of $\log \mathrm{H/He} = -5$ and -2. Here and in the remainder of this paper, we rely on the evolutionary models described in Bédard et al. (2020) with C/O cores, $q(\mathrm{He}) \equiv \log M_{\mathrm{He}}/M_{\star} = 10^{-2}$ and $q(\mathrm{H}) = 10^{-4}$, which are representative of H-atmosphere white dwarfs, and $q(\mathrm{He}) = 10^{-2}$ and $q(\mathrm{H}) = 10^{-10}$, which are representative of He-atmosphere white dwarfs. As discussed at length by Bergeron et al. (2019a), a trace of hydrogen is required to match the observed sequence of He-rich objects in Figure 4.1 with 0.6 $M_{\odot}$ models, in particular the DC and DZ white dwarfs. Such a trace of hydrogen is predicted by the transformation of DA stars into He-rich white dwarfs through convective mixing (see Figure 4 of Bédard et al. 2022b). Note in particular how the DZ stars overlap nicely with the DC white dwarfs in this colour-magnitude diagram.

The pure H sequence in Figure 4.1 follows perfectly the observed DA sequence, except at the faint end where the predicted magnitudes fall below the observed sequence. The problem is exacerbated at even lower luminosities where the observed DC sequence – presumably the extension of the DA sequence at lower temperatures when Hα disappears – lies significantly above the 0.6 $M_{\odot}$ pure H sequence. The problem is even worse if one assumes a pure He or mixed H/He compositions, as seen in Figure 4.1. This discrepancy between observed and predicted colours translates into low inferred masses at low temperatures when the photometric method is applied to this data set, as illustrated in Figure 12 of Bergeron et al. (2019a), and even more so when assuming He-rich atmospheres. The origin of this problem is still unknown.

Also observed at higher luminosities in Figure 4.1 is the crystallization sequence (the so-called Q-branch) composed of a pile up of massive DA stars caused by the release of latent heat and chemical fractionation, which decrease the cooling rate of a white dwarf (Tremblay et al., 2019b). In this particular color-magnitude diagram, this sequence of massive DA stars is well separated from the normal $\sim$0.6 $M_{\odot}$ DA white dwarfs.

Also of interest in Figure 4.1 is the small number of white dwarfs at faint luminosities in the region where He-rich objects should be located according to the model predictions. It is precisely this dearth of cool DC stars at low luminosities with colours consistent with pure

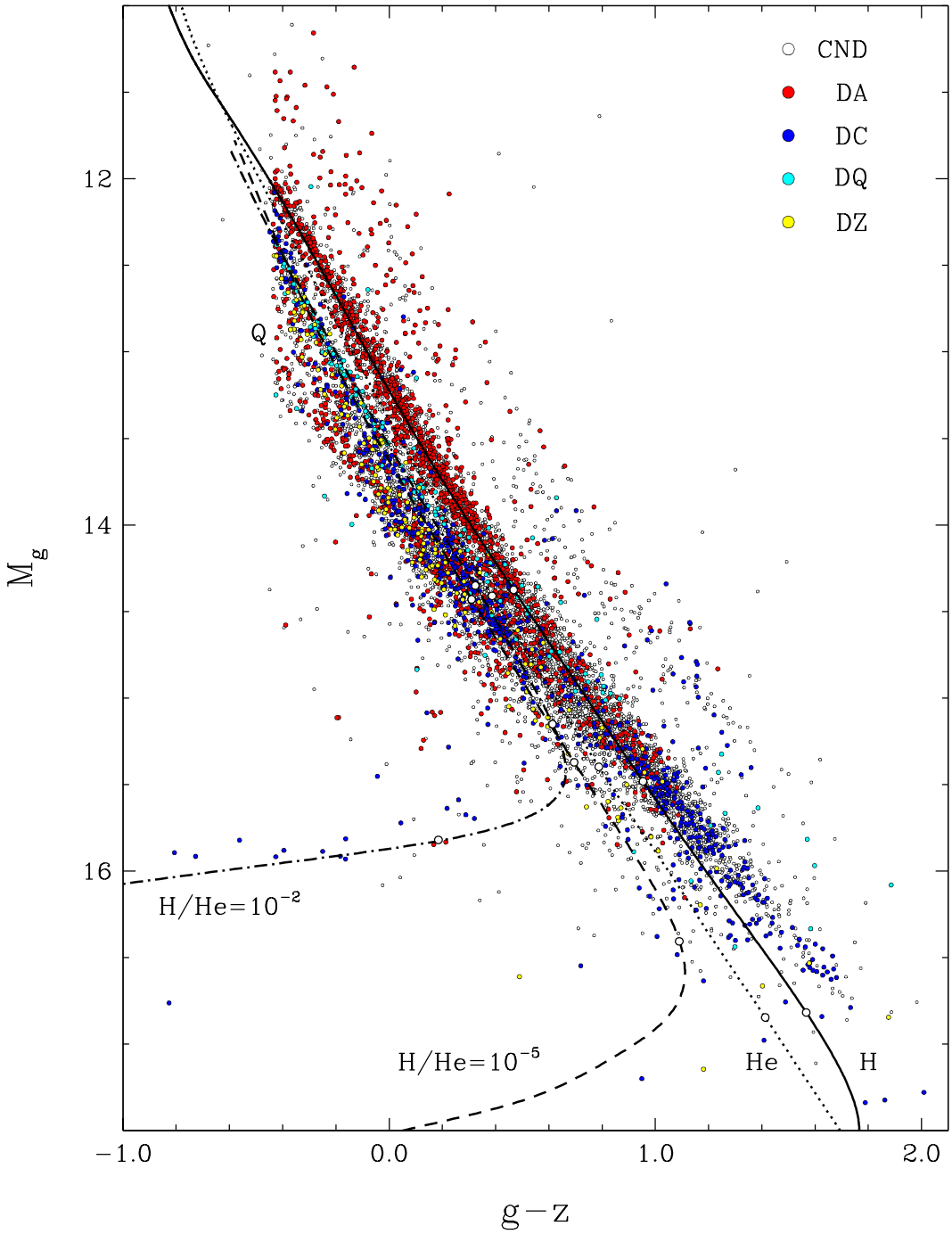

FIGURE 4.1 Pan-STARRS M_g versus $(g-z)$ colour-magnitude diagram for the 100 pc sample drawn from the MWDD. The various spectral types as well as the white dwarf candidates (CND) are identified with different colour symbols indicated in the legend. The various curves correspond to cooling sequences for 0.6 $M_\odot$ CO-core models with pure H, pure He, $\log \mathrm{H/He} = -5$ and -2 atmospheric compositions; white circles on each curve indicate $T_{\rm eff} = 6000$ K, 5000 K, and 4000 K. The crystallization sequence (the so-called Q-branch), composed of a pile up of massive DA stars, is also indicated by the letter Q.

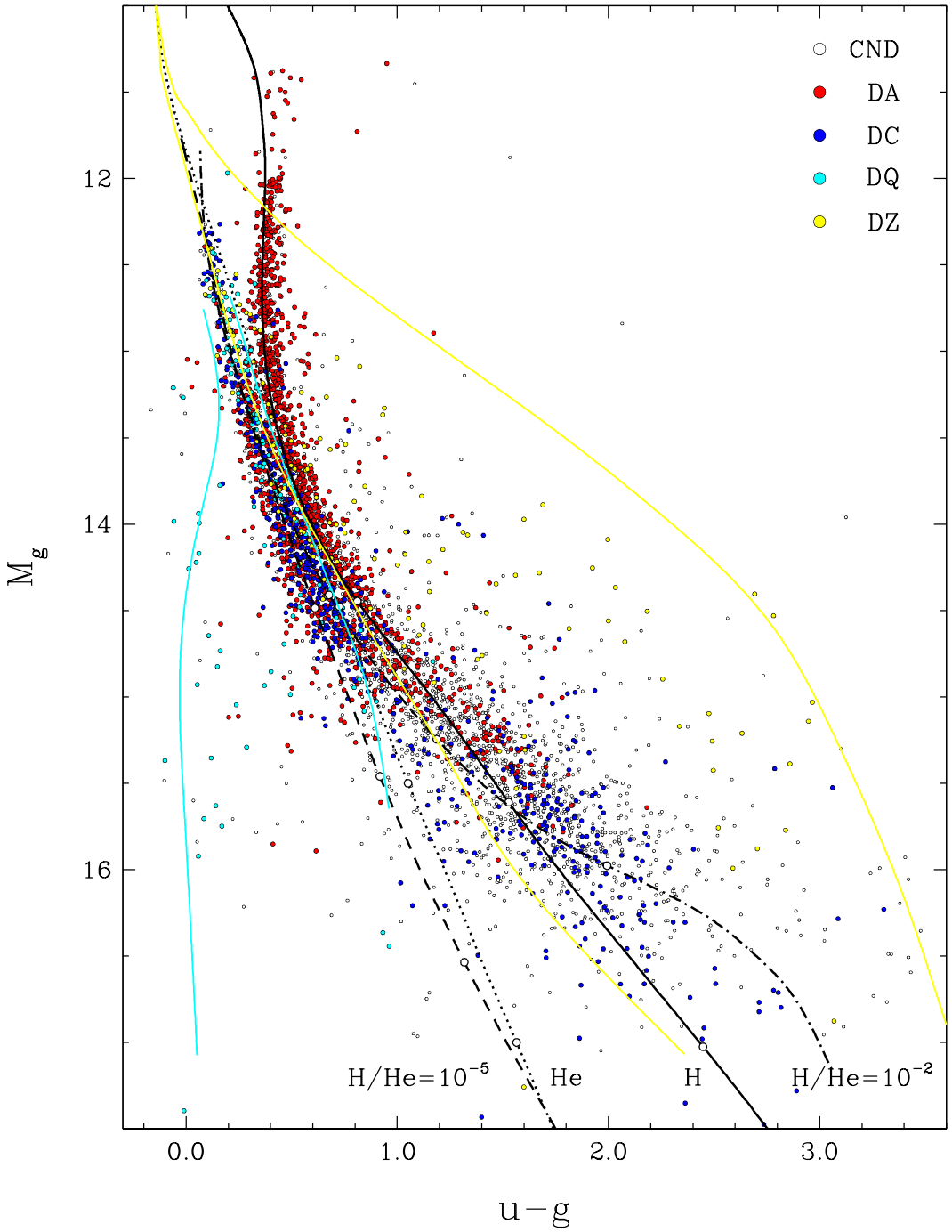

FIGURE 4.2 Same as Figure 4.1 but for the SDSS M_g versus $(u-g)$ colour-magnitude diagram. Also shown are cooling sequences for 0.6 $M_\odot$ CO-core models for DQ stars (cyan) with $\log \mathrm{C/He} = -5$ (left) and -7.5 (right), and for DZ stars (yellow) with $\log \mathrm{Ca/He} = -11.5$ (left) and -7 (right).

helium compositions that led Kowalski & Saumon (2006) to conclude that most cool, DC white dwarfs must have pure H atmospheres. We come back to this point below. Perhaps even more important is the existence of two distinct DC sequences, one at very low luminosities that appears as the extension of the DA sequence, but also a more luminous DC sequence, which terminates abruptly at $T_{\rm eff} \sim 5200$ K according to the theoretical models displayed in Figure 4.1. Moreover, there are very few DC stars connecting these two DC sequences. We can also see a deficiency of spectroscopically confirmed white dwarfs near $M_g \sim 15$ and $(g - z) \sim 0.7$, but this appears to be an observational bias since there are plenty of white dwarf candidates (CND) in the same region.

Figure 4.2 shows the M_g versus $(u - g)$ colour-magnitude diagram built from the sub-sample of objects with SDSS photometry (SDSS g here). In this particular diagram, the DA and DC sequences are well-separated at high luminosities as a result of the Balmer jump present in H atmospheres. The 0.6 $M_\odot$ pure H, pure He, and mixed H/He sequences are also reproduced in this figure, but in addition we show 0.6 $M_\odot$ white dwarf models for DQ stars with $\log {\rm C/He} = -7.5$ and 5.0, and for DZ stars with $\log {\rm Ca/He} = -11.5$ and -7.0, which correspond roughly to values that bracket the abundances measured for each spectral type in this temperature range (see Figures 8 and 12 of Coutu et al. 2019b). Interestingly, the effect on the predicted colours goes in the opposite direction when traces of carbon in DC stars and metals in DZ stars are gradually increased, in agreement with the location of these white dwarfs in this particular colour-magnitude diagram. Note again here the lack of He-atmosphere white dwarfs at faint luminosities, as well as the inability of pure H models to match the observed faint DC sequence.

4.3. Model Atmosphere Analysis

4.3.1. The Photometric Technique

The physical parameters of the white dwarfs in our sample can be measured using the so-called photometric technique, described at length in Bergeron et al. (1997b). Briefly, the optical and near-infrared photometry are first converted into average fluxes in each bandpass using the equations given in Holberg & Bergeron (2006b) appropriate for magnitudes on the AB system for the SDSS u and Pan-STARRS *grizy* optical photometry, or on the Vega system for the near-infrared *JHK* photometry, with zero points calculated for each filter system (2MASS, MKO, VISTA, Bessell, etc.). The synthetic photometry is calculated for each model grid described below, by integrating the monochromatic Eddington fluxes – which depend on $T_{\rm eff}$, $\log g$, and chemical composition – over each filter bandpass. The observed and model fluxes are related to each other by the solid angle, $\pi(R/D)^2$, where R is the stellar radius and D is the distance from Earth, which can be obtained from the Gaia

trigonometric parallax measurements ; given that our sample is limited to objects with $> 10\sigma$ significant parallax, it is justified to simply assume here $D = \varpi^{-1}$. A χ^2 value is calculated as the difference between observed and predicted fluxes summed over all bandpasses, and minimized using the nonlinear least-squares method of Levenberg-Marquardt (Press et al., 1986b), which is based on a steepest decent method. Only $T_{\rm eff}$ and the solid angle $\pi(R/D)^2$ are considered free parameters for an assumed chemical abundance, while the uncertainties of both parameters are obtained directly from the covariance matrix of the fit. The stellar radius is then converted into mass using the evolutionary models described in Section 4.2.3. We use thick ($q({\rm H}) = 10^{-4}$) and thin ($q({\rm H}) = 10^{-10}$) H-layer models for H- and He-dominated atmospheres, respectively. Bad photometric data points are excluded from our fits after visual inspection, and displayed in red in the fits presented below.

4.3.2. DA White Dwarfs

Our model atmospheres for DA white dwarfs are described at length in Tremblay et al. (2011) and references therein, and in Blouin et al. (2018b) for $T_{\rm eff} < 5000$ K, where additional nonideal effects are taken into account. We assume a pure hydrogen atmospheric composition for the 1764 DA stars in our sample [3]. This is a perfectly legitimate assumption, as discussed in Bergeron et al. (1997b, see also Blouin et al. 2019c). A fit to a typical DA star, J0034+1517, is displayed in Figure 4.3. We also provide the Gaia ID as well as the spectral type. The observed photometry is shown as error bars (1σ uncertainty) while the particular set of photometry used is indicated at the top left of the upper panel. In the case of the near-infrared *JHK* photometry, we use a lower subscript to specify the particular system used (M : MKO, 2 : 2MASS, B : Bessell, V : VISTA). Our best-fit model is represented by solid dots, with the corresponding parameters given in the upper panel. The bottom panel shows the optical spectrum, normalized to a continuum set to unity, compared to the model spectrum (in red) interpolated at the parameters obtained from the photometric solution and convolved with the appropriate spectral resolution. Hence, it is not a formal fit, but it is used instead to validate our photometric solution. An observed discrepancy might be indicative of an unresolved double degenerate binary (see Section 4.3.9), or of an incorrect assumption about the chemical composition (see Section 4.3.3). Depending on the spectral coverage, we show the region near Hα, Hβ, or even Hγ, in cases where the red part of the spectrum is contaminated by the presence of an M–dwarf companion. We also provide in the lower panel the spectral type with the temperature index defined as $50{,}400/T_{\rm eff}$.

Among our sample of DA white dwarfs, we also have 50 DAZ stars, where in the present context we refer to white dwarfs with H-dominated atmospheres and metal lines visible in their optical spectra, in particular the Ca II H & K doublet. If metal lines are detected, which

3. We exclude the 17 He-rich DAs and the 4 DA + DQ unresolved systems, which are analysed further below.

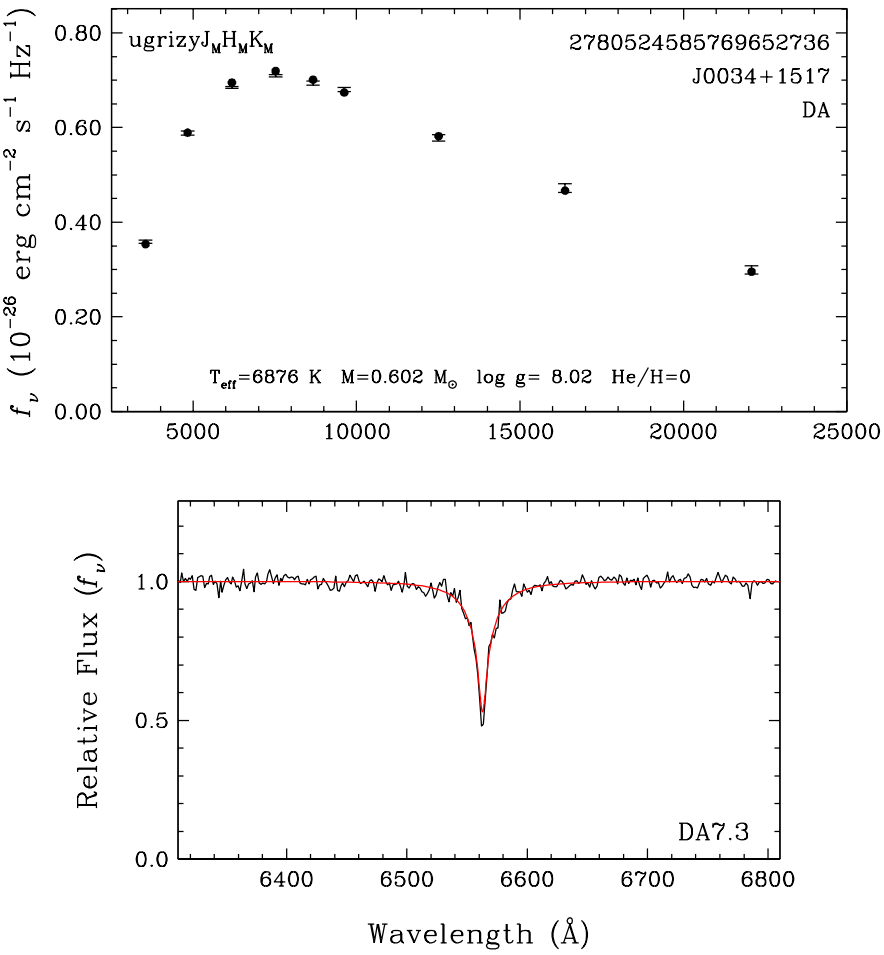

FIGURE 4.3 Best fit to a typical DA star in our sample. The observed photometry is shown as error bars (1σ uncertainty in all figures) and the photometric set used is indicated at the top left of the upper panel (see text). Our model atmosphere fit is shown as solid dots, with the parameters given in the upper panel. The lower panel shows the normalized optical spectrum (black), compared with the model spectrum (red) interpolated at the parameters obtained from the photometric solution.

is the case for 34 DAZ stars in our sample, we determine the Ca abundance by fitting the Ca II H & K doublet using a grid of model atmospheres with $T_{\rm eff} = 4500$ (500) 9000 K and $\log {\rm Ca/H} = -10.5$ (0.5) -5.5, where the numbers in parentheses indicate the step size. We assume chondritic abundance ratios with respect to Ca for other metals. The same model grid is also used in Section 4.3.5 to analyse cool H-atmosphere DZ and DZA white dwarfs.

The fits to all white dwarfs in our sample are provided as Supplementary Material [4]. For the fits to DA and DAZ white dwarfs, we display both the pure H and mixed H/He solutions (with H as a trace element, see Section 4.3.7) ; the entire spectrum is also shown in a third panel at the bottom. In some cases there is no optical spectrum available to us, and we simply

4. http ://www.astro.umontreal.ca/~bergeron/MNRAS

rely on the published spectral type. In general, the predicted model spectra are in excellent agreement with the observed absorption profiles. Exceptions include of course the magnetic DA white dwarfs (see, e.g., J0505−1722) since all our models are for non-magnetic stars (see also Section 4.3.8). We note that Hα can be detected in DA stars as cool as $T_{\rm eff} \sim 4800$ K (see J0717+1125), although this depends on the surface gravity of the white dwarf, and most importantly, on the signal-to-noise ratio of the optical spectrum.

4.3.3. He-rich DA White Dwarfs

Several DA stars in our sample have He-rich atmospheres. The origin of these so-called He-rich DA white dwarfs can be explained in terms of DA stars with thin hydrogen layers that turn into a He-rich white dwarf below $T_{\rm eff} \sim 12{,}000$ K as a result of convective mixing. If the object is hot enough, Hα might still be detectable as a shallow absorption feature, heavily broadened by van der Waals interactions. Classical He-rich DA white dwarfs include Ross 640, L745-46A, and GD 95, all three of which also show traces of metals (see Figure 14 of Giammichele et al. 2012b). Many additional He-rich DA white dwarfs have also been identified and analysed by Rolland et al. (2018b). As these stars cool off, the Hα absorption feature rapidly falls below the limit of visibility (see Figure 14 of Rolland et al. 2018b).

The 17 He-rich DA white dwarfs in our sample have been fitted using mixed H/He model atmospheres similar to those described above for DA stars, but with $\log {\rm H/He} = -5.0$, -4.0 (0.5) -1.0 (1.0) $+2.0$. We use the same photometric method as for DA stars, but this time we explore all values of H/He individually and simply adopt the solution that most closely matches the observed Hα profile. A fit to a typical He-rich DA star in our sample, J1024−0023, is displayed in Figure 4.4. Here we show both the pure H and mixed H/He solutions, as well as the corresponding predicted spectra at Hα. As can be seen, the observations at Hα clearly rule out the pure H solution for this object, whereas the mixed H/He solution constrained by Hα provides a much better fit to the observed photometry, in particular in the *ugr* passbands.

We also found in our sample what appears to be normal DA stars – with the complete Balmer series detected – for which we achieve a much better fit in the *ugr* passbands by assuming a mixed composition of $\log {\rm H/He} = -1.0$ (see J1611+1322 and J2138+2309 in the Supplementary Material), although we do not necessarily achieve better fits at Hα. Also, two He-rich DA stars in our sample (J0103−0522, J1159+0007) show asymmetric Balmer line profiles. Tremblay et al. (2020b) suggested that J0103−0522 was magnetic. However, the fact that J0103−0522 and J1159+0007 are almost identical twins, and that they both have He-rich atmospheres, suggests instead that the asymmetric profiles are the result of some unusual line broadening due to helium, unaccounted for in our models, a hypothesis supported by the recent calculations of Spiegelman et al. (2022, see their Figures 7 and 8).

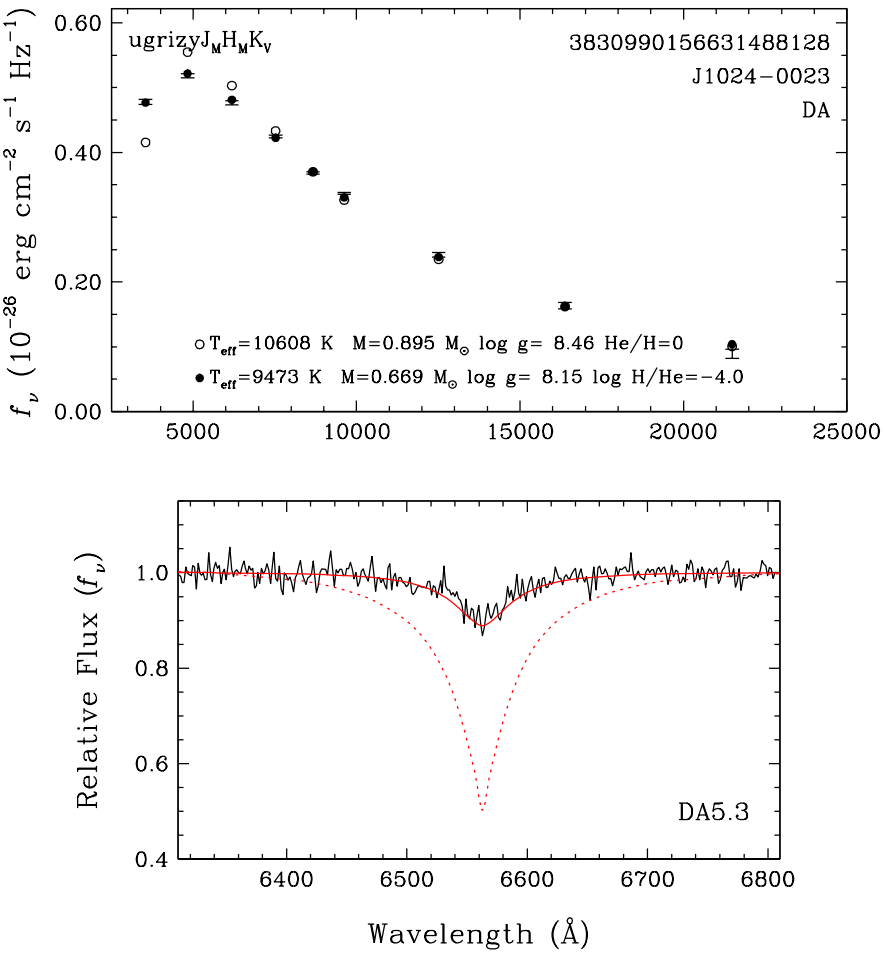

FIGURE 4.4 Best fit to a typical He-rich DA star in our sample. The observed photometry is shown as error bars and the photometric set used is indicated at the top left of the upper panel. Our model atmosphere fits for pure hydrogen and mixed H/He compositions are shown with different symbols, with parameters given in the upper panel. The lower panel shows the normalized optical spectrum (black), compared with the model spectra (red) interpolated at the parameters obtained from the photometric solution (solid line : mixed H/He solution, dotted line : pure H solution). Note that the y-axis begins at 0.4.

Similar asymmetric profiles can also be observed in the spectrum of GD 16 (see Figure 18 of Limoges et al. 2015b), another He-rich DA star (a DAZB white dwarf in this case). Clearly, these peculiar white dwarfs deserve further investigation.

4.3.4. DQ White Dwarfs

We fit the 146 DQ white dwarfs in our sample with spectra available (including the four DA + DQ systems) using a hybrid spectroscopic and photometric method outlined in Dufour et al. (2005b), although we rely here on the improved models of Blouin et al. (2018b, 2019c), and Blouin & Dufour (2019). We first assume a carbon abundance and fit the photometry

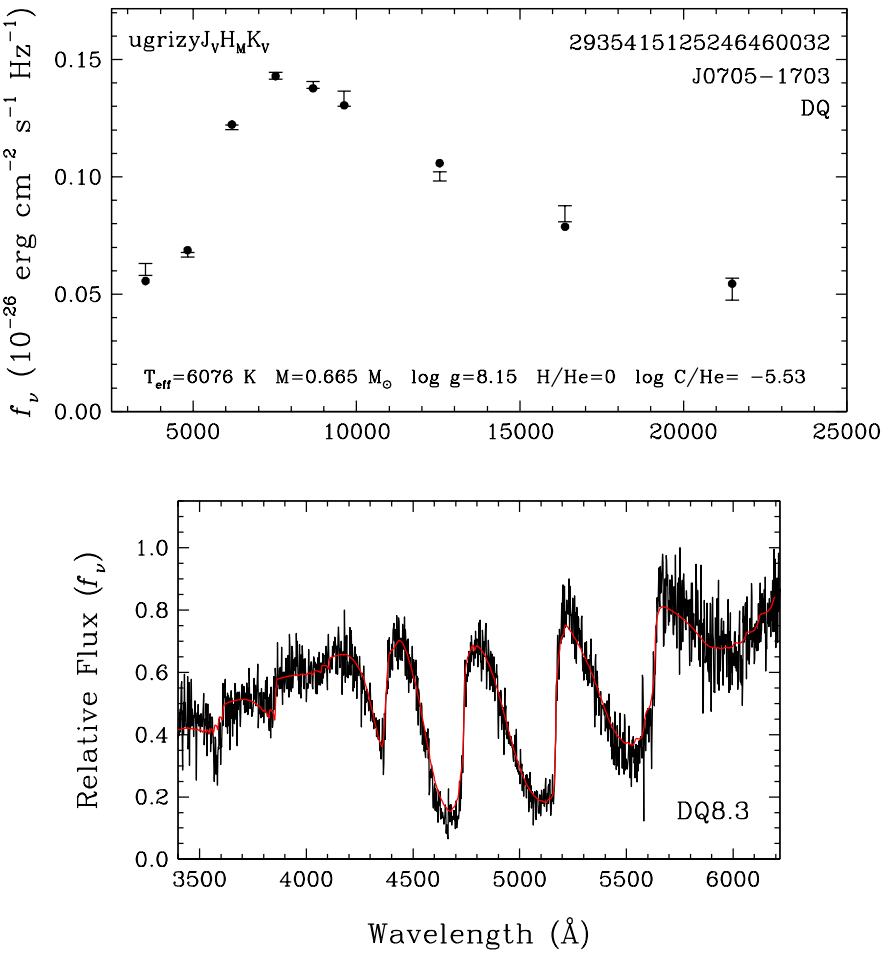

FIGURE 4.5 Best fit to a typical DQ white dwarf in our sample. Upper panel : The observed photometry, indicated at the top left, is shown by error bars, while the model atmosphere fit is shown by solid dots, with parameters given at the bottom. Lower panel : Optical spectrum (black) used to constrain the carbon abundance of the photometric solution, compared with the model spectrum (red).

using the same technique as before. We then fit the optical spectrum – neutral carbon lines or C_2 Swan bands – to measure the carbon abundance using the $T_{\rm eff}$ and $\log g$ values obtained from the photometric solution. We iterate this procedure until we reach an internal consistency between the photometric and spectroscopic solutions. A fit to a typical DQ star in our sample, J0705−1703, is displayed in Figure 4.5.

Some DQ stars in our sample also show a weak and broad Hα absorption feature (J0916+1011, J0950+3238, and J1147+0747) and are thus genuine DQA white dwarfs. In some cases, however, the presence of hydrogen lines is better explained as the result of an unresolved DA+DQ double degenerate binary (J0613+2050, J0928+2638, J1406+3401, and J1532+1356). In these cases, not only the object appears overluminous, but hydrogen lines are also much sharper, in contrast to the genuine DQA stars where Hα is heavily broadened

by van der Waals interactions in a He-dominated environment. For the three genuine DQA white dwarfs, we calculated a smaller set of model atmospheres that also include hydrogen with $\log \mathrm{H/He} = -5$, -4, and -3, and constrain the hydrogen abundance to the closest value set by the observations at Hα. For the four DA+DQ systems, we did not attempt to deconvolve the individual components, and simply fit these systems assuming a single DQ white dwarf; these are further discussed in Section 4.3.9.

Given the temperature range explored in our analysis, most DQ stars in our sample show only C_2 Swan bands, although some of the hottest ones (e.g., J0859+3257) also show neutral carbon lines. In general, the strong shift of the Swan bands, as modeled by Blouin & Dufour (2019) and references therein, is remarkably well reproduced (e.g., J1333+0016), although there are several exceptions and problematic cases (e.g., J1113+0146, J1618+0611), already discussed by Blouin & Dufour (see their Section 3.1). Possible explanations include problems with the simple model used to account for the distortion of the Swan bands, or the presence of a strong magnetic field, which has been confirmed by spectropolarimetric measurements in some objects.

Finally, we could not help noticing that some of the DQ white dwarfs in our sample appear to show some IR flux deficiency, the best example of which is J1442+4013. Other examples in our sample include J0033+1451, J0041−2221 (the well-studied LHS 1126; Wickramasinghe et al. 1982; Bergeron et al. 1994; Kilic et al. 2006; Blouin et al. 2019c), J0508−1450, J1045−1906, J1247+0646, and J1614+1728. Indeed, our poor photometric fits to these stars are reminiscent of the poor fits we obtain for the so-called IR-faint white dwarfs (see Section 4.3.6), when analysed with pure H or pure He models instead of mixed H/He models. In these cases, the IR-flux deficiency is the result of collision-induced absorptions (CIA) by molecular hydrogen due to collisions with helium. Perhaps the IR flux deficiency in these peculiar DQ stars is also the result of absorption by molecular hydrogen, thus offering the possibility of measuring H abundances in cool DQ white dwarfs. Unfortunately, our attempts to fit these DQ white dwarfs with mixed H/He/C model atmospheres were unsuccessful, the main problem being that a strong CH absorption feature is always predicted but not observed (with the possible exception of J1442+4013). Clearly, these objects deserve further investigation.

4.3.5. DZ White Dwarfs

The procedure used to fit the DZ and DZA white dwarfs in our sample is similar to the approach used for DQ stars, with model atmospheres described in Blouin et al. (2018b, see also Coutu et al. 2019b). The only exception here is that we also rely on optical spectra around Hα, if available, to measure (or constrain) the hydrogen abundance. Our solutions are provided in terms of the Ca abundance ($\log \mathrm{Ca/He}$), and we assume chondritic abundance ratios with respect to Ca for other metals, spectroscopically visible or not. Our model grid

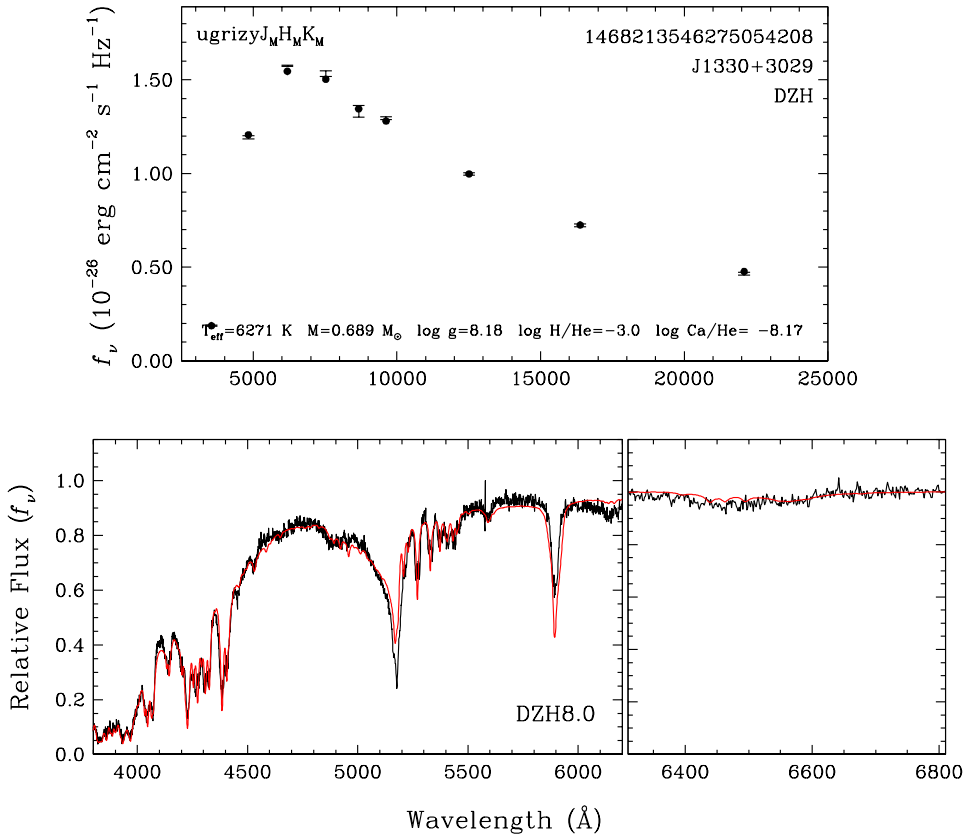

FIGURE 4.6 Best fit to a typical DZ white dwarf in our sample. Upper panel : The observed photometry, indicated at the top left, is shown by error bars, while the model atmosphere fit is shown by solid dots, with parameters given at the bottom. Lower panel : Optical spectrum (black) used to constrain the metal abundance (left) and hydrogen abundance (right) of the photometric solution, compared with the model spectra (red).

covers Ca abundances of $\log \mathrm{Ca/He} = -12.0$ (0.5) -7.0. As was the case for the He-rich DA white dwarfs, we do not attempt to fit the hydrogen abundance, but we simply explore the solutions with various hydrogen abundances ($\log \mathrm{H/He} = -5, -4, -3, -2, -1.5$, and -1) and adopt the value, or limit, consistent with the Hα spectrum. A fit to a typical DZ star in our sample, J1330+3029, is displayed in Figure 4.6. Even though the object shown here shows various metallic absorption features, most DZ stars in our sample only show the Ca II H & K doublet.

We have 9 DZ stars in our sample without optical spectra available to us. For 4 of those, we rely on Ca abundance published in the literature (J0124−2229, J0512−0505, J0823+0546, and J2343−1659), while we fit the remaining 5 (J0153+0911, J0733+2315, J1442+0635, J1551+1439, and J2147−2910) using the procedure for DC stars described in Section 4.3.7.

An important issue in our analysis is whether the cool DZ and DZA stars in our sample are H- or He-atmosphere white dwarfs (see, e.g., Blouin & Xu 2022). To explore this possibility,

we fitted all relevant objects with the He-atmosphere DZ model grid described above, and compared the solutions with those obtained from the model grid for H-atmosphere DAZ white dwarfs described in Section 4.3.2. We found out that it was rather easy to discriminate both solutions by simply looking at the quality of the fits. But more importantly, we also found that all cool, low-mass ($M < 0.45\ M_{\odot}$) DZ and DZA stars uncovered using He-atmosphere models turned out to be H-atmosphere white dwarfs, with much larger masses. A good example is displayed in Figure 4.7 for the DZA white dwarf J1627+4859, where we contrast both solutions. Here the mass obtained using H-atmosphere models, $M = 0.616\ M_{\odot}$, is significantly larger than that obtained using He-atmosphere models, $M = 0.413\ M_{\odot}$. The overall quality of the fit is also far superior using H-atmosphere models.

4.3.6. IR-faint White Dwarfs

Bergeron et al. (2022b) have recently demonstrated that white dwarfs showing a strong infrared flux deficiency resulting from collision-induced absorption (CIA) by molecular hydrogen – often referred to as ultracool white dwarfs – are not so cool after all. Indeed, model atmospheres including the high-density correction to the He^- free-free absorption coefficient of Iglesias et al. (2002) have been shown to yield significantly higher effective temperatures and larger stellar masses than previously reported. Hence, these objects should be more accurately referred to as IR-faint white dwarfs.

We have 47 IR-faint white dwarfs in our sample, 43 of which have been previously analysed in Bergeron et al. (2022b). With the exception of J0041−2221 (LHS 1126), which we analyzed above as a DQ white dwarf, we fit the IR-faint white dwarfs in our sample using the same models as those described at length in Bergeron et al. These are all DC white dwarfs with the exception of the four previously known DZ stars J0804+2239, J1824+1212, J1922+0233, and J2317+1830 (Blouin et al., 2018d; Tremblay et al., 2020b; Hollands et al., 2021). The four new IR-faint white dwarfs discovered in our analysis are J0223+2055, J0910+2554, J1801+5050, and J2347+0304. Three of these have comparable temperatures ($T_{\rm eff} \sim 4500$ K) and stellar masses ($M \sim 0.5\ M_{\odot}$), but more importantly, comparable chemical compositions in the range $\log {\rm H/He} \sim -1.0$ to 0.1 (i.e., nearly equal amounts of H and He compared to other IR-faint white dwarfs). Our best fit to J1801+5050 is displayed in Figure 4.8. These four new discoveries had not been identified as IR-faint candidates in Bergeron et al. because their colours in the Pan-STARRS M_g versus $(g - z)$ colour-magnitude diagram put them near the bulk of white dwarfs along the faint end of the main white dwarf sequence, making them impossible to identify without proper near-infrared photometry. We come back to this important point in Section 4.3.7.1.

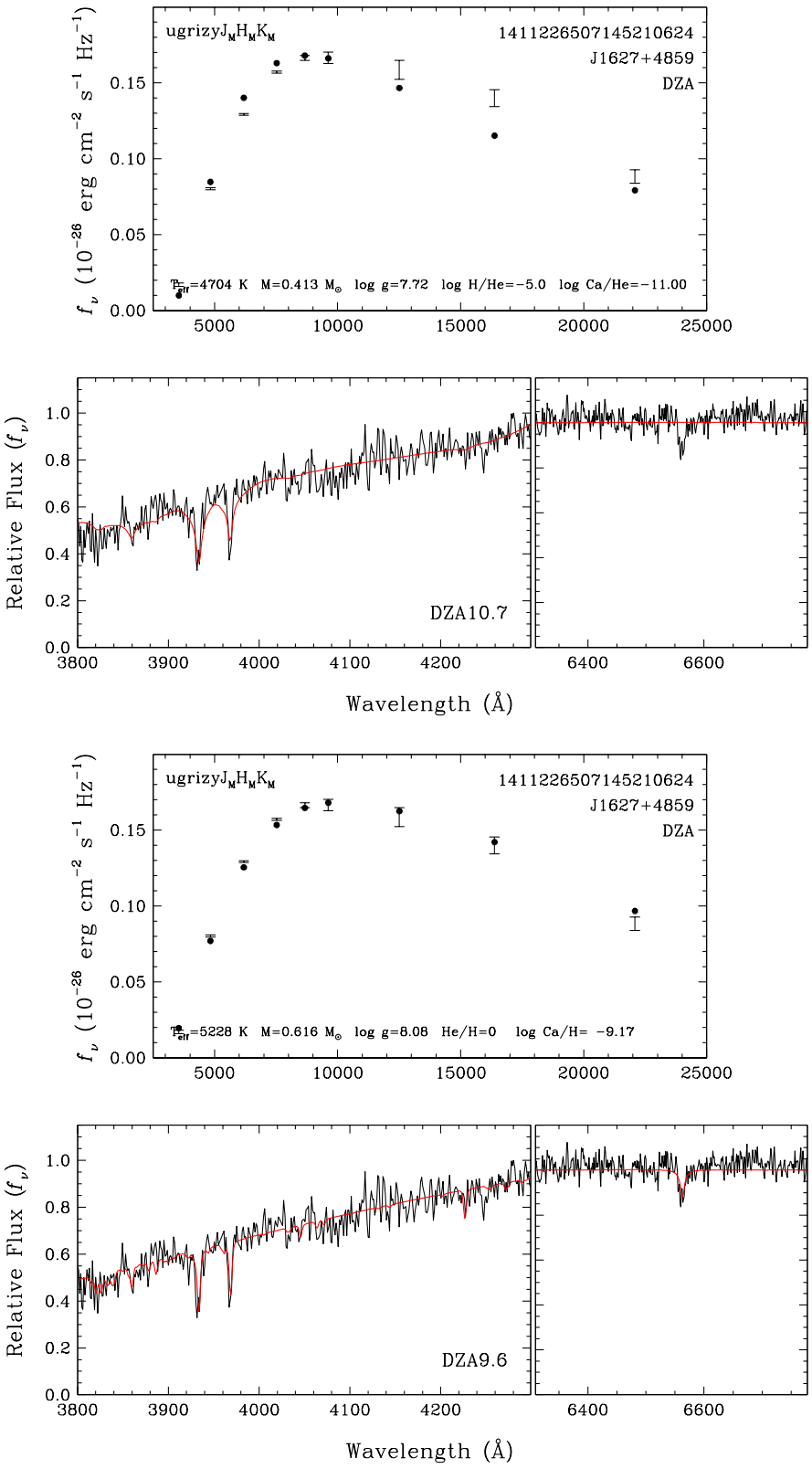

FIGURE 4.7 Same as Figure 4.6 but for a DZA star fitted under the assumption of a He-atmosphere (top two panels) and H-atmosphere (bottom two panels) white dwarf.

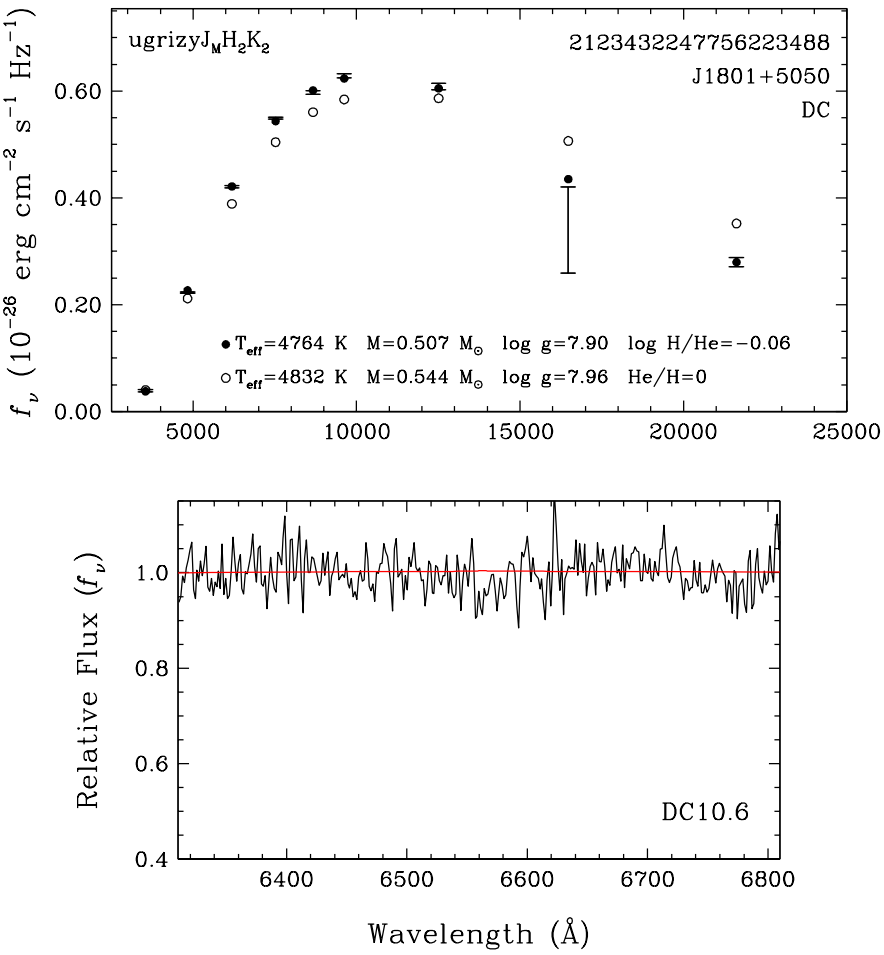

FIGURE 4.8 Best fit to a new IR-faint white dwarf identified in our sample. Upper panel : The observed photometry, indicated at the top left, is shown by error bars, while the model atmosphere fit is shown by solid dots for the mixed H/He solution, and open circles for the pure H solution, with parameters given at the bottom. Lower panel : Optical spectrum (black) compared with the model spectrum (red) interpolated at the parameters obtained from the pure H photometric solution.

4.3.7. DC White Dwarfs

The procedure used to fit the 810 DC white dwarfs in our sample (excluding the IR-faint DC stars) is identical to the approach used above for the DA stars (including the model atmospheres). A fit to a typical DC star in our sample, J1240+0932, is displayed in Figure 4.9. So far, it was possible for the previous spectral types to obtain an almost unique solution because the information contained in the optical spectrum (or the *JHK* photometry in the case of IR-faint white dwarfs) allowed us to constrain the chemical composition, whether it is the main constituent, hydrogen or helium, or traces of other elements (hydrogen, carbon, metals).

For genuine DC stars with featureless spectra, it becomes extremely difficult to determine even the main constituent of the atmosphere, unless the object is hot enough that Hα would be detected if the atmosphere were composed of hydrogen. The case of J1240+0932 displayed in Figure 4.9 is such an example. Moreover, as demonstrated in Bergeron et al. (2019a), invisible traces of hydrogen in He-atmosphere DC white dwarfs can affect the temperature and mass determinations significantly when using the photometric technique (see also Figure 5 of Blouin et al. 2019c), and the exact amount of hydrogen present is impossible to determine accurately. The only exception is for IR-faint DC white dwarfs where the presence of hydrogen can be inferred, and thus measured, from the strong infrared absorption resulting from collision-induced absorption by molecular hydrogen, whether it is due to H_2–H_2 or H_2–He interactions, but this becomes only possible at low effective temperatures ($T_{\rm eff} \lesssim 6000$ K) when molecular hydrogen starts to form.

In principle, it is theoretically possible to distinguish H-rich from He-rich white dwarfs over a wide range of effective temperatures due to the different behaviour of H and He continuum opacities, but this requires extremely precise photometry, and more importantly, a very accurate magnitude-to-flux conversion, which is not always the case, even for Pan-STARRS and SDSS magnitudes based on the AB photometric system, as discussed by Bergeron et al. (2019a). The problem becomes even more severe when multiple photometric systems are combined, for instance optical and infrared photometry. Consequently, it is extremely dangerous to allow the H/He abundance ratio to be a free parameter for fitting DC white dwarfs, as emphasized in Blouin et al. (2019c). We propose a different statistical approach below.

4.3.7.1. The Bottom of the Cooling Sequence. We first investigate in this section the nature of the cool DC white dwarfs at the faint end of the cooling sequence in the colour-magnitude diagrams displayed in Figures 4.1 and 4.2. In both diagrams, the 0.6 $M_\odot$ CO-core models with pure H (solid lines) and pure He (dotted lines) atmospheres fail to match the faint sequence of DC white dwarfs, although the pure H models are definitely much closer than the pure He models. Even though the mixed $\log {\rm H/He} = -5$ models (dash-dotted lines) match the DC sequence rather well in the SDSS M_g versus $(u-g)$ colour-magnitude diagram, they fail miserably in the Pan-STARRS M_g versus $(g-z)$ diagram due to the onset of CIA. We also notice that there are very few objects observed along the pure He sequence at faint luminosities, suggesting that most cool DC white dwarfs have H-dominated atmospheres, at least based on these diagrams. Furthermore, we can see in Figure 4.1 that the pure hydrogen sequence provides an excellent match to the DA stars at higher temperatures, and that the departure occurs below roughly $T_{\rm eff} \sim 5300$ K, when Hα becomes difficult to detect. But from an empirical point of view, the DA sequence at this temperature merges perfectly well with the cool DC sequence. All these observations strongly suggest a problem with the physics of pure-H model atmospheres at very low effective temperatures.

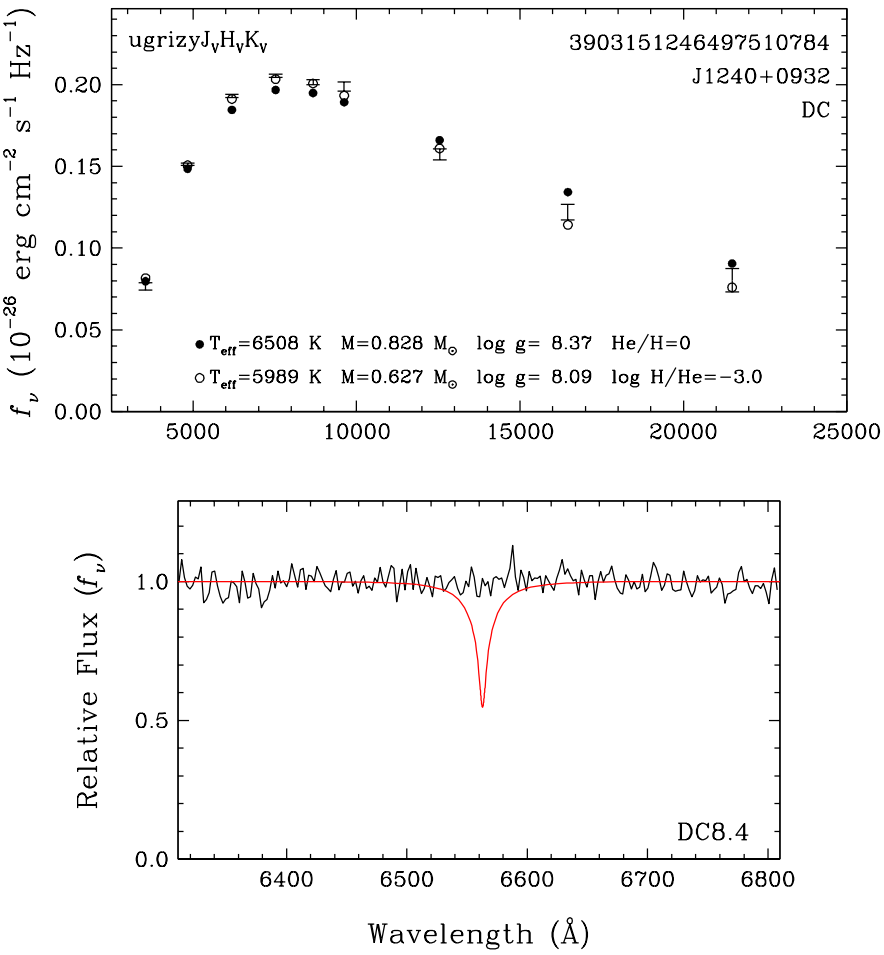

FIGURE 4.9 Best fit to a typical DC white dwarf in our sample. Upper panel : The observed photometry, indicated at the top left, is shown by error bars, while the model atmosphere fit is shown by solid dots for the pure H solution, and open circles for the mixed H/He solution, with parameters given at the bottom. Lower panel : Optical spectrum (black) compared with the model spectrum (red) interpolated at the parameters obtained from the pure H photometric solution.

We investigated this problem by looking at one of the coolest objects along the DC sequence, J1102+4112, with $M_g = 17.28$ and $(g - z) = 2.01$ (the reddest DC star in Figure 4.1). This object has also been analysed in detail by Hall et al. (2008). Our best photometric fit under the assumption of a pure H atmosphere is displayed in Figure 4.10. Here we show two fits, one by including the near-infrared *JHK* photometry (the solution shown in black), and the other solution (in red) where the *JHK* photometry has been omitted. Although both fits are far from perfect, they are significantly superior to those obtained with mixed H/He or pure He atmospheres (not shown here), two solutions that can be easily ruled out. Similar conclusions have been reached by Hall et al. (2008, see their Figures 4 and 5). The results shown in Figure 4.10 also indicate that the solution based solely on optical *ugrizy* photometry

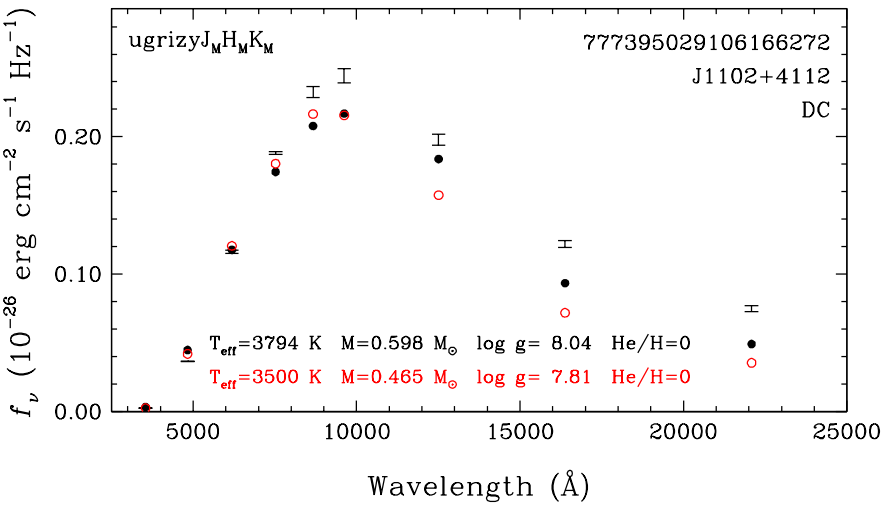

FIGURE 4.10 Best fits to one of the coolest DC white dwarfs in our sample assuming a pure H composition. The observed photometry, indicated at the top left, is shown by error bars. The filled black dots show the fit obtained by including the near-infrared *JHK* photometry, while the open red dots show the solution obtained by fitting only the optical *ugrizy* photometry. The corresponding parameters are given at the bottom.

yields a low temperature of $T_{\rm eff} = 3500$ K, and a low mass of $M = 0.465\ M_\odot$. However, the inclusion of the near-infrared *JHK* photometry has the effect of pushing the solution towards a higher temperature of $T_{\rm eff} = 3800$ K, and a much larger mass of $M = 0.598\ M_\odot$ – i.e., $\sim$0.13 $M_\odot$ larger – in much better agreement with the average mass of white dwarfs. [5]

We observe a similar effect in all cool DC white dwarfs in our sample, but to a lesser extent as we go up in temperature. And again, the pure He model atmospheres yield far worse solutions, in particular in terms of mass. This can be appreciated by examining the mass versus effective temperature distribution for all the cool ($T_{\rm eff} \lesssim 5500$ K) DC white dwarfs in our sample, displayed in Figure 4.11, obtained under the assumption of pure H (red symbols) and pure He (blue symbols) atmospheric compositions. Note that for the objects below 0.2 $M_\odot$, we rely on the He-core models described in Bergeron et al. (2022b, see their Figure 3), which are appropriate in the temperature range considered here. We can see that the $T_{\rm eff}$ and M values obtained under the assumption of pure He compositions are unrealistically low. This result is entirely consistent with the prediction of the 0.6 $M_\odot$, pure He sequence in the colour-magnitude diagram displayed in Figure 4.1 with respect to the location of these cool DC stars ; the models need to be more luminous, thus requiring larger

5. Note that Leggett et al. (2018) erroneously obtained a mixed H/He solution for this object (WD 1059+415 in their Table 4), although they also show (see the supplementary material) their best fit assuming a pure H composition, which is almost identical to that shown here. Their pure H solution fit even provides an excellent match to the Spitzer photometry.

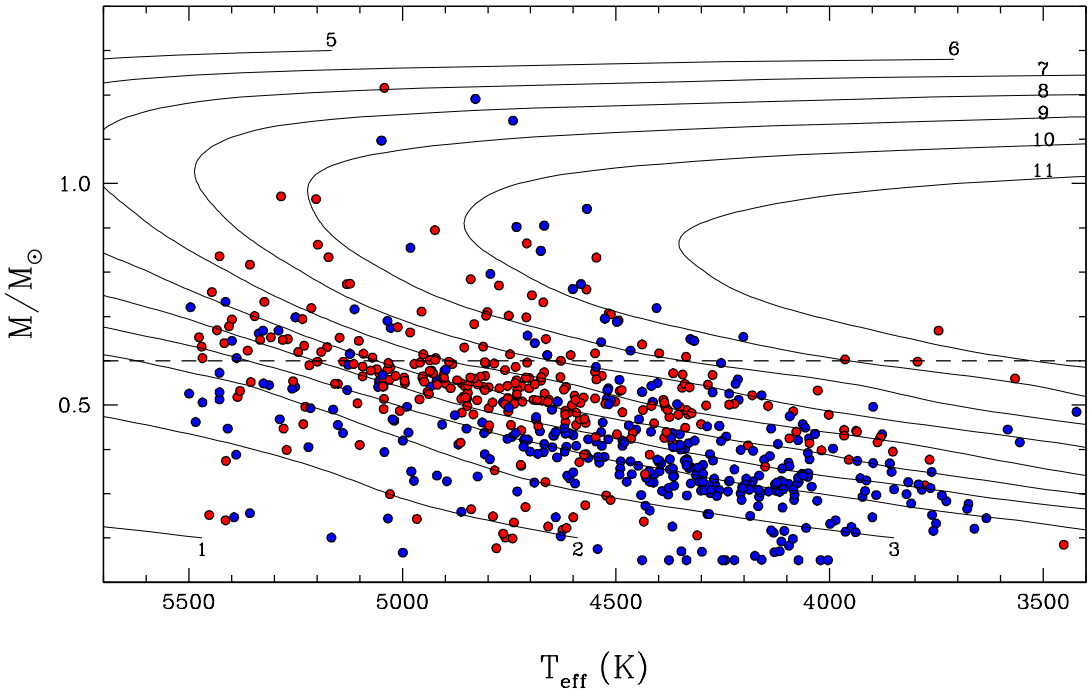

FIGURE 4.11 Mass as a function of effective temperature for the cool DC white dwarfs in our sample under the assumption of pure H (red dots) and pure He (blue dots) atmospheric compositions. The dashed line corresponds to 0.6 $M_{\odot}$, the average mass for white dwarfs. Solid curves are theoretical isochrones (white dwarf cooling age only), labeled in units of 10^9 yr, obtained from the CO-core cooling sequences described in Section 4.2.3 with thick H layers ($q(\mathrm{H}) = 10^{-4}$).

radii and smaller masses. In contrast, the masses obtained under the assumption of pure H models in Figure 4.11 are much closer to the mean mass of white dwarfs, although we see a definite trend towards lower masses at lower temperatures, another indication of problems with the physics of pure H model atmospheres at low effective temperatures, and thus higher photospheric densities, a conclusion also reached by Hall et al. (2008).

We can now understand more quantitatively the results displayed in Figure 12 of Bergeron et al. (2019a), which shows similar M versus $T_{\rm eff}$ distributions for all white dwarfs found in Gaia within a distance of 100 pc, including both spectroscopically identified white dwarfs as well as white dwarf candidates. In this case, the stellar parameters have been determined using photometric fits to Pan-STARRS *grizy* photometry only. Their solutions obtained from pure H (top panel) and pure He (middle panel) model atmospheres show the same behavior as in Figure 4.11, with the exception that our masses based on pure H models are larger due to the use of *JHK* photometry for many of our objects, but still not enough to reach the $\sim$0.6 $M_{\odot}$ average mass for white dwarfs for the coolest DC stars in our sample.

All the results above strongly support the idea, also suggested by Kowalski & Saumon (2006), that the bulk of cool ($T_{\rm eff} \lesssim 5000$ K) DC white dwarfs, but not all (see below), probably have H atmospheres. By taking into account the suspected problems with the H-atmosphere models, we did not find a single convincing case of a cool, pure He DC white dwarf in our sample. Note that we exclude from the discussion the cool DZ white dwarfs, which are discussed further below. The fact that the 0.6 $M_{\odot}$ pure H theoretical sequence in Figure 4.1 does not match the observed DC sequence is obviously related to the less-than-perfect fit displayed in Figure 4.10, in particular in the optical.

One possible explanation for this problem is the UV/blue opacity originating from the red wing of Lyα. Kowalski & Saumon (2006) performed such calculations and successfully demonstrated that models including this opacity show significant improvements in explaining the location of DC white dwarfs in colour-colour diagrams (see their Figure 4). Note that their calculations is based on the one-perturber approximation, H or H_2, and it is possible that the interaction from multiple perturbers (see, e.g., Allard & Kielkopf 2009) need to be taken account in the coolest white dwarfs where the densities are significantly larger. We also note that Saumon et al. (2014) analysed Hubble Space Telescope STIS spectra of eight very cool WDs (five DA and three DC stars) and showed that their fits become worse at lower $T_{\rm eff}$ and higher $\log g$ values. As the authors conclude, these are the stars with higher photospheric densities and more extreme physical conditions, implying that the microphysics of dense matter probably needs to be revised.

It is also possible that other sources of opacity might be responsible for the problems described above. For instance, the top panel of Figure 17 from Saumon et al. (2022) shows that at the photosphere of a pure H model at $T_{\rm eff} = 4000$ K, the opacity from the red wing of Lyα dominates in the UV, while the H^- bound-free opacity and the H_2-H_2 (and H_2-H) CIA opacity dominate in the optical and near-infrared, respectively. Perhaps the physics from these last two opacity sources needs te be revised as well.

As discussed above, the end of the cooling sequence in Figure 4.1 is composed mainly of DC stars that are better interpreted as H-atmosphere white dwarfs, but not all. The glaring exceptions are the IR-faint DC white dwarfs with mixed H/He compositions. We reproduce in Figure 4.12 the M_g versus $(g-z)$ colour-magnitude diagram from Bergeron et al. (2022b) together with the 105 IR-faint white dwarfs they analysed (in red) as well as the four new objects (in yellow) identified in our survey and discussed in Section 4.3.6. Most IR-faint white dwarfs in this diagram are located on the nearly horizontal branch, consistent with mixed H/He atmospheres with $\log {\rm H/He} \sim -2$, a result confirmed quantitatively by a more rigorous model atmosphere analysis (see Figure 15 of Bergeron et al. 2022b). However, these appear more common because they clearly stand out in such a colour-magnitude diagram, an obvious selection effect. But there are other IR-faint white dwarfs more difficult to detect, such as those found on the main branch at the end of the cooling sequence. These include three of

the four we identified in our analysis, thanks to the available *JHK* photometry, otherwise they would have gone unnoticed[6]. Note that the parameters determined for three of the new IR-faint white dwarfs identified in our survey ($M \sim 0.5\ M_{\odot}$, H/He ~ 1) are entirely consistent with their location in the colour-magnitude diagram, as illustrated in Figure 4.12, where we overplotted the corresponding cooling sequence (in green). It is therefore possible that many more are hiding in the same region of the colour-magnitude diagram. This stresses the importance of eventually securing *JHK* photometry for all spectroscopically confirmed white dwarfs at the end of the cooling sequence.

4.3.7.2. The Atmospheric Composition of DC White Dwarfs. As discussed above, it is possible to obtain a unique solution for the physical parameters of cool white dwarfs – effective temperature, stellar mass, atmospheric composition – using the photometric approach given that we have sufficient spectroscopic information (hydrogen, carbon, and metallic absorption features). Even in the case of IR-faint white dwarfs, the H/He abundance ratio can be determined from the CIA opacity in the near and far infrared. However, for most genuine featureless DC white dwarfs, the situation is nearly hopeless. Indeed, as discussed in Bergeron et al. (1997b), there are also subtle differences between pure H and pure He spectral energy distributions due to the presence (or absence) of the H^- opacity in the infrared (see their Figure 15), or to the onset of CIA absorption at low temperatures (see, e.g., Figure 1 of Blouin et al. 2019c), but such measurements can be extremely difficult and dangerous, in particular given the precision and accuracy (or even availability) of infrared photometric measurements. We adopt here a different approach for the DC white dwarfs in our sample.

Above some $T_{\rm eff}$ value, it is almost impossible to distinguish pure He models from models including a trace of hydrogen. Yet, as shown by Bergeron et al. (2019a), even undetectable traces of hydrogen can affect the temperature and mass determinations significantly at all temperatures of interest in our analysis. As a conservative estimate, we adopt $T_{\rm eff} = 6500$ K as the temperature above which all DC stars are assumed to have mixed H/He compositions. We adopt the same approach as in Kilic et al. (2020b, see their Section 3.5) and adjust the H/He abundance ratio as a function of $T_{\rm eff}$, from $\log {\rm H/He} = -5$ at $T_{\rm eff} = 11{,}000$ K, up to $\log {\rm H/He} = -3$ at $T_{\rm eff} = 6000$ K, thus following the predictions of the convective mixing scenario of Rolland et al. (2018b). However, we also found out that assuming $\log {\rm H/He} = -5$ throughout has little effect on the results (see below). It is of course possible that some of these DC white dwarfs may contain no hydrogen whatsoever, and thus their masses are probably underestimated here, but there is no possible way to identify those in our sample, neither spectroscopically, nor photometrically.

As discussed in the previous section, there is empirical evidence that most, but probably not all, extremely cool DC white dwarfs have pure H compositions. Here we adopt $T_{\rm eff} =$

6. These four IR-faint white dwarfs had not even been identified as potential candidates in the search for additional IR-faint candidates discussed in Section 5.4 of Bergeron et al. (2022b)

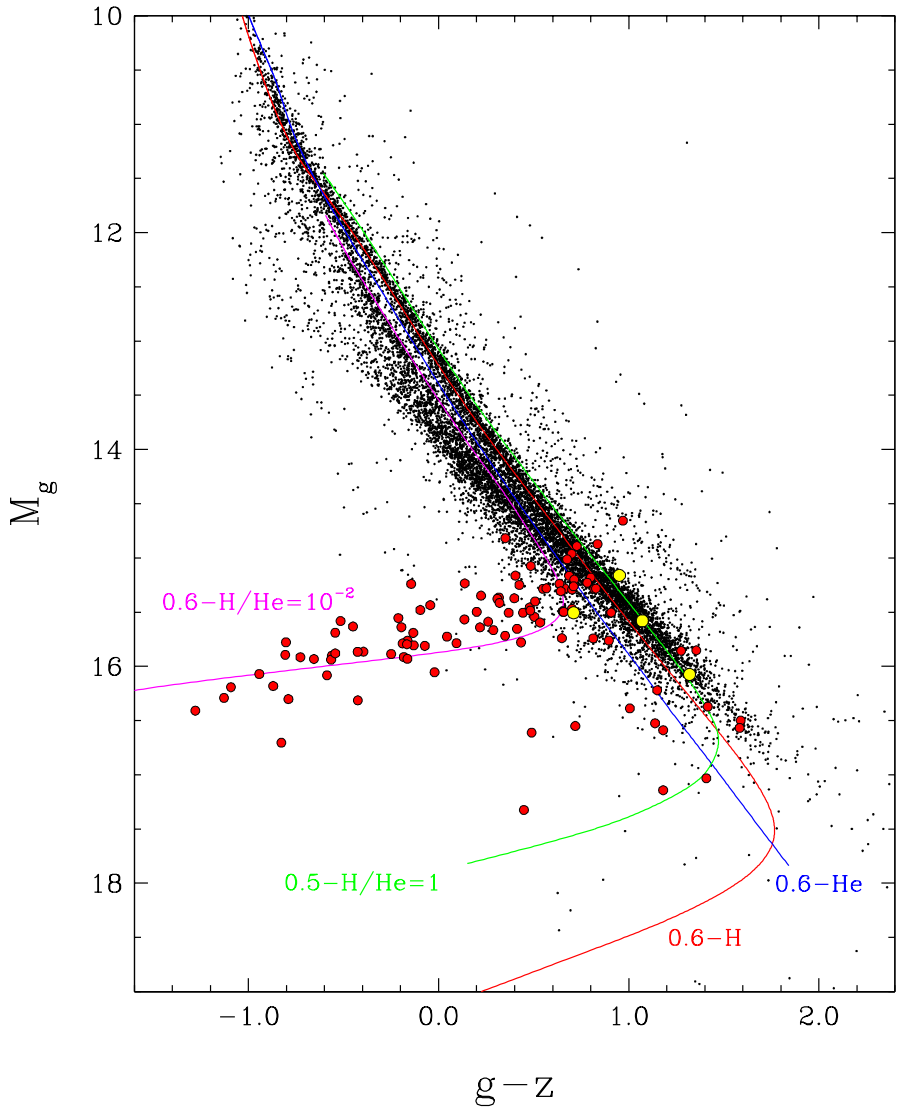

FIGURE 4.12 Pan-STARRS M_g versus $(g - z)$ colour-magnitude diagram for the 100 pc sample drawn from the MWDD. The red dots represent the IR-faint white dwarfs analysed in Bergeron et al. (2022b), while the yellow dots show the location of the four new objects identified in our analysis. Also overplotted are cooling sequences for 0.6 $M_\odot$ C/O-core models with pure H (red), pure He (blue), and $\log \mathrm{H/He} = -2$ (magenta) atmospheric compositions. The green sequence is for 0.5 $M_\odot$ C/O-core models with $\log \mathrm{H/He} = 0$ (i.e., H/He = 1).

5200 K as the temperature below which we assume a pure H atmospheric composition for the DC white dwarfs in our sample. This corresponds also roughly to the temperature above which it is possible to distinguish DA and DC stars from the detection of Hα. It is of course possible to detect theoretically Hα at much lower temperatures, a value that also depends on $\log g$, but the spectral classification is particularly sensitive to the signal-to-noise ratio of the observations. For instance, we can detect a weak Hα feature in the DA star J0700+3157

at $T_{\rm eff} \sim 4900$ K, but this is an extremely high S/N spectrum obtained with the Hale 5 m reflector at Palomar Observatory by Greenstein (1986), who contributed to reclassify many DC white dwarf as DA stars. Similar results have been reported by Bergeron et al. (1997b, 2001b).

Finally, there is a particular range in temperature between roughly $T_{\rm eff} = 5200$ K and 6500 K where the absence of Hα clearly rules out a pure H composition, but where the spectral energy distribution remains particularly sensitive to the presence of even small traces of hydrogen due to the onset of the H_2 CIA opacity. We determined that in this range of temperature, it is thus possible to differentiate pure H from He-rich white dwarfs by the presence of Hα, and to differentiate pure He from mixed H/He atmospheres by inspecting the spectral energy distribution. For instance, we compare in Figure 4.13 our best fits to two cool DC stars in this temperature range, obtained with pure He and mixed H/He ($\log {\rm H/He} = -5$) compositions. J1240+0932 (top) is an example of a DC star that is better fit under the assumption of a pure He atmosphere, while J0825+2242 (bottom) is better fit by a mixed H/He atmosphere, a conclusion that can be drawn by a simple inspection of the fits, but also confirmed from our χ^2 analysis. Note that the small trace of hydrogen of only $\log {\rm H/He} = -5$, which is much smaller than the hydrogen abundances inferred in IR-faint white dwarfs (see Figure 15 of Bergeron et al. 2022b), can affect both the temperature and mass determinations significantly. Moreover, a comparison of the $\log {\rm H/He} = -5$ solution for J1240+0932, displayed here, with the $\log {\rm H/He} = -3$ solution previously shown in Figure 4.9 for the same object, indicates that the particular H/He value used for DC stars in this temperature range (and above) does not affect the parameter determinations significantly.

To summarize, for temperatures between $T_{\rm eff} = 5200$ K and 6500 K, we adopt the pure H solution for DA stars, while for DC stars we adopt the pure He or mixed H/He solution based on a simple χ^2 analysis. We stress that this approach remains approximate because not all white dwarfs have near-infrared photometry available, and even for those that do, the quality of the photometry is highly variable.

4.3.8. Magnetic White Dwarfs

We have several magnetic white dwarfs in our sample of various spectral types. Among those, the more obvious are the magnetic DA stars, with Zeeman splitting in the form of a triplet at Hα for a moderate field (see, e.g., Figure 4.14), or with more displaced and distorted components if the magnetic field is much stronger. We also have several magnetic DQ white dwarfs, although in this case, these are restricted to the very cool DQ stars with strong and shifted C_2 Swan bands (see, e.g., J1038−2040 ≡ LP 790-29). We also have many cases of magnetic DZ stars (see, e.g., J1515+8230). In our analysis, we neglect the existence of these magnetic fields and apply the photometric method using non-magnetic model atmospheres.

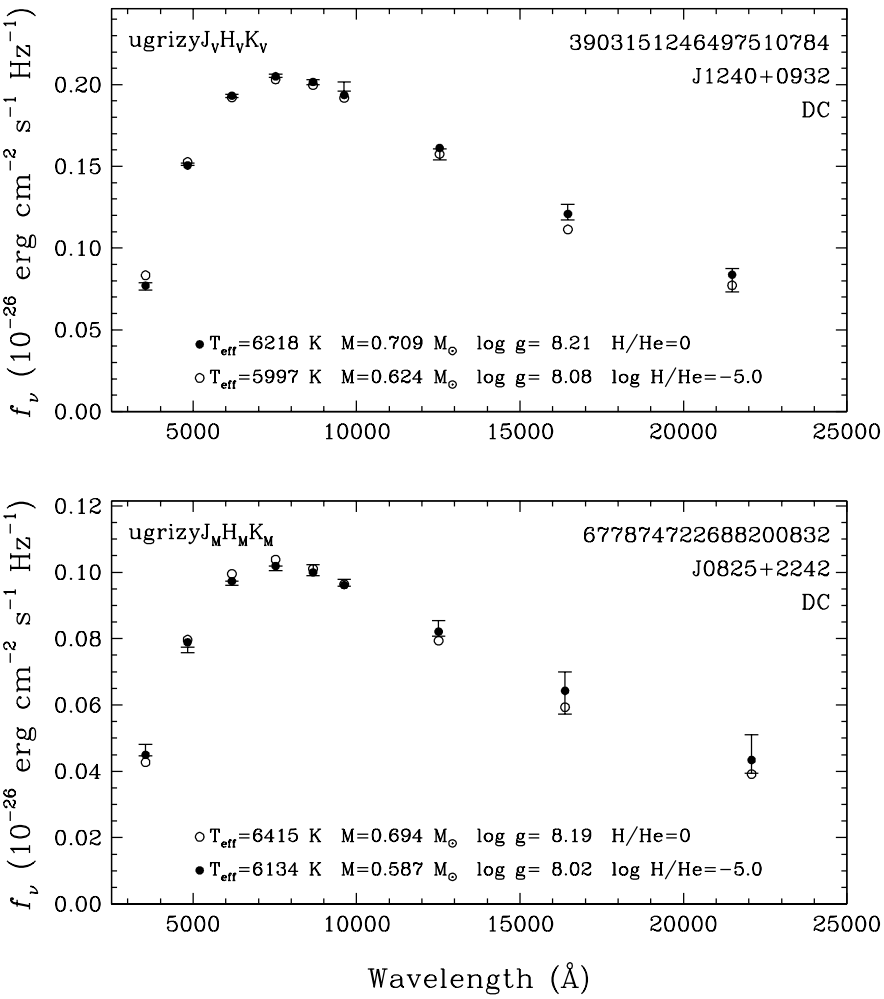

FIGURE 4.13 Two DC stars in our sample that are better fit with pure He (top) or mixed H/He (bottom) model atmospheres. The observed photometry is shown as error bars and the photometric set used is indicated at the top left of each panel. Our best model fit, pure He or mixed H/He ($\log \mathrm{H/He} = -5$), is shown as solid dots, while the other solution is shown as open circles with the model parameters given in each panel.

One obvious effect of using magnetic models is to change the predicted photometry due to absorption lines that are shifted to different wavelengths as a result of the magnetic field. However, we also found cases where even when line blanketing is unimportant, the continuum opacity seems to be affected, an example of which is displayed Figure 4.14, where we see that the energy distribution is better reproduced by a pure He model rather than a pure H model. We also observe a similar phenomenon in hotter magnetic DA stars, where the Balmer jump appears to be suppressed, in particular in objects with SDSS u magnitudes available (see, e.g., J1126+0906). Despite the better agreement with pure He (or He-rich) models for these stars, we still adopt the pure H solutions for all magnetic DA white dwarfs in our sample.

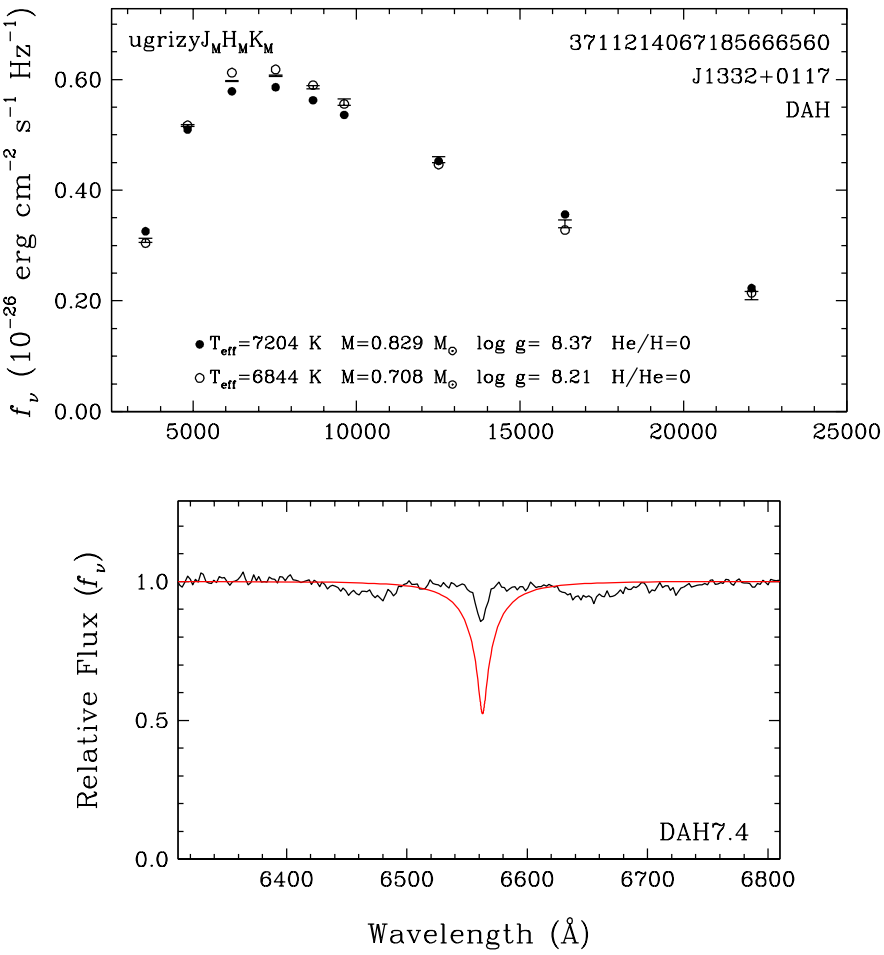

FIGURE 4.14 Best fit to a magnetic DA star in our sample. The observed photometry is shown as error bars and the photometric set used is indicated at the top left of the upper panel. Our pure H and pure He model atmosphere fits are shown as solid and open circles, respectively, with the parameters given in the upper panel. The lower panel shows the normalized optical spectrum, compared with the model spectrum (in red) interpolated at the parameters obtained from the pure H photometric solution.

4.3.9. Unresolved Double Degenerate Binaries

The existence of unresolved double degenerate binaries (DD) in our sample can already be inferred from the colour-magnitude diagram displayed in Figure 4.1 where they appear as overluminous objects above the main white dwarf sequence. Indeed, two unresolved white dwarfs of equal luminosity would appear ∼0.75 mag brighter than a single object, consistent with the location of most overluminous objects in Figure 4.1 (for systems composed of two ∼0.6 $M_\odot$ white dwarfs). We also note that most spectroscopically identified overluminous white dwarfs in Figure 4.1 are DA and DC stars, although we see a few DQ stars as well.

When applying the photometric technique to these DD systems assuming a single star, the radius measurement is usually overestimated since two objects contribute to the total luminosity, and the stellar mass is consequently underestimated as well. However, this may not necessarily be the case if one white dwarf component completely dominates the overall luminosity of the system, in which case the radius and mass measurements remain accurate. If an optical spectrum is available, the spectroscopic technique can be combined with the photometric method to deconvolve the stellar parameters of each component of the system, as done for instance by Bédard et al. (2017, see their Figures 14 to 16).

In our spectro-photometric analysis, we are able to detect the presence of DD systems in various ways. The first is of course when the stellar mass is very low ($M \lesssim 0.48\ M_{\odot}$), because such low-mass white dwarfs cannot have formed within the lifetime of our Galaxy, and can therefore only exist as a result of common envelope evolution. One example in our sample is the DA J0129+1022 with $M = 0.340\ M_{\odot}$. In this particular case, the predicted spectrum at Hα is in perfect agreement with the measured parameters obtained from the fit to the energy distribution assuming a single star. Hence, it is possible here that the luminosity of the brighter component of the system completely dominates that of the second component. Alternatively, if two DA components have similar parameters and contribute equally to the total luminosity of the system, we would also reach a perfect agreement between the photometric and spectroscopic solutions. It is of course impossible to distinguish between these two possibilities without a more refined analysis.

In most cases, however, it is expected that the individual components of DA + DA unresolved systems will have different stellar parameters, in which case we may observe a disagreement between the observed Hα profile and that predicted from the photometric solution assuming a single star. For instance, J0532+0624 ($M = 0.253\ M_{\odot}$) shows a distorted energy distribution that resembles a He-rich white dwarf, and moreover, the predicted Hα profile is at odds with the observations. Another example is J0138−0459 (L870-2, EG 11, WD 0135−052), a classical case of a DD system composed of two DA white dwarfs where both components contribute to the total luminosity of the system, but with significantly different parameters (Bergeron et al., 1989).

Even though all low mass white dwarfs must have formed through binary evolution, the reverse is not necessarily true, and there may exist more normal mass, or even massive, white dwarfs in our sample that are hidden in DD systems. For instance, J0611+0544 ($M = 0.594\ M_{\odot}$), J0904+1349 ($M = 0.611\ M_{\odot}$), and J0929−1732 ($M = 0.632\ M_{\odot}$) are good examples of normal mass white dwarfs with observed inconsistencies in there fits, while J0855−2637 ($M = 0.840\ M_{\odot}$) is a good example of a massive object.

It is also easy to detect the presence of DD systems when the spectral types of both components differ. A good example is J0110+2758 ($M = 0.301\ M_{\odot}$) where the broad and shallow Hα feature suggests the presence of a DC component in the system that dilutes

TABLEAU 4.2 Physical Parameters of the 100 pc White Dwarf Sample. This table is available in its entirety in machine-readable form.

Name	Gaia ID (DR2/EDR3*)	Sp Type	$T_{\rm eff}$ (K)	$M/M_{\odot}$	$\log g$	Comp	Metals	$\log L/L_{\odot}$	τ (Gyr)
J0000+0132	2738626591386423424	DA	10342 (32)	0.622 (0.007)	8.034 (0.008)	He/H=0	···	−2.79	0.61
J0000+1906	2774195552027050880	DC	5069 (54)	0.553 (0.055)	7.955 (0.066)	He/H=0	···	−4.00	4.86
J0001+3237	2874216647336589568	DC	5753 (56)	0.560 (0.034)	7.981 (0.041)	H/He=0	···	−3.80	3.06
J0001+3559	2877080497170502144	DC	6177 (73)	0.688 (0.031)	8.184 (0.035)	H/He=0	···	−3.79	3.49
J0001−1111	2422442334689173376	DC	6541 (48)	0.651 (0.024)	8.124 (0.027)	log H/He=−3.2	···	−3.65	2.41
J0002+0733	2745919102257342976	DA	7727 (44)	0.598 (0.015)	8.007 (0.018)	He/H=0	···	−3.29	1.23
J0002+0733	2745919106553695616	DAH	8130 (71)	0.805 (0.017)	8.331 (0.02)	He/H=0	···	−3.39	1.90
J0002+1610	2772241822943618176	DA	6684 (42)	0.613 (0.028)	8.037 (0.033)	He/H=0	···	−3.56	1.87
J0002+6357	431635455820288128	DC	4959 (23)	0.596 (0.01)	8.026 (0.011)	He/H=0	···	−4.08	6.55
J0003+6512	432177373309335424	DC	8595 (95)	0.506 (0.014)	7.874 (0.018)	log H/He=−4.0	···	−3.04	0.82

the Hα absorption profile. Similarly, we have 11 DQ stars with inferred masses below 0.4 $M_{\odot}$ (8 with $M < 0.3\ M_{\odot}$), although 4 of these are DD systems composed of a DQ and a cool DA white dwarf (J0613+2050, J0928+2638, J1406+3401, and J1532+1356). Perhaps the remaining 7 objects are also DD systems with the other component being a featureless DC white dwarf. Interestingly, we find no low-mass ($M < 0.4\ M_{\odot}$) DZ star in our sample; the only one is the IR-faint white dwarf J1824+1212 ($T_{\rm eff} \sim 4700$ K).

In what follows, we make no attempt to deconvolve the individual components of DD systems and simply assume that they are single white dwarfs. We just have to keep this in mind when interpreting the physical parameters obtained from our fits.

4.3.10. White Dwarfs + Companions

Because of the colour cut in the selection of our white dwarf sample, we avoid most WD + M–dwarf binaries, but these systems still exist in our sample, in particular if the M–dwarf has a late type that contaminates the colours, mostly in the near-infrared. In such cases, the M–dwarf companion may contribute significantly to the total flux, which leads to an overestimation of the white dwarf radius, and to an underestimation of its mass. Here we simply exclude the contaminated bandpasses from our photometric fits (these excluded bandpasses are shown in red in our figures). A good example is the DZ white dwarf J1651+6635. Contamination may also occur from different spectral types such as brown dwarfs, like in the case of the DA + L5 system J0135+1445 (NLTT 5306B, Casewell et al., 2020).

4.3.11. Adopted Parameters

The physical parameters for all white dwarfs in our sample are presented in Table 4.2, where for each object we provide the J name, Gaia ID (DR2; if not available the EDR3 is given and marked by a star symbol in Table 4.2), spectral type, effective temperature ($T_{\rm eff}$), mass ($M/M_{\odot}$), surface gravity ($\log g$), chemical composition (see below), luminosity ($\log L/L_{\odot}$), and white dwarf cooling age (τ in Gyr).

For clarity, we briefly summarize the procedure used to measure these parameters, and in particular the chemical composition. For DA stars, we assume a pure hydrogen composition

(He/H = 0), with the exception of He-rich DA stars for which the H/He ratio ($\log$ H/He) is adjusted to match the Hα absorption profile. For DQ stars, we provide the carbon abundance ($\log$ C/He) measured using the optical spectrum. For DZ stars – including DZA and DAZ stars as well –, we give the calcium abundance relative to helium ($\log$ Ca/He) or hydrogen ($\log$ Ca/H) depending on the main atmospheric constituent, measured using the metallic features observed in the optical spectrum (all other metals have chondritic abundance ratios with respect to Ca). For IR-faint white dwarfs, we provide the H/He ratio ($\log$ H/He) obtained from fits to the energy distribution. Finally, for DC stars, we assume a pure hydrogen composition (He/H = 0) for objects below $T_{\rm eff} = 5200$ K ; between $T_{\rm eff} = 5200$ K and 6500 K, we adopt the pure He (H/He = 0) or mixed H/He solution ($\log$ H/He) based on a χ^2 analysis ; for $T_{\rm eff} > 6500$ K, we also adopt a mixed H/He solution where the hydrogen abundance is adjusted as a function of $T_{\rm eff}$ (as discussed above, the precise hydrogen abundance has little effect on the measured parameters).

4.4. Selected Results

We can now explore the global properties of our sample, which is composed of all white dwarfs identified spectroscopically in the MWDD and with effective temperatures below $T_{\rm eff} \sim 10{,}000$ K. As such, it is by no means statistically complete in any sense, although we can expect with such a large sample that all spectral types are statistically well sampled at a given temperature, but probably not as a whole. For instance, Kilic et al. (2020b) increased significantly the number of spectroscopically confirmed white dwarfs within 100 pc in the SDSS footprint, but their sample was concentrated above ∼6000 K where DA stars could be easily identified. Hence, important selection effects are present in our sample, and we make no attempt in our analysis to restrict the results to any particular volume-limited sample.

4.4.1. Mass Distributions

The mass distribution, M versus $T_{\rm eff}$, for all 2880 spectroscopically confirmed white dwarfs in our sample are displayed in Figure 4.15, where the various spectral types are indicated with different colours. Also superposed are theoretical isochrones (WD cooling age only) obtained from cooling sequences with C/O-core compositions, q(He) = 10^{-2} and q(H) = 10^{-4} ; the other curves are described below. In terms of the overall analysis and model atmospheres, this figure is very similar to that shown in Figure 18 of Kilic et al. (2020b), with the exception that our analysis is not restricted to the SDSS footprint, it makes use of extensive sets of near-infrared *JHK* photometry, and more importantly, it is not restricted in temperature at the cool end of the white dwarf sequence (Kilic et al. restricted their analysis to $T_{\rm eff} \gtrsim 6000$ K). There are many interesting features observed in Figure 4.15, which we now discuss in turn.

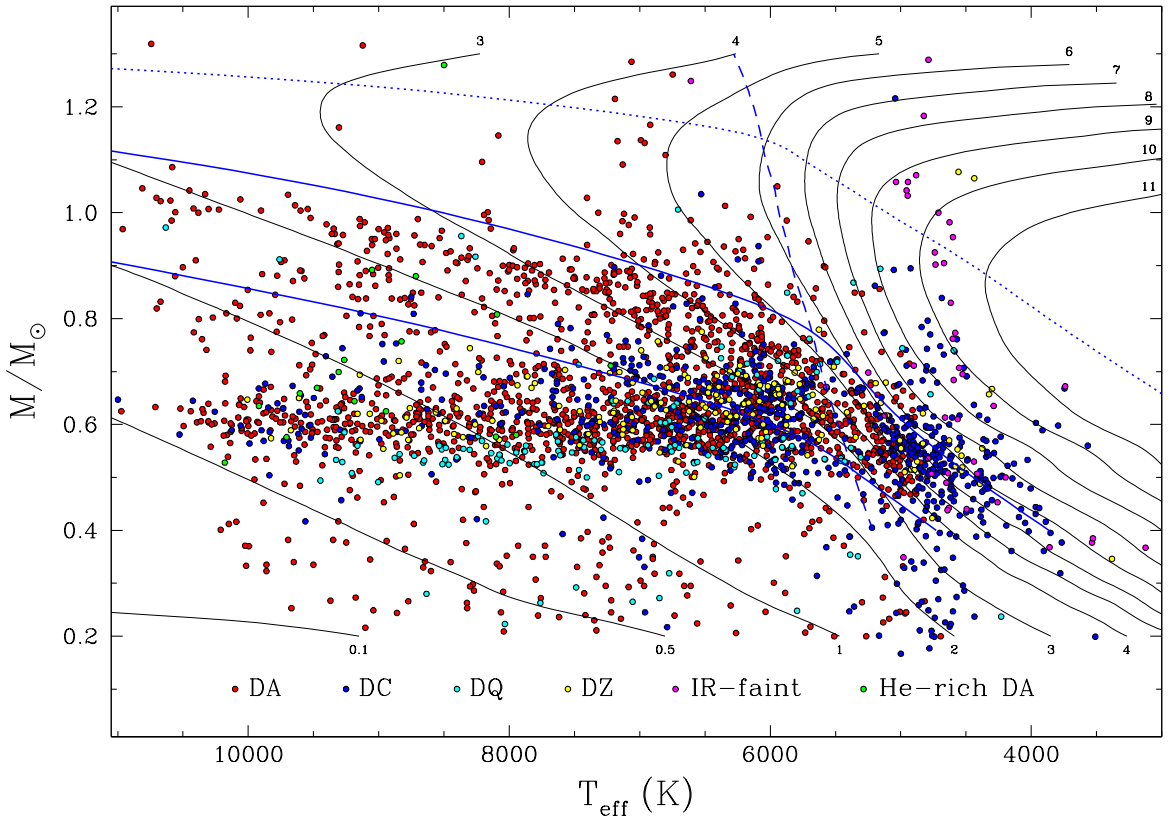

FIGURE 4.15 Mass distribution as a function of effective temperature for all 2880 spectroscopically confirmed white dwarfs in our sample for the various spectral types indicated in the legend. Solid black curves are theoretical isochrones (WD cooling age) labeled in units of Gyr, obtained from cooling sequences with C/O-cores, $q(\mathrm{He}) = 10^{-2}$ and $q(\mathrm{H}) = 10^{-4}$ (see Section 4.2.3). The lower blue solid curve indicates the onset of crystallization at the centre of evolving models, and the upper one indicates the locations where 80% of the total mass has solidified. The dashed curve indicates the onset of convective coupling, while the dotted curve corresponds to the transition between the classical to the quantum regime in the ionic plasma (see text).

We first focus on the region above $T_{\rm eff} \sim 6000$ K where we can see a nice clustering of objects around the mean mass for white dwarfs ($M \sim 0.6\ M_{\odot}$) composed mostly of DA stars, but also a significant fraction of non-DA stars including DC, DZ, and He-rich DA white dwarfs. Note that the normal masses obtained here for the DC stars can only be achieved with model atmospheres containing traces of hydrogen ($\log \mathrm{H/He} \sim -5$). The same conclusion applies to DZ white dwarfs, but in this case metals are the main source of free electrons. The DQ stars in the same temperature region also form a tight sequence, but with a mean mass $\sim$0.05 $M_{\odot}$ lower than average, consistent with the results obtained by Coutu et al. (2019b, see their Figure 13). There are at least two possible explanations for this lower mean mass, one involving problems with the physics of DQ model atmospheres (Coutu

et al., 2019b), and another one recently proposed by Bédard et al. (2022a), who suggested that carbon (and hence the DQ phenomenon) is preferentially detected in lower mass white dwarfs.

There are also two other regions where DA stars are concentrated. The first one is along the crystallization sequence at high mass. To illustrate this process, we indicated by the lower solid blue curve in Figure 4.15 the region where crystallization starts at the centre of the white dwarf, and by the upper solid blue curve the limit of 80% crystallization of the core resulting from the solidification front moving upward in the star with further cooling. When crystallization occurs, the release of latent heat and chemical fractionation decrease the cooling rate of a white dwarf, leading to this obvious pile up of objects in the M versus $T_{\rm eff}$ diagram observed in Figure 4.15. Note that the hot end of the crystallization sequence also contains several massive DQ, DC, and He-rich DA white dwarfs. Furthermore, we can clearly see the crystallization sequence merging with the normal-mass white dwarf sequence near $T_{\rm eff} \sim 5500$ K. Incidentally, this also coincides with the temperature where convective coupling occurs at $M \sim 0.6\ M_{\odot}$, that is, when the convection zone first reaches into the degenerate interior where all of the thermal energy of the star resides. This is illustrated by the dashed curve in Figure 4.15, which marks the effective temperature of the onset of convective coupling as a function of mass.

DA stars are also found in large numbers at very low masses ($M \lesssim 0.45\ M_{\odot}$). These are most likely unresolved DD binaries, and the low masses inferred here are simply the result of these objects being overluminous, as observed in Figure 4.1. For instance, we can calculate that two identical 0.6 $M_{\odot}$ unresolved DA white dwarfs would result in a $\sim$0.32 $M_{\odot}$ single object in this M versus $T_{\rm eff}$ diagram. But as discussed above, it is also possible that some of these low mass determinations are real if one component of the DD system completely dominates the overall luminosity. Not all low-mass white dwarfs are DA stars, however, and we can see several DQ and DC white dwarfs as well. Not surprisingly, the four DA + DQ unresolved binaries in our sample are found at such low masses. Actually, all four systems have inferred masses well below 0.3 $M_{\odot}$ (the DQ stars J0941+0901, J1135+5724, J1501+2100, and J1803+2320 also have masses below 0.3 $M_{\odot}$) ; if we assume that both the DA and DQ stars in these systems contribute equally to the luminosity, we can calculate the mass of the DQ components to be around 0.52 $M_{\odot}$, in excellent agreement with the bulk of single DQ white dwarfs in this temperature range. It is therefore possible that the remaining low-mass DQ white dwarfs in our sample are also DD systems composed of a DQ white dwarf and a featureless DC component. We come back to this point further below. Similarly, it is also possible that the low-mass DC white dwarfs above 6600 K are unresolved binaries, but composed of two normal-mass DC stars, a result that would be consistent with the absence of low-mass DB white dwarfs found in the spectroscopic analysis of Genest-Beaulieu & Bergeron (2019b).

We now turn our attention to the region below $T_{\rm eff} \sim 6000$ K, where the interpretation of our results becomes significantly more complicated. The most obvious feature in this temperature range is the trend of DA and DC white dwarfs towards lowers masses, reaching $M \sim 0.4\ M_{\odot}$ at the end of the cooling sequence. We remind the reader that we assumed pure H atmospheres for these DC stars. Had we used pure He or mixed H/He compositions, the situation would have been even worse (see Figure 4.11). We suggested that improved model atmospheres – most likely related to some inaccurate opacity source – could yield larger masses and higher effective temperatures for these cool DC white dwarfs, and cool DA stars as well, thus filling the apparent gap in the white dwarf distribution observed around $T_{\rm eff} \sim 5300$ K. Interestingly enough, we can also see that in the same temperature range, several DZ stars appear to follow the $\sim$0.6 $M_{\odot}$ sequence nicely, in contrast with the cool DA and DC white dwarfs. In such cool DZ stars, the presence of metals reduces the atmospheric pressure significantly, and thus the effect of collision-induced absorption by molecular hydrogen, if present. In fact, we found that traces of hydrogen have little effect on the measured stellar parameters in this temperature range. Also, we originally identified several low-mass DZ white dwarfs in this temperature range, but it turns out these were H-dominated rather than He-dominated DZ white dwarfs, as discussed in Section 4.3.5. Given these results, we also explored the possibility that the coolest DC stars in our sample have He-dominated atmospheres containing invisible traces of metals that could affect their temperature and mass determinations. However, the amount of metals required to affect the stellar parameters are large enough that the star would appear as a DZ white dwarf instead of a DC star, a conclusion previsouly reached by Blouin et al. (2018d). The fact that DZ white dwarfs behave normally at low temperatures again suggests that the low masses obtained for the cool DA and DC white dwarfs in our sample are most likely related to problems with the physics of pure-H model atmospheres.

Figure 4.15 includes 47 IR-faint white dwarfs, which all show strong collision-induced absorption by molecular hydrogen in the near-infrared, 43 of which are in common with the analysis of Bergeron et al. (2022b). Many of these appear to define the cool edge of our sample at all masses, and in particular in the upper right corner of the M versus $T_{\rm eff}$ diagram. The two DZ stars in the same region of the diagram are J1922+0233 and J2317+1830, also IR-faint white dwarfs (see Section 4.3.6). There is also one massive DC star overlapping this region, J1305+7022. Unfortunately, only Pan-STARRS *grizy* photometry is available, but our excellent fits with pure H or pure He models suggest that this is probably not an IR-faint white dwarf. As discussed at length in Bergeron et al. (2022b), the coolest and most massive IR-faint white dwarfs in Figure 4.15 are found in the Debye cooling phase, when the specific heat decreases quickly with cooling, thus rapidly depleting the reservoir of thermal energy and producing the extreme increase of the cooling rate observed in the upper right corner of Figure 4.15. To better illustrate this phenomenon, we indicated by a dotted curve the

so-called Debye cooling phase, i.e., the rapidly cooling phase resulting from the transition, in the solid phase, from the classical regime where the specific heat of a solid is independent of temperature, to the quantum regime where it goes down from that constant value with decreasing temperature. As described in Bergeron et al. (2022b), we define this transition from the classical to the quantum regime by isolating the evolving model where the central temperature becomes equal to 1/20 the central Debye temperature ($\theta_D/T = 20$), as defined in Althaus et al. (2007). Only a dozen or so objects in our sample have reached the Debye cooling phase. We also emphasize that the presence of cool, IR-faint white dwarfs in this particular cooling phase is the direct result of the improved model atmospheres described in Bergeron et al. (2022b), which led to higher $T_{\rm eff}$ and M values.

4.4.2. Low-Mass White Dwarfs

We now focus our attention towards the low-mass ($M < 0.45\ M_{\odot}$) white dwarfs in Figure 4.15, which include mostly DA stars, but also several DQ, DZ, and DC white dwarfs. We consider each of the non-DA spectral types in turn.

One of the DZ stars is J1824+1212, also an IR-faint white dwarf with an extremely low temperature of $T_{\rm eff} = 3381$ K (and $M = 0.346\ M_{\odot}$), where the physics of our model atmospheres is most uncertain. The other DZ star is J0045+1420, a problematic object in our sample, probably magnetic, with an energy distribution that is not well reproduced by our models. The low masses inferred for these two DZ white dwarfs are thus uncertain.

Among the low-mass DQ white dwarfs, we already discussed in Section 4.3.4 the four DA + DQ unresolved binaries in our sample. To go further, we show in Figure 4.16 the carbon abundance as a function of effective temperature for all DQ white dwarfs in our sample, with these four binaries displayed in blue (all of these have $M < 0.3\ M_{\odot}$), while the remaining DQs with $M < 0.45\ M_{\odot}$ are shown in red. Three of these binaries have C abundances near the bottom of the envelope defining the DQ sequence, as expected if there is a companion that dilutes the strength of the carbon Swan bands, resulting in C abundances being underestimated (the other DA + DQ system above the sequence is J0613+2050, an extreme case of contamination by a DA component). We note that other low-mass DQ stars in our sample have carbon abundances near the bottom of the envelope (red symbols in Figure 4.16), suggesting that these may also be unresolved double degenerates, but this time composed of a DQ white dwarf and a featureless DC component. The only exception is J1501+2100 ($M = 0.248\ M_{\odot}$), with a large carbon abundance above the sequence. Perhaps in this case there is indeed a low-mass DQ white dwarf in the system, dominating the luminosity, with a C abundance higher than average, which is expected in low-mass DQ white dwarfs, as discussed in Bédard et al. (2022a). Given these results, we inspected closely our fits to all low-mass DC white dwarfs and discovered that J0822+2023 ($M = 0.349\ M_{\odot}$)

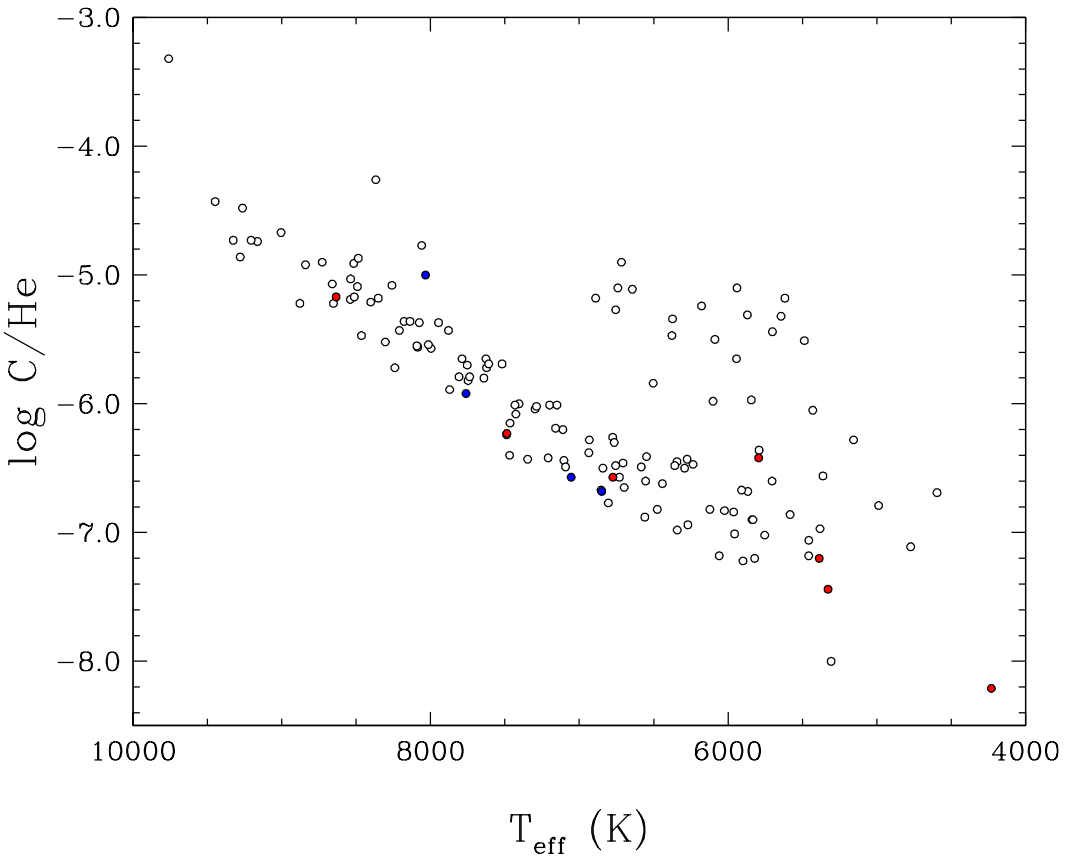

FIGURE 4.16 Carbon abundance as a function of effective temperature for all DQ white dwarfs in our sample. Coloured symbols all have $M < 0.45\ M_{\odot}$, with the blue dots representing the four unresolved DA + DQ double degenerate systems.

shows a weak absorption band near 5150 Å, indicating that this is probably an unresolved DQ + DC system as well.

With little evidence for low-mass single DQ white dwarfs, we examined the remaining low-mass ($M < 0.45\ M_{\odot}$) DC stars in our sample, but this time by restricting our inspection to $T_{\rm eff} > 5500$ K where the photometric analysis is less problematic. We find only 11 DC stars, three of which have no spectra available to us, and the spectral classification is thus difficult to confirm. A few of the remaining DCs have M–dwarf companions with bad photometric fits (see, e.g., J0200+1222 with $M = 0.217\ M_{\odot}$), while in some cases, we can even detect a hint of Hα (see J1325+4523), although the spectrum is rather noisy. Similarly, J1047+0007 ($M = 0.245\ M_{\odot}$) appears to show Zeeman splitting at Hα and could be magnetic. Hence, although we cannot completely rule out the existence of low-mass He-atmosphere white dwarfs in our sample, evidence suggests that most, if not all low-mass objects in our sample have hydrogen atmospheres. This result agrees with the conclusions of Genest-Beaulieu & Bergeron (2019b) who showed that there is no evidence for low-mass single DB white dwarfs, as determined

from spectroscopy ; several DB + DB systems have been identified by photometry, however, but these are probably composed of normal mass DB white dwarfs.

4.4.3. The Evolution of DA White Dwarfs

According to the analysis of Bédard et al. (2020), about 75% of all white dwarfs retain thick H layers and remain DA stars throughout their evolution. Hence a significant fraction of the DA white dwarfs in Figure 4.15 should remain DA stars in the temperature range displayed here, and eventually evolve into H-atmosphere DC stars at low temperatures when Hα disappears. We can see that the coolest DA stars indeed merge with the cool DC sequence near $T_{\rm eff} \sim 5000$ K, giving support to the idea that most cool DC stars in our sample have H-dominated atmospheres. Note also that in the temperature range considered in our analysis, it is possible for some of the DA stars to turn into He-rich DA or DC white dwarfs as a result of convective mixing. We come back to this point below.

What is particularly noteworthy in Figure 4.15 is the evolution of the crystallization sequence as a function of mass and $T_{\rm eff}$. The mass distribution of DA white dwarfs displayed in Figure 13 of Kilic et al. (2020b), based on spectroscopically confirmed DA stars hotter than 6000 K in the 100 pc sample and the SDSS footprint, shows a very strong peak at $\sim$0.6 $M_{\odot}$, and a smaller but very broad shoulder centred at $\sim$0.8 $M_{\odot}$ (see also Section 4.4.5 below). However, the results displayed in Figure 4.15 indicate that at $T_{\rm eff} \sim 9000$ K, say, nearly half of the DA stars lie within the crystallization boundaries near 1.0 $M_{\odot}$. As we go down in temperature, crystallization occurs at lower masses, until the crystallization sequence merges with the normal mass DA white dwarfs around 5500 K or so. Consequently, when the cumulative mass distribution is considered (N versus M), the normal mass white dwarfs accumulate in the mean peak, while the crystallized DA stars are smeared out over this broad shoulder.

With the exception of a few objects, most white dwarfs above 0.9 $M_{\odot}$ are DA stars, down to $T_{\rm eff} \sim 5500$ K, below which they seem to evolve into He-rich IR-faint white dwarfs. The obvious mechanism responsible for this transformation is convective mixing. However, as discussed at length in Bergeron et al. (2022b), the small H/He abundance ratios measured in these IR-faint white dwarfs ($\log {\rm H/He} = -4$ to -3) imply that the total amount of hydrogen in these stars is extremely small, such that mixing should have occurred at higher temperatures ($T_{\rm eff} \sim 9000$ K). Consequently, their immediate progenitors should be massive DC white dwarfs instead of DA stars. Two possible explanations are that the H abundance measured in these IR-faint white dwarfs is erroneous, or our understanding of convective mixing needs to be revised.

4.4.4. Magnetic White Dwarfs

Before discussing the evolution of He-atmosphere white dwarfs, it is worth investigating the magnetic objects in our sample and the role played by magnetism in the spectral evolution of these stars. Around 5% of the white dwarfs in our sample show signs of magnetism, whether it is through Zeeman splitting or polarization measurements. It is also detected in all spectral types (DA, DZ, DQ, DC) ; in the case of DQ white dwarfs, the strong C_2 Swan bands appear to be strongly shifted towards shorter wavelength. Various scenarios have been invoked to explain the origin of magnetic fields in white dwarfs (see the review by Ferrario et al. 2015), including a fossil origin, whether it was present in the forming stellar cloud or generated by a dynamo effect in rotating cores in the main sequence progenitor (Angel et al., 1981; Tout et al., 2004; Wickramasinghe & Ferrario, 2005; Ferrario et al., 2015). There is also strong evidence that binary evolution is responsible for producing magnetic fields in some white dwarfs (see, e.g., Tout et al. 2008; García-Berro et al. 2012). More recently, is has also been proposed that the onset of core crystallization in cooling white dwarfs might produce magnetic fields through a dynamo process triggered by the onset of convection in the liquid core due to phase separation (Isern et al., 2017; Schreiber et al., 2021; Ginzburg et al., 2022). It thus appears that several mechanisms for producing magnetic fields might be at play here, which probably vary as a function of mass and cooling age (see Figure 2 of Bagnulo & Landstreet 2022), or equivalently, as a function of decreasing effective temperature.

We show in Figure 4.17 the same M versus $T_{\rm eff}$ diagram as in Figure 4.15 but this time by highlighting with red symbols the magnetic white dwarfs in our sample. Our results conclusively demonstrate that the presence of a magnetic field in most, if not all white dwarfs in our sample is strongly correlated with the phenomenon of core crystallization, as showed by the two blue solid curves, where the lower curve indicates the onset of crystallization at the centre of evolving models, while the upper one indicates the locations where 80% of the total mass has solidified. Note that the number of magnetic white dwarfs at low temperatures is most likely underestimated given the difficulty of detecting Zeeman splitting in weak Hα absorption features. The situation is even worse in the case of DC stars, which would require spectropolarimetric measurements (e.g., Putney, 1997; Bagnulo & Landstreet, 2021; Berdyugin et al., 2022).

It has long been suggested that convective energy transport in cool white dwarfs ($T_{\rm eff} \lesssim$ 10,000 K) could be seriously impeded by the presence of a strong magnetic field. Tremblay et al. (2015) reexamined this problem using radiation magnetohydrodynamic simulations and indeed showed that magnetic fields of only tens of kG could significantly reduce the importance of convection to the point that the atmospheres become radiative. Model atmosphere analysis of magnetic white dwarfs can in principle be used to validate this finding by testing whether consistent fits can be obtained with non-convective atmospheres,

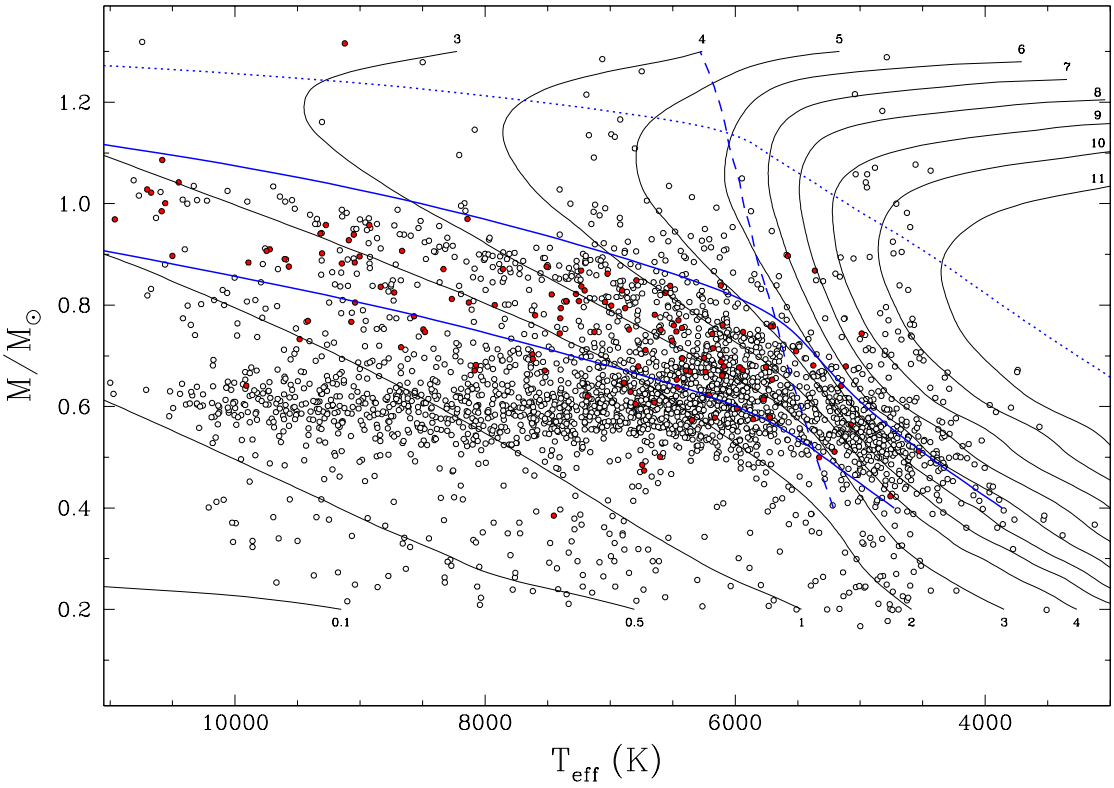

FIGURE 4.17 Same as Figure 4.15 but with magnetic white dwarfs shown as red dots (non-magnetic white dwarfs are shown with lighter circles to emphasize the magnetic objects).

but conflicting results have been reported (Lecavalier-Hurtubise & Bergeron, 2017; Gentile Fusillo et al., 2018). In any case, magnetic fields can plausibly inhibit (at least partially) convective transport and this may be the key physical mechanism responsible for turning He-atmosphere white dwarfs into H-atmosphere white dwarfs at low temperatures, a question we investigate in the next subsection.

4.4.5. The Evolution of He-atmosphere White Dwarfs

We first reexamine the M versus $T_{\rm eff}$ diagram displayed in Figure 4.15, but this time, instead of differentiating the white dwarfs in terms of their spectral type, we separate them in terms of their main atmospheric constituent, H or He. The results are displayed in Figure 4.18. Also indicated by small dots in this figure are the 5358 white dwarf candidates (i.e. without spectral classification) found in the MWDD, and analysed under the assumption of a pure H composition for all objects. We remind the reader that there are only 2880 spectroscopically confirmed white dwarfs in our 100 pc sample, hence less than 35% of the total sample.

He-atmosphere white dwarfs in our sample may have different origins. First, their immediate progenitors could be DB stars. In this case, it has been shown that as they cool off,

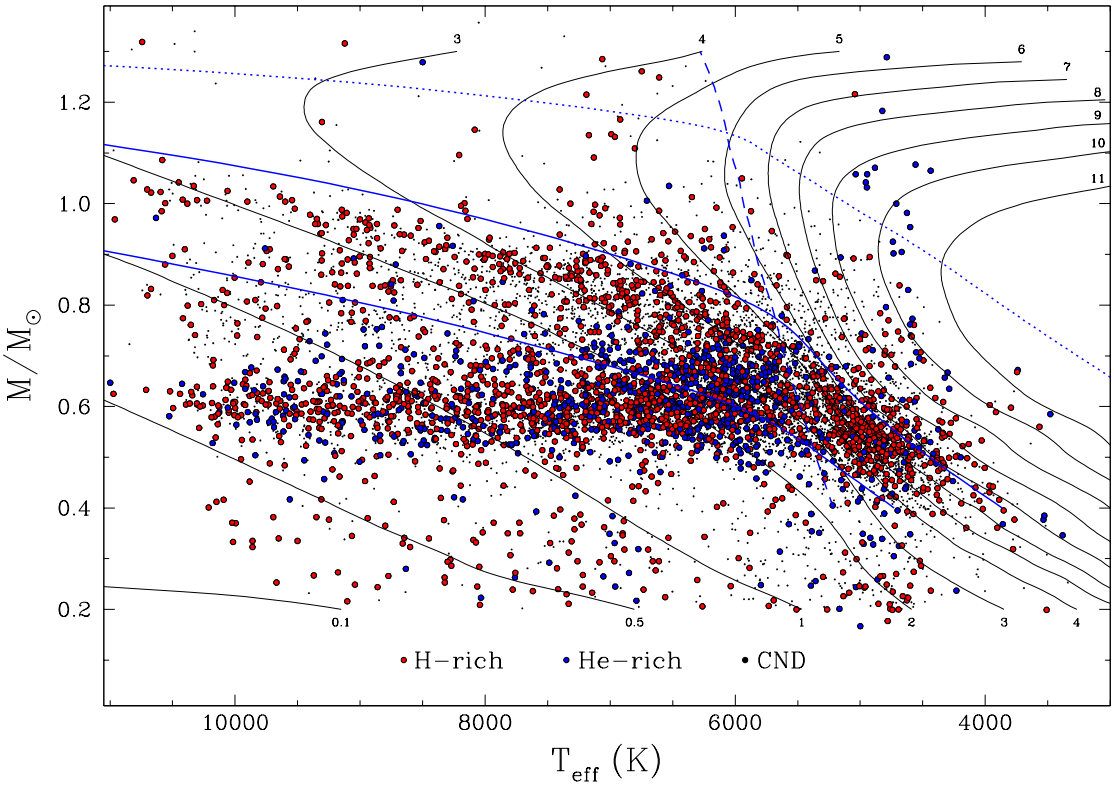

FIGURE 4.18 Same as Figure 4.15 with the exception that the objects are divided into H-atmosphere and He-atmosphere white dwarfs, as indicated in the legend. Also shown as small dots are the 5358 white dwarf candidates (without spectral classification) analysed under the assumption of a pure H composition.

the bottom of the He convection zone can reach deep into the interior where resides a massive hydrogen reservoir, resulting into traces of H being brought up to the surface, and thus producing a DBA star (Rolland et al. 2020, Bédard et al. 2022, submitted to ApJ). In some cases, however, there may be not enough hydrogen in the deep interior that the DB white dwarf retains a H-free atmosphere throughout its evolution. This particular channel is believed to be responsible for the origin of most DQ white dwarfs, while DQ stars with traces of hydrogen, such as those analysed in our study, are probably the result of convectively mixed DA stars below $T_{\rm eff} \sim$ 12,000 K (Bédard et al., 2022a). Convective mixing has also been invoked to account for the existence of the He-rich DA stars in our sample, as well as those reported in Rolland et al. (2018b). Similarly, He-atmosphere DZ and DZA white dwarfs may descend from DB stars, or from convectively mixed DA stars. Finally, as discussed in Section 4.3.7.2, featureless DC white dwarfs must contain some traces of hydrogen, otherwise their masses inferred from photometry are too large ; if they are devoid of hydrogen because of their prior evolution, it is believed they will become DQ white dwarfs instead. Thus, with the exception of some DQ stars, we expect the vast majoriy of cool, He-atmosphere white

dwarfs to contain residual amounts of hydrogen in their atmosphere and stellar envelope. This is obviously the case for IR-faint white dwarfs as well.

Going back to the results displayed in Figure 4.18, we must remember that a pure H composition was assumed for all DC stars below $T_{\rm eff} = 5200$ K. It is thus not a firm determination, but by far the most reasonable assumption given the results of our analysis. Indeed, as discussed in Section 4.2.3, such a sudden decrease of He-atmosphere white dwarfs in this temperature range is entirely consistent with the abrupt termination of the more luminous sequence of DC stars observed in the colour-magnitude diagram displayed in Figure 4.1. Given the location of this transition exactly in the range of mass and temperature where crystallization occurs, and given the correlation between the occurrence of magnetism and crystallization discussed in Section 4.4.4, it is tantalizing to suggest that the mechanism responsible for transforming most, but not all, He-atmosphere white dwarfs into H-atmosphere white dwarfs is the following sequence of events : First, crystallization occurs in the stellar core and the crystallization front moves outward as the white dwarf cools off. This process eventually creates a magnetic field through the dynamo mechanism described in Isern et al. (2017). Then, the presence of the magnetic field suppresses completely, or even partially, convective transport, allowing the hydrogen thoroughly diluted within the mixed H/He convective envelope to diffuse upward, gradually building a thick H layer sitting on top of a deeper He-rich envelope. While detailed evolutionary calculations are required to explore this suggestion more quantitatively, this is certainly the most promising explanation for the transition from He-atmosphere to H-atmosphere white dwarfs that occurs below $T_{\rm eff} = 5200$ K in Figure 4.18. Within this scenario, the few remaining cool ($T_{\rm eff} \lesssim 5000$ K) He-atmosphere white dwarfs identified in our survey, most of which are DZ stars, could be interpreted as objects with not enough hydrogen, or no hydrogen at all.

We now consider the peak of the mass distribution at $\sim$0.6 $M_{\odot}$ in Figure 4.18, but above $T_{\rm eff} = 6000$ K where we can easily identify DA stars. In Figure 4.15, we already noticed that both the DQ and DZ white dwarfs had very narrow mass distributions, but that the DQ sequence had a lower mean mass than the DZ counterpart, while the DC stars appear to share the same mass distribution as DZ white dwarfs. But if we now compare the mass distributions of H-atmosphere and He-atmosphere white dwarfs in the same temperature range, displayed in Figure 4.18, we notice that they are remarkably similar. We can explore this more quantitatively by looking at the cumulative mass distributions, N versus M, displayed in Figure 4.19, where we compare the mass distribution for the H-atmosphere DA stars above 6000 K with that for the He-atmosphere non-DA stars. For the latter, we also show the individual contributions from DC, DQ, and DZ white dwarfs. With the exception of the very broad shoulder observed for DA stars centred near $\sim$0.8 $M_{\odot}$ and already discussed in Section 4.4.3, we notice that the mass distributions of H- and He-atmosphere white dwarfs are indeed remarkably similar, although there are obviously more DA stars in the

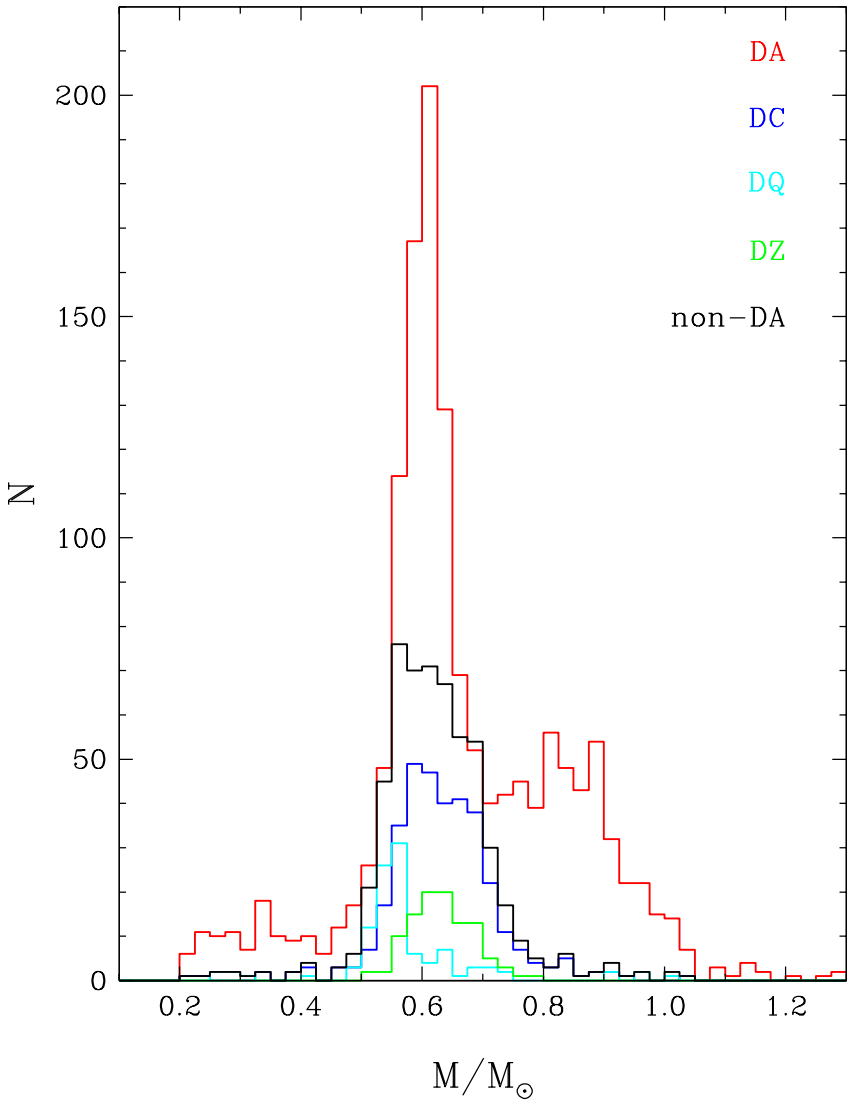

FIGURE 4.19 Mass distributions of all white dwarfs above $T_{\rm eff} = 6000$ K split into different spectral types, as indicated in the legend. The black histogram represents the sum of all non-DA types (DC, DQ, DZ).

central peak at 0.6 $M_\odot$, probably originating from the evolutionary channel consisting of white dwarfs retaining thick H layers throughout their cooling history (∼75% of the entire white dwarf population according to Bédard et al. 2020).

Given the results shown in Figure 4.19, is it possible that the non-DA stars form a more homogeneous population than previously believed ? First, as discussed in Bédard et al. (2022a), carbon can be more easily detected in lower mass DQ white dwarfs since the deep carbon diffusion tail sinks less rapidly in objects with lower surface gravity. Second, Blouin (2022) demonstrated that the simultaneous presence of metals at the photosphere of DQ white dwarfs can change the atmospheric structure significantly, to the point that carbon

features vanish, thus explaining the paucity of DQZ white dwarfs. This could partially explain the near absence of an overlap between the mass distributions of DQ and DZ white dwarfs, as observed in both Figures 4.15 and 4.19. Finally, given that DC and DZ white dwarfs probably differ only by the presence of surrounding material being accreted, it is then possible that a significant fraction of DC stars also result from the evolution of this so-called PG 1159–DO–DB–DQ scenario (see Bédard et al. 2022a and references therein), and that only a small fraction of non-DA stars above 6000 K originate from convectively mixed DA white dwarfs.

Although our sample is not statistically complete in any sense, we can still test this last hypothesis by looking at the variation of the fraction of He-atmosphere white dwarfs as a function of $T_{\rm eff}$, the results of which are displayed in Figure 4.20. Surprisingly, despite the ill-defined statistical properties of our sample, our results are entirely consistent with those displayed in Figure 8 of McCleery et al. (2020), which are based on the volume-limited 40 pc sample in the northern hemisphere. First, we can see that above $T_{\rm eff} \sim 6500$ K, the fraction of He-atmosphere white dwarfs remains nearly constant around 25%, which suggests that there is little evidence for convective mixing of DA white dwarfs into non-DA stars, at least not in the range of $T_{\rm eff}$ considered in our analysis. The situation changes drastically at lower temperatures, however, where the fraction increases to ∼45% around 6500 K, and gradually decreases to 15% around 4000 K. We have to be careful, however, not to overinterpret our results at very low $T_{\rm eff}$ values because this is the range of temperature where our spectrophotometric analysis is most uncertain, and also because this is where the fraction of white dwarf candidates (i.e., not spectroscopically confirmed) is the largest. Indeed, from the results displayed in Figure 4.18, we estimate that above 6000 K, 40% of our total sample of objects are spectroscopically confirmed white dwarfs, while this fraction drops to ∼25% below this temperature.

We thus conclude from the above discussion that convective mixing occurs in DA white dwarfs, but mostly at low effective temperature. In turn, this implies that most DA stars in the temperature range considered in our analysis have thick hydrogen layers around $\log q({\rm H}) \sim -7.5$ (at $M = 0.6\ M_{\odot}$) according to the results displayed in Figure 19 of Bergeron et al. (2022b), which explores the expected variation of the H/He ratio as a function of $T_{\rm eff}$ for DA models with various hydrogen layer masses.

4.5. Conclusions

We selected 8238 white dwarfs and white dwarf candidates from the MWDD within 100 pc from the Sun and below $T_{\rm eff} \sim 10{,}000$K, 2880 of which were spectroscopically confirmed degenerates (35% of the sample). Optical and infrared photometry as well as spectroscopic observations, when available, were combined to measure the stellar parameters for each

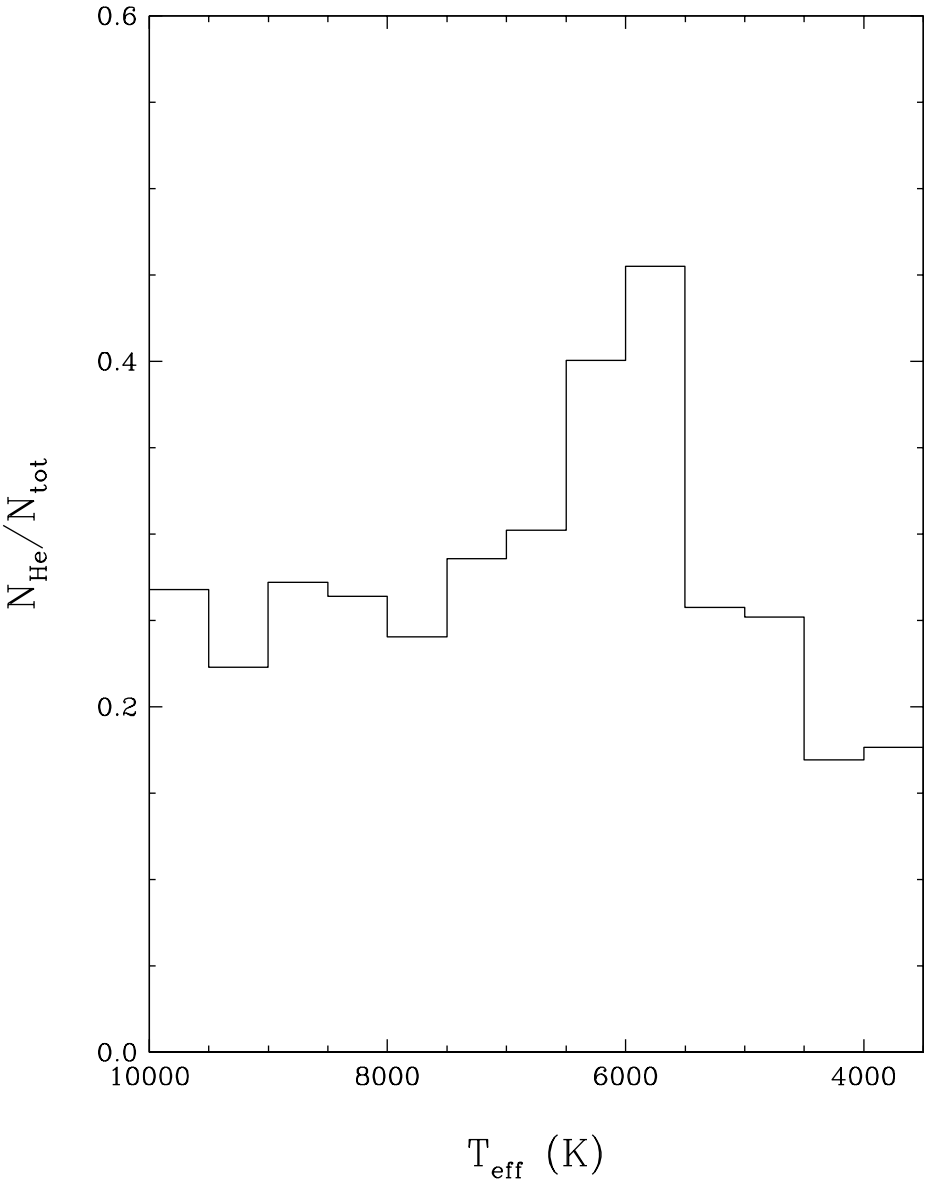

FIGURE 4.20 Ratio of He-atmosphere white dwarfs to the total number of stars as a function of effective temperature.

individual white dwarf in our sample using state-of-the-art model atmospheres appropriate for each spectral type. We can draw the following conclusions from our analysis :

1. There is now strong evidence that most, but probably not all, cool DC white dwarfs have H atmospheres. This conclusion is supported not only by the location of these objects in colour-magnitude diagrams, but also from our detailed photometric analysis. Effective temperature and stellar masses inferred from He-atmosphere models are unrealistically too low. However, our analysis has also revealed problems with the pure H model atmospheres, both in color-magnitude diagrams and photometric fits, which we attributed to inaccuracies

in the calculations of opacity sources, whether it is the red wing of Lα, the H^- bound-free opacity, or the CIA opacity from molecular hydrogen.

2. There is a more luminous observed sequence of DC white dwarfs in colour-magnitude diagrams that terminates around $T_{\rm eff} \sim 5200$ K. Our detailed photometric analysis suggests that below this temperature, He-atmosphere white dwarfs turn into H-atmosphere white dwarfs. The mechanism by which this transformation occurs appears to be related to the onset of crystallization and to the occurrence of magnetism being generated as a result of this process. The presence of a magnetic field would lead to a suppression, even partially, of convective transport, allowing hydrogen, thoroughly diluted within the deep stellar envelope, to float back to the surface.

3. Some DQ white dwarfs show traces of hydrogen in the form of an Hα absorption feature. In some cases, these are obviously unresolved DA + DQ binaries (due in part to their overluminosity), but other objects are genuine DQA stars, most likely originating from convectively mixed DA stars. We believe that we may also have identified a population of cool DQ white dwarfs in which the presence of hydrogen manifests itself as collision-induced absorption by molecular hydrogen in the near-infrared, although a more detailed analysis using model atmospheres including H, He, and C is required to confirm this interpretation.

4. We identified several unresolved double degenerate binaries in our sample, all of which have been analyzed under the assumption of a single object. These systems deserve further study to deconvolve the stellar parameters of the individual components, following the approach described in Bédard et al. (2017).

5. Our analysis reveals that most low-mass white dwarfs probably have H atmospheres, which would in turn indicate that common-envelope evolution most likely produces white dwarf remnants that retain thick H layers.

6. The mass distributions of DQ, DZ, and DC white dwarfs suggest that these may form a more homogeneous population than previously believed, with the DQ stars representing the low-mass component of the non-DA white dwarfs, in which carbon features can be more easily detected. Carbon features would be more difficult to detect in DZ and DC white dwarfs due to their higher mass and/or larger metal content. If this is indeed the case, it is possible that a larger fraction of non-DA white dwarfs below $T_{\rm eff} = 10{,}000$ K evolve from the so-called PG 1159–DO–DB–DQ scenario.

7. We found little evidence in our sample for the transformation of a large fraction of DA stars into He-atmosphere white dwarfs through the process of convective mixing between $T_{\rm eff} = 10{,}000$ K and $\sim$6500 K. The He-rich DA stars are the obvious exception, but there are very few of those in our sample (or even in the entire SDSS white dwarf sample for that matter, see Rolland et al. 2018b).

8. We do, however, find evidence for convective mixing below $T_{\rm eff} \sim 6500$ K, where the fraction of He-atmosphere white dwarfs increases to $\sim$45%, which suggests that most DA

stars in the temperature range considered in our analysis have thick hydrogen layers around $\log q(\mathrm{H}) \sim -7.5$.

9. Finally, there is an obvious need for more near-infrared photometry, with better accuracy and precision, required for the analysis of cool ($T_{\rm eff} < 6000$ K) white dwarfs, in particular for the determination of the chemical composition, and in some cases even the main atmospheric constituent.

Our understanding of the spectral evolution of cool white dwarfs is like a giant puzzle, where individual pieces are added one by one in order to build a better picture, as better observational data and theoretical models become available over the years. We feel we have added a few pieces of that puzzle in our analysis, but the overall picture remains incomplete. Even though we are convinced that progess can only be accomplished through tailored analyses of individual objects in a given sample, we felt we have reached the limit of human capacity to analyse individually each object in such a large sample of nearly 3000 white dwarfs. Better techniques for handling bigger data sets involving machine learning algorithms will eventually become necessary.

Acknowledgements

We are grateful to A. Bédard for enlightening discussions. This work was supported in part by NSERC Canada and by the Fund FRQ-NT (Québec). SB is a Banting Postdoctoral Fellow and a CITA National Fellow, supported by NSERC.

Funding for the Sloan Digital Sky Survey (`https://www.sdss.org`) has been provided by the Alfred P. Sloan Foundation, the U.S. Department of Energy Office of Science, and the Participating Institutions. SDSS-IV acknowledges support and resources from the Center for High-Performance Computing at the University of Utah, and is managed by the Astrophysical Research Consortium for the Participating Institutions of the SDSS Collaboration (Blanton et al., 2017).

This work has made use of data from the European Space Agency mission *Gaia* (`https://www.cosmos.esa.int/gaia`), processed by the *Gaia* Data Processing and Analysis Consortium (DPAC). Funding for the DPAC has been provided by national institutions, in particular the institutions participating in the *Gaia* Multilateral Agreement (Gaia Collaboration et al., 2018c).

This research has also made use of the NASA Astrophysics Data System Bibliographic Services ; the Montreal White Dwarf Database (Dufour et al., 2017b) ; the SIMBAD database, operated at the Centre de Données astronomiques de Strasbourg (Wenger et al., 2000) ; and the NASA/IPAC Infrared Science Archive, operated at the California Institute of Technology.

Data Availability

The astrometric, photometric and spectroscopic data underlying this article are available in the MWDD at http ://www.montrealwhitedwarfdatabase.org. The astrometric and photometric data are also available as online supplementary material.

Chapitre 5

Conclusion

Dans ce mémoire, nous avons construit un échantillon de 8238 naines blanches froides à l'intérieur de 100 pc du Soleil incluant 2880 avec un type spectral connu et 5358 candidates. L'échantillon rassemble des mesures de parallaxe Gaia DR2/EDR3 et de photométrie Pan-STARRS $grizy$ pour toutes les étoiles ainsi que de la photométrie SDSS u et infrarouge JHK si disponibles. Les données d'observation ainsi que l'ensemble des données spectroscopiques disponibles dans le MWDD ont été utilisées afin de déterminer les paramètres physiques des naines blanches connues de l'échantillon à l'aide de la méthode spectro-photométrique. Les différentes variations de cette méthode ainsi que des exemples de solutions typiques d'objets sont présentées pour chaque type de naine blanche présent dans l'échantillon, soit DA, DC, DQ, DZ, les DA riches en hélium et les IR-faint. Les difficultés rencontrées lors de la détermination des paramètres ainsi que les solutions permettant de surmonter ces problèmes sont discutées.

Un article scientifique résultant de ces travaux constitue l'essentiel de ce mémoire où l'analyse des résultats est discutée en détail. La validité des différents ensembles de données a d'abord été testée. Des diagrammes couleur-magnitude ont été générés avec la photométrie Pan-STARRS et SDSS incluant des séquences de couleurs théoriques correspondant à différentes compositions atmosphériques. Ces séquences ont indiqué que la majorité, si ce n'est la totalité, des étoiles DC froides ont une atmosphère dominée par l'hydrogène. De plus, l'analyse photométrique des étoiles DC froides permet de renforcer cette conclusion. Cependant, les analyses ont aussi révélé qu'il existe un problème avec la micro-physique des modèles purs en hydrogène à hautes densités et à basses températures, car ceux-ci ne parviennent pas à reproduire les couleurs observées des DC dans ce régime. Une explication possible serait l'opacité dans le bleu provenant de l'aile rouge de Lyα.

Différents graphiques de la masse en fonction de la température effective des étoiles de l'échantillon ont révélé certaines informations importantes. D'abord, les populations d'étoiles

DC, DQ et DZ semblent former un groupe beaucoup plus homogène que l'on croyait précédemment, avec les DQ ayant une masse moyenne plus faible que les DC et DZ. Ensuite, les naines blanches magnétiques sont majoritairement situées dans la zone de cristallisation, suggérant que ces deux mécanismes sont reliés. Ceci renforce l'hypothèse selon laquelle la présence d'un champ magnétique inhibe la convection dans les couches externes des naines blanches froides, permettant ainsi à l'hydrogène, dilué dans l'enveloppe dominée par l'hélium, de remonter vers la surface. Enfin, la distribution des étoiles selon leur constituant atmosphérique principal, H ou He, ne semble pas indiquer que le mélange convectif entre $T_{\rm eff}$ = 10,000 K et $T_{\rm eff}$ = 6500 K transforme une fraction significative de DA en non-DA. Par contre, entre $T_{\rm eff}$ = 6500 K et $T_{\rm eff}$ = 5500 K, la fraction de naines blanches avec une atmosphère riche en hélium atteint $\sim$45%, ce qui indique que dans ce régime de température, le mélange convectif transforme les atmosphères d'une fraction importante d'étoiles DA.

Des étoiles DQA ont également été analysées, ainsi qu'une possible population d'étoiles DQ froides montrant du CIA. Cette dernière nécessite toutefois des modèles d'atmosphère plus froids contenant à la fois du carbone et de l'hydrogène afin de les modéliser correctement. Enfin, l'exécution de ce travail a permis de constater que l'analyse d'un échantillon d'aussi grande taille ($\sim$3000 objets) est à la limite de ce qui est possible d'accomplir avec les méthodes d'analyse standards. L'échantillon de ce projet contient aussi une multitude d'objets exotiques qui requièrent une analyse plus approfondie. De plus, il existe probablement d'autres trésors cachés dans les étoiles candidates. Ce projet est donc un pas vers l'avant pour explorer les résultats possibles. Lorsque des spectres et de la photométrie infrarouge seront disponibles pour les candidates, il deviendra possible de les analyser aussi méticuleusement. Cependant, une technique faisant l'usage de l'intelligence artificielle est en cours de développement. Ceci serait un avantage afin de traiter la majorité des étoiles qui sont des cas triviaux et permettrait de passer plus de temps sur les cas spéciaux.

Bibliographie

1997, ESA Special Publication, Vol. 1200, The HIPPARCOS and TYCHO catalogues. Astrometric and photometric star catalogues derived from the ESA HIPPARCOS Space Astrometry Mission

Abazajian, K. N., Adelman-McCarthy, J. K., Agüeros, M. A., et al. 2009, ApJS, 182, 543

Abdurro'uf, Accetta, K., Aerts, C., et al. 2021, arXiv e-prints, arXiv :2112.02026

Ahumada, R., Prieto, C. A., Almeida, A., et al. 2020, ApJS, 249, 3

Akaike, H. 1974, IEEE Transactions on Automatic Control, 19, 716

Alam, S., Albareti, F. D., Allende Prieto, C., et al. 2015, ApJS, 219, 12

Allard, N. F., & Kielkopf, J. F. 2009, A&A, 493, 1155

Allard, N. F., Royer, A., Kielkopf, J. F., & Feautrier, N. 1999, Phys. Rev. A, 60, 1021

Althaus, L. G., García-Berro, E., Isern, J., Córsico, A. H., & Rohrmann, R. D. 2007, A&A, 465, 249

Anderson, D. R., & Burnham, K. P. 2002, The Journal of Wildlife Management, 66, 912. http://www.jstor.org/stable/3803155

Angel, J. R. P., Borra, E. F., & Landstreet, J. D. 1981, ApJS, 45, 457

Bagnulo, S., & Landstreet, J. D. 2021, MNRAS, 507, 5902

—. 2022, ApJ, 935, L12

Bédard, A., Bergeron, P., & Brassard, P. 2022a, ApJ, 930, 8

Bédard, A., Bergeron, P., Brassard, P., & Fontaine, G. 2020, ApJ, 901, 93

Bédard, A., Bergeron, P., & Fontaine, G. 2017, ApJ, 848, 11

Bédard, A., Brassard, P., Bergeron, P., & Blouin, S. 2021, arXiv e-prints, arXiv :2112.09989

—. 2022b, ApJ, 927, 128

Berdyugin, A. V., Piirola, V., Bagnulo, S., Landstreet, J. D., & Berdyugina, S. V. 2022, A&A, 657, A105

Bergeron, P., Dufour, P., Fontaine, G., et al. 2019a, ApJ, 876, 67

—. 2019b, ApJ, 876, 67

Bergeron, P., Kilic, M., Blouin, S., et al. 2022a, arXiv e-prints, arXiv :2206.03174

—. 2022b, arXiv e-prints, arXiv :2206.03174

Bergeron, P., Leggett, S. K., & Ruiz, M. T. 2001a, ApJS, 133, 413

—. 2001b, ApJS, 133, 413
Bergeron, P., Ruiz, M. T., & Leggett, S. K. 1997a, ApJS, 108, 339
—. 1997b, ApJS, 108, 339
Bergeron, P., Ruiz, M.-T., Leggett, S. K., Saumon, D., & Wesemael, F. 1994, ApJ, 423, 456
Bergeron, P., Saffer, R. A., & Liebert, J. 1992, ApJ, 394, 228
Bergeron, P., Wesemael, F., Liebert, J., & Fontaine, G. 1989, ApJ, 345, L91
Blanton, M. R., Bershady, M. A., Abolfathi, B., et al. 2017, AJ, 154, 28
Blouin, S. 2022, A&A, 666, L7
Blouin, S., & Dufour, P. 2019, MNRAS, 490, 4166
Blouin, S., Dufour, P., & Allard, N. F. 2018a, ApJ, 863, 184
—. 2018b, ApJ, 863, 184
Blouin, S., Dufour, P., Allard, N. F., & Kilic, M. 2018c, ApJ, 867, 161
—. 2018d, ApJ, 867, 161
Blouin, S., Dufour, P., Allard, N. F., et al. 2019a, ApJ, 872, 188
Blouin, S., Dufour, P., Thibeault, C., & Allard, N. F. 2019b, ApJ, 878, 63
—. 2019c, ApJ, 878, 63
Blouin, S., Kowalski, P. M., & Dufour, P. 2017, ApJ, 848, 36
Blouin, S., & Xu, S. 2022, MNRAS, 510, 1059
Casewell, S. L., Debes, J., Braker, I. P., et al. 2020, MNRAS, 499, 5318
Chambers, K. C., Magnier, E. A., Metcalfe, N., et al. 2016a, arXiv e-prints, arXiv :1612.05560
—. 2016b, arXiv e-prints, arXiv :1612.05560
Coutu, S., Dufour, P., Bergeron, P., et al. 2019a, ApJ, 885, 74
—. 2019b, ApJ, 885, 74
Dalton, G. B., Caldwell, M., Ward, A. K., et al. 2006, in Society of Photo-Optical Instrumentation Engineers (SPIE) Conference Series, Vol. 6269, Society of Photo-Optical Instrumentation Engineers (SPIE) Conference Series, ed. I. S. McLean & M. Iye, 62690X
Doi, M., Tanaka, M., Fukugita, M., et al. 2010, AJ, 139, 1628
Dufour, P., Bergeron, P., & Fontaine, G. 2005a, ApJ, 627, 404
—. 2005b, ApJ, 627, 404
Dufour, P., Blouin, S., Coutu, S., et al. 2017a, 509, 3
Dufour, P., Blouin, S., Coutu, S., et al. 2017b, in Astronomical Society of the Pacific Conference Series, Vol. 509, 20th European White Dwarf Workshop, ed. P. E. Tremblay, B. Gaensicke, & T. Marsh, 3
Dufour, P., Bergeron, P., Liebert, J., et al. 2007a, ApJ, 663, 1291
—. 2007b, ApJ, 663, 1291
Eisenstein, D. J., Liebert, J., Harris, H. C., et al. 2006, ApJS, 167, 40
Emerson, J., McPherson, A., & Sutherland, W. 2006, The Messenger, 126, 41
Evans, D. W., Riello, M., De Angeli, F., et al. 2018, A&A, 616, A4

Ferrario, L., Melatos, A., & Zrake, J. 2015, Space Sci. Rev., 191, 77
Flewelling, H. A., Magnier, E. A., Chambers, K. C., et al. 2020, ApJS, 251, 7
Fontaine, G., Brassard, P., & Bergeron, P. 2001, PASP, 113, 409
Gaia Collaboration, Babusiaux, C., & van Leeuwen, F. e. a. 2018a, A&A, 616, A10
Gaia Collaboration, Prusti, T., de Bruijne, J. H. J., et al. 2016a, A&A, 595, A1
Gaia Collaboration, Brown, A. G. A., Vallenari, A., et al. 2016b, A&A, 595, A2
—. 2018b, A&A, 616, A1
—. 2018c, A&A, 616, A1
Gaia Collaboration, Vallenari, A., Brown, A. G. A., et al. 2022, arXiv e-prints, arXiv :2208.00211
García-Berro, E., Lorén-Aguilar, P., Aznar-Siguán, G., et al. 2012, ApJ, 749, 25
Genest-Beaulieu, C., & Bergeron, P. 2019a, ApJ, 871, 169
—. 2019b, ApJ, 882, 106
Gentile Fusillo, N. P., Tremblay, P. E., Jordan, S., et al. 2018, MNRAS, 473, 3693
Gentile Fusillo, N. P., Tremblay, P.-E., Gänsicke, B. T., et al. 2019a, MNRAS, 482, 4570
—. 2019b, MNRAS, 482, 4570
Gentile Fusillo, N. P., Tremblay, P. E., Cukanovaite, E., et al. 2021, MNRAS, arXiv :2106.07669
Giammichele, N., Bergeron, P., & Dufour, P. 2012a, ApJS, 199, 29
—. 2012b, ApJS, 199, 29
Gianninas, A., Bergeron, P., & Ruiz, M. T. 2011, ApJ, 743, 138
Gianninas, A., Dufour, P., & Bergeron, P. 2004, ApJ, 617, L57
Ginzburg, S., Fuller, J., Kawka, A., & Caiazzo, I. 2022, MNRAS, 514, 4111
Greenstein, J. L. 1986, ApJ, 304, 334
Hall, P. B., Kowalski, P. M., Harris, H. C., et al. 2008, AJ, 136, 76
Hewett, P. C., Warren, S. J., Leggett, S. K., & Hodgkin, S. T. 2006, MNRAS, 367, 454
Holberg, J. B., & Bergeron, P. 2006a, AJ, 132, 1221
—. 2006b, AJ, 132, 1221
Hollands, M. A., Tremblay, P. E., Gänsicke, B. T., Gentile-Fusillo, N. P., & Toonen, S. 2018, MNRAS, 480, 3942
Hollands, M. A., Tremblay, P.-E., Gänsicke, B. T., Koester, D., & Gentile Fusillo, N. P. 2021, Nature Astronomy, 5, 451
Hummer, D. G., & Mihalas, D. 1988, ApJ, 331, 794
Iglesias, C. A., Rogers, F. J., & Saumon, D. 2002, ApJ, 569, L111
Isern, J., García-Berro, E., Külebi, B., & Lorén-Aguilar, P. 2017, ApJ, 836, L28
Kawka, A., Vennes, S., Schmidt, G. D., Wickramasinghe, D. T., & Koch, R. 2007, ApJ, 654, 499
Kepler, S. O., Pelisoli, I., Koester, D., et al. 2019a, MNRAS, 486, 2169

—. 2019b, MNRAS, 486, 2169
Kilic, M., Bergeron, P., Kosakowski, A., et al. 2020a, ApJ, 898, 84
—. 2020b, ApJ, 898, 84
Kilic, M., von Hippel, T., Mullally, F., et al. 2006, ApJ, 642, 1051
Kleinman, S. J., Kepler, S. O., Koester, D., et al. 2013a, ApJS, 204, 5
—. 2013b, ApJS, 204, 5
Koester, D., Voss, B., Napiwotzki, R., et al. 2009, A&A, 505, 441
Kowalski, P. M., Mazevet, S., Saumon, D., & Challacombe, M. 2007, Phys. Rev. B, 76, 075112
Kowalski, P. M., & Saumon, D. 2006, ApJ, 651, L137
Lecavalier-Hurtubise, É., & Bergeron, P. 2017, in Astronomical Society of the Pacific Conference Series, Vol. 509, 20th European White Dwarf Workshop, ed. P. E. Tremblay, B. Gaensicke, & T. Marsh, 169
Leggett, S. K., Bergeron, P., Subasavage, J. P., et al. 2018, ApJS, 239, 26
Liebert, J., Bergeron, P., & Holberg, J. B. 2005, ApJS, 156, 47
Limoges, M. M., Bergeron, P., & Lépine, S. 2015a, ApJS, 219, 19
—. 2015b, ApJS, 219, 19
Lindegren, L., Hernández, J., Bombrun, A., et al. 2018, A&A, 616, A2
Lindegren, L., Bastian, U., Biermann, M., et al. 2021, A&A, 649, A4
López-Sanjuan, C., Tremblay, P. E., Ederoclite, A., et al. 2022, A&A, 658, A79
Magnier, E. A., Schlafly, E., Finkbeiner, D., et al. 2013, ApJS, 205, 20
McCleery, J., Tremblay, P.-E., Gentile Fusillo, N. P., et al. 2020, MNRAS, 499, 1890
O'Brien, M. W., Tremblay, P. E., Gentile Fusillo, N. P., et al. 2022, arXiv e-prints, arXiv :2210.01608
Press, W. H., Flannery, B. P., & Teukolsky, S. A. 1986a, Numerical recipes. The art of scientific computing
—. 1986b, Numerical recipes. The art of scientific computing (Cambridge University Press)
Putney, A. 1997, ApJS, 112, 527
Rolland, B., Bergeron, P., & Fontaine, G. 2018a, ApJ, 857, 56
—. 2018b, ApJ, 857, 56
—. 2020, ApJ, 889, 87
Saumon, D., Blouin, S., & Tremblay, P.-E. 2022, Phys. Rep., 988, 1
Saumon, D., Holberg, J. B., & Kowalski, P. M. 2014, ApJ, 790, 50
Schreiber, M. R., Belloni, D., Gänsicke, B. T., Parsons, S. G., & Zorotovic, M. 2021, Nature Astronomy, 5, 648
Skrutskie, M. F., Cutri, R. M., Stiening, R., et al. 2006, AJ, 131, 1163
Spiegelman, F., Allard, N. F., & Kielkopf, J. F. 2022, A&A, 659, A157

Temmink, K. D., Toonen, S., Zapartas, E., Justham, S., & Gänsicke, B. T. 2020, A&A, 636, A31
Tonry, J. L., Stubbs, C. W., Lykke, K. R., et al. 2012a, ApJ, 750, 99
—. 2012b, ApJ, 750, 99
Tonry, J. L., Denneau, L., Heinze, A. N., et al. 2018, PASP, 130, 064505
Tout, C. A., Wickramasinghe, D. T., & Ferrario, L. 2004, MNRAS, 355, L13
Tout, C. A., Wickramasinghe, D. T., Liebert, J., Ferrario, L., & Pringle, J. E. 2008, MNRAS, 387, 897
Tremblay, P. E., Bergeron, P., & Gianninas, A. 2011, ApJ, 730, 128
Tremblay, P. E., Cukanovaite, E., Gentile Fusillo, N. P., Cunningham, T., & Hollands, M. A. 2019a, MNRAS, 482, 5222
Tremblay, P. E., Fontaine, G., Freytag, B., et al. 2015, ApJ, 812, 19
Tremblay, P. E., Ludwig, H. G., Steffen, M., & Freytag, B. 2013, A&A, 559, A104
Tremblay, P.-E., Fontaine, G., Gentile Fusillo, N. P., et al. 2019b, Nature, 565, 202
Tremblay, P. E., Hollands, M. A., Gentile Fusillo, N. P., et al. 2020a, MNRAS, 497, 130
—. 2020b, MNRAS, 497, 130
van Altena, W. F., Lee, J. T., & Hoffleit, E. D. 1995, The general catalogue of trigonometric [stellar] parallaxes
Wenger, M., Ochsenbein, F., Egret, D., et al. 2000, A&AS, 143, 9
Wickramasinghe, D. T., Allen, D. A., & Bessell, M. S. 1982, MNRAS, 198, 473
Wickramasinghe, D. T., & Ferrario, L. 2005, MNRAS, 356, 1576
Zuckerman, B., Koester, D., Melis, C., Hansen, B. M., & Jura, M. 2007, ApJ, 671, 872

Annexe A

Données utilisées et paramètres calculés dans ce projet.

Tableau A.1 – Données observationnelles des naines blanches de l'échantillon.

Name	Gaia DR2/EDR3*	Sp Type	ϖ (mas)	u	g	r	i	z	y	J	H	K
J0000+0132	2738626591386423424	DA	15.0 (0.1)	16.65	16.234	16.336	16.476	16.64	16.752	16.23	16.14	16.24
J0000+1906	2774195552027050880	DC	9.8 (0.5)	23.3	20.32	19.73	19.52	19.43	19.34	18.6	···	···
J0001+3237	2874216647336589568	DC	10.2 (0.3)	20.4	19.49	19.16	19.06	19.04	19.01	18.32	···	···
J0001+3559	2877080497170502144	DC*	11.7 (0.3)	20.0	19.03	18.85	18.83	18.58	18.45	17.81	···	···
J0001−1111	2422442334689173376	DC	13.5 (0.3)	19.09	18.48	18.28	18.28	18.31	18.35	17.72	···	17.7
J0002+0733	2745919102257342976	DA	11.9 (0.2)	18.31	17.845	17.764	17.775	17.83	17.87	17.23	17.07	17.1
J0002+0733	2745919106553695616	DAH	12.2 (0.2)	18.52	18.05	17.985	18.014	18.09	18.15	17.59	17.4	17.5
J0002+1610	2772241822943618176	DA	9.8 (0.3)	19.55	18.927	18.71	18.64	18.67	18.72	17.98	17.7	17.5
J0002+6357	431635455820288128	DC	38.1 (0.1)	···	17.64	16.993	16.723	16.65	16.59	15.8	15.6	15.5
J0003+6512	432177373309335424	DC	10.7 (0.1)	···	17.59	17.611	17.73	17.844	17.94	···	···	···
J0003−0111	2449594087142467712	DA	14.1 (0.5)	20.5	19.25	18.76	18.56	18.49	18.49	17.63	17.31	17.35
J0004−0340	2447889401738675072	DA	21.1 (0.1)	17.45	16.915	16.752	16.726	16.761	16.79	16.1	15.94	15.93
J0005+4003	2881925666956510848	DZA	15.5 (0.1)	···	16.81	16.863	16.986	17.131	17.25	16.69	···	···
J0005+4825	393365609282766848	DA	21.1 (0.1)	···	17.142	16.964	16.928	16.967	16.98	16.27	15.6	15.9
J0006+0755	2746037712074342784	DAH	10.2 (0.2)	18.31	18.03	17.98	18.057	18.15	18.22	17.55	17.6	17.5
J0006+1800	2773073470346643200	DQ	17.3 (0.1)	17.4	17.04	16.995	17.03	17.144	17.2	16.61	···	···
J0006−0505	2444446482939165824	DA	10.1 (0.3)	19.36	18.73	18.6	18.56	18.62	18.65	17.92	17.81	17.8
J0007+1230	2766234439302571904	DC	57.3 (0.1)	18.16	16.767	16.25	16.018	15.925	15.92	15.08	15.1	14.9
J0007+3403	2875903332533220992	DC	29.3 (0.1)	18.6	17.605	17.226	17.118	17.05	17.08	16.32	16.2	15.8
J0007+3947	383108338321272448	DC	29.0 (0.1)	···	17.25	16.533	16.228	16.124	16.062	15.17	14.8	14.6
J0007−0307	2448308212589610240	DA :	23.9 (0.4)	21.0	18.63	18.13	17.953	17.883	17.86	17.1	16.87	16.8
J0008−0353	2445187691214892416	DC	12.9 (0.4)	19.81	18.96	18.67	18.596	18.61	18.59	17.84	17.7	17.7
J0008−1435	2417481205081646592	DA	16.4 (0.3)	···	17.22	16.985	16.916	16.933	16.96	16.2	16.2	···
J0009+3108	2861792754354276352	DC	18.6 (0.1)	17.12	16.807	16.74	16.847	16.944	17.01	16.43	16.34	16.33
J0010−2021	2364836107306975872	DA	13.1 (0.1)	16.85	16.475	16.557	16.702	16.85	16.97	16.4	16.4	16.38
J0011+2824	2859908324567852416	DC	11.0 (0.1)	17.96	17.63	17.636	17.75	17.88	17.97	17.44	···	···
J0011+4240	384636109728592768	DA	42.71 (0.05)	···	15.417	15.265	15.235	15.283	15.31	14.602	14.35	14.4
J0011−0827	2429268309033277184	DC	10.2 (0.2)	18.25	18.02	18.038	18.158	18.3	18.4	17.81	···	17.5
J0011−0903	2429183303040388992	DA	18.0 (0.1)	18.61	17.85	17.517	17.42	17.39	17.43	16.6	16.0	···
J0012+5025	395234439752169344	DAH	91.98 (0.03)	···	14.516	14.27	14.204	14.207	14.224	13.452	13.25	13.19
J0013+0019	2545505281002947200	DA	25.0 (0.1)	15.779	15.376	15.416	15.53	15.66	15.76	15.15	15.12	15.16
J0013+5438	420531621029108608	DC	31.1 (0.2)	···	18.93	17.966	17.546	17.39	17.25	16.4	16.0	···

Tableau A.1 *suite page suivante*

Tableau A.1 *(suite)*

Name	Gaia DR2/EDR3*	Sp Type	ϖ (mas)	u	g	r	i	z	y	J	H	K
J0013−0213	2541549062071571968	DC	25.8 (0.2)	20.8	18.8	18.03	17.7	17.59	17.53	16.66	16.42	16.42
J0014+1503	2768536949794022656	DA	9.7 (0.5)	20.18	19.63	19.44	19.44	19.46	19.41	18.8	···	···
J0014−0758	2429392661221943040	DC	10.9 (0.4)	20.5	19.58	19.23	19.129	19.11	19.12	18.3	···	17.8
J0014−1311	2418116963320446720	DAH	53.8 (0.1)	···	16.12	15.758	15.623	15.609	15.625	14.81	14.5	14.6
J0015+1353	2768116146078155648	DA	12.5 (0.1)	17.64	17.26	17.25	17.306	17.4	17.48	16.89	16.8	16.8
J0016+0504	2741440172922171008	DA	10.5 (0.3)	19.12	18.63	18.5	18.46	18.515	18.61	···	···	···
J0017−0516	2443826805441462656	DA	21.4 (0.2)	19.02	17.91	17.517	17.35	17.32	17.27	16.48	16.26	16.13
J0018+0233	2548152217808246528	DQ	13.3 (0.1)	17.26	17.11	17.162	17.291	17.43	17.54	17.01	16.96	17.1
J0018+3055	2862337802883401856	DA	18.5 (0.1)	17.88	17.309	17.118	17.07	17.1	17.12	16.36	···	···
J0018+3441	2876148734080688256	DA	10.4 (0.2)	18.7	18.26	18.15	18.128	18.16	18.21	17.48	···	···
J0019+1414	2768190500551905408	DC*	11.4 (0.2)	18.37	18.01	18.0	18.07	18.17	18.26	17.65	17.6	17.7
J0019−1114	2424913628807069056	DC	11.2 (0.2)	18.21	17.98	17.937	18.01	18.14	18.24	···	···	···
J0020+0011	2545305410405677312	DA	10.5 (0.3)	19.14	18.61	18.44	18.41	18.45	18.49	17.81	17.6	17.7
J0020+0044	2546887573277984256	DA	21.2 (0.1)	17.07	16.727	16.735	16.829	16.93	17.01	16.41	16.31	16.29
J0020−1115	2424915789174828160	DA	10.6 (0.7)	20.3	19.52	19.25	19.15	19.16	19.13	···	···	···
J0021+1502	2792315366213367296	DAP*	14.2 (0.2)	18.69	18.149	17.97	17.978	18.01	18.06	17.5	17.6	17.3
J0021+2531	2855386170682263424	DA	35.7 (0.1)	15.93	15.43	15.492	15.3929	15.8	15.5	···	···	···
J0021+2640	2855790657816672000	DC	30.7 (0.1)	19.8	18.09	17.436	17.179	17.09	17.02	16.18	15.9	15.81
J0022+4236	385105360675267840	DC	29.3 (0.1)	···	16.75	16.354	16.207	16.17	16.182	15.38	15.1	14.9
J0024+6834	529594417061837824	DC	27.7 (0.1)	···	17.86	17.449	17.28	17.21	17.06	···	···	···
J0024−0030	2542192757410302720	DC	12.1 (0.9)	23.5	20.99	20.16	19.81	19.65	19.45	18.7	18.6	···
J0026+3533	366241825654658176	DA	10.0 (0.2)	18.31	17.877	17.86	17.921	18.06	18.11	17.51	···	···
J0026−1037	2424880574738721408	DA	11.3 (0.1)	16.76	16.203	16.265	16.39	16.519	16.601	16.0	15.8	15.7
J0027+0541	2555215995900584448	DA	46.1 (0.1)	17.54	16.371	15.944	15.783	15.75	15.755	14.905	14.636	14.56
J0027+0554	2747384888699406080	DC	27.3 (0.2)	20.3	18.565	17.964	17.724	17.75	17.874	17.49	17.8	17.8
J0027−0138	2541126609088680448	DA	11.5 (0.3)	20.2	19.31	19.0	18.85	18.84	18.81	18.09	17.8	17.9
J0028−0029	2543515813495903488	DC	9.6 (0.4)	20.4	19.61	19.37	19.33	19.34	19.37	18.6	18.7	18.7
J0030+0347	2553935752048977792	DC	36.0 (0.05)	17.0	16.33	16.107	16.045	16.053	16.09	15.5	15.2	15.2
J0030+2421	2807036078858147584	DC	11.5 (0.1)	17.25	17.13	17.196	17.37	17.5	17.61	17.13	···	···
J0030+2714	2856067008897130112	DC	14.6 (0.2)	19.72	18.79	18.47	18.374	18.37	18.39	17.66	···	···
J0031+1845	2794904441219064448	DA	12.7 (0.1)	18.26	17.82	17.743	17.757	17.82	17.89	17.29	···	···
J0031+2218	2799809779202757376	DA	19.7 (0.1)	18.78	17.938	17.606	17.484	17.48	17.47	16.69	16.3	···
J0032+1434	2780050795041827968	DC	10.3 (0.3)	19.84	19.16	18.96	18.87	18.92	19.0	18.2	17.9	17.9
J0032−0253	2528728726428345216	DC*	42.4 (0.1)	19.91	17.772	16.98	16.641	16.521	16.46	15.54	15.36	15.32

Tableau A.1 *suite page suivante*

Tableau A.1 *(suite)*

Name	Gaia DR2/EDR3*	Sp Type	ϖ (mas)	u	g	r	i	z	y	J	H	K
J0033+0540	2555356080553959168	DA	13.2 (0.2)	18.58	18.064	17.89	17.86	17.92	17.93	···	···	···
J0033+1451	2780434524599787136	DQ*	15.4 (0.2)	19.31	18.49	18.123	18.012	18.006	17.97	17.39	17.4	17.8
J0033+2506	2807462655009880320	DA	26.0 (0.1)	17.86	17.101	16.806	16.7	16.696	16.71	15.97	15.7	15.45
J0033+4444	388602146952607360	DA	13.0 (0.1)	···	16.545	16.64	16.778	16.952	17.05	16.48	16.2	···
J0034+0640	2555713215673881856	DA	14.3 (0.4)	21.0	19.35	18.87	18.66	18.59	18.55	17.77	17.6	17.5
J0034+1026	2751252493861856000	DA	10.3 (0.2)	18.86	18.43	18.295	18.29	18.36	18.4	17.68	17.7	17.5
J0034+1517	2780524585769652736	DA	22.3 (0.1)	17.55	16.98	16.811	16.773	16.8	16.82	16.08	15.86	15.83
J0034−1021	2425650847058388224	DC*	23.0 (0.2)	19.07	18.14	17.809	17.7	17.64	17.59	···	···	···
J0035+0011	2543230185287345664	DA	15.0 (0.1)	16.87	16.46	16.51	16.626	16.757	16.852	16.28	16.22	16.24
J0035+0153	2544456862306151680	DA	31.6 (0.1)	15.89	15.616	15.705	15.857	16.03	16.16	15.63	15.58	15.66
J0035+0958	2751172946772404224	DC	11.2 (0.2)	19.21	18.73	18.61	18.62	18.69	18.7	18.1	18.2	18.1
J0035+1530	2780622648462300160	DA	11.3 (0.4)	20.23	19.42	19.07	18.95	18.91	19.0	18.1	18.0	···
J0035−1718	2364319061964016512	DA	29.94 (0.04)	···	14.94	15.004	15.119	15.271	15.38	14.79	14.8	14.7
J0036+0552	2555403428272657792	DA	14.8 (0.2)	18.5	17.91	17.72	17.66	17.71	17.72	16.96	16.81	16.86
J0036+2422	2806614205695008256	DA	11.1 (0.2)	18.12	17.727	17.67	17.709	17.791	17.88	17.22	···	···
J0036−1112	2425347347488993408	DZ	19.1 (0.1)	17.54	17.04	17.004	17.106	17.24	17.3	16.7	16.7	16.3
J0038+0044	2543378511984771200	DC	11.1 (0.8)	22.1	20.86	20.26	19.97	19.93	19.9	···	···	···
J0038+3409	364978005758397952	DC	11.5 (0.1)	17.36	17.226	17.291	17.431	17.58	17.7	17.2	···	···
J0039+4229	381396329995329408	DA	13.0 (0.1)	16.91	16.51	16.579	16.714	16.882	16.98	16.38	···	···
J0040−0809	2522401586766106624	DA	26.9 (0.1)	18.44	17.57	17.223	17.09	17.08	17.09	16.32	16.3	16.05
J0041+3923	368639899170380672	DA	9.9 (0.1)	18.01	17.591	17.6	17.698	17.81	17.88	17.26	···	···
J0041+7321	536979286914485760	DQ	17.93 (0.05)	···	16.116	16.21	16.371	16.54	16.65	16.1	16.2	···
J0041−0226	2530119196321115776	DA	18.3 (0.1)	17.43	16.952	16.857	16.865	16.911	16.97	16.27	16.12	16.17
J0041−1104	2377643661128402048	DAH*	9.8 (0.4)	19.87	19.27	19.12	19.1	19.14	19.09	···	···	···
J0041−2221	2349916559152267008	DQ	109.88 (0.03)	15.76	14.756	14.288	14.111	14.06	14.032	13.396	13.48	13.719
J0042+2357	2803442840498734720	DA	12.0 (0.1)	17.78	17.392	17.387	17.43	17.56	17.6	17.0	···	···
J0043+1540	2781309637071878912	DA	13.4 (0.2)	18.9	18.271	18.072	18.02	18.03	18.07	17.34	17.12	17.1
J0044+0318	2550856260497950464	DA	14.7 (0.1)	18.4	17.83	17.63	17.59	17.63	17.66	16.9	16.76	16.73
J0044+0418	2551258990991085184	DZ	13.5 (0.2)	19.93	18.65	18.44	18.48	18.53	18.5	17.94	17.8	17.9
J0044+1518	2781085401124115328	DZ	9.6 (0.6)	20.11	19.37	19.13	19.08	19.03	19.053	···	···	···
J0044−2824	2342218942669916672	DC	15.4 (0.5)	···	20.38	19.5	19.18	19.02	18.8	18.07	17.97	17.82
J0045+0904	2558010366047159424	DA	11.8 (0.2)	18.46	18.01	17.931	17.92	17.99	18.0	···	···	···
J0045+1420	2776464325551066880	DZAH :*	17.4 (0.3)	22.1	19.1	18.46	18.23	18.145	18.1	17.24	16.99	16.89
J0045+1454	2781012734572656640	DA	15.6 (0.2)	18.84	18.291	18.1	18.064	18.09	18.1	···	···	···

Tableau A.1 *suite page suivante*

Tableau A.1 *(suite)*

Name	Gaia DR2/EDR3*	Sp Type	ϖ (mas)	u	g	r	i	z	y	J	H	K
J0045+2527	2808103391115590016	DA*	9.9 (0.5)	21.3	19.86	19.37	19.17	19.14	19.15	18.2	···	···
J0045−0608	2523840155996531456	DC	33.3 (0.2)	20.48	18.6	17.946	17.657	17.59	17.56	16.77	16.6	16.43
J0046+0635	2556270869932443648	DZ	9.8 (0.3)	19.34	18.82	18.68	18.66	18.71	18.75	18.3	17.9	17.7
J0048−0124	2530629365419780864	DA	14.5 (0.1)	17.36	17.11	17.2	17.336	17.54	17.6	17.06	17.05	17.0
J0049+0522	2552928187080872832	DZ	231.74 (0.04)	14.97	12.5	12.22	11.81	12.32	12.4	11.69	11.57	11.5
J0049+1727	2782037303315690752	DC	10.3 (0.5)	20.2	19.41	19.13	19.05	19.05	19.06	18.3	···	···
J0049+3841	367949367212923392	DA	10.3 (0.1)	17.78	17.148	17.217	17.348	17.52	17.59	17.03	···	···
J0050+4010	374172980983236352	DA	9.9 (0.2)	18.72	18.358	18.403	18.518	18.64	18.72	18.1	···	···
J0051−2028	2356519298275043200	DA	37.2 (0.1)	···	17.61	16.97	16.7	16.64	16.55	15.657	15.4	15.35
J0052+0453	2552643413569299968	DA	11.1 (0.3)	19.56	18.99	18.79	18.74	18.78	18.76	18.1	17.9	18.0
J0052−3036	5031709119620238336	DA	15.1 (0.1)	···	17.05	16.803	16.697	16.69	16.69	15.9	15.7	15.8
J0053+3927	368075574827351168	DA	20.9 (0.1)	17.15	16.66	16.562	16.557	16.62	16.68	16.01	15.8	15.4
J0054+1412	2777751372630874112	DC	10.2 (0.4)	20.05	19.36	19.14	19.11	19.13	19.16	18.4	18.6	···
J0054+2256	2803596046661176576	DA	27.5 (0.1)	16.52	16.17	16.23	16.346	16.47	16.55	15.98	16.1	15.5
J0054+4156	375131415820709632	DA	18.49 (0.05)	16.31	15.817	15.728	15.73	15.791	15.847	15.16	15.0	14.9
J0054−0952	2473754897386327808	DA	14.6 (0.1)	17.22	16.776	16.778	16.851	16.961	17.05	16.43	17.0	16.32
J0055+0850	2581058706745690752	DQ	11.4 (0.3)	18.99	18.53	18.387	18.38	18.43	18.49	17.81	17.9	17.8
J0055+1010	2582335342824976768	DA	37.7 (0.1)	17.09	16.321	16.037	15.948	15.936	15.953	15.2	15.0	14.9
J0055+1804	2788048780061707520	DA	12.1 (0.3)	19.18	18.5	18.28	18.195	18.23	18.25	17.46	···	···
J0055+3847	367799116372410752	DC	12.7 (0.2)	19.71	18.408	17.973	17.796	17.78	17.76	17.0	···	···
J0055+5948	426122397136335872	DC	43.8 (0.1)	···	17.54	16.79	16.482	16.369	16.3	15.4	15.2	15.0
J0055−1127	2472557872820632320	DA	44.57 (0.04)	···	15.36	15.191	15.14	15.168	15.196	14.51	14.35	14.3
J0056+4347	377196947196848128	DC	20.0 (0.2)	18.24	17.698	17.525	17.505	17.59	17.61	16.96	···	···
J0056−0614	2524394000619171840	DA	10.1 (0.4)	20.3	19.53	19.19	19.07	19.06	19.03	18.27	···	18.1
J0057+1756	2787939447373738880	DA	20.9 (0.2)	18.83	18.03	17.74	17.631	17.62	17.62	16.9	···	···
J0058+0639	2577467770489127296	DA	10.1 (0.2)	18.04	17.63	17.641	17.715	17.819	17.93	17.34	17.2	17.4
J0059+1623	2784445680457082368	DA	14.6 (0.2)	18.57	17.97	17.76	17.72	17.74	17.75	17.04	···	···
J0101−0252	2532236546477272192	DC	14.3 (0.2)	18.08	17.71	17.66	17.712	17.8	17.89	17.25	17.2	17.2
J0103+0008	2536332154276141696	DA	10.2 (0.2)	19.17	18.57	18.363	18.29	18.32	18.38	17.62	17.4	17.4
J0103+0504	2552121179905893888	DA	44.9 (0.1)	14.485	14.059	14.01	14.049	14.124	14.184	13.493	13.38	13.42
J0103+1401	2777098984278522752	DC	17.1 (0.3)	21.2	19.34	18.67	18.393	18.3	18.27	17.38	17.19	17.0
J0103−0325	2531407858307339264	DA	16.5 (0.1)	17.06	16.644	16.645	16.719	16.84	16.92	16.3	16.26	16.29
J0103−0522	2524879812959998592	DA*	34.6 (0.1)	17.7	17.41	17.44	17.486	17.6	17.69	17.11	17.14	17.1
J0103−2444	2344901720977366528	DC	12.7 (0.1)	···	16.703	16.801	16.959	17.112	17.2	16.65	16.5	16.74

Tableau A.1 *suite page suivante*

Tableau A.1 *(suite)*

Name	Gaia DR2/EDR3*	Sp Type	ϖ (mas)	u	g	r	i	z	y	J	H	K
J0104+2119	2790494815860044544	DA	30.7 (0.1)	19.61	18.21	17.662	17.456	17.38	17.344	16.56	16.32	16.21
J0104+2120	2790494850219788160	DC	31.0 (0.1)	···	18.45	17.76	17.47	17.36	17.32	16.7	16.3	15.6
J0104−0350	2531326283993100416	DA	27.9 (0.2)	19.78	18.27	17.764	17.55	17.51	17.48	16.5	16.4	···
J0105−0614	2476711101899811456	DA	10.2 (0.3)	19.9	19.05	18.74	18.636	18.62	18.6	17.86	···	17.6
J0105−0920	2473296504116465408	DA	14.4 (0.1)	17.68	17.23	17.179	17.223	17.31	17.37	16.67	17.3	16.7
J0106+0148	2538286403050847232	DA	10.2 (0.1)	17.73	17.28	17.236	17.292	17.392	17.448	16.82	16.69	16.7
J0106+3930	371070026026145792	DA	19.6 (0.1)	···	15.465	15.55	15.672	15.837	15.95	15.39	15.3	15.7
J0106+6119	522518883651891584	DC	23.0 (0.2)	···	19.18	18.34	17.98	17.85	17.75	···	···	···
J0107+0102	2537913801752406400	DQ	10.7 (0.2)	19.31	18.775	18.59	18.558	18.6	18.66	17.98	17.8	17.7
J0107+2107	2790417540424293120	DAZ	11.1 (0.4)	19.83	19.23	19.09	19.16	19.21	19.2	19.2	···	···
J0107+2650	306779618349361920	DZH*	14.6 (0.3)	23.4	19.22	18.81	18.7	18.77	18.75	18.05	···	···
J0108+7600	563004280465719040	DA	19.5 (0.1)	···	17.838	17.504	17.41	17.39	17.3	16.6	16.4	···
J0109+3300	313967881773971840	DA	11.7 (0.4)	20.1	19.38	19.03	18.9	18.89	18.85	18.2	···	···
J0109+3435	314956480167069696	DA	16.4 (0.2)	18.75	18.22	18.073	18.021	18.04	18.1	17.39	···	···
J0109−1042	2469900005324049280	DC	16.9 (0.2)	20.8	19.3	18.69	18.453	18.36	18.31	···	···	···
J0109−1042	2469900009618822656	DA	16.4 (0.1)	17.15	16.692	16.665	16.718	16.803	16.86	16.2	16.2	···
J0110+1239	2583892972844696448	DC	13.7 (0.3)	19.34	18.781	18.594	18.67	18.75	18.61	18.1	17.9	17.8
J0110+1439	2591091789004351104	DA	19.5 (0.1)	17.26	16.949	16.98	17.067	17.18	17.28	16.67	16.63	16.7
J0110+2758	307323228064848512	DA	26.3 (0.1)	17.4	19.05	18.49	18.15	17.94	17.82	15.2	15.0	14.9
J0110−1020	2469937908410307328	DC	14.1 (0.1)	18.0	17.63	17.563	17.62	17.696	17.78	···	···	···
J0111+2204	2790884008232725632	DA	15.6 (0.1)	17.91	17.548	17.533	17.622	17.72	17.79	17.26	···	···
J0112+3438	320903154445635456	DA	10.4 (0.1)	18.01	17.59	17.597	17.676	17.78	17.85	17.3	···	···
J0113+0603	2576622898882026624	DC	11.5 (0.2)	18.89	18.52	18.523	18.59	18.68	18.78	18.2	18.2	18.1
J0113+2558	294798377579784832	DC	11.5 (0.5)	22.2	20.09	19.36	19.02	18.9	18.8	17.71	···	···
J0113+3307	313996228559363840	DA	11.3 (0.3)	19.89	19.01	18.685	18.54	18.52	18.43	17.72	···	···
J0113−0510	2482721857094021760	DA	11.3 (0.3)	19.63	19.01	18.8	18.77	18.79	18.75	18.09	17.9	17.8
J0115+1227	2583651904920127232	DA	11.3 (0.3)	19.85	18.96	18.64	18.52	18.52	18.48	17.72	17.4	17.4
J0115+1435	2590924250920129920	DA	13.2 (0.2)	19.39	18.67	18.42	18.34	18.36	18.36	17.71	17.4	17.6
J0115+4733	401529105161219968	DZ	10.3 (0.5)	19.75	19.19	18.99	18.98	19.03	19.08	18.4	···	···
J0115−0133	2533575369771883648	DA	29.4 (0.1)	19.32	17.9	17.37	17.15	17.09	17.07	16.18	15.95	15.87
J0115−0146	2532059009708732288	DA	10.4 (0.1)	18.4	17.984	17.9	17.934	18.01	18.08	17.5	17.3	17.2
J0116+2050	2787507098786135552	DZ	13.6 (0.2)	19.95	18.178	18.002	18.07	18.18	18.25	17.66	···	···
J0116+2346	293138458619500800	DQ	11.2 (0.1)	18.01	17.77	17.778	17.87	17.98	18.07	17.42	···	···
J0116−0943	2471521269578009984	DA	10.8 (0.4)	20.01	19.33	19.07	18.96	19.0	18.96	18.19	···	17.8

Tableau A.1 *suite page suivante*

Tableau A.1 *(suite)*

Name	Gaia DR2/EDR3*	Sp Type	ϖ (mas)	u	g	r	i	z	y	J	H	K
J0116−1045	2470565072419060736	DA	9.6 (0.5)	21.2	20.02	19.6	19.45	19.4	19.5	···	···	···
J0117+4403	397531182099486080	DA	14.5 (0.1)	···	16.831	16.82	16.894	17.01	17.11	16.5	···	···
J0117−0439	2482813425794003200	DC :	23.9 (0.2)	20.4	18.58	17.922	17.643	17.544	17.49	16.6	16.41	16.32
J0117−0439	2482813430089468160	DC :	23.4 (0.2)	20.2	18.45	17.831	17.58	17.49	17.43	16.56	16.34	16.25
J0117−2648	5039601100551392896	DC	17.5 (0.2)	···	19.43	18.72	18.42	18.33	18.28	17.47	17.2	17.2
J0118+1610	2591754107321120896	DQ	59.61 (0.04)	14.04	13.837	13.91	14.029	14.1433	14.2648	13.704	13.68	13.73
J0119+1840	2785927684692570496	DA	10.8 (0.3)	19.39	18.782	18.567	18.51	18.52	18.51	17.81	···	···
J0119+2241	292790566268764288	DA	11.2 (0.4)	20.44	19.56	19.24	19.13	19.11	19.05	18.4	···	···
J0119+3055	310300323301763328	DC	9.7 (0.6)	23.7	20.6	19.83	19.51	19.44	19.4	18.3	···	···
J0119−1415	2456160271800004096	DA	39.4 (0.1)	···	17.27	16.67	16.4225	16.358	16.31	15.6	15.1	15.2
J0121+0951	2579280762084084736	DC :	12.5 (0.3)	19.63	18.92	18.65	18.6	18.61	18.63	18.0	18.0	18.1
J0121+3440	320029150076023808	DZ	25.7 (0.1)	17.23	16.75	16.65	16.672	16.747	16.81	16.17	16.1	15.88
J0121−0038	2533742048478056448	DC	13.0 (0.6)	22.3	20.57	19.75	19.37	19.24	19.13	18.2	18.0	18.1
J0122+3259	316773766729205632	DC	13.7 (0.3)	20.1	19.19	18.82	18.69	18.68	18.65	18.0	···	···
J0123−0209	2485211533668928640	DA	23.1 (0.2)	18.68	17.689	17.31	17.15	17.13	17.12	16.29	16.05	15.94
J0123−2748	5036250613743304192	DC	12.4 (0.4)	···	20.4	19.65	19.34	19.23	19.15	18.26	18.06	18.0
J0124+4023	372111985092019840	DA	37.0 (0.1)	18.93	17.41	16.876	16.668	16.607	16.57	15.74	15.5	15.3
J0124−1959	2353801065013205504	DA	14.2 (0.1)	18.25	17.78	17.64	17.66	17.73	17.75	17.09	···	17.0
J0124−2229	5043015122810735744	DZ	15.6 (0.1)	···	16.91	16.98	17.118	17.26	17.36	16.83	16.82	16.8
J0125−0417	2482521745974836352	DC	10.8 (0.6)	21.6	20.11	19.56	19.35	19.3	19.18	···	···	···
J0125−2600	5037084872486444928	DC	60.4 (0.03)	···	15.124	14.992	14.99	15.061	15.141	14.44	14.31	14.3
J0126−0840	2477282538708615680	DA	9.9 (0.2)	18.53	18.061	18.01	18.044	18.15	18.22	17.46	···	17.4
J0127+7328	535482641132742400	DA	18.6 (0.1)	···	17.046	16.88	16.83	16.83	16.59	14.76	···	···
J0128−0045	2485921779525500288	DA	22.1 (0.1)	18.92	17.862	17.44	17.273	17.24	17.23	16.44	16.16	16.05
J0128−0822	2477317211979980544	DA	12.6 (0.6)	18.84	18.56	18.29	18.36	18.3	18.41	17.44	···	17.3
J0129+1022	2585189473147457408	DA	34.1 (0.1)	14.988	14.42	14.424	14.488	14.586	14.675	14.032	13.928	13.954
J0129+3459	317446015009891328	DC	10.9 (0.5)	20.3	19.54	19.25	19.14	19.14	19.12	18.6	···	···
J0130+4414	396963005168870528	DZA	26.0 (0.1)	20.06	18.35	17.74	17.489	17.39	17.37	16.6	16.3	···
J0131+3147	315687277442204672	DA	12.0 (0.2)	18.21	17.78	17.693	17.706	17.8	17.83	17.17	···	···
J0132+0529	2564945432560219008	DAZ*	10.0 (0.2)	18.96	18.363	18.251	18.24	18.3	18.36	17.76	17.4	17.5
J0132+4604	398672715686799488	DA	26.0 (0.1)	15.398	15.0	15.116	15.263	15.436	15.553	14.99	15.1	15.2
J0135+0851	2572713104253752448	DA	10.8 (0.4)	20.0	19.31	19.03	18.93	18.91	18.9	18.2	18.0	17.9
J0135+1302	2586182156053386240	DZ	10.1 (0.4)	20.9	19.21	18.98	18.96	19.05	19.04	18.6	18.2	18.2
J0135+1445	2588874825669925504	DA	12.8 (0.1)	17.48	17.02	16.934	16.98	17.03	17.04	16.24	15.86	15.56

Tableau A.1 *suite page suivante*

Tableau A.1 *(suite)*

Name	Gaia DR2/EDR3*	Sp Type	ϖ (mas)	u	g	r	i	z	y	J	H	K
J0137−0207	2484544095751034496	DA	27.9 (0.1)	17.15	16.675	16.549	16.542	16.6	16.66	15.8	15.7	···
J0138+1527	2589304876450784128	DA	44.1 (0.1)	15.44	14.986	14.92	14.944	15.02	15.066	14.41	14.29	14.27
J0138−0356	2481212193266230400	DA	14.2 (0.1)	16.79	16.374	16.457	16.58	16.719	16.839	16.28	16.26	16.3
J0138−0459	2480523216087975040	DA+DA	79.21 (0.04)	14.98	12.95	13.076	12.789	12.83	12.863	12.12	11.94	11.92
J0138−1954	5139880551029408768	DA	41.01 (0.04)	16.01	15.598	15.579	15.656	15.75	15.84	15.23	15.1	15.2
J0139−0629	2479327870854949248	DA	11.1 (0.3)	19.82	18.96	18.67	18.56	18.53	18.59	17.76	···	17.6
J0140+3357	317634168937635200	DZ	9.8 (0.4)	19.69	19.06	18.88	18.89	18.93	18.94	18.5	···	···
J0141+2257	290602027028411136	DZ	13.6 (0.2)	18.28	17.44	17.388	17.517	17.71	17.76	17.23	···	···
J0141+3210	303958443311053824	DC	11.0 (0.3)	19.8	19.07	18.83	18.82	18.87	18.9	18.3	···	···
J0142+0730	2568588664341691520	DA	25.2 (0.1)	19.0	17.81	17.379	17.213	17.151	17.17	16.5	15.9	···
J0142+2239	290531967521897856	DC*	14.0 (0.4)	21.8	19.81	19.16	18.87	18.76	18.8	17.93	···	···
J0143+1310	2587491678697364224	DA	11.7 (0.2)	18.11	17.7	17.63	17.669	17.757	17.81	17.14	17.1	17.1
J0145+2317	290678477446232960	DQ	16.4 (0.1)	17.5	17.236	17.17	17.229	17.33	17.4	16.85	···	···
J0145+2918	302388929117252736	DC	24.5 (0.2)	19.94	18.49	17.919	17.7	17.62	17.6	16.71	16.1	15.51
J0145+3132	303637562009656704	DA	27.9 (0.1)	15.26	14.812	14.82	14.91	15.032	15.119	14.472	14.32	14.4
J0146+1404	2587993017344962688	DC	12.1 (0.5)	21.41	19.96	19.46	19.28	19.45	19.54	19.56	20.1	···
J0146+2154	98092934167683072	DA	37.75 (0.04)	15.48	15.072	15.116	15.202	15.333	15.42	14.803	14.8	14.7
J0146+2213	98381792193298176	DC	10.4 (0.3)	19.48	18.99	18.89	18.96	19.0	18.95	18.3	···	···
J0146−0826	2465343629137442816	DQ	14.0 (0.1)	18.07	17.69	17.63	17.667	17.744	17.81	17.2	···	17.1
J0147+3019	302740016924068608	DA	10.5 (0.2)	18.53	18.15	18.167	18.27	18.42	18.41	17.86	···	···
J0147−2711	5025127443016406144	DA	28.3 (0.1)	···	16.505	16.306	16.263	16.292	16.34	15.6	15.4	15.3
J0148+3615	318528007466920192	DA	28.5 (0.1)	···	17.077	16.753	16.658	16.649	16.66	15.86	15.5	15.4
J0148−0555	2467788122659245696	DA	17.2 (0.1)	16.92	16.53	16.514	16.589	16.7	16.77	16.12	···	16.09
J0148−1712	5142197118950177280	DA	13.0 (0.1)	18.23	17.71	17.57	17.56	17.62	17.65	17.0	16.94	16.95
J0149+2400	291186211300158592	DZA*	23.0 (0.1)	16.21	15.971	16.071	16.172	16.325	16.409	15.89	15.7	···
J0150+1524	90367383218249472	DA	11.9 (0.6)	20.3	19.31	19.05	18.93	18.92	18.95	18.13	18.2	17.7
J0150+1720	91460813172927488	DC	11.8 (0.3)	19.9	19.06	18.82	18.74	18.78	18.79	18.1	···	···
J0151+6425	518201792978858880	DA	57.77 (0.02)	14.85	14.041	14.028	14.16	14.22	14.26	···	···	···
J0151−1112	2460778770391950848	DA	15.7 (0.1)	···	16.499	16.545	16.644	16.75	16.851	16.5	16.0	···
J0151−1659	5142174201004781440	DA	10.7 (0.2)	18.62	17.87	17.701	17.65	17.8	17.68	···	···	···
J0151−1957	5136313563510213760	DA	21.0 (0.1)	···	15.79	15.81	15.932	16.081	16.19	15.6	15.5	15.5
J0152+0226	2512446810350495488	DA	11.7 (0.2)	19.03	18.42	18.21	18.174	18.19	18.22	17.49	17.26	17.2
J0152+1436	90076974709491968	DC	11.2 (0.2)	19.27	18.697	18.562	18.55	18.58	18.66	18.04	18.0	18.0
J0152+2418	99064833727036160	DZ	18.9 (0.1)	17.44	16.985	16.917	17.03	17.14	17.19	16.62	16.1	···

Tableau A.1 *suite page suivante*

Tableau A.1 *(suite)*

Name	Gaia DR2/EDR3*	Sp Type	ϖ (mas)	u	g	r	i	z	y	J	H	K
J0152+2553	297470774951165568	DA	28.7 (0.1)	16.23	15.79	15.681	15.684	15.759	15.807	15.15	15.1	15.2
J0153+0911	2569277680172652928	DZ :	12.9 (0.1)	17.25	17.14	17.194	17.31	17.45	17.5	···	···	···
J0153+1218	2575509780797922176	DA	10.7 (0.3)	19.64	19.12	18.98	18.93	18.96	19.01	18.3	18.1	···
J0153+1808	91980130553425536	DAH	21.8 (0.1)	16.86	16.528	16.548	16.653	16.75	16.854	16.27	16.4	···
J0153+3557	342283089327885184	DA	22.9 (0.2)	···	17.2	17.062	17.043	17.1	17.11	16.43	16.0	15.7
J0154+1403	77986298173874176	DQ	16.2 (0.2)	18.43	17.86	17.64	17.62	17.67	17.68	17.07	16.96	16.6
J0154+2537	297399444134124032	DAH	11.4 (0.2)	19.42	18.78	18.61	18.559	18.6	18.66	18.0	···	···
J0154−0426	2492027264515309696	DA	10.0 (0.3)	19.84	19.2	18.9	18.82	18.8	18.76	18.07	18.0	17.8
J0155+0135	2511020022215011072	DC :	11.9 (0.2)	19.0	18.53	18.5	18.521	18.51	18.53	17.88	17.8	17.9
J0156−0100	2505945535535013376	DC	10.8 (0.3)	19.25	18.74	18.57	18.56	18.62	18.68	18.02	17.9	17.8
J0157+1335	77708843286683904	DC	15.9 (0.4)	20.5	19.25	18.66	18.47	18.42	18.4	17.75	17.53	17.5
J0158+1238	2574848772446200960	DA	12.4 (0.1)	18.34	17.91	17.82	17.819	17.89	17.96	17.33	17.16	17.2
J0158+2530	105240786245136256	DC	26.2 (0.2)	22.0	19.33	18.32	17.91	17.73	17.63	16.8	···	···
J0159+1548	78629306318257536	DC	26.3 (0.1)	15.96	15.78	15.847	15.974	16.114	16.213	15.66	15.64	15.64
J0159+6858	521406968152848640	DA	10.2 (0.2)	18.97	18.61	18.51	18.56	18.63	18.68	···	···	···
J0159−1534	5147997450808347648	DA	15.4 (0.1)	18.17	17.656	17.495	17.474	17.53	17.58	···	···	···
J0200+0714	2567842095943560448	DQ	10.2 (0.3)	19.28	18.807	18.66	18.643	18.72	18.77	18.15	18.1	17.6
J0200+1222	2574640823015408128	DC	15.5 (0.2)	17.42	16.5	17.0	16.0	16.86	16.34	16.4	16.3	16.0
J0201+1212	2574620550768898432	DC	31.7 (0.1)	16.72	16.237	16.095	16.125	16.181	16.24	15.57	15.48	15.43
J0201−2650	5024591705975610752	DA	21.9 (0.1)	···	17.159	17.08	17.097	17.15	17.24	16.5	···	···
J0202+1602	78649033103100416	DZ	31.0 (0.1)	21.2	18.42	17.746	17.503	17.413	17.36	16.54	16.35	16.21
J0202+2615	105716359383595136	DA	12.1 (0.4)	20.26	19.34	18.96	18.85	18.79	18.74	18.1	···	···
J0203+2411	104118528470334720	DC	11.0 (0.2)	18.33	17.92	17.76	17.78	17.83	17.87	17.22	···	···
J0203−0701	2490494240363793792	DC	16.0 (0.1)	17.8	17.46	17.39	17.468	17.55	17.61	17.0	16.9	16.9
J0203−1229	5149836834976621056	DC	41.6 (0.1)	14.637	14.535	14.634	14.782	14.939	15.038	14.51	14.5	14.7
J0204+6954	521927243309686656	DA	12.3 (0.2)	19.17	18.54	18.32	18.22	18.25	18.28	···	···	···
J0205+2156	100567105912890496	DQ	9.5 (0.6)	21.1	19.86	19.54	19.47	19.5	19.5	18.8	···	···
J0205−0517	2490975272405858048	DC	30.9 (0.2)	21.31	19.06	18.11	17.66	17.47	17.44	16.56	16.53	16.46
J0206+1836	92597914738232448	DC	27.4 (0.2)	21.29	19.0	18.1	17.74	17.59	17.49	16.65	16.4	15.63
J0206−0057	2506507630789788032	DA	17.6 (0.2)	18.71	18.21	18.08	18.06	18.12	18.17	17.47	17.25	17.3
J0208+3729	330661599315957504	DA	30.2 (0.2)	···	18.07	17.668	17.511	17.476	17.46	16.66	···	···
J0208−0549	2490695859013226240	DA	12.2 (0.2)	19.17	18.52	18.303	18.242	18.25	18.25	17.48	17.29	17.4
J0209−0140	2494399362068211328	DA	17.9 (0.1)	16.57	16.18	16.201	16.318	16.448	16.53	15.92	15.91	15.95
J0210+6500	515466135029128576	DA	11.3 (0.2)	18.92	18.47	18.46	18.47	18.57	18.64	···	···	···

Tableau A.1 *suite page suivante*

Tableau A.1 *(suite)*

Name	Gaia DR2/EDR3*	Sp Type	ϖ (mas)	u	g	r	i	z	y	J	H	K
J0211+1644	80107603996819584	DC	14.8 (0.1)	17.6	17.338	17.351	17.45	17.572	17.66	17.16	···	···
J0211+2209	100445163201292800	DA	12.6 (0.4)	19.64	18.79	18.49	18.38	18.36	18.36	17.63	···	···
J0211+2613	106241174322991360	DA	11.1 (0.2)	18.25	17.927	18.018	18.16	18.31	18.42	17.9	···	···
J0211+3955	333010327952701696	DAZ	58.23 (0.04)	···	14.59	14.46	14.484	14.49	14.531	13.8	13.65	13.63
J0211+7119	522115156720215040	DC	37.0 (0.1)	19.02	17.5	16.94	16.693	16.64	16.59	15.8	15.4	15.3
J0211−0620	2487975808980333184	DA	10.8 (0.2)	18.96	18.5	18.43	18.46	18.53	18.57	17.9	17.68	17.7
J0212+3020	300313218667865344	DA	10.3 (0.3)	19.6	18.91	18.67	18.63	18.63	18.65	18.0	···	···
J0212−0040	2494852597081575808	DA	14.8 (0.3)	19.9	18.89	18.56	18.41	18.39	18.38	17.6	17.27	17.42
J0214+7745	561231932144411008	DC	25.2 (0.2)	···	18.96	18.3	18.0	17.89	17.84	16.5	17.5	15.89
J0214−0505	2488226252817987584	DAH	16.2 (0.2)	17.61	17.28	17.31	17.399	17.516	17.58	17.01	16.94	17.0
J0215+0104	2513144725356809216	DA	13.0 (0.2)	19.7	18.95	18.67	18.6	18.6	18.58	17.82	17.59	17.5
J0215+4453	352179415533582080	DAZ	10.2 (0.5)	19.79	19.04	18.87	18.789	18.82	18.83	18.0	···	···
J0216+3951	332820971434386432	DA	49.08 (0.04)	···	14.596	14.611	14.719	14.833	14.92	14.307	14.2	14.14
J0216+4257	351429930856438656	DA	48.9 (0.1)	···	16.442	15.985	15.791	15.736	15.673	14.98	14.73	14.52
J0217+3234	325134624944612992	DA	17.1 (0.2)	18.3	17.821	17.713	17.712	17.78	17.78	17.14	···	···
J0217−0043	2494710244685483520	DC	12.6 (0.2)	18.82	18.34	18.246	18.276	18.37	18.39	17.85	17.8	17.8
J0217−0656	2486955560973911424	DAZ	22.6 (0.2)	19.68	18.25	17.757	17.554	17.49	17.48	16.6	16.38	16.27
J0218+4648	353917571618022784	DA	12.9 (0.1)	18.37	17.89	17.723	17.72	17.78	17.8	17.16	···	···
J0218+5013	355669578975070976	DA	37.0 (0.1)	···	17.46	16.807	16.532	16.453	16.39	15.5	15.3	15.3
J0218−0919	5176159517007960576	DZ	10.4 (0.1)	17.48	17.36	17.461	17.615	17.79	17.9	17.41	···	17.5
J0219−0820	2486189510606565760	DA	10.4 (0.3)	20.16	19.56	19.32	19.23	19.21	19.17	18.52	···	18.2
J0220+3520	327766649623335296	DA	23.8 (0.1)	···	17.904	17.515	17.365	17.34	17.31	16.53	15.87	16.02
J0221+0445	2516606022320239104	DA	25.4 (0.1)	17.04	16.558	16.43	16.424	16.473	16.503	15.82	15.65	15.63
J0221+5333	455517329408362752	DC	34.4 (0.1)	···	16.347	16.147	16.12	16.12	15.9	15.0	15.0	15.1
J0223+2055	87648226538760064	DC	26.3 (0.2)	21.4	18.97	18.13	17.773	17.66	17.59	16.72	16.72	17.15
J0223+2629	103440095437050752	DA	12.0 (0.1)	18.32	17.81	17.71	17.74	17.795	17.83	17.18	···	···
J0223+5544	457474219590579328	DA	26.0 (0.1)	···	17.08	16.91	16.86	16.9	16.91	16.1	15.8	15.7
J0224+2325	101673523847748736	DA	16.0 (0.3)	21.0	19.22	18.63	18.39	18.3	18.24	17.38	···	···
J0224+4007	338094538438744320	DA	23.8 (0.1)	···	17.493	17.157	17.021	17.009	17.01	16.22	16.1	15.4
J0224−0242	2490455242060751360	DA	13.5 (0.4)	21.4	19.58	19.05	18.82	18.79	18.76	17.92	17.8	17.59
J0224−2854	5068532996689788544	DC	34.5 (0.1)	···	18.23	18.1	18.56	18.95	19.1	19.09	19.4	···
J0225+0545	2517080495947872896	DA	12.2 (0.3)	18.69	17.868	17.785	17.817	17.89	17.94	17.23	···	17.2
J0225+2410	101854122928108288	DC	13.6 (0.1)	17.82	17.526	17.5	17.583	17.7	17.79	17.18	···	···
J0225+4228	339492017717622016	DA	19.8 (0.2)	···	17.602	17.335	17.21	17.22	17.24	16.47	16.3	16.2

Tableau A.1 *suite page suivante*

Tableau A.1 *(suite)*

Name	Gaia DR2/EDR3*	Sp Type	ϖ (mas)	u	g	r	i	z	y	J	H	K
J0225+4228	339492052075797376	DC	19.9 (0.4)	···	19.8	18.94	18.57	18.42	18.36	17.47	···	···
J0225−1756	5131731035268115584	DA	14.9 (0.2)	19.31	18.467	18.15	18.044	18.04	18.01	17.25	···	16.9
J0225−1756	5131731039563630720	DC	14.9 (0.2)	17.79	17.48	17.403	17.477	17.56	17.65	17.04	···	16.9
J0226+6459	515289392829738624	DC	32.4 (0.1)	···	18.8	17.87	17.48	17.33	17.24	16.35	16.06	15.98
J0227+1807	85787470611883008	DA	26.7 (0.1)	···	15.58	15.572	15.642	15.736	15.7	15.2	15.0	14.9
J0227+5915	459237630076876672	DA	26.6 (0.1)	···	16.126	16.0	16.0	16.04	16.071	15.3	15.3	15.3
J0230+2508	102390302349905024	DAH	11.6 (0.3)	20.3	19.26	18.88	18.737	18.67	18.67	17.8	···	···
J0231+0810	19693180966870656	DC	25.7 (0.1)	···	17.512	17.17	17.034	17.017	17.0	16.27	16.15	16.31
J0231+2709	127366331745660288	DC*	35.5 (0.1)	19.58	17.74	17.061	16.793	16.69	16.63	15.8	15.4	15.3
J0231+2859	131188715200383872	DA	35.9 (0.4)	···	15.2401	15.058	15.036	15.066	15.096	14.41	14.2	14.3
J0232+0645	19252624696630016	DA	9.9 (0.2)	18.43	18.28	18.26	18.316	18.44	18.5	17.9	17.8	17.9
J0232+5211	452157015712452608	DA	12.6 (0.1)	···	16.99	17.029	17.14	17.267	17.35	16.75	···	···
J0232−1412	5146358426863612160	DA	60.0 (0.1)	···	16.023	15.558	15.372	15.34	15.292	14.473	14.26	14.13
J0233+2125	88996326578456192	DC	35.2 (0.1)	19.86	17.897	17.174	16.906	16.795	16.74	15.87	15.4	15.7
J0234+2407	102038286830643840	DA	14.9 (0.3)	20.24	18.99	18.55	18.36	18.32	18.27	17.46	···	···
J0234+2802	127700269747929344	DA	13.1 (0.4)	20.5	19.32	18.88	18.696	18.63	18.61	17.85	···	···
J0235+0118	2502097283492466560	DA :	30.2 (0.1)	16.99	16.38	16.179	16.134	16.149	16.167	15.44	15.22	15.22
J0235+0729	19399306419780224	DQ	12.5 (0.3)	19.45	19.27	18.73	18.59	18.67	18.74	18.16	···	···
J0235−2251	5125500927507946880	DA	21.5 (0.1)	···	17.322	17.084	16.992	17.01	17.03	16.24	15.8	16.04
J0235−2400	5125186299678747008	DC	54.07 (0.05)	···	16.29	15.673	15.38	15.299	15.21	14.45	14.34	14.1
J0237+1638	81606375784491520	DC	31.2 (0.1)	···	17.46	17.029	16.86	16.805	16.79	16.04	15.8	14.88
J0239+2609	126342377182577408	DA	48.0 (0.1)	17.55	16.354	15.95	15.777	15.73	15.711	14.91	14.61	14.5
J0239+7300	545997618721866624	DA	15.3 (0.1)	17.57	17.145	17.052	17.083	17.165	17.2	16.4	16.4	···
J0240+2701	126972461769858816	DA	21.5 (0.2)	20.5	19.03	18.49	18.274	18.2	18.21	···	···	···
J0240+3142	133116227803380224	DA	30.2 (0.1)	16.69	16.19	16.046	16.04	16.08	16.12	15.42	15.2	14.9
J0241+7442	548423278811480960	DA	20.59 (0.04)	16.39	16.01	16.05	16.097	16.2427	16.33	15.6	15.5	15.6
J0242+1112	25405350031335296	DAH	29.5 (0.1)	···	16.215	16.162	16.22	16.327	16.38	15.74	15.9	15.4
J0242+1655	81957772828837888	DQ	23.7 (0.1)	···	17.198	16.71	16.887	16.898	16.97	16.34	16.4	···
J0244−0142	2496042440461991296	DAH	15.9 (0.1)	17.08	17.064	17.117	17.222	17.381	17.46	16.88	···	17.0
J0245+2825	128707181880407680	DA	14.2 (0.3)	21.0	19.37	18.84	18.63	18.55	18.5	17.66	···	···
J0245−1951	5128633195616949120	DC	31.1 (0.1)	···	18.71	17.81	17.46	17.31	17.22	16.33	16.4	16.13
J0246−0227	2495751967528809216	DAZ	46.6 (0.1)	16.27	15.633	15.431	15.404	15.421	15.451	14.702	14.59	14.48
J0248+3408	139937559287208192	DQ	13.0 (0.3)	19.53	18.75	18.45	18.351	18.38	18.45	···	···	···
J0248+5423	453562088496088320	DAZ	92.03 (0.04)	···	15.71	15.087	14.861	14.758	14.716	13.858	13.54	13.47

Tableau A.1 *suite page suivante*

Tableau A.1 *(suite)*

Name	Gaia DR2/EDR3*	Sp Type	ϖ (mas)	u	g	r	i	z	y	J	H	K
J0249+1939	85008707141970304	DC	11.7 (0.4)	19.87	19.13	18.91	18.853	18.88	18.8	18.1	···	···
J0249+3307	139623068897753856	DA	28.0 (0.1)	18.48	17.373	16.978	16.82	16.784	16.78	15.97	15.5	15.4
J0249+4336	337449812306056832	DC	18.9 (0.3)	21.1	19.27	18.53	18.25	18.15	17.99	17.17	···	···
J0250+0817	20484382662003968	DC	26.0 (0.2)	···	18.75	17.937	17.606	17.48	17.421	16.2	16.3	···
J0250+2116	85469849190835968	DA	12.6 (0.2)	19.2	18.51	18.26	18.19	18.22	18.22	17.53	···	···
J0250−0437	5184589747536175104	DAH :	10.9 (0.2)	17.97	17.96	18.13	18.28	18.38	18.53	···	···	···
J0250−0910	5174110233491949312	DA	12.8 (0.5)	20.07	18.88	18.45	18.28	18.24	18.2	17.41	17.14	17.0
J0251+2925	128826375813389568	DC	12.2 (0.2)	18.95	18.48	18.34	18.331	18.39	18.48	17.82	···	···
J0251+7341	547501815051141248	DZ	16.3 (0.1)	17.68	17.26	17.226	17.301	17.43	17.52	16.93	16.85	16.84
J0253+0013	2498159515741377152	DA	14.7 (0.2)	17.79	17.34	17.277	17.273	17.35	17.41	16.79	16.65	16.5
J0253+3759	143076256963396480	DA	26.9 (0.1)	···	16.69	16.471	16.412	16.43	16.45	15.7	15.3	15.5
J0253−0033	2497895053130247040	DA	21.2 (0.1)	16.61	16.434	16.361	16.41	16.5	16.52	15.9	15.75	15.83
J0255+0237	1559111783825792	DA	14.8 (0.1)	17.66	17.267	17.287	17.329	17.449	17.53	16.92	···	···
J0255+2106	109247788869176448	DA	20.0 (0.1)	18.42	17.66	17.37	17.271	17.259	17.27	16.5	16.0	16.1
J0255−0715	5180494685197598464	DAH	10.0 (0.3)	19.23	18.72	18.6	18.584	18.64	18.69	18.02	···	17.9
J0256+0511	5526420319283584	DA	10.9 (0.4)	20.9	19.61	19.12	18.922	18.88	18.92	18.1	17.9	17.9
J0256+4954	439494077735062144	DA	26.6 (0.1)	···	17.428	17.096	16.968	16.961	16.96	16.19	15.8	15.45
J0256−0700	5180517706222368768	DC	16.3 (0.2)	20.7	18.87	18.09	17.8	17.72	17.66	16.71	16.62	16.5
J0257+0152	1268321022907264	DA	20.8 (0.2)	18.37	17.45	17.23	17.15	17.18	17.11	16.41	16.21	16.17
J0257+0620	7158988928491776	DA	12.1 (0.6)	21.5	20.08	19.39	19.16	19.07	18.98	···	···	···
J0258+0030	74698071455360	DA	14.5 (0.4)	20.04	19.11	18.84	18.74	18.73	18.75	18.05	17.7	17.7
J0258+3421	137141810455464192	DC	10.8 (0.3)	19.5	18.84	18.645	18.6	18.63	18.72	18.1	···	···
J0259+0811	8578256576520320	DAH	33.9 (0.1)	···	16.02	15.816	15.736	15.74	15.756	15.03	14.7	14.8
J0259+1725	35497904701569920	DA	14.3 (0.3)	···	19.21	18.637	18.4	18.32	18.26	17.43	···	···
J0300+5432	447366340472109440	DA	20.7 (0.1)	···	16.746	16.64	16.655	16.74	16.76	16.1	15.9	15.93
J0301−0044	5188044687948351872	DC	14.5 (0.5)	22.9	20.28	19.45	19.046	18.91	18.84	17.96	17.73	17.7
J0302+0622	7027562929324416	DA	11.6 (0.2)	19.05	18.44	18.25	18.2	18.22	18.18	17.63	17.44	17.4
J0303+0002	3266576684513815168	DA	10.4 (0.2)	18.27	17.85	17.81	17.869	17.97	18.04	17.31	17.36	17.4
J0303+0317	1843503042736512	DC	10.7 (0.5)	20.04	19.26	18.97	18.93	19.03	19.05	18.5	···	···
J0303+1921	60007152756147584	DC	14.9 (0.2)	19.13	18.49	18.27	18.2	18.23	18.29	17.52	···	···
J0303−0011	3266534357610950912	DC	15.5 (0.4)	21.3	19.21	18.57	18.288	18.18	18.14	17.29	16.98	17.0
J0305+2603	115409280235239296	DA	21.4 (0.2)	···	18.43	17.901	17.67	17.61	17.59	16.76	16.3	15.77
J0306−0638	5180178266367085312	DA	12.5 (0.2)	18.33	17.89	17.8	17.823	17.89	17.96	17.3	···	17.2
J0306−2029	5103714555575829888	DA	16.8 (0.1)	···	16.201	16.286	16.4	16.587	16.67	16.08	16.0	16.09

Tableau A.1 *suite page suivante*

Tableau A.1 *(suite)*

Name	Gaia DR2/EDR3*	Sp Type	ϖ (mas)	u	g	r	i	z	y	J	H	K
J0307+0936	14862584004642688	DC	20.6 (0.1)	18.53	17.668	17.49	17.5	17.57	17.61	16.94	···	···
J0307+1540	31322547949728256	DC :	17.3 (0.4)	···	20.11	19.17	18.79	18.67	18.49	17.72	···	···
J0307−0715	5179920984941553408	DA	32.9 (0.1)	18.59	17.57	17.169	17.027	17.0	16.97	16.2	15.95	15.87
J0308+0040	3267081566509086592	DA	11.3 (0.2)	18.86	18.31	18.23	18.25	18.29	18.34	17.71	17.6	17.6
J0308+4047	239109213145234560	DA	10.3 (0.5)	20.83	19.77	19.37	19.17	19.18	19.1	18.4	···	···
J0308+5128	439905192004402304	DA	27.2 (0.1)	···	18.0	17.451	17.25	17.172	17.11	16.2	15.9	15.6
J0309+0025	3266873724451739776	DC	23.3 (0.2)	19.24	18.16	17.715	17.532	17.482	17.48	16.64	16.54	16.87
J0309+0953	14895255820376064	DC	10.0 (0.3)	19.95	19.23	18.96	18.87	18.89	18.91	18.3	···	···
J0310+0757	13611477211053824	DAZ	15.2 (0.1)	···	16.211	16.313	16.458	16.625	16.73	16.18	16.0	···
J0310+5309	446263083632852608	DC	14.3 (0.1)	···	16.9	16.875	16.96	17.069	17.14	16.59	16.52	16.54
J0310+6633	492442090962517376	DC	26.1 (0.1)	···	18.591	17.865	17.56	17.46	17.406	16.6	16.3	15.31
J0311−0551	5181816233750415488	DC	31.4 (0.2)	···	19.05	18.06	17.638	17.48	17.38	16.7	···	···
J0311−0853	5167424240722533760	DA	25.7 (0.2)	···	18.16	17.58	17.342	17.243	17.21	16.6	16.0	···
J0312+2218	62311183668001664	DA	15.7 (0.1)	···	17.19	16.923	16.833	16.825	16.83	16.07	15.9	15.9
J0313+3251	125339755721933440	DA	9.9 (0.2)	···	17.31	17.372	17.501	17.623	17.76	17.19	···	17.2
J0314−0105	3265311627666274944	DA	16.0 (0.2)	19.61	18.52	18.144	17.993	17.94	17.93	17.08	16.82	16.8
J0314−0815	5167525434447523712	DQ	14.3 (0.1)	16.98	16.832	16.91	17.053	17.19	17.3	16.74	16.89	16.7
J0316+3932	235842052999634944	DC	26.4 (0.1)	16.021	15.803	15.84	15.95	16.08	16.16	15.58	15.5	15.6
J0316−0816	5167510797199003904	DA	31.9 (0.1)	17.69	16.95	16.701	16.64	16.64	16.66	15.91	15.9	15.67
J0317−2911	5058635403471767680	DAZ	31.7 (0.1)	···	17.67	17.202	17.004	16.96	16.94	16.0	15.8	15.76
J0318+0212	3268703483599047296	DA	19.4 (0.2)	18.25	17.77	17.657	17.637	17.705	17.74	17.04	16.4	···
J0318+1414	30048866808843648	DA	13.4 (0.1)	···	17.121	17.181	17.329	17.472	17.57	17.0	···	···
J0319+3630	234469931207274112	DZ	31.2 (0.1)	···	16.46	16.325	16.377	16.477	16.53	15.93	15.8	15.4
J0319−2109	5100053078775660160	DA	20.4 (0.1)	···	15.74	15.805	15.933	16.077	16.2	15.597	15.6	15.58
J0320+1113	16166875378033664	DA	10.2 (0.2)	18.58	18.2	18.117	18.12	18.2	18.26	17.53	···	···
J0320+1113	16166875377576064	DA	10.6 (0.4)	19.86	19.09	18.88	18.8	18.85	18.85	18.14	···	···
J0320+2333	62884540326096896	DC	25.5 (0.2)	···	18.37	17.53	17.157	17.012	16.94	16.08	15.6	15.8
J0320+4337	241335036997623296	DC	10.1 (0.3)	19.75	19.15	18.96	18.93	18.97	19.17	18.4	···	···
J0321+1757	56048945255703680	DA	17.3 (0.2)	20.4	18.97	18.443	18.257	18.2	18.16	17.3	···	···
J0322+2708	117651695542992256	DA	10.7 (0.2)	···	18.024	17.96	17.97	18.04	18.1	17.49	16.7	17.2
J0324−0617	5169733318219971968	DA	11.0 (0.2)	18.73	18.21	18.099	18.08	18.16	18.16	17.43	···	17.4
J0325+1509	42174998299513728	DA	11.0 (0.2)	···	18.192	18.09	18.11	18.19	18.22	17.61	···	···
J0325+1509	42175002593812864	DC	11.5 (0.7)	···	0.0	20.01	19.75	19.59	19.53	18.8	···	···
J0325+1701	54993654611672704	DC	10.6 (0.2)	19.14	18.35	18.31	18.397	18.51	18.59	18.02	···	···

Tableau A.1 *suite page suivante*

Tableau A.1 *(suite)*

Name	Gaia DR2/EDR3*	Sp Type	ϖ (mas)	u	g	r	i	z	y	J	H	K
J0325+1824	55981600168846080	DA	9.9 (0.4)	19.85	19.09	18.84	18.768	18.78	18.79	···	···	···
J0325−0149	3261591090771914240	DAZH	59.1 (0.1)	···	16.4	15.868	15.6645	15.593	15.59	14.63	14.37	14.28
J0325−1722	5105681684956745728	DA	18.0 (0.1)	···	17.301	17.128	17.092	17.13	17.1	16.41	16.1	16.21
J0326+1557	54253618862057728	DA	26.1 (0.1)	···	17.792	17.402	17.261	17.23	17.24	16.4	16.4	···
J0327+0451	3275575603071739136	DC	9.6 (0.5)	21.0	19.92	19.59	19.43	19.35	19.39	18.5	18.2	17.7
J0327+1729	55103056018558592	DC*	14.6 (0.5)	21.1	19.68	19.17	18.96	18.94	18.98	18.7	···	···
J0327+4623	242802266545591936	DA	11.7 (0.1)	17.92	17.49	17.42	17.445	17.53	17.6	16.93	16.82	16.9
J0327−0636	5168947721457740288	DA	15.7 (0.2)	18.01	17.54	17.46	17.464	17.521	17.58	16.72	···	16.8
J0328+2631	117690801219527168	DA :	13.3 (0.2)	···	18.1	17.88	17.8	17.78	17.61	···	···	···
J0328−2718	5060587895604134400	DA	43.43 (0.04)	14.42	13.675	13.657	13.71	13.836	13.889	13.2	13.1	13.1
J0329−0555	3247469130928600960	DA	11.0 (0.4)	21.4	19.8	19.33	19.12	19.07	19.04	18.1	···	18.1
J0330+0037	3264828357946121984	DA	10.1 (0.4)	20.8	19.72	19.34	19.19	19.14	19.13	18.35	18.16	18.1
J0330+7401	544718680539607680	DC	18.5 (0.1)	···	16.892	16.84	16.92	17.01	17.06	16.5	16.2	···
J0331+4509	241745640169579776	DA	13.1 (0.1)	18.13	17.74	17.72	17.787	17.9	17.97	17.34	17.29	17.4
J0331+4736	248937133409693440	DA	11.6 (0.1)	17.89	17.511	17.479	17.55	17.662	17.73	17.15	17.08	17.26
J0333+0007	3264551560189562112	DAH	28.3 (0.1)	17.03	16.54	16.43	16.398	16.49	16.56	15.93	15.88	15.84
J0333+0656	3276355500412926336	DZ	10.1 (0.4)	19.27	18.63	18.55	18.616	18.73	18.81	18.16	···	···
J0333+4427	238653229356266752	DA	13.0 (0.2)	18.3	17.94	17.97	18.07	18.17	18.28	17.67	···	···
J0335+3211	121519060190456960	DA	20.9 (0.1)	···	15.454	15.55	15.705	15.862	15.988	15.43	15.4	15.41
J0336−2215	5088251195844051328	DAZ	26.0 (0.1)	···	17.31	16.959	16.826	16.814	16.79	16.0	15.6	15.68
J0338+0409	3274761620869767168	DA	14.5 (0.1)	17.1	16.706	16.701	16.771	16.883	16.98	16.37	16.27	16.27
J0339+1431	41518658576469760	DA	10.2 (0.4)	19.94	19.19	18.99	18.89	18.88	18.92	18.2	···	···
J0340+0537	3275218193073023360	DC	10.6 (0.3)	19.92	19.24	19.02	18.953	18.99	18.99	18.4	···	···
J0340−0029	3263484003117848832	DA	19.6 (0.1)	17.72	17.23	17.078	17.053	17.104	17.15	16.42	16.32	16.3
J0341+3818	224218080493203328	DA	10.6 (0.2)	19.37	18.89	18.75	18.75	18.78	18.85	···	···	18.2
J0342+3920	224331059611503232	DC	14.0 (0.1)	17.52	17.28	17.31	17.4	17.52	17.59	17.04	···	17.01
J0343+1958	63126196662620416	DA	48.1 (0.1)	···	15.81	15.66	15.642	15.68	15.73	15.02	14.81	14.81
J0344+1509	42871199614383616	DA	18.3 (0.1)	17.26	16.899	16.88	16.917	17.02	17.1	16.48	16.6	···
J0344+1510	42871268333859584	DC	18.4 (0.1)	16.97	16.534	16.519	16.569	16.668	16.75	16.1	16.2	···
J0344+1705	44478578238260864	DA	10.6 (0.2)	18.15	17.675	17.64	17.69	17.82	17.85	17.28	···	···
J0344+1825	44901791432527232	DQ	53.0 (0.05)	···	15.27	15.066	15.066	15.12	15.17	14.56	14.35	14.4
J0344+3532	221424221446885248	DA	11.6 (0.3)	19.65	18.93	18.699	18.6	18.6	18.62	···	···	17.5
J0345−0348	3249479592235301376	DA	32.2 (0.1)	···	17.721	17.13	16.881	16.782	16.75	15.8	16.0	15.7
J0345−0348	3249479592234269056	DC	32.2 (0.1)	···	18.59	17.735	17.381	17.242	17.18	16.3	16.4	···

Tableau A.1 *suite page suivante*

Tableau A.1 *(suite)*

Name	Gaia DR2/EDR3*	Sp Type	ϖ (mas)	u	g	r	i	z	y	J	H	K
J0346+2455	66837563803594880	DC	25.2 (0.3)	···	19.55	18.54	18.09	17.97	17.93	17.6	17.9	19.0
J0347+0138	3270079526697712768	DC	49.6 (0.1)	···	16.859	16.243	15.98	15.9	15.87	14.98	14.9	14.7
J0347+0520	3276414466021403264	DC	13.7 (0.2)	18.63	18.17	18.053	18.07	18.14	18.18	17.6	···	···
J0348+8048	568168544844912128	DC	16.6 (0.1)	18.57	17.946	17.732	17.698	17.77	17.77	···	···	···
J0352+3658	220421260684140288	DA	10.0 (0.3)	19.77	19.2	19.0	18.979	18.98	19.09	···	···	18.2
J0352+4941	250278709394343936	DA	17.7 (0.1)	17.87	17.393	17.252	17.26	17.32	17.35	16.68	16.53	16.54
J0353+1037	3303137301563100544	DC*	10.8 (0.4)	20.6	19.5	19.19	19.05	19.06	19.07	18.4	···	···
J0354+0523	3273645105468368000	DA	12.2 (0.1)	···	16.613	16.717	16.875	17.031	17.16	16.56	···	···
J0354−0044	3256598792586547584	DA	20.3 (0.1)	18.1	17.32	17.006	16.873	16.852	16.85	16.04	15.84	15.75
J0355+4525	244214799689691904	DA	31.7 (0.1)	···	17.71	17.133	16.904	16.826	16.78	16.0	15.7	···
J0357+1915	50456318016101120	DAH	15.4 (0.2)	19.47	18.53	18.197	18.076	18.05	18.01	17.35	17.12	17.2
J0358+2157	53278867446391040	DAZ	27.6 (0.1)	···	16.868	16.675	16.621	16.653	16.68	16.1	15.6	15.6
J0358+2538	67156078578517888	DC :	14.7 (0.2)	···	18.62	18.27	18.06	18.03	18.0	17.54	17.37	17.27
J0358+5549	468737616704971136	DA	18.2 (0.1)	···	16.627	16.578	16.624	16.713	16.79	16.14	16.01	16.09
J0359+7055	495058241441193728	DC	15.2 (0.2)	···	18.85	18.52	18.24	18.14	17.88	···	···	···
J0359−1118	3193194629937678464	DC	18.0 (0.1)	18.14	17.62	17.45	17.441	17.47	17.56	16.93	···	16.8
J0400+0814	3301319572621418368	DA	53.8 (0.1)	···	16.129	15.69	15.49	15.444	15.428	14.584	14.3	14.1
J0401+5131	250862824946594816	DC	39.9 (0.1)	19.36	17.669	17.08	16.85	16.792	16.76	15.94	15.67	15.58
J0402+1527	39387328302768640	DC	27.1 (0.1)	17.31	16.8	16.659	16.66	16.74	16.79	16.13	15.9	16.0
J0404−0523	3197508598168785408	DA	11.2 (0.1)	17.97	17.57	17.537	17.599	17.71	17.79	17.14	···	17.2
J0405+2643	162653160663515008	DC	22.9 (0.3)	···	19.69	18.64	18.194	18.03	17.93	17.09	17.04	17.7
J0406+3323	170648503898774912	DA	10.6 (0.1)	···	17.543	17.544	17.636	17.74	17.82	···	···	17.3
J0406−0432	3251618000616770560	DA	20.3 (0.1)	18.12	17.43	17.16	17.105	17.111	17.13	16.32	16.1	16.09
J0406−0515	3197515087862709888	DA	10.3 (0.3)	19.99	19.3	19.12	19.05	19.1	19.14	18.4	···	···
J0406−0644	3197019139399144320	DA	13.7 (0.2)	18.87	17.963	17.594	17.446	17.44	17.42	16.59	16.44	16.27
J0408+2921	164297449857329408	DA	16.1 (0.1)	···	17.076	16.995	17.037	17.105	17.16	16.5	16.44	16.36
J0410+1954	48829075167625472	DC	34.2 (0.2)	19.65	18.02	17.454	17.23	17.145	17.12	16.26	16.03	15.82
J0411+1558	45293488153371776	DC :	12.4 (0.3)	19.93	19.07	18.74	18.618	18.64	18.66	18.0	···	···
J0412+2354	149824883240282496	DC :	12.8 (0.2)	···	18.7	18.53	18.54	18.59	18.8	18.0	···	18.0
J0412+7549	551153263105246208	DAH :*	28.48 (0.05)	···	15.916	15.9	15.948	16.047	16.12	15.5	15.4	15.5
J0412−1117	3189621320226676736	DAP	28.5 (0.1)	···	15.547	15.424	15.426	15.49	15.55	14.81	14.7	14.7
J0413+1512	3311801796791224192	DC	11.5 (0.8)	22.3	20.58	19.84	19.52	19.46	19.35	18.4	···	18.5
J0413+1522	3311813685256807040	DC	14.6 (0.2)	19.53	18.8	18.497	18.39	18.38	18.4	17.75	···	17.5
J0413+2433	149884909703520000	DC	10.9 (0.4)	20.05	19.18	18.94	18.86	18.85	18.8	18.4	···	18.1

Tableau A.1 *suite page suivante*

Tableau A.1 *(suite)*

Name	Gaia DR2/EDR3*	Sp Type	ϖ (mas)	u	g	r	i	z	y	J	H	K
J0413−0801	3195883481327214848	DA	17.5 (0.1)	···	16.298	16.31	16.403	16.531	16.605	16.0	15.7	15.94
J0416+2947	165677710612522752	DZ	10.9 (0.2)	19.12	18.5	18.39	18.427	18.54	18.65	18.1	···	17.9
J0416+5456	276438530560644864	DC	13.9 (0.1)	18.07	17.718	17.64	17.681	17.784	17.834	17.29	···	17.2
J0418+3022	166091096919353088	DC	10.9 (0.3)	19.69	19.0	18.78	18.73	18.76	18.78	18.12	18.0	18.0
J0418+4210	229143725086190336	DA	33.7 (0.1)	···	17.54	16.949	16.72	16.633	16.6	15.7	15.4	15.34
J0419−0934	3191738120628213760	DAP	27.5 (0.1)	···	17.64	17.308	17.191	17.22	17.19	16.4	15.8	16.2
J0420+1952	49013483883923968	DA	15.8 (0.2)	18.75	18.04	17.785	17.705	17.726	17.75	17.02	···	···
J0420+2617	150577636388844160	DA	11.2 (0.2)	19.34	18.62	18.4	18.331	18.33	18.36	17.67	···	17.4
J0421+4607	232990572675079296	DA	37.62 (0.04)	···	15.27	15.201	15.232	15.309	15.374	14.72	14.51	14.4
J0421+5535	276576484910598912	DC	16.9 (0.1)	18.24	17.8	17.66	17.67	17.75	17.83	17.12	17.11	17.0
J0421−1600	3175193288128400896	DA	21.3 (0.1)	···	17.55	17.28	17.21	17.277	17.2	16.49	16.1	16.3
J0422+0038	3254930932230273664	DZ	12.5 (0.3)	19.23	18.501	18.35	18.39	18.44	18.51	17.9	···	···
J0422+2641	152091973137497216	DC	15.5 (0.3)	20.39	19.03	18.6	18.41	18.37	18.35	···	17.1	17.2
J0422+3357	175817750438186240	DA	10.5 (0.2)	19.12	18.552	18.372	18.319	18.36	18.35	···	···	17.6
J0423+5006	270485053053115648	DC	18.4 (0.1)	···	16.14	16.234	16.384	16.55	16.67	16.14	···	16.01
J0423+5745	470639806179201792	DC	26.7 (0.1)	···	16.724	16.596	16.63	16.716	16.77	16.1	···	···
J0424+3038	165401149074789504	DC	10.2 (0.3)	19.15	18.7	18.58	18.599	18.66	18.7	18.1	17.9	18.3
J0425+1211	3307009304776119936	DC	62.38 (0.04)	···	15.567	15.289	15.188	15.203	15.222	14.485	14.35	14.2
J0425+2834	152931141027253888	DZ	15.5 (0.3)	19.45	18.5	18.233	18.168	18.19	18.23	17.56	17.37	17.34
J0425+4614	256832412872262656	DC	26.9 (0.3)	···	19.25	18.53	18.21	18.0	17.97	16.42	15.96	15.78
J0426+0432	3283853143218651264	DA	47.0 (0.1)	···	17.479	16.825	16.557	16.45	16.43	15.55	15.2	15.2
J0426−0347	3204665315057342336	DC	16.1 (0.2)	19.38	18.6	18.262	18.136	18.143	18.12	···	···	···
J0427−0708	3198881613315343872	DC	25.2 (0.1)	···	16.904	16.754	16.75	16.809	16.84	16.3	16.1	15.6
J0428+0006	3254620732512634624	DA	11.4 (0.4)	19.24	18.61	18.42	18.39	18.41	18.42	17.73	···	···
J0428+0052	3278914205706332928	DA	11.5 (0.1)	17.24	16.82	16.92	17.062	17.213	17.34	16.77	···	···
J0428+1044	3305972018634634880	DA	15.1 (0.1)	···	16.923	17.014	17.149	17.3	17.43	16.9	···	16.9
J0429+2159	145429108768875008	DC	22.9 (0.1)	16.85	16.562	16.541	16.629	16.737	16.81	16.22	16.21	16.21
J0429+4945	258761510321879424	DA	18.5 (0.1)	···	16.53	16.496	16.555	16.658	16.74	16.11	16.0	16.07
J0430+0941	3293635012838798464	DA	11.2 (0.2)	18.99	18.45	18.3	18.25	18.27	18.29	17.59	···	17.4
J0430+1611	3312860733860742272	DA	17.7 (0.1)	···	16.537	16.525	16.58	16.683	16.77	16.16	16.07	16.06
J0431+5858	470826482635701376	DC	181.28 (0.05)	···	12.9	0.0	13.555	13.16	12.62	11.84	11.73	11.68
J0432−1920	2978374522004181888	DA	29.4 (0.1)	···	17.27	16.895	16.732	16.7	16.7	16.0	15.6	15.7
J0433+0414	3282093301842469376	DA	41.2 (0.1)	···	17.495	16.866	16.621	16.54	16.49	15.65	15.3	15.2
J0433+5527	277090540953615616	DA	13.5 (0.1)	17.25	16.96	16.952	17.05	17.15	17.18	16.67	16.56	16.73

Tableau A.1 *suite page suivante*

Tableau A.1 *(suite)*

Name	Gaia DR2/EDR3*	Sp Type	ϖ (mas)	u	g	r	i	z	y	J	H	K
J0433−2753	4891567154251463680	DA*	43.0 (0.1)	···	17.11	16.552	16.331	16.269	16.227	15.342	15.1	14.99
J0434+3054	159277625222514048	DC	29.4 (0.2)	···	18.47	17.8	17.516	17.41	17.39	16.51	16.28	16.19
J0435−2240	4898310149826754304	DA	13.0 (0.1)	···	16.5	16.602	16.75	16.9	17.03	16.46	···	16.51
J0436+2709	151650935831913216	DA	57.5 (0.1)	···	16.04	15.61	15.439	15.38	15.38	14.6	14.12	14.21
J0436+4047	203828633790026496	DA	13.5 (0.1)	···	16.6	16.684	16.819	16.97	17.1	16.53	16.44	16.55
J0436+5537	277138090534130560	DA	13.4 (0.2)	18.62	18.13	17.99	17.97	18.02	18.05	17.42	17.28	17.4
J0437−0849	3186021141200137472	DQ	106.27 (0.02)	···	13.863	13.617	13.582	13.656	13.67	13.0	12.85	12.79
J0439+0928	3293451020735654272	DC	13.1 (0.1)	17.25	17.123	17.17	17.3	17.46	17.56	17.13	···	17.2
J0439−0405	3201594074140023936	DA	19.1 (0.1)	16.96	16.559	16.501	16.538	16.65	16.68	···	···	···
J0440+0923	3292685210887016192	DA	30.8 (0.1)	17.84	17.093	16.83	16.71	16.75	16.75	15.96	15.6	15.6
J0441+2042	3411147173483832320	DA	11.1 (0.2)	18.35	17.85	17.733	17.748	17.8	17.84	17.11	···	16.9
J0441−0042	3229556024930689024	DC	14.0 (0.2)	19.46	18.6	18.27	18.17	18.16	18.14	17.37	···	17.1
J0441−0551	3200232157189930880	DQ	15.2 (0.1)	17.63	17.35	17.307	17.371	17.5	17.53	16.8	···	···
J0441−1519	3173236054352419072	DA	27.1 (0.1)	···	17.189	16.862	16.75	16.734	16.71	15.94	15.9	15.62
J0443+5106	260218878625842816	DA	23.2 (0.1)	···	15.976	15.954	16.019	16.12	16.2	15.566	15.46	15.47
J0443−0607	3199980330371548800	DA	10.7 (0.4)	21.0	19.85	19.4	19.18	19.17	19.11	18.3	···	···
J0445+0050	3230171064244273024	DZ	12.8 (0.3)	19.74	18.66	18.469	18.49	18.54	18.61	17.93	···	···
J0445−0618	3187950092615927552	DA	16.3 (0.1)	18.52	17.869	17.626	17.542	17.55	17.59	16.81	···	16.6
J0445−2726	4881098119928195456	DC*	25.0 (0.1)	···	16.755	16.6	16.608	16.685	16.73	16.03	15.8	15.89
J0447+0106	3231702860037325824	DZ	15.5 (0.2)	19.17	18.45	18.22	18.141	18.17	18.2	17.43	···	···
J0449−1806	2979519903882838528	DA :*	24.82 (0.04)	···	16.05	15.977	15.996	16.07	16.13	15.46	···	15.32
J0452−0043	3226718494654224256	DA	10.2 (0.4)	20.3	19.39	19.09	18.99	18.95	18.98	18.19	···	17.8
J0453−0457	3188530840914150144	DC	14.0 (0.2)	17.52	17.27	17.272	17.38	17.522	17.59	17.02	16.97	16.95
J0454+1027	3294543969653440256	DA	18.9 (0.1)	···	16.868	16.78	16.79	16.83	16.86	16.19	15.9	15.97
J0454+1218	3295332796231463168	DA	10.5 (0.3)	19.43	18.82	18.58	18.56	18.45	18.36	17.72	···	17.3
J0455+3840	199060743352070528	DA	30.9 (0.2)	···	17.95	17.375	17.135	17.06	17.03	16.17	15.92	17.8
J0458+2548	3419918875386344576	DA	10.1 (0.2)	17.86	17.51	17.62	17.78	17.94	18.05	17.56	···	17.54
J0458+6410	479163220314358784	DC	13.5 (0.1)	···	16.66	16.757	16.933	17.11	17.2	···	···	···
J0459+2317	3418592726925673728	DA	11.3 (0.1)	18.35	17.89	17.791	17.81	17.886	17.93	17.29	···	17.3
J0500−0624	3211353408067754368	DA	21.4 (0.1)	···	16.699	16.608	16.609	16.68	16.72	16.01	15.9	15.91
J0502+2402	3418741367154043648	DAH :*	12.3 (0.1)	17.85	17.49	17.55	17.69	17.83	17.94	17.37	···	17.3
J0502+2522	3420019270246122112	DA	10.3 (0.2)	18.8	18.412	18.35	18.387	18.46	18.5	17.84	···	18.0
J0505−1722	2982808337003815040	DAH	51.68 (0.04)	···	16.255	15.7875	15.59	15.512	15.47	14.55	14.33	14.23
J0505−1731	2976789094955826560	DA	25.9 (0.1)	···	17.394	17.108	16.998	16.994	16.98	16.2	16.0	15.97

Tableau A.1 *suite page suivante*

Tableau A.1 *(suite)*

Name	Gaia DR2/EDR3*	Sp Type	ϖ (mas)	u	g	r	i	z	y	J	H	K
J0508−1450	2986577153625081344	DQ	28.8 (0.1)	···	17.524	17.05	16.88	16.85	16.83	16.23	16.1	16.5
J0508−1523	2986473765172532864	DA	26.7 (0.1)	···	18.12	17.59	17.365	17.317	17.23	16.4	16.1	16.1
J0512−0505	3211784863301909504	DZ	21.1 (0.1)	20.7	17.81	17.414	17.435	17.533	17.55	16.91	16.77	16.68
J0513−0522	3208758831207224704	DA	12.2 (0.2)	19.28	18.59	18.33	18.249	18.27	18.26	17.47	17.26	17.2
J0514+0800	3242153305741855744	DA	46.6 (0.1)	···	16.028	15.797	15.732	15.73	15.769	15.0	14.9	14.9
J0515+2839	3422405214775411840	DAH	33.3 (0.1)	···	16.675	16.415	16.3404	16.341	16.36	15.62	15.3	15.4
J0515+5021	261664427174056320	DA	26.0 (0.1)	···	15.274	15.321	15.44	15.575	15.683	15.09	···	···
J0519−0545	3209958746287926528	DA	17.1 (0.1)	16.85	16.539	16.526	16.602	16.72	16.8	16.18	16.12	16.23
J0520+0114	3222138444609365248	DAH	11.7 (0.2)	19.58	18.9	18.68	18.62	18.63	18.67	···	···	···
J0521+1622	3394087945636978432	DA	13.6 (0.1)	16.83	16.4129	16.506	16.451	16.19	15.897	14.624	···	···
J0521+3321	181170585358665088	DA	19.7 (0.1)	···	16.108	16.12	16.21	16.333	16.36	15.4	15.1	14.8
J0524−0604	3209150124204756224	DC	25.0 (0.1)	17.94	17.298	17.086	17.04	17.08	17.12	16.41	16.32	16.25
J0526+0339	3236259854698180480	DA	12.4 (0.1)	17.8	17.5	17.59	17.687	17.82	17.92	···	···	···
J0526+4435	208021900557436800	DC	25.8 (0.2)	···	18.66	17.92	17.64	17.52	17.45	16.61	16.37	18.3
J0529+4300	195470288131984128	DQ	27.9 (0.1)	···	15.603	15.625	15.748	15.872	15.96	15.5	15.4	15.4
J0530+3939	190802650815160960	DA	29.5 (0.1)	···	17.435	16.965	16.783	16.723	16.71	16.0	15.5	15.6
J0531+0009	3220982720449432448	DA	11.4 (0.4)	21.0	19.73	19.25	19.07	19.05	19.06	···	···	···
J0532+0624	3333830379107891968	DA	10.9 (0.1)	17.1	16.669	16.631	16.682	16.78	16.85	···	···	···
J0533−0750	3016329285438157312	DA	12.3 (0.1)	16.75	16.21	16.284	16.419	16.571	16.68	16.11	···	16.08
J0535+0526	3332761855668238464	DA	12.2 (0.1)	18.11	17.81	17.822	17.878	17.98	18.07	···	···	···
J0535+5715	269226279739467904	DC	24.3 (0.2)	···	18.52	17.873	17.619	17.521	17.49	16.6	16.18	16.29
J0536+4129	194394347281717504	DA	30.99 (0.04)	···	14.82	14.702	14.708	14.75	14.787	14.09	13.94	13.82
J0537+6759	481698110012697728	DAH	28.6 (0.1)	···	16.41	16.31	16.347	16.418	16.47	15.9	15.9	15.55
J0538+1832	3397839440654502656	DA	15.3 (0.2)	18.96	18.28	18.002	17.95	17.94	17.94	17.22	···	···
J0538+4436	197328114893527680	DA	22.6 (0.1)	···	17.475	17.181	17.062	17.05	17.05	16.28	15.77	15.85
J0538+6222	286251461381258624	DA	10.6 (0.2)	19.63	18.85	18.6	18.53	18.56	18.56	···	···	···
J0539+4352	197048460976343168	DC	25.3 (0.1)	···	17.607	17.286	17.165	17.166	17.17	16.5	16.1	···
J0541+3959	190998058945380608	DA	27.5 (0.1)	···	17.62	17.267	17.112	17.05	17.04	16.25	16.07	16.62
J0542+0144	3222969370457259648	DA	16.7 (0.1)	17.21	16.883	16.903	17.005	17.121	17.21	16.7	16.6	···
J0542+8219	558036098518042752	DA	16.2 (0.1)	19.27	18.32	17.99	17.85	17.85	17.74	···	···	···
J0543+0036	3219428015303785856	DA	11.3 (0.2)	19.28	18.64	18.42	18.36	18.36	18.41	···	···	···
J0543+3637	3455921181049073280	DAZ	45.01 (0.04)	···	15.826	15.578	15.496	15.505	15.512	14.78	14.6	14.5
J0543+6338	286925049691578496	DA	12.8 (0.2)	19.15	18.45	18.215	18.147	18.16	18.13	···	···	···
J0544+2602	3429296884940000000	DC	27.7 (0.1)	···	17.578	16.793	16.586	16.42	16.46	15.82	15.29	15.14

Tableau A.1 *suite page suivante*

Tableau A.1 *(suite)*

Name	Gaia DR2/EDR3*	Sp Type	ϖ (mas)	u	g	r	i	z	y	J	H	K
J0544+2720	3441551143893533312	DA	13.6 (0.1)	···	17.097	16.942	16.931	16.98	17.016	16.34	···	16.13
J0546+1115	3337021260634868224	DC	27.3 (0.2)	···	18.26	17.66	17.39	17.296	17.25	16.41	16.1	15.6
J0546+4338	196156864422578432	DA	18.4 (0.1)	···	16.93	16.849	16.869	16.94	16.98	16.27	···	···
J0547+5759	269694160592289664	DA	22.1 (0.1)	···	15.6	15.675	15.798	15.94	16.06	15.47	15.4	15.3
J0548+1325	3346603611845335424	DC	28.2 (0.2)	···	19.33	18.32	17.895	17.725	17.65	16.8	···	···
J0548+4655	210000437370798976	DC	11.3 (0.1)	17.15	17.06	17.146	17.319	17.48	17.59	17.09	···	···
J0549+2329	3427482725113315200	DC*	19.3 (0.2)	···	18.852	18.048	17.729	17.58	17.55	16.65	16.42	16.35
J0550+3257	3451263611151284480	DC	15.1 (0.2)	19.82	18.8	18.48	18.39	18.34	18.33	17.64	17.51	17.6
J0551−0010	3218697767783768320	DQ	89.17 (0.03)	15.306	14.772	14.403	14.348	14.386	14.438	13.708	13.68	13.563
J0553+2550	3429114022412106752	DA	10.3 (0.1)	···	17.008	17.11	17.27	17.44	17.56	17.01	16.97	17.04
J0553+6348	286977585732431488	DA	12.6 (0.1)	18.43	18.02	17.941	17.955	18.05	18.08	···	···	···
J0554−1035	3011223668834627328	DZ	65.35 (0.03)	···	15.085	14.88	14.829	14.883	14.918	14.19	14.14	14.0
J0555+4430	196617731593326976	DC	14.2 (0.2)	19.55	18.68	18.37	18.226	18.25	18.29	17.32	···	···
J0555+4650	198027266851070848	DA	33.4 (0.1)	···	17.525	16.98	16.741	16.65	16.626	15.79	15.5	15.5
J0555−0410	3022956969731332096	DZ	155.25 (0.03)	···	14.847	14.219	13.962	13.86	13.841	13.05	12.9	12.81
J0559−0414	3024247796382652800	DA	26.2 (0.1)	···	17.299	16.99	16.88	16.87	16.88	16.07	15.84	15.8
J0600+2343	3424863550977729536	DA	15.2 (0.1)	17.46	17.002	16.966	17.016	17.109	17.18	16.55	16.44	16.42
J0601−0101	3026097243659561600	DA	12.6 (0.3)	19.1	18.45	18.239	18.161	18.19	18.2	17.44	···	17.3
J0602+0904	3329569015639064192	DA	26.9 (0.1)	···	17.169	16.843	16.717	16.686	16.7	15.9	15.5	15.25
J0602+1553	3348678699526809600	DA	26.5 (0.1)	···	16.949	16.782	16.75	16.78	16.805	16.11	15.9	15.88
J0605+0505	3318463707678938368	DA	12.5 (0.1)	17.21	16.803	16.87	16.996	17.17	17.3	16.72	···	···
J0607+7331	1114054838014073984	DA	31.1 (0.1)	···	17.277	17.03	16.96	16.97	16.97	16.2	16.1	···
J0608+0016	3122380407457501824	DA	12.8 (0.1)	18.11	17.67	17.574	17.6	17.67	17.75	17.02	···	···
J0609+3525	3453292832862501120	DAZ	20.6 (0.1)	16.08	15.677	15.754	15.905	16.08	16.16	15.61	15.3	···
J0611+0544	3318722672728544384	DA	10.6 (0.3)	19.26	18.67	18.43	18.38	18.43	18.45	17.74	···	···
J0611+2429	3425920250370248832	DA	14.6 (0.2)	18.08	17.57	17.44	17.439	17.49	17.55	16.82	16.68	16.6
J0613+2050	3375135698070213632	DA+DQ	17.4 (0.1)	···	15.89	15.874	15.95	16.076	16.173	14.87	14.7	14.6
J0613−0104	3121223102749655808	DA	12.2 (0.2)	18.87	18.467	18.39	18.41	18.49	18.55	17.92	···	17.8
J0615+4638	968662184929578496	DA	11.5 (0.1)	17.63	17.29	17.376	17.518	17.66	17.78	17.27	···	···
J0618+6204	1007682723024253184	DC	25.3 (0.2)	···	18.74	18.025	17.7	17.59	17.51	16.7	16.3	···
J0620+0645	3324181683539044224	DA	41.5 (0.1)	17.57	16.598	16.231	16.092	16.062	16.055	15.257	14.976	14.91
J0620+0700	3324963367588643968	DA	11.2 (0.1)	16.69	16.27	16.375	16.54	16.69	16.79	16.19	16.14	16.19
J0620+3443	3440684419492448128	DA	14.6 (0.1)	16.91	16.539	16.61	16.749	16.89	16.98	16.46	16.48	16.48
J0620+4205	960039814744267520	DAH*	26.6 (0.1)	···	17.238	17.018	16.985	17.03	17.05	16.4	···	15.9

Tableau A.1 *suite page suivante*

Tableau A.1 *(suite)*

Name	Gaia DR2/EDR3*	Sp Type	ϖ (mas)	u	g	r	i	z	y	J	H	K
J0620+8247	1143693887630730240	DA	12.1 (0.1)	18.54	18.046	17.91	17.93	17.98	18.04	···	···	···
J0624−0056	3118424948738692352	DA	10.5 (0.3)	19.46	18.838	18.582	18.54	18.53	18.55	17.89	···	17.7
J0624−0104	3118420619409587712	DC	10.1 (0.3)	19.83	19.19	18.97	18.93	18.98	19.01	18.33	···	18.3
J0627+1002	3327488430402704000	DZ	18.9 (0.1)	···	16.56	16.59	16.696	16.834	16.92	16.34	16.31	16.34
J0627+3500	942461445610425856	DA	18.7 (0.2)	18.18	17.52	17.33	17.27	17.288	17.29	16.57	···	···
J0627−1934	2940050734981714432	DA	18.9 (0.1)	17.59	17.06	16.898	16.893	16.95	16.99	16.24	···	16.08
J0630−0205	3117320802840630400	DA	46.71 (0.04)	···	15.447	15.241	15.185	14.9141	15.19	14.358	···	14.04
J0630−1900	2940003108087120640	DA	14.6 (0.3)	20.0	18.99	18.67	18.54	18.53	18.52	17.82	···	17.3
J0632+2230	3382277296672027136	DA	26.8 (0.1)	···	17.674	17.23	17.046	16.996	16.97	16.17	15.8	15.76
J0632+5559	995112350178946048	DAH	27.09 (0.04)	···	15.873	15.944	16.062	16.21	16.327	15.7	15.7	15.8
J0634−2834	2895487456076198656	DC	34.6 (0.1)	···	18.92	17.89	17.435	17.24	17.15	16.0	16.0	···
J0635+1013	3327647271174824704	DA	11.2 (0.5)	19.47	18.96	18.86	18.81	18.87	18.85	18.15	18.0	17.9
J0635−0044	3119203643485532416	DA	16.2 (0.2)	17.94	17.447	17.315	17.32	17.32	17.38	16.66	16.49	16.56
J0636+4054	957295438016687616	DA	25.2 (0.1)	···	16.8	16.713	16.75	16.82	16.881	16.23	16.1	15.8
J0639+3639	942347092105836160	DA	13.6 (0.1)	18.03	17.56	17.494	17.52	17.582	17.65	17.01	···	···
J0640+3327	938351982245743360	DC	15.5 (0.1)	···	17.312	17.26	17.338	17.47	17.51	16.97	···	···
J0641−0432	3103811515783541504	DC	48.9 (0.1)	···	17.99	17.002	16.59	16.43	16.32	15.4	15.4	15.2
J0641−2027	2927186036623328256	DA	15.3 (0.1)	16.79	16.373	16.47	16.617	16.784	16.91	16.32	···	16.3
J0644+0926	3326650224581677312	DAH*	33.3 (0.1)	17.53	16.73	16.42	16.357	16.312	16.32	15.55	15.32	15.29
J0644+2731	3386162214851684864	DA	26.0 (0.1)	17.71	17.15	16.976	16.943	16.962	17.03	16.27	16.8	16.38
J0644−2832	2918665577420228480	DA	15.4 (0.1)	···	16.461	16.491	16.59	16.74	16.78	16.2	···	···
J0645+2715	3385389606068550144	DA	10.2 (0.3)	18.96	18.54	18.55	18.62	18.72	18.76	18.22	···	···
J0647+0231	3126453655659835136	DA	55.25 (0.05)	···	15.77	15.636	15.605	15.66	15.675	14.963	14.792	14.77
J0649+1519	3354582217971214464	DC	23.0 (0.2)	···	18.35	17.944	17.743	17.72	17.78	17.02	···	···
J0649+7521	1115546944012493696	DAH	26.3 (0.1)	···	17.186	16.933	16.87	16.892	16.91	16.1	15.8	15.46
J0650+1657	3358418684623972864	DA	34.3 (0.1)	···	17.703	17.144	16.931	16.86	16.83	15.99	15.7	15.3
J0651+6242	1100089318058003328	DAH	18.0 (0.1)	···	17.67	17.5	17.439	17.478	17.491	···	···	···
J0652+1416	3354222505874657280	DC	16.4 (0.1)	16.34	16.285	16.384	16.557	16.72	16.83	16.35	···	···
J0653+6355	1100267237077449728	DA	36.0 (0.1)	···	16.585	16.269	16.161	16.12	16.16	15.28	15.1	14.9
J0653+6403	1100655330324351616	DA	35.8 (0.1)	···	16.84	16.485	16.349	16.333	16.32	15.5	15.4	15.3
J0654+2834	887534135357644416	DC	10.8 (0.4)	21.7	20.05	19.45	19.18	19.12	19.03	18.2	···	···
J0654+3148	889391077355387392	DA	15.3 (0.1)	···	16.612	16.646	16.752	16.86	16.97	16.43	16.3	···
J0654+3938	950361883331847424	DZ	20.2 (0.1)	16.03	15.921	16.023	16.192	16.34	16.471	15.97	15.9	16.0
J0657+0240	3127761765259717632	DC	25.0 (0.1)	···	16.166	16.203	16.309	16.445	16.55	16.01	15.97	15.97

Tableau A.1 *suite page suivante*

Tableau A.1 *(suite)*

Name	Gaia DR2/EDR3*	Sp Type	ϖ (mas)	u	g	r	i	z	y	J	H	K
J0657+0550	3129655296079487872	DC	25.7 (0.1)	18.5	17.564	17.28	17.188	17.179	17.21	16.4	16.0	···
J0657+3009	888152408786189952	DA	15.3 (0.2)	17.57	17.128	17.054	17.085	17.173	17.2	16.53	16.0	···
J0657+4007	950478049312082688	DA	18.4 (0.2)	···	17.246	17.05	16.991	17.02	17.04	16.27	15.9	17.11
J0658−0115	3112162508466471808	DA	26.9 (0.3)	···	18.51	17.858	17.57	17.48	17.46	16.7	15.9	···
J0658−1650	2935589908933376896	DA	12.1 (0.2)	18.82	18.32	18.12	18.08	18.11	18.13	17.44	···	17.3
J0659+1225	3160815489969826944	DA	27.1 (0.1)	19.85	18.144	17.543	17.3	17.22	17.18	16.4	16.0	···
J0700+0530	3128834506352463104	DC	16.1 (0.1)	17.12	16.916	16.92	17.009	17.147	17.24	16.69	16.72	17.4
J0700+3157	890661253803216896	DA	51.0 (0.1)	···	16.972	16.32	16.031	15.93	15.9	15.03	14.67	14.7
J0700−0734	3052418589963163264	DC	39.5 (0.1)	···	16.928	16.466	16.384	16.423	16.51	15.77	15.45	15.29
J0701−0628	3052844272764398208	DA	48.31 (0.04)	···	15.57	15.33	15.259	15.254	15.27	14.54	14.2	14.4
J0703+7805	1140292479690791296	DA	41.51 (0.04)	···	16.716	16.227	16.046	15.985	15.96	15.09	14.9	14.7
J0703−1656	2935446392608812032	DZ	11.6 (0.2)	18.57	18.21	18.11	18.164	18.24	18.28	17.65	17.71	17.4
J0704+1151	3160571600249678720	DA	9.8 (0.3)	19.6	18.92	18.71	18.65	18.71	18.72	18.2	···	···
J0704+7111	1109924900541714304	DC	13.2 (0.2)	···	19.146	18.69	18.48	18.42	18.27	···	···	···
J0705+5142	980918204822332416	DA	25.4 (0.2)	···	18.59	18.01	17.756	17.69	17.63	16.84	···	···
J0705−1703	2935415125246460032	DQ	12.8 (0.3)	19.48	19.34	18.69	18.51	18.54	18.59	17.96	17.73	17.8
J0708+2044	3366672379112835328	DA	24.8 (0.1)	···	17.44	17.022	16.86	16.81	16.784	16.0	15.73	15.39
J0710+3740	946030529073021440	DQ	41.0 (0.05)	···	15.705	15.541	15.539	15.586	15.65	14.98	14.8	14.8
J0711+4607	977441274176008192	DC :	13.7 (0.2)	···	19.77	19.07	18.79	18.69	18.6	17.79	···	···
J0712−0428	3059515898856688000	DA	27.5 (0.1)	···	17.94	17.47	17.267	17.2	17.19	16.3	16.1	15.5
J0717+1125	3156974449176326528	DA	33.7 (0.1)	···	17.87	17.182	16.915	16.82	16.77	15.9	15.6	15.1
J0717+3630	898002379406954752	DZ	10.0 (0.2)	19.15	18.53	18.44	18.512	18.62	18.67	18.04	···	···
J0718+1229	3166062806131275136	DA	23.9 (0.1)	···	16.35	16.26	16.23	16.41	16.33	15.63	15.2	15.1
J0718+4547	974375354722176768	DC	28.12 (0.05)	···	15.172	15.265	15.417	15.573	15.685	15.12	15.2	15.0
J0718+5514	987361166866000128	DC	10.4 (0.7)	···	20.44	19.81	19.51	19.44	19.31	18.7	···	···
J0719+3343	896326002132552320	DC	10.4 (0.4)	19.18	18.71	18.59	18.592	18.66	18.74	18.14	···	···
J0721+3955	948173369860748160	DZ	10.4 (0.2)	19.25	18.438	18.32	18.39	18.46	18.55	17.93	···	···
J0722+2806	885100916128136064	DA	27.4 (0.1)	···	18.028	17.485	17.273	17.2	17.17	16.4	···	15.5
J0723+6602	1101763324511186304	DA	10.2 (0.1)	18.61	18.14	18.033	18.053	18.14	18.14	···	···	···
J0724+0431	3139699128636949248	DA	17.1 (0.2)	···	18.4	17.984	17.82	17.79	17.74	17.0	···	···
J0724+3206	892944179243357056	DA	11.5 (0.2)	17.78	17.45	17.502	17.611	17.76	17.86	17.33	···	···
J0724+4400	973275770078523520	DC	14.2 (0.2)	19.65	18.78	18.49	18.4	18.39	18.42	17.74	···	···
J0724−1338	3032020450247993600	DA	27.6 (0.2)	20.1	18.36	17.72	17.49	17.41	17.4	16.2	16.1	···
J0726+2216	866081701427025536	DZ	11.9 (0.2)	18.97	17.99	17.953	18.05	18.17	18.2	···	···	···

Tableau A.1 *suite page suivante*

Tableau A.1 *(suite)*

Name	Gaia DR2/EDR3*	Sp Type	ϖ (mas)	u	g	r	i	z	y	J	H	K
J0726+3531	896951830406797568	DA	12.1 (0.2)	18.71	18.2	18.05	18.03	18.06	18.11	17.4	···	···
J0727+1434	3166841329084630784	DA	32.0 (0.1)	18.19	17.092	16.691	16.533	16.51	16.5	15.66	15.3	15.2
J0729+2716	872009447786700672	DA	17.2 (0.1)	16.66	16.255	16.301	16.41	16.537	16.63	16.07	15.9	15.97
J0729+3552	898473932456801024	DC	12.2 (0.2)	17.59	17.448	17.481	17.594	17.74	17.81	17.33	···	···
J0730+3412	893633710472340992	DA	12.2 (0.2)	18.68	18.16	18.004	17.968	18.02	18.04	17.35	···	···
J0730+5332	983979721933760768	DC	27.6 (0.2)	···	18.67	17.88	17.574	17.488	17.47	16.8	···	···
J0731+4022	900399039877540096	DA*	21.5 (0.4)	20.9	19.02	18.31	18.033	17.93	17.88	17.01	···	···
J0731−0015	3086397068370475392	DA	14.5 (0.1)	16.85	16.452	16.52	16.65	16.796	16.9	16.35	···	16.6
J0732+2822	873303774834413056	DA	11.9 (0.2)	18.58	18.04	17.875	17.871	17.9	17.98	17.28	···	···
J0733+2315	866574493091351936	DZ	12.0 (0.1)	17.72	17.517	17.52	17.634	17.77	17.87	17.33	···	···
J0733+3910	899434463238910720	DC	9.9 (0.1)	18.04	17.87	17.915	18.007	18.135	18.23	17.64	···	···
J0733+6409	1089400763661597440	DAP	49.97 (0.05)	···	16.54	15.97	15.753	15.679	15.642	14.81	14.52	14.4
J0736+2917	879383936697674496	DA	11.2 (0.2)	18.92	18.385	18.237	18.22	18.232	18.3	···	···	···
J0736+4033	924374548053164800	DAH :	9.7 (0.3)	20.22	19.51	19.28	19.19	19.26	19.3	18.6	···	···
J0736+4118	924478859922238720	DZ	12.5 (0.6)	25.7	20.12	19.34	19.26	19.3	19.25	18.7	···	···
J0738+1101	3150099301752709504	DC	13.1 (0.2)	19.51	18.78	18.56	18.48	18.52	18.56	17.89	···	···
J0738+4227	925003537421986304	DC*	12.9 (0.4)	21.72	19.6	19.08	18.81	18.74	18.58	···	···	···
J0738+4326	925258860342797568	DC	24.8 (0.1)	18.37	17.599	17.29	17.208	17.22	17.24	16.5	···	···
J0739+2347	867440427218037120	DA	11.2 (0.1)	17.92	17.54	17.513	17.589	17.68	17.74	17.14	17.1	17.0
J0739+2504	868706888517664000	DA	10.2 (0.4)	19.01	18.58	18.488	18.51	18.61	18.67	17.99	17.6	18.0
J0740+2218	866962856917166208	DAZ	16.7 (0.2)	19.53	18.56	18.196	18.027	18.01	18.01	17.21	16.94	17.0
J0740−1724	5717278911884258176	DZA	109.22 (0.03)	···	13.104	13.0337	13.2	13.21	13.271	12.65	12.61	12.58
J0741+0136	3087094163041546240	DC	18.4 (0.2)	···	18.581	18.19	18.01	18.0	17.92	17.15	···	···
J0742+2857	878635723331279360	DA	10.3 (0.2)	18.19	17.73	17.722	17.785	17.86	17.95	17.32	17.09	16.88
J0742+3157	880354496226790400	DAH	15.0 (0.1)	17.16	16.85	16.89	16.988	17.101	17.23	16.63	···	···
J0742+4223	924219890574729856	DA	14.5 (0.2)	18.67	18.05	17.845	17.79	17.82	17.85	17.11	···	···
J0744+4649	927618687178189056	DZ	17.9 (0.3)	22.4	19.24	18.465	18.321	18.35	18.34	17.61	···	···
J0745+2626	874900643675606912	DC	25.3 (0.4)	21.9	19.774	18.71	18.212	18.04	17.96	17.12	17.09	17.2
J0746+3557	894957694270675584	DA	13.9 (0.2)	18.75	18.134	17.95	17.885	17.93	17.94	···	···	···
J0747+1107	3151407827963355136	DA	36.2 (0.1)	17.12	16.74	16.693	16.716	16.815	16.86	16.22	15.8	15.6
J0747+2438	867739936760402560	DA	18.3 (0.2)	19.47	18.32	17.911	17.759	17.73	17.73	16.78	16.58	16.53
J0747+2438	867740005479885184	DC	18.7 (0.2)	21.1	19.15	18.5	18.27	18.17	18.12	17.16	16.99	16.85
J0748+1125	3151443115414582016	DC	21.5 (0.1)	16.75	16.524	16.583	16.749	16.87	16.97	16.45	···	···
J0748+2134	674479430781455872	DA	9.8 (0.2)	18.93	18.429	18.313	18.3	18.36	18.5	17.7	17.5	17.5

Tableau A.1 *suite page suivante*

Tableau A.1 *(suite)*

Name	Gaia DR2/EDR3*	Sp Type	ϖ (mas)	u	g	r	i	z	y	J	H	K
J0748+3506	894591075862208128	DZA	21.1 (0.2)	19.51	18.23	17.89	17.788	17.79	17.78	16.9	···	···
J0749+1732	668127242870832768	DA	11.8 (0.3)	19.67	19.09	18.918	18.87	18.91	18.84	18.22	···	···
J0749+3124	880840789603989504	DZ	10.9 (0.3)	19.31	18.68	18.548	18.56	18.61	18.7	18.05	···	···
J0750+0711	3144837318276010624	DC	54.9 (0.1)	19.73	17.44	16.574	16.184	16.05	16.0	15.03	14.9	14.8
J0750+0711	3144837112117580800	DC	55.1 (0.1)	18.96	17.03	16.307	16.01	15.911	15.84	15.0	14.7	14.6
J0750+0918	3148732406937031936	DA	22.6 (0.2)	20.06	18.48	17.89	17.66	17.607	17.54	16.73	···	···
J0750+1740	668317840636534912	DA	18.9 (0.1)	17.77	17.285	17.12	17.098	17.112	17.15	16.46	16.3	15.7
J0750+2538	873994719110827264	DC	14.6 (0.1)	18.13	17.757	17.696	17.741	17.84	17.87	17.34	17.3	17.2
J0751+1416	3164518640833807872	DC	13.3 (0.3)	19.57	18.812	18.532	18.462	18.48	18.46	17.8	···	···
J0751+6707	1096117955074105088	DA	18.6 (0.2)	19.79	18.66	18.23	18.059	18.0	18.0	···	···	···
J0752+4447	926374594063195904	DC :	14.1 (0.1)	17.07	16.883	16.941	17.097	17.244	17.36	16.81	···	···
J0752+4724	933421359789700736	DC	11.5 (0.3)	19.18	18.68	18.55	18.57	18.64	18.73	17.98	···	···
J0752−0307	3080914632816248448	DC	27.0 (0.2)	···	18.71	17.92	17.6	17.45	17.28	16.6	16.0	···
J0753+4229	925532265076649472	DC	36.5 (0.2)	19.97	17.976	17.19	16.884	16.776	16.713	15.69	15.49	15.47
J0753+5229	984190381489031424	DC	45.82 (0.05)	16.1	15.663	15.58	15.598	15.689	15.76	15.09	15.2	15.1
J0753+6122	1084764020047940096	DC	28.5 (0.1)	···	16.063	16.014	16.087	16.176	16.28	15.6	15.4	15.2
J0753−0009	3084195266274202752	DA	12.9 (0.1)	17.01	16.596	16.669	16.804	16.967	17.06	16.5	···	16.5
J0753−2523	5602379190877207936	DA	56.1 (0.1)	···	16.636	16.023	15.763	15.68	15.624	14.75	14.47	14.3
J0754+1614	666999556257654784	DA	10.5 (0.1)	18.15	17.691	17.63	17.658	17.73	17.81	17.15	···	···
J0754+6611	1094919590481107968	DC	24.2 (0.1)	17.46	16.9	16.745	16.743	16.788	16.9	16.2	···	···
J0755+0813	3145370645837100160	DA	15.1 (0.2)	20.1	18.97	18.53	18.367	18.34	18.32	17.54	···	···
J0755+3621	906771229452899584	DA	24.6 (0.1)	16.57	16.1487	16.07	16.1	16.147	16.21	15.53	15.4	15.9
J0756+3646	918886709424112896	DA	15.2 (0.3)	19.12	18.48	18.235	18.154	18.17	18.11	17.35	···	···
J0756+4139	922434906461782272	DA	30.5 (0.1)	17.44	16.87	16.666	16.622	16.662	16.72	15.96	15.8	15.9
J0756+4242	922621269386513152	DA	11.5 (0.3)	19.37	18.796	18.6	18.543	18.57	18.53	17.83	···	···
J0756+5741	1081813343155426560	DC	33.96 (0.05)	···	15.054	15.114	15.27	15.409	15.54	14.99	15.0	15.0
J0756−2001	5714040261719110784	DC	23.8 (0.2)	···	19.01	18.72	19.34	19.82	20.0	···	···	···
J0757+3230	881146316398060672	DA	10.4 (0.4)	20.14	19.24	18.91	18.79	18.81	18.8	18.03	···	···
J0757+6453	1094608119452121856	DC	11.6 (0.1)	18.08	17.88	17.899	18.005	18.11	18.23	···	···	···
J0759+4335	923023248261420672	DCP	45.6 (0.1)	16.73	16.27	16.257	16.19	16.1	16.12	15.43	15.2	15.3
J0759+4735	933095015289999872	DA	20.2 (0.1)	16.62	16.24	16.22	16.312	16.445	16.52	15.93	15.7	15.9
J0800+0655	3144237908341731712	DAH	11.3 (0.2)	17.93	17.78	17.977	18.122	18.17	18.25	17.71	···	···
J0800+2052	670842761712806912	DC	10.8 (0.3)	19.02	18.59	18.533	18.57	18.67	18.74	18.22	18.0	18.1
J0800−0840	3039671225803688320	DZ	13.6 (0.2)	18.57	18.05	17.931	17.996	18.1	18.18	17.49	···	17.5

Tableau A.1 *suite page suivante*

Tableau A.1 *(suite)*

Name	Gaia DR2/EDR3*	Sp Type	ϖ (mas)	u	g	r	i	z	y	J	H	K
J0801+3618	907000821224488832	DC	12.0 (0.2)	18.45	18.02	17.94	17.999	18.05	18.04	17.43	···	···
J0801+3949	921281480108851200	DC	14.1 (0.5)	22.3	20.07	19.37	19.1	18.99	18.9	18.2	···	···
J0801+4852	933287876501371520	DA	27.9 (0.1)	19.47	17.92	17.382	17.147	17.08	17.05	16.17	15.78	15.68
J0801+5329	936641833642799744	DZ	12.1 (0.1)	17.75	17.475	17.48	17.64	17.7	17.57	17.26	···	···
J0802+5646	1081514379072280320	DC	24.9 (0.2)	···	19.091	18.3	17.91	17.78	17.67	17.0	16.4	···
J0803+0022	3084427916062349440	DA	13.7 (0.2)	19.0	18.33	18.079	18.0	18.01	18.04	17.28	···	···
J0804+0716	3145766676180517760	DA	10.7 (0.2)	18.62	18.159	18.036	18.021	18.1	18.12	17.45	···	···
J0804+1714	668796162553518720	DQ	14.9 (0.3)	19.89	18.99	18.44	18.29	18.25	18.22	17.54	···	···
J0804+2239	680099824985004288	DZ	25.3 (0.1)	19.82	18.158	17.613	17.411	17.36	17.28	16.71	16.92	17.3
J0804+3538	906160863060179072	DA	14.3 (0.1)	17.74	17.412	17.44	17.538	17.69	17.76	17.14	···	···
J0804+4213	922686832063591168	DA	13.5 (0.1)	17.27	16.89	16.902	16.991	17.12	17.25	16.57	···	···
J0805+0724	3097756127294671488	DQ	12.8 (0.4)	20.4	19.48	18.89	18.72	18.66	18.72	18.3	···	···
J0805+0735	3145802036649641472	DA	29.1 (0.1)	19.23	17.83	17.337	17.141	17.097	17.067	16.25	16.0	15.6
J0805+1820	669024203839693056	DA	12.3 (0.2)	19.12	18.53	18.29	18.235	18.25	18.27	17.54	17.4	17.5
J0805+3833	908962109449446656	DA	48.5 (0.1)	19.04	17.218	16.576	16.313	16.216	16.18	15.34	15.2	14.9
J0805+4720	932855386179190272	DA	10.6 (0.2)	19.03	18.498	18.325	18.296	18.34	18.38	17.67	···	···
J0805+4821	933057593239584000	DA	10.3 (0.3)	19.3	18.89	18.85	18.89	18.97	19.1	18.4	···	···
J0805+4957	934937139647967232	DA	10.6 (0.3)	19.35	18.78	18.635	18.61	18.64	18.65	18.05	···	···
J0805+5339	1032545631568349056	DC	10.0 (0.3)	19.5	18.92	18.74	18.728	18.79	18.78	18.2	···	···
J0805+6624	1095169656358227456	DZ	10.4 (0.2)	19.44	18.88	18.71	18.72	18.78	18.85	···	···	···
J0805−0654	3063960605892490368	DC	12.4 (0.3)	20.0	19.13	18.85	18.76	18.69	18.77	18.08	···	18.0
J0806+2215	677060225090183552	DA	20.2 (0.2)	19.35	18.128	17.75	17.6	17.57	17.56	16.77	16.51	16.45
J0806+4058	921642532239821440	DZH*	11.1 (0.3)	20.6	19.03	18.78	18.79	18.89	18.9	18.3	···	···
J0807+2557	681934703732973824	DA	10.4 (0.3)	19.36	18.76	18.63	18.518	18.51	18.52	17.81	17.6	17.7
J0807+4431	928937074630507392	DA	22.4 (0.2)	18.59	17.804	17.53	17.423	17.43	17.42	16.71	16.6	···
J0807+4854	934555334235313664	DA	14.4 (0.2)	18.91	18.25	18.027	17.955	17.98	17.98	17.25	···	···
J0807−0753	3063650376111451136	DC	14.0 (0.1)	17.01	16.855	16.934	17.085	17.24	17.34	16.82	···	16.8
J0808+1854	669444943132791424	DA	19.3 (0.1)	19.23	18.17	17.76	17.6	17.561	17.55	16.77	16.4	16.24
J0808+4640	929774314079963264	DQ	9.7 (0.7)	20.7	20.4	19.42	19.13	19.15	19.23	18.4	···	···
J0808−0431	3067956368587354368	DC	18.7 (0.2)	···	18.82	18.3	18.078	17.99	17.96	···	···	···
J0809+0245	3091044532222339584	DA	14.3 (0.2)	18.94	18.417	18.272	18.237	18.3	18.33	17.63	···	···
J0809+1112	649672906567630976	DZ	19.0 (0.1)	18.36	17.71	17.54	17.541	17.579	17.63	16.7	16.8	···
J0809+2250	677196843705878272	DA	18.1 (0.2)	18.47	17.819	17.591	17.543	17.56	17.59	16.86	16.61	16.6
J0809+2920	876571935709366272	DA	30.9 (0.1)	16.84	16.26	16.101	16.07	16.115	16.153	15.41	15.24	15.25

Tableau A.1 *suite page suivante*

Tableau A.1 *(suite)*

Name	Gaia DR2/EDR3*	Sp Type	ϖ (mas)	u	g	r	i	z	y	J	H	K
J0809+3527	905923368548465152	DA	28.39 (0.05)	15.54	15.159	15.164	15.227	15.345	15.42	14.806	14.8	14.7
J0810+0041	3083765357227100800	DA	10.6 (0.1)	16.94	16.52	16.612	16.753	16.91	17.03	16.46	···	···
J0811+2321	677593660028220544	DA	10.3 (0.3)	19.79	19.0	18.77	18.67	18.71	18.73	17.98	17.9	17.6
J0811+4816	931487524994983808	DA	9.8 (0.2)	18.62	18.222	18.149	18.185	18.27	18.19	17.75	···	···
J0812+0942	3146576878812071168	DA	10.2 (0.5)	20.9	20.05	19.82	19.69	19.7	19.7	19.0	···	···
J0813+0935	3146523896095375744	DA*	12.2 (0.2)	19.81	18.89	18.58	18.47	18.45	18.46	17.7	···	···
J0813+1130	649041786893358336	DA	12.0 (0.1)	17.04	16.653	16.753	16.897	17.072	17.18	16.66	16.6	···
J0813+1220	650230771279461760	DA	15.2 (0.2)	19.32	18.475	18.162	18.06	18.06	18.07	17.37	···	···
J0813+1957	675615677264385536	DC	28.1 (0.2)	21.3	19.28	18.285	17.877	17.7	17.63	16.6	16.4	···
J0814+1300	650340408909616896	DA	12.9 (0.2)	18.7	18.26	18.17	18.19	18.27	18.31	17.7	···	···
J0814+2455	682315757527779584	DQ	17.0 (0.1)	17.18	16.916	16.92	17.009	17.14	17.23	16.66	16.61	16.6
J0814+3300	902414964384353408	DC*	13.9 (0.5)	21.3	19.96	19.41	19.38	19.67	19.8	···	···	···
J0814+3437	902857685316692352	DC	14.7 (0.2)	18.78	18.23	18.08	18.069	18.14	18.18	17.48	···	···
J0814+4845	931573222477949696	DC	58.48 (0.04)	15.757	15.158	14.97	14.943	14.976	15.01	14.314	14.13	14.1
J0815+1633	655808799925588992	DA	14.0 (0.2)	20.8	18.87	18.14	17.84	17.74	17.7	16.85	16.1	15.7
J0815+5339	1031832946170531456	DA	13.0 (0.1)	17.89	17.483	17.545	17.647	17.78	17.89	17.35	···	···
J0815+5814	1035222289547372800	DA	16.8 (0.1)	18.16	17.72	17.624	17.64	17.72	17.74	17.1	···	···
J0816+1313	650432664805355392	DC	14.4 (0.2)	19.88	18.894	18.51	18.36	18.32	18.31	17.48	···	···
J0816+2137	676031052142751488	DA	25.4 (0.1)	17.95	17.146	16.865	16.749	16.75	16.749	15.97	15.73	15.67
J0817+2008	675590693439332096	DAH*	13.7 (0.2)	18.83	18.3	18.16	18.132	18.2	18.23	17.64	···	···
J0817+2822	684152216824047104	DC	18.8 (0.3)	21.7	19.36	18.619	18.3	18.14	18.08	17.33	17.01	16.9
J0817+2902	684258010458273152	DC	11.1 (0.3)	20.09	19.36	19.1	19.01	19.07	19.05	18.4	18.3	18.0
J0818+4144	915672081021495552	DAH :*	10.4 (0.2)	18.5	18.135	18.095	18.176	18.28	18.36	17.69	···	···
J0818+4449	928440365957680256	DC	10.7 (0.3)	20.05	19.32	19.05	18.97	18.95	18.97	18.3	···	···
J0819+1321	650400263572196480	DC	11.5 (0.4)	20.01	19.29	18.994	18.86	18.8	18.79	18.1	···	···
J0819+1948	663601481211006592	DA	15.5 (0.2)	20.12	18.792	18.38	18.22	18.18	18.18	17.38	···	···
J0819+3159	901360494077262208	DC	16.6 (0.3)	21.7	19.59	18.888	18.59	18.49	18.42	17.47	17.32	17.2
J0819+5732	1035126803834023296	DZ	18.4 (0.1)	18.61	17.834	17.596	17.549	17.57	17.66	16.94	···	···
J0820+0855	600139357979417344	DC	13.1 (0.2)	18.86	18.34	18.227	18.235	18.31	18.38	17.73	···	···
J0820+1523	652438247031965056	DC	12.7 (0.1)	17.16	17.081	17.18	17.323	17.47	17.59	17.06	···	···
J0820+3834	908364559240386944	DA	22.4 (0.1)	17.06	16.58	16.475	16.486	16.558	16.602	15.92	15.8	15.6
J0820+4310	916276228300814976	DA	10.9 (0.1)	18.22	17.662	17.472	17.448	17.477	17.5	16.77	16.1	15.7
J0820+4803	931304937345481344	DA	22.2 (0.1)	18.0	17.279	17.016	16.942	16.93	16.97	16.16	16.0	15.8
J0821+3727	908048587085834752	DA	18.5 (0.2)	21.0	19.04	18.428	18.167	18.1	18.07	17.25	17.0	16.85

Tableau A.1 *suite page suivante*

Tableau A.1 *(suite)*

Name	Gaia DR2/EDR3*	Sp Type	ϖ (mas)	u	g	r	i	z	y	J	H	K
J0822+0300	3090505359208876288	DA	10.2 (0.3)	19.59	18.91	18.7	18.659	18.67	18.69	17.99	17.9	17.7
J0822+2023	664021842547278592	DC	23.3 (0.1)	16.75	16.267	16.145	16.159	16.223	16.29	15.66	15.5	15.4
J0823+0546	3093722358432322176	DZ	20.9 (0.1)	19.52	17.431	17.17	17.202	17.31	17.35	16.69	16.58	16.52
J0823+4833	930966979254089472	DA	21.5 (0.1)	18.76	17.95	17.659	17.57	17.55	17.52	16.81	···	···
J0823+8237	1145602571097053952	DC	15.1 (0.2)	22.11	19.73	19.12	18.81	18.71	18.5	···	···	···
J0824+3104	709051168734737024	DA :*	12.9 (0.1)	17.94	17.646	17.601	17.669	17.78	17.84	17.28	···	···
J0825+2242	677874722688200832	DC	10.7 (0.3)	19.77	19.19	18.94	18.89	18.89	18.94	18.18	18.0	17.9
J0825+5049	1028072371590379136	DC	20.9 (0.2)	21.1	19.19	18.45	18.1	17.98	17.93	17.08	16.83	16.74
J0825+6003	1035806851776104448	DA	12.7 (0.1)	17.06	16.644	16.73	16.875	17.04	17.14	16.6	16.5	···
J0826+3249	902972034525449088	DAZ	15.2 (0.2)	19.28	18.41	18.09	17.96	17.952	17.93	17.18	···	···
J0826+4645	930242465515189376	DC	16.4 (0.2)	17.96	17.578	17.534	17.542	17.58	17.6	17.07	16.8	16.4
J0826−0539	3065135949463337984	DA	11.0 (0.1)	18.48	18.09	17.994	18.023	18.09	18.15	17.52	···	17.3
J0827+2607	679723276611814400	DA	12.2 (0.2)	18.69	18.213	18.079	18.07	18.11	18.14	17.45	17.4	17.2
J0827+4553	918126843809713280	DA	15.1 (0.6)	19.76	19.21	19.01	18.98	19.04	19.0	···	···	···
J0828+0208	3079642326059886208	DA*	15.9 (0.1)	18.46	17.803	17.569	17.5	17.52	17.52	16.81	16.61	16.51
J0828+0942	599922307511771776	DC	19.3 (0.2)	21.1	19.02	18.18	17.85	17.695	17.64	16.76	···	···
J0828+3131	709004920527186816	DC	15.0 (0.2)	19.03	18.39	18.15	18.1	18.116	18.15	17.42	···	···
J0828+3527	903847348860521856	DC	14.5 (0.5)	21.5	19.72	19.03	18.79	18.69	18.68	···	···	···
J0828−0141	3076010742232557952	DA	11.6 (0.3)	25.8	18.88	18.61	18.55	18.54	18.6	17.84	17.5	17.3
J0829+2539	679636484296738304	DC	17.7 (0.8)	21.45	19.24	18.62	18.25	18.17	18.15	17.46	16.82	16.6
J0829+4419	917707418778058368	DC	13.2 (0.3)	19.7	18.89	18.6	18.507	18.52	18.53	17.88	···	···
J0829+5312	1028955489881696768	DA	10.9 (0.1)	17.66	17.242	17.298	17.421	17.58	17.69	17.15	···	···
J0829+5641	1034060277555338368	DC	10.2 (0.1)	17.43	17.326	17.393	17.563	17.71	17.83	17.33	···	···
J0830+3241	710766750855439360	DA	44.7 (0.1)	16.28	15.802	15.682	15.674	15.74	15.78	15.06	15.0	14.9
J0830+4139	915116621490557440	DA	10.2 (0.1)	17.54	17.15	17.23	17.362	17.53	17.65	17.06	···	···
J0830+4520	918044247294118656	DA	20.4 (0.1)	15.513	15.06	15.166	15.312	15.482	15.607	15.02	15.0	14.8
J0831+1641	658781771991055104	DA	17.5 (0.1)	17.82	17.312	17.144	17.125	17.18	17.22	16.52	···	···
J0831+1905	662716271271960320	DA	10.9 (0.3)	19.98	19.09	18.785	18.68	18.67	18.7	17.88	17.8	17.7
J0831+3331	710947963731953792	DA	25.0 (0.1)	18.72	17.7	17.315	17.17	17.132	17.11	16.34	···	···
J0831−1643	5709868512742196608	DC	27.9 (0.3)	···	19.22	18.29	17.88	17.75	17.69	16.5	···	···
J0832+3139	710452358868303232	DA	19.5 (0.1)	18.66	17.992	17.714	17.55	17.53	17.55	16.8	···	···
J0832+5714	1034473453408991360	DA	12.8 (0.2)	20.15	19.205	18.83	18.67	18.63	18.59	17.8	···	···
J0832+6507	1092515229130044544	DA	14.1 (0.2)	19.4	18.728	18.447	18.375	18.39	18.41	···	···	···
J0832−0207	3073014263809462528	DA	13.7 (0.1)	18.04	17.71	17.749	17.858	17.985	18.1	17.52	17.5	17.5

Tableau A.1 *suite page suivante*

Tableau A.1 *(suite)*

Name	Gaia DR2/EDR3*	Sp Type	ϖ (mas)	u	g	r	i	z	y	J	H	K
J0832−0408	3065744460430556032	DQ	12.2 (0.2)	18.88	18.93	18.47	18.263	18.37	18.5	17.83	···	17.8
J0833+2914	707673416242396160	DA	14.2 (0.2)	18.77	18.14	17.935	17.848	17.885	17.88	17.17	16.93	16.9
J0834+0321	3080205580955810432	DA	12.0 (0.4)	20.5	19.4	19.08	18.98	18.99	19.0	18.24	17.9	17.7
J0834+0727	595867686585664256	DA	10.6 (0.2)	17.62	17.2	17.254	17.373	17.51	17.6	16.98	16.92	16.92
J0834+3659	910087768838947456	DA	20.2 (0.1)	16.45	16.06	16.077	16.154	16.289	16.36	15.77	15.6	15.4
J0835+4718	918648974394418816	DA	14.7 (0.2)	18.71	18.034	17.799	17.73	17.74	17.76	17.04	···	···
J0835+4758	1014793672740325248	DA	10.5 (0.2)	18.95	18.56	18.486	18.54	18.61	18.68	18.0	···	···
J0835+5332	1030289712881895296	DAH	10.3 (0.2)	18.54	18.22	18.17	18.27	18.36	18.47	17.8	···	···
J0835−0435	3065513047592503552	DC	12.3 (0.1)	17.27	17.166	17.226	17.37	17.53	17.66	17.04	···	17.2
J0836+1452	657598147723622912	DA	12.9 (0.3)	18.65	18.263	18.192	18.21	18.3	18.34	17.7	···	···
J0836+2216	665991789427730432	DA	11.4 (0.2)	18.49	18.06	17.99	18.017	18.11	18.17	17.48	17.4	17.4
J0836+2432	678537968717235072	DQ	10.2 (0.9)	20.4	19.5	18.936	18.76	18.72	18.69	17.99	17.9	18.0
J0836+3506	711527372000026624	DA	10.7 (0.3)	19.71	18.86	18.596	18.485	18.49	18.47	17.64	···	···
J0836+4556	918237791404732416	DC	14.8 (0.5)	21.5	19.81	19.16	18.88	18.78	18.78	17.9	17.7	17.59
J0836+5104	1027695136022450432	DC	13.4 (0.3)	20.1	19.16	18.82	18.7	18.68	18.72	···	···	···
J0837+3154	709769115467848448	DC	11.1 (0.3)	19.65	19.01	18.767	18.73	18.75	18.8	18.2	···	···
J0837+4613	918336060256260480	DA	13.8 (0.2)	19.23	18.44	18.18	18.095	18.1	18.08	17.32	···	···
J0837+5100	1027704894188127232	DA	10.8 (0.1)	18.01	17.49	17.36	17.34	17.39	17.44	16.74	···	···
J0837+5427	1030621658018969856	DC	10.9 (0.3)	19.22	18.72	18.55	18.54	18.57	18.67	18.01	···	···
J0838+1321	603155765049434752	DC*	12.6 (0.2)	19.1	18.55	18.36	18.349	18.4	18.43	17.76	···	···
J0838+2322	666207736086203648	DZ	11.8 (0.3)	20.38	19.14	18.86	18.84	18.85	18.9	18.24	···	···
J0838+2804	704316671665447296	DC	17.1 (0.3)	20.6	19.04	18.507	18.292	18.23	18.19	17.33	17.07	17.04
J0840+0939	598240497102033024	DA	11.0 (0.1)	17.66	17.188	17.301	17.444	17.62	17.73	17.82	16.91	16.96
J0840+1518	657673498630210176	DAZ	11.0 (0.3)	19.78	19.05	18.77	18.722	18.67	18.73	18.03	···	···
J0840+2244	666111739274159360	DC	13.9 (0.2)	19.16	18.56	18.38	18.3	18.37	18.32	17.81	17.5	17.6
J0840+3431	711260465552649216	DA	13.3 (0.2)	19.09	18.55	18.4	18.35	18.42	18.44	17.77	···	···
J0840+3714	909928404076399744	DC	13.3 (0.3)	19.44	18.74	18.5	18.449	18.48	18.51	17.88	···	···
J0841+0223	3079104660578372480	DAH	10.6 (0.3)	19.56	18.97	18.79	18.75	18.8	18.83	18.12	18.0	18.4
J0841+3329	710392886455231360	DQ	18.8 (0.9)	18.92	18.46	18.31	18.309	18.36	18.39	17.7	···	···
J0841+4737	1014548520302641536	DA	11.7 (0.1)	17.59	17.199	17.19	17.246	17.37	17.4	···	···	···
J0842+1406	609236712891803264	DZ	10.1 (0.2)	19.29	18.28	18.202	18.29	18.44	18.5	17.94	···	···
J0842+2409	690287663506579328	DA	26.2 (0.1)	18.36	17.391	17.028	16.877	16.859	16.85	16.1	15.9	15.6
J0842+5959	1040866941726072064	DC	12.0 (0.2)	19.87	19.12	18.82	18.751	18.78	18.81	···	···	···
J0842−1347	5734737438536674432	DZ	67.55 (0.04)	···	16.005	15.541	15.419	15.4	15.415	14.612	14.4	14.33

Tableau A.1 *suite page suivante*

Tableau A.1 *(suite)*

Name	Gaia DR2/EDR3*	Sp Type	ϖ (mas)	u	g	r	i	z	y	J	H	K
J0843+0002	3075067700558242176	DA	11.2 (0.2)	18.58	18.25	18.24	18.34	18.42	18.55	17.92	17.8	17.6
J0843+3412	716446797477471104	DA	9.8 (0.1)	17.4	17.04	17.076	17.17	17.303	17.4	···	···	···
J0843+5414	1030381796981255936	DA	10.9 (0.2)	19.0	18.46	18.269	18.236	18.28	18.24	17.59	···	···
J0844+1035	598769843231677056	DA	11.7 (0.2)	19.71	18.926	18.645	18.55	18.56	18.58	17.91	···	···
J0844+4536	917321936874346880	DA	16.0 (0.1)	16.45	15.969	15.968	16.034	16.132	16.23	15.58	15.6	15.6
J0845+3214	710026160671981440	DA	11.3 (0.2)	18.1	17.621	17.58	17.7	17.56	17.49	16.84	···	···
J0845+3801	910341618586847232	DA	24.8 (0.1)	16.48	16.06	16.001	16.023	16.116	16.16	15.51	15.4	15.4
J0845+6117	1042071701528617728	DAH	28.5 (0.1)	18.28	17.34	16.974	16.84	16.812	16.82	16.2	15.7	···
J0845+6117	1042071701528617856	DA	28.4 (0.1)	18.85	17.6	17.159	16.979	16.941	16.91	16.1	15.9	15.8
J0845+6143	1042192506072573312	DQ	13.1 (0.1)	17.75	17.515	17.49	17.58	17.69	17.803	···	···	···
J0845−2701	5646089927728820736	DC	19.6 (0.3)	···	19.85	19.06	18.691	18.52	18.6	17.57	···	17.7
J0846+0514	582729312907277568	DA	12.5 (0.3)	19.2	18.53	18.29	18.194	18.2	18.19	17.46	17.31	17.2
J0846+3538	717393648787722624	DZA	40.68 (0.05)	15.056	14.774	14.832	14.952	15.13	15.23	14.658	14.6	14.6
J0846+6352	1044109229717304064	DA	15.3 (0.1)	17.58	17.189	17.132	17.17	17.244	17.32	···	···	···
J0846+6944	1118460924702185088	DC	21.8 (0.1)	···	18.64	18.02	17.78	17.68	17.62	···	···	···
J0847+1830	660222170879118208	DQ	13.7 (0.1)	17.32	17.094	17.129	17.233	17.37	17.46	16.93	16.89	17.0
J0848+3548	717762977319125632	DZ	11.2 (0.2)	18.47	18.14	18.13	18.189	18.33	18.4	17.86	···	···
J0849+0923	597646245427109376	DA	10.1 (0.1)	18.13	17.734	17.704	17.779	17.88	17.95	17.33	17.23	17.3
J0849+1827	660212752014880256	DZ	11.3 (0.3)	19.7	18.95	18.71	18.69	18.74	18.8	18.2	18.0	18.2
J0849+3319	716112442863454464	DA	21.9 (0.1)	17.05	16.576	16.482	16.495	16.557	16.6	15.93	15.9	15.7
J0849+3429	716504796716020352	DA	32.4 (0.1)	16.19	15.73	15.621	15.614	15.691	15.73	15.04	14.8	14.9
J0849+4439	914211487199415680	DC	22.1 (0.3)	18.75	17.934	17.633	17.52	17.51	17.5	16.77	16.03	16.18
J0849+5942	1040991259555635328	DA	14.8 (0.2)	19.34	18.44	18.104	17.985	17.97	17.97	17.18	···	···
J0849−0156	3073747187092773632	DC	35.8 (0.1)	19.6	17.745	17.089	16.819	16.73	16.69	15.8	15.57	15.46
J0851+1543	609898313949732608	DZ	10.4 (0.3)	20.3	18.97	18.75	18.8	18.94	18.82	18.5	···	···
J0851+1624	611645983387812992	DC	32.4 (0.1)	17.91	16.916	16.586	16.48	16.493	16.5	15.8	15.7	15.7
J0851+5426	1029968414968983424	DA	13.1 (0.1)	17.82	17.63	17.68	17.767	17.9	18.04	17.45	···	···
J0852+1850	660431181166277120	DAZ	10.2 (0.1)	18.4	17.92	17.88	17.912	18.0	18.04	17.4	17.33	17.4
J0852+3209	712789886226437632	DC	16.5 (0.2)	19.19	18.324	18.01	17.89	17.89	17.9	17.16	···	···
J0852−0144	5764001760847057280	DC	12.6 (0.3)	19.58	18.91	18.662	18.59	18.63	18.61	17.94	17.7	17.7
J0853−0137	5764027015254831488	DA	10.2 (0.3)	20.1	19.25	18.94	18.83	18.81	18.85	18.02	17.9	17.7
J0853−2446	5652718097353105664	DC	38.9 (0.2)	···	18.6	17.74	17.66	17.88	18.02	17.17	···	16.18
J0854+2752	692904776058392064	DA	15.2 (0.2)	18.22	17.7	17.515	17.463	17.48	17.53	16.78	16.6	16.6
J0854+2926	705484593532621952	DA :	16.6 (0.3)	20.9	19.18	18.62	18.4	18.3	18.27	17.45	17.1	17.1

Tableau A.1 *suite page suivante*

Tableau A.1 *(suite)*

Name	Gaia DR2/EDR3*	Sp Type	ϖ (mas)	u	g	r	i	z	y	J	H	K
J0854+3503	716743042845256576	DC	18.6 (0.5)	23.2	20.28	19.38	19.107	19.1	18.98	18.44	18.23	17.98
J0855+0639	584402318633098624	DQ	13.1 (0.2)	18.19	17.85	17.75	17.8	17.877	17.93	17.36	17.27	17.3
J0855+3700	718682620012682112	DA	19.1 (0.1)	18.8	17.923	17.48	17.294	17.25	17.23	16.37	16.17	16.08
J0855−0833	5755957119598921728	DC	29.9 (0.2)	···	18.373	17.6	17.291	17.2	17.12	16.1	15.8	···
J0855−2637	5649105922480851200	DA	18.8 (0.1)	···	17.017	16.99	17.046	17.168	17.25	16.61	···	16.6
J0855−2637	5649105926779602432	DA	18.7 (0.1)	···	16.899	16.819	16.84	16.94	17.01	16.31	16.2	16.24
J0857+1808	612262122214240512	DA	19.1 (0.2)	17.96	17.347	17.144	17.09	17.137	17.118	16.41	16.1	16.4
J0857+2542	691600338653939328	DA	15.7 (0.4)	19.28	18.43	18.111	17.986	17.962	17.97	17.16	···	···
J0857+3901	719707193051500928	DA	14.4 (0.2)	18.83	18.16	17.933	17.86	17.872	17.91	17.1	···	···
J0857+4150	912788233820354560	DC	11.6 (0.3)	19.46	18.87	18.68	18.663	18.74	18.73	18.1	···	···
J0857+6308	1043885758275341184	DC	10.7 (0.1)	17.71	17.571	17.63	17.775	17.919	18.02	···	···	···
J0858+4126	912718071240545152	DAH	26.1 (0.1)	17.58	17.026	16.873	16.87	16.93	16.96	16.31	···	15.7
J0858+6813	1117334024067935872	DC	26.1 (0.1)	···	18.835	18.07	17.775	17.67	17.58	16.4	···	···
J0859+3257	712888090655562624	DQ	43.4 (0.1)	15.107	15.142	15.1624	15.318	15.49	15.62	15.16	15.2	15.3
J0859+5934	1038018828652951296	DA	13.2 (0.4)	21.4	19.67	19.11	18.847	18.76	18.69	17.92	···	···
J0859+6016	1038076351151065088	DQ	23.9 (0.1)	16.72	16.407	16.327	16.402	16.51	16.591	16.0	15.6	15.91
J0859−0058	5764485618978306176	DC	54.7 (0.1)	18.38	16.682	16.078	15.828	15.736	15.715	14.83	14.6	14.7
J0900−0008	5764602334714811904	DC	10.3 (0.4)	20.06	19.29	19.05	19.01	19.06	19.06	18.4	18.4	18.1
J0900−2213	5655188871777035520	DC	13.7 (0.2)	···	18.72	18.29	18.08	18.0	17.8649	17.11	···	16.7
J0901+3037	711612103114782592	DC	10.4 (0.4)	19.88	19.21	19.0	18.96	19.02	19.03	···	···	···
J0901+3846	719266799987963392	DC*	11.5 (0.2)	18.59	18.2	18.13	18.17	18.243	18.35	17.66	···	···
J0901+4946	1015799828959492352	DC	11.1 (0.4)	21.6	19.99	19.51	19.29	19.22	19.2	18.3	···	···
J0901−0141	5764107760640582656	DA	12.2 (0.2)	18.53	18.1	18.002	18.0	18.07	18.11	17.44	17.29	17.2
J0902+1535	610411820238973056	DC	20.8 (0.2)	20.4	18.4	17.664	17.34	17.24	17.18	16.29	16.1	15.2
J0902+2010	684598618544000384	DQ	25.9 (0.2)	18.95	18.9	17.752	17.26	17.3	17.362	16.7	···	···
J0902+3120	711744456827031680	DA	29.5 (0.1)	15.592	15.26	15.302	15.423	15.583	15.679	15.09	15.05	15.1
J0902+5630	1036295206737529856	DA	10.8 (0.3)	20.9	19.48	18.9	18.66	18.58	18.54	···	···	···
J0902+6503	1044511002434919936	DZ	12.0 (0.2)	19.38	18.62	18.45	18.508	18.6	18.61	···	···	···
J0903+0838	585164761227127424	DA	19.0 (0.2)	20.11	18.76	18.27	18.079	18.04	18.0	17.19	16.9	16.9
J0903+2012	636651837034002944	DA	17.9 (0.1)	17.57	17.066	16.92	16.909	16.967	16.98	16.26	16.2	15.9
J0903+2139	685402357248747648	DA	11.7 (0.3)	18.91	18.49	18.4	18.44	18.54	18.52	···	···	···
J0903+2444	688314207636275328	DA	10.3 (0.2)	18.16	17.76	17.73	17.816	17.95	17.96	17.39	···	···
J0904+0211	577342113952420224	DA	14.4 (0.3)	19.68	18.86	18.58	18.47	18.49	18.52	17.72	17.5	17.3
J0904+1349	606938634805314944	DA	17.8 (0.1)	17.1	16.7	16.655	16.707	16.792	16.84	16.2	16.0	15.8

Tableau A.1 *suite page suivante*

Tableau A.1 *(suite)*

Name	Gaia DR2/EDR3*	Sp Type	ϖ (mas)	u	g	r	i	z	y	J	H	K
J0904+1349	606938634805314816	DA	17.7 (0.1)	16.46	16.128	16.173	16.296	16.433	16.52	15.95	15.8	15.7
J0904+3017	699628147926656768	DA	12.7 (0.2)	18.92	18.31	18.1	18.041	18.06	18.06	17.36	17.1	17.2
J0904+3403	713438705462521728	DC	21.2 (0.2)	20.08	18.64	18.083	17.876	17.86	17.9	17.23	16.93	16.8
J0905+0904	591207406550605312	DQ	16.8 (0.1)	16.94	16.72	16.76	16.873	16.99	17.11	16.58	16.54	16.55
J0905+1124	604127802048700032	DC	11.0 (0.2)	19.27	18.75	18.6	18.55	18.62	18.69	18.2	17.9	18.0
J0905+2315	685671909396428544	DA	10.4 (0.4)	20.3	19.46	19.2	19.07	19.09	18.9	18.2	···	···
J0905+3653	715502037814544384	DC	10.5 (0.4)	19.76	19.2	19.04	19.022	19.09	19.12	···	···	···
J0905+5143	1016617865610081152	DA	13.3 (0.2)	18.55	18.144	18.07	18.115	18.21	18.25	17.59	···	···
J0905+7314	1123700235048742016	DC	38.9 (0.1)	···	17.276	16.73	16.506	16.433	16.404	15.6	15.3	15.1
J0905−0154	5763373596110853248	DAZ	11.8 (0.2)	19.12	18.52	18.3	18.25	18.27	18.24	17.53	17.33	17.2
J0906+0122	577026966432521088	DA	10.7 (0.4)	19.79	19.29	19.1	19.09	19.11	19.13	18.5	18.4	18.5
J0906+0128	577035178410047616	DC	10.3 (0.3)	19.65	19.06	18.84	18.81	18.87	19.0	18.17	18.1	18.0
J0906+4702	1012210992942502144	DQ	11.7 (0.4)	20.5	20.33	19.42	19.03	19.07	19.1	18.5	···	···
J0907+1042	592019425952313600	DA	12.1 (0.1)	18.17	17.72	17.591	17.6	17.646	17.7	17.0	16.81	16.8
J0907+2736	692134636881870208	DA	12.1 (0.3)	18.51	18.08	17.96	17.97	18.03	18.07	17.38	···	···
J0907+3643	715437789400182016	DA	19.4 (0.1)	17.08	16.719	16.697	16.777	16.89	16.96	16.34	16.2	15.8
J0907+5138	1016560970179771264	DC	10.1 (0.2)	19.08	18.65	18.54	18.549	18.6	18.67	18.1	···	···
J0908+4431	1009518284670371840	DA	10.6 (0.2)	18.35	18.02	18.05	18.14	18.28	18.37	17.72	···	···
J0909+0828	590316282441032704	DA	10.3 (0.3)	19.68	19.002	18.74	18.66	18.66	18.7	17.92	17.73	17.6
J0909+4700	1011466005095102464	DC	16.1 (0.3)	20.7	19.25	18.69	18.47	18.433	18.47	18.11	18.6	19.1
J0909+6019	1039435691120199936	DA	21.0 (0.1)	16.72	16.339	16.318	16.391	16.5	16.59	16.0	15.7	15.5
J0909−2246	5651964996310470144	DC	25.4 (0.2)	···	19.03	18.24	17.92	17.78	17.75	16.6	···	···
J0910+2156	685295640197734528	DA	20.0 (0.1)	18.66	17.61	17.24	17.075	17.05	17.02	16.22	16.1	16.0
J0910+2554	688818750329816192	DC*	16.2 (0.4)	20.7	19.46	18.97	18.79	18.75	18.79	18.3	···	···
J0910+3744	716010802461047552	DC	14.2 (1.2)	23.1	21.58	20.48	19.98	19.79	19.66	18.8	···	···
J0910+4929	1013058162355432832	DA	10.0 (0.2)	18.82	18.28	18.12	18.18	18.27	18.29	17.61	···	···
J0911+1354	606216148291719680	DA	13.0 (0.1)	17.37	16.965	17.006	17.11	17.24	17.34	16.74	···	···
J0911+1515	607535218647587328	DC	17.6 (0.4)	21.0	19.261	18.62	18.33	18.24	18.16	17.34	···	···
J0911−0012	3842126835031738368	DA	16.8 (0.2)	18.87	18.05	17.756	17.647	17.64	17.62	16.88	16.66	16.56
J0912+0808	590183142750379136	DZ	15.8 (0.2)	18.76	17.974	17.828	17.85	17.91	17.97	17.3	17.21	17.1
J0912+1951	636732410620758016	DA	29.4 (0.2)	19.69	18.059	17.46	17.229	17.15	17.13	16.26	15.9	15.8
J0912+2251	686867284694206336	DC	22.2 (0.2)	20.5	18.71	18.08	17.83	17.74	17.67	16.89	16.5	16.0
J0912+2538	688606063549945600	DA	26.5 (0.1)	17.55	16.879	16.647	16.579	16.599	16.6	15.86	15.44	15.08
J0913+0112	3843483151343659776	DA	14.7 (0.2)	18.74	18.25	18.11	18.11	18.17	18.22	17.48	17.33	17.3

Tableau A.1 *suite page suivante*

Tableau A.1 *(suite)*

Name	Gaia DR2/EDR3*	Sp Type	ϖ (mas)	u	g	r	i	z	y	J	H	K
J0913+2627	688954024621015040	DZ	9.4 (0.8)	23.3	20.21	19.79	19.72	19.67	19.7	19.2	···	···
J0913+3116	699920381797443712	DZ	18.2 (0.4)	20.6	18.83	18.43	18.31	18.28	18.25	17.53	17.2	17.3
J0913+4047	815429197896495104	DA	18.0 (0.1)	17.99	17.4	17.19	17.141	17.18	17.2	16.47	16.1	15.5
J0913+5933	1038500174228188416	DA	12.8 (0.2)	19.27	18.67	18.51	18.47	18.52	18.5	17.8	···	···
J0913+6205	1040160612880069888	DA	31.7 (0.1)	18.31	17.226	16.837	16.69	16.656	16.63	15.8	15.5	15.4
J0915+2719	695023530668813952	DA	10.6 (0.5)	19.49	18.84	18.618	18.55	18.549	18.53	17.9	···	···
J0915+5325	1022780838737369216	DCP	97.29 (0.04)	14.453	13.9353	13.9	13.87	13.92	13.999	13.22	13.15	13.09
J0915+6631	1068706339918614016	DA	12.7 (0.1)	18.23	17.87	17.777	17.815	17.88	17.95	···	···	···
J0916+0548	579835153490062976	DA	17.5 (0.1)	18.63	17.884	17.633	17.554	17.54	17.57	16.9	16.53	16.51
J0916+1011	591040864898749312	DQZA	25.8 (0.1)	15.98	15.79	15.823	15.938	16.08	16.17	15.61	15.56	15.56
J0916+2259	638935758908460288	DA	18.5 (0.3)	19.52	18.496	18.111	17.965	17.948	17.92	17.18	···	···
J0916+2540	687914432080614528	DZ	21.6 (0.2)	21.4	18.15	17.476	17.404	17.58	17.5	16.84	···	···
J0916+4359	818602457173176192	DA	29.83 (0.05)	15.79	15.377	15.379	15.464	15.556	15.64	15.01	14.9	14.9
J0918+0124	3844228070471625216	DC	10.1 (0.3)	19.96	19.23	18.952	18.89	18.92	18.89	18.22	18.0	18.3
J0918+1057	592605431290049152	DC	19.2 (0.2)	20.4	18.74	18.153	17.935	17.873	17.81	16.99	16.71	16.61
J0918+3222	701552327634833280	DA	9.8 (0.3)	18.48	18.032	17.96	17.98	18.04	18.12	17.48	17.4	17.2
J0918+3737	811059120212556416	DC	10.2 (0.5)	20.17	19.56	19.31	19.26	19.3	19.23	18.6	···	···
J0918−0205	3838626849001351168	DC	13.3 (0.2)	19.36	18.566	18.368	18.332	18.37	18.38	17.71	17.6	17.5
J0919+0113	3844209481853063296	DA	16.1 (0.2)	19.1	18.293	18.0	17.89	17.87	17.89	17.1	16.83	16.9
J0919+7723	1131562121144696960	DA	21.45 (0.03)	···	15.18	15.191	15.304	15.434	15.53	14.9	14.9	14.9
J0920+1935	635777617916154368	DA	14.9 (0.3)	19.15	18.43	18.14	18.03	18.034	18.05	17.28	···	···
J0920+5442	1023278947569264896	DC	9.8 (0.2)	19.44	18.97	18.85	18.85	19.04	19.0	18.4	···	···
J0920−1728	5681814336118618368	DA	18.2 (0.2)	···	17.9296	17.66	17.56	17.57	17.56	16.76	···	16.5
J0921+1729	632270313262592640	DA	9.6 (0.6)	20.25	19.56	19.33	19.25	19.272	19.27	18.6	···	···
J0921+5935	1038360708050042496	DC	11.4 (0.3)	20.15	19.34	19.07	18.99	19.0	18.96	18.4	···	···
J0922+0103	3843957354387777152	DAZ	30.8 (0.1)	17.68	16.806	16.495	16.381	16.376	16.37	15.6	15.33	15.31
J0922+0504	585488567401589248	DAH	19.5 (0.2)	19.42	18.34	17.942	17.79	17.76	17.73	16.95	16.68	16.54
J0922+2121	637716641031134848	DC :	12.8 (0.3)	19.12	18.52	18.34	18.33	18.38	18.42	17.71	···	···
J0922+2628	694006757290271360	DA	10.8 (0.3)	19.32	18.66	18.468	18.42	18.45	18.499	17.64	···	···
J0922+4125	812885610888282880	DA	10.4 (0.3)	19.61	18.86	18.6	18.488	18.48	18.51	17.74	···	···
J0923+0105	3844051225193053440	DC	15.2 (0.2)	18.63	18.12	18.002	18.02	18.09	18.17	17.5	17.4	17.4
J0923+0559	585700189030449920	DA	13.0 (0.2)	18.9	17.893	17.512	17.348	17.33	17.31	16.52	16.25	16.13
J0923+1842	632656894678554624	DQ	11.7 (0.2)	18.94	18.49	18.35	18.36	18.45	18.51	···	···	···
J0923+2413	639439884989423616	DA	12.1 (0.3)	19.09	18.53	18.4	18.39	18.44	18.49	17.82	···	···

Tableau A.1 *suite page suivante*

Tableau A.1 *(suite)*

Name	Gaia DR2/EDR3*	Sp Type	ϖ (mas)	u	g	r	i	z	y	J	H	K
J0923+4819	1011870071322756096	DA	13.5 (0.2)	19.07	18.52	18.39	18.39	18.4	18.49	17.75	···	···
J0924+0521	585513959248023936	DA	12.4 (0.3)	19.76	18.94	18.65	18.52	18.54	18.53	17.71	17.5	17.2
J0924+2107	637527525030988160	DAZ	14.3 (0.3)	19.51	18.64	18.35	18.242	18.26	18.3	17.54	···	···
J0924+3120	700531568527365376	DC	26.4 (0.3)	20.5	18.62	17.925	17.65	17.549	17.5	16.63	16.41	16.4
J0925+3130	700557819367554432	DZ	12.1 (0.3)	21.0	18.93	18.61	18.64	18.73	18.76	···	···	···
J0925+3539	798602271945568256	DA	14.5 (0.2)	18.41	17.842	17.687	17.674	17.726	17.78	···	···	···
J0925+6120	1039163458912998272	DA	36.4 (0.03)	15.458	15.054	14.984	15.025	15.108	15.173	14.5	14.36	14.3
J0926+1321	594116366425186944	DA	9.6 (0.8)	18.79	18.35	18.38	18.5	18.63	18.7	18.2	···	···
J0926+1932	634225902066816640	DA	14.6 (0.2)	18.01	17.51	17.402	17.4	17.47	17.52	16.83	···	···
J0926+3642	810799665531428608	DA	11.5 (0.4)	20.11	19.23	18.925	18.81	18.81	18.85	18.1	···	···
J0926+4725	819574013135499776	DQ	10.7 (0.2)	18.79	18.385	18.27	18.29	18.39	18.45	17.81	···	···
J0927+0028	3840946062621774592	DA	10.4 (0.3)	19.24	18.82	18.73	18.76	18.83	18.87	18.21	18.0	18.1
J0927+0207	3844512328587119616	DC	10.5 (0.3)	19.42	18.94	18.74	18.75	18.78	18.9	18.1	18.0	18.2
J0927+0947	589285627728700160	DA	11.5 (0.1)	18.1	17.785	17.859	17.99	18.18	18.26	17.74	17.7	18.0
J0928+1458	618571635330439040	DC*	22.4 (0.3)	19.56	18.48	18.043	17.86	17.83	17.79	17.06	···	···
J0928+1841	633911196927706880	DA	27.6 (0.1)	17.02	16.663	16.58	16.59	16.676	16.72	16.03	16.3	15.7
J0928+1937	634307433430523648	DZ	12.6 (0.3)	19.62	18.636	18.424	18.447	18.51	18.57	17.94	···	···
J0928+2638	694176429973819520	DQ+DA	9.9 (0.2)	18.2	17.806	17.705	17.72	17.796	17.86	17.22	···	···
J0928+3622	798742730259141376	DC	16.4 (0.1)	17.87	17.506	17.438	17.495	17.6	17.66	17.09	···	···
J0928+3737	811237923994639744	DC	11.4 (0.3)	19.53	18.89	18.71	18.708	18.75	18.85	18.2	···	···
J0928+4300	814576110016081920	DC*	14.6 (0.4)	22.1	19.95	19.18	18.86	18.74	18.67	17.79	···	···
J0928+6049	1039078998380506880	DC	11.2 (0.7)	21.8	20.56	20.14	20.45	20.7	0.0	···	···	···
J0929+3310	701307621874580864	DQ	11.0 (0.3)	18.89	18.87	18.37	18.23	18.33	18.41	17.87	17.8	···
J0929+6649	1068317142866278016	DA	10.3 (0.3)	20.4	19.51	19.17	19.04	19.06	19.06	···	···	···
J0929−1732	5681903877596752640	DA	30.3 (0.2)	···	16.057	15.966	15.954	15.99	16.03	15.4	15.2	15.1
J0930+0628	586075122495366400	DC	17.5 (0.5)	19.49	18.87	18.7	18.66	18.72	18.78	18.11	18.1	18.1
J0930+3845	811435114533149056	DA	10.5 (0.3)	19.89	19.09	18.747	18.63	18.62	18.65	17.82	···	···
J0930+5941	1038698805623461376	DA	11.1 (0.1)	18.29	17.83	17.89	17.98	18.16	18.12	17.67	···	···
J0931+2100	634839219101579136	DC*	11.9 (0.3)	20.03	19.13	18.843	18.74	18.76	18.69	18.1	···	···
J0933+2911	696261653777188864	DA	33.9 (0.1)	16.4	16.02	15.969	16.024	16.124	16.19	15.55	15.4	15.3
J0933+3743	799278226781362048	DZA	14.2 (0.2)	20.45	18.92	18.5	18.368	18.35	18.35	17.63	17.37	17.26
J0934+1910	633295848373672320	DA	15.5 (0.1)	16.99	16.62	16.639	16.744	16.87	16.96	16.34	16.1	···
J0934+5637	1025040880593486720	DA	11.4 (0.2)	19.72	19.08	18.87	18.83	18.87	18.91	···	···	···
J0935+0024	3841045053027974912	DQ	12.9 (0.4)	20.28	20.1	19.15	18.63	18.7	18.71	18.11	17.8	18.1

Tableau A.1 *suite page suivante*

Tableau A.1 *(suite)*

Name	Gaia DR2/EDR3*	Sp Type	ϖ (mas)	u	g	r	i	z	y	J	H	K
J0936+0428	3851443134492197888	DA	10.4 (0.3)	20.24	19.36	19.08	18.99	18.99	19.01	18.19	18.2	17.8
J0936+0747	587767202170593536	DA	12.1 (0.2)	17.81	17.41	17.397	17.45	17.56	17.62	17.01	16.93	16.9
J0936+8221	1145020139172129536	DA	11.8 (0.1)	17.53	17.17	17.18	17.293	17.43	17.51	16.7	16.1	···
J0938+0711	3854286918237953536	DC	10.1 (0.5)	19.48	18.98	18.8	18.76	18.83	18.87	18.5	18.1	18.3
J0938+5412	1021408850089922560	DA	11.1 (0.2)	18.53	18.08	18.1	18.19	18.32	18.37	17.72	···	···
J0939+1021	588813460499195264	DA	10.5 (0.2)	18.25	17.82	17.781	17.849	17.924	18.01	17.37	17.23	17.2
J0939+1341	617587538064096640	DA	13.4 (0.2)	19.46	18.59	18.295	18.199	18.19	18.21	···	···	···
J0939+4951	826275295988399232	DA	29.2 (0.1)	18.45	17.54	17.22	17.103	17.106	17.092	16.32	16.3	15.53
J0939+5201	1020158400426591872	DQ	13.6 (0.1)	17.39	17.189	17.21	17.335	17.49	17.59	17.05	···	···
J0939+5550	1022128244227188224	DZA	14.6 (0.1)	17.01	16.75	16.83	16.978	17.157	17.24	16.75	···	···
J0939+5911	1026514226174393344	DC	10.6 (0.3)	20.14	19.36	19.12	19.04	19.08	19.06	18.4	···	···
J0939+6018	1050825733935333376	DA	11.2 (0.2)	18.8	18.25	18.12	18.1	18.13	18.13	···	···	···
J0939−1458	5688717241916173568	DC	28.2 (0.1)	···	19.03	18.1798	17.808	17.64	17.59	16.65	···	16.5
J0940+0210	3847322577227869952	DQ	19.2 (0.1)	17.63	17.246	17.13	17.175	17.29	17.35	16.75	16.67	16.54
J0940+0906	588349771535238912	DQ	11.0 (0.4)	19.47	18.83	18.57	18.51	18.55	18.56	17.88	17.8	17.9
J0940+0907	588349805894986624	DC	20.4 (0.3)	20.04	18.48	17.95	17.738	17.67	17.62	16.82	16.58	16.44
J0941+0901	588332900903805824	DQ	11.2 (0.1)	16.96	16.804	16.845	16.974	17.098	17.2	16.68	16.59	16.6
J0941+6511	1064978578888570496	DC	21.9 (0.2)	21.54	19.24	18.4	18.05	17.91	17.82	···	···	···
J0942+0117	3846462656056088448	DA	12.8 (0.3)	19.92	19.05	18.75	18.65	18.64	18.64	17.88	17.6	17.6
J0942+0347	3848159236857539584	DA	10.0 (0.3)	19.18	18.75	18.69	18.68	18.82	18.82	18.2	18.3	18.0
J0942+0942	588530847356236672	DA	22.1 (0.2)	19.92	18.422	17.92	17.7	17.64	17.6	16.76	16.14	15.44
J0942+4437	820899298308206208	DC	12.6 (0.2)	21.4	19.31	18.56	18.232	18.15	18.07	17.15	16.97	16.86
J0942+4654	824743882449610752	DA	15.1 (0.1)	···	16.522	16.557	16.658	16.798	16.87	16.28	···	···
J0942+6600	1065088220813167744	DC	10.5 (0.2)	18.93	18.58	18.52	18.575	18.68	18.77	···	···	···
J0943+5134	1020076452450631296	DC	21.6 (0.2)	20.6	18.8	18.11	17.833	17.734	17.69	16.72	16.6	16.5
J0943−0703	3820383996887145088	DA	34.8 (0.1)	···	16.592	16.26	16.136	16.131	16.12	15.289	15.06	14.98
J0944+4407	820169737983275904	DA	11.2 (0.3)	19.56	19.0	18.78	18.74	18.77	18.8	18.12	···	···
J0944+4807	825049851623687296	DC	15.2 (0.2)	19.26	18.53	18.3	18.22	18.26	18.27	17.53	···	···
J0944+6037	1050892563625773184	DA	11.1 (0.1)	17.76	17.41	17.434	17.542	17.68	17.74	···	···	···
J0945+0154	3846557660732848384	DA	18.5 (0.1)	18.02	17.414	17.24	17.215	17.24	17.28	16.57	16.36	16.39
J0945+2327	641625576666483584	DA	16.1 (0.1)	17.99	17.424	17.301	17.29	17.339	17.38	16.67	16.3	16.0
J0945+2327	641625576666484480	DA	15.9 (0.1)	18.19	17.599	17.434	17.44	17.45	17.46	16.72	16.3	···
J0945+4035	801512095107318144	DA	13.0 (0.2)	18.79	18.14	17.976	17.94	17.97	17.99	17.19	···	···
J0945+6850	1070129451562454400	DC	14.1 (0.1)	17.85	17.594	17.68	17.815	17.92	17.96	···	···	···

Tableau A.1 *suite page suivante*

Tableau A.1 *(suite)*

Name	Gaia DR2/EDR3*	Sp Type	ϖ (mas)	u	g	r	i	z	y	J	H	K
J0946+2255	641362724667841536	DA	10.3 (0.4)	19.54	18.91	18.67	18.607	18.63	18.63	18.0	···	···
J0946+3251	793575201703625984	DA	22.7 (0.1)	17.88	17.27	17.058	17.001	17.03	17.04	16.35	16.0	15.8
J0946+6738	1069735341067492224	DA	12.3 (0.2)	19.03	18.41	18.2	18.15	18.2	18.17	···	···	···
J0947+4459	820969357814798080	DC	18.5 (0.4)	20.7	19.39	18.85	18.95	19.34	19.63	19.7	20.3	21.0
J0947+4500	820969357814799872	DA	18.1 (0.3)	21.0	19.48	18.76	18.516	18.45	18.34	17.43	17.24	17.11
J0948+1232	613553056239392768	DQ	12.4 (0.2)	18.67	18.28	18.15	18.16	18.23	18.3	17.65	17.6	17.7
J0948+1319	614379236149119360	DA	18.2 (0.2)	18.01	17.48	17.27	17.216	17.25	17.27	16.53	16.1	16.51
J0948+1519	616394263005286272	DA	12.7 (0.3)	18.59	18.182	18.104	18.12	18.18	18.29	17.64	···	···
J0948+2023	639665392247496576	DC	27.2 (0.2)	20.5	18.43	17.76	17.489	17.38	17.33	16.47	16.3	15.7
J0948+2441	643229626692471040	DA	12.1 (0.1)	17.74	17.356	17.36	17.439	17.573	17.68	17.04	···	···
J0948+5252	1020268248510254464	DA	9.8 (0.2)	19.11	18.58	18.45	18.42	18.48	18.5	17.77	···	···
J0950+1509	616396182856185728	DC	25.9 (0.3)	19.15	17.85	17.392	17.195	17.15	17.12	16.3	16.0	15.36
J0950+3238	793334404360693632	DQA	11.0 (0.5)	17.67	17.453	17.449	17.55	17.66	17.76	···	···	···
J0950+5315	1020653077580086784	DQ	36.31 (0.05)	15.441	15.179	15.178	15.274	15.404	15.484	14.94	14.9	14.9
J0951+1009	3879201783004024832	DA	13.2 (0.2)	18.75	18.135	17.939	17.896	17.89	17.95	17.21	17.01	17.0
J0951+1900	627240597321087488	DC	20.3 (0.2)	18.94	18.06	17.679	17.532	17.49	17.51	16.79	16.4	17.33
J0951+2045	628067498784238208	DC	9.8 (0.4)	19.68	19.05	18.825	18.79	18.81	18.8	18.3	···	···
J0951+4033	807280785942808320	DZA	13.8 (0.1)	17.8	17.55	17.547	17.65	17.79	17.87	17.32	···	···
J0951+8039	1132614349476009728	DC	10.9 (0.2)	19.81	19.15	18.89	18.89	18.92	19.09	···	···	···
J0952+0602	3850381865253059328	DC	13.3 (0.3)	18.56	18.06	17.946	17.99	18.04	18.15	17.48	17.4	17.4
J0952+4454	820542992117501952	DA+dM	16.1 (0.1)	16.29	15.89	16.03	16.2	16.36	16.4	···	···	···
J0952+4807	823393402996648960	DA	11.6 (0.1)	18.29	17.79	17.739	17.759	17.84	17.88	17.24	···	···
J0954+3046	744878171010647552	DC	10.3 (0.5)	20.06	19.29	19.063	18.98	19.01	19.02	18.27	···	···
J0954+3129	745127553991482368	DA	10.9 (0.2)	19.06	18.46	18.28	18.23	18.25	18.27	17.51	···	···
J0954+6022	1050272718241775488	DC	13.7 (0.2)	19.34	18.63	18.38	18.353	18.35	18.38	···	···	···
J0954+6702	1066726497434084864	DA	39.2 (0.1)	18.0	16.95	16.55	16.388	16.35	16.358	15.5	15.3	15.5
J0955+5056	826954824238274048	DA	11.7 (0.1)	18.6	18.1	17.97	17.958	18.01	18.07	17.38	···	···
J0956+2114	628141337862068864	DA	13.1 (0.3)	18.37	18.042	18.03	18.093	18.19	18.28	···	···	···
J0957+0515	3850056169293341824	DC	13.2 (0.2)	18.42	17.91	17.789	17.8	17.86	17.97	17.22	17.22	17.1
J0957+2432	642685200933153408	DA	36.3 (0.1)	15.364	15.108	15.088	15.151	15.263	15.343	14.678	14.7	14.7
J0957−0107	3832801498958855552	DA	13.6 (0.1)	18.16	17.73	17.633	17.647	17.73	17.77	17.13	17.02	17.1
J0958+0846	3877871477014130048	DA	16.8 (0.1)	18.31	17.684	17.494	17.458	17.487	17.51	16.79	16.64	16.61
J0958+4345	808268967721645696	DA	11.6 (0.2)	19.34	18.63	18.37	18.301	18.3	18.32	17.57	···	···
J0959+0257	3836456103811208064*	DA	11.1 (0.2)	18.77	18.25	18.134	18.116	18.16	18.21	17.54	17.37	17.3

Tableau A.1 *suite page suivante*

Tableau A.1 *(suite)*

Name	Gaia DR2/EDR3*	Sp Type	ϖ (mas)	u	g	r	i	z	y	J	H	K
J0959+1445	615705144092773376	DC	14.9 (0.2)	18.29	17.86	17.75	17.767	17.86	17.9	17.31	···	···
J0959+1528	616587738397098240	DA	12.6 (0.1)	18.18	17.702	17.615	17.61	17.68	17.75	···	···	···
J0959+2513	642837135401004672	DA	12.8 (0.2)	18.91	18.31	18.12	18.08	18.12	18.16	17.41	···	···
J0959+2556	643650361688870656	DZ	17.5 (0.2)	16.75	16.555	16.599	16.721	16.88	16.96	16.43	16.3	···
J1000+1231	3881473820703514752	DA	10.3 (0.2)	18.15	17.73	17.746	17.835	17.94	17.99	17.39	17.31	17.5
J1000+4236	807222713688595200	DC	17.7 (0.4)	21.7	19.5	18.74	18.462	18.37	18.34	17.47	17.23	17.13
J1001+1441	615733593956317568	DC	51.5 (0.1)	16.1	15.522	15.334	15.299	15.342	15.355	14.698	14.5	14.5
J1001+2428	642463713764824192	DA	11.2 (0.3)	19.61	19.08	18.92	18.89	18.9	18.99	18.4	···	···
J1001+3903	803211596486728064	DC	15.3 (0.6)	21.4	19.96	19.6	19.99	20.35	···	20.6	21.0	···
J1001+4656	822352371643412352	DC	24.3 (0.3)	21.3	19.13	18.3	17.94	17.83	17.74	16.79	16.7	17.0
J1002+4326	808030648576069760	DC	28.5 (0.2)	20.45	18.45	17.72	17.447	17.349	17.26	16.42	···	···
J1002+6108	1050402662475992320	DC	23.6 (0.2)	21.8	19.29	18.42	18.04	17.919	17.86	16.8	16.7	16.72
J1003+3303	746736796632638976	DA	12.3 (0.1)	17.24	16.882	16.917	17.03	17.183	17.28	16.69	17.7	16.1
J1003+3543	795686191013196544	DA	10.1 (0.4)	19.05	18.63	18.6	18.648	18.75	18.8	18.2	···	···
J1003+5401	852604201427010816	DA	10.2 (0.1)	17.66	17.253	17.333	17.446	17.6	17.69	17.13	···	···
J1003−0337	3828424828500179584	DA	30.0 (0.1)	···	15.481	15.454	15.512	15.62	15.676	15.01	14.9	15.0
J1004+1052	3880219037418284160	DA	10.5 (0.4)	19.81	19.29	19.09	19.06	19.1	19.13	18.5	18.4	18.3
J1004+2003	626844326458669568	DA	13.6 (0.2)	18.37	18.064	18.027	18.1	18.18	18.26	17.72	···	···
J1004+3405	747348704918599552	DA	11.1 (0.3)	19.78	19.052	18.81	18.722	18.72	18.69	18.1	···	···
J1004−0506	3822028007288795264	DC	28.3 (0.1)	···	19.117	18.163	17.784	17.7	17.73	17.8	18.3	···
J1005+0308	3836605980989228928	DA	11.7 (0.2)	18.16	17.675	17.62	17.678	17.77	17.84	17.19	17.05	16.98
J1005+5354	852433880203843712	DA	17.9 (0.1)	18.66	18.012	17.835	17.793	17.83	17.89	···	···	···
J1006+0711	3874412413432643328	DC	18.5 (0.3)	21.1	19.26	18.586	18.3	18.23	18.18	17.35	17.03	16.96
J1006+0712	3874412413432647680	DA	18.4 (0.1)	16.41	16.0	16.065	16.173	16.32	16.44	15.84	15.75	15.77
J1006−1828	5672600772274345600	DC	20.0 (0.2)	···	18.93	18.25	17.95	17.84	17.78	16.94	16.5	16.6
J1007+1541	621824987157964544	DA	13.9 (0.2)	18.2	17.68	17.556	17.544	17.61	17.64	16.93	···	···
J1007+1623	621979502901486720	DAH	11.7 (0.1)	18.03	17.711	17.81	17.97	18.13	18.23	17.76	···	···
J1007+3229	745895322345421568	DA	10.1 (0.1)	18.06	17.77	17.798	17.924	18.07	18.14	17.61	···	···
J1009+3621	801684301820413952	DA	13.3 (0.2)	18.92	18.21	17.951	17.88	17.9	17.94	17.16	···	···
J1010+4028	803585018126670208	DA	15.5 (0.2)	19.37	18.48	18.13	18.009	18.01	18.05	17.23	···	···
J1010+6155	1051954485699665280	DA	11.2 (0.2)	19.39	18.87	18.7	18.64	18.67	18.66	18.1	18.0	17.68
J1011+0029	3831947801194371072	DAH	24.6 (0.1)	18.1	17.326	17.01	16.924	16.91	16.9	16.1	15.9	···
J1011+2647	739253825436690432	DA	22.4 (0.2)	19.54	18.178	17.69	17.51	17.44	17.41	16.58	16.2	15.6
J1011+2845	740483560857296768	DQ*	67.8 (0.1)	18.27	18.26	16.404	15.968	16.005	16.01	15.11	14.7	14.5

Tableau A.1 *suite page suivante*

Tableau A.1 *(suite)*

Name	Gaia DR2/EDR3*	Sp Type	ϖ (mas)	u	g	r	i	z	y	J	H	K
J1011+3727	801851053926004608	DAH :	11.7 (0.3)	19.68	18.862	18.61	18.52	18.58	18.6	17.81	···	···
J1011+4958	823804585985883776	DAH	13.1 (0.2)	19.81	18.97	18.67	18.556	18.55	18.56	17.82	···	···
J1012+6116	1051676171819127040	DA	10.6 (0.2)	20.02	19.16	18.83	18.72	18.71	18.65	···	···	···
J1012−1843	5669427512997660800	DZ	55.3 (0.1)	···	15.564	15.33	15.29	15.343	15.385	14.662	14.5	14.49
J1013+0305	3835861439819152128	DA	19.8 (0.3)	20.17	18.61	18.069	17.83	17.753	17.73	16.86	16.56	16.46
J1013+1733	622536749138267904	DC	11.4 (0.3)	19.47	18.96	18.79	18.79	18.82	18.92	18.3	···	···
J1014+0305	3835866563715176192	DA	21.0 (0.4)	20.08	18.54	17.99	17.778	17.72	17.68	16.79	16.54	16.46
J1014+0401	3860751256335185408	DA	19.5 (0.2)	17.31	16.813	16.73	16.708	16.78	16.86	16.12	15.95	15.94
J1014+2027	625415030061614336	DA	11.9 (0.1)	17.48	17.126	17.151	17.234	17.38	17.46	16.87	···	···
J1014+4226	805470233890349440	DA	32.0 (0.1)	16.77	16.357	16.27	16.279	16.355	16.41	15.72	15.5	15.3
J1014+5027	847884509109410816	DA	12.6 (0.2)	18.3	17.81	17.702	17.716	17.785	17.82	17.15	···	···
J1015+0806	3875651975353757440	DC	33.5 (0.3)	20.32	18.2	17.423	17.136	16.997	16.96	16.08	15.8	15.81
J1015+0806	3875652014008894720	DA	33.8 (0.1)	16.78	16.14	15.93	15.87	15.893	15.918	15.138	14.93	14.9
J1015+0907	3876618892751168000	DAH	11.8 (0.3)	19.13	18.62	18.44	18.433	18.5	18.51	17.86	17.69	17.7
J1015+1850	624921521139276800	DC	14.8 (0.2)	21.3	19.24	18.473	18.15	18.02	17.93	17.14	16.97	16.5
J1016+1817	624090737025312000	DC*	10.5 (0.3)	19.46	18.94	18.84	18.81	18.91	18.93	18.2	···	···
J1016+1932	625075796364911360	DA	10.7 (0.1)	17.74	17.372	17.43	17.479	17.631	17.72	17.09	···	···
J1016−0119	3830623164560911872	DA	21.5 (0.1)	15.885	15.41	15.349	15.35	15.438	15.488	14.798	14.65	14.62
J1017+0838	3875789001991057536	DQ	22.8 (0.1)	16.79	16.422	16.38	16.451	16.547	16.627	16.0	15.9	15.93
J1017+2336	725478112972149504	DAH :	12.7 (0.2)	17.77	17.6	17.666	17.82	17.97	18.09	17.56	···	···
J1017+7619	1127701323501940224	DA	22.0 (0.1)	···	16.869	16.679	16.67	16.72	16.76	16.1	15.7	15.47
J1018+0111	3832329434808415744	DAH	20.1 (0.1)	16.54	16.337	16.434	16.577	16.747	16.87	16.35	16.34	16.32
J1018+0547	3861407596057614080	DA	11.0 (0.8)	20.04	19.32	19.0	18.92	18.91	18.94	18.11	18.0	17.7
J1018+3421	752524965144307584	DA	15.9 (0.3)	19.85	19.29	19.17	19.14	19.17	19.26	18.6	···	···
J1018−0442	3780210350269115776	DAZ	16.5 (0.2)	···	17.148	17.065	17.101	17.18	17.25	16.54	16.42	16.4
J1019+3138	742962753035089792	DA	12.3 (0.2)	19.07	18.62	18.44	18.43	18.49	18.53	17.88	···	···
J1019+5214	848290091460808448	DA	20.1 (0.1)	19.87	18.42	17.94	17.747	17.68	17.65	16.89	16.7	···
J1021+1905	624600566824086016	DA	12.0 (0.2)	19.38	18.66	18.38	18.3	18.28	18.3	17.56	···	···
J1021+2503	726057456815979904	DA	10.7 (0.2)	18.2	17.786	17.74	17.795	17.91	18.0	17.34	···	···
J1021+4257	805697489201014272	DA	13.9 (0.2)	19.21	18.48	18.2	18.128	18.16	18.16	17.43	···	···
J1021−1034	3767515389014753152	DAH*	21.0 (0.1)	···	16.375	16.457	16.603	16.784	16.87	16.34	16.34	16.35
J1022+0708	3863287692225892736	DA	11.9 (0.2)	19.64	18.83	18.59	18.48	18.46	18.47	17.76	17.57	17.7
J1022+1328	3886816622581111552	DA	12.3 (0.4)	19.13	18.491	18.28	18.205	18.24	18.28	17.51	17.25	17.4
J1022+1658	3890322415406225408	DA	13.5 (0.2)	18.86	18.18	18.0	17.944	17.98	17.97	17.19	···	···

Tableau A.1 *suite page suivante*

Tableau A.1 *(suite)*

Name	Gaia DR2/EDR3*	Sp Type	ϖ (mas)	u	g	r	i	z	y	J	H	K
J1022+2523	726160806613850624	DA	11.9 (0.2)	18.0	17.63	17.595	17.657	17.77	17.83	17.23	···	···
J1022+3904	755877620910173696	DZ	25.7 (0.1)	18.73	17.531	17.28	17.233	17.28	17.32	16.6	16.28	16.45
J1022+4600	833452873535333760	DA	14.4 (0.1)	17.17	16.731	16.619	16.647	16.726	16.78	16.11	16.1	15.8
J1022+4612	833470465721350784	DA	30.3 (0.1)	16.91	16.395	16.264	16.244	16.29	16.32	15.61	15.5	15.6
J1022+5344	851806982481563264	DA	9.7 (0.3)	19.32	18.8	18.56	18.544	18.58	18.55	17.88	···	···
J1022+8243	1146403741412820864	DA	25.0 (0.1)	···	18.248	17.84	17.68	17.67	17.62	16.6	16.2	···
J1023+3319	749177746806827264	DC :	12.2 (0.2)	18.11	17.87	17.81	17.903	18.01	18.09	17.48	···	···
J1023+6327	1052520154368111872	DA	62.73 (0.02)	15.458	14.828	14.619	14.57	14.625	14.65	13.87	13.73	13.69
J1023+6348	1052563683861162880	DA	16.8 (0.1)	18.92	18.094	17.793	17.69	17.68	17.67	···	···	···
J1024+8019	1133810794221801856	DA	12.7 (0.1)	18.2	17.74	17.63	17.668	17.74	17.76	···	···	···
J1024−0023	3830990156631488128	DA	13.6 (0.2)	17.24	17.11	17.2	17.33	17.484	17.581	17.02	17.01	17.2
J1025+0521	3860625435268868864	DA	9.9 (0.2)	18.1	17.699	17.69	17.78	17.89	18.0	17.39	17.19	17.2
J1025+6142	1048769578471443072	DC	13.7 (0.2)	19.88	18.99	18.65	18.519	18.52	18.53	···	···	···
J1025+6407	1053321934567306752	DC	11.4 (0.2)	19.37	18.97	18.77	18.68	18.67	18.69	···	···	···
J1026+1439	3887433414244718464	DA	12.1 (0.2)	17.56	17.138	17.145	17.24	17.37	17.44	16.86	16.5	16.62
J1026+5807	1047132925349510784	DQ	14.5 (0.1)	17.33	17.113	17.142	17.23	17.36	17.47	16.94	···	···
J1027+1218	3883495444630204672	DQ	10.3 (0.3)	19.01	18.59	18.486	18.54	18.62	18.68	18.09	17.9	18.3
J1027+1644	3890141958060313984	DA	11.0 (0.3)	18.49	18.2	18.24	18.316	18.45	18.56	···	···	···
J1027+1928	624510170646474112	DA	22.3 (0.1)	17.87	17.382	17.23	17.23	17.26	17.27	16.62	16.5	16.94
J1027+5019	847272257226467840	DZ	13.7 (0.4)	20.1	18.98	18.65	18.55	18.56	18.53	17.84	···	···
J1028+0344	3857118439852847744	DA	13.3 (0.1)	17.91	17.54	17.46	17.47	17.56	17.68	16.96	16.8	16.9
J1028+1451	3888929097950924416	DAH	15.4 (0.2)	19.51	18.53	18.15	18.006	17.98	17.96	17.21	···	···
J1028+3512	752814274140797568	DQ	13.5 (0.2)	19.67	19.31	18.61	18.44	18.51	18.53	17.9	···	···
J1028+3750	754853769426521856	DA	10.2 (0.2)	19.35	18.81	18.55	18.55	18.56	18.52	17.85	···	···
J1028+5815	1047228922162323968	DC	14.4 (0.1)	18.46	17.898	17.714	17.678	17.741	17.79	17.17	···	···
J1029+1127	3882611201058534400	DAH	29.7 (0.1)	17.34	16.71	16.518	16.494	16.53	16.61	15.88	15.76	15.71
J1029+2300	722391440239688064	DA	10.9 (0.3)	19.65	19.08	18.89	18.83	18.85	18.97	18.2	···	···
J1029+7931	1132966468074614272	DA	15.1 (0.2)	19.95	19.12	18.84	18.73	18.74	18.7	···	···	···
J1029−2624	5469171261208778240	DA	29.1 (0.1)	···	17.266	16.891	16.735	16.7	16.68	15.84	15.6	15.52
J1030+0845	3863974783909961600	DA	12.4 (0.2)	19.64	18.787	18.47	18.37	18.34	18.38	17.62	17.3	17.3
J1030−1423	3750749378584132992	DA	36.2 (0.1)	···	16.84	16.506	16.399	16.38	16.365	15.65	15.4	15.4
J1031+1203	3883044266905679488	DZ	9.9 (0.3)	18.24	17.882	17.94	18.09	18.25	18.36	17.8	17.6	17.8
J1032+0218	3856005626711298560	DA	12.3 (0.1)	17.04	16.597	16.701	16.85	17.027	17.13	16.6	16.57	16.58
J1032+1516	3889004478921783296	DC	13.6 (0.3)	20.15	19.1	18.7	18.549	18.53	18.51	···	···	···

Tableau A.1 *suite page suivante*

Tableau A.1 *(suite)*

Name	Gaia DR2/EDR3*	Sp Type	ϖ (mas)	u	g	r	i	z	y	J	H	K
J1032+4104	756515161560637952	DA	16.4 (0.1)	18.38	17.79	17.59	17.539	17.568	17.58	16.87	···	···
J1032−0205	3781742343628799232	DA	11.7 (0.5)	19.62	18.91	18.64	18.55	18.55	18.56	17.77	17.5	17.5
J1033+1446	3885878502939219712	DA	12.1 (0.3)	18.57	18.035	17.92	17.9	17.94	18.01	···	···	···
J1033+2839	729219716681441280	DA	10.9 (0.1)	17.58	17.107	17.178	17.299	17.44	17.55	17.0	···	···
J1034+2245	721648380828681984	DZ	24.5 (0.1)	17.34	16.637	16.574	16.69	16.806	16.87	16.27	16.4	15.75
J1034+3949	755466845943050368	DA	15.0 (0.6)	20.4	19.97	19.79	19.75	19.8	19.71	19.1	···	···
J1035+0430	3858586012997916160	DC	15.1 (0.2)	18.53	18.024	17.9	17.921	17.992	18.05	17.49	17.3	17.3
J1035+0727	3862830334039617408	DA	11.3 (0.3)	18.88	18.37	18.22	18.182	18.24	18.28	17.55	17.3	17.4
J1035+2126	721244821406496640	DAH	18.9 (0.1)	17.96	17.383	17.217	17.18	17.24	17.26	16.63	16.8	15.6
J1035+4041	780275504757613568	DA*	17.5 (0.3)	20.22	18.79	18.23	18.03	17.96	17.93	17.07	···	···
J1036+0732	3862858165427681536	DC	17.7 (0.4)	22.2	19.81	18.93	18.54	18.4	18.3	17.51	17.6	17.3
J1036+7110	1076941716370493696	DC	56.7 (0.1)	···	17.28	16.56	16.27	16.19	16.12	15.19	14.8	15.0
J1037+4227	780712285751716224	DA	14.6 (0.4)	19.69	18.91	18.65	18.574	18.59	18.55	17.85	···	···
J1037+6304	1049324629980448256	DA	10.1 (0.1)	18.35	17.863	17.74	17.732	17.8	17.82	···	···	···
J1038+0202	3855792630692650112	DA	11.5 (0.3)	18.89	18.34	18.19	18.185	18.22	18.27	17.56	17.4	17.5
J1038+3402	750160156150755328	DZ	13.6 (0.5)	20.25	19.14	18.74	18.63	18.63	18.58	17.97	···	···
J1038−2040	3553682127126319360	DQP*	70.8 (0.1)	···	16.64	15.725	15.724	15.721	15.669	14.642	14.35	14.08
J1039+1803	3986005971704112256	DQ	9.7 (0.8)	20.67	19.79	19.26	19.14	19.19	19.1	18.7	···	···
J1039+3800	752057981939651584	DA	12.9 (0.1)	18.52	17.99	17.83	17.81	17.86	17.88	17.2	···	···
J1039+4135	780429608184054912	DA	12.9 (0.2)	18.2	17.76	17.637	17.65	17.719	17.74	17.11	···	···
J1039+4614	830472368094495232	DC	10.2 (0.8)	20.8	19.81	19.54	19.43	19.44	19.37	18.6	···	···
J1040+1003	3870354528331257984	DC	26.9 (0.1)	18.2	17.391	17.078	16.979	16.981	16.99	16.0	16.3	16.1
J1040+2407	723361209490895744	DZ	10.7 (0.3)	21.6	19.22	18.82	18.86	19.02	19.0	18.6	···	···
J1040+3943	779223787525884928	DA	11.3 (0.2)	18.21	17.78	17.699	17.728	17.818	17.87	17.22	···	···
J1041+1415	3884899559633556224	DC*	26.5 (0.1)	17.05	16.58	16.466	16.486	16.56	16.64	15.94	15.87	15.81
J1042+1017	3870346934829606528	DC	18.3 (0.2)	19.14	18.383	18.12	18.034	18.06	18.07	17.42	17.22	17.1
J1042+2412	723319324969842304	DA	10.1 (0.5)	20.37	19.66	19.37	19.29	19.3	19.3	18.6	···	···
J1042+4448	829441717689202816	DC	10.3 (0.4)	20.23	19.42	19.13	19.062	19.07	19.04	18.5	···	···
J1042+4932	835731057331866880	DC	14.4 (0.2)	20.7	19.11	18.574	18.382	18.33	18.32	17.51	17.32	17.32
J1042−2108	3553408245652181760	DA :	11.2 (0.1)	···	17.27	17.36	17.4	17.64	17.62	17.38	···	17.3
J1043+3516	750713313579071232	DZ	11.7 (0.3)	20.7	18.9	18.62	18.622	18.71	18.71	18.1	···	···
J1044+0214	3809230860172408320	DA	13.5 (0.2)	18.47	17.909	17.787	17.748	17.809	17.85	17.13	16.96	16.89
J1044+2023	3987528623509801984	DZ	11.2 (0.2)	18.03	17.763	17.779	17.906	18.0	18.12	17.53	···	···
J1044+2645	730811362842136704	DA	11.4 (0.2)	18.21	17.77	17.745	17.79	17.89	17.97	17.35	···	···

Tableau A.1 *suite page suivante*

Tableau A.1 *(suite)*

Name	Gaia DR2/EDR3*	Sp Type	ϖ (mas)	u	g	r	i	z	y	J	H	K
J1044+2921	734744453373358848	DA	9.9 (0.5)	20.31	19.43	19.11	19.0	18.99	18.94	18.3	···	···
J1044+5513	850713449448779008	DC	10.4 (0.3)	19.48	18.95	18.79	18.77	18.86	18.96	···	···	···
J1045+5904	855361055035055104	DQ	17.5 (0.1)	17.75	17.78	17.697	17.761	17.92	18.04	17.74	···	17.96
J1045−1906	3554395813252626048	DQ	53.1 (0.1)	···	15.82	15.38	15.1	15.18	15.06	14.62	14.41	14.36
J1046+2424	723524383888419840	DZ	16.9 (0.2)	18.69	18.02	17.83	17.81	17.85	17.88	17.22	···	···
J1047+0007	3806529291383459456	DC	11.9 (0.2)	17.87	17.428	17.298	17.31	17.374	17.4	16.8	16.6	16.58
J1047+3453	750469737393655936	DA	12.7 (0.1)	16.97	16.5	16.462	16.516	16.62	16.69	16.0	16.0	15.7
J1047+3736	775758092515293696	DA	9.6 (0.6)	20.5	19.45	19.12	18.97	18.96	18.96	18.1	···	···
J1047+4509	829430275896255232	DA	9.9 (0.2)	18.31	17.84	17.79	17.839	17.93	17.97	17.33	···	···
J1047+5912	855387061061127168	DQ	9.9 (0.1)	18.01	17.809	17.834	17.95	18.09	18.17	17.64	···	17.6
J1047−0924	3761499853524374784	DA	18.3 (0.1)	···	16.493	16.546	16.653	16.779	16.86	16.3	16.27	16.27
J1048+2113	3989101543613421184	DA	10.5 (0.7)	19.9	19.35	19.12	19.09	19.09	19.08	18.3	···	···
J1048+6334	1055313016981775488	DA	29.1 (0.1)	19.43	17.829	17.29	17.084	17.019	16.96	16.1	15.8	15.5
J1049+0958	3869429224872527744	DA	19.6 (0.2)	18.18	17.614	17.438	17.39	17.43	17.45	16.74	16.57	16.55
J1049+4543	830949079408842752	DC	14.8 (0.4)	22.0	19.9	19.15	18.84	18.72	18.7	17.89	···	···
J1049+4752	832162626703637888	DA	11.2 (0.6)	21.5	19.79	19.27	19.069	19.0	18.88	18.17	···	···
J1049+5154	836823151552466304	DZ	12.5 (0.2)	18.69	17.94	17.872	17.933	18.05	18.11	17.58	···	···
J1049−0008	3806277464565712256	DA	11.2 (0.3)	18.99	18.42	18.192	18.13	18.165	18.17	17.5	17.3	17.3
J1050+3225	737619062099922688	DA	23.1 (0.1)	19.14	17.95	17.52	17.359	17.32	17.32	16.49	16.49	16.09
J1050+3306	737721346745881728	DA	10.5 (0.3)	20.8	19.51	19.11	18.95	18.93	18.9	18.2	···	···
J1050+3426	738375899762150912	DA	11.7 (0.2)	19.32	18.61	18.36	18.296	18.3	18.28	···	···	···
J1052+4050	776762672481353984	DC	29.4 (0.1)	17.67	16.96	16.692	16.643	16.61	16.668	15.97	15.5	15.21
J1053+2425	3996172640334271872	DA	23.4 (0.2)	18.94	17.962	17.587	17.46	17.43	17.43	16.69	16.3	16.12
J1055+0403	3809758930696054784	DC	11.6 (0.3)	19.51	18.92	18.71	18.68	18.72	18.79	18.22	18.0	18.2
J1055+2111	3988212592756945152	DAH	21.1 (0.2)	18.7	17.8	17.492	17.39	17.382	17.39	16.63	17.09	15.8
J1055+2525	729726763340729600	DAH	12.2 (0.4)	19.0	18.46	18.29	18.28	18.322	18.37	17.68	···	···
J1055+4130	778305557877833088	DC	9.7 (0.4)	19.99	19.39	19.11	19.08	19.13	19.14	···	···	···
J1055+5241	837242890116333312	DA	10.7 (0.2)	18.35	17.959	17.97	18.066	18.18	18.28	17.77	···	···
J1056+0644	3864754303293985792	DC :	10.4 (0.2)	18.82	18.42	18.34	18.381	18.46	18.53	17.95	18.0	17.8
J1056+2336	3989883777417007232	DA	22.5 (0.2)	19.9	18.307	17.78	17.57	17.5	17.47	16.62	16.6	16.25
J1056+3852	775531009004593664	DA	17.6 (0.2)	19.66	18.61	18.2	18.07	18.04	18.03	17.25	···	···
J1056+5714	857165662854257792	DZ	10.6 (0.1)	18.74	18.38	18.29	18.32	18.41	18.41	17.86	···	17.79
J1056−2252	3549471753507182592	DA	27.6 (0.1)	16.55	16.13	15.978	16.028	16.11	16.143	15.441	15.4	15.31
J1057+0411	3815759279181364864	DAH	12.9 (0.1)	18.08	17.669	17.58	17.608	17.683	17.75	17.12	17.06	17.0

Tableau A.1 *suite page suivante*

Tableau A.1 *(suite)*

Name	Gaia DR2/EDR3*	Sp Type	ϖ (mas)	u	g	r	i	z	y	J	H	K
J1057+1158	3871736820606012928	DA	10.7 (0.2)	18.37	17.99	17.94	17.992	18.07	18.15	17.47	17.45	17.4
J1057+3008	733294781652279680	DC	20.5 (0.2)	18.19	17.547	17.343	17.271	17.31	17.31	16.65	···	···
J1057+3208	736984742674902912	DC	13.9 (0.2)	18.71	18.09	17.944	17.932	18.0	18.02	17.36	···	···
J1057+4145	778326792196212352	DC	11.8 (0.2)	18.93	18.468	18.33	18.34	18.39	18.47	17.9	···	···
J1057−0413	3789156870225942656	DZ	27.5 (0.1)	···	16.626	16.488	16.523	16.59	16.64	15.98	15.92	15.84
J1057−0731	3763445409285757824	DC	81.46 (0.04)	···	14.388	14.286	14.307	14.378	14.45	13.755	13.684	13.637
J1058+3503	762295264123316864	DC	15.3 (0.2)	18.0	17.656	17.621	17.7	17.77	17.81	17.24	···	···
J1058+4748	831785498511369344	DC	13.7 (0.6)	22.7	20.47	19.55	19.19	19.05	18.98	18.1	···	···
J1059+2700	730264772419060608	DC	11.4 (0.4)	20.38	19.44	19.14	19.02	19.04	18.98	18.2	···	···
J1059−1748	3556190937783724928	DA	11.0 (0.3)	19.34	18.71	18.49	18.4	18.47	18.44	17.68	···	17.4
J1101+1942	3984813379545559424	DA	10.5 (0.5)	19.84	19.14	18.9	18.81	18.8	18.83	18.01	···	···
J1102+0214	3808536101967194368	DZ	10.4 (0.5)	21.4	19.44	19.19	19.16	19.23	19.3	18.5	18.5	18.4
J1102+2054	3985469616188225152	DS*	14.8 (0.1)	17.57	17.27	17.28	17.379	17.46	17.6	17.04	···	···
J1102+4030	777221198894621440	DA	18.6 (0.2)	20.4	18.81	18.246	18.02	17.94	17.91	17.09	16.78	16.67
J1102+4112	777395029106166272	DC	28.6 (0.3)	22.96	19.993	18.74	18.21	17.98	17.93	17.24	17.33	17.34
J1102+6707	1059423708705441152	DC	15.1 (0.2)	21.2	19.53	18.95	18.68	18.6	18.6	17.76	17.49	17.41
J1103+0902	3866845986727270400	DA	12.4 (0.3)	20.16	19.28	18.96	18.82	18.84	18.84	18.02	17.8	17.7
J1103+3935	776981269136616960	DAZ	25.8 (0.2)	20.01	18.29	17.663	17.414	17.328	17.3	16.42	···	···
J1103+4248	778845108849112704	DC	12.3 (0.6)	19.77	18.903	18.6	18.47	18.43	18.44	17.63	···	···
J1104+0436	3815105615223622144	DC	18.8 (0.3)	22.1	19.71	18.88	18.53	18.44	18.31	17.42	17.3	17.3
J1104−1837	3552845261339955200	DA	25.0 (0.1)	16.43	16.035	15.972	16.006	16.09	16.17	15.507	15.3	15.38
J1106+2539	3996544137821457664	DC	9.6 (0.4)	19.6	19.01	18.98	18.94	18.98	19.04	18.3	···	···
J1106+4518	782378320745502336	DA	24.6 (0.2)	17.44	16.972	16.862	16.868	16.945	17.0	16.3	16.0	15.9
J1106+6210	862260868456553856	DA	12.0 (0.1)	17.67	17.314	17.395	17.519	17.71	17.79	···	···	···
J1107+1446	3968635204109066880	DA	26.0 (0.1)	17.38	16.751	16.541	16.472	16.489	16.53	15.79	15.56	15.53
J1107+4059	777512951728187392	DQ	18.4 (0.2)	17.71	17.23	17.1	17.107	17.14	17.15	16.63	···	···
J1107+4855	831946229073235200	DC	20.8 (0.3)	21.6	19.3	18.53	18.21	18.1	18.07	17.05	17.0	16.9
J1107+5246	842498482680906496	DA	10.4 (0.2)	19.01	18.49	18.34	18.313	18.34	18.43	17.67	···	···
J1107+5246	842504358196167680	DA	10.3 (0.2)	19.37	18.79	18.57	18.489	18.51	18.57	17.8	···	···
J1107−0220	3791246075462610304	DA	10.6 (0.1)	17.68	17.35	17.438	17.57	17.75	17.87	17.3	17.28	17.5
J1108+0801	3818473629793533312	DA	26.4 (0.1)	16.64	16.17	16.07	16.081	16.14	16.23	15.52	15.36	15.35
J1108+1349	3968318334306923264	DQ	11.1 (0.2)	18.49	18.11	18.05	18.122	18.2	18.28	17.73	17.62	17.7
J1108+3021	732841233105592320	DA	10.5 (0.5)	20.02	19.37	19.21	19.14	19.19	19.23	18.6	···	···
J1109+1226	3964744479135122560	DC	14.5 (0.2)	19.1	18.59	18.45	18.45	18.46	18.55	···	···	···

Tableau A.1 *suite page suivante*

Tableau A.1 *(suite)*

Name	Gaia DR2/EDR3*	Sp Type	ϖ (mas)	u	g	r	i	z	y	J	H	K
J1109+4249	778707154499553792	DQ	11.4 (0.2)	17.53	17.372	17.42	17.568	17.72	17.85	17.31	···	···
J1109+5512	843807902246527232	DA	27.9 (0.1)	17.82	17.266	17.107	17.073	17.137	17.16	16.46	16.4	···
J1109−0312	3790932787663209344	DC	11.8 (0.2)	18.09	17.82	17.79	17.871	17.99	18.08	17.47	17.5	17.5
J1109−2601	3532509621985958912	DC	24.7 (0.1)	···	17.67	17.336	17.233	17.23	17.24	16.55	···	16.4
J1110+0054	3810397128476695424	DA	11.9 (0.1)	17.84	17.45	17.45	17.538	17.64	17.74	17.12	17.0	17.1
J1110+0110	3810416820902223616	DC	21.0 (0.1)	18.24	17.63	17.42	17.41	17.46	17.51	16.84	16.71	16.6
J1110+2026	3990494251184010496	DC	36.0 (0.2)	19.97	18.03	17.33	17.05	16.9	16.85	15.95	15.69	15.62
J1111+0337	3812098863243533824	DA	20.4 (0.2)	19.38	18.32	17.92	17.778	17.76	17.699	16.98	16.7	16.67
J1111+2519	3995728953028752768	DC	16.1 (0.7)	20.19	19.13	18.7	18.55	18.52	18.48	17.7	···	···
J1111+3848	764725833360592640	DC	15.6 (0.3)	20.1	18.74	18.15	17.91	17.86	17.85	17.1	···	···
J1111+5604	855892153511070080	DA	12.4 (0.1)	17.29	16.87	16.89	16.97	17.1	17.19	16.58	16.0	···
J1112+0858	3819003074706435200	DC	13.6 (0.4)	21.6	20.09	19.27	18.948	18.84	18.74	17.94	17.7	17.7
J1112+1524	3970216984735025792	DC	10.0 (0.5)	19.38	18.93	18.79	18.83	18.89	18.96	18.28	18.2	18.0
J1113+0032	3810134246413902848	DC	18.1 (0.2)	18.43	17.76	17.52	17.38	17.68	17.7	17.1	16.98	16.7
J1113+0146	3810552434493888768	DQH*	22.9 (0.2)	18.65	19.25	18.47	18.25	18.12	18.06	17.02	16.81	16.62
J1113+0324	3812052855548962816*	DA	11.8 (0.3)	19.26	18.56	18.32	18.225	18.25	18.22	···	···	···
J1113+2859	3999033225988190720	DA	19.9 (0.5)	20.22	18.399	17.716	17.45	17.37	17.31	16.43	15.8	15.87
J1113+2922	3999150942451828480	DA	10.8 (0.2)	18.57	17.965	17.779	17.77	17.79	17.84	17.05	···	···
J1113−1903	3557916273390162560	DC	21.2 (0.2)	···	18.661	18.07	17.84	17.76	17.7	16.84	16.1	16.5
J1114+3638	763471702912929024	DC	12.0 (0.5)	19.64	18.96	18.77	18.702	18.75	18.73	18.0	···	···
J1114+6546	1056003918305358592	DZ	14.3 (0.2)	19.86	18.71	18.48	18.44	18.54	18.52	···	···	···
J1115+0033	3810099989754827136	DA	25.2 (0.1)	19.5	17.841	17.25	17.016	16.91	16.84	15.8	15.6	15.6
J1115+2315	3992108467396622464	DA	10.0 (0.4)	18.45	17.82	17.596	17.504	17.51	17.56	16.78	···	···
J1116+0627	3817262208497857024	DA	26.7 (0.1)	17.62	16.881	16.64	16.544	16.549	16.59	15.79	15.59	15.55
J1116+0925	3915111042492943360	DA	16.4 (0.2)	20.27	18.98	18.468	18.251	18.199	18.19	17.31	17.09	16.98
J1116−0032	3791951961927535616	DA*	16.7 (0.2)	19.26	18.37	17.991	17.86	17.844	17.82	17.03	16.8	16.7
J1116−1035	3566532561902107648	DA	11.7 (0.3)	20.4	19.39	18.978	18.82	18.8	18.77	18.0	17.8	17.5
J1116−1035	3566532561902107904	DA	11.5 (0.2)	19.26	18.58	18.318	18.244	18.25	18.26	17.51	17.34	17.2
J1116−1252	3565057738851555840	DA	10.5 (0.2)	18.37	17.93	17.861	17.92	18.03	18.06	17.4	17.4	17.3
J1117+1821	3971863297233655040	DA	10.7 (0.5)	18.63	18.3	18.355	18.445	18.57	18.74	18.2	···	···
J1117+3029	4023258765683278720	DA	11.2 (0.2)	18.68	18.269	18.21	18.22	18.35	18.41	17.82	···	···
J1117+4851	789712823515276416	DA	11.3 (0.2)	19.16	18.48	18.255	18.2	18.21	18.23	17.54	···	···
J1117+5010	837941213142775680	DC	18.6 (0.3)	21.1	19.21	18.56	18.27	18.18	18.16	17.24	17.07	16.97
J1118+2836	3998830061150314368	DA	18.5 (0.1)	16.93	16.578	16.561	16.62	16.735	16.81	16.15	16.1	16.17

Tableau A.1 *suite page suivante*

Tableau A.1 *(suite)*

Name	Gaia DR2/EDR3*	Sp Type	ϖ (mas)	u	g	r	i	z	y	J	H	K
J1118−0314	3790040465258127616	DQ	27.3 (0.1)	15.428	15.313	15.371	15.533	15.708	15.812	15.27	15.32	15.3
J1119+3224	757272896870658176	DA	13.5 (0.3)	19.91	18.96	18.67	18.53	18.53	18.5	17.9	···	···
J1119+4708	788592386816314752	DA	10.6 (0.1)	18.08	17.64	17.566	17.611	17.702	17.74	17.11	···	···
J1119−0107	3791660630001113344	DC	16.2 (0.4)	22.1	19.81	19.07	18.77	18.68	18.64	17.76	17.55	17.41
J1119−0831	3783206210217512320	DA	33.0 (0.1)	···	17.24	16.779	16.637	16.6	16.59	15.8	15.6	15.2
J1119−1038	3566494186369726720	DA	12.9 (0.1)	17.16	16.653	16.512	16.497	16.552	16.59	15.85	15.7	15.67
J1120+3745	763955591105229056	DA	12.5 (0.2)	18.07	17.6116	17.53	17.55	17.65	17.68	17.04	···	···
J1120+4734	788619668448368512	DC	15.4 (0.2)	19.17	18.407	18.153	18.095	18.11	18.16	17.38	···	···
J1121+1553	3967492742808436864	DA	12.6 (0.3)	18.33	17.8	17.68	17.687	17.75	17.79	17.15	16.96	17.1
J1121+3756	763981296484951936	DA	24.9 (0.1)	15.88	15.517	15.541	15.672	15.83	15.908	15.3	15.2	15.1
J1122+2839	4022081429247669632	DA	21.9 (0.2)	19.39	18.2	17.81	17.63	17.61	17.59	16.5	16.99	16.18
J1122+4708	788768476168350976	DA	13.5 (0.2)	19.55	18.762	18.487	18.392	18.41	18.4	17.64	···	···
J1123+0956	3915026861134449664	DAH	10.5 (0.2)	18.11	17.69	17.738	17.87	18.0	18.09	···	17.4	17.6
J1123+1446	3966812278254805248	DA	13.8 (0.2)	18.12	17.63	17.518	17.533	17.59	17.64	16.98	16.81	16.7
J1123+5844	857552239974460160	DA	10.3 (0.2)	19.67	18.91	18.67	18.59	18.6	18.63	···	···	···
J1124+1705	3970693313784409344	DA	9.7 (0.3)	19.17	18.64	18.6	18.64	18.75	18.8	18.0	···	···
J1125+2111	3978862277154958592	DC	26.2 (0.1)	17.87	17.17	16.894	16.818	16.842	16.87	16.13	16.2	15.7
J1125+4223	771517005584473600	DA	17.6 (0.1)	16.84	16.4	16.457	16.59	16.723	16.83	16.23	16.2	15.7
J1126+0906	3914160793864337280	DAH	12.1 (0.2)	18.13	17.93	18.004	18.18	18.3	18.41	17.88	17.8	17.8
J1126+1433	3967110520783248640	DA	13.1 (0.2)	19.3	18.52	18.24	18.152	18.13	18.14	17.42	17.14	17.0
J1126+5919	859082970614616448	DA	39.36 (0.03)	15.441	15.1192	15.22	15.359	15.519	15.66	15.05	15.2	15.1
J1126−0653	3785295862130129792	DC	20.4 (0.4)	22.0	19.83	19.03	18.7	18.56	18.49	17.59	17.5	17.1
J1127+0623	3814445324131846272	DA	13.8 (0.1)	17.52	17.1	17.061	17.135	17.257	17.32	16.67	16.54	16.6
J1127+7531	1080303919849120128	DC	18.4 (0.1)	16.95	16.706	16.706	16.78	16.916	16.99	16.4	···	···
J1127−0138	3796601418644353536	DZ	10.5 (0.2)	18.71	18.106	18.08	18.197	18.36	18.41	17.81	17.7	17.9
J1127−2940	3482983495102507904	DA	29.7 (0.1)	···	15.056	15.066	15.186	15.329	15.414	14.803	14.71	14.76
J1128+0736	3913666009336762624	DA	10.4 (0.3)	19.99	19.25	19.01	18.96	19.01	18.97	···	···	···
J1128+1825	3976920329166692736	DA	12.5 (0.2)	18.84	18.262	18.114	18.107	18.14	18.19	17.56	···	···
J1128+4150	771045212017101952	DA	12.1 (0.2)	17.66	17.26	17.273	17.368	17.502	17.58	16.96	16.4	···
J1130+1002	3914686699729551744	DA	19.3 (0.3)	20.5	18.81	18.23	18.0	17.92	17.89	17.1	16.85	16.8
J1130+6647	1057653804222121600	DC :*	13.3 (0.1)	18.62	18.16	17.99	18.024	18.05	18.12	···	···	···
J1131+0643	3910338303034941824	DA	14.5 (0.1)	17.83	17.341	17.234	17.251	17.318	17.36	16.69	16.5	16.51
J1131+4920	789242022082351616	DA	14.2 (0.2)	19.69	18.81	18.478	18.354	18.35	18.3	17.52	···	···
J1131+4938	790014605097236224	DA	10.1 (0.1)	16.82	16.368	16.455	16.63	16.8	16.9	16.28	16.2	15.8

Tableau A.1 *suite page suivante*

Tableau A.1 *(suite)*

Name	Gaia DR2/EDR3*	Sp Type	ϖ (mas)	u	g	r	i	z	y	J	H	K
J1132+2328	3993006940195159552	DA	10.3 (0.2)	18.61	18.16	18.072	18.07	18.12	18.12	17.41	···	···
J1132+2809	4018868591847502208	DAH	19.6 (0.1)	17.53	17.006	16.91	16.92	16.981	17.05	16.38	16.1	16.0
J1132+3634	759949799663166464	DA	12.5 (0.1)	17.45	17.09	17.1	17.18	17.28	17.36	16.74	···	···
J1132−0532	3785855994584716288	DA	11.4 (0.4)	19.56	18.95	18.75	18.69	18.75	18.73	18.04	17.9	18.2
J1133+3301	4025333681563592960	DA	22.7 (0.1)	16.99	16.694	16.678	16.774	16.89	16.99	16.35	···	···
J1133+6243	862946654474456832	DA+DC	21.86 (0.05)	17.09	16.506	16.275	16.221	16.249	16.28	15.57	15.39	15.56
J1134+6108	859567752163281792	DA	35.58 (0.04)	15.922	15.53	15.435	15.424	15.505	15.539	14.89	14.7	14.6
J1135+1240	3917662149987657472	DC	21.1 (0.8)	21.0	18.73	18.16	17.96	17.81	17.5	16.89	16.61	16.62
J1135+2717	4018536882933053056*	DC	23.0 (0.2)	21.1	19.06	18.28	17.97	17.85	17.8	···	···	···
J1135+5724	845973046799769984	DQ	17.1 (0.05)	16.81	16.475	16.403	16.47	16.554	16.62	16.03	15.9	15.9
J1135+6429	864111582748403968	DA	13.0 (0.1)	18.28	17.96	17.97	18.05	18.18	18.24	···	···	···
J1136+0802	3910941183300119808	DA	20.3 (0.2)	19.51	18.215	17.81	17.62	17.46	17.1	16.64	16.37	16.21
J1136+0838	3911257636490384512	DA	18.0 (0.2)	18.41	17.76	17.521	17.452	17.46	17.5	16.7	16.47	16.47
J1136+1530	3972493871447452032	DA	11.7 (0.2)	18.47	17.97	17.839	17.849	17.9	17.94	17.26	17.09	17.1
J1137+0343	3800902265750001664	DZ	15.4 (0.2)	18.4	17.85	17.74	17.769	17.857	17.92	17.3	17.21	17.1
J1137+1347	3918024679587352960	DC	11.1 (0.6)	19.71	19.01	18.74	18.69	18.72	18.78	18.05	18.0	17.9
J1137+2005	3979898652273088128	DZ	10.5 (0.4)	20.02	19.29	19.041	18.993	19.04	19.09	18.4	···	···
J1137+2041	3979070527235441792	DA	13.3 (0.2)	17.92	17.47	17.368	17.38	17.46	17.52	16.81	16.4	16.41
J1137+2451	4017215231301573376	DA	9.9 (0.2)	18.52	17.88	17.84	17.72	17.98	17.77	17.4	···	···
J1137+3117	4024105492715825152	DA	12.9 (0.4)	19.84	18.94	18.59	18.48	18.44	18.46	17.64	···	···
J1137+4019	767724270288678784	DC	10.5 (0.2)	18.74	18.3	18.2	18.242	18.35	18.33	17.88	···	···
J1137+5740	845982667526493440	DAH	21.1 (0.1)	17.37	16.891	16.777	16.79	16.87	16.93	16.27	15.8	15.7
J1138+1323	3917811443050820736	DA	10.8 (0.5)	19.61	18.97	18.75	18.695	18.73	18.75	18.01	17.7	17.8
J1138+3610	765628876004078464	DA	10.7 (0.8)	20.7	20.11	19.95	19.91	19.98	19.82	19.4	···	···
J1138+6438	864108971408318848	DC	15.3 (0.2)	19.4	18.74	18.57	18.54	18.64	18.64	···	···	···
J1138−1313	3585097235918075776	DC	37.3 (0.1)	···	16.72	16.434	16.297	16.328	16.37	15.6	15.5	15.7
J1139+2613	4017476365313408512	DA	18.9 (0.2)	18.55	17.91	17.67	17.6	17.62	17.62	16.89	···	···
J1139−2852	3483746453090944896	DC	9.8 (0.7)	···	20.87	20.02	19.71	19.53	19.4	18.6	···	18.2
J1140+0112	3790009353404271488	DA	20.8 (0.1)	16.25	15.78	15.864	15.979	16.127	16.188	15.64	15.56	15.58
J1140+1245	3917712246486088064	DC :	17.3 (0.1)	18.64	17.985	17.741	17.705	17.742	17.75	17.07	16.91	16.9
J1140+5938	858407492517973888	DA	10.8 (0.1)	19.09	18.51	18.33	18.3	18.34	18.38	17.67	···	···
J1141+3836	766499483055284864	DQ	12.6 (0.4)	19.8	19.92	19.04	18.63	18.68	18.78	17.97	···	···
J1141−0132	3793871056394569600	DA	12.6 (0.3)	18.98	18.5	18.4	18.35	18.41	18.44	17.81	17.7	17.5
J1142+1538	3972360517007764096	DA	12.0 (0.4)	20.6	19.49	19.07	18.94	18.9	18.83	18.11	17.8	17.6

Tableau A.1 *suite page suivante*

Tableau A.1 *(suite)*

Name	Gaia DR2/EDR3*	Sp Type	ϖ (mas)	u	g	r	i	z	y	J	H	K
J1142−0208	3793038176336413568	DA	11.4 (0.3)	19.33	18.86	18.69	18.68	18.73	18.78	18.1	17.9	17.8
J1143+1448	3924198849694079488	DC	11.8 (0.5)	19.27	18.57	18.38	18.36	18.39	18.52	17.79	17.6	17.7
J1143+4053	769043546803129216	DA	9.8 (0.3)	19.65	19.04	18.81	18.761	18.79	18.81	18.1	···	···
J1143+7036	1062419637373273728	DA	10.6 (0.2)	19.93	19.209	18.9	18.77	18.75	18.65	···	···	···
J1143−0131	3793132257595347200	DA	25.3 (0.1)	18.06	17.4	17.174	17.11	17.125	17.162	16.38	16.13	16.17
J1144+0621	3909703579883878528	DC	12.2 (0.3)	20.6	19.39	19.01	18.83	18.81	18.77	···	···	···
J1144+1132	3916509896161613056	DA	20.9 (0.1)	18.27	17.464	17.17	17.068	17.06	17.073	···	···	···
J1144+1218	3916712206301454720	DZ	19.8 (0.2)	20.7	18.32	17.866	17.777	17.79	17.81	17.07	16.93	16.9
J1144+6629	1056998259069523584	DAH	16.0 (0.1)	18.13	17.5	17.283	17.245	17.276	17.31	16.5	16.3	···
J1145+1523	3924625975601987968	DA	13.6 (0.6)	21.1	19.55	18.98	18.76	18.65	18.63	···	···	···
J1145+6305	863131372427958912	DA	41.64 (0.05)	17.83	16.624	16.171	16.01	15.945	15.91	15.12	14.8	14.7
J1146+0514	3897015868534544000	DA	16.0 (0.1)	17.68	17.02	16.81	16.737	16.774	16.8	16.06	15.84	15.77
J1146−0136	3794567429507510528	DA	30.5 (0.1)	17.15	16.4811	16.28	16.24	16.222	16.25	15.47	15.26	15.24
J1147+0747	3911460633824772224	DQA*	23.3 (0.1)	16.08	15.88	15.909	16.049	16.209	16.32	15.74	15.74	15.73
J1147+2001	3976193895578807296	DC	12.1 (0.2)	18.21	17.882	17.84	17.891	18.0	18.06	17.48	···	···
J1147+2218	3979704120809463808	DC	12.7 (0.6)	19.88	19.11	18.84	18.75	18.73	18.75	18.1	···	···
J1147+2220	3979751266665795456	DC	16.4 (0.6)	20.29	19.208	18.72	18.68	18.98	19.3	19.2	···	···
J1147+3009	4020794214664565120	DC	16.6 (0.1)	18.35	17.806	17.64	17.64	17.69	17.74	17.09	17.12	16.66
J1147+4303	769543893313272576	DC	19.3 (0.2)	20.8	18.985	18.33	18.045	17.95	17.91	17.04	16.84	16.72
J1148+3541	4032410520652747648	DA	13.8 (0.2)	18.82	18.2	17.993	17.931	17.96	17.93	17.18	···	···
J1148−0126	3794415245931016320	DQ	14.7 (0.2)	17.36	17.42	17.46	17.641	17.84	17.95	17.56	17.48	17.5
J1149+2353	4004175916749342592	DC	22.9 (0.2)	20.2	18.56	17.955	17.69	17.62	17.59	16.72	16.0	17.03
J1149−0221	3602129564384942848	DC	10.6 (0.3)	19.52	18.916	18.75	18.697	18.74	18.79	18.08	18.1	17.9
J1149−2921	3480776843983381632	DA	32.2 (0.1)	···	17.56	17.173	17.031	17.003	17.0	16.16	15.7	15.91
J1150+0342	3895853993981558400	DA	21.2 (0.2)	18.89	17.925	17.58	17.42	17.4	17.42	16.57	16.33	16.26
J1150+2518	4005438916307756928	DA	19.8 (0.1)	16.07	15.66	15.74	15.884	16.042	16.149	15.62	15.6	15.7
J1150+6831	1058284412796260480	DA	58.51 (0.03)	15.98	15.368	15.15	15.107	15.133	15.153	14.46	14.22	14.2
J1150−0636	3598424931753893888	DA	24.3 (0.1)	···	16.52	16.513	16.58	16.71	16.76	16.13	16.06	16.1
J1151+1253	3922795941576557184	DC	14.1 (0.4)	20.8	19.33	18.82	18.63	18.543	19.8	17.64	17.41	17.45
J1151+5411	840622479622035712	DA	13.0 (0.1)	17.15	16.718	16.782	16.897	17.054	17.14	16.63	16.3	···
J1151−2732	3487220772397809536	DQ	39.8 (0.1)	···	15.947	15.733	15.728	15.772	15.8	15.088	14.9	14.9
J1152+1803	3974607884414675584	DA	12.8 (0.3)	18.69	18.14	17.95	17.93	17.96	18.01	···	···	···
J1153−0312	3601778888894719616	DA	10.7 (0.2)	18.7	18.14	18.015	18.014	18.09	18.14	17.41	17.21	17.22
J1154+0441	3896315612771069184	DC*	13.2 (0.2)	19.16	18.48	18.29	18.25	18.25	18.32	17.63	17.37	17.7

Tableau A.1 *suite page suivante*

Tableau A.1 *(suite)*

Name	Gaia DR2/EDR3*	Sp Type	ϖ (mas)	u	g	r	i	z	y	J	H	K
J1154+2422	4004395720290994048	DA	37.6 (0.1)	15.93	15.627	15.625	15.685	15.799	15.88	15.25	15.1	15.4
J1154+3749	4034132866962718848	DA	12.2 (0.2)	18.11	17.68	17.606	17.657	17.72	17.79	17.18	···	···
J1154+7914	1129251428738666880	DA	16.88 (0.05)	···	15.825	15.902	16.06	16.252	16.38	15.7	15.7	15.9
J1156+0503	3896442675083660288	DA	12.4 (0.2)	17.95	17.53	17.493	17.539	17.65	17.71	17.07	17.0	···
J1156+1822	3926968661219149184	DC	37.5 (0.1)	16.1	15.672	15.598	15.628	15.719	15.802	15.14	15.2	15.1
J1156+3233	4027510375284724608	DC*	14.9 (0.2)	18.06	17.7	17.621	17.69	17.78	17.87	17.27	···	···
J1157+0631	3898377201369256576	DA	13.0 (0.2)	17.81	17.365	17.32	17.351	17.447	17.51	16.85	16.69	16.66
J1157+0854	3899975238440888064	DA	15.4 (0.1)	18.37	17.57	17.293	17.192	17.187	17.19	16.44	16.19	16.15
J1157+2308	4001198168679083648	DC	15.3 (0.2)	18.68	18.12	17.955	17.9	17.938	18.04	17.34	···	···
J1158+0005	3795052348495488896	DC	29.0 (0.2)	20.8	18.71	17.866	17.5	17.4	17.35	16.36	16.31	16.18
J1158+0739	3899642425719062400	DA	13.7 (0.2)	19.61	18.77	18.44	18.28	18.22	17.72	···	···	···
J1158+2853	4007991157673846144	DA	14.5 (0.1)	17.17	16.76	16.787	16.882	17.002	17.1	16.52	16.45	15.85
J1159+0007	3891115064506627840	DA	35.4 (0.1)	16.02	15.774	15.817	15.885	16.018	16.13	15.56	15.54	15.53
J1159+1300	3919950955240152832	DQ	16.1 (0.2)	18.24	18.185	17.76	17.703	17.81	17.91	17.38	17.3	17.1
J1159+3538	4031471636506212352	DA	21.5 (0.1)	18.01	17.46	17.346	17.341	17.406	17.43	16.72	···	···
J1159+4842	786717135370412800	DA	23.2 (0.1)	18.65	17.682	17.323	17.192	17.169	17.17	16.36	16.0	16.1
J1200+4237	1537367257087358592	DQ	10.8 (0.3)	19.82	19.22	18.94	18.91	18.92	18.96	18.3	···	···
J1200+4335	1537794524729363712	DA	26.76 (0.05)	16.31	15.825	15.762	15.8	15.863	15.93	15.23	15.2	15.3
J1200+4833	1546270625514967168	DA	11.2 (0.1)	18.05	17.657	17.612	17.659	17.769	17.8	17.27	···	···
J1200−1032	3575728709655386752	DA	29.6 (0.1)	···	16.404	16.33	16.38	16.465	16.52	15.8	15.6	15.3
J1201+0847	3900013579612540672	DAH	11.0 (0.4)	19.13	18.65	18.5	18.51	18.59	18.57	17.9	17.8	17.8
J1201+3400	4028120776036373760	DQ	24.7 (0.1)	18.24	17.7	17.258	17.19	17.22	17.27	16.55	15.95	15.53
J1202+4929	1546780420950246912	DA :	12.0 (0.4)	22.1	20.12	19.48	19.19	19.08	19.04	18.2	···	···
J1202+5344	1549208138324951936	DA	12.4 (0.2)	18.51	18.17	18.134	18.199	18.26	18.33	17.72	···	···
J1202−0313	3600899515814587904	DC	16.2 (0.3)	22.3	19.81	19.05	18.76	18.65	18.6	17.61	17.6	17.5
J1202−1004	3575770010060921728	DA	31.6 (0.1)	···	15.86	15.889	15.978	16.112	16.21	15.6	15.54	15.54
J1203+0426	3894780007343533184	DC	20.5 (0.2)	19.58	18.11	17.47	17.23	17.141	17.12	16.39	16.49	16.9
J1203+0834	3899809757644549632	DZ	15.9 (0.3)	19.11	18.002	17.863	17.878	17.95	18.02	···	17.19	17.1
J1203+1330	3920078086272085888	DC	10.4 (0.3)	18.93	18.51	18.41	18.43	18.52	18.59	17.96	17.9	17.8
J1203+1422	3921843867586039808	DC	13.7 (0.2)	18.68	18.17	17.994	17.98	18.045	18.09	17.46	17.3	17.3
J1203+5910	1576088036528753408	DC :	10.8 (0.1)	18.2	18.046	18.054	18.175	18.31	18.4	17.9	···	···
J1204+2316	4001074538044978816	DC	17.8 (0.3)	20.9	19.21	18.55	18.314	18.22	18.18	17.32	···	···
J1204+6222	1582945145090883200	DC	19.6 (0.2)	20.9	19.11	18.41	18.134	18.034	17.98	17.07	16.86	16.8
J1204+6259	1582991152779542400	DA	14.0 (0.2)	19.48	18.63	18.34	18.217	18.21	18.23	···	···	···

Tableau A.1 *suite page suivante*

Tableau A.1 *(suite)*

Name	Gaia DR2/EDR3*	Sp Type	ϖ (mas)	u	g	r	i	z	y	J	H	K
J1205+0449	3894911089745430656	DC	13.6 (0.3)	19.42	18.4	17.983	17.816	17.791	17.77	16.95	16.85	16.7
J1205+1607	3925475283910531328	DA	12.6 (0.1)	17.48	17.09	17.167	17.31	17.43	17.57	17.01	···	···
J1205−0042	3698611842864771328	DC	9.8 (0.4)	19.6	18.96	18.754	18.727	18.75	18.81	18.16	18.0	17.8
J1205−2333	3489719481290397696	DAZ	95.84 (0.05)	···	12.834	12.8	13.0	13.0	13.07	12.616	12.3	12.35
J1206+0823	3904993787466857472	DA	16.0 (0.1)	17.41	16.99	16.945	16.989	17.07	17.15	16.49	16.32	16.37
J1206+2353	4002617427736191872	DC	16.5 (0.4)	20.9	19.25	18.67	18.435	18.34	18.31	17.5	17.24	17.2
J1207+2916	4013877015215909632	DC	11.7 (0.2)	19.93	19.12	18.82	18.72	18.74	18.74	18.07	17.9	17.6
J1207+3953	1536034236678159232	DA	10.9 (0.1)	18.02	17.62	17.604	17.685	17.788	17.86	17.24	···	···
J1208+0312	3893651289938122496	DA	13.0 (0.3)	19.64	18.79	18.457	18.338	18.32	18.35	17.54	17.33	17.1
J1208+0845	3905035495893288448	DA	21.9 (0.2)	20.4	18.66	18.03	17.79	17.701	17.65	16.75	16.51	16.4
J1208+2343	4001862578644425344	DA	10.0 (0.2)	18.51	18.12	18.095	18.17	18.28	18.33	17.65	17.58	17.4
J1208+5429	1573121554156399872	DA	15.2 (0.1)	17.74	17.27	17.21	17.228	17.31	17.38	16.78	16.5	···
J1209+0939	3905948159264050432	DA	15.3 (0.3)	19.9	19.08	18.76	18.64	18.64	18.64	17.9	17.7	17.3
J1211+0724	3904628406009296896	DA	39.5 (0.1)	18.62	17.074	16.535	16.311	16.261	16.234	15.367	15.09	14.99
J1211+1046	3906450326840122368	DA	11.3 (0.2)	18.6	18.14	18.014	17.98	18.07	18.07	17.43	17.09	17.2
J1211+2053	3951770649948609920	DA	10.0 (0.2)	18.38	17.748	17.546	17.483	17.527	17.53	16.81	···	15.9
J1211+2815	4012821445398156416	DC	10.2 (0.3)	19.38	18.9	18.79	18.83	18.89	18.94	18.4	18.2	17.9
J1211+3653	4030292070983358208	DA	10.1 (0.1)	17.65	17.24	17.35	17.463	17.62	17.74	17.13	···	···
J1211+4953	1548117972546002560	DA	14.1 (0.2)	20.3	19.11	18.66	18.48	18.42	18.38	17.61	···	···
J1211+5724	1575357587146077056	DAZ	50.1 (0.03)	16.97	15.97	15.604	15.478	15.485	15.46	14.658	14.4	14.5
J1211−0242	3598349645270793984	DA	12.3 (0.3)	18.86	18.601	18.5	18.52	18.6	18.7	17.9	17.9	17.9
J1212+0440	3894294439815819904	DC	16.8 (0.4)	22.1	19.87	19.08	18.77	18.64	18.56	17.67	17.5	17.5
J1212+3834	1532708866839099648	DC	10.9 (0.2)	19.01	18.642	18.59	18.625	18.75	18.8	18.3	···	···
J1212+4345	1538365922883198336	DA	14.3 (0.3)	20.6	19.3	18.78	18.59	18.53	18.49	17.69	17.45	17.28
J1212+5452	1573476112296657408	DQ	10.6 (0.1)	18.09	17.88	17.876	17.97	18.13	18.19	17.59	···	···
J1212−0622	3596192953212776704	DA	23.0 (0.1)	···	17.197	16.92	16.83	16.84	16.88	16.04	15.89	15.78
J1214+6216	1582663189077609088	DA*	19.1 (0.1)	20.08	18.46	18.063	17.87	17.8	17.76	16.8	16.2	···
J1214+7822	1717341818608187648	DZ	30.6 (0.1)	···	18.05	17.379	17.122	17.028	17.0	16.2	15.6	15.6
J1214−0142	3694595296825212288	DA	15.0 (0.3)	20.9	19.42	18.84	18.62	18.54	18.5	17.65	17.4	17.4
J1214−0234	3694399755554510720	DZH*	26.2 (0.2)	20.9	18.23	17.79	17.6	17.56	17.58	16.76	16.6	16.42
J1215+0948	3905534918987016576	DA	10.1 (0.2)	18.38	17.96	18.013	18.099	18.26	18.4	17.93	17.7	17.9
J1215+0948	3905533368502667520	DA	10.3 (0.2)	18.31	17.88	17.839	17.888	17.99	18.07	17.44	17.37	17.3
J1215+4630	1545050717357814272	DA	22.0 (0.1)	17.87	17.25	17.032	16.981	17.006	17.01	16.29	16.07	15.74
J1215−0056	3698040337339931776	DAH	11.0 (0.3)	19.75	19.06	18.83	18.79	18.8	18.82	18.14	18.0	18.0

Tableau A.1 *suite page suivante*

Tableau A.1 *(suite)*

Name	Gaia DR2/EDR3*	Sp Type	ϖ (mas)	u	g	r	i	z	y	J	H	K
J1216+0338	3893925965982400384	DA	10.7 (0.3)	20.15	19.23	18.911	18.76	18.76	18.71	18.05	17.7	17.8
J1216+3023	4013717723468865152	DC*	9.8 (0.3)	19.14	18.7	18.63	18.7	18.78	18.79	18.32	18.1	18.0
J1217+0403	3893966162580541184	DA	9.8 (0.4)	20.7	19.45	18.97	18.78	18.74	18.71	···	···	···
J1217+3044	4013798537573517568	DA	10.1 (0.3)	18.99	18.44	18.313	18.28	18.33	18.36	17.66	17.4	17.7
J1217+3205	4016142868162408576	DC	22.3 (0.1)	17.56	17.1	16.952	16.99	16.98	16.96	16.39	16.24	16.3
J1217+3226	4016204440813547520	DA	12.4 (0.1)	18.35	17.87	17.74	17.7	17.75	17.8	17.09	16.0	15.3
J1217+3656	1531580424311162880	DC	14.1 (0.2)	19.76	18.86	18.525	18.39	18.36	18.38	17.62	···	···
J1217+6404	1584734595969095424	DA	10.6 (0.1)	17.86	17.36	17.23	17.24	17.29	17.34	···	···	···
J1217+6848	1683330453627242752	DA	30.5 (0.1)	17.81	17.13	16.886	16.83	16.822	16.88	16.1	15.9	···
J1219+4015	1533299819978845312	DA	11.1 (0.2)	19.51	18.78	18.52	18.44	18.45	18.47	17.8	···	···
J1219+4715	1545014807135001088	DC*	14.3 (0.1)	18.08	17.67	17.55	17.59	17.69	17.74	17.12	···	···
J1219+5827	1575107070293783296	DA	13.5 (0.1)	17.24	16.824	16.84	16.953	17.06	17.17	16.64	16.3	···
J1220+4414	1538625407627245056	DA	20.7 (0.1)	18.2	17.669	17.5	17.474	17.521	17.56	16.82	···	···
J1221+3306	4016670251491467520	DA	10.9 (0.1)	18.43	17.99	17.887	17.91	17.99	18.03	17.38	···	···
J1221+5320	1572216243769902336	DA	11.1 (0.2)	19.08	18.65	18.53	18.55	18.6	18.65	18.02	···	···
J1221+6520	1680980518105612672	DC	12.6 (0.2)	19.42	18.75	18.52	18.5	18.5	18.48	···	···	···
J1223+5410	1572454940873010176	DZ	11.3 (0.3)	20.9	19.46	19.05	18.94	18.92	18.85	18.3	···	···
J1223+5645	1574853491129437440	DC	10.9 (0.2)	19.4	18.83	18.66	18.65	18.67	18.68	18.1	···	···
J1223−1852	3519617951228451328	DC	20.8 (0.1)	···	16.509	16.53	16.656	16.77	16.872	16.28	16.1	16.24
J1224+2838	4010119017615780608	DZ	12.2 (0.4)	22.4	19.67	19.2	19.07	19.08	19.04	18.27	18.2	18.1
J1224−0018	3696633688303809664	DA	20.6 (0.1)	18.16	17.51	17.274	17.19	17.21	17.23	16.46	16.25	16.23
J1225+1522	3945304834382891008	DA	12.0 (0.4)	20.02	19.37	19.11	19.04	19.06	19.06	···	···	···
J1225+2836	4010090670831602432	DC	12.5 (0.3)	19.71	18.84	18.56	18.479	18.51	18.53	17.82	17.7	18.0
J1226+1836	3947104533054775168	DC	28.0 (0.1)	16.76	16.36	16.295	16.33	16.398	16.5	15.84	15.5	15.7
J1226+1949	3949023868038967808	DA	11.0 (0.4)	19.65	19.03	18.84	18.81	18.83	18.84	18.1	···	···
J1226+2936	4011709259321463808	DZ	11.7 (0.7)	23.3	20.38	19.74	19.56	19.51	19.52	18.8	18.2	18.5
J1226+3513	1518943638389520384	DA	28.7 (0.1)	19.39	17.78	17.199	16.953	16.91	16.85	15.99	16.1	···
J1226+3632	1519362376225775744	DA	11.6 (0.4)	20.5	19.35	18.96	18.84	18.81	18.77	18.1	···	···
J1227+0407	3707668520142907392	DA	12.7 (0.2)	18.4	17.97	17.88	17.891	17.95	18.02	17.33	17.2	17.2
J1227+3150	4015547856277853824	DA	25.8 (0.1)	17.49	16.834	16.587	16.515	16.53	16.555	15.77	15.5	15.5
J1227+6330	1583921850718408960	DZ	10.3 (0.1)	18.9	18.17	18.16	18.27	18.42	18.49	···	···	···
J1228+0022	3696778892558087552	DA	30.94 (0.04)	15.356	14.991	15.031	15.121	15.266	15.37	14.742	14.68	14.72
J1228+1256	3907977484067188096	DA	19.3 (0.1)	17.51	16.999	16.859	16.867	16.919	16.95	16.22	16.08	16.08
J1228+2056	3952478391839564928	DAZ	19.0 (0.1)	18.88	17.976	17.655	17.533	17.523	17.51	16.74	···	···

Tableau A.1 *suite page suivante*

Tableau A.1 *(suite)*

Name	Gaia DR2/EDR3*	Sp Type	ϖ (mas)	u	g	r	i	z	y	J	H	K
J1228+3300	4015951102167164032	DC	19.2 (0.2)	20.7	18.78	17.968	17.651	17.533	17.49	16.56	16.2	16.0
J1228+4150	1534836250044023168	DC	13.7 (0.2)	19.9	18.98	18.57	18.43	18.41	18.42	17.69	···	···
J1228−0247	3693624423762089216	DA	12.7 (0.1)	18.41	17.86	17.739	17.741	17.8	17.86	17.17	16.98	16.91
J1229+4126	1534719152051775616	DAH	10.3 (0.3)	19.74	18.95	18.67	18.6	18.62	18.6	17.9	···	···
J1229+5047	1544707665434144640	DC	10.0 (0.2)	19.32	18.78	18.645	18.66	18.74	18.76	···	···	···
J1229−0432	3681000076065709312	DC	20.6 (0.1)	···	16.665	16.66	16.751	16.867	16.98	16.3	16.28	16.19
J1229−0707	3583402849843287680	DA	28.3 (0.1)	···	17.942	17.338	17.078	16.992	16.958	15.9	15.9	15.5
J1231+0531	3708253980021111168	DA	11.9 (0.1)	17.88	17.46	17.444	17.504	17.61	17.7	17.04	16.93	16.9
J1231+1452	3933031020441648384	DA	22.2 (0.2)	19.49	18.36	17.99	17.84	17.81	17.77	17.02	16.76	16.7
J1231+3924	1533568375694548480	DA	16.0 (0.2)	20.11	18.88	18.47	18.316	18.29	18.23	17.45	···	···
J1233+0607	3708578473389974528	DA	26.5 (0.2)	19.6	18.21	17.7	17.524	17.47	17.462	16.58	16.3	16.26
J1233+0824	3902698243410506112	DQ	12.2 (0.3)	19.15	18.62	18.37	18.313	18.35	18.4	17.71	17.61	17.6
J1233+1253	3931756484602030848	DQ	19.9 (0.1)	17.8	17.288	17.13	17.127	17.18	17.19	16.61	16.48	16.4
J1233+2825	4010592357371458944	DA	13.5 (0.3)	20.2	19.15	18.81	18.67	18.63	18.63	17.84	17.6	17.9
J1233+6008	1581483997215646208	DA	12.4 (0.3)	17.39	16.97	16.93	17.0	17.07	17.17	16.5	···	···
J1233+6745	1682417167486191360	DA	10.1 (0.1)	17.46	16.993	17.055	17.19	17.34	17.46	16.6	···	···
J1234+0109	3697125646741428224	DA	12.1 (0.3)	21.3	19.77	19.25	19.03	18.95	18.94	18.19	17.91	17.79
J1234+0547	3708366954839619328	DA	19.8 (0.1)	17.89	17.44	17.324	17.345	17.4	17.45	16.78	16.67	16.68
J1234+1248	3931751257626586880	DA	11.2 (0.1)	17.81	17.41	17.341	17.376	17.45	17.5	16.8	16.82	16.78
J1234+1503	3933386712453327360	DA+DC*	14.4 (0.3)	19.53	18.673	18.36	18.274	18.26	18.24	17.55	17.4	17.5
J1234+4911	1544285079309656064	DA	11.1 (0.1)	18.43	17.97	17.857	17.863	17.92	17.96	17.33	···	···
J1234+6045	1583023618437189504	DA	12.6 (0.1)	18.58	18.0	17.85	17.847	17.89	17.94	···	···	···
J1234+6605	1680532535836237440	DA	14.6 (0.2)	20.6	19.24	18.74	18.53	18.47	18.44	17.56	17.38	17.24
J1235+2107	3949551801124462976	DC	13.9 (0.2)	19.4	18.57	18.311	18.27	18.28	18.33	17.59	···	···
J1235+2318	3958889751516035200	DA	14.6 (0.2)	17.77	17.35	17.26	17.275	17.34	17.41	16.69	16.58	16.54
J1235+3918	1533514911941019008	DQ	12.6 (0.1)	17.23	17.168	17.244	17.4	17.558	17.65	17.14	···	···
J1235+5503	1571109898850692608	DA	10.1 (0.1)	17.5	17.04	16.985	17.062	17.18	17.23	16.58	16.0	16.4
J1236+3307	1514736047908364928	DC	11.5 (0.1)	17.73	17.579	17.63	17.754	17.91	17.98	17.46	···	···
J1237+1814	3947604806549970560	DC	13.7 (0.1)	17.0	16.84	16.892	17.06	17.199	17.34	16.8	···	···
J1237+3448	1518352719609121280	DA	12.6 (0.1)	17.88	17.52	17.54	17.61	17.73	17.82	17.24	···	···
J1237+4156	1534384148897669248	DQP	27.7 (0.1)	17.81	17.79	17.09	16.851	16.929	16.97	16.35	16.5	···
J1237+6023	1580009552123749888	DA	21.5 (0.1)	20.16	18.4	17.876	17.679	17.62	17.62	16.7	16.0	15.6
J1238+3502	1518373537314807552	DC	12.5 (1.0)	24.73	21.5	20.26	19.89	20.09	20.2	21.2	···	···
J1238+3933	1521599470071180672	DA	14.5 (0.2)	19.12	18.46	18.219	18.17	18.19	18.18	···	···	···

Tableau A.1 *suite page suivante*

Tableau A.1 *(suite)*

Name	Gaia DR2/EDR3*	Sp Type	ϖ (mas)	u	g	r	i	z	y	J	H	K
J1238+4931	1544353553970169728	DA	10.2 (0.3)	20.13	19.43	19.18	19.11	19.13	19.12	18.4	···	···
J1238+5122	1568579647717853184	DA	15.5 (0.1)	17.85	17.367	17.26	17.253	17.31	17.35	16.65	···	···
J1238+5840	1578256136019422080	DC	10.1 (0.3)	20.09	19.37	19.11	19.04	19.05	19.09	18.5	···	···
J1238−0045	3695839596094423296	DA	12.2 (0.2)	19.28	18.63	18.4	18.306	18.3	18.32	17.59	17.41	17.6
J1239+4525	1541286711100812160	DA	37.2 (0.1)	17.36	16.637	16.38	16.302	16.29	16.32	15.58	15.2	···
J1240+0932	3903151246497510784	DC	16.0 (0.2)	19.23	18.45	18.19	18.118	18.14	18.15	17.47	17.3	17.3
J1240+1807	3935942939548822272	DA	25.4 (0.1)	19.19	17.91	17.43	17.23	17.18	17.16	16.34	15.9	15.8
J1240−0310	3682835848166848896	DA	23.5 (0.1)	16.29	15.959	16.026	16.178	16.323	16.427	15.87	15.81	15.82
J1240−2317	3501922067493606272	DA	23.8 (0.1)	17.92	16.77	16.341	16.16	16.11	16.08	15.35	15.1	14.9
J1241+2614	3961323069532233984	DQ	12.2 (0.3)	19.82	19.085	18.69	18.57	18.57	18.5	17.87	17.74	18.0
J1241+4706	1542933401563275136	DA	10.9 (0.1)	17.56	17.17	17.225	17.327	17.45	17.56	···	···	···
J1241+5407	1570797397030134912	DA	10.1 (0.1)	17.72	17.326	17.381	17.492	17.65	17.76	17.21	···	···
J1241−0733	3676222491884053376	DA	12.1 (0.2)	17.24	16.799	16.878	17.02	17.163	17.28	16.67	16.66	16.7
J1241−1506	3526928874624208128	DAH	11.5 (0.2)	19.05	18.6	18.53	18.57	18.66	18.74	18.15	18.1	18.1
J1242+1123	3927653893186082176	DA	12.5 (0.3)	19.64	18.95	18.69	18.6	18.59	18.59	17.8	17.6	17.7
J1242+1311	3929166408868873344	DC	22.1 (0.2)	20.4	18.65	18.043	17.81	17.7	17.65	16.83	16.57	16.47
J1242+2733	3962296416495937152	DA	19.6 (0.2)	19.57	18.43	18.02	17.859	17.83	17.81	17.01	16.88	16.72
J1242+2957	4011194202932877696	DA	18.5 (0.2)	21.2	19.27	18.64	18.34	18.2	18.21	17.39	17.08	17.0
J1242+6542	1680452683804651520	DA	17.7 (0.1)	18.29	17.654	17.43	17.367	17.387	17.4	16.6	17.14	16.1
J1242−0211	3683074094297008128	DA	14.9 (0.3)	19.32	18.48	18.15	18.022	18.01	18.03	17.28	17.01	16.91
J1243+6712	1682144424177509888	DA :	10.8 (0.2)	19.53	18.96	18.77	18.77	18.86	18.83	···	···	···
J1244−1051	3530399693530713344	DA	24.8 (0.04)	15.222	14.765	14.709	14.74	14.83	14.887	14.23	14.07	14.1
J1244−1947	3503786766199868416	DA	12.0 (0.3)	19.57	18.94	18.76	18.694	18.73	18.73	17.99	···	18.0
J1245+1205	3928077827935031168	DA	12.2 (0.3)	19.19	18.514	18.3	18.23	18.26	18.27	17.59	17.29	17.3
J1245+4238	1540371883066128768	DA*	14.1 (0.1)	17.3	17.132	17.163	17.291	17.431	17.52	···	···	···
J1245−1837	3521882906526249088	DA	10.3 (0.3)	19.52	19.008	18.84	18.794	18.84	18.84	18.22	···	17.7
J1245−1946	3503777905682327552	DA	18.5 (0.1)	16.71	16.348	16.444	16.601	16.781	16.892	16.33	···	16.37
J1246+1155	3928060510626899200	DZ	12.5 (0.1)	17.87	17.442	17.462	17.604	17.773	17.85	17.29	17.27	17.3
J1247+0646	3709565658737443200	DQ	19.1 (0.3)	21.0	19.93	18.67	18.41	18.35	18.32	17.55	17.54	17.35
J1247+3030	1465214177336901376	DA	12.2 (0.1)	18.54	18.06	17.95	17.96	18.0	18.09	17.4	17.29	17.4
J1247−0111	3683627840135415808	DA	21.3 (0.1)	17.49	16.97	16.812	16.773	16.83	16.86	16.1	15.92	15.91
J1248+1222	3928101738016062336	DA	10.5 (0.2)	18.8	18.28	18.146	18.133	18.2	18.22	17.56	17.4	17.2
J1248+1230	3928119295842399360	DA	13.9 (0.2)	19.46	18.78	18.54	18.5	18.5	18.52	17.77	17.51	17.6
J1248+2942	1465092887460185600	DA	15.6 (0.1)	18.44	17.788	17.591	17.55	17.585	17.62	16.93	16.81	16.8

Tableau A.1 *suite page suivante*

Tableau A.1 *(suite)*

Name	Gaia DR2/EDR3*	Sp Type	ϖ (mas)	u	g	r	i	z	y	J	H	K
J1248+4104	1527940564084210816	DAH*	15.3 (0.1)	18.4	17.88	17.73	17.736	17.79	17.86	17.21	···	···
J1248−1028	3530520910392199680	DC	25.2 (0.1)	17.43	16.968	16.849	16.879	16.944	17.02	16.3	···	···
J1249+2742	3961972747760766720	DA	10.9 (0.2)	19.05	18.52	18.33	18.3	18.34	18.38	17.69	17.5	17.5
J1249+2800	3961998375830065152	DQ	10.7 (0.3)	18.88	18.52	18.45	18.51	18.59	18.69	18.05	18.0	17.9
J1249+3407	1515081328918440064	DQ	13.9 (0.1)	17.34	17.14	17.15	17.278	17.42	17.52	16.95	16.85	17.0
J1250+1955	3942229672158400640	DA	12.4 (0.2)	18.58	18.164	18.106	18.162	18.24	18.3	17.64	···	···
J1250+5446	1570514066627694336	DC	42.1 (0.1)	21.09	18.33	17.31	16.863	16.7	16.6	15.72	15.67	15.63
J1251+0753	3709760890770697856	DA	10.1 (0.2)	18.56	18.27	18.33	18.42	18.59	18.7	18.11	18.2	17.9
J1251+2912	1464837457164974976	DC	10.9 (0.8)	22.4	20.53	19.8	19.51	19.4	19.3	18.4	18.3	18.3
J1251+4403	1528861748669458432	DC	21.1 (0.8)	···	20.14	20.37	20.8	21.0	20.9	21.8	···	···
J1252+1943	3942041105914664832	DQ	11.9 (0.4)	18.19	17.775	17.63	17.619	17.67	17.72	17.06	17.0	···
J1252+2153	3954943428189717504	DAZ	10.9 (0.3)	20.03	19.01	18.73	18.63	18.63	18.62	18.0	···	···
J1252−0234	3682469122383597056	DC	12.9 (0.1)	18.02	17.59	17.51	17.53	17.62	17.69	17.05	16.95	16.92
J1253+0355	3704624487842182656	DA	13.7 (0.2)	19.18	18.47	18.197	18.12	18.12	18.12	17.41	17.14	17.0
J1253+2203	3954947379559880064	DC	19.0 (0.2)	20.7	18.97	18.38	18.156	18.066	18.0	···	···	···
J1253+3437	1515869884914637824	DC	17.0 (0.3)	21.4	19.45	18.76	18.48	18.35	18.33	17.45	17.2	17.2
J1254+1432	3930720057454344960	DC	13.3 (0.1)	17.08	16.953	17.023	17.174	17.343	17.44	16.9	16.97	17.0
J1254+2054	3942685179209931008	DA	11.4 (0.2)	19.35	18.79	18.63	18.57	18.62	18.63	···	···	···
J1254+3620	1517239773324267904	DC	35.0 (0.1)	19.78	17.82	17.115	16.83	16.745	16.69	15.81	15.7	15.4
J1254+4918	1555410036744248832	DAH	10.3 (0.2)	20.0	19.28	19.04	18.96	19.0	19.0	18.2	···	···
J1254−0236	3682412703692940032	DZ	12.7 (0.2)	18.88	18.39	18.29	18.32	18.4	18.5	17.85	17.77	17.8
J1255+4655	1531097433767946240	DC	27.0 (0.2)	21.06	19.07	18.33	18.04	17.92	17.87	16.87	16.8	16.7
J1256+1355	3929872707650824320	DA	10.1 (0.3)	20.12	19.27	18.97	18.854	18.84	18.82	18.03	17.9	17.7
J1256+1551	3931506719368273792	DA	12.4 (0.2)	18.23	17.85	17.861	17.91	18.03	18.1	17.57	17.43	17.5
J1256+1839	3941103359935056640	DA	10.1 (0.3)	19.86	19.15	18.93	18.88	18.93	18.94	18.3	···	···
J1257+2312	3956630388264212992	DA	10.3 (0.4)	20.5	19.49	19.14	19.03	18.99	19.01	18.21	17.9	17.9
J1257+2911	1464134289414972288	DA	13.7 (0.1)	18.68	18.02	17.82	17.775	17.8	17.84	17.1	16.84	17.0
J1257+3414	1515693894335906688	DAH	18.1 (0.1)	17.11	16.798	16.825	16.93	17.08	17.162	16.6	16.5	16.62
J1257+5127	1557524191442926336	DA	10.3 (0.2)	19.41	18.959	18.84	18.872	18.95	18.93	···	···	···
J1258+1946	3941619958601686016	DC	16.5 (0.3)	21.7	19.71	18.94	18.62	18.48	18.45	17.53	···	···
J1258+5014	1555883930548870400	DA	20.0 (0.1)	17.02	16.601	16.572	16.621	16.71	16.78	16.15	16.1	15.6
J1259+0442	3705109338109763712	DC	19.3 (0.3)	21.3	19.31	18.61	18.32	18.22	18.16	17.4	17.2	16.9
J1259+2734	1460689760003983232	DAZ	30.3 (0.1)	15.853	15.43	15.422	15.5	15.604	15.686	15.066	14.95	14.99
J1259+2754	1460807304669403136	DQ	10.3 (0.1)	17.53	17.46	17.5	17.68	17.84	17.96	17.4	17.5	17.4

Tableau A.1 *suite page suivante*

Tableau A.1 *(suite)*

Name	Gaia DR2/EDR3*	Sp Type	ϖ (mas)	u	g	r	i	z	y	J	H	K
J1259+6234	1675850407304241536	DC	19.4 (0.1)	18.61	17.97	17.769	17.737	17.774	17.78	···	···	···
J1300+0130	3690395231125833600	DA	27.7 (0.1)	19.11	17.74	17.26	17.037	16.99	16.98	16.15	15.88	15.85
J1300+0328	3704392873140270336	DA	60.8 (0.2)	17.2	16.05	15.633	15.47	15.418	15.43	14.573	14.319	14.254
J1300+0836	3733693754214402816	DA	11.9 (0.3)	19.87	19.13	18.81	18.68	18.7	18.66	17.99	17.64	17.7
J1300+1817	3940853397134158848	DA	11.9 (0.1)	16.84	16.49	16.517	16.62	16.75	16.85	16.26	16.0	16.1
J1300+3931	1523861990123367808	DQ	10.9 (0.4)	20.32	20.54	19.64	19.29	19.33	19.42	18.7	···	···
J1300+5904	1578748824604827648	DAH	15.6 (0.1)	19.07	18.22	17.911	17.819	17.83	17.81	17.06	···	···
J1301+1520	3930500666228897536	DC	12.4 (0.2)	19.26	18.63	18.44	18.41	18.45	18.47	17.83	17.7	17.9
J1301+2600	1460293317343353344	DA	15.4 (0.1)	18.31	17.747	17.556	17.525	17.542	17.56	16.88	16.67	16.7
J1301+6713	1679365202380970880	DA	32.46 (0.05)	17.3	16.66	16.436	16.383	16.41	16.42	15.6	15.3	15.3
J1301−0235	3685203985758805120	DA	10.7 (0.4)	20.2	19.68	19.52	19.48	19.58	19.56	18.9	18.6	18.8
J1302+2120	3944082692848953088	DC	12.4 (0.2)	19.48	18.765	18.53	18.45	18.48	18.5	17.67	···	···
J1303+1949	3941482519648231296	DA	11.8 (0.2)	19.03	18.37	18.19	18.15	18.17	18.15	17.48	···	···
J1303+2603	1459546263999675264	DC	26.3 (0.2)	21.6	19.26	18.37	17.972	17.83	17.76	16.89	16.71	16.7
J1303+3854	1523586253222618112	DC	10.7 (0.3)	20.13	19.45	19.15	19.05	19.03	19.05	···	···	···
J1303+7510	1691837787408390400	DC	24.0 (0.1)	···	16.57	16.468	16.53	16.627	16.68	16.16	15.79	15.27
J1303−0323	3684329706511747840	DA	15.5 (0.1)	17.41	16.896	16.76	16.73	16.8	16.833	16.13	15.94	15.93
J1304+0126	3691095100341397632	DC*	13.5 (0.5)	21.3	19.99	19.42	19.38	19.77	19.98	20.1	···	···
J1304−0528	3629758603668233728	DA	34.7 (0.1)	···	17.491	16.952	16.735	16.672	16.634	15.8	15.6	15.5
J1305+1525	3936440262402010368	DA	10.3 (0.1)	17.73	17.324	17.382	17.517	17.66	17.76	17.21	17.22	17.2
J1305+6034	1579314622119638400	DC :	10.5 (0.1)	18.22	17.99	18.008	18.11	18.24	18.31	···	···	···
J1305+7022	1686322048672412288	DC	28.9 (0.2)	···	19.9	19.27	19.05	18.95	18.92	···	···	···
J1306+1811	3938160280840704000	DA	13.6 (0.2)	18.27	17.93	17.917	17.968	18.07	18.14	17.54	···	···
J1306+4355	1529609897612606592	DA	12.0 (0.1)	19.1	18.41	18.2	18.14	18.15	18.14	17.44	···	···
J1307+4910	1554850591480752384	DA	12.9 (0.2)	20.3	19.19	18.776	18.61	18.56	18.59	17.75	···	···
J1308+8502	1726678630833373824	DAP	60.72 (0.04)	···	16.307	15.76	15.58	15.52	15.487	14.69	14.5	14.3
J1309+3715	1522443933657255936	DA	10.3 (0.1)	17.72	17.31	17.349	17.451	17.59	17.71	17.1	···	···
J1309+4913	1554843655110340992	DZ	12.7 (0.1)	17.62	17.381	17.41	17.531	17.671	17.75	···	···	···
J1310+1214	3736695803210593664	DA	10.6 (0.1)	18.13	17.773	17.729	17.79	17.89	17.93	17.32	17.2	17.2
J1310+1404	3743905507112335616	DA	17.9 (0.1)	16.78	16.409	16.363	16.43	16.526	16.61	16.01	15.88	15.89
J1310+6117	1675399401377503360	DC	10.9 (0.6)	22.4	20.8	19.87	19.57	19.45	19.6	···	···	···
J1310+6118	1675399225287958272	DC	10.7 (0.3)	20.8	19.52	19.09	18.92	18.833	18.89	···	···	···
J1310+6746	1679458897091659008	DC	13.9 (0.2)	19.59	18.89	18.64	18.59	18.6	18.57	···	···	···
J1310+7236	1688070959355309312	DA	17.3 (0.1)	···	16.94	16.86	16.903	16.98	17.02	16.03	16.0	15.24

Tableau A.1 *suite page suivante*

Tableau A.1 *(suite)*

Name	Gaia DR2/EDR3*	Sp Type	ϖ (mas)	u	g	r	i	z	y	J	H	K
J1310−0202	3684909561456453248	DA :	13.7 (0.3)	19.4	18.66	18.4	18.329	18.33	18.38	17.61	17.49	17.5
J1311+2923	1462641629366243712	DQ	18.4 (0.2)	19.63	19.49	18.46	17.91	17.92	18.0	17.36	17.22	16.9
J1311+3837	1523116177642231808	DC	12.9 (0.2)	19.31	18.67	18.46	18.43	18.47	18.49	17.78	···	···
J1311−0034	3687414210289577344	DA	12.2 (0.3)	19.78	19.07	18.79	18.728	18.74	18.75	18.08	17.85	17.6
J1312+5805	1566603962760532736	DA	31.3 (0.2)	14.53	14.068	14.17	14.342	14.495	14.6	14.053	14.0	14.1
J1313+0226	3691685882071367936	DC	32.3 (0.2)	21.0	18.72	17.83	17.443	17.281	17.251	16.25	16.22	16.1
J1313+1057	3733305179932909312	DA :	15.7 (0.3)	20.01	18.85	18.45	18.32	18.31	18.28	17.56	17.33	17.2
J1313+1341	3743646365965636352	DC	16.0 (0.1)	17.24	17.05	17.108	17.223	17.35	17.47	16.86	16.87	16.87
J1313+5738	1566553007268519168	DZA	14.7 (0.1)	17.04	16.85	16.89	17.033	17.19	17.28	16.75	···	···
J1313−0223	3684741301817503872	DA*	19.4 (0.1)	18.32	17.627	17.363	17.28	17.3	17.3	16.776	16.3	16.26
J1314+0700	3729759568466399488	DA	10.8 (0.1)	17.6	17.17	17.21	17.341	17.471	17.59	17.01	16.94	17.0
J1314+1456	3744078023062858624	DA	17.9 (0.1)	19.1	18.27	17.98	17.87	17.88	17.89	17.18	16.93	16.92
J1314+1732	3937174942327932544	DAH	12.3 (0.2)	19.14	18.6	18.45	18.45	18.5	18.54	17.9	···	···
J1314+5327	1563260687202320256	DC	13.3 (0.1)	16.91	16.806	16.896	17.053	17.22	17.33	16.6	16.0	···
J1315+4711	1551346520939849728	DQ	11.8 (0.1)	18.08	17.75	17.712	17.792	17.9	17.99	17.47	···	···
J1315+6046	1663349849153677952	DA	12.2 (0.1)	18.99	18.368	18.2	18.17	18.2	18.3	···	···	···
J1316+0149	3688402091422432128	DA :*	13.1 (0.3)	19.04	18.43	18.183	18.1	18.13	18.14	17.36	17.18	17.14
J1316+0810	3731530843043705216	DQ	11.4 (0.3)	19.03	18.526	18.38	18.37	18.43	18.51	17.85	17.7	17.7
J1316−2007	3506567328028533120	DZ	43.1 (0.1)	···	17.46	16.92	16.77	16.72	16.72	15.86	15.6	15.5
J1317+0621	3717651845204820864	DA	22.2 (0.2)	20.01	18.52	17.969	17.74	17.67	17.65	16.86	16.74	16.7
J1317+2157	3943650619138622848	DC	31.5 (0.1)	17.6	16.94	16.694	16.626	16.66	16.69	16.02	15.8	···
J1317+4434	1550492952021749248	DC :	13.6 (0.1)	19.28	18.62	18.41	18.355	18.42	18.45	17.75	···	···
J1317+4833	1556005701461744640	DA	25.5 (0.1)	18.44	17.49	17.124	16.965	16.97	16.92	···	···	···
J1317+6005	1663262163101591936	DC	16.6 (0.1)	18.01	17.506	17.403	17.431	17.517	17.58	···	···	···
J1317−1121	3623233040812235904	DA	25.1 (0.1)	···	15.621	15.64	15.739	15.851	15.941	15.29	15.24	15.23
J1318+1241	3742597358857731712	DA	11.5 (0.3)	19.68	18.92	18.65	18.54	18.524	18.54	17.78	17.49	17.5
J1318+5003	1556577584947193856	DC	11.4 (0.1)	17.19	17.08	17.18	17.344	17.49	17.59	17.2	···	···
J1319−2148	3506061587037686144	DA	50.5 (0.1)	···	16.9	16.542	16.401	16.39	16.36	15.53	15.3	15.26
J1320+2801	1461469893567499904	DC	11.2 (0.6)	24.32	20.73	19.88	19.48	19.4	19.2	18.4	18.3	18.0
J1320+3942	1524536884104266368	DA	12.1 (0.9)	20.07	19.55	19.41	19.4	19.45	19.42	18.7	···	···
J1320+4712	1551402252435630592	DA	12.6 (0.1)	18.02	17.583	17.502	17.519	17.614	17.66	16.96	16.9	17.2
J1320+5530	1563853976804546688	DC	10.4 (0.3)	20.6	19.52	19.21	19.13	19.1	19.13	18.5	···	···
J1320−0224	3638148805100101888	DA	17.0 (0.5)	21.0	19.25	18.65	18.38	18.29	18.25	17.3	17.13	17.0
J1321+1645	3746179365877952256	DAH*	12.8 (0.1)	18.44	17.965	17.85	17.852	17.92	17.97	17.34	···	···

Tableau A.1 *suite page suivante*

Tableau A.1 *(suite)*

Name	Gaia DR2/EDR3*	Sp Type	ϖ (mas)	u	g	r	i	z	y	J	H	K
J1321+3345	1472821908743764096	DA	13.7 (0.1)	18.2	17.882	17.88	17.949	18.09	18.19	17.53	17.4	17.4
J1323+1756	3746422113133965696	DC :	10.2 (0.3)	19.95	19.4	19.18	19.12	19.14	19.15	18.6	···	···
J1324+0857	3731853549706103680	DA	17.2 (0.1)	17.09	16.642	16.604	16.641	16.74	16.82	16.15	16.04	15.99
J1324+4149	1525359868557998336	DA	12.8 (0.2)	20.9	19.3	18.81	18.65	18.58	18.52	17.76	···	···
J1324+6226	1663956268471724288	DA	15.8 (0.05)	16.63	16.192	16.29	16.421	16.579	16.71	16.2	16.0	16.0
J1325+0852	3731848189586855040	DA	13.3 (0.1)	17.44	17.081	17.14	17.26	17.39	17.54	16.94	16.86	16.94
J1325+4523	1550208900064886656	DC	10.2 (0.2)	20.03	19.19	18.89	18.76	18.75	18.7	···	···	···
J1326+0504	3716300103033172608	DA	9.9 (0.2)	18.66	18.01	17.8	17.745	17.76	17.79	···	···	···
J1326+5025	1553656418774428032	DA	11.4 (0.2)	19.18	18.61	18.37	18.33	18.37	18.39	17.68	···	···
J1327+5755	1566012013187728768	DA	24.6 (0.1)	17.45	16.78	16.609	16.55	16.602	16.58	15.85	15.7	15.7
J1327+5805	1566020598826667904	DC	11.6 (0.2)	20.4	19.5	19.18	19.05	19.03	19.0	18.3	···	···
J1328+4450	1550124654283201920	DC	10.4 (0.2)	18.9	18.34	18.26	18.28	18.41	18.39	···	···	···
J1329+0746	3719493011785709056	DQ	14.3 (0.1)	17.57	17.31	17.298	17.403	17.51	17.62	17.0	17.02	16.9
J1329+2450	1447925976193082368	DC	23.1 (0.2)	22.3	19.8	18.758	18.33	18.14	18.1	17.2	17.11	17.0
J1329+3109	1468305213760240384	DC	10.4 (0.5)	22.9	20.7	19.91	19.62	19.5	19.3	18.6	18.6	···
J1329+3927	1476702321500114432	DA	10.0 (0.1)	18.38	17.92	17.844	17.88	17.95	18.02	17.39	···	···
J1329−0134	3638457669084084224	DA	18.5 (0.1)	17.73	17.205	17.08	17.04	17.09	17.13	16.44	16.28	16.25
J1329−0238	3637209066255998592	DA	10.2 (0.3)	18.36	17.98	17.99	18.06	18.18	18.27	17.68	17.6	17.5
J1330+2329	1443266623871074816	DA	14.8 (0.3)	19.87	18.99	18.71	18.61	18.58	18.61	17.78	17.57	17.6
J1330+3029	1468213546275054208	DZH	39.15 (0.05)	18.26	16.21	15.907	15.94	16.09	16.12	15.48	15.4	15.36
J1330+5445	1565012935076040832	DA	20.71 (0.05)	17.33	16.87	16.767	16.775	16.839	16.89	16.19	15.9	15.4
J1330+6435	1666074615061406336	DC*	11.6 (0.9)	24.1	21.4	20.81	20.08	19.95	19.8	···	···	···
J1331+6809	1684555515739151360	DA	17.82 (0.04)	···	16.118	16.162	16.277	16.41	16.51	15.82	15.67	16.1
J1332+0117	3711214067185666560	DAH	24.1 (0.1)	17.71	17.116	16.96	16.942	16.98	17.03	16.33	16.22	16.22
J1332+1043	3738162616145822208	DC	9.9 (0.3)	19.51	18.93	18.79	18.768	18.82	18.85	18.25	18.0	17.8
J1332+2740	1448881864114808448	DQZ	13.9 (0.1)	17.43	17.19	17.22	17.331	17.47	17.563	16.99	16.94	16.94
J1333+0016	3662951038644235776	DQ	24.5 (0.4)	19.09	19.5	18.36	18.12	18.2	18.21	17.38	17.05	16.73
J1333+0649	3718579386342034816	DA	14.4 (0.2)	18.45	18.01	17.9	17.922	17.977	18.03	17.37	17.13	17.3
J1333+1550	3744991824600484864	DA	13.8 (0.2)	18.4	18.033	18.028	18.077	18.18	18.25	···	···	···
J1333+2450	1444926572896853376	DC	20.6 (0.2)	21.4	19.33	18.548	18.221	18.11	18.05	17.17	16.92	16.9
J1333+4225	1501320872177341952	DAZ	9.9 (0.3)	20.15	19.48	19.35	19.28	19.3	19.31	18.6	···	···
J1334+0647	3718388689794769664	DA	10.8 (0.2)	18.7	18.27	18.16	18.188	18.25	18.29	17.75	17.5	17.2
J1334+4704	1551761857160285312	DC	10.5 (0.2)	20.0	19.3	19.03	19.0	19.02	19.04	18.3	···	···
J1334+6601	1666261218505739008	DA	18.5 (0.1)	19.28	18.346	18.021	17.897	17.89	17.87	···	···	···

Tableau A.1 *suite page suivante*

Tableau A.1 *(suite)*

Name	Gaia DR2/EDR3*	Sp Type	ϖ (mas)	u	g	r	i	z	y	J	H	K
J1335+3322	1469189191046042112	DA	10.7 (0.1)	17.56	17.07	17.079	17.13	17.27	17.33	16.74	16.6	16.7
J1335+3610	1471998511973713152	DA	12.6 (0.1)	17.02	16.65	16.726	16.872	17.032	17.13	16.6	16.49	16.6
J1335−0542	3633287421812873600	DA	22.3 (0.1)	···	16.351	16.27	16.305	16.38	16.45	15.6	15.5	15.3
J1336+3034	1456253707325896960	DA	9.9 (0.3)	20.0	19.27	18.95	18.86	18.84	18.83	18.03	17.9	17.6
J1336+3547	1471788161655374080	DZH*	16.8 (0.1)	19.49	17.79	17.641	17.715	17.83	17.88	17.33	17.1	17.2
J1336+3623	1472029470098019072	DA	28.2 (0.1)	17.06	16.47	16.288	16.246	16.271	16.292	15.55	15.3	15.3
J1336+3648	1472094341284011904	DA	19.0 (0.1)	18.85	17.951	17.65	17.516	17.497	17.43	16.78	16.2	···
J1336+3727	1472500473391093120	DA	23.3 (0.1)	17.45	17.066	16.974	16.992	17.066	17.13	16.44	16.3	···
J1336+5403	1561941170170300288	DA	12.0 (0.2)	20.0	19.03	18.72	18.59	18.58	18.56	17.9	···	···
J1337+0001	3662779171232754688	DC	18.7 (0.7)	20.83	19.47	19.13	19.56	20.03	19.8	20.4	20.7	···
J1337+6110	1662871286717909632	DA	22.8 (0.1)	19.41	18.103	17.64	17.47	17.43	17.41	16.5	16.4	15.6
J1337−1203	3610422798340344704	DC	14.8 (0.2)	···	18.195	17.99	17.95	18.01	18.03	17.35	17.3	17.3
J1338+3213	1468882118064381696	DA	10.2 (0.2)	20.13	19.28	18.95	18.83	18.83	18.82	18.02	17.8	17.8
J1338−0045	3661843349398271232	DA	13.8 (0.4)	19.6	18.7	18.42	18.29	18.3	18.29	17.53	17.3	17.17
J1339+6010	1662524184641472640	DA	11.4 (0.1)	18.34	17.92	17.858	17.889	17.98	17.99	···	···	···
J1339−0020	3661954022115425536	DA	10.6 (0.3)	18.54	18.12	18.03	18.06	18.13	18.14	17.56	17.3	17.4
J1340+0203	3663664003222454528	DA	24.7 (0.2)	19.28	18.06	17.61	17.456	17.42	17.41	16.59	16.33	16.27
J1340+3228	1456903763514134272	DA	14.0 (0.1)	17.36	16.92	16.924	16.98	17.119	17.2	16.57	16.45	16.51
J1340+4033	1500140065408640512	DC	16.5 (0.4)	21.3	19.32	18.631	18.36	18.28	18.18	17.31	17.01	16.84
J1341+0227	3713218786120541824	DQ	24.9 (0.1)	18.37	17.928	17.32	17.17	17.18	17.18	16.5	15.7	···
J1341+0500	3714914271705535360	DC	68.2 (0.1)	19.64	17.26	16.301	15.883	15.725	15.64	14.7	14.59	14.5
J1341+0721	3724485756648081920	DA	10.9 (0.3)	19.85	18.97	18.63	18.502	18.48	18.46	17.75	17.5	17.3
J1341+2156	1249747212968218496	DC	19.4 (0.2)	21.1	19.16	18.46	18.178	18.07	18.01	17.12	···	···
J1341+4150	1501012287368950528	DA	17.1 (0.1)	18.04	17.66	17.606	17.62	17.7	17.74	17.07	···	···
J1342+4436	1503203059990907648	DC	11.7 (0.2)	19.65	19.0	18.708	18.64	18.67	18.66	18.04	···	···
J1343+1157	3728216571400055040	DA	12.2 (0.3)	19.09	18.591	18.5	18.52	18.59	18.66	17.92	17.9	17.7
J1344+4349	1503091085900019712	DA	16.5 (0.1)	19.37	18.58	18.3	18.177	18.19	18.2	···	···	···
J1345+1514	3741324506644465280	DC	15.4 (0.5)	23.6	20.62	19.6	19.18	18.99	18.85	18.07	18.0	18.2
J1345+4200	1500607765872799616	DC	26.7 (0.1)	19.73	17.74	17.01	16.694	16.59	16.54	15.6	15.4	15.0
J1346+0918	3725166869742133248	DA	17.3 (0.2)	20.1	18.75	18.23	18.03	17.97	17.93	17.11	16.83	16.73
J1346−1350	3606199608537728768	DA	11.3 (0.1)	···	15.89	15.921	16.051	16.17	16.267	15.7	15.6	15.4
J1347+1021	3725570772761744384	DAZ*	48.08 (0.04)	15.8	15.211	15.035	15.05	15.074	15.101	14.41	14.1	14.2
J1347+2552	1444528416543875456	DA	15.4 (0.1)	18.11	17.604	17.46	17.43	17.472	17.51	16.78	16.62	16.62
J1347+5036	1558872261424381184	DA	16.6 (0.2)	20.7	19.05	18.49	18.265	18.18	18.14	17.29	17.07	16.91

Tableau A.1 *suite page suivante*

Tableau A.1 *(suite)*

Name	Gaia DR2/EDR3*	Sp Type	ϖ (mas)	u	g	r	i	z	y	J	H	K
J1348+2334	1251824057289839744	DC	84.27 (0.04)	18.12	16.039	15.309	14.99	14.871	14.82	13.92	13.67	13.62
J1348+4618	1503808066264043136	DA	9.9 (0.1)	18.22	17.79	17.77	17.84	17.95	18.03	17.43	···	···
J1348−0152	3658513620167922816	DC	10.5 (0.4)	20.4	19.47	19.17	19.08	19.06	19.13	18.37	18.22	18.1
J1349+1155	3728074738695246336	DC	35.4 (0.2)	20.6	18.54	17.83	17.438	17.26	17.21	16.43	16.29	16.26
J1349+2755	1451566149955227520	DA	33.3 (0.1)	16.96	16.445	16.329	16.303	16.35	16.4	15.69	15.54	15.52
J1349+4332	1502284452385828864	DA	11.2 (0.1)	18.66	18.29	18.273	18.34	18.45	18.47	···	···	···
J1351+1214	3728063945441922176	DC	10.7 (10.2)	22.7	20.8	20.02	19.77	19.65	19.6	18.8	18.57	18.48
J1351+1719	1244753299874351488	DAH	14.5 (0.1)	17.9	17.58	17.59	17.711	17.78	17.91	17.34	···	···
J1351+3654	1495325853747745536	DA	10.2 (0.1)	19.05	18.51	18.31	18.291	18.34	18.36	17.71	···	···
J1351+4141	1500444625834675200	DA	10.3 (0.2)	19.01	18.63	18.56	18.623	18.7	18.77	···	···	···
J1351+4253	1502063317405058304	DZ	25.4 (0.1)	17.61	17.04	16.867	16.844	16.92	16.94	16.3	15.9	···
J1351+4653	1509842495314395264	DA	11.2 (0.3)	20.9	19.98	19.64	19.51	19.49	19.48	···	···	···
J1351+6623	1672147149062665472	DQ	10.0 (0.1)	17.84	17.71	17.76	17.89	18.07	18.15	···	···	···
J1351−2734	6177238676273826304	DA	26.6 (0.1)	···	15.157	15.2057	15.325	15.47	15.5	14.9	14.8	14.8
J1352+0818	3721801956139414400	DA	10.1 (0.2)	19.04	18.47	18.289	18.26	18.3	18.33	17.66	17.5	17.5
J1352+0907	3722192007889372800	DC	21.1 (0.3)	20.9	19.2	18.61	18.41	18.3	18.36	17.49	17.23	17.17
J1352+1053	3727155340815968256	DA	28.2 (0.1)	17.97	17.083	16.752	16.628	16.606	16.603	15.83	15.57	15.52
J1352−0054	3659054987910568320	DA	14.6 (0.1)	18.27	17.737	17.562	17.542	17.58	17.61	16.92	16.69	16.8
J1353+2928	1452337006389928960	DA	17.0 (0.1)	17.96	17.5	17.4	17.398	17.47	17.51	16.85	16.7	16.67
J1353−0916	3618657732410663808	DAP	50.73 (0.04)	···	14.62	14.636	14.715	14.821	14.893	14.19	14.08	14.14
J1353−2738	6177179298350278016	DA	18.3 (0.1)	···	16.93	16.835	16.84	16.91	16.94	16.1	16.1	15.9
J1354+6009	1661023419988816256	DA	10.9 (0.1)	18.75	18.4	18.38	18.462	18.57	18.63	···	···	···
J1354−0051	3658879826259633664	DA	20.1 (0.1)	17.68	17.247	17.136	17.15	17.195	17.25	16.57	16.39	16.42
J1355+3636	1495340933377121792	DQ	11.7 (0.1)	17.9	17.72	17.69	17.764	17.89	17.95	17.39	···	···
J1355+4553	1508988758895110656	DC	10.2 (0.1)	18.25	17.96	17.97	18.074	18.19	18.27	···	···	···
J1355−2622	6178524211524592640	DA	30.6 (0.1)	···	16.93	16.619	16.507	16.484	16.51	15.8	15.6	···
J1356+1336	1230679413599906176	DC	12.2 (0.4)	19.98	19.13	18.78	18.67	18.65	18.65	17.88	17.77	17.8
J1356+2416	1257923215792065152	DZ	9.9 (0.3)	20.4	18.98	18.73	18.76	18.86	18.96	18.4	18.1	18.2
J1356+5853	1659211974581862912	DA	15.8 (0.1)	18.6	18.07	17.935	17.93	17.99	18.02	17.32	···	···
J1356−0009	3660622479174640640	DQ	12.8 (0.2)	19.0	18.61	18.315	18.264	18.32	18.35	17.77	17.59	17.5
J1356−0920	3615616169715231104	DA	11.9 (0.1)	17.8	17.35	17.335	17.4	17.51	17.58	16.93	16.8	16.9
J1357+2954	1453676525085505408	DC	12.7 (0.1)	18.55	18.09	17.99	18.024	18.11	18.16	17.55	17.42	17.5
J1357+6028	1660937971614743808	DC	20.1 (0.1)	18.84	18.02	17.73	17.64	17.63	17.68	···	···	···
J1358+1442	1231038060549269120	DC	12.0 (0.2)	18.32	18.03	18.0	18.069	18.2	18.26	17.67	17.54	17.7

Tableau A.1 *suite page suivante*

Tableau A.1 *(suite)*

Name	Gaia DR2/EDR3*	Sp Type	ϖ (mas)	u	g	r	i	z	y	J	H	K
J1358+3704	1483371791532150784	DAZ	11.9 (0.2)	20.7	19.44	18.95	18.779	18.74	18.67	17.95	17.66	17.67
J1359−2333	6275184065428686464	DA	29.97 (0.05)	···	15.029	15.069	15.187	15.326	15.41	14.787	14.7	14.76
J1401+3659	1483683911099065088	DZ	11.9 (0.2)	19.88	18.77	18.56	18.543	18.59	18.64	···	···	···
J1402−0254	3645620879964502016	DA	10.0 (0.5)	19.65	19.08	18.92	18.87	18.9	18.89	18.24	18.06	18.0
J1402−0736	3616350265525122816	DA	23.9 (0.1)	17.09	16.7362	16.727	16.791	16.88	16.94	16.2	15.9	···
J1402−0902	3615906062827657344	DC	14.7 (0.2)	18.4	18.021	17.97	18.01	18.11	18.17	···	···	···
J1403+0452	3671751946324947584	DA	19.4 (0.1)	16.63	16.243	16.257	16.335	16.448	16.54	···	15.81	15.86
J1403+0644	3672656947473710592	DC	20.4 (0.1)	18.02	17.444	17.273	17.271	17.321	17.38	16.69	16.61	16.51
J1403+4052	1497899703093177728	DA	10.2 (0.1)	18.57	18.128	18.03	18.055	18.123	18.16	17.51	···	···
J1403+4533	1505825635741455872	DC	29.1 (0.2)	20.16	18.87	18.98	19.55	19.97	20.1	20.2	20.6	20.9
J1403+5206	1512752769450543488	DA	23.6 (0.1)	17.03	16.522	16.41	16.42	16.49	16.48	15.83	15.7	15.1
J1403+6439	1670992421335403904	DA*	14.3 (0.1)	17.0	16.878	16.949	17.096	17.24	17.36	16.8	···	···
J1403−0914	3615854321357005824	DA	12.2 (0.1)	17.27	16.813	16.875	17.003	17.15	17.26	16.7	···	···
J1403−1514	6300991145225638272	DC	20.5 (0.2)	···	18.65	18.159	17.96	17.94	17.95	17.5	17.7	18.3
J1404+0936	3723164143671997952	DA	12.9 (0.1)	16.89	16.471	16.551	16.695	16.861	16.97	16.4	16.1	16.38
J1404+1330	1229916112012470528	DC	13.7 (0.4)	20.8	19.55	19.02	18.828	18.92	19.08	18.8	19.18	19.7
J1404+1349	1229959542721326080	DAZ	10.5 (0.4)	20.7	19.59	19.2	19.04	19.02	18.98	18.24	17.9	17.9
J1404+3620	1483427385588999936	DZ	12.2 (0.2)	19.97	18.708	18.5	18.53	18.64	18.7	17.9	···	···
J1404+5020	1511457265578685440	DC	16.4 (0.1)	20.06	18.75	18.31	18.01	18.05	17.78	···	···	···
J1404+5243	1512865022715710464	DA	10.8 (0.1)	18.36	17.95	17.89	17.933	18.0	18.07	17.47	···	···
J1405+4300	1499290379143445760	DC	12.7 (0.1)	19.28	18.51	18.34	18.34	18.41	18.46	17.8	···	···
J1405+6648	1671668067321674368	DC	27.2 (0.1)	···	19.41	18.369	17.93	17.76	17.68	···	···	···
J1406+0849	3722502856146928256	DA	11.0 (0.4)	19.97	19.26	19.01	18.93	18.93	19.0	18.2	17.9	18.0
J1406+1608	1231446224176456064	DA	17.9 (0.1)	18.22	17.61	17.389	17.339	17.34	17.35	16.63	16.3	17.28
J1406+1812	1245468295966061952	DA	22.7 (0.1)	17.81	17.28	17.145	17.118	17.189	17.23	16.52	16.4	···
J1406+2003	1246230047071154944	DC	10.8 (0.2)	18.64	18.24	18.18	18.2	18.251	18.2617	···	···	···
J1406+3130	1454347089739329152	DC	25.4 (0.2)	20.5	18.6	17.92	17.651	17.53	17.48	16.6	15.88	16.1
J1406+3401	1481854770426696704	DQ+DA	10.1 (0.1)	18.36	17.9	17.79	17.802	17.87	17.92	17.23	···	···
J1407+1133	1226206806457202432	DA	18.6 (0.2)	20.1	18.74	18.23	18.024	17.95	17.92	17.08	16.86	16.78
J1407+5509	1609392862209121664	DA	18.9 (0.3)	20.17	19.45	19.23	19.22	19.24	19.2	18.7	···	···
J1407−0626	3643555726544985088	DA	40.64 (0.04)	···	15.098	15.071	15.133	15.231	15.3	14.7	14.55	14.6
J1408−2649	6270584739570554880	DC	25.0 (0.1)	···	17.13	16.967	16.946	16.999	17.05	16.4	16.3	15.7
J1409+1511	1230575131794474752	DZ	11.5 (0.2)	19.35	18.75	18.597	18.572	18.64	18.68	18.0	···	···
J1409+3828	1485197354494658176	DA	10.2 (0.1)	18.83	18.34	18.24	18.22	18.25	18.31	17.57	···	···

Tableau A.1 *suite page suivante*

Tableau A.1 *(suite)*

Name	Gaia DR2/EDR3*	Sp Type	ϖ (mas)	u	g	r	i	z	y	J	H	K
J1409+4216	1498447607777405312	DA	27.78 (0.03)	15.434	15.08	15.162	15.283	15.444	15.545	14.95	14.9	14.9
J1410+0245	3667514634669861120	DAZ	36.1 (0.1)	18.09	16.926	16.503	16.344	16.304	16.27	15.439	15.2	15.08
J1411+1630	1232925891949581824	DA	10.4 (0.1)	17.81	17.358	17.357	17.464	17.58	17.64	17.01	···	···
J1411+2206	1253353890280943104	DC	19.0 (0.1)	18.17	17.58	17.429	17.411	17.465	17.52	16.86	16.3	16.99
J1412+1129	1226246251436497152	DA	10.7 (0.2)	19.14	18.64	18.575	18.598	18.67	18.75	18.13	18.0	18.0
J1412+1532	1232045934759720192	DA*	27.1 (0.2)	20.23	18.48	17.85	17.598	17.49	17.48	16.62	16.4	16.1
J1412+1815	1233764059112037632	DA	11.3 (0.4)	20.13	19.22	18.93	18.86	18.84	18.93	···	···	···
J1412+4216	1498271406743008640	DAH :*	10.7 (0.2)	18.95	18.466	18.28	18.27	18.3	18.35	17.67	···	···
J1412−1842	6296317052576778240	DC	30.1 (0.1)	···	17.323	16.942	16.804	16.774	16.77	15.96	15.8	15.69
J1413+1205	1226307755368045824	DA	12.6 (0.3)	19.2	18.58	18.35	18.321	18.34	18.38	17.62	17.5	17.5
J1413+3256	1478514389681253248	DA	11.9 (0.1)	17.15	16.703	16.8	16.939	17.127	17.233	16.8	16.5	···
J1413−0014	3659914737283635840	DA	11.2 (0.2)	18.34	18.031	18.109	18.222	18.37	18.48	17.9	18.0	18.3
J1413−0026	3647875570291353344	DA	11.6 (0.1)	17.78	17.428	17.48	17.587	17.71	17.77	17.24	17.13	17.2
J1414+2237	1253770497813126144	DA*	14.8 (0.1)	17.53	17.29	17.268	17.32	17.44	17.5	16.92	···	···
J1414+2906	1260898494256935040	DA	14.4 (0.1)	18.35	17.91	17.75	17.739	17.789	17.76	···	···	···
J1414+4336	1504443450842002176	DA	20.2 (0.1)	18.25	17.53	17.264	17.18	17.19	17.21	16.44	15.76	15.67
J1415+4337	1504453896202493568	DA	14.7 (0.1)	18.57	17.99	17.8	17.758	17.789	17.83	17.08	16.7	···
J1416+2822	1260609838099260928	DC	9.9 (0.3)	19.69	19.07	18.93	18.9	18.95	18.93	···	···	···
J1416−0902	3638957019161984640	DA+DA	12.2 (0.1)	···	15.903	15.975	16.098	16.25	16.34	15.7	15.7	···
J1417+0346	3667872216467035776	DA	13.3 (0.2)	19.56	18.62	18.325	18.236	18.24	18.24	17.45	17.34	17.17
J1417+1805	1233598174590839296	DAH	14.5 (0.1)	17.9	17.55	17.59	17.69	17.79	17.88	17.25	···	···
J1417+4941	1508482266288333952	DC	11.3 (0.1)	17.37	17.21	17.3	17.445	17.62	17.75	17.18	···	···
J1417+5735	1611509353373118336	DAH	9.7 (0.4)	21.0	20.1	19.71	19.53	19.48	19.42	18.7	···	···
J1417−0012	3653854572788715520	DC	13.3 (0.1)	18.41	17.98	17.878	17.9	17.97	18.03	17.33	17.32	17.25
J1418+0408	3669400430255790336	DA	16.1 (0.2)	18.2	17.776	17.701	17.731	17.83	17.89	17.25	17.03	17.0
J1418+1452	1228760220348642304	DA	14.8 (0.8)	17.24	16.8	16.71	16.71	16.72	16.77	16.0	15.7	15.5
J1419+1103	1225189552042779904	DC	13.5 (0.1)	17.95	17.63	17.58	17.654	17.77	17.82	17.23	17.25	17.2
J1419+2543	1258934014870979712	DAH	13.5 (0.1)	17.78	17.414	17.453	17.537	17.66	17.73	17.11	···	···
J1420+0351	3669328034286134016	DC	12.7 (0.3)	19.97	19.13	18.76	18.66	18.68	18.73	18.01	17.83	17.6
J1420+4656	1506805751574450048	DA	10.1 (0.1)	16.93	16.41	16.499	16.655	16.82	16.936	16.33	···	···
J1420+5322	1608061254844374784	DA	15.8 (0.1)	17.45	16.96	16.851	16.867	16.931	16.99	16.31	15.9	···
J1420−0905	6329136310728635776	DA	27.0 (0.1)	···	15.457	15.383	15.394	15.47	15.52	14.798	14.67	14.66
J1421+0709	3673479966286848640	DC	11.0 (0.4)	19.84	19.1	18.84	18.78	18.79	18.82	18.11	18.0	18.0
J1421+0930	1176784239825009280	DA	13.0 (0.1)	17.52	17.025	17.088	17.203	17.34	17.38	16.9	16.86	16.79

Tableau A.1 *suite page suivante*

Tableau A.1 *(suite)*

Name	Gaia DR2/EDR3*	Sp Type	ϖ (mas)	u	g	r	i	z	y	J	H	K
J1421+1436	1228599279334490496	DA	9.6 (0.4)	20.3	19.32	18.99	18.78	18.56	18.24	16.75	···	···
J1421+2147	1252685559010039424	DA	16.4 (0.1)	17.11	16.76	16.737	16.81	16.92	17.0	16.37	15.9	17.16
J1421+4226	1492278518615941504	DA	21.8 (0.1)	17.66	17.4	17.39	17.492	17.605	17.72	17.13	···	···
J1421−0046	3653562656746977792	DA	10.2 (0.1)	18.03	17.603	17.601	17.673	17.776	17.84	17.2	17.1	17.1
J1422+0459	3669573053580577536	DC	18.4 (0.3)	21.0	19.34	18.58	18.29	18.2	18.14	17.15	17.1	17.02
J1422+3056	1285142833024133760	DA	16.2 (0.1)	17.43	17.09	17.11	17.186	17.305	17.4	16.8	···	···
J1423+3037	1284932139108595712	DA	14.6 (0.1)	19.43	18.08	17.573	17.372	17.307	17.28	16.43	16.2	15.7
J1423−1820	6284524274971664000	DA	11.4 (0.3)	19.25	18.7	18.591	18.61	18.68	18.7	···	···	···
J1424+0319	3668476222012308480	DA	15.1 (0.2)	18.51	17.99	17.85	17.807	17.87	17.88	17.14	16.99	17.1
J1424+1743	1238591671072637184	DC	10.3 (0.4)	20.4	19.5	19.2	19.13	19.1	19.18	18.4	···	···
J1424+2028	1240475993483896832	DA	10.4 (0.2)	18.38	18.0	17.93	17.97	18.07	18.11	···	···	···
J1424+2546	1256240383181740928	DA	13.2 (0.1)	18.12	17.48	17.281	17.22	17.24	17.04	16.49	···	···
J1424+4405	1492836834300292992	DC	16.5 (0.1)	18.03	17.5	17.34	17.32	17.38	17.46	16.82	···	···
J1424+6246	1666805889078252928	DA	20.5 (0.1)	20.4	18.73	18.13	17.888	17.78	17.76	···	···	···
J1425−0050	3652865390281317120	DZ	14.1 (0.2)	18.46	18.036	17.926	17.98	18.07	18.13	17.46	17.32	17.3
J1426+0937	1176378520034381952	DC	13.5 (0.4)	20.9	19.29	18.76	18.55	18.48	18.42	17.62	17.36	17.17
J1426+4455	1494432053873688448	DC :	12.5 (0.2)	19.34	18.69	18.45	18.37	18.42	18.5	17.8	···	···
J1426+4921	1507571286545131648	DC	29.5 (0.1)	17.57	16.961	16.755	16.726	16.773	16.826	16.1	15.9	···
J1427+0532	3669936102871625600	DC	23.9 (0.1)	17.59	17.02	16.866	16.845	16.9	16.94	16.24	16.13	15.98
J1427+4126	1491559506730816384	DC	10.8 (0.3)	20.13	19.46	19.26	19.2	19.24	19.27	18.5	···	···
J1427+4536	1494485758144731520	DC	23.4 (0.1)	17.29	16.83	16.718	16.74	16.844	16.91	16.26	16.3	17.2
J1427+6110	1666378698746614528	DQ	23.3 (0.1)	17.71	17.126	16.91	16.884	16.926	16.95	16.3	16.2	16.1
J1428+4403	1494157691363079168	DZ	22.3 (0.1)	17.93	17.01	16.876	16.954	17.068	17.15	16.51	16.0	16.0
J1428+4531	1494564162771398016	DC	11.1 (0.2)	20.4	19.35	19.04	18.93	18.95	18.87	18.1	···	···
J1429+0925	1176312965948448512	DC	13.0 (0.2)	19.15	18.52	18.33	18.294	18.34	18.39	17.69	17.6	17.4
J1430+0438	3669065354086975872	DA	16.3 (0.1)	17.55	17.149	17.062	17.086	17.16	17.24	16.58	16.42	16.43
J1430+2811	1280674894509973760	DAH	14.0 (0.1)	18.0	17.71	17.7	17.78	17.9	17.99	17.39	···	···
J1430−2403	6272326022391660928	DC	30.7 (0.1)	···	18.068	17.38	17.132	17.03	16.974	16.0	16.0	···
J1431+2921	1284194603029215104	DA	15.7 (0.2)	18.89	18.26	18.073	18.031	18.06	18.08	17.36	···	···
J1431+4848	1603370081109395200	DC	10.5 (0.3)	19.98	19.24	18.88	18.77	18.79	18.73	···	···	···
J1433+1026	1176494381072110848	DAH	15.8 (0.2)	18.86	18.21	18.036	17.98	18.01	18.02	17.32	17.25	17.2
J1433+1326	1179764607826002688	DA	18.9 (0.1)	16.61	16.254	16.34	16.466	16.633	16.76	16.18	16.14	16.19
J1433+1907	1239213243034520192	DA	20.2 (0.2)	20.4	18.67	18.09	17.85	17.79	17.77	16.9	16.07	15.33
J1433+3751	1487362258530962944	DA	10.2 (0.1)	17.76	17.379	17.46	17.61	17.77	17.9	17.37	···	···

Tableau A.1 *suite page suivante*

Tableau A.1 *(suite)*

Name	Gaia DR2/EDR3*	Sp Type	ϖ (mas)	u	g	r	i	z	y	J	H	K
J1435+5052	1604147165248626048	DA	12.9 (0.1)	17.36	16.911	16.955	17.063	17.21	17.31	16.7	···	···
J1436+0537	1171041215714699904	DC	17.6 (0.4)	22.0	20.09	19.33	18.86	18.58	18.47	17.62	17.66	17.49
J1436+2107	1241188721832696704	DC	16.1 (0.1)	17.56	17.3	17.28	17.373	17.478	17.57	16.97	···	···
J1436+4332	1493367245581725184	DC	36.9 (0.1)	19.89	17.89	17.167	16.875	16.78	16.74	15.78	15.62	15.51
J1436+4753	1591250718488330112	DA	16.8 (0.1)	17.79	17.41	17.367	17.41	17.49	17.56	···	···	···
J1436+5635	1610657197502002048	DA	10.1 (0.2)	19.27	18.68	18.48	18.434	18.47	18.46	17.7	···	···
J1437+2003	1240776435036602368	DC	13.0 (0.2)	18.36	17.977	17.89	17.938	18.03	18.09	17.4	···	···
J1437+4151	1492944375984949504	DC	18.0 (0.2)	20.12	18.95	18.45	18.24	18.167	18.16	17.43	17.76	18.4
J1440+0112	3654870693331906304	DC*	20.8 (0.4)	22.9	19.99	18.99	18.56	18.39	18.29	17.59	17.39	17.33
J1440+0310	3656509794586217984	DA*	13.5 (0.1)	18.54	17.69	17.38	17.25	17.24	17.23	16.41	16.2	16.11
J1440+0626	1171211743096194560	DA	17.8 (0.3)	19.41	18.83	18.63	18.6	18.63	18.69	18.1	17.7	17.9
J1440+0807	1172780578685760512	DA	23.6 (0.2)	19.22	17.942	17.499	17.306	17.262	17.23	16.5	15.9	16.3
J1440+0958	1174728432253334784	DQ	13.8 (0.1)	17.56	17.305	17.305	17.43	17.54	17.63	17.11	17.03	17.03
J1440+1318	1179626958418884864	DC	18.3 (0.2)	20.12	18.76	18.26	18.05	17.96	17.96	17.15	16.93	16.83
J1440−0232	3648790157806712448	DZ	10.0 (0.2)	19.2	18.64	18.51	18.51	18.58	18.63	18.0	17.9	···
J1441+0518	1159061967810978432	DA	10.9 (0.3)	19.69	18.95	18.75	18.69	18.7	18.7	18.02	17.8	17.9
J1441+0831	1172831907840206848	DZ	9.9 (0.4)	19.02	18.544	18.46	18.485	18.59	18.66	18.1	17.9	18.1
J1441+4511	1493934284343845504	DA	10.3 (0.1)	17.7	17.27	17.31	17.419	17.56	17.66	···	···	···
J1441+5322	1605951944865784960	DC	11.0 (0.2)	19.64	19.0	18.83	18.79	18.84	18.85	18.3	···	···
J1441+5639	1607738921843325440	DA	11.8 (0.1)	19.05	18.55	18.41	18.41	18.48	18.51	17.85	···	···
J1441+5816	1616879612977156352	DA	15.5 (0.1)	18.67	18.0	17.784	17.718	17.75	17.74	16.99	···	···
J1441+6228	1618920714579089280	DA	12.1 (0.1)	18.64	18.105	17.95	17.92	17.96	18.06	···	···	···
J1442+0027	3651747667992161920	DAH :*	12.1 (0.2)	18.44	18.04	17.97	18.015	18.09	18.17	17.55	17.5	17.4
J1442+0635	1171581179003421312	DZ :	14.7 (0.2)	18.97	18.33	18.07	17.98	17.95	18.01	17.21	17.0	17.0
J1442+4013	1488064949540111104	DQP	12.5 (0.2)	20.3	19.45	18.8	18.653	18.64	18.67	18.15	18.24	18.2
J1442+5546	1607546129351189888	DA	15.0 (0.2)	20.8	19.4	18.89	18.68	18.6	18.58	17.76	17.52	17.4
J1442−1947	6281523986913711872	DC :	24.2 (0.2)	···	18.47	17.96	17.72	17.66	17.63	16.8	···	16.6
J1443−1437	6310804634396281984	DA	34.9 (0.1)	···	16.44	16.23	16.168	16.193	16.217	15.5	15.4	15.5
J1444+1048	1175242896321238400	DC	14.8 (0.3)	19.14	18.4	18.15	18.07	18.1	18.1	17.43	17.26	17.3
J1444+1848	1237419351158798336	DA	11.6 (0.2)	18.82	18.245	18.08	18.07	18.11	18.15	17.44	···	···
J1444+3759	1486801267085903488	DC	10.8 (0.3)	20.43	19.43	19.11	19.03	19.03	18.99	18.4	···	···
J1444+4717	1590192369827025152	DA	13.6 (0.05)	16.89	16.472	16.549	16.683	16.823	16.94	16.5	15.9	15.6
J1444−0052	3651305423799211008	DA	11.1 (0.4)	19.16	18.55	18.38	18.343	18.41	18.42	17.74	17.5	17.5
J1445+2921	1282448170543051520	DA	26.0 (0.1)	19.22	17.804	17.33	17.156	17.1	17.08	16.3	15.9	···

Tableau A.1 *suite page suivante*

Tableau A.1 *(suite)*

Name	Gaia DR2/EDR3*	Sp Type	ϖ (mas)	u	g	r	i	z	y	J	H	K
J1445−0208	3648744214542134912	DZ	11.4 (0.2)	19.43	18.75	18.58	18.59	18.65	18.73	18.0	18.1	17.8
J1446+2130	1238445745263425536	DA	13.6 (0.2)	19.89	18.87	18.48	18.34	18.27	18.32	17.53	···	···
J1446+2512	1267289165075531008	DC	10.7 (0.2)	19.93	19.2	18.9	18.83	18.76	18.83	18.1	···	···
J1446+2825	1281584774741482880	DC	10.9 (0.2)	18.67	18.33	18.25	18.34	18.42	18.54	18.0	···	···
J1447+2014	1238026522095817728	DA	10.4 (0.3)	20.32	19.51	19.17	19.05	19.02	19.0	18.2	···	···
J1447+5427	1606475479904001792	DC	12.9 (0.2)	21.3	19.31	18.62	18.32	18.24	18.19	17.3	17.2	17.1
J1447−1742	6282457918962299776	DC	75.2 (0.1)	···	16.76	16.13	15.874	15.786	15.71	14.98	14.84	14.65
J1447−3035	6217739938701063808	DA	17.9 (0.1)	···	17.41	17.24	17.22	17.26	17.264	16.6	16.3	···
J1448+0157	3652390092020688128	DA	16.0 (0.2)	18.23	17.65	17.47	17.439	17.48	17.5	16.79	16.66	16.6
J1448+1047	1175204104176381696	DZ	11.3 (0.3)	20.18	18.77	18.62	18.68	18.76	18.88	18.16	18.2	18.0
J1448+1456	1186165582270482688	DA	10.7 (0.2)	19.15	18.51	18.34	18.28	18.31	18.32	···	···	···
J1448−0047	3650615686411758080	DQ	11.2 (0.3)	18.82	18.42	18.281	18.322	18.37	18.4	17.68	17.7	17.6
J1448−0232	6338811188419479040	DA	12.6 (0.1)	17.38	16.985	17.014	17.112	17.242	17.335	16.75	16.72	16.6
J1449+1030	1174996090320432000	DA	12.6 (0.3)	18.97	18.517	18.391	18.4	18.45	18.48	17.81	17.7	17.7
J1449+2054	1238352149340737536	DAH :	13.2 (0.3)	20.5	19.42	19.0	18.83	18.78	18.82	17.95	···	···
J1450+0742	1173230210222240640	DA	10.9 (0.2)	18.64	18.25	18.17	18.21	18.29	18.41	17.68	17.6	17.6
J1450+2403	1265985590961480192	DC*	14.8 (0.2)	18.7	18.202	18.05	18.05	18.11	18.16	17.55	···	···
J1450+5753	1613862480054872320	DA	14.5 (0.1)	18.56	18.01	17.85	17.816	17.85	17.89	17.17	···	···
J1450−1454	6310405202436481024	DA :*	24.4 (0.1)	···	16.357	16.242	16.249	16.312	16.23	15.5	15.8	···
J1450−1914	6281218357040987136	DA	20.5 (0.1)	···	15.873	15.75	15.74	15.786	15.827	15.068	14.9	14.89
J1451+0243	1154456216681249536	DA	13.4 (0.3)	18.48	18.09	18.09	18.11	18.21	18.27	17.6	17.5	17.5
J1451+4221	1489418418289775616	DA	16.52 (0.04)	16.63	16.221	16.25	16.376	16.52	16.58	16.03	···	···
J1452+4049	1488715482466110080	DC	13.8 (0.3)	21.9	19.9	19.22	18.95	18.86	18.76	17.9	···	···
J1452+4522	1586838374030594048	DC	10.7 (0.3)	21.6	19.88	19.33	19.3	19.34	19.4	18.6	18.43	18.37
J1452+4746	1590462948470580480	DA	10.9 (0.3)	20.18	19.4	19.084	18.96	18.98	18.97	18.2	···	···
J1452−0011	3651028381228835456	DA	22.7 (0.2)	19.89	18.36	17.81	17.595	17.51	17.51	16.67	16.4	16.32
J1452−0051	3650426742210702976	DC :	14.4 (0.3)	20.5	19.25	18.78	18.59	18.53	18.53	17.66	17.48	17.42
J1453+0925	1174070610767977728	DA	12.4 (0.2)	18.04	17.74	17.826	17.985	18.15	18.25	17.69	17.6	17.7
J1453+3244	1289485349902909440	DC	17.4 (0.2)	20.9	19.21	18.59	18.342	18.26	18.24	17.43	17.2	17.0
J1453+4225	1489504004102020864	DA	13.6 (0.2)	20.17	19.12	18.75	18.6	18.56	18.57	17.83	···	···
J1454+0603	1160054281350128384	DA	19.1 (0.2)	18.9	18.23	18.03	17.95	17.97	17.99	17.28	17.1	17.1
J1454+1253	1181607110141081984	DA	11.1 (0.4)	20.6	19.51	19.08	18.94	18.88	18.91	18.07	17.7	17.9
J1454+4406	1586427298416103296	DA	11.7 (0.1)	18.31	17.855	17.76	17.778	17.87	17.9	17.18	···	···
J1454−0110	3650730589671206528	DC	16.7 (0.6)	21.9	19.89	19.164	18.81	18.69	18.65	17.76	17.64	17.49

Tableau A.1 *suite page suivante*

Tableau A.1 *(suite)*

Name	Gaia DR2/EDR3*	Sp Type	ϖ (mas)	u	g	r	i	z	y	J	H	K
J1455+0141	1154089117236952960	DC	12.3 (0.2)	19.29	18.66	18.442	18.41	18.45	18.43	17.71	17.6	17.6
J1455+3725	1295170344710806400	DA	13.0 (0.1)	18.08	17.62	17.547	17.58	17.657	17.72	17.06	···	···
J1457+2107	1261421999231535616	DQ	12.0 (0.3)	19.68	19.08	18.68	18.58	18.56	18.57	17.87	···	···
J1457+2827	1269774649765271552	DA	10.2 (0.1)	17.94	17.524	17.57	17.67	17.79	17.92	···	···	···
J1457+2952	1282030970304135296	DA	15.6 (0.2)	20.9	18.92	18.43	18.27	18.22	18.13	17.38	···	···
J1457+3331	1289812355829447040	DC	11.1 (0.1)	17.71	17.49	17.532	17.659	17.8	17.92	17.35	17.38	17.3
J1458+0605	1160021841461912448	DA	10.6 (0.6)	19.71	19.11	18.91	18.85	18.85	18.91	18.17	17.9	18.1
J1458+1146	1181245508254835584	DC	14.6 (0.4)	20.7	18.74	18.01	17.711	17.61	17.58	16.63	16.47	16.3
J1458+2937	1281989124439286912	DAZ	35.01 (0.03)	16.16	15.669	15.538	15.549	15.608	15.654	14.93	14.6	14.7
J1458+3416	1290050262657404544	DC*	12.1 (0.2)	19.26	18.63	18.484	18.492	18.54	18.58	18.1	···	···
J1459+0851	1161820298887863424	DA	13.8 (0.3)	21.0	19.44	18.98	18.78	18.73	18.66	17.91	17.65	17.6
J1500+0512	1159705388271330176	DA	11.3 (0.6)	20.3	19.24	18.9	18.8	18.75	18.65	18.09	17.9	17.5
J1500+3600	1294793345366747776	DC :	12.8 (0.2)	21.6	19.72	19.05	18.69	18.65	18.65	17.8	···	···
J1501+0719	1160623343042019968	DA	11.0 (0.5)	19.6	19.01	18.81	18.77	18.79	18.82	18.09	17.9	18.2
J1501+2100	1261253842671908096	DQ	10.8 (0.2)	19.17	18.667	18.18	18.03	18.04	18.06	17.34	···	···
J1501+6138	1619166249269416832	DA	14.2 (0.1)	18.83	17.79	17.39	17.24	17.2	17.2	16.29	16.05	16.13
J1502+0920	1167866620703225984	DA	11.4 (0.3)	19.64	19.03	18.83	18.79	18.8	18.83	···	18.1	17.9
J1502+4933	1592242645479324288	DZ	10.9 (0.2)	19.51	18.67	18.55	18.59	18.68	18.74	18.1	···	···
J1503+2956	1275981324189764608	DC	11.9 (0.1)	18.34	17.84	17.72	17.731	17.8	17.86	17.22	···	···
J1504+0750	1160759923002231936	DA	11.7 (0.3)	19.4	18.7	18.49	18.45	18.45	18.45	17.69	17.62	17.6
J1504+2302	1262123144052263040	DC	12.5 (0.2)	19.53	18.85	18.61	18.57	18.57	18.6	17.95	···	···
J1505+3259	1289020673097509760	DA	12.3 (0.1)	17.13	16.795	16.828	16.917	16.951	16.87	15.726	15.3	14.8
J1505−0714	6332763530870415488	DAH	37.0 (0.1)	···	16.003	15.795	15.735	15.755	15.782	15.041	14.9	14.84
J1506+0151	1153544794556784384	DC	11.2 (0.3)	19.96	19.2	18.88	18.78	18.79	18.78	18.08	17.9	17.8
J1506+0638	1160300056558791168	DA	10.0 (0.1)	17.07	16.58	16.65	16.78	16.93	17.03	16.45	16.38	16.36
J1506+2934	1275760219272654080	DA	10.6 (0.1)	18.03	17.58	17.55	17.615	17.712	17.78	17.15	···	···
J1506+4152	1392973720770987392	DZ	10.5 (0.1)	17.76	17.6	17.653	17.802	17.95	18.05	17.46	···	···
J1507+3218	1288658006059681408	DA	10.5 (0.3)	19.56	19.18	19.136	19.18	19.25	19.29	18.79	18.3	18.5
J1508+0135	4420124124769394176	DA*	13.6 (0.2)	18.26	17.97	17.961	18.037	18.13	18.22	17.6	17.6	17.7
J1508+1826	1211862818279517824	DC	15.0 (0.4)	21.0	19.41	18.843	18.628	18.55	18.52	···	···	···
J1509+5020	1592629707931918720	DC	12.1 (0.2)	19.34	18.67	18.45	18.41	18.44	18.5	17.79	···	···
J1509+6332	1620030637207462912	DA	28.66 (0.03)	···	14.713	14.813	14.972	15.14	15.264	14.72	14.6	14.82
J1510+0627	1157317008497672320	DC	10.4 (0.3)	20.12	19.4	19.11	19.0	19.0	19.1	···	···	···
J1510+1248	1182318120502368256	DA	11.4 (0.5)	19.97	19.17	18.85	18.73	18.74	18.73	18.0	···	···

Tableau A.1 *suite page suivante*

Tableau A.1 *(suite)*

Name	Gaia DR2/EDR3*	Sp Type	ϖ (mas)	u	g	r	i	z	y	J	H	K
J1510+1453	1183956427187401344	DA	20.2 (0.1)	17.76	17.332	17.251	17.278	17.357	17.41	16.72	···	···
J1510−1045	6318882711964895872	DA	16.8 (0.1)	15.85	15.4	15.499	15.638	15.784	15.905	15.32	15.29	15.31
J1511+4048	1392065975139109504	DA	18.17 (0.04)	16.16	15.754	15.713	15.774	15.856	15.93	15.26	15.1	14.8
J1511+5624	1600882264252963072	DA	17.4 (0.1)	16.71	16.32	16.328	16.429	16.555	16.643	16.05	15.7	15.9
J1512−0946	6319467136754514176	DA	16.1 (0.1)	16.53	16.13	16.209	16.332	16.49	16.581	16.06	15.95	15.84
J1513+2359	1263732043096088320	DC	11.3 (0.8)	24.1	20.83	20.0	19.62	19.51	19.44	18.6	···	···
J1513+3022	1275492999287723392	DA	17.1 (0.1)	19.28	18.54	18.3	18.232	18.245	18.31	17.55	17.34	17.2
J1514+0157	4421694158655153664	DA	16.8 (0.1)	17.3	16.666	16.737	16.866	17.0	16.94	16.52	16.45	16.36
J1514+1941	1212425463290645504	DA	10.9 (0.1)	17.77	17.406	17.426	17.517	17.64	17.67	17.2	···	···
J1515+3707	1292166062330701056	DC	10.4 (0.2)	20.12	19.36	19.08	18.974	18.99	18.97	18.3	···	···
J1515+6642	1645204475617697536	DA	26.23 (0.03)	15.81	15.431	15.514	15.645	15.81	15.94	15.3	15.2	15.2
J1515+8230	1722236328978172928	DZH	26.1 (0.1)	···	18.9	18.12	17.75	17.67	17.57	···	···	···
J1516+0647	1163166719594895872	DA	14.1 (0.3)	19.46	18.8	18.56	18.517	18.52	18.53	17.83	17.6	17.7
J1516+2316	1215408610135114112	DA	10.4 (0.1)	18.57	17.97	17.795	17.751	17.79	17.82	17.08	···	···
J1516+2803	1271649969930799872	DAH	21.2 (0.1)	17.02	16.597	16.527	16.55	16.64	16.74	16.07	16.3	15.7
J1517+2256	1215384313505335424	DQ	12.6 (0.1)	18.18	17.86	17.798	17.843	17.932	18.01	···	···	···
J1518+0506	1156006287558141056	DZ	14.5 (0.5)	22.0	19.37	18.87	18.79	18.77	18.83	18.1	17.9	17.9
J1519+1239	1170279945646967424	DA	11.3 (0.2)	17.61	17.19	17.208	17.32	17.433	17.53	16.94	16.5	16.4
J1519+3214	1278042010837800192	DA	10.8 (0.1)	18.68	18.352	18.38	18.45	18.58	18.7	18.0	···	···
J1520+3355	1278756555956826624	DA	13.4 (0.2)	19.83	19.06	18.75	18.66	18.69	18.7	···	···	···
J1520+3903	1388493176528426752	DA	10.6 (0.1)	17.44	17.018	16.956	17.004	17.08	17.15	16.47	16.52	15.83
J1520−0238	4414809875835433216	DA	9.9 (0.1)	17.6	17.168	17.273	17.429	17.6	17.72	17.19	17.1	17.1
J1521+0748	1163714413825307776	DC	9.8 (0.6)	22.7	20.57	19.83	19.56	19.46	19.37	···	···	···
J1521+1358	1170894503927889024	DC	13.1 (0.1)	16.87	16.695	16.787	16.94	17.109	17.24	16.6	16.76	16.19
J1522+2535	1270140821499608832	DC	10.4 (0.1)	17.77	17.56	17.606	17.726	17.88	17.99	17.5	···	···
J1522−0206	4415230812694612864	DA	9.8 (0.3)	19.34	18.81	18.72	18.7	18.75	18.75	18.2	18.1	17.8
J1523+1607	1207403993686544256	DA	14.1 (0.2)	19.08	18.344	18.068	17.97	17.964	17.98	···	···	···
J1525+5629	1602197696772907648	DA*	30.9 (0.1)	18.38	17.18	16.72	16.555	16.504	16.49	15.66	15.2	15.1
J1525−0421	4401558183740868480	DA	13.4 (0.1)	···	16.48	16.584	16.72	16.89	16.99	16.37	16.5	16.4
J1526+2936	1273685372108354176	DA	43.1 (0.1)	18.63	17.032	16.468	16.24	16.156	16.144	15.245	14.99	14.92
J1527+2442	1222024990079978368	DA	13.9 (0.1)	18.06	17.713	17.725	17.807	17.91	18.01	17.37	···	···
J1528+3254	1277756687570196096	DC	16.2 (0.2)	20.7	19.21	18.67	18.46	18.38	18.3	17.53	17.3	17.17
J1529+1304	1193808772927091712	DA	15.3 (0.1)	17.07	16.898	16.963	17.104	17.24	17.35	16.78	16.4	16.1
J1529−0038	4416948833973175168	DA	13.0 (0.3)	19.55	19.0	18.83	18.79	18.85	18.91	18.0	18.1	17.9

Tableau A.1 *suite page suivante*

Tableau A.1 *(suite)*

Name	Gaia DR2/EDR3*	Sp Type	ϖ (mas)	u	g	r	i	z	y	J	H	K
J1530+0235	4421098773108860928	DA	18.6 (0.1)	17.3	16.84	16.751	16.756	16.812	16.88	16.22	16.03	16.06
J1530+0630	1162536355835288320	DC	14.7 (0.3)	18.94	18.46	18.38	18.396	18.46	18.5	17.99	17.8	18.0
J1530+4650	1395759333479862016	DA	10.5 (0.1)	19.27	18.62	18.4	18.31	18.36	18.38	17.71	···	···
J1531+2514	1222254066452610176	DC	15.0 (0.2)	19.37	18.67	18.446	18.39	18.43	18.48	···	···	···
J1531+4240	1391331222197901696	DZ	11.5 (0.1)	18.75	18.21	18.12	18.174	18.27	18.36	17.66	···	···
J1531+4421	1394479501945576064	DC*	11.1 (0.4)	21.6	20.36	19.82	19.81	20.1	19.9	···	···	···
J1532+1356	1193974077628437760	DA+DQ	14.3 (0.2)	16.87	16.6	16.579	16.653	16.752	16.82	16.12	15.92	16.44
J1533+0717	1164185283975493120	DA	11.1 (0.1)	17.18	16.71	16.82	16.974	17.135	17.27	16.73	16.65	16.76
J1533+2109	1211355290583415168	DA	11.2 (0.2)	19.83	18.81	18.64	18.46	18.48	18.23	18.2	···	···
J1534+0037	4417527967363383680	DA	12.7 (0.2)	17.87	17.48	17.453	17.48	17.61	17.67	17.03	16.91	16.92
J1534+0218	4424031479858305408	DA	29.6 (0.1)	16.66	16.307	16.277	16.334	16.4	16.48	15.83	15.76	15.76
J1534+0711	4430709068108076544	DA	17.0 (0.2)	20.6	19.06	18.503	18.287	18.2	18.16	17.44	17.09	17.06
J1534+1010	1165926910393567872	DA	12.7 (0.2)	18.49	17.929	17.773	17.76	17.77	17.81	17.14	16.96	16.9
J1534+1010	1165926910393568384	DA	12.8 (0.2)	19.02	18.36	18.1	18.05	18.04	18.06	···	···	···
J1534+4146	1390295486540598656	DQZ	15.2 (0.1)	17.51	17.23	17.187	17.294	17.396	17.5	16.93	···	···
J1534+4649	1401010605309570816	DC	32.4 (0.1)	21.0	18.61	17.74	17.376	17.23	17.21	16.17	16.12	16.04
J1534+5624	1601489813146914176	DC	10.7 (0.5)	21.7	20.22	19.57	19.37	19.32	19.26	···	···	···
J1535+1115	1166330259362301440	DC	24.1 (0.1)	15.554	15.47	15.557	15.726	15.9	16.017	15.4	15.5	15.8
J1535+1247	1193520666521113344	DZP	51.9 (0.1)	18.02	15.93	15.509	15.466	15.54	15.55	14.857	14.73	14.7
J1535+1645	1197139189352207232	DC	15.6 (0.3)	21.0	19.33	18.786	18.55	18.45	18.47	···	···	···
J1535+2125	1211378350265079808	DA	21.4 (0.1)	18.25	17.502	17.235	17.14	17.139	17.17	16.38	16.1	16.98
J1536+1717	1197240000824171648	DA	11.5 (0.3)	20.33	19.34	18.93	18.75	18.72	18.7	···	···	···
J1536+3626	1374676889508967680	DC	13.4 (0.1)	19.03	18.42	18.19	18.15	18.2	18.28	17.55	···	···
J1536+5013	1402721307964211072	DA	14.59 (0.03)	16.28	15.849	15.856	15.934	16.039	16.14	15.52	15.3	15.1
J1537+1041	1166063073741131520	DA	11.3 (0.7)	20.7	19.63	19.21	19.05	18.994	19.0	18.3	···	···
J1537+6501	1641386833807056640	DA	34.63 (0.02)	15.26	14.65	14.702	14.828	14.962	15.074	14.46	14.45	14.5
J1537−0030	4416438420059253248	DC	9.8 (0.3)	19.87	19.21	19.0	18.95	18.96	18.97	18.34	18.24	17.9
J1538+0206	4423790579436883072	DA	11.5 (0.5)	20.37	19.43	19.11	18.97	18.91	18.98	18.09	18.1	17.9
J1538+0842	1164767677244452096	DAH	12.1 (0.2)	18.24	17.9	17.937	18.04	18.15	18.16	17.58	17.56	17.47
J1538+5211	1596812426258489600	DA	14.6 (0.1)	17.38	16.981	16.952	17.011	17.104	17.15	16.46	···	···
J1539+0153	4423768662219609088	DA	11.3 (0.1)	17.85	17.45	17.46	17.518	17.63	17.72	17.06	16.92	16.9
J1539+5241	1596840493868996864	DA	11.4 (0.2)	20.11	19.27	18.97	18.87	18.85	18.9	···	···	···
J1539+5811	1602106536090424832	DA	14.0 (0.1)	18.48	17.86	17.682	17.652	17.7	17.75	17.03	17.6	15.7
J1540+3308	1370654257498865536	DA	33.84 (0.03)	15.509	15.15	15.13	15.189	15.312	15.41	14.759	14.7	14.5

Tableau A.1 *suite page suivante*

Tableau A.1 *(suite)*

Name	Gaia DR2/EDR3*	Sp Type	ϖ (mas)	u	g	r	i	z	y	J	H	K
J1541+2053	1216353051968362112	DA	12.1 (0.2)	20.0	19.19	18.9	18.789	18.77	18.78	18.2	···	···
J1541+2557	1223091649497003264	DA	10.5 (0.3)	19.69	19.185	19.01	18.96	18.99	19.06	18.4	···	···
J1542+0153	4423803223819720704	DA	11.8 (0.2)	19.32	18.73	18.517	18.459	18.47	18.52	17.9	17.6	17.5
J1542+2329	1218051664291152000	DA	36.0 (0.1)	17.9	16.95	16.598	16.456	16.426	16.42	15.64	15.5	15.8
J1542+4614	1397791368407211264	DA	11.9 (0.1)	18.95	18.39	18.2	18.18	18.21	18.24	17.5	···	···
J1542+7247	1696660893947352704	DC	13.6 (0.1)	···	18.38	18.11	18.02	18.03	17.85	···	···	···
J1542−0341	4402583302239225600	DA	18.6 (0.5)	···	15.19	15.279	15.414	15.58	15.67	15.055	15.0	15.04
J1542−1356	6265350823707860480	DC	15.2 (0.2)	···	19.03	18.52	18.31	18.29	18.21	···	···	···
J1544+2548	1222865601075380480	DC	12.9 (0.2)	19.23	18.6	18.383	18.34	18.35	18.35	17.76	···	···
J1545+6021	1627064973301021056	DA	16.0 (0.1)	18.76	17.96	17.688	17.629	17.63	17.64	···	···	···
J1546+0458	4426297740826647680	DA	10.5 (0.4)	20.33	19.49	19.19	19.09	19.09	19.0	···	···	···
J1546+2437	1219722127394433920	DAH	13.6 (0.2)	19.44	18.75	18.49	18.401	18.4	18.44	···	···	···
J1546+4548	1397898124114691456	DA	10.3 (0.2)	20.11	19.242	18.98	18.82	18.84	18.9	18.1	···	···
J1546+4911	1401717243394126464	DA	13.4 (0.1)	18.95	18.29	18.08	18.02	18.02	18.06	17.28	···	···
J1547+0659	4430165650933432576	DZ	11.4 (0.1)	17.74	17.45	17.497	17.647	17.78	17.93	17.36	17.3	17.3
J1547+5426	1597468108851256192	DC	10.4 (0.3)	20.5	19.59	19.29	19.19	19.2	19.21	···	···	···
J1548+5708	1598771000065137536	DC	26.4 (0.1)	18.55	17.68	17.35	17.208	17.19	17.21	16.44	16.2	···
J1549+2009	1204095391402194944	DA	11.6 (0.1)	17.67	17.235	17.262	17.346	17.46	17.51	16.95	16.3	···
J1549+4802	1401366366041668224	DC	23.8 (0.1)	18.0	17.38	17.167	17.114	17.139	17.18	16.44	15.85	16.75
J1549−0149	4403335028894782464	DC	11.2 (0.2)	19.17	18.633	18.478	18.468	18.49	18.56	17.81	17.6	18.0
J1550+0838	4455205894384768256	DA	12.5 (0.2)	19.72	19.02	18.75	18.65	18.67	18.72	17.93	17.7	17.8
J1550+2200	1216863676336891520	DA	14.5 (0.1)	17.01	16.634	16.738	16.889	17.06	17.175	16.7	16.3	···
J1551+0824	4454432667131057792	DQ	13.9 (0.1)	18.5	18.03	17.877	17.883	17.944	17.98	17.37	17.2	17.2
J1551+1439	1192571822348252160	DZA	9.8 (0.2)	17.82	17.69	17.786	17.911	18.07	18.17	17.67	···	17.9
J1551+3222	1369772925913456768	DA	11.7 (0.1)	17.93	17.484	17.472	17.526	17.638	17.69	17.07	···	···
J1551+6227	1639910911246160896	DQ	18.0 (0.1)	17.14	16.84	16.816	16.9	17.018	17.1	16.4	···	15.4
J1551−1638	6261001052630781312	DA	10.7 (0.1)	17.85	17.36	17.287	17.323	17.41	17.44	16.8	···	16.63
J1552+1852	1203637376090060928	DA	14.7 (0.1)	16.99	16.53	16.451	16.471	16.533	16.59	15.92	15.7	15.4
J1552+3419	1371714251131163264	DC	10.8 (0.1)	18.85	18.38	18.3	18.34	18.43	18.52	18.0	···	···
J1552+4638	1398051402907424512	DA	10.9 (0.3)	21.6	20.05	19.48	19.275	19.19	19.18	18.3	···	···
J1552−0219	4403059253334693248	DZ	10.6 (0.2)	18.45	18.063	18.024	18.115	18.24	18.34	17.76	···	···
J1553−0114	4409340076070042496	DA	11.0 (0.2)	18.6	18.102	17.996	18.01	18.07	18.09	17.38	17.26	17.2
J1554+0336	4425127624234553984	DQ	9.8 (0.3)	19.43	18.86	18.68	18.66	18.69	18.73	18.1	···	···
J1554+0401	4425202936481819520	DA	10.4 (0.3)	19.48	18.99	18.84	18.83	18.88	18.9	18.2	···	···

Tableau A.1 *suite page suivante*

Tableau A.1 *(suite)*

Name	Gaia DR2/EDR3*	Sp Type	ϖ (mas)	u	g	r	i	z	y	J	H	K
J1554+1408	1192479390353665280	DA	12.1 (0.1)	17.78	17.351	17.334	17.39	17.5	17.55	16.9	···	···
J1554+1735	1202552914026910976	DZ	17.7 (0.1)	18.75	17.58	17.432	17.5	17.62	17.69	17.06	···	···
J1554+2657	1223443630657641728	DA	10.3 (0.3)	21.9	20.15	19.59	19.34	19.3	19.25	18.56	18.2	18.0
J1554+5730	1622769245794819968	DA	10.8 (0.2)	19.28	18.67	18.43	18.378	18.4	18.42	17.77	···	···
J1554+6145	1627811571760152960	DA	10.2 (0.3)	20.9	19.88	19.61	19.48	19.53	19.5	···	···	···
J1555+0647	4427021425634792832	DA	16.3 (0.3)	20.02	18.93	18.535	18.36	18.33	18.35	17.52	17.26	17.2
J1555+3153	1321738565727229184	DA	16.6 (0.1)	18.37	17.726	17.5	17.442	17.47	17.49	16.75	···	···
J1555+5025	1403348682426861568	DA	32.7 (0.05)	17.55	16.721	16.423	16.303	16.299	16.317	15.55	15.0	15.0
J1556+1153	4456309700985355264	DC	13.2 (0.5)	21.79	19.97	19.32	19.03	18.95	18.85	···	···	···
J1556+3810	1373569711363357056	DC	16.4 (0.1)	18.94	18.207	17.93	17.87	17.87	17.93	17.24	···	···
J1557+0746	4454109681291473536	DA	11.8 (0.2)	19.01	18.36	18.17	18.131	18.163	18.23	17.46	17.37	17.2
J1557+0953	4455760769799431040	DC	10.8 (0.3)	20.03	19.27	18.97	18.87	18.9	18.91	18.2	···	···
J1557+1108	4456018914514270592	DC	11.9 (0.2)	19.03	18.533	18.409	18.408	18.46	18.53	···	···	···
J1557+1412	1191742717564070528	DC	22.2 (0.2)	21.1	19.0	18.29	17.981	17.857	17.8	16.92	···	···
J1558+0417	4425632987265111680	DC	44.5 (0.1)	16.85	16.224	15.99	15.991	16.07	16.21	15.48	15.3	14.8
J1558+0736	4451097882722882432	DA	12.2 (0.2)	19.76	18.9	18.614	18.536	18.53	18.55	···	···	···
J1558+0840	4454328930782860800	DA	11.1 (0.2)	18.86	18.31	18.13	18.114	18.12	18.19	17.46	···	···
J1558+2512	1219957873855946240	DZ	18.5 (0.1)	17.66	17.226	17.144	17.2	17.29	17.364	16.73	16.66	16.59
J1559+2529	1220062430539961344	DA	18.5 (0.1)	16.99	16.57	16.533	16.575	16.69	16.74	16.09	15.95	16.01
J1600+5038	1403545284553914880	DA	12.9 (0.2)	19.95	19.09	18.78	18.655	18.65	18.68	17.9	···	···
J1600−1654	6250213984568447872	DC	32.9 (0.2)	21.97	19.02	17.97	17.56	17.39	17.301	16.6	16.3	···
J1601+1334	1191779830379112192	DA	9.8 (0.2)	18.77	18.46	18.494	18.6	18.73	18.87	18.3	···	···
J1601+2735	1316607896578157824	DA	14.8 (0.1)	18.3	17.76	17.592	17.562	17.6	17.65	16.94	···	···
J1601+4120	1383292181587562496	DC	18.4 (0.2)	21.3	19.19	18.454	18.144	18.008	17.93	17.07	···	···
J1601+5317	1404831472640252928	DA	26.54 (0.04)	17.28	16.692	16.482	16.435	16.453	16.49	15.74	15.6	15.4
J1602+1630	1199192840852373376	DA	23.2 (0.1)	18.41	17.389	16.98	16.814	16.768	16.76	15.93	15.7	15.7
J1602+1858	1203132627235232256	DA	11.0 (0.4)	20.4	19.43	19.02	18.84	18.83	18.78	17.93	···	···
J1602+2336	1218800393053400576	DA	13.7 (0.2)	20.07	19.26	18.95	18.85	18.86	18.86	18.16	···	···
J1602+2644	1316238426312036096	DA	11.7 (0.1)	18.82	18.25	18.097	18.064	18.11	18.15	17.46	17.19	17.3
J1602+3323	1323407624377828224	DA	10.0 (0.1)	18.87	18.34	18.24	18.219	18.28	18.32	17.65	···	···
J1603+0808	4451552182885460480	DA	14.3 (0.1)	18.05	17.591	17.467	17.452	17.49	17.54	16.8	···	···
J1604+0055	4411572123331402880	DC	30.9 (0.1)	19.9	18.02	17.39	17.109	17.007	16.974	16.07	16.0	15.5
J1604+4908	1400157173832960384	DAH	11.6 (0.1)	18.21	17.91	17.93	18.01	18.126	18.24	17.59	···	···
J1604−0727	4349513797276615680	DC	37.1 (0.2)	···	18.64	17.81	17.67	17.555	17.34	16.32	16.18	16.1

Tableau A.1 *suite page suivante*

Tableau A.1 *(suite)*

Name	Gaia DR2/EDR3*	Sp Type	ϖ (mas)	u	g	r	i	z	y	J	H	K
J1604−1331	4341773063622911872	DA	26.6 (0.1)	···	18.005	17.4	17.15	17.068	17.04	16.2	15.8	···
J1605+5311	1428781653392160128	DA	10.0 (0.2)	19.54	18.9	18.67	18.609	18.61	18.61	17.81	···	···
J1605+5556	1621523537776065280	DA	11.1 (0.1)	18.33	17.74	17.554	17.505	17.55	17.58	16.81	···	16.62
J1605−0028	4406733207018066944	DA	14.4 (0.1)	17.03	16.65	16.683	16.795	16.91	17.026	16.37	16.37	16.28
J1606+0518	4449634256649531776	DC	10.1 (0.3)	19.67	19.1	18.9	18.863	18.89	18.92	18.21	···	···
J1606+2547	1315371255234720896	DA*	18.8 (0.2)	21.1	19.14	18.446	18.182	18.06	18.05	17.07	17.1	16.8
J1606+6733	1643544689800386176	DC*	14.6 (0.1)	···	17.02	17.11	17.248	17.38	17.5	···	···	···
J1606+7022	1647162396588999552	DA	27.86 (0.04)	···	16.83	16.596	16.516	16.53	16.57	15.8	15.6	···
J1607+1343	4458454611944673408	DA	12.9 (0.1)	18.06	17.83	17.811	17.893	18.0	18.1	17.57	···	···
J1607+3423	1323922779935068160	DA	29.1 (0.1)	18.61	17.4	16.964	16.796	16.746	16.74	15.9	15.7	15.6
J1607−0230	4405080812841630592	DA	12.8 (0.2)	18.33	17.84	17.733	17.726	17.77	17.83	17.15	···	17.0
J1607−1404	4341495230772911616	DAH	36.3 (0.1)	···	16.81	16.46	16.31	16.27	16.14	15.4	15.4	15.4
J1608+1723	1199686173677816576	DA	14.2 (0.2)	18.56	18.143	18.07	18.096	18.176	18.19	17.62	···	···
J1608+4235	1384938730313376512	DC	16.3 (0.2)	21.1	19.34	18.73	18.487	18.4	18.39	17.42	17.3	17.2
J1608+4256	1384982332821602560	DA	12.4 (0.1)	17.66	17.258	17.247	17.301	17.403	17.49	16.81	···	···
J1609+0655	4450425359563998720	DQ	11.7 (0.1)	18.04	17.74	17.71	17.813	17.93	18.03	17.45	···	···
J1609+1619	1198427031003111552	DA	15.4 (0.1)	18.12	17.628	17.473	17.461	17.51	17.57	16.81	···	···
J1609+2441	1303034120592956160	DA	17.0 (0.1)	18.92	18.386	18.24	18.196	18.23	18.29	17.55	17.4	17.5
J1609+5222	1427746463194276736	DAM	20.6 (0.1)	18.95	18.28	18.04	17.969	17.999	18.03	···	···	···
J1609−0031	4406683522836435968	DA	10.1 (0.2)	19.31	18.77	18.554	18.51	18.54	18.53	17.8	17.6	17.7
J1610+0619	4449818459207085696	DC*	11.8 (0.9)	21.8	20.55	20.24	20.57	20.98	0.0	···	···	···
J1610+1327	4458251064854338176	DAH	22.5 (0.1)	17.77	17.148	16.899	16.84	16.85	16.887	16.17	···	···
J1610−2513	6049555929998115072	DA	22.7 (0.1)	···	15.188	15.273	15.415	15.558	15.69	15.09	15.02	15.04
J1611+0451	4437515851806126208	DQ	14.8 (0.2)	19.44	18.64	18.27	18.16	18.12	18.18	17.47	···	···
J1611+1322	4458207634145130368	DA	44.85 (0.05)	15.364	15.13	15.168	15.253	15.377	15.474	14.886	14.8	14.9
J1611+6141	1628349890076998912	DA	14.39 (0.04)	16.69	16.285	16.4	16.542	16.725	16.83	16.2	16.2	···
J1613+4428	1385719147346936064	DA	33.1 (0.1)	24.6	17.4	16.873	16.59	16.54	16.23	···	···	···
J1614+0905	4452997701376633728	DC	35.8 (0.1)	19.69	17.837	17.145	16.85	16.753	16.72	15.9	15.8	15.4
J1614+1728	1198984345958836864	DQ	18.4 (0.1)	19.19	18.65	17.88	17.747	17.81	17.93	17.43	···	···
J1615+1503	4464661728744046848	DC	9.8 (0.2)	19.08	18.66	18.543	18.59	18.65	18.75	18.0	···	···
J1615+1819	1200578152485877376	DC	13.6 (0.2)	19.15	18.57	18.38	18.344	18.38	18.42	17.75	···	···
J1615+4449	1385742821206707456	DC	16.0 (0.3)	21.1	19.5	18.83	18.563	18.45	18.44	17.44	17.24	17.3
J1615+4602	1386704545987569280	DA :	12.8 (0.3)	21.7	19.79	19.23	18.88	18.79	18.53	···	···	···
J1616+3924	1380443823700583552	DQ	10.7 (0.1)	18.68	18.3	18.22	18.252	18.36	18.47	···	···	···

Tableau A.1 *suite page suivante*

Tableau A.1 *(suite)*

Name	Gaia DR2/EDR3*	Sp Type	ϖ (mas)	u	g	r	i	z	y	J	H	K
J1616+4600	1386691867244096000	DZ	12.0 (0.1)	19.45	18.72	18.51	18.49	18.54	18.52	17.93	···	···
J1616+6310	1629354495811136384	DA	12.3 (0.1)	18.93	18.444	18.35	18.36	18.41	18.5	···	···	···
J1618+0611	4438164190006954880	DQ	12.9 (0.2)	18.42	18.27	18.25	18.447	18.52	18.5	···	···	···
J1619−1831	6246049446837287680	DAH :*	25.9 (0.2)	···	18.413	17.97	17.798	17.75	17.77	···	···	···
J1620+0756	4451874958268328960	DA	12.0 (0.2)	19.57	18.79	18.53	18.433	18.42	18.43	17.62	···	···
J1620+1256	4463278336956814208	DA	13.1 (0.1)	18.57	18.21	18.12	18.16	18.25	18.28	···	···	···
J1620+1436	4464010508621809664	DA	13.4 (0.3)	21.0	19.65	19.08	18.83	18.7	18.49	···	···	···
J1620+1809	1200428928142394496	DQ	9.9 (0.2)	18.4	18.089	18.077	18.146	18.3	18.33	···	···	···
J1620+2044	1202123726533582848	DA	14.7 (0.2)	17.25	16.774	16.749	16.809	16.91	16.98	16.3	16.0	16.89
J1621+0552	4437908587914479360	DA	14.0 (0.2)	18.34	17.944	17.919	17.961	18.05	18.14	17.48	···	···
J1621−0552	4355229123137665792	DC	25.6 (0.2)	···	18.59	17.843	17.55	17.428	17.389	16.4	···	···
J1622+0532	4437884055061048064	DA	14.2 (0.1)	17.3	16.8559	16.73	16.735	16.77	16.83	15.92	15.85	15.22
J1622+0713	4439766762564880512	DA	10.8 (0.2)	18.24	17.82	17.8	17.877	17.98	18.0	···	···	···
J1622+1309	4463261431966304768	DC*	13.2 (0.4)	20.5	19.36	18.9	18.725	18.64	18.64	17.95	···	···
J1622+1822	1200416902234462464	DA	10.1 (0.3)	20.02	19.39	19.12	19.021	19.0	18.99	18.3	···	···
J1622+2651	1305209190813293440	DC	10.8 (0.2)	19.81	19.05	18.77	18.69	18.7	18.72	18.0	17.7	17.7
J1622+2919	1317956898562626176	DC	21.1 (0.2)	21.7	19.68	18.86	18.52	18.39	18.25	17.46	17.36	17.3
J1622+6701	1642588149044082688	DA	11.1 (0.1)	···	18.69	18.6	18.618	18.69	18.77	···	···	···
J1623+1336	4463651999111841024	DC	19.3 (0.2)	21.3	19.38	18.66	18.36	18.24	18.18	17.35	···	···
J1623+3340	1325705942981586176	DA	10.0 (0.2)	19.39	18.86	18.67	18.62	18.65	18.62	17.93	···	···
J1623+4650	1410031887762012800	DA	14.4 (0.1)	17.26	17.13	17.204	17.311	17.465	17.58	17.03	···	···
J1623+5642	1429800419634352000	DC	10.2 (0.3)	20.3	19.5	19.19	19.09	19.08	19.15	18.5	···	···
J1624+1347	4463664815294536192	DA	10.6 (0.2)	19.2	18.59	18.41	18.364	18.4	18.44	17.64	···	···
J1624+1448	4464073180784561408	DQ	10.4 (0.2)	20.2	19.36	19.03	18.92	18.94	18.94	18.3	···	···
J1624+2013	1201304517354978688	DC	14.3 (0.3)	20.6	19.45	18.97	18.782	18.72	18.74	···	···	···
J1625+1752	4466984859374027904	DC	11.6 (0.2)	19.79	19.03	18.78	18.72	18.73	18.72	18.1	···	···
J1625+2835	1305852233317101184	DA	10.0 (0.1)	18.49	17.95	17.83	17.811	17.84	17.91	17.19	16.98	17.0
J1625+3759	1332001785217988992	DA	14.3 (0.1)	18.88	18.5	18.39	18.05	18.2	18.31	17.6	···	···
J1626+0210	4432834444826809088	DC	20.0 (0.2)	···	18.11	17.53	17.28	17.1	16.93	15.6	···	···
J1626+0552	4438653541403499776	DAH	11.9 (0.1)	18.01	17.55	17.59	17.69	17.82	17.88	17.32	···	···
J1626+1355	4463681655863346816	DA	17.7 (0.1)	18.08	17.45	17.276	17.23	17.254	17.28	16.54	16.2	15.85
J1626+1938	1201036206454896000	DA	36.3 (0.1)	17.64	16.802	16.505	16.379	16.377	16.38	15.6	15.3	15.4
J1626+4738	1410897688745546752	DA	13.0 (0.1)	16.91	16.462	16.474	16.524	16.627	16.731	16.08	···	···
J1626+4918	1411292580922301312	DA	15.53 (0.04)	16.92	16.492	16.544	16.647	16.78	16.89	16.29	16.4	16.1

Tableau A.1 *suite page suivante*

Tableau A.1 *(suite)*

Name	Gaia DR2/EDR3*	Sp Type	ϖ (mas)	u	g	r	i	z	y	J	H	K
J1627+0028	4407614499946419200	DA	22.4 (0.1)	18.63	17.692	17.334	17.2	17.175	17.187	16.37	···	···
J1627+0912	4452521234885949184	DA	39.88 (0.05)	16.84	16.241	16.064	16.014	16.052	16.1	15.32	15.2	15.0
J1627+3726	1331208070965684224	DC	18.1 (0.2)	21.8	19.7	18.96	18.64	18.53	18.48	···	···	···
J1627+4859	1411226507145210624	DZA	16.5 (0.2)	20.9	19.14	18.622	18.41	18.35	18.35	17.48	17.18	17.16
J1628+2332	1299122058220640512	DAH	12.9 (0.1)	18.84	18.31	18.19	18.202	18.28	18.34	17.66	···	···
J1628+3646	1331106782752978688	DZA	62.91 (0.02)	14.219	13.85	13.907	14.004	14.13	14.25	13.662	13.65	13.58
J1628+7053	1653044367185115264	DA	30.4 (0.1)	···	18.1	17.49	17.22	17.14	17.08	16.1	15.8	15.63
J1628−1739	4323956302321933952	DA	30.9 (0.1)	···	17.92	17.269	17.0	16.9	16.87	16.1	15.8	15.7
J1629+0045	4431665212995124608	DA	11.3 (0.1)	17.95	17.62	17.674	17.79	17.93	18.03	17.49	···	···
J1629+2022	1297161594628972672	DA	10.5 (0.1)	17.49	17.07	17.155	17.302	17.47	17.54	17.01	···	···
J1629+5357	1425374610454574464	DA	12.7 (0.1)	18.3	17.917	17.938	18.013	18.14	18.27	···	···	···
J1631−0516	4352651700380171392	DA	11.6 (0.2)	19.3	18.66	18.429	18.351	18.34	18.34	···	···	···
J1632+0851	4440264291578812928	DA	77.35 (0.03)	16.4	15.316	14.903	14.72	14.689	14.672	13.85	13.61	13.49
J1632+2426	1300727345195414272	DC	23.8 (0.2)	21.3	19.5	18.74	18.51	18.49	18.51	17.67	18.1	18.04
J1633+5231	1424245175791207936	DA	19.1 (0.1)	18.14	17.475	17.25	17.171	17.184	17.22	16.44	16.2	15.7
J1633+5521	1430007784951049216	DC	12.0 (0.1)	18.44	17.982	17.92	17.996	18.11	18.17	17.55	···	···
J1634+0934	4446506356529203968	DA	12.1 (0.1)	18.77	18.09	17.898	17.836	17.86	17.91	17.15	···	···
J1634+1736	4466388790929771904	DAZ	39.05 (0.03)	14.37	13.4	13.47	14.2	13.528	13.654	13.05	12.99	13.08
J1634+3350	1325899461324069376	DC	17.9 (0.1)	17.51	17.135	17.063	17.103	17.199	17.25	16.4	···	···
J1634+5710	1431176943768691328	DQ	67.32 (0.02)	···	15.146	14.839	14.756	14.78	14.812	14.02	13.98	14.0
J1634+7558	1703379704562897280	DA	29.87 (0.03)	15.2	14.072	14.554	14.678	0.0	14.558	···	···	···
J1634−0901	4338593516506343424	DA	10.3 (0.1)	18.29	17.827	17.819	17.871	17.96	18.08	···	···	···
J1635+4317	1405343643196929536	DAZ	68.97 (0.02)	15.646	14.974	14.748	14.677	14.691	14.72	13.905	13.77	13.61
J1636+1255	4459666716138776576	DC	13.2 (0.3)	20.6	19.4	19.02	18.89	18.89	18.85	18.15	···	···
J1636+1619	4465939601772584448	DZ	14.5 (0.5)	24.7	20.39	19.53	19.3	19.22	19.1	···	···	···
J1636+2049	4564212061278453248	DA	9.8 (0.3)	19.51	19.02	18.89	18.9	18.96	19.01	18.4	···	···
J1637+0110	4384056565671592576	DA	14.9 (0.1)	18.22	17.682	17.53	17.498	17.531	17.58	16.86	···	···
J1637+1110	4447152865064276736	DA	15.0 (0.2)	20.19	18.91	18.44	18.256	18.2	18.18	17.41	···	···
J1637+1340	4461228611063376128	DAZ	21.9 (0.1)	17.61	16.97	16.84	16.7964	16.81	16.861	16.1	15.7	15.7
J1637+5133	1425397189098547200	DA	18.1 (0.1)	17.97	17.39	17.245	17.246	17.299	17.37	16.7	16.4	···
J1637−0204	4358066107952246784	DA	16.3 (0.1)	17.4	16.92	16.88	16.922	17.006	17.07	16.4	···	16.26
J1638+0540	4435778215414219520	DA	27.8 (0.1)	···	16.427	16.41	16.451	16.56	16.6373	15.96	15.9	···
J1638−2035	4130191322368475392	DA	23.2 (0.1)	···	15.94	15.922	15.997	16.08	16.19	15.6	15.4	15.8
J1639+1036	4447039585308297088	DAH	13.2 (0.2)	19.51	18.8	18.54	18.45	18.47	18.48	17.68	···	···

Tableau A.1 *suite page suivante*

Tableau A.1 *(suite)*

Name	Gaia DR2/EDR3*	Sp Type	ϖ (mas)	u	g	r	i	z	y	J	H	K
J1639+3325	1326398777041821568	DA	32.82 (0.03)	15.036	14.631	14.72	14.844	15.02	15.118	14.551	14.47	14.4
J1639+4030	1355979969155873792	DA	16.0 (0.1)	17.48	17.07	17.05	17.087	17.184	17.26	16.59	16.4	15.7
J1639+8038	1710386067532886272	DC	16.5 (0.1)	···	18.78	18.42	18.32	18.28	18.16	···	···	···
J1640+2229	1299314816353108992	DAZ	14.2 (0.1)	18.17	17.67	17.554	17.56	17.62	17.7	16.99	16.4	···
J1640+5341	1425909733315616000	DAH	49.65 (0.03)	15.55	15.124	15.002	15.041	15.119	15.19	14.526	14.48	14.4
J1640+7310	1654560662439820416	DQ	18.6 (0.1)	···	16.54	16.565	16.672	16.8	16.925	16.5	16.3	···
J1641+1512	4462612140287443840	DA	31.5 (0.1)	16.29	15.782	15.66	15.643	15.708	15.778	15.04	15.0	15.1
J1641+2543	1301111585855899136	DA	10.0 (0.2)	19.14	18.63	18.47	18.46	18.51	18.54	17.87	···	···
J1641+4833	1410448259071414528	DQ	10.9 (0.1)	18.42	18.11	18.05	18.127	18.23	18.36	17.72	···	···
J1643+1422	4461739604794187520	DZ	13.2 (0.2)	19.02	18.42	18.246	18.22	18.27	18.33	17.72	···	···
J1643+4438	1405848383457312512	DC	13.5 (0.3)	21.5	19.73	19.16	18.88	18.78	18.78	17.9	···	···
J1644+2253	1299436415467829888	DC	12.1 (0.1)	18.47	18.118	18.058	18.12	18.23	18.3	17.63	···	···
J1644+7628	1704918191912744192	DA	18.2 (0.1)	18.17	17.559	17.373	17.306	17.342	17.37	···	···	···
J1645+3059	1311660540930405632	DAZ	11.0 (0.1)	19.11	18.6	18.44	18.418	18.46	18.47	17.77	17.65	17.5
J1645+4958	1412228093519039744	DA	14.2 (0.1)	18.55	17.925	17.709	17.65	17.66	17.72	16.8	···	···
J1646+0303	4385909109622569088	DA	10.7 (0.1)	18.16	17.692	17.678	17.74	17.83	17.91	17.3	···	···
J1646+3246	1314253292427950720	DA	11.6 (0.2)	20.38	19.25	18.86	18.68	18.67	18.66	17.87	···	···
J1647+2636	1307226283551364224	DZ	19.8 (0.1)	17.51	17.016	16.92	16.985	17.092	17.177	16.57	···	···
J1647+3946	1352743419240352384	DC	11.4 (0.5)	24.4	21.29	20.31	19.9	19.74	19.6	18.8	···	···
J1648+3939	1352692734330406912	DC	10.5 (0.1)	20.22	18.8	18.33	18.137	18.1	18.06	17.19	17.3	17.6
J1649−2155	4126670518631322880	DA	27.5 (0.2)	···	18.091	17.51	17.28	17.27	17.55	16.4	15.8	···
J1650−1004	4334670557801027840	DA	11.7 (0.2)	18.33	17.87	17.805	17.8	17.87	17.73	···	···	···
J1651+4249	1356633384004567168	DZH*	11.4 (0.3)	22.3	19.68	19.17	19.04	19.16	19.15	···	···	···
J1651+6635	1636125872530936192	DZ	16.1 (0.1)	···	16.59	16.651	16.79	16.93	17.07	16.33	15.93	14.81
J1652+1324	4449419409503701376	DA	9.9 (0.4)	21.2	19.83	19.3	19.09	19.01	19.05	18.1	···	···
J1652+1346	4449495546386664832	DA	12.1 (0.3)	19.84	18.92	18.598	18.49	18.46	18.47	17.64	···	···
J1652−0114	4379328051494006784	DA	33.1 (0.1)	···	17.564	17.128	16.964	16.91	16.901	16.2	16.0	···
J1653+6253	1631578537252535040	DC	32.5 (0.1)	19.65	18.36	17.87	18.16	18.54	18.87	18.33	18.9	19.2
J1654+1243	4449057326579614592	DA	16.1 (0.2)	20.4	18.95	18.46	18.281	18.21	18.2	17.4	···	···
J1654+3157	1313265900922425856	DQ	15.8 (0.1)	17.89	17.524	17.421	17.464	17.538	17.63	16.94	···	···
J1654+3829	1351956512512484480	DAZ	36.6 (0.1)	17.97	16.93	16.587	16.433	16.401	16.42	15.59	15.4	15.3
J1654+5742	1436666805326235648	DA	17.5 (0.1)	···	16.062	16.085	16.177	16.285	16.4	15.73	16.0	15.2
J1655+1850	4559800992425812096	DA	11.1 (0.2)	19.56	18.81	18.56	18.46	18.45	18.47	17.69	···	···
J1656+4911	1409166984427845632	DC	11.2 (0.2)	20.3	19.3	19.02	18.96	18.98	18.9	···	···	···

Tableau A.1 *suite page suivante*

Tableau A.1 *(suite)*

Name	Gaia DR2/EDR3*	Sp Type	ϖ (mas)	u	g	r	i	z	y	J	H	K
J1657+2126	4565048312887877888	DA	47.6 (0.02)	14.537	14.14	14.167	14.27	14.396	14.48	13.863	13.82	13.86
J1657+2414	4572405140891735296	DC	10.5 (0.5)	23.2	20.71	19.98	19.7	19.55	19.6	···	···	···
J1658+2210	4565386996828484224	DA	11.7 (0.2)	19.19	18.53	18.32	18.245	18.29	18.22	17.53	···	···
J1658−0617	4340322876499078400	DA	31.5 (0.1)	18.59	17.402	16.974	16.789	16.733	16.74	15.8	15.6	15.4
J1659+1705	4558448219470271616	DA	10.4 (0.1)	17.93	17.527	17.554	17.66	17.779	17.86	17.3	···	···
J1659+3203	1313405848136604672	DA	26.7 (0.1)	18.36	17.607	17.36	17.27	17.273	17.29	16.52	···	15.7
J1659+4425	1358325021299899136	DA	35.06 (0.05)	18.28	16.986	16.559	16.382	16.336	16.32	15.4	15.2	15.0
J1701+4124	1354610798005917312	DA	10.5 (0.1)	18.0	17.59	17.69	17.811	17.98	18.07	17.58	···	···
J1702+1022	4444590625015876864	DA	34.0 (0.1)	19.81	18.19	17.63	17.398	17.33	17.31	16.45	16.0	17.04
J1704+1852	4560373769265200640	DC	10.2 (0.5)	21.1	20.03	19.67	19.53	19.48	19.49	···	···	···
J1704+2007	4561641991506408448	DA	19.1 (0.1)	18.45	17.72	17.461	17.359	17.37	17.38	16.61	16.5	16.1
J1704+3608	1339274053906752896	DC	23.3 (0.1)	20.7	18.61	17.948	17.653	17.574	17.5	16.62	16.34	16.3
J1704−1446	4139348334376604928	DA	30.5 (0.1)	···	16.599	16.46	16.459	16.509	16.56	15.7	15.4	15.3
J1705+0423	4391500847801807104	DA	21.8 (0.1)	···	16.181	16.149	16.189	16.28	16.37	15.7	15.6	15.4
J1705+2605	4573071139998034048	DA	28.9 (0.1)	18.26	17.35	17.04	16.91	16.91	16.88	16.14	···	···
J1705+4803	1408135749896104192	DA	25.38 (0.03)	14.756	14.447	14.471	14.565	14.681	14.745	14.112	14.07	14.1
J1705−0145	4379812558164849408	DC	35.3 (0.1)	19.9	18.035	17.308	17.022	16.925	16.87	16.1	15.7	···
J1706+6316	1631186458277453440	DAH	10.1 (0.1)	18.07	17.737	17.834	17.974	18.15	18.29	···	···	···
J1706−1238	4140966708116861440	DQ	10.1 (0.4)	19.8	19.18	18.89	18.81	18.85	18.8	18.1	···	···
J1707+6413	1632041328568823424	DA	10.9 (0.1)	18.49	18.022	17.91	17.928	17.99	18.09	···	···	···
J1708+0257	4388138816124225792	DZ	55.97 (0.03)	···	15.276	15.12	15.117	15.2	15.254	14.6	14.5	14.5
J1709+2332	4571723134445705856	DC	11.5 (0.2)	19.44	18.85	18.639	18.59	18.62	18.68	18.0	···	···
J1709+6820	1636757232723867264	DA	18.3 (0.1)	···	17.525	17.303	17.223	17.25	17.27	···	···	···
J1711+0932	4443586358581794176	DA	11.4 (0.1)	18.47	17.977	17.871	17.866	17.914	18.0	17.3	···	···
J1711−1447	4139531467491239680	DQ	44.1 (0.04)	···	14.28	14.38	14.532	14.681	14.79	14.15	14.2	14.1
J1712+3559	1338388813904333952	DC	14.1 (0.1)	17.41	17.108	17.14	17.244	17.37	17.48	16.88	16.3	17.2
J1712+3921	1341599143042727680	DAH	12.6 (0.2)	19.81	18.91	18.62	18.508	18.5	18.5	17.7	···	···
J1712+5629	1432420624562923520	DA	13.1 (0.1)	18.38	17.888	17.712	17.687	17.74	17.77	17.1	···	···
J1713+3240	1334374153353733888	DQ	14.4 (0.1)	17.6	17.345	17.329	17.398	17.51	17.6	17.01	···	···
J1713+4053	1342008814203085440	DA	15.9 (0.1)	17.87	17.49	17.534	17.61	17.73	17.79	17.2	···	···
J1713−0032	4368448074699014528	DA	12.3 (0.1)	17.73	17.334	17.311	17.357	17.456	17.53	···	···	···
J1714+2127	4567158653660872064	DC	25.0 (0.1)	17.18	16.73	16.611	16.628	16.698	16.743	16.11	16.0	···
J1714+3918	1341543072245722752	DAH	25.26 (0.04)	17.15	16.52	16.313	16.261	16.295	16.34	15.57	15.4	15.4
J1714−0534	4361621688038664064	DA*	38.24 (0.05)	···	14.667	14.715	14.833	14.976	15.071	14.459	···	14.45

Tableau A.1 *suite page suivante*

Tableau A.1 *(suite)*

Name	Gaia DR2/EDR3*	Sp Type	ϖ (mas)	u	g	r	i	z	y	J	H	K
J1716+2612	4573650303451549952	DA	10.2 (0.1)	18.14	17.699	17.68	17.713	17.8	17.9	17.18	···	···
J1716+4129	1348007784003797376	DC	10.0 (0.2)	19.12	18.65	18.56	18.584	18.68	18.73	18.1	···	···
J1716−0821	4359722208685335552	DQ	26.0 (0.1)	···	17.079	16.769	16.685	16.709	16.74	15.9	15.7	···
J1717+6136	1438490650303065984	DA	11.4 (0.3)	20.2	19.55	19.31	19.22	19.18	19.2	···	···	···
J1719−0130	4367353266060378624	DC :	26.2 (0.3)	···	18.78	18.06	17.74	17.61	17.55	16.67	···	16.42
J1720+1022	4491748511228743808	DC	26.7 (0.1)	20.1	18.218	17.621	17.376	17.3	17.26	16.2	16.4	···
J1720+4253	1360235560190381440	DC	19.0 (0.1)	···	18.88	18.384	18.169	18.12	18.1	17.4	···	···
J1722+2848	4598568230530318592	DA	17.4 (0.2)	20.8	19.06	18.59	18.36	18.28	18.19	17.43	17.28	17.3
J1722+3221	1333697880686680960	DA	10.1 (0.2)	19.42	18.782	18.58	18.54	18.55	18.55	17.9	···	···
J1722+5752	1433166540130924544	DC	16.2 (0.2)	20.4	19.21	18.75	18.56	18.5	18.49	17.74	17.84	18.8
J1723+0458	4390134326651497728	DA	15.0 (0.1)	···	16.939	16.92	16.98	17.067	17.13	16.4	16.0	15.86
J1723+0905	4490607183799536896	DA	10.9 (0.1)	18.46	17.86	17.692	17.638	17.68	17.71	16.98	···	···
J1724+2756	4598266758185956864	DA	26.0 (0.1)	18.55	17.628	17.318	17.2	17.174	17.19	16.41	···	···
J1725+6209	1439283711720415872	DA	14.5 (0.1)	17.78	17.34	17.253	17.267	17.31	17.4	···	···	···
J1726+3112	4599998179762051200	DA	14.0 (0.1)	17.75	17.239	17.184	17.207	17.288	17.37	16.5	···	···
J1726+3245	4600426645699105664	DA*	10.5 (0.2)	19.02	18.42	18.261	18.24	18.27	18.3	17.61	···	···
J1727+0808	4490300553197280256	DC	10.9 (0.6)	21.3	20.21	19.65	19.48	19.57	19.77	···	···	···
J1728+0211	4376680324417193472	DA	23.0 (0.1)	···	16.31	16.26	16.31	16.4	16.47	15.7	15.9	15.9
J1729+1435	4542785981266940416	DC	31.4 (0.2)	···	18.63	17.947	17.669	17.56	17.54	16.7	···	···
J1729+2916	4598830738931385984	DA	24.5 (0.1)	17.73	17.13	17.006	16.978	17.023	17.05	16.3	16.8	···
J1730+1346	4542521278141244288	DA	24.72 (0.04)	···	15.064	15.17	15.322	15.49	15.62	15.09	15.05	15.17
J1731+3705	1336442472164656000	DAZB	17.78 (0.04)	16.29	16.01	16.144	16.272	16.448	16.561	16.01	···	···
J1732+0213	4376589580346060928	DA	16.7 (0.1)	···	17.006	16.848	16.813	16.861	16.9	16.14	16.15	15.51
J1733+2705	4595011409196652544	DA	10.6 (0.2)	19.87	19.06	18.78	18.701	18.69	18.75	17.9	···	···
J1733+2903	4598775557191664384	DC	25.3 (0.1)	18.02	17.271	17.031	16.965	16.993	17.03	16.4	15.9	16.0
J1733+3013	4598979924619296384	DZ	16.9 (0.1)	17.65	16.888	16.92	17.067	17.215	17.32	···	···	···
J1733+7949	1706631093589103872	DC	37.2 (0.1)	···	17.29	16.919	16.763	16.75	16.77	16.1	16.1	15.48
J1734+4236	1347620038652968192	DA	14.03 (0.05)	···	16.83	16.691	16.655	16.705	16.72	15.95	15.91	15.39
J1734+4423	1348795004265872000	DA	26.7 (0.1)	19.88	18.24	17.66	17.446	17.35	17.34	16.5	16.0	···
J1737+0138	4375699353885688448	DA	21.4 (0.1)	···	16.958	16.836	16.83	16.883	16.91	16.18	15.76	15.07
J1738+0516	4485626636646013696	DA	21.9 (0.1)	···	15.937	15.944	16.037	16.145	16.22	15.6	15.6	15.4
J1738−0826	4168312459956062208	DAZ	32.9 (0.1)	···	16.056	15.903	15.882	15.928	15.949	15.19	···	15.02
J1739+4404	1350007967453813632	DA	13.1 (0.1)	18.04	17.62	17.571	17.604	17.7	17.76	17.08	···	···
J1739+6043	1435776922462177408	DA	17.4 (0.1)	18.24	17.61	17.387	17.33	17.34	17.4	16.5	···	···

Tableau A.1 *suite page suivante*

Tableau A.1 *(suite)*

Name	Gaia DR2/EDR3*	Sp Type	ϖ (mas)	u	g	r	i	z	y	J	H	K
J1741+2401	4581383928942599296	DA	31.7 (0.1)	17.28	16.607	16.466	16.455	16.5	16.54	15.81	15.6	15.7
J1742+4338	1349256249394224128	DA	31.8 (0.1)	18.67	17.373	16.912	16.713	16.656	16.642	15.77	15.7	···
J1742+5136	1368236912466084352	DA	23.5 (0.04)	16.31	15.915	15.914	15.966	16.072	16.15	15.6	15.4	15.6
J1743+0502	4473632403597115776	DA	10.9 (17.1)	20.6	19.89	19.71	19.63	19.73	19.7	19.2	19.0	···
J1743+1434	4500646618315862144	DC	29.18 (0.05)	···	14.858	14.968	15.132	15.2882	15.39	14.89	14.83	15.05
J1743+1701	4549622027311531904	DC	29.9 (0.1)	21.3	18.9	18.042	17.681	17.53	17.47	16.3	15.7	15.8
J1745+4825	1363721110836082176	DA	11.8 (0.1)	18.27	17.82	17.75	17.761	17.842	17.88	17.27	···	···
J1746−1234	4150020774057837440	DA	27.1 (0.1)	···	17.52	17.23	17.12	17.1	17.16	16.3	15.8	···
J1747+2859	4596322473734130304	DC	27.4 (0.1)	···	18.131	17.47	17.216	17.11	17.07	16.2	16.2	16.16
J1748+0052	4372558083524803072	DAH	18.8 (0.1)	17.25	16.901	16.926	17.006	17.133	17.21	16.59	···	···
J1748+4503	1350517492310172416	DC	33.43 (0.03)	15.816	15.601	15.628	15.733	15.846	15.94	15.32	15.2	15.2
J1748+7052	1638979384378696704	DXP	160.98 (0.01)	···	14.288	13.807	13.521	13.434	13.464	12.71	12.53	12.51
J1749+8247	1711005951573009792	DA	61.16 (0.02)	···	14.4338	14.232	14.218	14.27	14.3234	13.63	13.47	13.43
J1749−2355	4068499305485306240	DAZ	37.54 (0.04)	···	15.58	15.478	15.45	15.518	15.56	14.97	15.5	14.62
J1751+4455	1349726324974648192	DC	15.3 (0.1)	18.11	17.67	17.576	17.593	17.68	17.73	17.0	···	···
J1752+0947	4488750108662714624	DA	22.7 (0.1)	···	15.62	15.724	15.876	16.04	16.09	15.62	15.6	15.6
J1752+5037	1367469041032593024	DA	18.4 (0.05)	16.7	16.332	16.356	16.46	16.585	16.68	16.1	15.8	···
J1753+5039	1367551813642685952	DA	14.6 (0.1)	17.81	17.46	17.456	17.53	17.64	17.71	17.08	···	···
J1754+3846	4610983121260366336	DAH	19.1 (0.1)	18.58	17.85	17.601	17.518	17.53	17.546	···	···	···
J1754+5938	1423078520938173056	DA	10.0 (0.2)	19.82	19.11	18.84	18.75	18.7	18.74	17.94	···	···
J1757+1021	4494877446445481472	DZ	22.5 (0.1)	16.51	16.142	16.186	16.298	16.449	16.54	15.92	15.97	15.35
J1757+3900	4610819951159775616	DA	10.1 (0.3)	19.79	19.21	19.01	18.987	19.02	19.05	18.3	···	···
J1757+4052	4611543459874840832	DC	32.3 (0.1)	18.51	17.436	16.987	16.79	16.75	16.76	15.95	15.9	15.8
J1757+5441	1417200020676904704	DA	15.5 (0.1)	17.71	17.23	17.143	17.161	17.212	17.26	16.58	···	···
J1758+1417	4499839473701254400	DA	47.0 (0.1)	···	16.538	16.078	15.876	15.814	15.8	14.93	14.7	14.7
J1758+2310	4577666681988285696	DC	11.2 (0.3)	20.28	19.31	19.01	18.89	18.88	19.0	18.3	···	···
J1758+5201	1367876852471768320	DA	12.2 (0.1)	18.45	18.05	18.016	18.059	18.2	18.21	17.6	···	···
J1759+3924	4611204329256349312	DC	25.4 (0.1)	20.9	18.78	18.02	17.711	17.58	17.54	16.7	···	···
J1801+0846	4476287041283507840	DA	19.3 (0.1)	···	17.88	17.47	17.301	17.257	17.24	16.42	16.0	15.53
J1801+5050	2123432247756223488	DC	32.3 (0.1)	19.97	18.03	17.34	17.051	16.96	16.9	16.02	16.2	15.94
J1802+1354	4496751667093478016	DAZ	25.0 (0.1)	···	16.068	16.025	16.088	16.18	16.234	15.5	15.4	15.3
J1803+2320	4577545533852426624	DQ	15.3 (0.3)	21.41	20.15	18.85	18.51	18.27	18.19	17.13	···	···
J1806+2312	4578278903808759040	DA	11.9 (0.1)	18.53	18.17	18.19	18.271	18.39	18.45	17.82	···	···
J1807+0356	4470233817461336704	DA	33.18 (0.04)	14.991	14.608	14.71	14.854	15.012	15.13	14.57	14.5	14.5

Tableau A.1 *suite page suivante*

Tableau A.1 *(suite)*

Name	Gaia DR2/EDR3*	Sp Type	ϖ (mas)	u	g	r	i	z	y	J	H	K
J1807−1955	4095056359580563328	DC	16.1 (0.2)	17.69	17.38	17.409	17.5157	17.612	17.78	17.23	17.6	17.4
J1811+2213	4577915996250307968	DA	10.0 (0.2)	18.8	18.35	18.225	18.24	18.29	18.34	17.74	···	···
J1811+2423	4578464515115212672	DA	13.5 (0.1)	17.8	17.35	17.303	17.359	17.473	17.51	16.86	···	···
J1813+3248	4592910074976281472	DA	22.62 (0.05)	···	16.445	16.355	16.366	16.434	16.49	15.77	15.7	15.8
J1813+3248	4592910105037219072	DA	22.5 (0.1)	···	17.17	16.94	16.871	16.885	16.9	16.13	16.0	15.8
J1814+1301	4497001870409825280	DC	11.5 (0.1)	17.71	17.5	17.53	17.647	17.76	17.88	17.35	···	···
J1815+3158	4592623171160970112	DA	21.8 (0.1)	···	18.5	17.908	17.659	17.577	17.54	16.67	16.3	16.07
J1815−1140	4153937891610652928	DC	25.5 (0.2)	···	18.45	17.768	17.505	17.42	17.37	16.4	16.01	15.78
J1816+2454	4578913738632417920	DAP	26.6 (0.1)	···	17.043	16.8702	16.81	16.82	16.87	16.17	16.1	15.5
J1817+1328	4497414466452138496	DA	66.1 (0.1)	18.03	16.2314	15.593	15.325	15.232	15.191	14.292	15.1	15.0
J1817−1335	4146666271458052352	DA	30.7 (0.1)	···	17.46	17.09	16.981	16.97	16.965	16.1	···	···
J1819+1739	4523585076572785408	DC	29.3 (0.1)	···	18.31	17.634	17.36	17.27	17.18	16.36	16.02	16.0
J1819−1934	4094555467661923328	DC	25.4 (0.3)	···	18.97	18.12	17.8151	17.69	17.51	16.54	16.26	···
J1820+2619	4585067258532443776	DA	25.1 (0.1)	···	18.778	18.178	17.91	17.83	17.79	···	···	···
J1820+7454	2268813145513879808	DA	14.0 (0.1)	···	16.709	16.763	16.881	17.02	17.15	16.5	···	···
J1821+5509	2149253075743572224	DA	32.4 (0.1)	···	17.78	17.216	16.964	16.854	16.74	15.97	···	···
J1821+6100	2158285185808357504	DA	72.92 (0.03)	···	16.033	15.3636	15.092	14.984	14.948	14.08	13.81	13.8
J1822+2257	4530172280800983808	DA	11.2 (0.3)	20.05	19.32	19.07	18.95	19.0	18.9	18.2	···	···
J1823+2022	4528439381757452928	DC	26.0 (0.1)	···	18.45	17.82	17.552	17.48	17.39	16.6	16.2	···
J1823−1123	4154063678315488640	DA	27.6 (0.1)	···	17.537	17.178	17.03	17.01	17.04	···	···	···
J1824+1209	4484277256704949376	DA	30.4 (0.1)	···	17.896	17.343	17.119	17.034	17.02	16.1	15.9	15.6
J1824+1212	4484289866726156160	DZ	25.5 (0.2)	···	19.502	18.51	18.04	17.924	18.0	18.1	···	···
J1824−1308	4152557420406043264	DAZ	52.4 (0.1)	···	15.73	15.4	15.286	15.292	15.252	14.53	14.28	14.21
J1825+1135	4484184592790777728	DA	50.9 (0.1)	···	16.9	16.28	16.019	15.895	15.845	14.98	14.7	14.7
J1826+1120	4483974792231866624	DA	36.9 (0.1)	···	17.5253	16.898	16.597	16.54	16.19	14.8	···	···
J1827+0621	4477166581862730752	DC*	10.6 (0.1)	···	16.946	17.04	17.23	17.38	17.48	16.85	···	···
J1828+4149	2111294734600515072	DA	10.3 (0.2)	19.8	19.192	18.97	18.89	18.89	18.8	18.2	···	···
J1829−0429	4257461275049675008	DA	38.8 (0.6)	···	14.63	14.644	14.74	14.851	14.933	14.285	14.255	14.32
J1829−0536	4257063458004688896	DA	25.2 (0.1)	···	17.84	17.4	17.212	17.16	17.12	16.26	15.99	15.98
J1829−0536	4257063453704172416	DC	25.1 (0.1)	···	17.07	16.85	16.798	16.83	16.822	···	···	···
J1830+2529	4537112917885892608	DC	11.3 (0.5)	···	20.67	20.25	20.54	20.8	···	···	···	···
J1830+5447	2150504594853811456	DXP	58.7 (0.03)	···	15.721	15.445	15.424	15.499	15.63	14.83	14.5	14.5
J1831+4658	2118649750133781376	DA	42.92 (0.03)	···	15.246	15.144	15.132	15.186	15.245	14.52	14.38	14.4
J1833+1945	4525569007873380736	DQ	25.4 (0.1)	16.89	16.498	16.398	16.433	16.503	16.58	15.93	16.0	15.6

Tableau A.1 *suite page suivante*

Tableau A.1 *(suite)*

Name	Gaia DR2/EDR3*	Sp Type	ϖ (mas)	u	g	r	i	z	y	J	H	K
J1833+3217	4589139574728058880	DZA	25.42 (0.04)	···	16.106	16.1	16.17	16.32	16.41	···	15.6	15.3
J1834+1215	4508113436149576960	DQ*	11.1 (0.1)	···	17.89	17.86	17.93	18.04	18.13	17.57	···	···
J1835+6421	2256410856215182464	DC	33.1 (0.1)	19.85	18.01	17.345	17.072	16.97	16.94	15.9	15.6	···
J1835+6429	2256422164865057536	DQ	18.7 (0.1)	17.68	17.65	17.234	17.168	17.28	17.39	16.6	···	···
J1838+6251	2160181598552871040	DC	11.5 (0.2)	19.97	19.08	18.8	18.716	18.74	18.78	···	···	···
J1841+4107	2110551602180192256	DA	10.4 (0.3)	20.5	19.46	19.09	18.955	18.9	18.87	18.1	···	···
J1842−1108	4107012041007171456	DA	41.44 (0.05)	···	14.22	14.2939	14.45	14.588	14.673	14.14	14.0	14.2
J1843+0420	4280632829779587072	DA	40.21 (0.04)	···	14.833	14.836	14.926	15.037	15.12	14.44	14.4	14.6
J1847+2820	4539227892919675648	DC	24.9 (0.2)	···	19.11	18.39	18.1	17.97	17.93	17.11	···	···
J1848+6852	2259262581356603136	DA	11.3 (0.1)	···	17.565	17.419	17.387	17.43	17.46	16.5	16.4	···
J1849−0736	4252064631569619712	DC	28.5 (0.1)	···	17.15	16.892	16.852	16.832	16.83	16.15	16.09	16.1
J1851+7738	2292861388958880640	DC	32.9 (0.1)	19.13	17.55	17.008	16.789	16.715	16.67	15.9	15.8	14.93
J1852+1833	4517521407404432512	DAH	20.5 (0.1)	17.28	16.949	16.92	17.02	17.11	17.19	16.52	···	···
J1855+5359	2146645790077864704	DC	35.7 (0.1)	···	18.04	17.307	17.004	16.873	16.83	16.0	15.8	15.4
J1857+2026	4518917168694695168	DA+DC :*	30.8 (0.1)	17.52	16.93	16.63	16.58	16.58	16.62	15.89	15.6	16.11
J1857+5330	2146576589564898688	DC	40.4 (0.1)	···	17.604	16.909	16.625	16.518	16.47	15.57	15.4	15.5
J1857−2651	4073522222505044224	DA*	25.3 (0.1)	···	16.593	16.41	16.374	16.424	16.45	15.7	15.5	15.5
J1859+1158	4313658585693385984	DA	20.2 (0.1)	···	15.606	15.675	15.814	15.942	16.08	15.424	15.4	15.46
J1900+3922	2100304020669107328	DA	22.51 (0.03)	16.07	15.654	15.712	15.811	15.939	16.044	15.47	15.4	15.2
J1906+4446	2106132596228948480	DA	15.5 (0.1)	···	17.328	17.211	17.224	17.27	17.34	16.65	···	···
J1912+0242	4268167357267580160	DZ	31.6 (0.1)	···	16.72	16.509	16.535	16.63	16.641	16.1	···	···
J1913+2949	2039140284770609152	DA	26.9 (0.1)	···	17.258	16.97	16.851	16.83	16.84	16.06	15.7	15.48
J1914+1428	4320303621677848832	DA	25.5 (0.1)	···	16.94	16.76	16.712	16.73	16.78	16.02	15.87	15.85
J1914+4936	2132684535027576448	DA	15.3 (0.1)	···	16.726	16.735	16.813	16.92	16.99	16.38	···	···
J1916+8044	2295446546953958272	DA	28.2 (0.1)	···	17.89	17.379	17.193	17.14	17.1	16.3	16.1	15.21
J1918+3843	2052891361294411520	DC	84.21 (0.02)	15.424	14.752	14.5	14.431	14.443	14.457	13.723	13.67	13.52
J1918+3851	2100934448852549760	DA	10.1 (0.2)	19.0	18.58	18.55	18.59	18.71	18.8	18.2	···	···
J1918+6258	2252512954353689344	DA	12.7 (0.1)	18.19	17.712	17.64	17.655	17.75	17.82	···	···	···
J1921+0613	4293873732939569920	DA	55.03 (0.04)	···	15.945	15.619	15.49	15.458	15.47	14.61	14.41	14.4
J1922+0233	4288942973032203904	DZ	25.4 (0.3)	···	19.59	19.06	18.94	19.1	19.47	···	···	···
J1922+7137	2264228628701507200	DA	14.0 (0.2)	···	17.362	17.289	17.304	17.39	17.345	···	···	···
J1923+2141	2018864362679341824	DA	28.2 (0.2)	···	14.707	14.723	14.81	14.93	15.04	14.3	14.19	14.3
J1924+3751	2052569921645067008	DC	12.2 (0.2)	19.8	18.994	18.77	18.7	18.72	18.7	18.03	···	···
J1924+5506	2140241890760529408	DA	11.0 (0.1)	···	17.142	17.203	17.309	17.46	17.54	16.98	···	···

Tableau A.1 *suite page suivante*

Tableau A.1 *(suite)*

Name	Gaia DR2/EDR3*	Sp Type	ϖ (mas)	u	g	r	i	z	y	J	H	K
J1926+4620	2127566548919332608	DA	29.69 (0.03)	···	15.96	15.896	15.94	16.025	16.09	15.4	15.4	···
J1927+5644	2142307563871222912	DA	31.5 (0.1)	···	16.958	16.73	16.665	16.69	16.69	16.0	15.7	15.8
J1930−0057	4215241712185612544	DC	28.6 (0.1)	···	16.288	16.222	16.274	16.36	16.45	15.7	15.6	···
J1935−1724	4180014832789446400	DC	25.0 (0.2)	···	19.39	18.6	18.28	18.1	18.07	17.18	···	16.8
J1939+6619	2248748668919802496	DC	28.3 (0.1)	···	18.22	17.678	17.46	17.39	17.36	16.5	···	15.7
J1940+4240	2077905319548753664	DA+DA	15.5 (0.1)	···	16.504	16.535	16.65	16.781	16.869	16.2	16.3	···
J1940+8348	2301882675705225472	DC	27.9 (0.2)	···	18.93	18.23	17.95	17.861	17.77	16.7	16.24	16.96
J1943+5011	2134968663059016832	DA	10.2 (0.1)	···	17.07	17.165	17.332	17.49	17.61	17.07	···	···
J1944−0425	4209580395521652352	DC	10.5 (0.6)	···	20.7	19.99	19.72	19.71	19.61	···	···	···
J1945+4650	2080526555267050496	DA	34.7 (0.1)	···	17.45	16.9615	16.758	16.7	16.67	15.84	15.5	15.5
J1945+4650	2080526555267049984	DA	34.7 (0.1)	···	17.82	17.17	16.87	16.8	16.733	15.87	15.5	15.3
J1945−1719	6871494782188972672	DC	19.0 (0.2)	···	18.49	18.03	17.852	17.8	17.79	16.94	···	16.6
J1946+0937	4301829970867752704	DA	23.2 (0.1)	···	17.367	17.08	16.973	16.9584	16.99	16.2	15.7	15.5
J1948+6122	2240605346504273280	DA	11.2 (0.2)	19.9	19.07	18.725	18.618	18.59	18.59	···	···	···
J1949+0747	4298029268399256704	DA	27.37 (0.04)	···	15.425	15.45	15.547	15.677	15.77	15.16	15.3	15.2
J1949−0855	4195385769125206144	DC	11.1 (0.4)	19.35	18.88	18.71	18.7	18.74	18.8	18.1	···	17.7
J1950+0033	4240231824768647040	DA	27.9 (0.1)	···	17.206	16.84	16.699	16.68	16.667	15.8	15.5	15.7
J1951+4026	2073772770741915264	DC	25.1 (0.1)	···	18.76	18.04	17.831	17.87	18.01	17.59	···	···
J1951+4209	2078430778727685632	DA	26.0 (0.1)	···	18.36	17.732	17.48	17.415	17.36	16.2	16.1	···
J1954+0115	4240366136980012416	DA	11.3 (0.3)	20.2	19.3	19.05	18.94	18.96	18.95	18.2	···	···
J1955−0030	4237044301894347392	DA	10.2 (0.2)	18.55	18.2	18.211	18.28	18.39	18.48	17.91	···	17.9
J1956−0102	4235280071072332672	DA	86.48 (0.03)	14.259	13.75	13.65	14.1	13.706	13.791	13.127	13.03	13.009
J2004+0109	4237555506083389568	DA	30.8 (0.1)	24.64	16.9	16.1849	16.64	16.63	16.37	15.1	15.6	···
J2004−1058	4190734280885088128	DA	10.7 (0.2)	18.83	18.45	18.35	18.35	18.43	18.49	17.81	···	17.9
J2005−1056	4190813690536580608	DC	57.8 (0.1)	19.41	17.408	16.651	16.321	16.217	16.137	15.31	15.14	15.09
J2006+6143	2237893023118101504	DA	29.8 (0.1)	18.18	16.84	16.341	16.142	16.095	16.049	15.17	14.9	14.7
J2006−2101	6865904860773722496	DA	25.5 (0.1)	···	18.17	17.592	17.367	17.28	17.249	16.5	16.1	15.6
J2007+3222	2055059112897283712	DA	12.4 (0.3)	20.09	19.32	19.05	18.92	18.917	18.9	18.25	18.0	···
J2008−1619	6874124023727679104	DC	26.1 (0.1)	···	18.158	17.77	17.598	17.57	17.56	16.4	···	···
J2009+5955	2236900335916533248	DC	10.9 (0.1)	17.99	17.823	17.886	18.018	18.18	18.29	···	···	···
J2009−0059	4236208432541189376	DA	10.5 (0.2)	19.52	19.0	18.817	18.79	18.84	18.85	18.2	···	18.1
J2010−1126	6880851931079280512	DA	11.0 (0.2)	19.68	18.92	18.62	18.526	18.54	18.52	17.71	···	17.6
J2010−2146	6853784501721502720	DA	37.16 (0.03)	···	14.4151	14.48	14.581	14.7446	14.85	14.231	14.2	14.21
J2011+0913	4299397713684601088	DA	14.6 (0.1)	18.07	17.492	17.307	17.25	17.28	17.3	16.55	···	···

Tableau A.1 *suite page suivante*

Tableau A.1 *(suite)*

Name	Gaia DR2/EDR3*	Sp Type	ϖ (mas)	u	g	r	i	z	y	J	H	K
J2012−1307	6879638761736608768	DC	13.1 (0.1)	17.09	16.982	17.059	17.209	17.37	17.45	16.98	···	16.9
J2012−2210	6853523539508720000	DC	28.1 (0.1)	···	17.745	17.33	17.169	17.133	17.13	16.4	16.1	···
J2013+0642	4249667902270614272	DC	43.62 (0.05)	16.47	15.902	15.69	15.655	15.68	15.731	14.97	14.83	14.76
J2015+0001	4230380819051252736	DC	39.3 (0.1)	19.45	17.65	16.996	16.732	16.64	16.58	15.7	···	···
J2015−1222	6879784584465884544	DC	11.1 (0.1)	17.32	17.228	17.302	17.442	17.6	17.72	17.16	···	17.2
J2020−0005	4230332092645516672	DA	15.1 (0.1)	18.25	17.72	17.524	17.491	17.53	17.53	16.79	···	16.7
J2021+5454	2185261016407220224	DC	26.3 (0.1)	···	17.567	17.245	17.142	17.14	17.14	16.4	···	···
J2022+8333	2302010356492847744	DC	26.0 (0.1)	···	17.53	17.18	17.04	17.04	17.04	16.2	16.4	15.99
J2023+0759	1752188773770447872	DC	11.6 (0.3)	19.51	18.88	18.662	18.61	18.62	18.68	18.05	···	···
J2027+0523	4246381595156273792	DA	16.7 (0.1)	17.93	17.39	17.228	17.195	17.23	17.27	16.57	15.9	15.46
J2030+0655	1748816983925915776	DA	24.3 (0.1)	18.62	17.68	17.324	17.181	17.16	17.16	16.36	···	···
J2030+0729	1748922296525519872	DC	24.18 (0.04)	···	16.124	16.109	16.191	16.311	16.39	15.66	16.08	15.6
J2030+4015	2067343097310013056	DC	11.4 (0.2)	19.89	19.19	18.94	18.84	18.87	18.86	18.23	18.1	18.2
J2031+3934	2064284054100290048	DC	28.5 (0.1)	···	18.55	17.82	17.54	17.39	17.12	16.0	···	14.9
J2031−1450	6875432476922523520	DC	26.2 (0.2)	21.2	19.05	18.26	17.932	17.802	17.76	16.5	···	···
J2031−1658	6862687522250677376	DAZ	43.8 (0.1)	···	16.524	16.077	15.899	15.853	15.82	15.005	14.8	14.69
J2033+3954	2064689567732385792	DA	48.19 (0.04)	17.51	16.584	16.232	16.087	16.084	16.073	15.3	15.2	14.9
J2034+1345	1756261467922806784	DA	12.7 (0.2)	19.19	18.66	18.52	18.51	18.57	18.6	17.9	···	···
J2038+0037	4231193525645520768	DA	10.1 (0.3)	19.15	18.65	18.5	18.46	18.52	18.53	17.92	17.7	17.7
J2041+4320	2069588300054515200	DA	16.6 (0.1)	18.23	17.635	17.452	17.43	17.449	17.49	16.78	16.6	16.66
J2041−0520	6914243308941804288	DC	18.9 (0.2)	20.9	19.2	18.54	18.287	18.199	18.13	17.25	16.97	16.93
J2042+0031	4228210894197669760	DC	15.8 (0.3)	21.9	19.85	19.09	18.75	18.63	18.59	17.65	17.45	17.36
J2042+3752	2063293355469201152	DA	11.5 (0.3)	20.6	19.76	19.39	19.3	19.3	19.3	18.9	18.1	17.7
J2044+4030	2066035777984385792	DAH	17.1 (0.1)	18.32	17.83	17.683	17.679	17.74	17.82	17.11	16.98	16.96
J2045+0227	4231922059473951616	DA	16.1 (0.1)	17.37	17.07	17.153	17.309	17.466	17.59	17.08	···	···
J2045+0424	1735171735387308160	DA	11.8 (0.4)	20.3	19.51	19.28	19.188	19.17	19.17	18.5	···	···
J2045+4146	2066251179185657856	DC	11.8 (0.1)	17.45	17.35	17.396	17.531	17.67	17.74	17.24	17.28	17.4
J2045+8105	2298135638862051968	DA	15.02 (0.04)	···	16.51	16.445	16.49	16.59	16.61	16.2	16.1	···
J2045−0016	4227915744043939584	DA*	10.9 (0.3)	18.68	18.16	18.013	17.99	18.044	18.09	17.39	17.4	17.3
J2045−0710	6907079269131974912	DA*	11.7 (0.2)	21.0	19.27	18.626	18.36	18.25	18.21	17.32	17.1	17.03
J2045−1612	6886287332455279104	DA	12.0 (0.3)	18.41	17.967	17.838	17.836	17.91	17.95	17.2	···	17.0
J2046−0644	6907108371830928768	DA	11.5 (0.1)	17.46	17.08	17.116	17.236	17.363	17.44	16.76	···	···
J2046−0710	6907031749613795968	DAH	11.6 (0.2)	18.25	17.95	17.92	17.983	18.09	18.18	17.6	···	···
J2046−1413	6887386745296346624	DA	15.7 (0.1)	17.16	16.74	16.728	16.783	16.89	16.96	16.31	15.8	16.26

Tableau A.1 *suite page suivante*

Tableau A.1 *(suite)*

Name	Gaia DR2/EDR3*	Sp Type	ϖ (mas)	u	g	r	i	z	y	J	H	K
J2048+5110	2169971345155578752	DC	26.0 (0.1)	···	18.49	17.815	17.542	17.442	17.41	16.56	16.29	16.25
J2050+2630	1844125748497557632	DA	52.35 (0.05)	17.7	16.0	15.387	15.12	15.0194	14.98	14.12	13.83	13.79
J2050+7740	2290785163113859712	DC	18.6 (0.1)	···	19.0	18.4	18.14	18.071	18.03	···	···	···
J2051+5636	2189957816542364800	DA	12.7 (0.1)	18.63	18.08	17.94	17.9	17.93	17.97	17.26	···	···
J2051−2452	6805808514433280000	DA	37.3 (0.1)	···	15.57	15.459	15.464	15.54	15.59	14.854	14.7	14.7
J2052+0133	4228576550540445184	DC*	20.7 (0.1)	19.1	18.142	17.708	17.54	17.53	17.59	···	···	···
J2052−2206	6808651507904773888	DC	49.22 (0.05)	···	15.067	15.001	15.057	15.152	15.246	14.57	14.6	14.6
J2053−0702	6909994246262080000	DQ	10.2 (0.3)	19.27	19.19	18.77	18.67	18.75	18.83	18.27	18.04	18.2
J2056+0621	1736555475066523008	DA	11.5 (0.1)	17.04	16.56	16.608	16.721	16.844	16.944	16.33	···	···
J2056+4313	2162041628635165824	DZ	13.5 (0.1)	···	17.074	17.114	17.241	17.39	17.49	16.95	16.89	17.03
J2056−0450	6913810483611035776	DC	61.8 (0.1)	···	17.17	16.32	15.94	15.821	15.75	14.7	14.6	14.3
J2056−2717	6801786157301360896	DA	12.2 (0.2)	···	17.19	17.198	17.274	17.4	17.471	16.85	16.83	16.8
J2057+0944	1750460792464604672	DA	12.0 (0.3)	19.16	18.66	18.52	18.495	18.54	18.61	17.96	···	···
J2057+2316	1839493604790492032	DC	12.7 (0.2)	19.61	18.48	18.348	18.397	18.48	18.51	17.9	···	···
J2058+1657	1764481588648685440	DZA*	12.8 (0.3)	19.95	19.078	18.74	18.62	18.59	18.61	17.86	···	···
J2059+5517	2188860027203347968	DC	44.1 (0.1)	19.97	17.85	17.035	16.693	16.57	16.52	15.62	15.4	15.5
J2059−0033	6917473674103954560	DA	13.1 (0.1)	18.13	17.689	17.58	17.581	17.631	17.7	17.03	16.89	16.9
J2100+5051	2169025009235266816	DA	29.35 (0.03)	···	15.109	15.155	15.263	15.434	15.51	14.82	15.0	14.9
J2101+3148	1864760695541016832	DQ	31.03 (0.03)	···	15.031	15.105	15.261	15.43	15.53	14.99	14.9	15.0
J2102+1912	1789361097242243584	DA	30.4 (0.1)	···	16.472	16.267	16.207	16.224	16.251	15.5	15.6	15.4
J2102+2457	1841254644460354688	DA	35.8 (0.1)	17.59	16.763	16.451	16.329	16.318	16.31	15.51	15.2	15.1
J2103−0024	2690065251596080384	DC	16.7 (0.4)	19.15	18.41	18.123	18.036	18.04	18.05	17.34	17.15	17.1
J2103−0055	6917223054171248256	DC	13.2 (0.4)	21.7	20.0	19.27	19.0	18.91	18.85	18.1	17.7	17.6
J2105+0602	1736329589850340736	DA	10.0 (0.3)	20.15	19.31	19.01	18.903	18.91	18.94	18.1	···	···
J2106+0106	2690697646876721152	DA	25.8 (0.1)	17.98	17.183	16.866	16.753	16.742	16.744	15.9	15.8	···
J2107+0740	1737167215848315264	DA	26.1 (0.1)	17.06	16.537	16.376	16.356	16.411	16.44	15.74	15.8	15.14
J2108−0033	2689915958535673472	DA	11.6 (0.3)	19.78	19.02	18.73	18.633	18.64	18.57	17.87	17.6	17.5
J2108−0312	6912866381081015552	DC	28.5 (0.1)	18.98	17.73	17.261	17.064	16.981	16.97	16.0	15.9	16.0
J2109+0131	2690830511689102336	DA	13.1 (0.3)	20.17	19.24	18.932	18.83	18.83	18.78	18.2	···	···
J2109+0628	1733833492297878656	DA	12.0 (0.4)	19.61	19.05	18.85	18.82	18.86	18.83	18.2	···	···
J2109−0111	2688986325747403264	DA	11.6 (0.2)	18.62	18.17	18.062	18.07	18.13	18.17	17.54	17.3	17.4
J2110−2129	6831993452567326592	DA	31.4 (0.1)	···	16.979	16.652	16.521	16.495	16.501	15.71	15.5	15.45
J2111−0036	2689129601561746560	DQ	10.6 (0.2)	18.64	18.29	18.19	18.22	18.31	18.33	17.7	17.7	17.6
J2112+0622	1733782571164433408	DC	17.3 (0.1)	16.32	16.229	16.313	16.472	16.62	16.75	16.21	···	···

Tableau A.1 *suite page suivante*

Tableau A.1 *(suite)*

Name	Gaia DR2/EDR3*	Sp Type	ϖ (mas)	u	g	r	i	z	y	J	H	K
J2112−2922	6788656957673130112	DC	30.4 (0.1)	···	15.161	15.227	15.368	15.531	15.642	15.14	15.0	15.2
J2113+0727	1739921801713625600	DA	34.1 (0.1)	17.04	16.298	16.055	15.993	15.98	16.0	15.21	15.0	14.8
J2113+2621	1841683423932168832	DA	32.3 (0.3)	···	14.74	14.697	14.74	14.81	14.87	14.204	14.12	14.1
J2115+0400	1732272185785761408	DAH	10.0 (0.3)	19.82	19.07	18.831	18.78	18.81	18.82	17.9	···	···
J2115−0741	6898489884295407488	DA	14.5 (0.1)	17.86	17.461	17.406	17.44	17.54	17.58	16.95	···	16.8
J2116−0724	6898521877506794880	DC	24.7 (0.1)	20.3	18.327	17.586	17.283	17.166	17.112	16.16	16.02	15.9
J2118+1120	1746315255670491904	DA	17.9 (0.2)	19.38	18.42	18.1	17.963	17.94	17.94	17.18	···	···
J2118−0737	6898455661995166336	DC	16.2 (0.5)	22.8	20.51	19.47	19.043	18.84	18.78	17.9	17.82	17.81
J2118−0737	6898453913943607040	DC	10.4 (0.6)	19.78	19.19	18.98	18.94	18.96	19.01	18.29	···	18.1
J2119−0300	2685318075783946368	DA	10.8 (0.1)	17.32	16.873	16.871	16.963	17.06	17.17	16.5	16.47	16.54
J2120+1303	1747132467687929600	DA	12.6 (0.1)	17.53	17.138	17.139	17.204	17.319	17.4	16.83	···	···
J2120+2320	1792207664128299776	DA	10.6 (0.3)	20.1	19.25	18.95	18.85	18.86	18.83	18.0	···	···
J2120+5819	2191146977029443584	DA	25.76 (0.04)	···	16.02	15.951	15.968	16.07	16.12	15.44	···	···
J2121−0130	2685959542034846464	DA	28.6 (0.1)	17.42	16.733	16.49	16.418	16.43	16.458	15.72	15.52	15.43
J2122+0413	2693095097621419648	DA	41.3 (0.1)	18.85	17.139	16.507	16.252	16.157	16.12	15.26	15.0	14.9
J2123+1917	1785659488269249408	DA	12.6 (0.1)	17.25	16.86	16.924	17.039	17.195	17.32	16.71	···	···
J2124+0638	1738863620555712512	DC	13.1 (0.3)	19.54	18.86	18.609	18.551	18.58	18.58	17.94	···	···
J2125+2752	1847460116290325888	DA	10.4 (0.3)	20.1	19.29	18.947	18.81	18.81	18.83	18.0	···	···
J2126+0729	1739397914486670208	DA	13.7 (0.3)	19.42	18.76	18.55	18.487	18.5	18.52	17.78	···	···
J2127+0229	2691890685712023552	DA	10.1 (0.4)	19.69	19.08	18.93	18.91	18.96	19.0	18.3	···	···
J2127+2632	1847118992806013568	DA	12.2 (0.2)	19.26	18.53	18.31	18.209	18.22	18.28	17.48	···	···
J2129+0013	2687768066863960576	DA	15.2 (0.1)	16.02	15.597	15.616	15.698	15.807	15.9	15.25	15.16	15.23
J2130+1817	1786065654735928064	DC	10.5 (0.2)	18.23	18.018	18.004	18.089	18.21	18.26	17.64	···	···
J2130+2537	1798927947915336448	DC	15.3 (0.2)	19.03	18.31	18.008	17.91	17.92	17.97	17.25	···	···
J2131+0659	1739109601921701120	DAH :	9.6 (0.5)	19.79	19.18	18.97	18.92	18.95	18.91	18.3	···	···
J2132+2654	1847190701579945856	DC	16.4 (0.2)	19.05	18.269	18.009	17.93	17.94	17.99	17.27	···	···
J2133+2414	1797472370615364992	DA	28.5 (0.1)	18.11	17.37	17.1	17.01	17.023	17.05	16.2	15.8	···
J2133−0611	2670770991487735424	DC	14.2 (0.3)	19.46	18.643	18.302	18.23	18.205	18.26	17.5	17.6	17.7
J2134+3655	1951870157081161216	DA	25.34 (0.05)	···	16.504	16.382	16.392	16.459	16.5	15.9	15.9	15.4
J2135+0106	2688307166863547264	DA	9.7 (0.4)	19.98	19.152	18.845	18.72	18.63	0.0	17.86	17.6	17.8
J2135+4633	1977417206669775744	DA	25.8 (0.1)	···	18.38	17.77	17.441	17.4	17.12	16.43	16.12	15.99
J2136−1318	6842831888437047680	DA	42.7 (0.1)	···	13.669	13.752	13.893	14.062	14.158	13.546	13.58	13.541
J2138+1123	1766620929036759808	DAH	10.1 (0.1)	17.51	17.389	17.401	17.53	17.67	17.74	17.2	···	···
J2138+2309	1794118516552814336	DA	23.95 (0.04)	15.48	15.24	15.329	15.462	15.62	15.728	15.16	15.1	14.8

Tableau A.1 *suite page suivante*

Tableau A.1 *(suite)*

Name	Gaia DR2/EDR3*	Sp Type	ϖ (mas)	u	g	r	i	z	y	J	H	K
J2138−0056	2686607906002083328	DC	13.6 (0.3)	21.3	19.53	19.0	18.79	18.71	18.7	18.3	18.8	···
J2139−1245	6844375121726139520	DA	27.2 (0.1)	···	16.5	16.46	16.455	16.58	16.66	16.0	15.7	···
J2140+2140	1793628851625008512	DA	10.2 (0.1)	17.46	17.016	17.122	17.26	17.423	17.56	17.01	···	···
J2141+0923	1741417790361772160	DA	19.0 (0.1)	16.29	15.865	15.906	16.004	16.144	16.24	15.63	15.4	15.4
J2142+0805	2701893698904233216	DA	33.4 (0.1)	19.53	17.67	17.015	16.751	16.66	16.602	15.77	15.27	15.18
J2142+1328	1767494804558717824	DA	21.3 (0.1)	···	16.642	16.54	16.527	16.59	16.644	16.02	15.7	15.5
J2142+1329	1767494868982336000	DC :	21.7 (0.2)	···	18.52	18.02	17.817	17.75	17.74	16.94	···	···
J2142+2059	1792830060723673472	DQ	90.64 (0.03)	13.91	13.356	13.5	13.372	13.477	13.573	12.979	12.93	12.92
J2142+2252	1794409921493969792	DZ	21.4 (0.1)	16.07	15.91	15.978	16.109	16.264	16.37	15.86	15.74	15.54
J2142−0036	2675091174536113792	DC*	12.7 (0.3)	19.13	18.619	18.442	18.42	18.46	18.53	17.9	17.8	17.8
J2143+1934	1786444230333492480	DA	10.2 (0.3)	20.12	19.24	18.94	18.83	18.81	18.77	18.1	···	···
J2143+2829	1801199745097109632	DA	10.7 (0.3)	20.12	19.22	18.9	18.77	18.72	18.64	18.0	···	···
J2143−0659	2667464656943675392	DA	55.11 (0.05)	14.93	14.61	14.605	14.681	14.796	14.883	14.23	14.17	14.16
J2144+4753	1977776953135753856	DA	13.6 (0.1)	18.05	17.58	17.48	17.496	17.56	17.57	16.92	16.78	17.1
J2145+1106	1765847182089067008	DC	15.6 (0.8)	23.4	20.87	19.92	19.51	19.244	19.33	18.4	···	···
J2145+1106	1765847186383576832	DC	15.3 (1.4)	23.8	21.4	20.2	19.77	19.54	19.5	18.9	···	···
J2146+1550	1772407315138035584	DA	13.4 (0.3)	17.13	16.61	16.56	16.569	16.65	16.71	16.0	15.7	15.53
J2146+4626	1974579637737581568	DC	10.0 (0.3)	20.3	19.62	19.28	19.18	19.2	19.0	18.5	···	···
J2147+1127	1765881576187554432	DA :	19.0 (0.3)	20.9	19.09	18.43	18.164	18.06	18.05	17.14	16.84	16.79
J2147−0647	2667108891917960960	DA	12.9 (0.2)	18.27	17.807	17.702	17.702	17.76	17.86	17.11	16.99	16.9
J2147−0824	2666306798185155200	DA	20.5 (0.1)	18.59	17.708	17.376	17.25	17.233	17.22	16.43	···	16.13
J2147−2910	6809585263858474240	DZ	10.4 (0.2)	···	18.23	18.18	18.27	18.4	18.4	17.85	···	18.0
J2148−2821	6809702159983236992	DC	11.3 (0.9)	···	20.62	20.17	20.52	20.9	···	···	···	···
J2149+0415	2696628687474414208	DA	28.4 (0.1)	18.7	17.159	16.634	16.398	16.329	16.29	15.42	15.2	15.1
J2150+1953	1780497934010525312	DA	10.1 (0.2)	18.33	17.953	17.93	17.98	18.09	18.19	17.53	···	···
J2150−0113	2674012072593383168	DQ	11.1 (0.2)	17.73	17.48	17.535	17.67	17.805	17.94	17.39	17.37	17.4
J2150−0439	2669936427801840256	DC	28.2 (0.1)	19.58	18.25	17.721	17.529	17.59	17.8	17.68	18.2	18.8
J2151+0031	2681243457490130304	DC*	12.6 (0.3)	18.15	17.86	17.837	17.912	18.028	18.1	···	···	···
J2151+2305	1795037875776233984	DA	13.5 (0.2)	17.78	17.47	17.49	17.576	17.705	17.79	17.21	···	···
J2151+5917	2202703050401536000	DAH	118.12 (0.02)	···	14.922	14.367	14.16	14.089	13.964	13.0	12.8	12.7
J2153+0726	2700725635303873024	DA	10.4 (0.1)	18.04	17.63	17.63	17.699	17.809	17.88	17.31	···	···
J2153+2948	1897310564741680512	DA	12.1 (0.3)	19.97	19.13	18.83	18.737	18.73	18.73	18.0	···	···
J2154+1300	1767957488499891968	DAZ*	18.9 (0.2)	20.19	18.96	18.349	18.073	17.97	17.93	17.09	···	···
J2154+2657	1799905929149972352	DA	11.2 (0.2)	19.42	18.67	18.452	18.39	18.39	18.377	17.64	···	···

Tableau A.1 *suite page suivante*

Tableau A.1 *(suite)*

Name	Gaia DR2/EDR3*	Sp Type	ϖ (mas)	u	g	r	i	z	y	J	H	K
J2155+1201	1766164322474245376	DA	12.7 (0.7)	19.73	18.834	18.53	18.39	18.37	18.35	17.68	···	···
J2155+4103	1959573541696236032	DZ	16.9 (0.1)	···	18.17	17.98	17.97	18.0	18.07	17.42	15.8	15.8
J2155−2750	6617996741403360128	DC	42.5 (0.1)	···	16.706	16.272	16.084	16.053	16.03	15.17	15.1	14.85
J2156+0559	2697327113581223936	DQ	10.3 (0.2)	19.2	18.72	18.55	18.558	18.6	18.62	18.1	···	···
J2157+2705	1892992267183979776	DC	27.0 (0.2)	20.68	18.555	17.786	17.465	17.36	17.27	16.4	16.1	···
J2158+1814	1779145878305570944	DA	11.8 (0.3)	18.4	18.064	18.09	18.198	18.32	18.45	17.9	···	···
J2158+5804	2199338643594260352	DA	14.2 (0.1)	···	17.73	17.58	17.51	17.51	17.49	16.2	15.5	15.5
J2158−0239	2676567307551465088	DC	35.7 (0.1)	19.57	17.706	17.062	16.792	16.711	16.65	15.8	15.7	15.2
J2158−0240	2676566272464334720	DC	35.5 (0.3)	19.7	17.791	17.11	16.834	16.736	16.687	15.8	15.7	15.1
J2200+5822	2199371701965748992	DA	26.2 (0.1)	···	17.76	17.309	17.129	17.08	17.06	16.22	15.98	15.86
J2201+0219	2683345934175922176	DZ	15.7 (0.4)	22.3	19.66	19.074	18.854	18.79	18.8	···	···	···
J2202+0237	2683452758602312192	DA	33.5 (0.2)	18.24	17.223	16.844	16.691	16.668	16.66	15.7	15.6	15.5
J2202+3848	1956112657053495296	DA	18.93 (0.04)	···	15.984	16.024	16.139	16.28	16.35	15.79	15.5	15.5
J2203+2434	1795467063268699264	DC	11.8 (0.2)	19.36	18.73	18.52	18.48	18.52	18.51	17.82	···	···
J2204−0109	2677191860220980480	DC	13.4 (0.6)	21.9	20.05	19.33	19.03	18.91	18.82	18.01	17.68	17.7
J2204−0331	2675503117734361344	DC	11.0 (0.6)	20.31	0.0	19.676	19.52	19.45	0.0	18.4	···	···
J2206+0825	2722195455261832448	DA	11.5 (0.6)	20.3	19.56	19.24	19.1	19.05	19.06	18.5	···	···
J2206−0103	2677172996724050048	DAP*	11.3 (0.5)	19.51	18.89	18.61	18.66	18.58	18.5	17.66	17.5	17.1
J2206−0112	2677157569201482624	DC	10.2 (0.9)	20.8	20.11	19.8	19.72	19.74	19.7	19.0	···	···
J2207+3428	1900382604528495744	DA	25.2 (0.04)	···	15.172	15.251	15.397	15.562	15.672	15.14	15.03	15.1
J2208+2221	1782874287875828864	DA	14.3 (0.2)	18.02	17.723	17.72	17.81	17.94	18.04	17.41	···	···
J2209+1429	2735175263041913088	DA	36.86 (0.05)	16.11	15.669	15.562	15.568	15.637	15.69	14.98	14.8	14.8
J2211+1136	2727596187657230592	DAH	14.7 (0.6)	19.53	19.28	19.31	19.38	19.48	19.6	19.1	···	···
J2212+1916	1777927516344108416	DA	9.7 (0.4)	20.0	19.4	19.22	19.187	19.2	19.28	18.6	···	···
J2212−1429	2600033326799287296	DA	26.34 (0.04)	···	15.137	15.048	15.08	15.147	15.191	14.496	14.4	14.35
J2213+0349	2707796667595813248	DC	24.7 (0.3)	19.99	18.255	17.61	17.367	17.28	17.26	16.43	16.17	16.11
J2213+2925	1894996161487458048	DA	17.6 (0.2)	18.92	18.41	18.2	18.15	18.16	18.21	17.48	···	···
J2214+0650	2720807150033137024	DC	13.0 (0.3)	19.93	19.08	18.75	18.638	18.66	18.62	···	···	···
J2214+3727	1955134710179436672	DC	34.3 (0.1)	···	17.1	16.82	16.784	16.84	16.89	16.14	16.1	15.6
J2215+3158	1898875311527105152	DA	19.7 (0.1)	17.65	17.137	16.995	16.986	17.039	17.1	16.34	16.0	15.7
J2215−0728	2619561508006403712	DA	10.3 (0.6)	20.8	19.8	19.44	19.27	19.24	19.18	18.5	···	18.3
J2217+3707	1907041590544054656	DC	49.1 (0.1)	···	17.57	16.773	16.433	16.307	16.23	15.37	15.2	15.0
J2218+0319	2706795626682842752	DA	14.6 (0.1)	17.34	16.905	16.897	16.986	17.084	17.17	16.56	16.45	16.47
J2218+2123	1778839767397091200	DQ	10.4 (0.2)	18.17	17.954	17.948	18.041	18.14	18.24	17.7	···	···

Tableau A.1 *suite page suivante*

Tableau A.1 *(suite)*

Name	Gaia DR2/EDR3*	Sp Type	ϖ (mas)	u	g	r	i	z	y	J	H	K
J2218+3908	1956838712683591296	DZ	20.7 (0.1)	16.55	16.189	16.234	16.377	16.546	16.614	16.09	···	···
J2218+4839	1999615350008375552	DA+DC*	25.2 (0.04)	···	16.186	16.036	16.026	16.08	16.11	15.41	15.3	15.3
J2218+5602	2006217676803960960	DC	25.3 (0.1)	···	18.83	18.01	17.657	17.53	17.48	16.59	16.4	16.43
J2219+1353	2734163982926890624	DC	10.1 (0.4)	19.37	18.84	18.73	18.749	18.77	18.87	···	···	···
J2219+2122	1778836056545324160	DC	18.6 (0.2)	20.27	18.42	17.708	17.434	17.32	17.28	16.41	···	16.0
J2219+4805	1987576380575220352	DA	18.4 (0.1)	···	17.9	17.62	17.527	17.51	17.53	16.79	···	···
J2219−0930	2615280147167407104	DA	10.3 (0.4)	19.9	19.32	19.14	19.12	19.18	19.22	18.5	···	···
J2220−0041	2677851743291189888	DA	13.7 (0.2)	17.92	17.47	17.383	17.401	17.456	17.45	16.8	16.6	15.7
J2220−0600	2625820512307604352	DA	12.5 (0.4)	20.3	19.35	19.03	18.92	18.9	18.9	18.13	18.0	17.8
J2221−0408	2626677723354947968	DA	16.6 (0.4)	16.85	16.441	16.443	16.543	16.66	16.71	15.9	15.81	15.76
J2223+2319	1878189370339859328	DAH	13.3 (0.2)	18.27	17.93	17.903	17.98	18.09	18.19	17.63	···	···
J2224+2158	1874951106733026048	DA	16.8 (0.1)	17.29	16.88	16.82	16.864	16.94	17.037	16.39	16.4	···
J2224+2716	1881612734154248320	DAM	16.0 (0.2)	16.98	16.572	16.64	16.76	16.56	0.0	···	···	···
J2224−1615	2595728287804350720	DAZ	18.7 (0.1)	···	16.027	16.091	16.24	16.391	16.51	15.9	15.8	15.82
J2225+1835	1777269424274555776	DC	23.3 (0.1)	17.22	16.798	16.697	16.744	16.82	16.9	16.34	···	···
J2225+3005	1894563160062140416	DA	13.0 (0.2)	18.6	18.18	18.1	18.143	18.22	18.27	17.55	···	···
J2225+6357	2205493129867600256	DC	26.3 (0.1)	···	18.04	17.44	17.213	17.15	17.12	···	···	···
J2225−0113	2629899631727265920	DA	12.8 (0.9)	21.4	19.78	19.15	18.91	18.82	18.76	17.96	17.7	17.4
J2225−0114	2629899631727265280	DA	13.8 (0.4)	19.68	18.5	18.12	17.951	17.9	17.91	17.12	16.89	17.0
J2226+0112	2702527013306504064	DC*	15.5 (0.3)	18.57	18.077	17.95	17.966	18.03	18.07	17.4	17.41	17.3
J2227+1753	2737921155893258496	DAZ	24.0 (0.1)	17.49	16.89	16.659	16.618	16.622	16.644	15.94	15.6	15.5
J2228+1207	2730508416002618752	DZ	29.5 (0.1)	16.95	16.319	16.221	16.276	16.365	16.44	15.85	15.8	15.9
J2229+2327	1875613386395668864	DA	27.4 (0.2)	20.1	18.36	17.79	17.529	17.44	17.42	16.6	16.0	···
J2229+3024	1900545847646195840	DA	11.0 (0.1)	16.66	16.17	16.303	16.44	16.54	16.52	15.52	15.22	15.02
J2229+3927	1909045549271308928	DA	17.7 (0.1)	18.59	18.036	17.865	17.839	17.87	17.92	17.21	···	···
J2230+1256	2730989658498251776	DA	23.6 (0.1)	17.63	17.159	17.067	17.06	17.124	17.16	16.48	16.3	15.7
J2230+1523	2736054627915080448	DA	26.3 (0.2)	19.61	18.114	17.605	17.436	17.36	17.36	16.51	16.3	15.9
J2230+2254	1875301369907249024	DC	32.2 (0.1)	18.19	17.31	16.962	16.839	16.797	16.823	16.1	15.7	···
J2230−0023	2630076966632012160	DA	22.7 (0.1)	15.85	15.434	15.475	15.588	15.718	15.82	15.207	15.16	15.21
J2230−0945	2609067704606647680	DA	14.5 (0.1)	18.11	17.503	17.361	17.361	17.42	17.48	16.78	16.1	16.67
J2231+0137	2702619273499003776	DA	13.3 (0.3)	19.17	18.47	18.273	18.208	18.22	18.31	17.54	17.39	17.4
J2231+0906	2711092621203766912	DZ	11.1 (0.5)	20.7	19.22	18.93	18.86	18.88	18.97	18.2	···	···
J2231−0204	2628823381642484864	DC	9.8 (0.4)	20.2	19.53	19.27	19.21	19.22	19.2	18.6	18.4	···
J2231−0902	2621138310760174592	DA	12.1 (0.3)	19.8	18.98	18.656	18.527	18.52	18.46	17.74	···	17.4

Tableau A.1 *suite page suivante*

Tableau A.1 *(suite)*

Name	Gaia DR2/EDR3*	Sp Type	ϖ (mas)	u	g	r	i	z	y	J	H	K
J2232+2155	1874375473741569664	DA	11.9 (0.3)	19.02	18.44	18.32	18.306	18.36	18.42	17.79	···	···
J2232+3205	1901175799087508608	DA	15.1 (0.2)	18.7	18.013	17.752	17.666	17.644	17.64	16.83	···	···
J2232−0744	2621565333592122496	DQ	18.3 (0.2)	18.48	18.43	17.8	17.678	17.79	17.87	17.35	···	16.8
J2234+1456	2733055335904034432	DA	29.5 (0.1)	17.54	16.779	16.515	16.432	16.424	16.431	15.67	15.3	···
J2234+5543	2006489634151514112	DA	18.2 (0.1)	···	17.435	17.26	17.229	17.256	17.31	16.56	16.34	16.32
J2235+6439	2205619397609830656	DC	14.6 (0.2)	20.74	19.38	18.85	18.63	18.56	18.54	···	···	···
J2236+5303	2002232359484482304	DC	12.1 (0.1)	···	16.786	16.89	17.059	17.209	17.31	16.81	16.79	17.4
J2237+3206	1901132845117712256	DA	12.3 (0.2)	19.68	18.93	18.714	18.635	18.65	18.65	18.09	···	···
J2238+1313	2731772377633104128	DAZ	15.7 (0.1)	17.49	17.058	16.999	17.041	17.12	17.18	16.56	16.4	15.5
J2239+0018	2654379433485461632	DC	13.8 (1.4)	21.5	19.99	19.48	19.46	19.67	···	19.7	···	···
J2239+1904	2833291244003645440	DC	10.2 (0.9)	20.8	20.02	19.76	19.64	19.65	19.7	18.9	···	···
J2239−0011	2653903963426062208	DA	11.5 (0.3)	19.27	18.79	18.69	18.701	18.74	18.73	18.2	18.0	18.0
J2240−0303	2625541412447911424	DC	19.7 (0.2)	20.5	18.88	18.3	18.047	17.98	17.94	17.02	16.6	16.7
J2241+0432	2704955971931335168	DQ	16.2 (0.2)	18.98	18.289	17.944	17.836	17.83	17.89	17.15	16.99	17.0
J2241+0801	2715786505062211840	DA	15.5 (0.2)	19.72	18.68	18.29	18.142	18.11	18.11	17.36	17.06	17.0
J2241+1332	2731866347221858432	DA	28.1 (0.2)	18.43	17.519	17.16	17.031	17.013	17.02	16.2	···	···
J2241+3646	1904585689586580736	DA	19.2 (0.1)	···	17.205	17.066	17.053	17.108	17.16	16.43	16.2	16.98
J2241−1940	2400975126071250944	DC	10.2 (0.4)	···	19.86	19.47	19.23	19.2	19.15	18.4	···	18.1
J2242+0048	2654423998066862464	DC	19.0 (0.3)	21.8	19.47	18.65	18.303	18.19	18.26	18.06	18.7	19.2
J2242+1403	2731922422315395968	DA	12.0 (0.2)	18.16	17.72	17.651	17.671	17.753	17.8	17.17	···	···
J2243−0127	2652784694950778624	DA	18.2 (0.1)	16.67	16.23	16.245	16.346	16.463	16.55	15.93	15.86	15.91
J2244+1305	2731591469315403520	DA	9.9 (0.3)	19.05	18.45	18.218	18.154	18.2	18.22	17.49	···	···
J2244+1513	2732515029018125312	DA	17.1 (0.2)	19.45	18.37	17.97	17.82	17.786	17.78	···	···	···
J2244+3835	1929002200706278144	DC	15.2 (0.3)	···	19.49	18.86	18.6	18.51	18.5	17.6	···	···
J2245−1002	2608247533357159424	DA	17.6 (0.2)	17.38	17.021	17.022	17.08	17.2	17.26	16.63	···	16.57
J2248+0436	2705188999676567936	DA	11.9 (0.1)	17.33	16.952	17.02	17.143	17.27	17.402	16.85	16.72	16.8
J2249+2236	2836609093355562496	DA	56.1 (0.1)	14.719	14.385	14.47	14.609	14.762	14.912	14.32	14.32	14.4
J2249+3623	1903614958258305536	DA	23.0 (0.1)	···	18.6	17.994	17.753	17.67	17.65	16.6	16.2	17.12
J2249−0608	2611836167511100800	DC	10.1 (0.9)	19.9	19.44	19.43	19.36	19.35	19.35	18.7	18.6	···
J2250+0351	2656959231361709056	DA	12.4 (0.3)	19.69	18.97	18.73	18.63	18.64	18.65	18.0	17.6	17.8
J2251+2939	1884744525522874880	DA	51.5 (0.1)	···	15.75	15.35	15.17	15.13	15.12	14.23	13.98	13.87
J2251−1015	2605271846869877632	DA	19.6 (0.2)	18.98	18.057	17.773	17.613	17.58	17.5	16.72	···	16.52
J2252+3928	1929287700069881856	DC	25.3 (0.1)	···	18.54	17.89	17.633	17.531	17.46	16.5	···	···
J2253+8130	2286958798223194624	DC	26.7 (0.1)	···	18.01	17.52	17.08	17.242	16.99	15.7	···	···

Tableau A.1 *suite page suivante*

Tableau A.1 *(suite)*

Name	Gaia DR2/EDR3*	Sp Type	ϖ (mas)	u	g	r	i	z	y	J	H	K
J2253−0647	2611561706216413696	DZ	117.15 (0.05)	19.64	16.321	15.335	15.023	14.918	14.863	14.01	13.68	13.5
J2253−1438	2410908771246898176	DC :	27.3 (0.1)	···	17.985	17.48	17.288	17.21	17.22	16.33	16.3	16.05
J2254+1323	2719852224183359360	DC	21.8 (0.2)	21.7	19.349	18.5	18.128	18.0	17.95	17.04	16.88	16.85
J2255+0545	2711324446359728384	DA	40.4 (0.1)	17.36	16.391	16.039	15.911	15.85	15.81	15.066	14.82	14.8
J2255−0750	2610488514148351360	DA	27.8 (0.1)	17.24	16.555	16.367	16.321	16.31	16.37	15.59	15.3	15.38
J2256+3735	1928174375826595072	DA :*	16.7 (0.1)	···	16.429	16.513	16.673	16.832	16.95	16.43	16.1	···
J2257+1205	2718818202217242240	DC	13.1 (0.5)	20.2	19.26	18.9	18.8	18.77	18.78	18.09	17.8	17.6
J2257+1921	2831963931606829312	DA	15.1 (0.1)	17.28	16.88	16.868	16.935	17.042	17.13	16.52	···	···
J2257+5130	1989342372349280384	DA	27.35 (0.05)	···	16.91	16.69	16.772	16.79	16.84	16.2	···	···
J2258+6430	2208752769527485568	DA	15.6 (0.1)	17.71	17.326	17.25	17.263	17.31	17.37	16.6	···	···
J2258−0054	2651505207011569152	DC	11.9 (0.5)	22.2	20.06	19.477	19.22	19.14	19.25	18.34	18.1	18.1
J2259+5717	2010066242392545792	DA	17.6 (0.2)	···	18.84	18.27	18.04	18.0	17.92	17.17	15.93	15.2
J2259−0828	2607380156121387648	DAH	14.3 (0.2)	19.75	18.885	18.57	18.462	18.45	18.47	17.59	···	17.4
J2300+2204	2835805586577740288	DZ	16.4 (0.1)	17.99	17.49	17.409	17.45	17.547	17.61	17.04	···	···
J2300+6408	2208530698238308736	DC	27.5 (0.1)	20.7	18.68	17.919	17.59	17.47	17.43	···	···	···
J2301+2323	2842112183412398336	DA	19.3 (0.1)	16.18	16.039	16.14	16.299	16.452	16.58	16.03	···	···
J2301+4056	1930213488860610176	DA	14.2 (0.1)	···	16.69	16.757	16.86	17.014	17.09	16.53	···	···
J2302+2430	2843077206728009472	DQ	13.8 (0.2)	18.62	18.14	17.99	17.97	18.02	18.08	17.46	···	···
J2302+4312	1931838292168404480	DA	19.1 (0.1)	···	16.588	16.525	16.565	16.642	16.7	16.05	16.0	17.03
J2303+4632	1936315366080098432	DC	25.3 (0.2)	···	19.04	18.29	17.97	17.87	17.83	16.96	···	···
J2304+2415	2842312874347797632	DZ	11.5 (0.3)	22.2	19.77	19.18	19.07	19.09	19.08	18.3	···	···
J2304−0701	2634608741244388096	DC	18.1 (0.5)	22.2	19.75	18.97	18.6	18.48	18.41	17.47	17.3	17.1
J2304−0701	2634608741244966016	DC	18.2 (0.1)	17.61	17.19	17.11	17.155	17.246	17.28	16.69	16.6	16.5
J2305+3922	1929838143078434432	DC	28.1 (0.1)	···	18.21	17.77	17.88	18.25	18.45	18.3	···	···
J2305+4334	1931870929622075008	DC	21.2 (0.1)	···	18.81	18.11	17.831	17.74	17.67	16.83	16.04	16.47
J2307+0821	2713617271700011008	DC	10.6 (0.5)	20.2	19.4	19.15	19.11	19.12	19.25	···	···	···
J2307+1400	2815415285174565248	DC*	12.2 (0.3)	20.09	19.13	18.757	18.63	18.61	18.59	17.82	17.46	17.48
J2308+0553	2663502184540697856	DA	13.1 (0.4)	20.03	19.13	18.768	18.67	18.64	18.65	17.91	17.7	17.8
J2308+2414	2842462137347560320	DC	25.2 (0.2)	20.5	18.49	17.803	17.54	17.44	17.39	16.5	···	···
J2309+5506	1996725077535283200	DA	60.91 (0.04)	···	16.036	15.597	15.423	15.387	15.334	14.27	13.9	13.9
J2309−0705	2631652528139944832	DA	13.3 (0.2)	17.86	17.31	17.274	17.3	17.37	17.4203	16.61	16.67	16.6
J2310−0243	2638053472519840256	DC	11.2 (0.3)	19.62	18.98	18.76	18.69	18.75	18.85	18.2	18.0	17.7
J2310−2948	6605335899369392128	DA	15.1 (0.1)	···	17.11	17.044	17.06	17.12	17.2	16.53	16.1	16.4
J2312+1310	2812250821990695936	DA :	31.4 (0.1)	19.18	17.67	17.111	16.88	16.8	16.78	15.9	15.5	15.3

Tableau A.1 *suite page suivante*

Tableau A.1 *(suite)*

Name	Gaia DR2/EDR3*	Sp Type	ϖ (mas)	u	g	r	i	z	y	J	H	K
J2312+2133	2838537563735201664	DA	12.3 (0.2)	19.94	19.02	18.67	18.54	18.53	18.56	···	···	···
J2312−0030	2651072927142789632	DA	13.8 (0.5)	20.9	19.84	19.51	19.37	19.36	19.35	18.4	18.7	18.2
J2312−2722	2379201119352265472	DA :	13.6 (0.1)	···	16.98	17.039	17.174	17.331	17.43	16.9	···	16.9
J2314+0109	2657451056656635648	DA	11.0 (0.2)	18.33	17.84	17.784	17.813	17.88	17.95	17.33	17.1	17.2
J2314+2333	2839397832801325952	DA :*	14.5 (0.1)	17.49	16.934	16.768	16.751	16.79	16.81	16.2	16.0	15.7
J2314−0632	2631876970245863552	DQ	38.7 (0.1)	15.8	15.438	15.365	15.432	15.52	15.61	14.981	14.93	14.89
J2315+6831	2214678175128464256	DA	22.9 (0.04)	···	16.046	16.038	16.126	16.234	16.33	15.9	15.8	15.4
J2315−0209	2638553754605793408	DZ	33.6 (0.1)	17.21	16.43	16.22	16.196	16.269	16.298	15.63	15.54	15.49
J2315−1440	2407167579853954688	DA	34.67 (0.05)	···	15.56	15.557	15.632	15.754	15.85	15.22	15.1	15.0
J2316+1720	2818727009902345600	DC	15.2 (0.1)	20.3	18.43	17.758	17.49	17.39	17.34	16.47	16.6	15.6
J2316−0938	2437933525811466112	DC	10.1 (0.3)	19.3	18.85	18.74	18.77	18.86	18.91	18.3	···	18.3
J2317+1830	2818957013992481280	DZ	26.5 (0.5)	21.8	20.03	19.31	18.99	18.85	18.81	18.1	···	18.4
J2317−0840	2630264429069509888	DA	9.9 (0.2)	19.01	18.35	18.19	18.14	18.2	18.23	17.44	···	17.2
J2318+2117	2837909055400871424	DC	12.6 (0.2)	19.77	19.05	18.74	18.671	18.66	18.64	17.96	···	···
J2318+2345	2839231634746334976	DC	10.3 (0.3)	19.99	19.29	18.99	18.9	18.88	18.86	18.2	···	···
J2318+2345	2839231634746334848	DA	10.4 (0.5)	21.4	19.917	19.39	19.204	19.13	19.05	18.4	···	···
J2319−0229	2637741490390750080	DA	24.1 (0.1)	18.99	17.48	16.911	16.666	16.593	16.55	15.72	15.44	15.39
J2319−0613	2631967439437024384	DC	27.6 (0.3)	20.62	18.58	17.78	17.459	17.36	17.29	16.3	15.8	16.08
J2320+1945	2825325213544431360	DA	16.8 (0.3)	20.0	19.07	18.76	18.64	18.63	18.65	17.91	···	···
J2321+0102	2645295921252503424	DA	16.2 (0.3)	20.6	19.22	18.82	18.642	18.584	18.61	17.84	17.62	17.8
J2321+0102	2645295955612242688	DC	15.9 (0.4)	21.7	19.7	18.97	18.65	18.523	18.52	17.63	17.36	17.4
J2321+5511	1996831828951826176	DA	13.6 (0.1)	18.29	17.8	17.655	17.633	17.68	17.75	16.95	···	···
J2321+6925	2214973561500636544	DC	16.0 (0.1)	17.96	17.608	17.49	17.545	17.675	17.73	···	···	···
J2321−1327	2408844399510334464	DC	12.6 (0.4)	···	19.03	18.63	18.52	18.5	18.56	17.83	···	17.6
J2322+0946	2762076666146759040	DC :	13.7 (0.3)	19.93	18.92	18.53	18.37	18.34	18.25	17.58	17.3	17.1
J2323+1135	2810953668852136064	DA	12.9 (0.3)	19.31	18.729	18.546	18.479	18.51	18.54	17.87	17.68	17.8
J2323+7255	2228616684031896192	DA	20.2 (0.1)	17.57	16.53	16.428	16.426	16.494	16.55	15.8	15.8	16.16
J2324+2835	2869130517001766400	DA	25.5 (0.1)	16.97	16.474	16.322	16.32	16.353	16.38	15.68	15.2	15.4
J2324+3014	2870129010998688512	DA	11.9 (0.1)	18.0	17.56	17.5	17.526	17.62	17.68	17.05	···	···
J2324−0216	2637627549202579328	DAZ	12.2 (0.2)	19.27	18.53	18.29	18.219	18.22	18.24	17.46	17.4	17.1
J2325+0949	2762042070184969216	DC :	9.9 (0.3)	19.17	18.67	18.538	18.554	18.64	18.67	18.2	18.0	17.9
J2325+1403	2813020961166816512	DA	42.3 (0.1)	18.04	16.70	15.772	15.54	15.464	15.423	14.51	14.37	14.4
J2325+2511	2841283151645302272	DA	10.1 (0.1)	17.55	17.15	17.201	17.31	17.38	17.31	16.95	···	···
J2325+2552	2841348430852439680	DA	21.5 (0.1)	18.11	17.23	16.86	16.71	16.69	16.68	15.85	15.4	15.5

Tableau A.1 *suite page suivante*

Tableau A.1 *(suite)*

Name	Gaia DR2/EDR3*	Sp Type	ϖ (mas)	u	g	r	i	z	y	J	H	K
J2325−0936	2437760730687096192	DA	10.1 (0.2)	18.35	17.85	17.8	17.841	17.93	18.0	17.36	···	17.1
J2326+1600	2814629409239942272	DC	29.5 (0.1)	15.172	15.07	15.167	15.316	15.458	15.58	15.05	14.9	14.9
J2327+0415	2659860636389069312	DA	13.5 (0.2)	18.42	17.9	17.755	17.73	17.782	17.79	17.1	16.92	16.9
J2327+1444	2813447365520332672	DA	9.9 (0.2)	18.25	17.83	17.788	17.867	17.954	18.04	17.45	17.2	17.6
J2327+2638	2841680934336159104	DC	21.8 (0.2)	20.6	18.92	18.24	18.0	17.91	17.86	17.0	···	···
J2327+2638	2841680934336158976	DA	21.7 (0.1)	18.49	17.82	17.6	17.535	17.56	17.6	16.84	···	···
J2328+7059	2227233773282607488	DA	11.3 (0.1)	18.85	17.32	17.28	17.36	17.46	17.52	···	···	···
J2329+0047	2645449715440904960	DA	14.6 (0.2)	19.26	18.53	18.23	18.127	18.14	18.12	17.36	17.22	17.0
J2329+6159	2015698348961991552	DC	18.9 (0.1)	···	18.02	17.78	17.699	17.73	17.81	···	···	···
J2330+0028	2644672498158933248	DC	16.9 (0.4)	22.1	19.74	18.98	18.63	18.5	18.42	17.63	17.36	17.32
J2330+0100	2645480299903701504	DA	22.0 (0.1)	18.14	17.505	17.27	17.23	17.233	17.22	16.5	16.31	16.23
J2330+0120	2645509810623287552	DC	17.5 (0.2)	18.58	17.94	17.71	17.64	17.676	17.706	16.96	16.84	16.8
J2331+3001	2869685285040721536	DA	10.3 (0.4)	20.05	19.34	19.15	19.09	19.09	19.1	18.4	···	···
J2332+2658	2865535629374939520	DAH	34.3 (0.1)	15.73	15.341	15.402	15.521	15.67	15.766	15.17	15.1	15.0
J2332+3353	2872712618509070080	DA	10.5 (0.1)	18.1	17.69	17.661	17.724	17.83	17.89	17.29	···	···
J2335+1230	2764723912188128896	DC	12.1 (0.2)	19.42	18.78	18.57	18.55	18.63	18.61	18.1	18.3	···
J2336+3252	2872373629627611520	DA	17.2 (0.2)	18.64	18.08	17.9	17.86	17.91	17.95	17.25	···	···
J2337+0032	2645946252315491200	DA	19.3 (0.2)	19.26	18.198	17.803	17.642	17.61	17.6	16.78	16.49	16.51
J2338+0627	2756665763266917888	DA	10.7 (0.6)	19.92	19.16	18.91	18.82	18.82	18.82	18.1	18.0	17.8
J2338+2101	2826254713186397440	DA	25.4 (0.1)	19.62	18.14	17.648	17.45	17.37	17.28	16.51	16.2	15.14
J2338+3101	2871162547632415744	DA	10.5 (0.3)	19.69	18.99	18.78	18.698	18.69	18.7	18.03	···	···
J2338−1826	2393875961742886656	DA	26.8 (0.1)	···	15.614	15.549	15.57	15.64	15.697	15.06	14.9	14.7
J2339+2843	2866228901519900544	DA	13.0 (0.3)	20.1	19.17	18.83	18.69	18.69	18.67	17.82	···	···
J2339+4919	1943422948539962240	DC	10.5 (0.3)	20.26	19.44	19.15	19.08	19.02	19.02	18.5	···	···
J2339+5316	1993289138054372480	DA	23.0 (0.1)	···	17.29	17.02	16.93	16.93	16.97	16.19	15.48	15.6
J2340+4357	1925701917774697344	DA	13.5 (0.1)	17.69	17.275	17.269	17.349	17.43	17.51	16.94	···	···
J2342+0950	2760011096114471040	DA	11.6 (0.4)	19.63	18.93	18.71	18.66	18.67	18.69	17.97	18.0	17.5
J2342−1001	2435433202010203264	DA	20.3 (0.2)	20.7	18.81	18.227	17.961	17.87	17.82	17.1	16.9	16.8
J2343+0837	2759588063311504768	DA	17.5 (0.1)	18.1	17.5	17.3	17.243	17.274	17.28	16.56	16.42	16.33
J2343+1309	2764079838893099136	DC :	9.8 (0.3)	19.64	19.16	19.12	19.13	19.07	18.96	18.4	18.2	···
J2343+4725	1939308236730745472	DC	19.2 (0.1)	19.46	18.34	17.931	17.772	17.74	17.67	16.91	···	···
J2343−1659	2394366515727615104	DZ	40.3 (0.2)	···	17.66	17.094	16.882	16.8	16.79	15.95	16.0	15.63
J2344+1429	2771071908211662464	DA	11.9 (0.3)	21.3	19.77	19.18	18.98	18.9	18.87	18.1	18.0	17.6
J2346+1158	2763719512612656000	DC	27.5 (0.1)	18.26	17.415	17.13	17.039	17.044	17.038	16.34	16.21	16.14

Tableau A.1 *suite page suivante*

Tableau A.1 *(suite)*

Name	Gaia DR2/EDR3*	Sp Type	ϖ (mas)	u	g	r	i	z	y	J	H	K
J2346+2728	2865060636057386112	DA	11.4 (0.3)	19.55	18.78	18.49	18.38	18.4	18.37	17.56	···	···
J2347+0223	2646617809106367360	DA	14.4 (0.3)	20.03	18.49	17.913	17.71	17.63	17.58	16.73	16.39	16.41
J2347+0304	2742789930821144320	DC	39.7 (0.1)	19.13	17.16	16.525	16.296	16.218	16.207	15.5	15.71	16.33
J2347+0656	2744932943406490112	DA	10.6 (0.5)	20.1	19.5	19.25	19.2	19.2	19.22	18.3	18.4	18.0
J2348+4300	1922778419431649280	DC	18.9 (0.1)	20.31	18.52	17.818	17.5	17.41	17.39	16.49	15.9	15.7
J2349+1423	2770647462363429376	DC	15.0 (0.2)	19.71	18.84	18.472	18.333	18.32	18.3	17.56	17.4	17.5
J2349+2933	2867032958053059200	DA	47.7 (0.1)	16.88	15.96	15.61	15.47	15.412	15.424	14.609	14.34	14.2
J2350−0846	2436043980719301504	DA	16.3 (0.3)	20.4	19.02	18.582	18.4	18.37	18.36	17.52	17.27	17.19
J2351+4103	1921255247935490944	DC	10.1 (0.4)	19.47	19.01	18.91	18.93	19.02	18.9	18.4	···	···
J2351+5839	1999250788878655360	DA	13.7 (0.2)	19.4	18.7	18.39	18.251	18.24	18.26	17.46	···	···
J2352+0212	2739624711723101312	DA	11.2 (0.5)	21.3	19.92	19.41	19.21	19.14	19.13	18.4	17.7	17.8
J2352+2531	2851868317587963136	DA	9.9 (0.4)	19.39	18.96	18.92	18.959	19.08	19.1	18.6	···	···
J2352−0253	2448933731627261824	DA	33.1 (0.1)	17.18	16.98	17.066	17.21	17.369	17.49	16.95	16.91	17.0
J2353+2051	2823398800448735104	DA	17.5 (0.1)	17.23	16.674	16.536	16.533	16.583	16.63	15.89	15.9	15.6
J2354+0548	2743812644136889600	DA	11.6 (0.4)	19.38	18.63	18.36	18.263	18.25	18.26	···	17.3	17.2
J2354+4027	1921351390779081600	DQ	45.22 (0.03)	···	14.972	14.898	14.98	15.097	15.16	14.573	14.5	14.5
J2354+6522	2017484922210746368	DC	17.7 (0.3)	···	19.53	18.84	18.53	18.45	18.4	···	···	···
J2354+6522	2017484922214792576	DQ	17.3 (0.1)	···	18.156	17.78	17.634	17.66	17.68	···	···	···
J2355+2314	2848334010475644288	DC	14.7 (0.1)	16.82	16.671	16.755	16.927	17.093	17.19	16.69	16.4	···
J2355−1916	2389966854309408512	DA	14.8 (0.1)	17.19	16.77	16.779	16.857	16.98	17.05	···	···	···
J2356+0537	2745244002118134400	DA	12.3 (0.2)	19.09	18.43	18.192	18.12	18.11	18.15	17.36	17.21	17.2
J2356−2054	2341622358827194880	DZ	15.4 (0.6)	···	20.9	20.48	19.27	19.03	19.0	18.2	18.3	18.0
J2357+1949	2822330113802737408	DZ	24.9 (0.1)	20.2	17.344	16.919	16.964	17.063	17.11	16.4	16.3	15.9
J2357+2602	2853372247632375040	DA	13.0 (0.1)	17.83	17.414	17.353	17.404	17.465	17.55	16.9	···	···
J2357+5057	1944042802521121024	DA	15.3 (0.2)	20.24	18.9	18.51	18.38	18.35	18.34	17.59	···	···
J2359+2733	2854727528856212992	DC	12.6 (0.5)	21.9	20.02	19.36	19.09	18.97	18.92	···	···	···

Tableau A.2 – Paramètres physiques des naines blanches de l'échantillon.

Name	Gaia DR2/EDR3*	Sp Type	$T_{\rm eff}$ (K)	$M/M_{\odot}$	$\log g$	Composition	Métaux	$\log L/L_{\odot}$	τ (Gyr)
J0000+0132	2738626591386423424	DA	10342 (32)	0.622 (0.007)	8.034 (0.008)	He/H=0	···	−2.79	0.61
J0000+1906	2774195552027050880	DC	5069 (54)	0.553 (0.055)	7.955 (0.066)	He/H=0	···	−4.00	4.86
J0001+3237	2874216647336589568	DC	5753 (56)	0.560 (0.034)	7.981 (0.041)	H/He=0	···	−3.80	3.06
J0001+3559	2877080497170502144	DC*	6177 (73)	0.688 (0.031)	8.184 (0.035)	H/He=0	···	−3.79	3.49
J0001−1111	2422442334689173376	DC	6541 (48)	0.651 (0.024)	8.124 (0.027)	log H/He=−3.2	···	−3.65	2.41
J0002+0733	2745919102257342976	DA	7727 (44)	0.598 (0.015)	8.007 (0.018)	He/H=0	···	−3.29	1.23
J0002+0733	2745919106553695616	DAH	8130 (71)	0.805 (0.017)	8.331 (0.02)	He/H=0	···	−3.39	1.90
J0002+1610	2772241822943618176	DA	6684 (42)	0.613 (0.028)	8.037 (0.033)	He/H=0	···	−3.56	1.87
J0002+6357	431635455820288128	DC	4959 (23)	0.596 (0.01)	8.026 (0.011)	He/H=0	···	−4.08	6.55
J0003+6512	432177373309335424	DC	8595 (95)	0.506 (0.014)	7.874 (0.018)	log H/He=−4.0	···	−3.04	0.82
J0003−0111	2449594087142467712	DA	5421 (34)	0.607 (0.037)	8.037 (0.043)	He/H=0	···	−3.92	3.82
J0004−0340	2447889401738675072	DA	7209 (26)	0.604 (0.007)	8.020 (0.008)	He/H=0	···	−3.41	1.50
J0005+4003	2881925666956510848	DZA	8979 (95)	0.607 (0.012)	8.048 (0.014)	log H/He=−4.0	log Ca/He=−10.27	−3.06	0.93
J0005+4825	393365609282766848	DA	6926 (23)	0.636 (0.006)	8.073 (0.007)	He/H=0	···	−3.51	1.80
J0006+0755	2746037712074342784	DAH	8672 (70)	0.717 (0.023)	8.194 (0.026)	He/H=0	···	−3.19	1.21
J0006+1800	2773073470346643200	DQ	7405 (41)	0.500 (0.009)	7.869 (0.012)	H/He=0	log C/He=−6.00	−3.30	1.19
J0006−0505	2444446482939165824	DA	7097 (58)	0.687 (0.031)	8.153 (0.034)	He/H=0	···	−3.52	1.91
J0007+1230	2766234439302571904	DC	4804 (9)	0.594 (0.005)	8.042 (0.005)	H/He=0	···	−4.15	6.57
J0007+3403	2875903332533220992	DC	5567 (15)	0.669 (0.006)	8.157 (0.006)	H/He=0	···	−3.96	5.22
J0007+3947	383108338321272448	DC	4759 (12)	0.201 (0.003)	7.046 (0.007)	He/H=0	···	−3.64	2.42
J0007−0307	2448308212589610240	DA :	5589 (43)	0.899 (0.02)	8.482 (0.022)	He/H=0	···	−4.14	6.96
J0008−0353	2445187691214892416	DC	5992 (49)	0.624 (0.032)	8.084 (0.035)	log H/He=−3.0	···	−3.79	3.22
J0008−1435	2417481205081646592	DA	6534 (30)	0.341 (0.012)	7.499 (0.021)	He/H=0	···	−3.31	1.03
J0009+3108	2861792754354276352	DC	7885 (45)	0.550 (0.008)	7.955 (0.01)	log H/He=−3.8	···	−3.23	1.14
J0010−2021	2364836107306975872	DA	10138 (51)	0.565 (0.008)	7.938 (0.01)	He/H=0	···	−2.77	0.56
J0011+2824	2859908324567852416	DC	8405 (78)	0.534 (0.015)	7.925 (0.019)	log H/He=−4.0	···	−3.11	0.93
J0011+4240	384636109728592768	DA	7068 (20)	0.590 (0.004)	7.997 (0.004)	He/H=0	···	−3.44	1.52
J0011−0827	2429268309033277184	DC	8674 (85)	0.666 (0.024)	8.143 (0.027)	log H/He=−4.0	···	−3.17	1.16
J0011−0903	2429183303040388992	DA	6181 (32)	0.543 (0.011)	7.922 (0.013)	He/H=0	···	−3.63	1.92
J0012+5025	395234439752169344	DAH	6470 (17)	0.748 (0.004)	8.249 (0.004)	He/H=0	···	−3.74	3.35
J0013+0019	2545505281002947200	DA	9507 (22)	0.591 (0.004)	7.986 (0.004)	He/H=0	···	−2.91	0.71
J0013+5438	420531621029108608	DC	4047 (45)	0.414 (0.016)	7.709 (0.023)	He/H=0	···	−4.27	6.34

Tableau A.2 *suite page suivante*

Tableau A.2 *(suite)*

Name	Gaia DR2/EDR3*	Sp Type	$T_{\rm eff}$ (K)	$M/M_{\odot}$	$\log g$	Composition	Métaux	$\log L/L_{\odot}$	τ (Gyr)
J0013−0213	2541549062071571968	DC	4615 (23)	0.539 (0.012)	7.936 (0.014)	He/H=0	···	−4.16	6.83
J0014+1503	2768536949794022656	DA	6920 (87)	0.959 (0.043)	8.568 (0.053)	He/H=0	···	−3.83	4.45
J0014−0758	2429392661221943040	DC	5725 (53)	0.651 (0.041)	8.129 (0.046)	H/He=0	···	−3.89	4.47
J0014−1311	2418116963320446720	DAH	5937 (21)	0.747 (0.006)	8.251 (0.006)	He/H=0	···	−3.89	4.38
J0015+1353	2768116146078155648	DA	8735 (53)	0.605 (0.012)	8.014 (0.015)	He/H=0	···	−3.07	0.91
J0016+0504	2741440172922171008	DA	7309 (46)	0.721 (0.028)	8.205 (0.031)	He/H=0	···	−3.50	1.97
J0017−0516	2443826805441462656	DA	5711 (20)	0.564 (0.009)	7.963 (0.011)	He/H=0	···	−3.79	2.51
J0018+0233	2548152217808246528	DQ	9313 (60)	0.625 (0.011)	8.076 (0.014)	log H/He=−4.4	···	−3.01	0.88
J0018+3055	2862337802883401856	DA	6834 (26)	0.554 (0.008)	7.936 (0.01)	He/H=0	···	−3.46	1.52
J0018+3441	2876148734080688256	DA	7402 (56)	0.572 (0.017)	7.964 (0.021)	He/H=0	···	−3.34	1.29
J0019+1414	2768190500551905408	DC*	7903 (59)	0.623 (0.023)	8.076 (0.026)	log H/He=−3.8	···	−3.30	1.34
J0019−1114	2424913628807069056	DC	8192 (76)	0.635 (0.022)	8.095 (0.025)	log H/He=−3.8	···	−3.25	1.25
J0020+0011	2545305410405677312	DA	7091 (59)	0.655 (0.027)	8.103 (0.03)	He/H=0	···	−3.49	1.77
J0020+0044	2546887573277984256	DA	8921 (48)	0.895 (0.008)	8.465 (0.009)	He/H=0	···	−3.32	1.99
J0020−1115	2424915789174828160	DA	6287 (59)	0.820 (0.06)	8.358 (0.067)	He/H=0	···	−3.86	4.42
J0021+1502	2792315366213367296	DAP*	7352 (41)	0.808 (0.016)	8.337 (0.017)	He/H=0	···	−3.57	2.74
J0021+2531	2855386170682263424	DA	8211 (91)	0.721 (0.014)	8.201 (0.016)	He/H=0	···	−3.29	1.41
J0021+2640	2855790657816672000	DC	4972 (21)	0.593 (0.01)	8.022 (0.01)	He/H=0	···	−4.07	6.42
J0022+4236	385105360675267840	DC	5357 (14)	0.256 (0.003)	7.332 (0.006)	H/He=0	···	−3.61	1.64
J0024+6834	529594417061837824	DC	5129 (26)	0.534 (0.011)	7.942 (0.013)	H/He=0	···	−3.98	5.01
J0024−0030	2542192757410302720	DC	4336 (54)	0.609 (0.078)	8.051 (0.088)	He/H=0	···	−4.33	9.18
J0026+3533	366241825654658176	DA	8621 (67)	0.647 (0.02)	8.083 (0.023)	He/H=0	···	−3.14	1.03
J0026−1037	2424880574738721408	DA	9177 (30)	0.273 (0.004)	7.262 (0.01)	He/H=0	···	−2.58	0.33
J0027+0541	2555215995900584448	DA	5633 (8)	0.584 (0.003)	7.997 (0.003)	He/H=0	···	−3.83	2.79
J0027+0554	2747384888699406080	DC	4594 (23)	0.684 (0.009)	8.182 (0.014)	log H/He=−1.61	···	−4.30	7.77
J0027−0138	2541126609088680448	DA	6005 (62)	0.710 (0.033)	8.195 (0.037)	He/H=0	···	−3.84	3.75
J0028−0029	2543515813495903488	DC	5932 (73)	0.651 (0.044)	8.127 (0.05)	log H/He=−3.0	···	−3.83	3.76
J0030+0347	2553935752048977792	DC	6132 (21)	0.510 (0.005)	7.894 (0.007)	log H/He=−3.0	···	−3.64	2.00
J0030+2421	2807036078858147584	DC	9727 (78)	0.569 (0.014)	7.981 (0.017)	log H/He=−4.4	···	−2.88	0.69
J0030+2714	2856067008897130112	DC	5838 (47)	0.633 (0.019)	8.100 (0.021)	H/He=0	···	−3.84	3.85
J0031+1845	2794904441219064448	DA	7946 (67)	0.695 (0.015)	8.163 (0.017)	He/H=0	···	−3.33	1.45
J0031+2218	2799809779202757376	DA	6095 (21)	0.641 (0.009)	8.086 (0.011)	He/H=0	···	−3.75	2.65
J0032+1434	2780050795041827968	DC	6154 (67)	0.573 (0.033)	8.000 (0.039)	log H/He=−3.0	···	−3.69	2.30
J0032−0253	2528728726428345216	DC*	4525 (6)	0.503 (0.005)	7.874 (0.006)	He/H=0	···	−4.16	6.63

Tableau A.2 *suite page suivante*

Tableau A.2 *(suite)*

Name	Gaia DR2/EDR3*	Sp Type	$T_{\rm eff}$ (K)	$M/M_{\odot}$	$\log g$	Composition	Métaux	$\log L/L_{\odot}$	τ (Gyr)
J0033+0540	2555356080553959168	DA	7074 (41)	0.623 (0.015)	8.050 (0.018)	He/H=0	···	−3.46	1.65
J0033+1451	2780434524599787136	DQ*	5821 (21)	0.524 (0.014)	7.920 (0.017)	H/He=0	log C/He=−7.20	−3.75	2.53
J0033+2506	2807462655009880320	DA	6191 (19)	0.572 (0.006)	7.972 (0.007)	He/H=0	···	−3.65	2.06
J0033+4444	388602146952607360	DA	10005 (46)	0.583 (0.011)	7.970 (0.013)	He/H=0	···	−2.81	0.61
J0034+0640	2555713215673881856	DA	5329 (43)	0.637 (0.028)	8.087 (0.032)	He/H=0	···	−3.98	4.95
J0034+1026	2751252493861856000	DA	7518 (63)	0.658 (0.022)	8.106 (0.025)	He/H=0	···	−3.39	1.53
J0034+1517	2780524585769652736	DA	6876 (27)	0.602 (0.007)	8.018 (0.008)	He/H=0	···	−3.50	1.69
J0034−1021	2425650847058388224	DC*	5666 (45)	0.709 (0.017)	8.217 (0.018)	H/He=0	···	−3.96	5.31
J0035+0011	2543230185287345664	DA	9505 (49)	0.585 (0.008)	7.977 (0.009)	He/H=0	···	−2.90	0.70
J0035+0153	2544456862306151680	DA	10811 (20)	1.046 (0.002)	8.704 (0.004)	He/H=0	···	−3.16	1.86
J0035+0958	2751172946772404224	DC	7002 (76)	0.712 (0.026)	8.217 (0.028)	log H/He=−3.4	···	−3.59	2.43
J0035+1530	2780622648462300160	DA	6095 (60)	0.758 (0.036)	8.267 (0.039)	He/H=0	···	−3.85	4.17
J0035−1718	2364319061964016512	DA	9670 (54)	0.606 (0.007)	8.012 (0.008)	He/H=0	···	−2.90	0.70
J0036+0552	2555403428272657792	DA	6869 (41)	0.612 (0.016)	8.034 (0.018)	He/H=0	···	−3.51	1.73
J0036+2422	2806614205695008256	DA	8226 (42)	0.588 (0.015)	7.987 (0.018)	He/H=0	···	−3.16	1.02
J0036−1112	2425347347488993408	DZ	7572 (31)	0.703 (0.007)	8.202 (0.008)	log H/He=−4.0	log Ca/He=−8.96	−3.45	1.79
J0038+0044	2543378511984771200	DC	5053 (66)	0.892 (0.068)	8.473 (0.077)	He/H=0	···	−4.32	9.44
J0038+3409	364978005758397952	DC	9591 (60)	0.592 (0.015)	8.021 (0.018)	log H/He=−4.4	···	−2.93	0.75
J0039+4229	381396329995329408	DA	9860 (45)	0.535 (0.009)	7.886 (0.011)	He/H=0	···	−2.79	0.57
J0040−0809	2522401586766106624	DA	6089 (31)	0.772 (0.009)	8.288 (0.01)	He/H=0	···	−3.87	4.33
J0041+3923	368639899170380672	DA	8866 (59)	0.564 (0.015)	7.944 (0.019)	He/H=0	···	−3.01	0.80
J0041+7321	536979286914485760	DQ	9447 (36)	0.494 (0.005)	7.849 (0.006)	H/He=0	log C/He=−4.43	−2.86	0.62
J0041−0226	2530119196321115776	DA	7656 (34)	0.602 (0.008)	8.013 (0.01)	He/H=0	···	−3.31	1.27
J0041−1104	2377643661128402048	DAH*	7021 (85)	0.862 (0.04)	8.419 (0.044)	He/H=0	···	−3.71	3.67
J0041−2221	2349916559152267008	DQ	5307 (7)	0.538 (0.003)	7.948 (0.003)	H/He=0	log C/He=−8.00	−3.92	4.42
J0042+2357	2803442840498734720	DA	8624 (31)	0.607 (0.012)	8.017 (0.014)	He/H=0	···	−3.10	0.94
J0043+1540	2781309637071878912	DA	6745 (35)	0.649 (0.016)	8.094 (0.018)	He/H=0	···	−3.57	2.00
J0044+0318	2550856260497950464	DA	6921 (35)	0.581 (0.012)	7.982 (0.014)	He/H=0	···	−3.46	1.57
J0044+0418	2551258990991085184	DZ	6018 (35)	0.672 (0.019)	8.159 (0.021)	log H/He=−4.0	log Ca/He=−9.84	−3.82	3.74
J0044+1518	2781085401124115328	DZ	6133 (40)	0.619 (0.057)	8.075 (0.066)	log H/He=−2.0	log Ca/He=−10.46	−3.74	2.75
J0044−2824	2342218942669916672	DC	4285 (41)	0.546 (0.038)	7.949 (0.046)	He/H=0	···	−4.29	8.06
J0045+0904	2558010366047159424	DA	7567 (66)	0.627 (0.021)	8.056 (0.024)	He/H=0	···	−3.35	1.39
J0045+1420	2776464325551066880	DZAH :*	4758 (25)	0.423 (0.017)	7.739 (0.024)	He/H=0	log Ca/H=−8.50	−4.01	4.17
J0045+1454	2781012734572656640	DA	6950 (33)	0.843 (0.011)	8.391 (0.013)	He/H=0	···	−3.70	3.60

Tableau A.2 *suite page suivante*

Tableau A.2 *(suite)*

Name	Gaia DR2/EDR3*	Sp Type	$T_{\rm eff}$ (K)	$M/M_{\odot}$	$\log g$	Composition	Métaux	$\log L/L_{\odot}$	τ (Gyr)
J0045+2527	2808103391115590016	DA*	5363 (48)	0.524 (0.048)	7.898 (0.06)	He/H=0	···	−3.87	2.80
J0045−0608	2523840155996531456	DC	4924 (22)	0.895 (0.008)	8.478 (0.01)	He/H=0	···	−4.36	9.82
J0046+0635	2556270869932443648	DZ	6641 (63)	0.561 (0.031)	7.979 (0.037)	log H/He=−4.0	log Ca/He=−11.17	−3.55	1.81
J0048−0124	2530629365419780864	DA	9264 (65)	0.722 (0.012)	8.227 (0.013)	log H/He=−3.0	···	−3.11	1.11
J0049+0522	2552928187080872832	DZ	5908 (87)	0.637 (0.021)	8.105 (0.023)	log H/He=−4.0	log Ca/He=−10.15	−3.82	3.66
J0049+1727	2782037303315690752	DC	6049 (67)	0.646 (0.048)	8.118 (0.053)	H/He=0	···	−3.79	3.34
J0049+3841	367949367212923392	DA	9830 (53)	0.589 (0.013)	7.982 (0.015)	He/H=0	···	−2.85	0.65
J0050+4010	374172980983236352	DA	9337 (75)	0.960 (0.019)	8.564 (0.022)	He/H=0	···	−3.31	2.16
J0051−2028	2356519298275043200	DA	4988 (14)	0.576 (0.007)	7.994 (0.008)	He/H=0	···	−4.05	5.95
J0052+0453	2552643413569299968	DA	6854 (60)	0.807 (0.031)	8.337 (0.034)	He/H=0	···	−3.69	3.38
J0052−3036	5031709119620238336	DA	6262 (39)	0.206 (0.004)	7.061 (0.014)	He/H=0	···	−3.17	0.68
J0053+3927	368075574827351168	DA	7577 (33)	0.586 (0.007)	7.988 (0.009)	He/H=0	···	−3.31	1.26
J0054+1412	2777751372630874112	DC	6178 (55)	0.658 (0.037)	8.137 (0.042)	log H/He=−3.0	···	−3.76	3.15
J0054+2256	2803596046661176576	DA	9522 (74)	0.990 (0.008)	8.613 (0.01)	He/H=0	···	−3.31	2.25
J0054+4156	375131415820709632	DA	7618 (16)	0.236 (0.001)	7.152 (0.006)	He/H=0	···	−2.86	0.46
J0054−0952	2473754897386327808	DA	9449 (44)	0.668 (0.009)	8.115 (0.01)	He/H=0	···	−3.00	0.86
J0055+0850	2581058706745690752	DQ	6841 (43)	0.604 (0.026)	8.049 (0.029)	H/He=0	log C/He=−6.50	−3.53	1.84
J0055+1010	2582335342824976768	DA	6286 (11)	0.624 (0.003)	8.057 (0.004)	He/H=0	···	−3.67	2.26
J0055+1804	2788048780061707520	DA	6546 (38)	0.591 (0.028)	8.002 (0.033)	He/H=0	···	−3.57	1.87
J0055+3847	367799116372410752	DC	5166 (18)	0.201 (0.006)	7.094 (0.019)	H/He=0	···	−3.54	2.07
J0055+5948	426122397136335872	DC	4673 (16)	0.510 (0.007)	7.884 (0.008)	He/H=0	···	−4.11	6.13
J0055−1127	2472557872820632320	DA	7028 (38)	0.586 (0.007)	7.990 (0.009)	He/H=0	···	−3.44	1.53
J0056+4347	377196947196848128	DC	6649 (35)	0.709 (0.013)	8.214 (0.014)	log H/He=−3.2	···	−3.68	2.88
J0056−0614	2524394000619171840	DA	6069 (59)	0.696 (0.036)	8.172 (0.041)	He/H=0	···	−3.80	3.42
J0057+1756	2787939447373738880	DA	6260 (25)	0.798 (0.01)	8.325 (0.011)	He/H=0	···	−3.84	4.26
J0058+0639	2577467770489127296	DA	8975 (62)	0.617 (0.017)	8.032 (0.02)	He/H=0	···	−3.04	0.87
J0059+1623	2784445680457082368	DA	6801 (47)	0.606 (0.015)	8.025 (0.018)	He/H=0	···	−3.52	1.75
J0101−0252	2532236546477272192	DC	7668 (45)	0.652 (0.014)	8.123 (0.015)	log H/He=−3.6	···	−3.38	1.53
J0103+0008	2536332154276141696	DA	6757 (38)	0.514 (0.023)	7.866 (0.029)	He/H=0	···	−3.44	1.42
J0103+0504	2552121179905893888	DA	8094 (13)	0.337 (0.002)	7.472 (0.004)	He/H=0	···	−2.92	0.59
J0103+1401	2777098984278522752	DC	4887 (29)	0.538 (0.019)	7.932 (0.023)	He/H=0	···	−4.05	5.72
J0103−0325	2531407858307339264	DA	9010 (34)	0.658 (0.008)	8.100 (0.009)	He/H=0	···	−3.07	0.95
J0103−0522	2524879812959998592	DA*	8499 (59)	1.279 (0.003)	9.247 (0.008)	log H/He=−1.5	···	−4.03	2.51
J0103−2444	2344901720977366528	DC	9838 (40)	0.504 (0.009)	7.866 (0.011)	log H/He=−4.6	···	−2.80	0.57

Tableau A.2 *suite page suivante*

Tableau A.2 *(suite)*

Name	Gaia DR2/EDR3*	Sp Type	$T_{\rm eff}$ (K)	$M/M_{\odot}$	$\log g$	Composition	Métaux	$\log L/L_{\odot}$	τ (Gyr)
J0104+2119	2790494815860044544	DA	5352 (20)	0.849 (0.008)	8.408 (0.009)	He/H=0	···	−4.17	7.80
J0104+2120	2790494850219788160	DC	4832 (24)	0.683 (0.01)	8.163 (0.012)	He/H=0	···	−4.20	8.59
J0104−0350	2531326283993100416	DA	5280 (18)	0.774 (0.009)	8.296 (0.009)	He/H=0	···	−4.12	7.45
J0105−0614	2476711101899811456	DA	6141 (49)	0.523 (0.027)	7.886 (0.035)	He/H=0	···	−3.62	1.86
J0105−0920	2473296504116465408	DA	8202 (50)	0.620 (0.011)	8.041 (0.013)	He/H=0	···	−3.20	1.11
J0106+0148	2538286403050847232	DA	8329 (39)	0.376 (0.009)	7.567 (0.015)	He/H=0	···	−2.92	0.61
J0106+3930	371070026026145792	DA	9952 (41)	0.496 (0.006)	7.813 (0.007)	He/H=0	···	−2.73	0.51
J0106+6119	522518883651891584	DC	4382 (23)	0.439 (0.013)	7.756 (0.017)	He/H=0	···	−4.15	5.79
J0107+0102	2537913801752406400	DQ	6554 (28)	0.574 (0.023)	8.000 (0.027)	H/He=0	log C/He=−6.60	−3.58	1.92
J0107+2107	2790417540424293120	DAZ	7404 (169)	1.028 (0.037)	8.700 (0.05)	He/H=0	log Ca/H=−7.50	−3.82	3.71
J0107+2650	306779618349361920	DZH*	5151 (18)	0.641 (0.025)	8.114 (0.027)	log H/He=−4.0	log Ca/He=−9.50	−4.07	6.21
J0108+7600	563004280465719040	DA	6031 (24)	0.573 (0.009)	7.974 (0.01)	He/H=0	···	−3.70	2.21
J0109+3300	313967881773971840	DA	6064 (53)	0.759 (0.034)	8.269 (0.037)	He/H=0	···	−3.86	4.24
J0109+3435	314956480167069696	DA	7061 (40)	0.894 (0.012)	8.467 (0.014)	He/H=0	···	−3.73	3.87
J0109−1042	2469900005324049280	DC	5070 (33)	0.607 (0.019)	8.042 (0.021)	He/H=0	···	−4.05	6.07
J0109−1042	2469900009618822656	DA	8233 (36)	0.526 (0.008)	7.880 (0.01)	He/H=0	···	−3.10	0.89
J0110+1239	2583892972844696448	DC	6641 (36)	0.828 (0.024)	8.392 (0.026)	log H/He=−3.2	···	−3.79	3.81
J0110+1439	2591091789004351104	DA	9345 (47)	0.970 (0.007)	8.581 (0.008)	He/H=0	···	−3.32	2.23
J0110+2758	307323228064848512	DA	5972 (23)	0.301 (0.006)	7.401 (0.013)	He/H=0	···	−3.42	1.16
J0110−1020	2469937908410307328	DC	7528 (56)	0.567 (0.012)	7.986 (0.014)	log H/He=−3.6	···	−3.33	1.33
J0111+2204	2790884008232725632	DA	8918 (52)	0.952 (0.009)	8.553 (0.011)	He/H=0	···	−3.38	2.41
J0112+3438	320903154445635456	DA	8882 (57)	0.608 (0.014)	8.019 (0.016)	He/H=0	···	−3.05	0.88
J0113+0603	2576622898882026624	DC	7859 (66)	0.846 (0.022)	8.416 (0.024)	log H/He=−3.8	···	−3.51	2.59
J0113+2558	294798377579784832	DC	4523 (38)	0.296 (0.036)	7.435 (0.067)	He/H=0	···	−3.95	3.01
J0113+3307	313996228559363840	DA	5961 (44)	0.535 (0.028)	7.910 (0.036)	He/H=0	···	−3.69	2.08
J0113−0510	2482721857094021760	DA	6786 (48)	0.815 (0.028)	8.350 (0.032)	He/H=0	···	−3.72	3.58
J0115+1227	2583651904920127232	DA	6027 (29)	0.541 (0.022)	7.920 (0.027)	He/H=0	···	−3.67	2.05
J0115+1435	2590924250920129920	DA	6512 (49)	0.735 (0.02)	8.230 (0.022)	He/H=0	···	−3.72	3.13
J0115+4733	401529105161219968	DZ	6495 (63)	0.725 (0.049)	8.238 (0.054)	log H/He=−3.0	log Ca/He=−10.88	−3.73	3.26
J0115−0133	2533575369771883648	DA	5318 (29)	0.665 (0.01)	8.131 (0.01)	He/H=0	···	−4.01	5.54
J0115−0146	2532059009708732288	DA	8055 (49)	0.603 (0.016)	8.014 (0.019)	He/H=0	···	−3.22	1.11
J0116+2050	2787507098786135552	DZ	6263 (28)	0.591 (0.015)	8.030 (0.018)	log H/He=−4.0	log Ca/He=−8.87	−3.68	2.26
J0116+2346	293138458619500800	DQ	7996 (52)	0.527 (0.014)	7.915 (0.018)	H/He=0	log C/He=−5.57	−3.19	1.04
J0116−0943	2471521269578009984	DA	6392 (62)	0.778 (0.037)	8.296 (0.041)	He/H=0	···	−3.79	3.83

Tableau A.2 *suite page suivante*

Tableau A.2 *(suite)*

Name	Gaia DR2/EDR3*	Sp Type	$T_{\rm eff}$ (K)	$M/M_{\odot}$	$\log g$	Composition	Métaux	$\log L/L_{\odot}$	τ (Gyr)
J0116−1045	2470565072419060736	DA	5664 (92)	0.704 (0.055)	8.188 (0.061)	He/H=0	···	−3.94	4.52
J0117+4403	397531182099486080	DA	8896 (48)	0.594 (0.009)	7.995 (0.011)	He/H=0	···	−3.03	0.85
J0117−0439	2482813425794003200	DC :	4952 (19)	0.565 (0.011)	7.976 (0.012)	He/H=0	···	−4.05	5.92
J0117−0439	2482813430089468160	DC :	5044 (25)	0.542 (0.012)	7.936 (0.014)	He/H=0	···	−4.00	4.76
J0117−2648	5039601100551392896	DC	4922 (31)	0.606 (0.019)	8.043 (0.022)	He/H=0	···	−4.10	6.96
J0118+1610	2591754107321120896	DQ	8660 (14)	0.528 (0.002)	7.915 (0.002)	H/He=0	log C/He=−5.07	−3.05	0.85
J0119+1840	2785927684692570496	DA	6702 (45)	0.641 (0.031)	8.083 (0.036)	He/H=0	···	−3.58	1.99
J0119+2241	292790566268764288	DA	6067 (62)	0.807 (0.038)	8.340 (0.042)	He/H=0	···	−3.91	4.71
J0119+3055	310300323301763328	DC	4715 (137)	0.422 (0.071)	7.720 (0.101)	He/H=0	···	−4.01	4.03
J0119−1415	2456160271800004096	DA	5098 (21)	0.546 (0.008)	7.943 (0.01)	He/H=0	···	−3.98	4.49
J0121+0951	2579280762084084736	DC :	5898 (43)	0.579 (0.021)	8.013 (0.026)	log H/He=−3.0	···	−3.77	2.90
J0121+3440	320029150076023808	DZ	6798 (28)	0.627 (0.007)	8.086 (0.008)	log H/He=−4.0	log Ca/He=−10.85	−3.57	1.97
J0121−0038	2533742048478056448	DC	4389 (57)	0.512 (0.049)	7.891 (0.06)	He/H=0	···	−4.22	7.27
J0122+3259	316773766729205632	DC	5677 (54)	0.676 (0.027)	8.168 (0.03)	H/He=0	···	−3.93	4.93
J0123−0209	2485211533668928640	DA	5827 (17)	0.578 (0.009)	7.986 (0.01)	He/H=0	···	−3.77	2.45
J0123−2748	5036250613743304192	DC	4502 (74)	0.508 (0.045)	7.882 (0.056)	He/H=0	···	−4.17	6.79
J0124+4023	372111985092019840	DA	5237 (16)	0.638 (0.007)	8.091 (0.007)	He/H=0	···	−4.02	5.59
J0124−1959	2353801065013205504	DA	7537 (52)	0.688 (0.013)	8.153 (0.014)	He/H=0	···	−3.41	1.64
J0124−2229	5043015122810735744	DZ	9145 (116)	0.694 (0.013)	8.185 (0.015)	log H/He=−4.0	log Ca/He=−9.40	−3.11	1.07
J0125−0417	2482521745974836352	DC	5190 (48)	0.620 (0.057)	8.062 (0.065)	He/H=0	···	−4.02	5.54
J0125−2600	5037084872486444928	DC	6846 (32)	0.692 (0.006)	8.187 (0.006)	log H/He=−3.4	···	−3.61	2.43
J0126−0840	2477282538708615680	DA	7982 (46)	0.589 (0.019)	7.991 (0.022)	He/H=0	···	−3.22	1.11
J0127+7328	535482641132742400	DA	6772 (75)	0.443 (0.019)	7.728 (0.028)	He/H=0	···	−3.37	1.20
J0128−0045	2485921779525500288	DA	5715 (14)	0.560 (0.007)	7.957 (0.008)	He/H=0	···	−3.79	2.48
J0128−0822	2477317211979980544	DA	6747 (154)	0.704 (0.055)	8.181 (0.062)	He/H=0	···	−3.62	2.40
J0129+1022	2585189473147457408	DA	8449 (13)	0.340 (0.002)	7.475 (0.003)	He/H=0	···	−2.84	0.53
J0129+3459	317446015009891328	DC	6052 (91)	0.751 (0.049)	8.279 (0.052)	H/He=0	···	−3.88	4.46
J0130+4414	396963005168870528	DZA	4998 (18)	0.555 (0.009)	7.977 (0.011)	He/H=0	log Ca/H=−9.70	−4.04	5.67
J0131+3147	315687277442204672	DA	7831 (60)	0.602 (0.016)	8.013 (0.019)	He/H=0	···	−3.27	1.20
J0132+0529	2564945432560219008	DAZ*	7355 (41)	0.562 (0.02)	7.977 (0.024)	He/H=0	log Ca/H=−7.44	−3.37	1.40
J0132+4604	398672715686799488	DA	10520 (46)	0.630 (0.005)	8.047 (0.006)	He/H=0	···	−2.77	0.59
J0135+0851	2572713104253752448	DA	6297 (72)	0.739 (0.036)	8.237 (0.039)	He/H=0	···	−3.78	3.56
J0135+1302	2586182156053386240	DZ	5878 (66)	0.599 (0.042)	8.045 (0.049)	log H/He=−2.0	log Ca/He=−9.25	−3.80	3.24
J0135+1445	2588874825669925504	DA	7720 (48)	0.350 (0.007)	7.510 (0.014)	He/H=0	···	−3.02	0.69

Tableau A.2 *suite page suivante*

Tableau A.2 *(suite)*

Name	Gaia DR2/EDR3*	Sp Type	$T_{\rm eff}$ (K)	$M/M_{\odot}$	$\log g$	Composition	Métaux	$\log L/L_{\odot}$	τ (Gyr)
J0137−0207	2484544095751034496	DA	7367 (32)	0.807 (0.006)	8.336 (0.008)	He/H=0	···	−3.57	2.72
J0138+1527	2589304876450784128	DA	7920 (20)	0.642 (0.004)	8.078 (0.005)	He/H=0	···	−3.28	1.28
J0138−0356	2481212193266230400	DA	10051 (33)	0.588 (0.006)	7.979 (0.008)	He/H=0	···	−2.81	0.61
J0138−0459	2480523216087975040	DA+DA	7144 (126)	0.233 (0.009)	7.154 (0.027)	He/H=0	···	−2.98	0.55
J0138−1954	5139880551029408768	DA	8533 (45)	0.952 (0.007)	8.554 (0.007)	He/H=0	···	−3.46	2.73
J0139−0629	2479327870854949248	DA	6163 (42)	0.582 (0.025)	7.989 (0.03)	He/H=0	···	−3.67	2.15
J0140+3357	317634168937635200	DZ	6420 (70)	0.622 (0.042)	8.079 (0.047)	log H/He=−4.0	log Ca/He=−10.93	−3.66	2.32
J0141+2257	290602027028411136	DZ	7829 (25)	0.669 (0.013)	8.149 (0.014)	log H/He=−3.0	log Ca/He=−7.50	−3.36	1.50
J0141+3210	303958443311053824	DC	6190 (58)	0.612 (0.033)	8.065 (0.038)	log H/He=−3.0	···	−3.72	2.56
J0142+0730	2568588664341691520	DA	5601 (17)	0.624 (0.008)	8.062 (0.008)	He/H=0	···	−3.88	3.42
J0142+2239	290531967521897856	DC*	4932 (44)	0.578 (0.033)	7.998 (0.039)	He/H=0	···	−4.07	6.34
J0143+1310	2587491678697364224	DA	8136 (46)	0.609 (0.016)	8.024 (0.018)	He/H=0	···	−3.20	1.10
J0145+2317	290678477446232960	DQ	7627 (29)	0.568 (0.009)	7.987 (0.01)	H/He=0	log C/He=−5.65	−3.31	1.29
J0145+2918	302388929117252736	DC	4687 (24)	0.473 (0.012)	7.836 (0.017)	H/He=0	···	−4.08	5.22
J0145+3132	303637562009656704	DA	8799 (27)	0.365 (0.003)	7.536 (0.006)	He/H=0	···	−2.80	0.51
J0146+1404	2587993017344962688	DC	4439 (38)	0.530 (0.042)	7.936 (0.071)	log H/He=−2.52	···	−4.23	6.49
J0146+2154	98092934167683072	DA	9151 (22)	0.784 (0.003)	8.295 (0.003)	He/H=0	···	−3.16	1.24
J0146+2213	98381792193298176	DC	7011 (77)	0.757 (0.033)	8.285 (0.035)	log H/He=−3.4	···	−3.63	2.84
J0146−0826	2465343629137442816	DQ	7347 (42)	0.570 (0.012)	7.991 (0.015)	H/He=0	log C/He=−6.43	−3.38	1.43
J0147+3019	302740016924068608	DA	9099 (102)	0.890 (0.023)	8.456 (0.026)	He/H=0	···	−3.28	1.82
J0147−2711	5025127443016406144	DA	6811 (28)	0.601 (0.007)	8.016 (0.008)	He/H=0	···	−3.51	1.72
J0148+3615	318528007466920192	DA	6095 (20)	0.624 (0.006)	8.058 (0.007)	He/H=0	···	−3.73	2.49
J0148−0555	2467788122659245696	DA	8766 (42)	0.599 (0.007)	8.003 (0.008)	He/H=0	···	−3.06	0.89
J0148−1712	5142197118950177280	DA	7614 (72)	0.591 (0.017)	7.996 (0.019)	He/H=0	···	−3.31	1.26
J0149+2400	291186211300158592	DZA*	8762 (28)	0.631 (0.005)	8.086 (0.005)	log H/He=−3.0	log Ca/He=−8.45	−3.12	1.04
J0150+1524	90367383218249472	DA	6154 (54)	0.805 (0.045)	8.337 (0.05)	He/H=0	···	−3.88	4.53
J0150+1720	91460813172927488	DC	6245 (55)	0.702 (0.027)	8.205 (0.03)	H/He=0	···	−3.78	3.48
J0151+6425	518201792978858880	DA	8561 (30)	0.631 (0.005)	8.057 (0.006)	He/H=0	···	−3.13	1.01
J0151−1112	2460778770391950848	DA	9180 (40)	0.589 (0.007)	7.985 (0.009)	He/H=0	···	−2.97	0.77
J0151−1659	5142174201004781440	DA	6696 (75)	0.318 (0.016)	7.438 (0.03)	He/H=0	···	−3.24	0.92
J0151−1957	5136313563510213760	DA	9396 (48)	0.590 (0.006)	7.985 (0.008)	He/H=0	···	−2.93	0.73
J0152+0226	2512446810350495488	DA	6767 (40)	0.587 (0.019)	7.993 (0.023)	He/H=0	···	−3.51	1.69
J0152+1436	90076974709491968	DC	6692 (42)	0.615 (0.024)	8.067 (0.027)	log H/He=−3.2	···	−3.58	2.00
J0152+2418	99064833727036160	DZ	7459 (31)	0.625 (0.009)	8.081 (0.01)	log H/He=−4.0	log Ca/He=−9.45	−3.40	1.55

Tableau A.2 *suite page suivante*

Tableau A.2 *(suite)*

Name	Gaia DR2/EDR3*	Sp Type	$T_{\rm eff}$ (K)	$M/M_{\odot}$	$\log g$	Composition	Métaux	$\log L/L_{\odot}$	τ (Gyr)
J0152+2553	297470774951165568	DA	7748 (18)	0.538 (0.004)	7.903 (0.006)	He/H=0	···	−3.22	1.06
J0153+0911	2569277680172652928	DZ :	9139 (61)	0.571 (0.011)	7.988 (0.013)	log H/He=−4.2	···	−2.99	0.82
J0153+1218	2575509780797922176	DA	7095 (71)	0.890 (0.029)	8.462 (0.033)	He/H=0	···	−3.72	3.80
J0153+1808	91980130553425536	DAH	9304 (45)	0.902 (0.007)	8.475 (0.008)	He/H=0	···	−3.25	1.78
J0153+3557	342283089327885184	DA	7189 (47)	0.809 (0.012)	8.339 (0.013)	He/H=0	···	−3.61	2.95
J0154+1403	77986298173874176	DQ	6475 (34)	0.542 (0.013)	7.947 (0.015)	H/He=0	log C/He=−6.82	−3.58	1.85
J0154+2537	297399444134124032	DAH	6849 (53)	0.752 (0.021)	8.253 (0.023)	He/H=0	···	−3.64	2.81
J0154−0426	2492027264515309696	DA	6408 (64)	0.648 (0.031)	8.094 (0.035)	He/H=0	···	−3.66	2.28
J0155+0135	2511020022215011072	DC :	7023 (59)	0.690 (0.022)	8.184 (0.024)	log H/He=−3.4	···	−3.57	2.21
J0156−0100	2505945535535013376	DC	6714 (51)	0.590 (0.033)	8.027 (0.038)	log H/He=−3.2	···	−3.56	1.87
J0157+1335	77708843286683904	DC	5055 (38)	0.554 (0.03)	7.976 (0.035)	H/He=0	···	−4.02	5.50
J0158+1238	2574848772446200960	DA	7866 (57)	0.691 (0.015)	8.156 (0.016)	He/H=0	···	−3.34	1.48
J0158+2530	105240786245136256	DC	3903 (31)	0.361 (0.013)	7.598 (0.02)	He/H=0	···	−4.28	5.85
J0159+1548	78629306318257536	DC	9147 (36)	0.668 (0.006)	8.145 (0.006)	log H/He=−4.2	···	−3.08	1.01
J0159+6858	521406968152848640	DA	7996 (78)	0.830 (0.021)	8.368 (0.024)	He/H=0	···	−3.44	2.24
J0159−1534	5147997450808347648	DA	7173 (37)	0.622 (0.011)	8.049 (0.012)	He/H=0	···	−3.44	1.59
J0200+0714	2567842095943560448	DQ	6775 (28)	0.607 (0.026)	8.053 (0.029)	H/He=0	log C/He=−6.26	−3.55	1.90
J0200+1222	2574640823015408128	DC	6790 (97)	0.217 (0.011)	7.163 (0.029)	log H/He=−3.4	···	−3.11	0.64
J0201+1212	2574620550768898432	DC	6948 (19)	0.589 (0.005)	8.023 (0.005)	log H/He=−3.4	···	−3.49	1.72
J0201−2650	5024591705975610752	DA	7723 (39)	0.873 (0.008)	8.434 (0.009)	He/H=0	···	−3.55	2.91
J0202+1602	78649033103100416	DZ	4392 (9)	0.488 (0.006)	7.864 (0.008)	log H/He=−4.0	log Ca/He=−10.15	−4.21	6.05
J0202+2615	105716359383595136	DA	5899 (41)	0.712 (0.034)	8.198 (0.037)	He/H=0	···	−3.87	4.00
J0203+2411	104118528470334720	DC	6964 (47)	0.331 (0.013)	7.513 (0.025)	log H/He=−3.4	···	−3.23	0.91
J0203−0701	2490494240363793792	DC	7657 (52)	0.638 (0.012)	8.101 (0.013)	log H/He=−3.6	···	−3.37	1.50
J0203−1229	5149836834976621056	DC	9870 (33)	0.677 (0.005)	8.157 (0.006)	log H/He=−4.6	···	−2.96	0.85
J0204+6954	521927243309686656	DA	6599 (55)	0.628 (0.019)	8.062 (0.022)	He/H=0	···	−3.59	2.00
J0205+2156	100567105912890496	DQ	5867 (54)	0.730 (0.062)	8.248 (0.067)	H/He=0	log C/He=−6.68	−3.92	4.83
J0205−0517	2490975272405858048	DC	4274 (25)	0.568 (0.012)	7.985 (0.014)	He/H=0	···	−4.32	8.51
J0206+1836	92597914738232448	DC	4351 (25)	0.496 (0.012)	7.862 (0.015)	He/H=0	···	−4.22	7.13
J0206−0057	2506507630789788032	DA	7318 (52)	1.000 (0.01)	8.633 (0.014)	He/H=0	···	−3.78	4.20
J0208+3729	330661599315957504	DA	5707 (24)	0.946 (0.007)	8.552 (0.009)	He/H=0	···	−4.16	6.71
J0208−0549	2490695859013226240	DA	6618 (38)	0.628 (0.017)	8.061 (0.02)	He/H=0	···	−3.59	1.98
J0209−0140	2494399362068211328	DA	9520 (55)	0.619 (0.008)	8.034 (0.01)	He/H=0	···	−2.93	0.75
J0210+6500	515466135029128576	DA	8049 (99)	0.900 (0.019)	8.475 (0.022)	He/H=0	···	−3.50	2.80

Tableau A.2 *suite page suivante*

Tableau A.2 *(suite)*

Name	Gaia DR2/EDR3*	Sp Type	$T_{\rm eff}$ (K)	$M/M_{\odot}$	$\log g$	Composition	Métaux	$\log L/L_{\odot}$	τ (Gyr)
J0211+1644	80107603996819584	DC	8569 (45)	0.703 (0.01)	8.201 (0.011)	log H/He=−4.0	···	−3.23	1.29
J0211+2209	100445163201292800	DA	6134 (38)	0.616 (0.033)	8.046 (0.038)	He/H=0	···	−3.71	2.38
J0211+2613	106241174322991360	DA	10224 (80)	1.006 (0.013)	8.637 (0.017)	He/H=0	···	−3.20	1.93
J0211+3955	333010327952701696	DAZ	7191 (41)	0.533 (0.007)	7.929 (0.008)	He/H=0	log Ca/H=−8.50	−3.38	1.38
J0211+7119	522115156720215040	DC	5176 (19)	0.631 (0.008)	8.079 (0.008)	He/H=0	···	−4.03	5.85
J0211−0620	2487975808980333184	DA	7761 (72)	0.804 (0.021)	8.330 (0.024)	He/H=0	···	−3.47	2.24
J0212+3020	300313218667865344	DA	6606 (48)	0.633 (0.026)	8.069 (0.03)	He/H=0	···	−3.60	2.02
J0212−0040	2494852597081575808	DA	5924 (36)	0.736 (0.019)	8.234 (0.021)	He/H=0	···	−3.88	4.27
J0214+7745	561231932144411008	DC	4804 (49)	0.702 (0.02)	8.193 (0.022)	He/H=0	···	−4.23	8.95
J0214−0505	2488226252817987584	DAH	9317 (59)	0.941 (0.01)	8.535 (0.013)	He/H=0	···	−3.29	2.05
J0215+0104	2513144725356809216	DA	6306 (58)	0.771 (0.021)	8.285 (0.023)	He/H=0	···	−3.81	3.90
J0215+4453	352179415533582080	DAZ	6583 (65)	0.664 (0.047)	8.145 (0.052)	He/H=0	log Ca/H=−8.15	−3.66	2.48
J0216+3951	332820971434386432	DA	8977 (26)	0.790 (0.004)	8.306 (0.003)	He/H=0	···	−3.20	1.32
J0216+4257	351429930856438656	DA	5547 (10)	0.622 (0.004)	8.061 (0.005)	He/H=0	···	−3.90	3.58
J0217+3234	325134624944612992	DA	7496 (40)	0.875 (0.011)	8.438 (0.013)	He/H=0	···	−3.60	3.19
J0217−0043	2494710244685483520	DC	7200 (48)	0.704 (0.02)	8.204 (0.022)	log H/He=−3.4	···	−3.54	2.13
J0217−0656	2486955560973911424	DAZ	5366 (18)	0.604 (0.009)	8.034 (0.011)	He/H=0	···	−3.94	4.05
J0218+4648	353917571618022784	DA	7368 (54)	0.603 (0.015)	8.018 (0.017)	He/H=0	···	−3.38	1.41
J0218+5013	355669578975070976	DA	4925 (15)	0.468 (0.006)	7.806 (0.008)	He/H=0	···	−3.97	3.89
J0218−0919	5176159517007960576	DZ	10007 (86)	0.647 (0.015)	8.109 (0.017)	log H/He=−5.0	log Ca/He=−10.13	−2.90	0.76
J0219−0820	2486189510606565760	DA	6557 (53)	0.888 (0.031)	8.460 (0.034)	He/H=0	···	−3.85	4.55
J0220+3520	327766649623335296	DA	5638 (21)	0.642 (0.009)	8.092 (0.01)	He/H=0	···	−3.89	3.64
J0221+0445	2516606022320239104	DA	7396 (15)	0.673 (0.005)	8.131 (0.005)	He/H=0	···	−3.43	1.66
J0221+5333	455517329408362752	DC	6364 (46)	0.548 (0.013)	7.958 (0.016)	log H/He=−3.2	···	−3.61	1.96
J0223+2055	87648226538760064	DC	4258 (31)	0.453 (0.008)	7.799 (0.014)	log H/He=0.11	···	−4.23	5.89
J0223+2629	103440095437050752	DA	7590 (53)	0.573 (0.014)	7.965 (0.017)	He/H=0	···	−3.29	1.21
J0223+5544	457474219590579328	DA	6781 (36)	0.770 (0.008)	8.281 (0.008)	He/H=0	···	−3.68	3.12
J0224+2325	101673523847748736	DA	4999 (30)	0.505 (0.019)	7.871 (0.024)	He/H=0	···	−3.98	4.19
J0224+4007	338094538438744320	DA	5977 (23)	0.589 (0.009)	8.001 (0.01)	He/H=0	···	−3.73	2.36
J0224−0242	2490455242060751360	DA	5302 (32)	0.663 (0.028)	8.129 (0.031)	He/H=0	···	−4.02	5.62
J0224−2854	5068532996689788544	DC	4882 (24)	1.071 (0.002)	8.774 (0.005)	log H/He=−3.83	···	−4.60	7.04
J0225+0545	2517080495947872896	DA	7052 (36)	0.537 (0.022)	7.906 (0.027)	He/H=0	···	−3.39	1.35
J0225+2410	101854122928108288	DC	8065 (50)	0.601 (0.013)	8.041 (0.014)	log H/He=−3.8	···	−3.24	1.21
J0225+4228	339492017717622016	DA	6261 (15)	0.568 (0.008)	7.965 (0.01)	He/H=0	···	−3.63	1.99

Tableau A.2 *suite page suivante*

Tableau A.2 *(suite)*

Name	Gaia DR2/EDR3*	Sp Type	$T_{\rm eff}$ (K)	$M/M_{\odot}$	$\log g$	Composition	Métaux	$\log L/L_{\odot}$	τ (Gyr)
J0225+4228	339492052075797376	DC	4366 (42)	0.572 (0.027)	7.992 (0.032)	He/H=0	···	−4.28	8.34
J0225−1756	5131731035268115584	DA	6114 (23)	0.621 (0.014)	8.054 (0.016)	He/H=0	···	−3.72	2.45
J0225−1756	5131731039563630720	DC	7764 (46)	0.599 (0.013)	8.039 (0.015)	log H/He=−3.8	···	−3.31	1.32
J0226+6459	515289392829738624	DC	4345 (25)	0.539 (0.013)	7.937 (0.014)	He/H=0	···	−4.26	7.78
J0227+1807	85787470611883008	DA	8436 (45)	0.550 (0.008)	7.920 (0.01)	He/H=0	···	−3.08	0.88
J0227+5915	459237630076876672	DA	7265 (36)	0.506 (0.007)	7.847 (0.008)	He/H=0	···	−3.31	1.16
J0230+2508	102390302349905024	DAH	5724 (37)	0.579 (0.025)	7.988 (0.031)	He/H=0	···	−3.80	2.59
J0231+0810	19693180966870656	DC	6016 (17)	0.605 (0.006)	8.054 (0.006)	log H/He=−3.0	···	−3.76	2.89
J0231+2709	127366331745660288	DC*	4849 (15)	0.515 (0.007)	7.891 (0.009)	He/H=0	···	−4.04	5.39
J0231+2859	131188715200383872	DA	7048 (8)	0.362 (0.008)	7.547 (0.012)	He/H=0	···	−3.20	0.90
J0232+0645	19252624696630016	DA	9151 (79)	0.864 (0.018)	8.416 (0.02)	He/H=0	···	−3.24	1.58
J0232+5211	452157015712452608	DA	9223 (60)	0.601 (0.01)	8.005 (0.012)	He/H=0	···	−2.97	0.78
J0232−1412	5146358426863612160	DA	5556 (10)	0.637 (0.004)	8.084 (0.004)	He/H=0	···	−3.91	3.81
J0233+2125	88996326578456192	DC	4739 (12)	0.511 (0.006)	7.885 (0.007)	He/H=0	···	−4.08	5.85
J0234+2407	102038286830643840	DA	5515 (25)	0.599 (0.019)	8.024 (0.022)	He/H=0	···	−3.89	3.30
J0234+2802	127700269747929344	DA	5582 (33)	0.642 (0.031)	8.092 (0.034)	He/H=0	···	−3.90	3.82
J0235+0118	2502097283492466560	DA :	6786 (18)	0.599 (0.004)	8.013 (0.005)	He/H=0	···	−3.52	1.73
J0235+0729	19399306419780224	DQ	6373 (18)	0.747 (0.023)	8.272 (0.024)	H/He=0	log C/He=−5.34	−3.79	3.68
J0235−2251	5125500927507946880	DA	6537 (12)	0.610 (0.006)	8.032 (0.006)	He/H=0	···	−3.59	1.96
J0235−2400	5125186299678747008	DC	5100 (21)	0.410 (0.007)	7.687 (0.01)	He/H=0	···	−3.85	2.56
J0237+1638	81606375784491520	DC	5312 (25)	0.545 (0.01)	7.960 (0.011)	H/He=0	···	−3.93	4.51
J0239+2609	126342377182577408	DA	5608 (11)	0.606 (0.004)	8.033 (0.005)	He/H=0	···	−3.86	3.11
J0239+7300	545997618721866624	DA	7823 (41)	0.552 (0.009)	7.927 (0.01)	He/H=0	···	−3.22	1.07
J0240+2701	126972461769858816	DA	5297 (23)	0.847 (0.012)	8.406 (0.013)	He/H=0	···	−4.19	8.10
J0240+3142	133116227803380224	DA	7244 (25)	0.641 (0.006)	8.080 (0.006)	He/H=0	···	−3.44	1.62
J0241+7442	548423278811480960	DA	8946 (48)	0.584 (0.006)	7.977 (0.007)	He/H=0	···	−3.01	0.81
J0242+1112	25405350031335296	DAH	8333 (30)	0.871 (0.005)	8.429 (0.006)	He/H=0	···	−3.41	2.30
J0242+1655	81957772828837888	DQ	6343 (17)	0.552 (0.006)	7.965 (0.007)	H/He=0	log C/He=−6.45	−3.62	2.00
J0244−0142	2496042440461991296	DAH	9722 (58)	0.910 (0.008)	8.487 (0.01)	He/H=0	···	−3.18	1.57
J0245+2825	128707181880407680	DA	5175 (33)	0.554 (0.025)	7.954 (0.03)	He/H=0	···	−3.96	4.14
J0245−1951	5128633195616949120	DC	4323 (32)	0.482 (0.012)	7.837 (0.016)	He/H=0	···	−4.22	6.94
J0246−0227	2495751967528809216	DAZ	6818 (10)	0.675 (0.004)	8.160 (0.003)	He/H=0	log Ca/H=−10.48	−3.60	2.29
J0248+3408	139937559287208192	DQ	6024 (25)	0.577 (0.02)	8.009 (0.023)	H/He=0	log C/He=−6.83	−3.73	2.57
J0248+5423	453562088496088320	DAZ	5048 (15)	0.644 (0.005)	8.102 (0.005)	He/H=0	···	−4.09	6.95

Tableau A.2 *suite page suivante*

Tableau A.2 *(suite)*

Name	Gaia DR2/EDR3*	Sp Type	$T_{\rm eff}$ (K)	$M/M_\odot$	$\log g$	Composition	Métaux	$\log L/L_\odot$	τ (Gyr)
J0249+1939	85008707141970304	DC	6034 (56)	0.649 (0.036)	8.124 (0.04)	log H/He=−3.0	···	−3.80	3.43
J0249+3307	139623068897753856	DA	5706 (13)	0.580 (0.006)	7.990 (0.006)	He/H=0	···	−3.81	2.63
J0249+4336	337449812306056832	DC	4738 (29)	0.503 (0.021)	7.872 (0.026)	He/H=0	···	−4.08	5.72
J0250+0817	20484382662003968	DC	4498 (20)	0.434 (0.011)	7.746 (0.015)	He/H=0	···	−4.10	5.21
J0250+2116	85469849190835968	DA	6563 (41)	0.633 (0.017)	8.069 (0.019)	He/H=0	···	−3.61	2.05
J0250−0437	5184589747536175104	DAH :	10451 (151)	1.042 (0.016)	8.698 (0.022)	He/H=0	···	−3.21	2.01
J0250−0910	5174110233491949312	DA	5574 (27)	0.442 (0.034)	7.741 (0.047)	He/H=0	···	−3.72	1.96
J0251+2925	128826375813389568	DC	6923 (46)	0.650 (0.021)	8.121 (0.023)	log H/He=−3.4	···	−3.55	1.98
J0251+7341	547501815051141248	DZ	7618 (39)	0.635 (0.009)	8.097 (0.01)	log H/He=−3.0	log Ca/He=−9.32	−3.37	1.51
J0253+0013	2498159515741377152	DA	7906 (47)	0.622 (0.013)	8.045 (0.016)	He/H=0	···	−3.27	1.22
J0253+3759	143076256963396480	DA	6563 (36)	0.563 (0.008)	7.954 (0.01)	He/H=0	···	−3.54	1.73
J0253−0033	2497895053130247040	DA	8143 (42)	0.620 (0.008)	8.042 (0.01)	He/H=0	···	−3.21	1.13
J0255+0237	1559111783825792	DA	8764 (41)	0.776 (0.009)	8.285 (0.01)	He/H=0	···	−3.23	1.36
J0255+2106	109247788869176448	DA	6252 (23)	0.593 (0.008)	8.007 (0.01)	He/H=0	···	−3.66	2.13
J0255−0715	5180494685197598464	DAH	7403 (55)	0.744 (0.03)	8.240 (0.033)	He/H=0	···	−3.50	2.05
J0256+0511	5526420319283584	DA	5469 (32)	0.545 (0.034)	7.933 (0.042)	He/H=0	···	−3.85	2.75
J0256+4954	439494077735062144	DA	5713 (14)	0.588 (0.006)	8.003 (0.006)	He/H=0	···	−3.81	2.68
J0256−0700	5180517706222368768	DC	4739 (42)	0.235 (0.012)	7.252 (0.03)	He/H=0	···	−3.78	2.06
J0257+0152	1268321022907264	DA	6294 (25)	0.598 (0.01)	8.015 (0.011)	He/H=0	···	−3.65	2.12
J0257+0620	7158988928491776	DA	4957 (43)	0.560 (0.049)	7.968 (0.058)	He/H=0	···	−4.05	5.78
J0258+0030	74698071455360	DA	6193 (39)	0.914 (0.023)	8.501 (0.026)	He/H=0	···	−3.98	5.30
J0258+3421	137141810455464192	DC	6380 (46)	0.550 (0.029)	7.961 (0.036)	log H/He=−3.2	···	−3.61	1.95
J0259+0811	8578256576520320	DAH	6601 (28)	0.501 (0.006)	7.842 (0.007)	He/H=0	···	−3.47	1.46
J0259+1725	35497904701569920	DA	5108 (30)	0.446 (0.023)	7.759 (0.031)	He/H=0	···	−3.88	2.85
J0300+5432	447366340472109440	DA	7650 (28)	0.627 (0.007)	8.055 (0.007)	He/H=0	···	−3.33	1.35
J0301−0044	5188044687948351872	DC	4375 (29)	0.473 (0.035)	7.821 (0.046)	He/H=0	···	−4.19	6.58
J0302+0622	7027562929324416	DA	6964 (57)	0.645 (0.02)	8.087 (0.022)	He/H=0	···	−3.51	1.82
J0303+0002	3266576684513815168	DA	8375 (64)	0.621 (0.019)	8.042 (0.022)	He/H=0	···	−3.16	1.05
J0303+0317	1843503042736512	DC	5837 (79)	0.577 (0.042)	8.010 (0.05)	log H/He=−3.0	···	−3.79	3.04
J0303+1921	60007152756147584	DC	6209 (37)	0.638 (0.018)	8.105 (0.019)	log H/He=−3.0	···	−3.73	2.82
J0303−0011	3266534357610950912	DC	4878 (29)	0.402 (0.027)	7.675 (0.04)	He/H=0	···	−3.92	3.18
J0305+2603	115409280235239296	DA	5283 (25)	0.574 (0.013)	7.985 (0.016)	He/H=0	···	−3.94	3.87
J0306−0638	5180178266367085312	DA	7877 (60)	0.700 (0.015)	8.171 (0.018)	He/H=0	···	−3.35	1.50
J0306−2029	5103714555575829888	DA	9918 (35)	0.653 (0.007)	8.087 (0.008)	He/H=0	···	−2.89	0.73

Tableau A.2 *suite page suivante*

Tableau A.2 *(suite)*

Name	Gaia DR2/EDR3*	Sp Type	$T_{\rm eff}$ (K)	$M/M_{\odot}$	$\log g$	Composition	Métaux	$\log L/L_{\odot}$	τ (Gyr)
J0307+0936	14862584004642688	DC	6286 (26)	0.668 (0.01)	8.152 (0.011)	log H/He=−3.2	···	−3.74	3.03
J0307+1540	31322547949728256	DC :	4094 (41)	0.425 (0.025)	7.732 (0.036)	He/H=0	···	−4.26	6.45
J0307−0715	5179920984941553408	DA	5846 (20)	0.861 (0.007)	8.423 (0.008)	He/H=0	···	−4.03	5.70
J0308+0040	3267081566509086592	DA	7602 (71)	0.739 (0.02)	8.231 (0.022)	He/H=0	···	−3.45	1.83
J0308+4047	239109213145234560	DA	5757 (47)	0.693 (0.045)	8.170 (0.05)	He/H=0	···	−3.90	4.08
J0308+5128	439905192004402304	DA	5178 (20)	0.568 (0.009)	7.978 (0.011)	He/H=0	···	−3.97	4.43
J0309+0025	3266873724451739776	DC	5570 (31)	0.671 (0.008)	8.160 (0.011)	log H/He=−1.14	···	−3.96	5.23
J0309+0953	14895255820376064	DC	5892 (72)	0.486 (0.032)	7.852 (0.042)	log H/He=−3.0	···	−3.69	2.19
J0310+0757	13611477211053824	DAZ	10184 (33)	0.607 (0.007)	8.011 (0.009)	He/H=0	···	−2.80	0.61
J0310+5309	446263083632852608	DC	8248 (59)	0.421 (0.009)	7.710 (0.014)	log H/He=−3.8	···	−3.03	0.74
J0310+6633	492442090962517376	DC	4719 (8)	0.508 (0.006)	7.881 (0.007)	He/H=0	···	−4.09	5.90
J0311−0551	5181816233750415488	DC	3966 (19)	0.444 (0.009)	7.768 (0.012)	He/H=0	···	−4.33	7.22
J0311−0853	5167424240722533760	DA	5083 (24)	0.527 (0.011)	7.910 (0.014)	He/H=0	···	−3.97	4.12
J0312+2218	62311183668001664	DA	6303 (26)	0.258 (0.005)	7.262 (0.011)	He/H=0	···	−3.26	0.88
J0313+3251	125339755721933440	DA	9814 (57)	0.615 (0.021)	8.025 (0.024)	He/H=0	···	−2.88	0.69
J0314−0105	3265311627666274944	DA	5726 (27)	0.560 (0.015)	7.956 (0.018)	He/H=0	···	−3.78	2.46
J0314−0815	5167525434447523712	DQ	9163 (41)	0.560 (0.008)	7.968 (0.01)	H/He=0	log C/He=−4.74	−2.98	0.79
J0316+3932	235842052999634944	DC	8670 (26)	0.597 (0.005)	8.031 (0.006)	log H/He=−4.0	···	−3.11	0.99
J0316−0816	5167510797199003904	DA	6500 (23)	0.817 (0.005)	8.354 (0.006)	He/H=0	···	−3.80	4.03
J0317−2911	5058635403471767680	DAZ	5486 (26)	0.723 (0.008)	8.218 (0.009)	He/H=0	···	−4.01	5.53
J0318+0212	3268703483599047296	DA	7403 (37)	0.939 (0.01)	8.536 (0.012)	He/H=0	···	−3.69	3.74
J0318+1414	30048866808843648	DA	9838 (61)	0.810 (0.011)	8.333 (0.012)	He/H=0	···	−3.06	1.08
J0319+3630	234469931207274112	DZ	6467 (29)	0.670 (0.007)	8.155 (0.008)	log H/He=−4.0	log Ca/He=−9.26	−3.69	2.73
J0319−2109	5100053078775660160	DA	9787 (44)	0.611 (0.006)	8.019 (0.007)	He/H=0	···	−2.88	0.69
J0320+1113	16166875378033664	DA	7846 (64)	0.622 (0.021)	8.047 (0.024)	He/H=0	···	−3.28	1.25
J0320+1113	16166875377576064	DA	6502 (65)	0.721 (0.035)	8.209 (0.038)	He/H=0	···	−3.71	2.98
J0320+2333	62884540326096896	DC	4435 (14)	0.237 (0.006)	7.266 (0.014)	He/H=0	···	−3.91	2.56
J0320+4337	241335036997623296	DC	6567 (62)	0.682 (0.035)	8.172 (0.04)	log H/He=−3.2	···	−3.68	2.70
J0321+1757	56048945255703680	DA	5323 (21)	0.634 (0.015)	8.083 (0.016)	He/H=0	···	−3.98	4.94
J0322+2708	117651695542992256	DA	7793 (52)	0.596 (0.017)	8.004 (0.02)	He/H=0	···	−3.27	1.20
J0324−0617	5169733318219971968	DA	7329 (54)	0.596 (0.019)	8.005 (0.022)	He/H=0	···	−3.38	1.40
J0325+1509	42174998299513728	DA	7803 (58)	0.693 (0.02)	8.160 (0.022)	He/H=0	···	−3.36	1.52
J0325+1509	42175002593812864	DC	4801 (72)	0.710 (0.068)	8.205 (0.074)	He/H=0	···	−4.24	9.06
J0325+1701	54993654611672704	DC	6926 (51)	0.555 (0.023)	7.967 (0.028)	log H/He=−3.4	···	−3.47	1.60

Tableau A.2 *suite page suivante*

Tableau A.2 *(suite)*

Name	Gaia DR2/EDR3*	Sp Type	$T_{\rm eff}$ (K)	$M/M_{\odot}$	$\log g$	Composition	Métaux	$\log L/L_{\odot}$	τ (Gyr)
J0325+1824	55981600168846080	DA	6384 (47)	0.608 (0.036)	8.030 (0.041)	He/H=0	···	−3.63	2.08
J0325−0149	3261591090771914240	DAZH	5185 (17)	0.592 (0.006)	8.037 (0.007)	He/H=0	log Ca/H=−9.55	−4.01	5.57
J0325−1722	5105681684956745728	DA	6990 (33)	0.569 (0.008)	7.962 (0.011)	He/H=0	···	−3.44	1.49
J0326+1557	54253618862057728	DA	5785 (15)	0.731 (0.007)	8.228 (0.008)	He/H=0	···	−3.92	4.55
J0327+0451	3275575603071739136	DC	5428 (85)	0.573 (0.056)	8.005 (0.066)	H/He=0	···	−3.92	4.47
J0327+1729	55103056018558592	DC*	5027 (62)	0.674 (0.041)	8.166 (0.044)	H/He=0	···	−4.14	6.83
J0327+4623	242802266545591936	DA	8144 (50)	0.522 (0.011)	7.871 (0.014)	He/H=0	···	−3.12	0.90
J0327−0636	5168947721457740288	DA	7635 (43)	0.710 (0.015)	8.187 (0.016)	He/H=0	···	−3.41	1.67
J0328+2631	117690801219527168	DA :	6146 (89)	0.402 (0.021)	7.648 (0.033)	He/H=0	···	−3.50	1.39
J0328−2718	5060587895604134400	DA	8324 (28)	0.263 (0.002)	7.241 (0.006)	He/H=0	···	−2.75	0.42
J0329−0555	3247469130928600960	DA	5331 (52)	0.584 (0.042)	8.002 (0.05)	He/H=0	···	−3.94	3.83
J0330+0037	3264828357946121984	DA	5769 (63)	0.672 (0.039)	8.138 (0.044)	He/H=0	···	−3.87	3.75
J0330+7401	544718680539607680	DC	7660 (40)	0.538 (0.008)	7.935 (0.01)	log H/He=−3.6	···	−3.27	1.19
J0331+4509	241745640169579776	DA	8738 (72)	0.849 (0.013)	8.395 (0.014)	He/H=0	···	−3.31	1.77
J0331+4736	248937133409693440	DA	9015 (42)	0.687 (0.011)	8.146 (0.013)	He/H=0	···	−3.10	1.01
J0333+0007	3264551560189562112	DAH	7857 (33)	0.871 (0.006)	8.430 (0.006)	He/H=0	···	−3.52	2.75
J0333+0656	3276355500412926336	DZ	7156 (55)	0.699 (0.036)	8.196 (0.039)	log H/He=−3.0	log Ca/He=−8.95	−3.54	2.13
J0333+4427	238653229356266752	DA	9146 (98)	0.988 (0.015)	8.610 (0.019)	He/H=0	···	−3.38	2.48
J0335+3211	121519060190456960	DA	10163 (43)	0.580 (0.006)	7.965 (0.007)	He/H=0	···	−2.78	0.58
J0336−2215	5088251195844051328	DAZ	5926 (18)	0.573 (0.006)	7.975 (0.007)	He/H=0	···	−3.73	2.31
J0338+0409	3274761620869767168	DA	8838 (36)	0.532 (0.009)	7.886 (0.011)	He/H=0	···	−2.98	0.75
J0339+1431	41518658576469760	DA	6470 (52)	0.712 (0.035)	8.194 (0.04)	He/H=0	···	−3.71	2.92
J0340+0537	3275218193073023360	DC	6147 (61)	0.630 (0.032)	8.094 (0.036)	log H/He=−3.0	···	−3.75	2.87
J0340−0029	3263484003117848832	DA	7311 (35)	0.697 (0.009)	8.167 (0.01)	He/H=0	···	−3.48	1.81
J0341+3818	224218080493203328	DA	7353 (59)	0.852 (0.023)	8.403 (0.025)	He/H=0	···	−3.61	3.16
J0342+3920	224331059611503232	DC	8541 (55)	0.620 (0.011)	8.069 (0.013)	log H/He=−4.0	···	−3.16	1.09
J0343+1958	63126196662620416	DA	7158 (28)	0.889 (0.005)	8.460 (0.005)	He/H=0	···	−3.70	3.71
J0344+1509	42871199614383616	DA	8599 (43)	0.774 (0.008)	8.282 (0.009)	He/H=0	···	−3.26	1.42
J0344+1510	42871268333859584	DC	7591 (26)	0.393 (0.006)	7.654 (0.008)	log H/He=−3.6	···	−3.15	0.86
J0344+1705	44478578238260864	DA	8395 (47)	0.579 (0.016)	7.971 (0.019)	He/H=0	···	−3.12	0.95
J0344+1825	44901791432527232	DQ	6548 (29)	0.560 (0.006)	7.978 (0.008)	H/He=0	log C/He=−6.41	−3.57	1.87
J0344+3532	221424221446885248	DA	6426 (42)	0.695 (0.023)	8.169 (0.027)	He/H=0	···	−3.70	2.78
J0345−0348	3249479592235301376	DA	5057 (14)	0.530 (0.007)	7.914 (0.008)	He/H=0	···	−3.98	4.35
J0345−0348	3249479592234269056	DC	4387 (18)	0.506 (0.009)	7.881 (0.01)	He/H=0	···	−4.21	7.18

Tableau A.2 *suite page suivante*

Tableau A.2 *(suite)*

Name	Gaia DR2/EDR3*	Sp Type	$T_{\rm eff}$ (K)	$M/M_{\odot}$	$\log g$	Composition	Métaux	$\log L/L_{\odot}$	τ (Gyr)
J0346+2455	66837563803594880	DC	3534 (66)	0.377 (0.01)	7.586 (0.022)	log H/He=0.25	···	−4.42	12.13
J0347+0138	3270079526697712768	DC	5045 (10)	0.553 (0.005)	7.955 (0.005)	He/H=0	···	−4.01	5.03
J0347+0520	3276414466021403264	DC	7085 (50)	0.676 (0.016)	8.162 (0.018)	log H/He=−3.4	···	−3.54	2.03
J0348+8048	568168544844912128	DC	6339 (36)	0.548 (0.011)	7.957 (0.014)	log H/He=−3.2	···	−3.62	1.98
J0352+3658	220421260684140288	DA	6913 (57)	0.818 (0.029)	8.353 (0.033)	He/H=0	···	−3.69	3.41
J0352+4941	250278709394343936	DA	7491 (27)	0.718 (0.008)	8.200 (0.008)	He/H=0	···	−3.45	1.81
J0353+1037	3303137301563100544	DC*	5660 (52)	0.607 (0.042)	8.060 (0.048)	H/He=0	···	−3.87	4.13
J0354+0523	3273645105468368000	DA	10188 (43)	0.579 (0.008)	7.963 (0.01)	He/H=0	···	−2.77	0.58
J0354−0044	3256598792586547584	DA	6095 (18)	0.409 (0.005)	7.664 (0.008)	He/H=0	···	−3.52	1.44
J0355+4525	244214799689691904	DA	5136 (22)	0.555 (0.009)	7.956 (0.01)	He/H=0	···	−3.98	4.41
J0357+1915	50456318016101120	DAH	6113 (33)	0.688 (0.016)	8.160 (0.019)	He/H=0	···	−3.78	3.23
J0358+2157	53278867446391040	DAZ	6765 (30)	0.712 (0.007)	8.218 (0.008)	He/H=0	log Ca/H=−7.39	−3.65	2.75
J0358+2538	67156078578517888	DC :	5389 (104)	0.388 (0.034)	7.664 (0.051)	H/He=0	···	−3.76	2.49
J0358+5549	468737616704971136	DA	8389 (27)	0.615 (0.005)	8.032 (0.006)	He/H=0	···	−3.15	1.03
J0359+7055	495058241441193728	DC	4896 (58)	0.328 (0.021)	7.532 (0.035)	H/He=0	···	−3.86	2.73
J0359−1118	3193194629937678464	DC	6754 (37)	0.598 (0.01)	8.039 (0.011)	log H/He=−3.4	···	−3.55	1.88
J0400+0814	3301319572621418368	DA	5481 (6)	0.555 (0.003)	7.950 (0.004)	He/H=0	···	−3.86	2.82
J0401+5131	250862824946594816	DC	5123 (10)	0.774 (0.005)	8.298 (0.006)	He/H=0	···	−4.18	8.36
J0402+1527	39387328302768640	DC	6873 (27)	0.669 (0.007)	8.151 (0.008)	log H/He=−3.4	···	−3.58	2.17
J0404−0523	3197508598168785408	DA	8587 (60)	0.611 (0.014)	8.025 (0.017)	He/H=0	···	−3.11	0.96
J0405+2643	162653160663515008	DC	3777 (30)	0.319 (0.014)	7.501 (0.024)	He/H=0	···	−4.30	5.20
J0406+3323	170648503898774912	DA	9021 (48)	0.629 (0.014)	8.053 (0.015)	He/H=0	···	−3.04	0.88
J0406−0432	3251618000616770560	DA	6462 (22)	0.580 (0.007)	7.983 (0.008)	He/H=0	···	−3.58	1.88
J0406−0515	3197515087862709888	DA	6728 (68)	0.846 (0.031)	8.396 (0.034)	He/H=0	···	−3.76	3.96
J0406−0644	3197019139399144320	DA	5885 (21)	0.282 (0.008)	7.350 (0.018)	He/H=0	···	−3.43	1.15
J0408+2921	164297449857329408	DA	8049 (29)	0.622 (0.007)	8.045 (0.009)	He/H=0	···	−3.23	1.17
J0410+1954	48829075167625472	DC	5130 (19)	0.773 (0.008)	8.296 (0.008)	He/H=0	···	−4.17	8.31
J0411+1558	45293488153371776	DC :	5882 (48)	0.606 (0.026)	8.056 (0.03)	H/He=0	···	−3.80	3.32
J0412+2354	149824883240282496	DC :	6932 (160)	0.787 (0.032)	8.329 (0.035)	log H/He=−3.4	···	−3.68	3.16
J0412+7549	551153263105246208	DAH :*	8494 (49)	0.752 (0.008)	8.249 (0.008)	He/H=0	···	−3.26	1.40
J0412−1117	3189621320226676736	DAP	7450 (32)	0.385 (0.005)	7.596 (0.009)	He/H=0	···	−3.13	0.83
J0413+1512	3311801796791224192	DC	4708 (80)	0.596 (0.078)	8.028 (0.088)	He/H=0	···	−4.17	7.68
J0413+1522	3311813685256807040	DC	6087 (43)	0.711 (0.021)	8.218 (0.022)	H/He=0	···	−3.84	3.97
J0413+2433	149884909703520000	DC	5824 (54)	0.555 (0.032)	7.974 (0.039)	log H/He=−3.0	···	−3.77	2.80

Tableau A.2 *suite page suivante*

Tableau A.2 *(suite)*

Name	Gaia DR2/EDR3*	Sp Type	$T_{\rm eff}$ (K)	$M/M_{\odot}$	$\log g$	Composition	Métaux	$\log L/L_{\odot}$	τ (Gyr)
J0413−0801	3195883481327214848	DA	8980 (18)	0.564 (0.004)	7.943 (0.006)	He/H=0	···	−2.98	0.77
J0416+2947	165677710612522752	DZ	6912 (47)	0.644 (0.02)	8.112 (0.022)	log H/He=−4.0	log Ca/He=−9.70	−3.55	1.96
J0416+5456	276438530560644864	DC	7632 (29)	0.610 (0.01)	8.056 (0.011)	log H/He=−3.6	···	−3.35	1.42
J0418+3022	166091096919353088	DC	6190 (45)	0.569 (0.026)	7.993 (0.032)	log H/He=−3.0	···	−3.68	2.23
J0418+4210	229143725086190336	DA	5107 (16)	0.522 (0.007)	7.899 (0.009)	He/H=0	···	−3.96	3.85
J0419−0934	3191738120628213760	DAP	6115 (29)	0.839 (0.008)	8.388 (0.009)	He/H=0	···	−3.92	4.91
J0420+1952	49013483883923968	DA	6482 (30)	0.618 (0.013)	8.045 (0.014)	He/H=0	···	−3.62	2.04
J0420+2617	150577636388844160	DA	6542 (40)	0.568 (0.018)	7.963 (0.022)	He/H=0	···	−3.55	1.77
J0421+4607	232990572675079296	DA	7862 (34)	0.605 (0.006)	8.019 (0.006)	He/H=0	···	−3.26	1.20
J0421+5535	276576484910598912	DC	7071 (44)	0.702 (0.011)	8.202 (0.011)	log H/He=−3.4	···	−3.56	2.27
J0421−1600	3175193288128400896	DA	6506 (51)	0.690 (0.011)	8.160 (0.012)	He/H=0	···	−3.67	2.59
J0422+0038	3254930932230273664	DZ	6861 (34)	0.757 (0.021)	8.286 (0.023)	log H/He=−2.0	log Ca/He=−8.74	−3.67	3.03
J0422+2641	152091973137497216	DC	5019 (41)	0.465 (0.024)	7.820 (0.032)	H/He=0	···	−3.96	4.27
J0422+3357	175817750438186240	DA	6907 (31)	0.577 (0.022)	7.975 (0.026)	He/H=0	···	−3.46	1.56
J0423+5006	270485053053115648	DC	9413 (48)	0.544 (0.008)	7.940 (0.009)	log H/He=−4.4	···	−2.92	0.71
J0423+5745	470639806179201792	DC	7099 (34)	0.678 (0.007)	8.166 (0.008)	log H/He=−3.4	···	−3.54	2.04
J0424+3038	165401149074789504	DC	7070 (63)	0.619 (0.028)	8.072 (0.032)	log H/He=−3.4	···	−3.49	1.75
J0425+1211	3307009304776119936	DC	5999 (17)	0.664 (0.004)	8.147 (0.004)	H/He=0	···	−3.82	3.71
J0425+2834	152931141027253888	DZ	5957 (27)	0.656 (0.017)	8.135 (0.019)	log H/He=−2.0	log Ca/He=−10.41	−3.83	3.75
J0425+4614	256832412872262656	DC	4569 (48)	0.761 (0.024)	8.281 (0.026)	He/H=0	···	−4.37	10.21
J0426+0432	3283853143218651264	DA	4933 (12)	0.715 (0.006)	8.212 (0.006)	He/H=0	···	−4.19	8.62
J0426−0347	3204665315057342336	DC	5897 (38)	0.639 (0.017)	8.109 (0.018)	H/He=0	···	−3.83	3.73
J0427−0708	3198881613315343872	DC	6698 (36)	0.598 (0.008)	8.039 (0.01)	log H/He=−3.2	···	−3.57	1.92
J0428+0006	3254620732512634624	DA	6805 (53)	0.664 (0.035)	8.117 (0.04)	He/H=0	···	−3.57	2.03
J0428+0052	3278914205706332928	DA	10126 (43)	0.599 (0.01)	7.998 (0.012)	He/H=0	···	−2.81	0.61
J0428+1044	3305972018634634880	DA	10402 (64)	0.910 (0.009)	8.484 (0.01)	He/H=0	···	−3.06	1.23
J0429+2159	145429108768875008	DC	8232 (31)	0.710 (0.006)	8.211 (0.006)	log H/He=−3.8	···	−3.31	1.45
J0429+4945	258761510321879424	DA	8683 (40)	0.642 (0.007)	8.075 (0.008)	He/H=0	···	−3.12	1.00
J0430+0941	3293635012838798464	DA	7023 (56)	0.625 (0.022)	8.054 (0.025)	He/H=0	···	−3.48	1.69
J0430+1611	3312860733860742272	DA	8700 (43)	0.613 (0.008)	8.027 (0.01)	He/H=0	···	−3.09	0.93
J0431+5858	470826482635701376	DC	6936 (136)	0.595 (0.026)	8.035 (0.03)	log H/He=−3.4	···	−3.50	1.75
J0432−1920	2978374522004181888	DA	5773 (38)	0.611 (0.011)	8.041 (0.012)	He/H=0	···	−3.82	2.83
J0433+0414	3282093301842469376	DA	5035 (14)	0.651 (0.006)	8.113 (0.006)	He/H=0	···	−4.10	7.15
J0433+5527	277090540953615616	DA	9265 (71)	0.631 (0.012)	8.055 (0.014)	He/H=0	···	−2.99	0.83

Tableau A.2 *suite page suivante*

Tableau A.2 *(suite)*

Name	Gaia DR2/EDR3*	Sp Type	$T_{\rm eff}$ (K)	$M/M_{\odot}$	$\log g$	Composition	Métaux	$\log L/L_{\odot}$	τ (Gyr)
J0433−2753	4891567154251463680	DA*	5230 (14)	0.634 (0.005)	8.083 (0.006)	He/H=0	···	−4.01	5.54
J0434+3054	159277625222514048	DC	4955 (17)	0.711 (0.009)	8.205 (0.01)	He/H=0	···	−4.18	8.47
J0435−2240	4898310149826754304	DA	10304 (74)	0.604 (0.009)	8.006 (0.011)	He/H=0	···	−2.78	0.59
J0436+2709	151650935831913216	DA	5536 (12)	0.606 (0.005)	8.035 (0.005)	He/H=0	···	−3.89	3.34
J0436+4047	2038286337900264 96	DA	10068 (59)	0.638 (0.009)	8.063 (0.011)	He/H=0	···	−2.85	0.68
J0436+5537	277138090534130560	DA	7423 (45)	0.757 (0.014)	8.259 (0.015)	He/H=0	···	−3.50	2.14
J0437−0849	3186021141200137472	DQ	6275 (7)	0.519 (0.002)	7.907 (0.002)	H/He=0	log C/He=−6.43	−3.61	1.91
J0439+0928	3293451020735654272	DC	9660 (73)	0.673 (0.014)	8.150 (0.016)	log H/He=−4.4	···	−2.99	0.89
J0439−0405	3201594074140023936	DA	8149 (37)	0.582 (0.008)	7.978 (0.009)	He/H=0	···	−3.17	1.03
J0440+0923	3292685210887016192	DA	6340 (23)	0.786 (0.007)	8.308 (0.008)	He/H=0	···	−3.81	4.00
J0441+2042	3411147173483832320	DA	7415 (52)	0.477 (0.016)	7.791 (0.022)	He/H=0	···	−3.24	1.03
J0441−0042	3229556024930689024	DC	5813 (32)	0.489 (0.018)	7.858 (0.024)	H/He=0	···	−3.72	2.33
J0441−0551	3200232157189930880	DQ	7623 (44)	0.550 (0.011)	7.957 (0.012)	H/He=0	log C/He=−5.72	−3.29	1.24
J0441−1519	3173236054352419072	DA	6065 (18)	0.610 (0.006)	8.035 (0.006)	He/H=0	···	−3.73	2.42
J0443+5106	260218878625842816	DA	8537 (33)	0.599 (0.006)	8.004 (0.007)	He/H=0	···	−3.11	0.95
J0443−0607	3199980330371548800	DA	5484 (69)	0.640 (0.043)	8.090 (0.048)	He/H=0	···	−3.93	4.16
J0445+0050	3230171064244273024	DZ	6083 (38)	0.644 (0.025)	8.115 (0.027)	log H/He=−4.0	log Ca/He=−10.13	−3.78	3.21
J0445−0618	3187950092615927552	DA	6547 (28)	0.586 (0.011)	7.993 (0.013)	He/H=0	···	−3.57	1.85
J0445−2726	4881098119928195456	DC*	6809 (34)	0.552 (0.007)	7.962 (0.008)	log H/He=−3.4	···	−3.50	1.66
J0447+0106	3231702860037325824	DZ	6186 (42)	0.692 (0.016)	8.189 (0.017)	log H/He=−2.0	log Ca/He=−10.92	−3.79	3.50
J0449−1806	2979519903882838528	DA :*	7927 (46)	0.561 (0.007)	7.943 (0.01)	He/H=0	···	−3.21	1.06
J0452−0043	3226718494654224256	DA	6082 (65)	0.661 (0.038)	8.117 (0.043)	He/H=0	···	−3.77	2.90
J0453−0457	3188530840914150144	DC	8494 (54)	0.606 (0.014)	8.048 (0.016)	log H/He=−4.0	···	−3.16	1.07
J0454+1027	3294543969653440256	DA	7417 (39)	0.550 (0.009)	7.926 (0.01)	He/H=0	···	−3.31	1.22
J0454+1218	3295332796231463168	DA	6471 (55)	0.549 (0.027)	7.929 (0.034)	He/H=0	···	−3.55	1.73
J0455+3840	199060743352070528	DA	5177 (16)	0.656 (0.008)	8.119 (0.009)	He/H=0	···	−4.05	6.33
J0458+2548	3419918875386344576	DA	10672 (97)	0.832 (0.021)	8.364 (0.024)	He/H=0	···	−2.94	0.92
J0458+6410	479163220314358784	DC	9990 (111)	0.564 (0.015)	7.973 (0.019)	log H/He=−4.6	···	−2.83	0.63
J0459+2317	3418592726925673728	DA	7858 (52)	0.602 (0.016)	8.014 (0.018)	He/H=0	···	−3.26	1.19
J0500−0624	3211353408067754368	DA	7669 (29)	0.640 (0.006)	8.076 (0.007)	He/H=0	···	−3.34	1.39
J0502+2402	3418741367154043648	DAH :*	9893 (92)	0.884 (0.014)	8.446 (0.016)	He/H=0	···	−3.12	1.32
J0502+2522	3420019270246122112	DA	8108 (63)	0.791 (0.021)	8.308 (0.023)	He/H=0	···	−3.38	1.80
J0505−1722	2982808337003815040	DAH	5328 (9)	0.500 (0.004)	7.855 (0.005)	He/H=0	···	−3.86	2.70
J0505−1731	2976789094955826560	DA	6230 (21)	0.719 (0.006)	8.207 (0.007)	He/H=0	···	−3.78	3.44

Tableau A.2 *suite page suivante*

Tableau A.2 *(suite)*

Name	Gaia DR2/EDR3*	Sp Type	$T_{\rm eff}$ (K)	$M/M_{\odot}$	$\log g$	Composition	Métaux	$\log L/L_{\odot}$	τ (Gyr)
J0508−1450	2986577153625081344	DQ	5458 (11)	0.536 (0.007)	7.943 (0.008)	H/He=0	log C/He=−7.18	−3.87	3.77
J0508−1523	2986473765172532864	DA	5295 (25)	0.655 (0.01)	8.116 (0.01)	He/H=0	···	−4.01	5.51
J0512−0505	3211784863301909504	DZ	5606 (21)	0.580 (0.01)	8.017 (0.01)	log H/He=−4.0	log Ca/He=−8.99	−3.87	3.92
J0513−0522	3208758831207224704	DA	6422 (34)	0.591 (0.017)	8.002 (0.02)	He/H=0	···	−3.61	1.97
J0514+0800	3242153305741855744	DA	6627 (16)	0.806 (0.004)	8.336 (0.004)	He/H=0	···	−3.75	3.72
J0515+2839	3422405214775411840	DAH	6505 (20)	0.730 (0.005)	8.222 (0.005)	He/H=0	···	−3.71	3.08
J0515+5021	261664427174056320	DA	9469 (26)	0.586 (0.004)	7.978 (0.005)	He/H=0	···	−2.91	0.71
J0519−0545	3209958746287926528	DA	9130 (37)	0.647 (0.007)	8.082 (0.008)	He/H=0	···	−3.04	0.89
J0520+0114	3222138444609365248	DAH	6596 (54)	0.751 (0.023)	8.254 (0.025)	He/H=0	···	−3.71	3.19
J0521+1622	3394087945636978432	DA	10258 (85)	0.602 (0.014)	8.003 (0.016)	He/H=0	···	−2.79	0.60
J0521+3321	181170585358665088	DA	8699 (34)	0.546 (0.006)	7.912 (0.007)	He/H=0	···	−3.02	0.81
J0524−0604	3209150124204756224	DC	6373 (21)	0.662 (0.007)	8.142 (0.008)	log H/He=−3.2	···	−3.71	2.80
J0526+0339	3236259854698180480	DA	9778 (78)	0.881 (0.014)	8.441 (0.015)	He/H=0	···	−3.14	1.36
J0526+4435	208021900557436800	DC	4693 (24)	0.512 (0.012)	7.888 (0.014)	He/H=0	···	−4.10	6.08
J0529+4300	1954702881319841 28	DQ	8491 (40)	0.533 (0.006)	7.924 (0.007)	H/He=0	log C/He=−5.09	−3.09	0.90
J0530+3939	190802650815160960	DA	5451 (17)	0.539 (0.007)	7.923 (0.008)	He/H=0	···	−3.85	2.73
J0531+0009	3220927204494324 48	DA	5508 (51)	0.664 (0.039)	8.128 (0.044)	He/H=0	···	−3.95	4.49
J0532+0624	3333830379107891968	DA	8322 (35)	0.253 (0.005)	7.204 (0.013)	He/H=0	···	−2.73	0.39
J0533−0750	3016329285438157312	DA	9694 (53)	0.382 (0.007)	7.568 (0.011)	He/H=0	···	−2.65	0.41
J0535+0526	3332761855668238464	DA	8900 (79)	0.838 (0.015)	8.378 (0.018)	He/H=0	···	−3.26	1.59
J0535+5715	269226279739467904	DC	4949 (21)	0.553 (0.01)	7.956 (0.012)	He/H=0	···	−4.04	5.67
J0536+4129	194394347281717504	DA	7348 (18)	0.230 (0.002)	7.134 (0.005)	He/H=0	···	−2.92	0.49
J0537+6759	481698110012697728	DAH	7600 (28)	0.780 (0.005)	8.294 (0.006)	He/H=0	···	−3.48	2.17
J0538+1832	3397839440654502656	DA	6473 (31)	0.678 (0.016)	8.142 (0.018)	He/H=0	···	−3.67	2.51
J0538+4436	197328114893527680	DA	5879 (22)	0.516 (0.008)	7.876 (0.01)	He/H=0	···	−3.69	2.05
J0538+6222	286251461381258624	DA	6371 (37)	0.566 (0.023)	7.960 (0.028)	He/H=0	···	−3.60	1.89
J0539+4352	197048460976343168	DC	5786 (20)	0.617 (0.009)	8.075 (0.01)	H/He=0	···	−3.84	3.81
J0541+3959	190998058945380608	DA	5852 (27)	0.733 (0.009)	8.230 (0.01)	He/H=0	···	−3.90	4.40
J0542+0144	3222969370457259648	DA	9247 (43)	0.805 (0.008)	8.327 (0.008)	He/H=0	···	−3.17	1.27
J0542+8219	558036098518042752	DA	5906 (33)	0.556 (0.013)	7.947 (0.015)	He/H=0	···	−3.72	2.24
J0543+0036	3219428015303785856	DA	6625 (35)	0.606 (0.02)	8.025 (0.023)	He/H=0	···	−3.56	1.88
J0543+3637	3455921181049073280	DAZ	6447 (13)	0.607 (0.004)	8.055 (0.004)	He/H=0	log Ca/H=−8.55	−3.64	2.18
J0543+6338	286925049691578496	DA	6463 (41)	0.593 (0.016)	8.005 (0.019)	He/H=0	···	−3.60	1.95
J0544+2602	3429296884940000000	DC	5029 (14)	0.299 (0.005)	7.429 (0.01)	He/H=0	···	−3.75	2.00

Tableau A.2 *suite page suivante*

Tableau A.2 *(suite)*

Name	Gaia DR2/EDR3*	Sp Type	$T_{\rm eff}$ (K)	$M/M_\odot$	$\log g$	Composition	Métaux	$\log L/L_\odot$	τ (Gyr)
J0544+2720	3441551143893533312	DA	7308 (26)	0.334 (0.006)	7.472 (0.011)	He/H=0	···	−3.10	0.77
J0546+1115	3337021260634868224	DC	5033 (8)	0.595 (0.007)	8.025 (0.008)	He/H=0	···	−4.05	6.07
J0546+4338	196156864422578432	DA	7695 (48)	0.610 (0.01)	8.026 (0.011)	He/H=0	···	−3.30	1.28
J0547+5759	269694160592289664	DA	9718 (37)	0.617 (0.005)	8.030 (0.006)	He/H=0	···	−2.90	0.71
J0548+1325	3346603611845335424	DC	3938 (59)	0.442 (0.02)	7.765 (0.027)	He/H=0	···	−4.34	7.26
J0548+4655	210000437370798976	DC	10126 (64)	0.589 (0.013)	8.015 (0.014)	log H/He=−4.6	···	−2.83	0.65
J0549+2329	3427482725113315200	DC*	4572 (8)	0.274 (0.007)	7.375 (0.014)	He/H=0	···	−3.90	2.71
J0550+3257	3451263611151284480	DC	5651 (41)	0.609 (0.019)	8.063 (0.022)	H/He=0	···	−3.88	4.19
J0551−0010	3218697767783768320	DQ	6235 (4)	0.701 (0.002)	8.202 (0.001)	H/He=0	log C/He=−6.47	−3.78	3.48
J0553+2550	3429114022412106752	DA	10440 (48)	0.625 (0.014)	8.040 (0.015)	He/H=0	···	−2.78	0.60
J0553+6348	286977585732431488	DA	7868 (79)	0.759 (0.017)	8.261 (0.018)	He/H=0	···	−3.40	1.77
J0554−1035	3011223668834627328	DZ	6089 (14)	0.574 (0.004)	8.003 (0.003)	log H/He=−4.0	log Ca/He=−11.60	−3.71	2.42
J0555+4430	196617731593326976	DC	5724 (44)	0.510 (0.02)	7.896 (0.025)	H/He=0	···	−3.77	2.63
J0555+4650	198027266851070848	DA	5191 (10)	0.555 (0.004)	7.956 (0.005)	He/H=0	···	−3.96	4.06
J0555−0410	3022959697313320 96	DZ	4534 (7)	0.541 (0.004)	7.955 (0.004)	H/He=0	log Ca/He=−11.15	−4.20	6.45
J0559−0414	3024247796382652800	DA	6116 (19)	0.649 (0.006)	8.099 (0.007)	He/H=0	···	−3.75	2.70
J0600+2343	3424863550977729536	DA	8305 (34)	0.601 (0.008)	8.009 (0.009)	He/H=0	···	−3.16	1.02
J0601−0101	3026097243659561600	DA	6646 (34)	0.630 (0.024)	8.064 (0.027)	He/H=0	···	−3.58	1.97
J0602+0904	3329569015639064192	DA	5713 (15)	0.486 (0.005)	7.824 (0.007)	He/H=0	···	−3.72	2.04
J0602+1553	3348678699526809600	DA	7008 (26)	0.786 (0.006)	8.305 (0.006)	He/H=0	···	−3.63	2.96
J0605+0505	3318463707678938368	DA	10058 (57)	0.649 (0.012)	8.080 (0.013)	He/H=0	···	−2.87	0.69
J0607+7331	1114054838014073984	DA	6435 (22)	0.907 (0.006)	8.489 (0.006)	He/H=0	···	−3.90	4.86
J0608+0016	3122380407457501824	DA	7771 (52)	0.602 (0.013)	8.013 (0.015)	He/H=0	···	−3.28	1.22
J0609+3525	3453292832862501120	DAZ	10031 (33)	0.633 (0.006)	8.054 (0.006)	He/H=0	···	−2.85	0.67
J0611+0544	3318722672728544384	DA	6772 (42)	0.594 (0.025)	8.005 (0.029)	He/H=0	···	−3.52	1.72
J0611+2429	3425920250370248832	DA	7361 (25)	0.591 (0.011)	7.997 (0.013)	He/H=0	···	−3.37	1.37
J0613+2050	3375135698070213632	DA+DQ	8033 (44)	0.223 (0.003)	7.161 (0.009)	H/He=0	log C/He=−5.00	−2.80	0.39
J0613−0104	3121223102749655808	DA	7969 (58)	0.929 (0.016)	8.519 (0.019)	He/H=0	···	−3.55	3.07
J0615+4638	968662184929578496	DA	10271 (98)	0.802 (0.014)	8.320 (0.016)	He/H=0	···	−2.98	0.95
J0618+6204	1007682723024253184	DC	4657 (25)	0.512 (0.013)	7.889 (0.016)	He/H=0	···	−4.11	6.25
J0620+0645	3324181683539044224	DA	5879 (5)	0.680 (0.003)	8.149 (0.003)	He/H=0	···	−3.85	3.59
J0620+0700	3324963367588643968	DA	9994 (57)	0.370 (0.008)	7.534 (0.014)	He/H=0	···	−2.57	0.36
J0620+3443	3440684419492448128	DA	10173 (51)	0.692 (0.008)	8.149 (0.009)	He/H=0	···	−2.89	0.74
J0620+4205	960039814744267520	DAH*	6790 (33)	0.849 (0.008)	8.401 (0.009)	He/H=0	···	−3.75	3.90

Tableau A.2 *suite page suivante*

Tableau A.2 *(suite)*

Name	Gaia DR2/EDR3*	Sp Type	$T_{\rm eff}$ (K)	$M/M_{\odot}$	$\log g$	Composition	Métaux	$\log L/L_{\odot}$	τ (Gyr)
J0620+8247	1143693887630730240	DA	7400 (46)	0.626 (0.013)	8.055 (0.015)	He/H=0	···	−3.39	1.48
J0624−0056	3118424948738692352	DA	6661 (40)	0.626 (0.026)	8.058 (0.029)	He/H=0	···	−3.57	1.94
J0624−0104	3118420619409587712	DC	6328 (64)	0.616 (0.035)	8.071 (0.04)	log H/He=−3.2	···	−3.68	2.39
J0627+1002	3327488430402704000	DZ	8490 (58)	0.607 (0.008)	8.049 (0.01)	log H/He=−4.0	log Ca/He=−10.19	−3.16	1.07
J0627+3500	942461445610425856	DA	6672 (30)	0.615 (0.01)	8.040 (0.012)	He/H=0	···	−3.56	1.88
J0627−1934	2940050734981714432	DA	7201 (30)	0.567 (0.007)	7.957 (0.009)	He/H=0	···	−3.38	1.37
J0630−0205	3117320802840630400	DA	6355 (13)	0.493 (0.003)	7.829 (0.004)	He/H=0	···	−3.53	1.58
J0630−1900	2940003108087120640	DA	5999 (53)	0.797 (0.021)	8.326 (0.023)	He/H=0	···	−3.92	4.75
J0632+2230	3382277296672027136	DA	5508 (18)	0.579 (0.008)	7.991 (0.009)	He/H=0	···	−3.87	3.04
J0632+5559	995112350178946048	DAH	9748 (37)	0.907 (0.005)	8.482 (0.005)	He/H=0	···	−3.17	1.53
J0634−2834	2895487456076198656	DC	3888 (31)	0.416 (0.011)	7.714 (0.016)	He/H=0	···	−4.34	6.86
J0635+1013	3327647271174824704	DA	7217 (82)	0.901 (0.037)	8.479 (0.042)	He/H=0	···	−3.70	3.73
J0635−0044	3119203643485532416	DA	7363 (34)	0.624 (0.011)	8.051 (0.013)	He/H=0	···	−3.40	1.49
J0636+4054	957295438016687616	DA	7887 (46)	0.881 (0.008)	8.446 (0.008)	He/H=0	···	−3.52	2.81
J0639+3639	942347092105836160	DA	7863 (40)	0.644 (0.01)	8.081 (0.011)	He/H=0	···	−3.30	1.31
J0640+3327	938351982245743360	DC	8026 (49)	0.623 (0.01)	8.077 (0.011)	log H/He=−3.8	···	−3.27	1.29
J0641−0432	3103811515783541504	DC	4078 (21)	0.440 (0.009)	7.760 (0.012)	He/H=0	···	−4.28	6.81
J0641−2027	2927186036623328256	DA	10177 (34)	0.681 (0.006)	8.132 (0.006)	He/H=0	···	−2.88	0.72
J0644+0926	3326650224581677312	DAH*	6237 (16)	0.668 (0.006)	8.127 (0.006)	He/H=0	···	−3.73	2.72
J0644+2731	3386162214851684864	DA	6975 (26)	0.843 (0.006)	8.391 (0.007)	He/H=0	···	−3.70	3.57
J0644−2832	2918665577420228480	DA	9073 (57)	0.542 (0.009)	7.903 (0.011)	He/H=0	···	−2.94	0.72
J0645+2715	3385389606068550144	DA	8595 (104)	0.937 (0.029)	8.530 (0.035)	He/H=0	···	−3.43	2.57
J0647+0231	3126453655659835136	DA	7132 (21)	0.984 (0.003)	8.607 (0.003)	He/H=0	···	−3.81	4.33
J0649+1519	3354582217971214464	DC	5496 (32)	0.721 (0.013)	8.235 (0.014)	H/He=0	···	−4.02	5.95
J0649+7521	1115546944012493696	DAH	5986 (22)	0.596 (0.006)	8.014 (0.008)	He/H=0	···	−3.74	2.40
J0650+1657	3358418684623972864	DA	5229 (13)	0.679 (0.007)	8.154 (0.007)	He/H=0	···	−4.06	6.40
J0651+6242	1100089318058003328	DAH	6775 (45)	0.679 (0.01)	8.142 (0.011)	He/H=0	···	−3.59	2.15
J0652+1416	3354222505874657280	DC	10424 (68)	0.645 (0.01)	8.104 (0.011)	log H/He=−4.8	···	−2.83	0.68
J0653+6355	1100267237077449728	DA	5999 (18)	0.599 (0.006)	8.018 (0.006)	He/H=0	···	−3.74	2.41
J0653+6403	1100655330324351616	DA	5910 (24)	0.666 (0.007)	8.127 (0.008)	He/H=0	···	−3.82	3.32
J0654+2834	887534135357644416	DC	5006 (49)	0.487 (0.04)	7.840 (0.051)	He/H=0	···	−3.96	3.80
J0654+3148	889391077355387392	DA	9404 (53)	0.645 (0.009)	8.077 (0.01)	He/H=0	···	−2.98	0.82
J0654+3938	950361883331847424	DZ	9673 (46)	0.589 (0.006)	8.015 (0.007)	log H/He=−3.0	log Ca/He=−8.88	−2.91	0.73
J0657+0240	3127761765259717632	DC	8972 (46)	0.752 (0.007)	8.273 (0.008)	log H/He=−4.2	···	−3.19	1.28

Tableau A.2 *suite page suivante*

Tableau A.2 *(suite)*

Name	Gaia DR2/EDR3*	Sp Type	$T_{\rm eff}$ (K)	$M/M_{\odot}$	$\log g$	Composition	Métaux	$\log L/L_{\odot}$	τ (Gyr)
J0657+0550	3129655296079487872	DC	5855 (24)	0.656 (0.009)	8.135 (0.01)	H/He=0	···	−3.85	4.07
J0657+3009	888152408786189952	DA	7841 (27)	0.559 (0.01)	7.940 (0.013)	He/H=0	···	−3.22	1.08
J0657+4007	950478049312082688	DA	6717 (25)	0.492 (0.01)	7.826 (0.013)	He/H=0	···	−3.43	1.37
J0658−0115	3112162508466471808	DA	4894 (22)	0.614 (0.014)	8.056 (0.016)	He/H=0	···	−4.12	7.25
J0658−1650	2935589908933376896	DA	7000 (46)	0.621 (0.016)	8.048 (0.019)	He/H=0	···	−3.48	1.69
J0659+1225	3160815489969826944	DA	5007 (13)	0.532 (0.007)	7.919 (0.009)	He/H=0	···	−4.00	4.77
J0700+0530	3128834506352463104	DC	9405 (42)	0.729 (0.009)	8.237 (0.009)	log H/He=−4.4	···	−3.09	1.08
J0700+3157	890661253803216896	DA	4911 (13)	0.550 (0.006)	7.952 (0.007)	He/H=0	···	−4.05	5.85
J0700−0734	3052418589963163264	DC	5682 (11)	0.688 (0.004)	8.185 (0.005)	H/He=0	···	−3.94	5.03
J0701−0628	3052844272764398208	DA	6474 (10)	0.596 (0.003)	8.010 (0.003)	He/H=0	···	−3.60	1.95
J0703+7805	1140292479690791296	DA	5417 (11)	0.528 (0.004)	7.905 (0.005)	He/H=0	···	−3.85	2.71
J0703−1656	2935446392608812032	DZ	7312 (60)	0.614 (0.017)	8.064 (0.019)	log H/He=−4.0	log Ca/He=−11.31	−3.43	1.59
J0704+1151	3160571600249678720	DA	6709 (53)	0.627 (0.03)	8.059 (0.034)	He/H=0	···	−3.56	1.91
J0704+7111	1109924900541714304	DC	4973 (30)	0.329 (0.018)	7.533 (0.032)	H/He=0	···	−3.84	2.63
J0705+5142	980918204822332416	DA	5147 (18)	0.737 (0.011)	8.243 (0.012)	He/H=0	···	−4.14	7.81
J0705−1703	2935415125246460032	DQ	6088 (24)	0.666 (0.022)	8.149 (0.023)	H/He=0	log C/He=−5.50	−3.79	3.47
J0708+2044	3366672379112835328	DA	5547 (17)	0.436 (0.006)	7.729 (0.009)	He/H=0	···	−3.72	1.95
J0710+3740	946030529073021440	DQ	6583 (14)	0.527 (0.004)	7.920 (0.004)	H/He=0	log C/He=−6.49	−3.53	1.71
J0711+4607	977441274176008192	DC :	4834 (53)	0.479 (0.026)	7.827 (0.034)	He/H=0	···	−4.02	4.65
J0712−0428	3059515898856688000	DA	5381 (22)	0.662 (0.009)	8.126 (0.01)	He/H=0	···	−3.99	5.12
J0717+1125	3156974449176326528	DA	4839 (20)	0.510 (0.009)	7.883 (0.011)	He/H=0	···	−4.04	5.34
J0717+3630	898002379406954752	DZ	7183 (56)	0.645 (0.025)	8.114 (0.028)	log H/He=−4.0	log Ca/He=−9.07	−3.49	1.78
J0718+1229	3166062806131275136	DA	7350 (63)	0.538 (0.013)	7.906 (0.015)	He/H=0	···	−3.32	1.21
J0718+4547	974375354722176768	DC	9613 (46)	0.551 (0.006)	7.951 (0.007)	log H/He=−4.4	···	−2.89	0.68
J0718+5514	987361166866000128	DC	4928 (73)	0.572 (0.07)	7.989 (0.082)	He/H=0	···	−4.07	6.23
J0719+3343	896326002132552320	DC	7025 (62)	0.630 (0.038)	8.090 (0.043)	log H/He=−3.4	···	−3.51	1.81
J0721+3955	948173369860748160	DZ	6582 (38)	0.501 (0.021)	7.875 (0.026)	log H/He=−3.0	log Ca/He=−9.79	−3.51	1.61
J0722+2806	885100916128136064	DA	5224 (16)	0.607 (0.008)	8.041 (0.009)	He/H=0	···	−3.99	5.02
J0723+6602	1101763324511186304	DA	7583 (58)	0.553 (0.016)	7.931 (0.02)	He/H=0	···	−3.28	1.16
J0724+0431	3139699128636949248	DA	5687 (37)	0.545 (0.015)	7.931 (0.018)	He/H=0	···	−3.78	2.42
J0724+3206	892944179243357056	DA	9905 (64)	0.807 (0.017)	8.328 (0.019)	He/H=0	···	−3.04	1.06
J0724+4400	973275770078523520	DC	5997 (41)	0.665 (0.018)	8.148 (0.02)	H/He=0	···	−3.82	3.73
J0724−1338	3032020450247993600	DA	5000 (45)	0.635 (0.019)	8.089 (0.021)	He/H=0	···	−4.10	7.08
J0726+2216	866081701427025536	DZ	7196 (33)	0.626 (0.016)	8.083 (0.018)	log H/He=−4.0	log Ca/He=−8.34	−3.46	1.70

Tableau A.2 *suite page suivante*

Tableau A.2 *(suite)*

Name	Gaia DR2/EDR3*	Sp Type	$T_{\rm eff}$ (K)	$M/M_{\odot}$	$\log g$	Composition	Métaux	$\log L/L_{\odot}$	τ (Gyr)
J0726+3531	896951830406797568	DA	7204 (55)	0.640 (0.018)	8.078 (0.02)	He/H=0	···	−3.45	1.64
J0727+1434	3166841329084630784	DA	5702 (14)	0.581 (0.006)	7.992 (0.006)	He/H=0	···	−3.81	2.64
J0729+2716	872009447786700672	DA	9264 (34)	0.588 (0.007)	7.983 (0.008)	He/H=0	···	−2.95	0.75
J0729+3552	898473932456801024	DC	9130 (61)	0.652 (0.018)	8.120 (0.021)	log H/He=−4.2	···	−3.07	0.98
J0730+3412	893633710472340992	DA	7148 (41)	0.615 (0.015)	8.038 (0.018)	He/H=0	···	−3.44	1.57
J0730+5332	983979721933760768	DC	4675 (24)	0.563 (0.011)	7.975 (0.013)	He/H=0	···	−4.15	7.05
J0731+4022	900399039877540096	DA*	4806 (18)	0.566 (0.02)	7.980 (0.023)	He/H=0	···	−4.11	6.57
J0731−0015	3086397068370475392	DA	10070 (38)	0.637 (0.007)	8.062 (0.008)	He/H=0	···	−2.85	0.67
J0732+2822	873303774834413056	DA	7203 (46)	0.555 (0.015)	7.937 (0.019)	He/H=0	···	−3.37	1.33
J0733+2315	866574493091351936	DZ	8787 (64)	0.613 (0.014)	8.058 (0.016)	log H/He=−4.2	···	−3.10	0.99
J0733+3910	899434463238910720	DC	8794 (60)	0.588 (0.017)	8.016 (0.019)	log H/He=−4.2	···	−3.08	0.94
J0733+6409	1089400763661597440	DAP	5205 (13)	0.511 (0.005)	7.879 (0.006)	He/H=0	···	−3.91	3.21
J0736+2917	879383936697674496	DA	7110 (37)	0.628 (0.017)	8.059 (0.019)	He/H=0	···	−3.46	1.65
J0736+4033	924374548053164800	DAH :	6559 (80)	0.824 (0.035)	8.363 (0.039)	He/H=0	···	−3.79	4.00
J0736+4118	924478859922238720	DZ	4830 (26)	0.621 (0.05)	8.085 (0.056)	log H/He=−5.0	log Ca/He=−9.41	−4.16	6.81
J0738+1101	3150099301752709504	DC	6001 (56)	0.602 (0.02)	8.049 (0.023)	log H/He=−3.0	···	−3.76	2.90
J0738+4227	925003537421986304	DC*	4723 (30)	0.365 (0.031)	7.598 (0.048)	He/H=0	···	−3.95	3.26
J0738+4326	925258860342797568	DC	6073 (18)	0.687 (0.007)	8.183 (0.007)	H/He=0	···	−3.82	3.75
J0739+2347	867440427218037120	DA	8613 (71)	0.599 (0.015)	8.004 (0.018)	He/H=0	···	−3.09	0.93
J0739+2504	868706888517664000	DA	7841 (90)	0.801 (0.037)	8.324 (0.042)	He/H=0	···	−3.45	2.13
J0740+2218	866962856917166208	DAZ	5904 (31)	0.659 (0.015)	8.139 (0.017)	He/H=0	log Ca/H=−8.78	−3.84	3.94
J0740−1724	5717278911884258176	DZA	7461 (145)	0.561 (0.022)	7.976 (0.026)	log H/He=−3.0	log Ca/He=−10.94	−3.34	1.34
J0741+0136	3087094163041546240	DC	5325 (29)	0.549 (0.016)	7.966 (0.019)	H/He=0	···	−3.93	4.51
J0742+2857	878635723331279360	DA	8155 (50)	0.531 (0.021)	7.889 (0.026)	He/H=0	···	−3.12	0.92
J0742+3157	880354496226790400	DAH	9484 (55)	0.733 (0.009)	8.216 (0.011)	He/H=0	···	−3.05	0.99
J0742+4223	924219890574729856	DA	6742 (42)	0.622 (0.014)	8.051 (0.016)	He/H=0	···	−3.55	1.86
J0744+4649	927618687178189056	DZ	4830 (16)	0.564 (0.017)	7.992 (0.02)	log H/He=−4.0	log Ca/He=−9.15	−4.11	6.16
J0745+2626	874900643675606912	DC	4028 (13)	0.533 (0.015)	7.929 (0.018)	He/H=0	···	−4.39	8.58
J0746+3557	894957694270675584	DA	6764 (27)	0.625 (0.015)	8.055 (0.017)	He/H=0	···	−3.55	1.86
J0747+1107	3151407827963355136	DA	8083 (29)	1.146 (0.003)	8.893 (0.005)	He/H=0	···	−3.81	3.83
J0747+2438	867739936760402560	DA	5645 (22)	0.568 (0.01)	7.970 (0.013)	He/H=0	···	−3.82	2.63
J0747+2438	867740005479885184	DC	4904 (19)	0.567 (0.015)	7.979 (0.018)	He/H=0	···	−4.07	6.25
J0748+1125	3151443115414582016	DC	9139 (44)	0.810 (0.007)	8.361 (0.008)	log H/He=−4.2	···	−3.22	1.42
J0748+2134	674479430781455872	DA	7402 (52)	0.598 (0.026)	8.008 (0.03)	He/H=0	···	−3.36	1.37

Tableau A.2 *suite page suivante*

Tableau A.2 *(suite)*

Name	Gaia DR2/EDR3*	Sp Type	$T_{\rm eff}$ (K)	$M/M_{\odot}$	$\log g$	Composition	Métaux	$\log L/L_{\odot}$	τ (Gyr)
J0748+3506	894591075862208128	DZA	5411 (21)	0.623 (0.012)	8.086 (0.014)	log H/He=−5.0	log Ca/He=−11.00	−3.96	5.20
J0749+1732	668127242870832768	DA	6882 (62)	0.907 (0.025)	8.489 (0.03)	He/H=0	···	−3.79	4.21
J0749+3124	880840789603989504	DZ	6774 (52)	0.670 (0.025)	8.153 (0.028)	log H/He=−2.0	log Ca/He=−9.46	−3.61	2.29
J0750+0711	3144837318276010624	DC	4354 (17)	0.478 (0.008)	7.831 (0.01)	He/H=0	···	−4.20	6.77
J0750+0711	3144837112117580800	DC	4736 (14)	0.550 (0.006)	7.953 (0.007)	He/H=0	···	−4.12	6.53
J0750+0918	3148732406937031936	DA	5134 (20)	0.571 (0.011)	7.984 (0.014)	He/H=0	···	−3.99	4.82
J0750+1740	668317840636534912	DA	7148 (27)	0.641 (0.008)	8.080 (0.009)	He/H=0	···	−3.46	1.68
J0750+2538	873994719110827264	DC	7635 (38)	0.682 (0.011)	8.170 (0.012)	log H/He=−3.6	···	−3.41	1.65
J0751+1416	3164518640833807872	DC	5882 (38)	0.578 (0.019)	8.010 (0.023)	log H/He=−3.0	···	−3.78	2.92
J0751+6707	1096117955074105088	DA	5653 (29)	0.720 (0.012)	8.213 (0.013)	He/H=0	···	−3.95	4.78
J0752+4447	926374594063195904	DC :	9297 (53)	0.590 (0.01)	8.018 (0.012)	log H/He=−4.4	···	−2.98	0.81
J0752+4724	933421359789700736	DC	6918 (64)	0.691 (0.025)	8.186 (0.028)	log H/He=−3.4	···	−3.59	2.33
J0752−0307	3080914632816248448	DC	4461 (36)	0.437 (0.016)	7.751 (0.021)	He/H=0	···	−4.12	5.42
J0753+4229	925532265076649472	DC	4619 (7)	0.487 (0.005)	7.844 (0.007)	He/H=0	···	−4.11	5.93
J0753+5229	984190381489031424	DC	7251 (16)	0.769 (0.003)	8.302 (0.004)	log H/He=−3.6	···	−3.58	2.66
J0753+6122	1084764020047940096	DC	7628 (32)	0.583 (0.006)	8.012 (0.006)	log H/He=−3.6	···	−3.32	1.33
J0753−0009	3084195266274202752	DA	9951 (47)	0.583 (0.008)	7.971 (0.01)	He/H=0	···	−2.82	0.62
J0753−2523	5602379190877207936	DA	5006 (9)	0.554 (0.004)	7.957 (0.005)	He/H=0	···	−4.02	5.32
J0754+1614	666999556257654784	DA	7994 (49)	0.489 (0.015)	7.812 (0.02)	He/H=0	···	−3.12	0.88
J0754+6611	1094919590481107968	DC	6702 (24)	0.564 (0.006)	7.984 (0.007)	log H/He=−3.2	···	−3.53	1.77
J0755+0813	3145370645837100160	DA	5676 (31)	0.671 (0.016)	8.137 (0.018)	He/H=0	···	−3.90	4.00
J0755+3621	906771229452899584	DA	7850 (19)	0.574 (0.005)	7.966 (0.006)	He/H=0	···	−3.23	1.11
J0756+3646	918886709424112896	DA	6501 (29)	0.764 (0.019)	8.273 (0.021)	He/H=0	···	−3.75	3.49
J0756+4139	922434906461782272	DA	6898 (21)	0.848 (0.005)	8.399 (0.005)	He/H=0	···	−3.72	3.72
J0756+4242	922621269386513152	DA	6772 (39)	0.724 (0.024)	8.212 (0.026)	He/H=0	···	−3.64	2.59
J0756+5741	1081813343155426560	DC	9497 (40)	0.650 (0.006)	8.115 (0.006)	log H/He=−4.4	···	−3.00	0.88
J0756−2001	5714040261719110784	DC	4711 (275)	1.000 (0.008)	8.656 (0.013)	log H/He=−3.63	···	−4.57	7.72
J0757+3230	881146316398060672	DA	6052 (40)	0.600 (0.037)	8.020 (0.043)	He/H=0	···	−3.72	2.36
J0757+6453	1094608119452121856	DC	8638 (69)	0.712 (0.015)	8.214 (0.017)	log H/He=−4.0	···	−3.22	1.29
J0759+4335	923023248261420672	DCP	6520 (17)	0.838 (0.004)	8.406 (0.004)	log H/He=−3.2	···	−3.83	4.04
J0759+4735	933095015289999872	DA	8943 (44)	0.655 (0.008)	8.094 (0.008)	He/H=0	···	−3.08	0.96
J0800+0655	3144237908341731712	DAH	10559 (105)	1.001 (0.014)	8.628 (0.018)	He/H=0	···	−3.14	1.72
J0800+2052	670842761712806912	DC	7521 (77)	0.744 (0.029)	8.265 (0.031)	log H/He=−3.6	···	−3.50	2.17
J0800−0840	3039671225803688320	DZ	6979 (60)	0.660 (0.017)	8.137 (0.018)	log H/He=−4.0	log Ca/He=−9.93	−3.55	2.00

Tableau A.2 *suite page suivante*

Tableau A.2 *(suite)*

Name	Gaia DR2/EDR3*	Sp Type	$T_{\rm eff}$ (K)	$M/M_{\odot}$	$\log g$	Composition	Métaux	$\log L/L_{\odot}$	τ (Gyr)
J0801+3618	907000821224488832	DC	7225 (40)	0.517 (0.017)	7.900 (0.021)	log H/He=−3.4	···	−3.36	1.32
J0801+3949	921281480108851200	DC	4811 (35)	0.632 (0.037)	8.085 (0.041)	He/H=0	···	−4.16	7.94
J0801+4852	933287876501371520	DA	5138 (14)	0.532 (0.007)	7.917 (0.009)	He/H=0	···	−3.96	3.90
J0801+5329	936641833642799744	DZ	8847 (70)	0.720 (0.015)	8.226 (0.016)	log H/He=−5.0	log Ca/He=−8.40	−3.19	1.24
J0802+5646	1081514379072280320	DC	4417 (13)	0.498 (0.012)	7.866 (0.014)	He/H=0	···	−4.20	6.95
J0803+0022	3084427916062349440	DA	6509 (35)	0.615 (0.015)	8.041 (0.018)	He/H=0	···	−3.60	2.01
J0804+0716	3145766676180517760	DA	7473 (37)	0.575 (0.016)	7.969 (0.02)	He/H=0	···	−3.32	1.27
J0804+1714	668796162553518720	DQ	5457 (18)	0.531 (0.023)	7.934 (0.028)	H/He=0	log C/He=−7.06	−3.87	3.69
J0804+2239	680099824985004288	DZ	4920 (26)	0.515 (0.006)	7.909 (0.009)	log H/He=−1.25	···	−4.04	5.30
J0804+3538	906160863060179072	DA	9307 (57)	0.888 (0.011)	8.453 (0.013)	He/H=0	···	−3.24	1.67
J0804+4213	922686832063591168	DA	9067 (55)	0.586 (0.01)	7.980 (0.012)	He/H=0	···	−2.99	0.79
J0805+0724	3097756127294671488	DQ	5382 (19)	0.556 (0.027)	7.977 (0.033)	H/He=0	log C/He=−6.97	−3.92	4.38
J0805+0735	3145802036649641472	DA	5378 (16)	0.665 (0.007)	8.131 (0.008)	He/H=0	···	−3.99	5.19
J0805+1820	669024203839693056	DA	6751 (57)	0.668 (0.022)	8.124 (0.024)	He/H=0	···	−3.59	2.10
J0805+3833	908962109449446656	DA	4909 (11)	0.627 (0.006)	8.076 (0.006)	He/H=0	···	−4.12	7.41
J0805+4720	932855386179190272	DA	7070 (34)	0.604 (0.02)	8.020 (0.024)	He/H=0	···	−3.45	1.57
J0805+4821	933057593239584000	DA	8157 (90)	0.986 (0.027)	8.609 (0.034)	He/H=0	···	−3.58	3.27
J0805+4957	934937139647967232	DA	7091 (59)	0.747 (0.029)	8.245 (0.032)	He/H=0	···	−3.58	2.43
J0805+5339	1032545631568349056	DC	6529 (42)	0.554 (0.026)	7.967 (0.031)	log H/He=−3.2	···	−3.57	1.85
J0805+6624	1095169656358227456	DZ	6622 (77)	0.643 (0.027)	8.111 (0.03)	log H/He=−3.0	log Ca/He=−10.86	−3.63	2.24
J0805−0654	3063960605892490368	DC	6008 (50)	0.689 (0.027)	8.185 (0.03)	H/He=0	···	−3.84	3.96
J0806+2215	677060225090183552	DA	5700 (18)	0.625 (0.01)	8.064 (0.011)	He/H=0	···	−3.85	3.18
J0806+4058	921642532239821440	DZH*	6090 (42)	0.679 (0.029)	8.170 (0.032)	log H/He=−3.0	log Ca/He=−9.10	−3.81	3.61
J0807+2557	681934703732973824	DA	6751 (37)	0.617 (0.028)	8.043 (0.032)	He/H=0	···	−3.54	1.84
J0807+4431	928937074630507392	DA	6309 (21)	0.787 (0.009)	8.310 (0.01)	He/H=0	···	−3.82	4.07
J0807+4854	934555334235313664	DA	6589 (35)	0.657 (0.016)	8.108 (0.018)	He/H=0	···	−3.62	2.19
J0807−0753	3063650376111451136	DC	9608 (48)	0.624 (0.009)	8.073 (0.011)	log H/He=−4.4	···	−2.95	0.81
J0808+1854	669444943132791424	DA	5687 (25)	0.556 (0.01)	7.949 (0.012)	He/H=0	···	−3.79	2.49
J0808+4640	929774314079963264	DQ	5430 (22)	0.530 (0.072)	7.934 (0.088)	H/He=0	log C/He=−6.05	−3.88	3.79
J0808−0431	3067956368587354368	DC	4907 (27)	0.456 (0.015)	7.802 (0.021)	H/He=0	···	−3.99	4.41
J0809+0245	3091044532222339584	DA	7198 (35)	0.888 (0.014)	8.459 (0.016)	He/H=0	···	−3.69	3.66
J0809+1112	649672906567630976	DZ	6375 (28)	0.645 (0.01)	8.116 (0.011)	log H/He=−4.0	log Ca/He=−11.15	−3.69	2.61
J0809+2250	677196843705878272	DA	6662 (20)	0.704 (0.01)	8.182 (0.011)	He/H=0	···	−3.65	2.52
J0809+2920	876571935709366272	DA	7049 (18)	0.649 (0.004)	8.094 (0.005)	He/H=0	···	−3.50	1.78

Tableau A.2 *suite page suivante*

Tableau A.2 *(suite)*

Name	Gaia DR2/EDR3*	Sp Type	$T_{\rm eff}$ (K)	$M/M_{\odot}$	$\log g$	Composition	Métaux	$\log L/L_{\odot}$	τ (Gyr)
J0809+3527	905923368548465152	DA	8867 (27)	0.502 (0.004)	7.830 (0.005)	He/H=0	···	−2.94	0.70
J0810+0041	3083765357227100800	DA	10091 (70)	0.416 (0.009)	7.645 (0.014)	He/H=0	···	−2.62	0.40
J0811+2321	677593660028220544	DA	6429 (50)	0.633 (0.028)	8.071 (0.032)	He/H=0	···	−3.64	2.17
J0811+4816	931487524994983808	DA	8116 (61)	0.662 (0.022)	8.110 (0.024)	He/H=0	···	−3.26	1.26
J0812+0942	3146576878812071168	DA	6346 (81)	1.013 (0.039)	8.657 (0.051)	He/H=0	···	−4.05	5.50
J0813+0935	3146523896095375744	DA*	6056 (31)	0.609 (0.02)	8.034 (0.022)	He/H=0	···	−3.73	2.42
J0813+1130	649041786893358336	DA	10393 (50)	0.604 (0.008)	8.004 (0.009)	He/H=0	···	−2.76	0.58
J0813+1220	650230771279461760	DA	6207 (27)	0.683 (0.013)	8.152 (0.015)	He/H=0	···	−3.75	2.98
J0813+1957	675615677264385536	DC	4085 (31)	0.486 (0.014)	7.845 (0.018)	He/H=0	···	−4.32	7.75
J0814+1300	650340408909616896	DA	7796 (64)	0.865 (0.017)	8.422 (0.019)	He/H=0	···	−3.52	2.77
J0814+2455	682315757527779584	DQ	8086 (21)	0.573 (0.007)	7.993 (0.008)	H/He=0	log C/He=−5.56	−3.21	1.12
J0814+3300	902414964384353408	DC*	4601 (58)	0.762 (0.032)	8.299 (0.046)	log H/He=−2.42	···	−4.37	8.19
J0814+3437	902857685316692352	DC	6665 (26)	0.659 (0.017)	8.137 (0.018)	log H/He=−3.2	···	−3.63	2.32
J0814+4845	931573222477949696	DC	6381 (11)	0.538 (0.003)	7.941 (0.003)	log H/He=−3.2	···	−3.60	1.90
J0815+1633	655808799925588992	DA	4693 (37)	0.200 (0.0)	7.027 (0.02)	He/H=0	···	−3.65	1.62
J0815+5339	1031832946170531456	DA	9592 (67)	0.890 (0.012)	8.455 (0.014)	He/H=0	···	−3.19	1.51
J0815+5814	1035222289547372800	DA	7725 (46)	0.861 (0.01)	8.415 (0.011)	He/H=0	···	−3.54	2.80
J0816+1313	650432664805355392	DC	5468 (25)	0.506 (0.018)	7.890 (0.022)	H/He=0	···	−3.84	3.27
J0816+2137	676031052142751488	DA	6193 (11)	0.579 (0.005)	7.984 (0.005)	He/H=0	···	−3.66	2.10
J0817+2008	675590693439332096	DAH*	7273 (44)	0.822 (0.015)	8.359 (0.017)	He/H=0	···	−3.60	2.98
J0817+2822	684152216824047104	DC	4612 (33)	0.483 (0.018)	7.838 (0.025)	He/H=0	···	−4.11	5.88
J0817+2902	684258010458273152	DC	5984 (63)	0.671 (0.03)	8.157 (0.033)	log H/He=−3.0	···	−3.83	3.83
J0818+4144	915672081021495552	DAH :*	8568 (56)	0.778 (0.02)	8.287 (0.022)	He/H=0	···	−3.27	1.45
J0818+4449	928440365957680256	DC	5920 (54)	0.600 (0.033)	8.047 (0.037)	log H/He=−3.0	···	−3.79	3.12
J0819+1321	650400263572196480	DC	5902 (51)	0.629 (0.04)	8.093 (0.045)	H/He=0	···	−3.82	3.58
J0819+1948	663601481211006592	DA	5563 (16)	0.595 (0.016)	8.016 (0.018)	He/H=0	···	−3.87	3.09
J0819+3159	901360494077262208	DC	4731 (34)	0.535 (0.024)	7.927 (0.029)	He/H=0	···	−4.11	6.28
J0819+5732	1035126803834023296	DZ	6055 (28)	0.560 (0.009)	7.980 (0.011)	log H/He=−3.0	log Ca/He=−11.12	−3.71	2.37
J0820+0855	600139357979417344	DC	6965 (48)	0.684 (0.019)	8.175 (0.021)	log H/He=−3.4	···	−3.58	2.21
J0820+1523	652438247031965056	DC	9919 (71)	0.668 (0.014)	8.143 (0.015)	log H/He=−4.6	···	−2.94	0.82
J0820+3834	908364559240386944	DA	7591 (29)	0.619 (0.006)	8.042 (0.007)	He/H=0	···	−3.34	1.35
J0820+4310	916276228300814976	DA	6966 (18)	0.295 (0.008)	7.369 (0.016)	He/H=0	···	−3.13	0.77
J0820+4803	931304937345481344	DA	6391 (21)	0.575 (0.007)	7.975 (0.007)	He/H=0	···	−3.60	1.92
J0821+3727	908048587085834752	DA	5028 (24)	0.578 (0.016)	7.997 (0.018)	He/H=0	···	−4.04	5.74

Tableau A.2 *suite page suivante*

Tableau A.2 *(suite)*

Name	Gaia DR2/EDR3*	Sp Type	$T_{\rm eff}$ (K)	$M/M_{\odot}$	$\log g$	Composition	Métaux	$\log L/L_{\odot}$	τ (Gyr)
J0822+0300	3090505359208876288	DA	6677 (40)	0.651 (0.028)	8.098 (0.031)	He/H=0	···	−3.59	2.06
J0822+2023	664021842547278592	DC	7005 (19)	0.349 (0.005)	7.557 (0.008)	log H/He=−3.4	···	−3.24	0.94
J0823+0546	3093722358432322176	DZ	5831 (14)	0.521 (0.007)	7.915 (0.009)	log H/He=−4.0	log Ca/He=−9.34	−3.74	2.49
J0823+4833	930966979254089472	DA	6240 (26)	0.786 (0.009)	8.308 (0.01)	He/H=0	···	−3.84	4.17
J0823+8237	1145602571097053952	DC	4817 (36)	0.564 (0.024)	7.975 (0.027)	He/H=0	···	−4.10	6.47
J0824+3104	709051168734737024	DA :*	7947 (35)	0.580 (0.012)	8.007 (0.013)	log H/He=−3.5	···	−3.25	1.20
J0825+2242	677874722688200832	DC	6177 (59)	0.606 (0.034)	8.054 (0.038)	log H/He=−3.0	···	−3.72	2.52
J0825+5049	1028072371590379136	DC	4667 (30)	0.526 (0.015)	7.913 (0.018)	He/H=0	···	−4.12	6.42
J0825+6003	1035806851776104448	DA	9999 (55)	0.597 (0.009)	7.994 (0.011)	He/H=0	···	−2.83	0.63
J0826+3249	902972034525449088	DAZ	6068 (27)	0.566 (0.015)	7.990 (0.018)	He/H=0	log Ca/H=−9.21	−3.71	2.40
J0826+4645	930242465515189376	DC	7334 (39)	0.646 (0.012)	8.114 (0.013)	log H/He=−3.6	···	−3.45	1.69
J0826−0539	3065135949463337984	DA	7981 (65)	0.679 (0.016)	8.137 (0.018)	He/H=0	···	−3.30	1.38
J0827+2607	679723276611814400	DA	7352 (34)	0.691 (0.018)	8.158 (0.02)	He/H=0	···	−3.46	1.76
J0827+4553	918126843809713280	DA	6991 (74)	1.137 (0.022)	8.877 (0.036)	He/H=0	···	−4.05	4.76
J0828+0208	3079642326059886208	DA*	6601 (27)	0.558 (0.01)	7.944 (0.013)	He/H=0	···	−3.53	1.68
J0828+0942	599922307511771776	DC	4513 (14)	0.286 (0.009)	7.410 (0.018)	He/H=0	···	−3.94	2.94
J0828+3131	709004920527186816	DC	6168 (33)	0.584 (0.018)	8.019 (0.02)	log H/He=−3.0	···	−3.70	2.35
J0828+3527	903847348860521856	DC	4898 (38)	0.548 (0.035)	7.948 (0.042)	He/H=0	···	−4.06	5.87
J0828−0141	3076010742232557952	DA	6422 (43)	0.675 (0.025)	8.137 (0.029)	He/H=0	···	−3.68	2.54
J0829+2539	679636484296738304	DC	4575 (29)	0.388 (0.041)	7.652 (0.061)	He/H=0	···	−4.03	3.97
J0829+4419	917707418778058368	DC	6072 (41)	0.659 (0.023)	8.139 (0.026)	H/He=0	···	−3.79	3.44
J0829+5312	1028955489881696768	DA	9827 (58)	0.671 (0.012)	8.118 (0.014)	He/H=0	···	−2.93	0.78
J0829+5641	1034060277555338368	DC	9882 (80)	0.569 (0.015)	7.981 (0.018)	log H/He=−4.6	···	−2.85	0.66
J0830+3241	710766750855439360	DA	7407 (19)	0.878 (0.004)	8.443 (0.005)	He/H=0	···	−3.63	3.32
J0830+4139	915116621490557440	DA	10012 (70)	0.609 (0.013)	8.015 (0.015)	He/H=0	···	−2.83	0.64
J0830+4520	918044247294118656	DA	10149 (33)	0.412 (0.004)	7.635 (0.006)	He/H=0	···	−2.60	0.39
J0831+1641	658781771991055104	DA	7199 (28)	0.599 (0.009)	8.011 (0.011)	He/H=0	···	−3.41	1.48
J0831+1905	662716271271960320	DA	6140 (44)	0.612 (0.029)	8.039 (0.033)	He/H=0	···	−3.71	2.35
J0831+3331	710947963731953792	DA	5817 (19)	0.658 (0.007)	8.114 (0.008)	He/H=0	···	−3.84	3.41
J0831−1643	5709868512742196608	DC	4181 (30)	0.522 (0.014)	7.909 (0.016)	He/H=0	···	−4.31	8.03
J0832+3139	710452358868303232	DA	6305 (27)	0.713 (0.011)	8.198 (0.012)	He/H=0	···	−3.75	3.23
J0832+5714	1034473453408991360	DA	5836 (30)	0.680 (0.02)	8.150 (0.023)	He/H=0	···	−3.86	3.70
J0832+6507	1092515229130044544	DA	6477 (34)	0.794 (0.016)	8.319 (0.018)	He/H=0	···	−3.78	3.85
J0832−0207	3073014263809462528	DA	9599 (82)	1.004 (0.011)	8.634 (0.014)	He/H=0	···	−3.31	2.28

Tableau A.2 *suite page suivante*

Tableau A.2 *(suite)*

Name	Gaia DR2/EDR3*	Sp Type	$T_{\rm eff}$ (K)	$M/M_{\odot}$	$\log g$	Composition	Métaux	$\log L/L_{\odot}$	τ (Gyr)
J0832−0408	3065744460430556032	DQ	6716 (29)	0.640 (0.016)	8.106 (0.018)	H/He=0	log C/He=−4.90	−3.60	2.11
J0833+2914	707673416242396160	DA	6667 (33)	0.617 (0.014)	8.043 (0.016)	He/H=0	···	−3.56	1.90
J0834+0321	3080205580955810432	DA	6056 (55)	0.821 (0.033)	8.361 (0.037)	He/H=0	···	−3.92	4.86
J0834+0727	595867686585664256	DA	9327 (56)	0.558 (0.018)	7.931 (0.022)	He/H=0	···	−2.91	0.69
J0834+3659	910087768838947456	DA	9012 (37)	0.596 (0.007)	7.998 (0.008)	He/H=0	···	−3.01	0.82
J0835+4718	918648974394418816	DA	6570 (28)	0.576 (0.013)	7.975 (0.016)	He/H=0	···	−3.55	1.78
J0835+4758	1014793672740325248	DA	8035 (108)	0.852 (0.025)	8.401 (0.027)	He/H=0	···	−3.46	2.41
J0835+5332	1030289712881895296	DAH	8727 (120)	0.825 (0.022)	8.359 (0.024)	He/H=0	···	−3.29	1.61
J0835−0435	3065513047592503552	DC	9564 (60)	0.618 (0.013)	8.064 (0.014)	log H/He=−4.4	···	−2.96	0.81
J0836+1452	657598147723622912	DA	8000 (54)	0.901 (0.02)	8.477 (0.022)	He/H=0	···	−3.52	2.85
J0836+2216	665991789427730432	DA	7985 (51)	0.714 (0.018)	8.191 (0.019)	He/H=0	···	−3.33	1.49
J0836+2432	678537968717235072	DQ	5328 (29)	0.351 (0.073)	7.583 (0.122)	H/He=0	log C/He=−7.44	−3.74	2.32
J0836+3506	711527372000026624	DA	6146 (35)	0.506 (0.026)	7.856 (0.034)	He/H=0	···	−3.60	1.77
J0836+4556	918237791404732416	DC	5011 (45)	0.676 (0.035)	8.153 (0.038)	He/H=0	···	−4.13	7.71
J0836+5104	1027695136022450432	DC	5727 (48)	0.668 (0.026)	8.154 (0.029)	H/He=0	···	−3.90	4.66
J0837+3154	709769115467848448	DC	6260 (52)	0.604 (0.032)	8.051 (0.037)	log H/He=−3.2	···	−3.69	2.36
J0837+4613	918336060256260480	DA	6279 (37)	0.602 (0.018)	8.021 (0.021)	He/H=0	···	−3.66	2.15
J0837+5100	1027704894188127232	DA	7331 (51)	0.312 (0.009)	7.410 (0.018)	He/H=0	···	−3.06	0.71
J0837+5427	1030621658018969856	DC	6732 (57)	0.599 (0.026)	8.042 (0.029)	log H/He=−3.2	···	−3.56	1.90
J0838+1321	603155765049434752	DC*	6566 (50)	0.615 (0.022)	8.067 (0.025)	log H/He=−3.2	···	−3.62	2.11
J0838+2322	666207736086203648	DZ	5880 (46)	0.684 (0.028)	8.178 (0.03)	log H/He=−3.0	log Ca/He=−9.91	−3.87	4.30
J0838+2804	704316671665447296	DC	4701 (28)	0.395 (0.016)	7.683 (0.024)	H/He=0	···	−4.00	3.83
J0840+0939	598240497102033024	DA	9608 (59)	0.650 (0.012)	8.084 (0.014)	He/H=0	···	−2.95	0.78
J0840+1518	657673498630210176	DAZ	6420 (34)	0.673 (0.025)	8.159 (0.028)	He/H=0	log Ca/H=−8.82	−3.71	2.84
J0840+2244	666111739274159360	DC	6418 (47)	0.667 (0.02)	8.151 (0.022)	log H/He=−3.2	···	−3.70	2.78
J0840+3431	711260465552649216	DA	7110 (42)	0.859 (0.017)	8.414 (0.019)	He/H=0	···	−3.68	3.52
J0840+3714	909928404076399744	DC	5948 (46)	0.585 (0.023)	8.022 (0.027)	log H/He=−3.0	···	−3.76	2.84
J0841+0223	3079104660578372480	DAH	6991 (74)	0.799 (0.03)	8.324 (0.034)	He/H=0	···	−3.65	3.11
J0841+3329	710392886455231360	DQ	6706 (53)	1.006 (0.036)	8.665 (0.045)	H/He=0	log C/He=−6.46	−3.96	4.36
J0841+4737	1014548520302641536	DA	8560 (53)	0.492 (0.012)	7.814 (0.016)	He/H=0	···	−3.00	0.75
J0842+1406	609236712891803264	DZ	7132 (36)	0.581 (0.021)	8.011 (0.025)	log H/He=−4.0	log Ca/He=−8.39	−3.44	1.58
J0842+2409	690287663506579328	DA	5901 (18)	0.602 (0.007)	8.024 (0.008)	He/H=0	···	−3.77	2.54
J0842+5959	1040866941726072064	DC	5849 (64)	0.610 (0.021)	8.063 (0.024)	log H/He=−3.0	···	−3.82	3.49
J0842−1347	5734737438536674432	DZ	5627 (14)	0.779 (0.004)	8.321 (0.004)	log H/He=−1.5	log Ca/He=−9.55	−4.04	5.95

Tableau A.2 *suite page suivante*

Tableau A.2 *(suite)*

Name	Gaia DR2/EDR3*	Sp Type	$T_{\rm eff}$ (K)	$M/M_{\odot}$	$\log g$	Composition	Métaux	$\log L/L_{\odot}$	τ (Gyr)
J0843+0002	3075067700558242176	DA	8945 (120)	0.948 (0.021)	8.547 (0.025)	He/H=0	···	−3.37	2.37
J0843+3412	716446797477471104	DA	9310 (51)	0.417 (0.009)	7.653 (0.013)	He/H=0	···	−2.76	0.50
J0843+5414	1030381796981255936	DA	6948 (47)	0.583 (0.017)	7.985 (0.021)	He/H=0	···	−3.46	1.56
J0844+1035	598769843231677056	DA	6329 (31)	0.668 (0.021)	8.127 (0.024)	He/H=0	···	−3.70	2.58
J0844+4536	917321936874346880	DA	8600 (26)	0.323 (0.004)	7.427 (0.008)	He/H=0	···	−2.79	0.48
J0845+3214	710026160671981440	DA	7286 (41)	0.379 (0.012)	7.584 (0.02)	He/H=0	···	−3.16	0.87
J0845+3801	910341618586847232	DA	8060 (38)	0.592 (0.007)	7.996 (0.008)	He/H=0	···	−3.21	1.09
J0845+6117	1042071701528617728	DAH	5940 (14)	0.672 (0.005)	8.136 (0.005)	He/H=0	···	−3.82	3.34
J0845+6117	1042071701528617856	DA	5534 (15)	0.616 (0.006)	8.050 (0.006)	He/H=0	···	−3.90	3.51
J0845+6143	1042192506072573312	DQ	7946 (24)	0.547 (0.009)	7.950 (0.011)	H/He=0	log C/He=−5.37	−3.22	1.11
J0845−2701	5646089927728820736	DC	4439 (71)	0.637 (0.03)	8.095 (0.034)	He/H=0	···	−4.31	9.30
J0846+0514	582729312907277568	DA	6489 (41)	0.602 (0.025)	8.020 (0.029)	He/H=0	···	−3.60	1.97
J0846+3538	717393648787722624	DZA	8563 (20)	0.623 (0.003)	8.075 (0.003)	log H/He=−4.0	log Ca/He=−8.69	−3.16	1.09
J0846+6352	1044109229717304064	DA	8116 (39)	0.639 (0.009)	8.072 (0.01)	He/H=0	···	−3.24	1.19
J0846+6944	1118460924702185088	DC	4960 (25)	0.513 (0.013)	7.886 (0.015)	He/H=0	···	−4.00	4.64
J0847+1830	660222170879118208	DQ	8464 (41)	0.524 (0.01)	7.908 (0.013)	H/He=0	log C/He=−5.47	−3.08	0.89
J0848+3548	717762977319125632	DZ	7860 (63)	0.691 (0.021)	8.183 (0.024)	log H/He=−4.0	log Ca/He=−10.45	−3.37	1.56
J0849+0923	597646245427109376	DA	8612 (43)	0.590 (0.013)	7.989 (0.016)	He/H=0	···	−3.08	0.91
J0849+1827	660212752014880256	DZ	6201 (52)	0.639 (0.026)	8.107 (0.029)	log H/He=−3.0	log Ca/He=−10.45	−3.74	2.85
J0849+3319	716112442863454464	DA	7627 (30)	0.605 (0.007)	8.019 (0.008)	He/H=0	···	−3.31	1.29
J0849+3429	716504796716020352	DA	7548 (22)	0.581 (0.005)	7.980 (0.006)	He/H=0	···	−3.31	1.25
J0849+4439	914211487199415680	DC	5907 (19)	0.669 (0.016)	8.155 (0.018)	H/He=0	···	−3.85	4.05
J0849+5942	1040991259555635328	DA	6017 (27)	0.565 (0.012)	7.961 (0.015)	He/H=0	···	−3.70	2.18
J0849−0156	3073747187092773632	DC	4892 (11)	0.562 (0.005)	7.971 (0.006)	He/H=0	···	−4.07	6.21
J0851+1543	609898313949732608	DZ	6408 (39)	0.692 (0.025)	8.188 (0.027)	log H/He=−3.0	log Ca/He=−8.80	−3.73	3.06
J0851+1624	611645983387812992	DC	5752 (19)	0.550 (0.007)	7.965 (0.008)	H/He=0	···	−3.79	2.94
J0851+5426	1029968414968983424	DA	8825 (65)	0.757 (0.014)	8.282 (0.015)	log H/He=−3.5	···	−3.23	1.35
J0852+1850	660431181166277120	DAZ	8108 (56)	0.561 (0.017)	7.973 (0.02)	He/H=0	log Ca/H=−6.94	−3.20	1.08
J0852+3209	712789886226437632	DC	5864 (30)	0.546 (0.016)	7.957 (0.019)	H/He=0	···	−3.75	2.60
J0852−0144	5764001760847057280	DC	6077 (55)	0.623 (0.03)	8.082 (0.034)	log H/He=−3.0	···	−3.76	2.95
J0853−0137	5764027015254831488	DA	6139 (55)	0.616 (0.03)	8.045 (0.035)	He/H=0	···	−3.71	2.38
J0853−2446	5652718097353105664	DC	3740 (37)	0.672 (0.004)	8.165 (0.006)	log H/He=−1.07	···	−4.65	9.11
J0854+2752	692904776058392064	DA	6954 (32)	0.562 (0.012)	7.949 (0.016)	He/H=0	···	−3.44	1.48
J0854+2926	705484593532621952	DA :	5106 (38)	0.587 (0.023)	8.010 (0.026)	He/H=0	···	−4.02	5.38

Tableau A.2 *suite page suivante*

Tableau A.2 *(suite)*

Name	Gaia DR2/EDR3*	Sp Type	$T_{\rm eff}$ (K)	$M/M_{\odot}$	$\log g$	Composition	Métaux	$\log L/L_{\odot}$	τ (Gyr)
J0854+3503	716743042845256576	DC	4738 (73)	0.925 (0.02)	8.540 (0.032)	log H/He=0.19	···	−4.48	7.99
J0855+0639	584402318633098624	DQ	7297 (34)	0.552 (0.015)	7.962 (0.019)	H/He=0	log C/He=−6.04	−3.37	1.39
J0855+3700	718682620012682112	DA	5768 (18)	0.447 (0.008)	7.749 (0.01)	He/H=0	···	−3.66	1.81
J0855−0833	5755957119598921728	DC	4619 (13)	0.478 (0.009)	7.827 (0.012)	He/H=0	···	−4.10	5.72
J0855−2637	5649105922480851200	DA	8542 (38)	0.840 (0.008)	8.382 (0.008)	He/H=0	···	−3.34	1.85
J0855−2637	5649105926779602432	DA	8035 (30)	0.680 (0.007)	8.138 (0.008)	He/H=0	···	−3.29	1.35
J0857+1808	612262122214240512	DA	6773 (13)	0.582 (0.008)	7.985 (0.01)	He/H=0	···	−3.50	1.67
J0857+2542	691600338653939328	DA	6075 (21)	0.633 (0.025)	8.074 (0.028)	He/H=0	···	−3.75	2.60
J0857+3901	719707193051500928	DA	6549 (31)	0.602 (0.015)	8.019 (0.018)	He/H=0	···	−3.58	1.92
J0857+4150	912788233820354560	DC	6514 (82)	0.666 (0.034)	8.148 (0.038)	log H/He=−3.2	···	−3.68	2.61
J0857+6308	1043885758275341184	DC	9304 (63)	0.625 (0.013)	8.076 (0.014)	log H/He=−4.4	···	−3.01	0.88
J0858+4126	912718071240545152	DAH	7232 (26)	0.868 (0.006)	8.428 (0.006)	He/H=0	···	−3.66	3.44
J0858+6813	1117334024067935872	DC	4630 (13)	0.563 (0.008)	7.976 (0.01)	He/H=0	···	−4.17	7.23
J0859+3257	712888090655562624	DQ	9760 (18)	0.912 (0.002)	8.513 (0.002)	H/He=0	log C/He=−3.32	−3.20	1.67
J0859+5934	1038018828652951296	DA	5061 (38)	0.545 (0.029)	7.940 (0.035)	He/H=0	···	−3.99	4.71
J0859+6016	1038076351151065088	DQ	7519 (11)	0.547 (0.004)	7.952 (0.004)	H/He=0	log C/He=−5.69	−3.32	1.28
J0859−0058	5764485618978306176	DC	5016 (10)	0.566 (0.003)	7.976 (0.005)	He/H=0	···	−4.03	5.52
J0900−0008	5764602334714811904	DC	6270 (58)	0.667 (0.038)	8.151 (0.042)	log H/He=−3.2	···	−3.75	3.05
J0900−2213	5655188871777035520	DC	5034 (55)	0.244 (0.018)	7.297 (0.039)	H/He=0	···	−3.71	1.87
J0901+3037	711612103114782592	DC	6251 (72)	0.632 (0.044)	8.096 (0.05)	log H/He=−3.2	···	−3.72	2.67
J0901+3846	719266799987963392	DC*	7439 (53)	0.610 (0.02)	8.057 (0.023)	log H/He=−3.6	···	−3.39	1.51
J0901+4946	1015799828959492352	DC	4877 (68)	0.477 (0.043)	7.842 (0.054)	H/He=0	···	−4.02	4.84
J0901−0141	5764107760640582656	DA	7655 (57)	0.713 (0.018)	8.191 (0.02)	He/H=0	···	−3.41	1.67
J0902+1535	610411820238973056	DC	4659 (20)	0.226 (0.009)	7.223 (0.021)	He/H=0	···	−3.80	2.12
J0902+2010	684598618544000384	DQ	5487 (7)	0.718 (0.007)	8.231 (0.008)	H/He=0	log C/He=−5.51	−4.03	5.96
J0902+3120	711744456827031680	DA	9823 (33)	0.737 (0.005)	8.220 (0.005)	He/H=0	···	−2.99	0.91
J0902+5630	1036295206737529856	DA	5121 (29)	0.312 (0.022)	7.460 (0.041)	He/H=0	···	−3.73	1.89
J0902+6503	1044511002434919936	DZ	6403 (49)	0.652 (0.019)	8.127 (0.021)	log H/He=−4.0	log Ca/He=−10.34	−3.69	2.64
J0903+0838	585164761227127424	DA	5444 (20)	0.695 (0.013)	8.176 (0.014)	He/H=0	···	−4.00	5.32
J0903+2012	636651837034002944	DA	7224 (27)	0.526 (0.008)	7.884 (0.01)	He/H=0	···	−3.33	1.23
J0903+2139	685402357248747648	DA	7805 (52)	0.872 (0.021)	8.432 (0.024)	He/H=0	···	−3.53	2.81
J0903+2444	688314207636275328	DA	8677 (83)	0.628 (0.023)	8.053 (0.027)	He/H=0	···	−3.11	0.98
J0904+0211	577342113952420224	DA	6265 (46)	0.816 (0.02)	8.353 (0.023)	He/H=0	···	−3.86	4.43
J0904+1349	606938634805314944	DA	8221 (35)	0.595 (0.007)	7.999 (0.009)	He/H=0	···	−3.17	1.04

Tableau A.2 *suite page suivante*

Tableau A.2 *(suite)*

Name	Gaia DR2/EDR3*	Sp Type	$T_{\rm eff}$ (K)	$M/M_{\odot}$	$\log g$	Composition	Métaux	$\log L/L_{\odot}$	τ (Gyr)
J0904+1349	606938634805314816	DA	9638 (38)	0.611 (0.007)	8.020 (0.008)	He/H=0	···	−2.90	0.71
J0904+3017	699628147926656768	DA	6725 (35)	0.597 (0.018)	8.011 (0.021)	He/H=0	···	−3.53	1.77
J0904+3403	713438705462521728	DC	4934 (23)	0.542 (0.014)	7.957 (0.016)	H/He=0	···	−4.06	5.66
J0905+0904	591207406550605312	DQ	8539 (36)	0.562 (0.007)	7.974 (0.009)	H/He=0	log C/He=−5.19	−3.10	0.95
J0905+1124	604127802048700032	DC	6759 (66)	0.630 (0.027)	8.091 (0.031)	log H/He=−3.4	···	−3.58	2.02
J0905+2315	685671909396428544	DA	6141 (48)	0.733 (0.041)	8.228 (0.045)	He/H=0	···	−3.82	3.78
J0905+3653	715502037814544384	DC	6613 (49)	0.746 (0.039)	8.269 (0.042)	log H/He=−3.2	···	−3.72	3.27
J0905+5143	1016617865610081152	DA	8009 (47)	0.889 (0.013)	8.457 (0.015)	He/H=0	···	−3.50	2.75
J0905+7314	1123700235048742016	DC	5199 (11)	0.598 (0.005)	8.027 (0.005)	He/H=0	···	−3.99	4.98
J0905−0154	5763373596110853248	DAZ	6701 (50)	0.579 (0.021)	8.008 (0.025)	He/H=0	log Ca/H=−9.14	−3.55	1.84
J0906+0122	577026966432521088	DA	7150 (71)	0.960 (0.029)	8.569 (0.035)	He/H=0	···	−3.78	4.17
J0906+0128	577035178410047616	DC	6440 (53)	0.607 (0.034)	8.055 (0.039)	log H/He=−3.2	···	−3.64	2.18
J0906+4702	1012210992942502144	DQ	5701 (34)	0.762 (0.035)	8.296 (0.038)	H/He=0	log C/He=−5.44	−4.00	5.64
J0907+1042	592019425952313600	DA	7474 (40)	0.503 (0.011)	7.840 (0.015)	He/H=0	···	−3.25	1.07
J0907+2736	692134636881870208	DA	7557 (58)	0.668 (0.026)	8.122 (0.029)	He/H=0	···	−3.39	1.55
J0907+3643	715437789400182016	DA	8710 (40)	0.774 (0.007)	8.281 (0.008)	He/H=0	···	−3.24	1.37
J0907+5138	1016560970179771264	DC	7089 (60)	0.593 (0.025)	8.030 (0.03)	log H/He=−3.4	···	−3.46	1.65
J0908+4431	1009518284670371840	DA	9223 (78)	0.865 (0.017)	8.418 (0.019)	He/H=0	···	−3.23	1.55
J0909+0828	590316282441032704	DA	6473 (34)	0.621 (0.031)	8.051 (0.035)	He/H=0	···	−3.62	2.07
J0909+4700	1011466005095102464	DC	4650 (39)	0.490 (0.018)	7.867 (0.031)	log H/He=−1.88	···	−4.11	5.54
J0909+6019	1039435691120199936	DA	8439 (32)	0.644 (0.006)	8.079 (0.006)	He/H=0	···	−3.17	1.09
J0909−2246	5651964996310470144	DC	4549 (33)	0.575 (0.016)	7.996 (0.019)	He/H=0	···	−4.21	7.80
J0910+2156	685295640197734528	DA	5739 (21)	0.393 (0.008)	7.636 (0.012)	He/H=0	···	−3.61	1.62
J0910+2554	688818750329816192	DC*	4900 (75)	0.711 (0.023)	8.222 (0.035)	log H/He=−2.15	···	−4.22	7.39
J0910+3744	716010802461047552	DC	3745 (129)	0.668 (0.099)	8.144 (0.108)	He/H=0	···	−4.63	11.32
J0910+4929	1013058162355432832	DA	7470 (58)	0.571 (0.019)	7.962 (0.024)	He/H=0	···	−3.32	1.26
J0911+1354	606216148291719680	DA	9324 (56)	0.632 (0.014)	8.055 (0.016)	He/H=0	···	−2.98	0.81
J0911+1515	607535218647587328	DC	4918 (20)	0.546 (0.022)	7.945 (0.027)	He/H=0	···	−4.05	5.71
J0911−0012	3842126835031738368	DA	6192 (26)	0.582 (0.013)	7.988 (0.015)	He/H=0	···	−3.66	2.12
J0912+0808	590183142750379136	DZ	6328 (32)	0.605 (0.015)	8.053 (0.016)	log H/He=−4.0	log Ca/He=−10.48	−3.67	2.29
J0912+1951	636732410620758016	DA	5087 (12)	0.615 (0.008)	8.055 (0.009)	He/H=0	···	−4.05	6.13
J0912+2251	686867284694206336	DC	4953 (18)	0.561 (0.013)	7.970 (0.016)	He/H=0	···	−4.05	5.83
J0912+2538	688606063549945600	DA	6338 (14)	0.552 (0.005)	7.936 (0.006)	He/H=0	···	−3.59	1.84
J0913+0112	3843483151343659776	DA	7329 (57)	0.873 (0.015)	8.435 (0.017)	He/H=0	···	−3.64	3.37

Tableau A.2 *suite page suivante*

Tableau A.2 *(suite)*

Name	Gaia DR2/EDR3*	Sp Type	$T_{\rm eff}$ (K)	$M/M_\odot$	$\log g$	Composition	Métaux	$\log L/L_\odot$	τ (Gyr)
J0913+2627	688954024621015040	DZ	5105 (47)	0.617 (0.086)	8.078 (0.097)	log H/He=−4.0	log Ca/He=−9.72	−4.06	6.10
J0913+3116	699920381797443712	DZ	4874 (19)	0.530 (0.025)	7.936 (0.03)	log H/He=−4.0	log Ca/He=−10.31	−4.07	5.62
J0913+4047	815429197896495104	DA	6723 (28)	0.532 (0.009)	7.898 (0.011)	He/H=0	···	−3.47	1.50
J0913+5933	1038500174228188416	DA	6927 (62)	0.832 (0.02)	8.375 (0.022)	He/H=0	···	−3.70	3.53
J0913+6205	1040160612880069888	DA	5744 (13)	0.650 (0.005)	8.104 (0.005)	He/H=0	···	−3.86	3.49
J0915+2719	695023530668813952	DA	6562 (42)	0.612 (0.046)	8.035 (0.053)	He/H=0	···	−3.59	1.95
J0915+5325	1022780838737369216	DCP	6837 (8)	0.629 (0.002)	8.089 (0.002)	log H/He=−3.4	···	−3.56	1.94
J0915+6631	1068706339918614016	DA	7995 (66)	0.720 (0.015)	8.201 (0.016)	He/H=0	···	−3.34	1.51
J0916+0548	579835153490062976	DA	6397 (25)	0.625 (0.01)	8.058 (0.011)	He/H=0	···	−3.65	2.15
J0916+1011	591040864898749312	DQZA	8516 (27)	0.553 (0.005)	7.959 (0.006)	log H/He=−4.0	log C/He=−4.91	−3.10	0.94
J0916+2259	638935758908460288	DA	5855 (19)	0.734 (0.015)	8.232 (0.016)	He/H=0	···	−3.90	4.41
J0916+2540	687914432080614528	DZ	5812 (13)	0.698 (0.009)	8.200 (0.01)	log H/He=−4.0	log Ca/He=−7.20	−3.91	4.68
J0916+4359	818602457173176192	DA	8695 (27)	0.610 (0.005)	8.023 (0.005)	He/H=0	···	−3.09	0.93
J0918+0124	3844228070471625216	DC	5956 (53)	0.508 (0.032)	7.891 (0.039)	log H/He=−3.0	···	−3.69	2.21
J0918+1057	592605431290049152	DC	5151 (22)	0.548 (0.014)	7.944 (0.017)	He/H=0	···	−3.96	4.15
J0918+3222	701552327634833280	DA	7957 (50)	0.555 (0.031)	7.933 (0.038)	He/H=0	···	−3.19	1.03
J0918+3737	811059120212556416	DC	6140 (61)	0.721 (0.046)	8.234 (0.05)	log H/He=−3.0	···	−3.83	3.93
J0918−0205	3838626849001351168	DC	5974 (31)	0.533 (0.018)	7.934 (0.022)	log H/He=−3.0	···	−3.71	2.31
J0919+0113	3844209481853063296	DA	6184 (25)	0.644 (0.015)	8.090 (0.016)	He/H=0	···	−3.72	2.54
J0919+7723	1131562121144696960	DA	9065 (44)	0.345 (0.004)	7.480 (0.007)	He/H=0	···	−2.72	0.44
J0920+1935	635777617916154368	DA	6326 (26)	0.669 (0.02)	8.129 (0.023)	He/H=0	···	−3.71	2.60
J0920+5442	1023278947569264896	DC	7124 (82)	0.717 (0.029)	8.225 (0.032)	log H/He=−3.4	···	−3.56	2.34
J0920−1728	5681814336118618368	DA	6217 (75)	0.623 (0.02)	8.056 (0.023)	He/H=0	···	−3.69	2.33
J0921+1729	632270313262592640	DA	6548 (39)	0.833 (0.055)	8.378 (0.062)	He/H=0	···	−3.80	4.11
J0921+5935	1038360708050042496	DC	6076 (66)	0.725 (0.033)	8.239 (0.035)	H/He=0	···	−3.85	4.14
J0922+0103	3843957354387777152	DAZ	6105 (11)	0.558 (0.004)	7.976 (0.005)	He/H=0	log Ca/H=−9.08	−3.69	2.28
J0922+0504	585488567401589248	DAH	5754 (23)	0.678 (0.01)	8.146 (0.012)	He/H=0	···	−3.88	3.87
J0922+2121	637716641031134848	DC :	6491 (52)	0.608 (0.028)	8.056 (0.032)	log H/He=−3.2	···	−3.63	2.14
J0922+2628	694006757290271360	DA	6675 (22)	0.593 (0.029)	8.004 (0.035)	He/H=0	···	−3.54	1.78
J0922+4125	812885610888282880	DA	6308 (45)	0.522 (0.031)	7.883 (0.04)	He/H=0	···	−3.57	1.73
J0923+0105	3844051225193053440	DC	6970 (56)	0.728 (0.017)	8.242 (0.018)	log H/He=−3.4	···	−3.61	2.63
J0923+0559	585700189030449920	DA	5732 (16)	0.207 (0.007)	7.089 (0.02)	He/H=0	···	−3.35	0.90
J0923+1842	632656894678554624	DQ	6932 (40)	0.641 (0.019)	8.108 (0.021)	H/He=0	log C/He=−6.28	−3.54	1.93
J0923+2413	639439884989423616	DA	7211 (58)	0.796 (0.024)	8.320 (0.027)	He/H=0	···	−3.59	2.79

Tableau A.2 *suite page suivante*

Tableau A.2 *(suite)*

Name	Gaia DR2/EDR3*	Sp Type	$T_{\rm eff}$ (K)	$M/M_{\odot}$	$\log g$	Composition	Métaux	$\log L/L_{\odot}$	τ (Gyr)
J0923+4819	1011870071322756096	DA	7200 (61)	0.883 (0.017)	8.451 (0.02)	He/H=0	···	−3.68	3.62
J0924+0521	585513959248023936	DA	6173 (39)	0.672 (0.025)	8.134 (0.029)	He/H=0	···	−3.75	2.88
J0924+2107	637527525030988160	DAZ	6230 (39)	0.685 (0.022)	8.178 (0.024)	He/H=0	log Ca/H=−8.29	−3.77	3.33
J0924+3120	700531568527365376	DC	4855 (19)	0.630 (0.013)	8.082 (0.014)	He/H=0	···	−4.14	7.73
J0925+3130	700557819367554432	DZ	5931 (38)	0.657 (0.025)	8.137 (0.027)	log H/He=−3.0	log Ca/He=−8.81	−3.83	3.84
J0925+3539	798602271945568256	DA	7101 (32)	0.640 (0.015)	8.078 (0.017)	He/H=0	···	−3.47	1.70
J0925+6120	1039163458912998272	DA	8031 (22)	0.514 (0.004)	7.857 (0.005)	He/H=0	···	−3.13	0.92
J0926+1321	594116366425186944	DA	9162 (135)	0.908 (0.068)	8.484 (0.079)	He/H=0	···	−3.29	1.92
J0926+1932	634225902066816640	DA	7525 (47)	0.605 (0.014)	8.020 (0.016)	He/H=0	···	−3.34	1.34
J0926+3642	810799665531428608	DA	6153 (38)	0.733 (0.033)	8.228 (0.036)	He/H=0	···	−3.81	3.76
J0926+4725	819574013135499776	DQ	7103 (32)	0.555 (0.023)	7.967 (0.027)	H/He=0	log C/He=−6.44	−3.42	1.50
J0927+0028	3840946062621774592	DA	7806 (84)	0.901 (0.029)	8.476 (0.033)	He/H=0	···	−3.56	3.05
J0927+0207	3844512328587119616	DC	6703 (99)	0.646 (0.036)	8.116 (0.04)	log H/He=−3.2	···	−3.61	2.17
J0927+0947	589285627728700160	DA	10382 (67)	1.000 (0.011)	8.627 (0.014)	He/H=0	···	−3.17	1.81
J0928+1458	618571635330439040	DC*	5290 (31)	0.668 (0.016)	8.156 (0.018)	H/He=0	···	−4.04	6.06
J0928+1841	633911196927706880	DA	7880 (33)	0.896 (0.006)	8.468 (0.008)	He/H=0	···	−3.54	2.94
J0928+1937	634307433430523648	DZ	6054 (35)	0.600 (0.025)	8.046 (0.029)	log H/He=−4.0	log Ca/He=−10.44	−3.75	2.74
J0928+2638	694176429973819520	DQ+DA	7054 (24)	0.265 (0.013)	7.327 (0.028)	H/He=0	log C/He=−6.57	−3.12	0.73
J0928+3622	798742730259141376	DC	7672 (36)	0.696 (0.01)	8.191 (0.011)	log H/He=−3.6	···	−3.42	1.68
J0928+3737	811237923994639744	DC	6546 (50)	0.680 (0.029)	8.170 (0.032)	log H/He=−3.2	···	−3.68	2.71
J0928+4300	814576110016081920	DC*	4599 (24)	0.475 (0.026)	7.822 (0.034)	He/H=0	···	−4.10	5.75
J0928+6049	1039078998380506880	DC	4668 (219)	0.905 (0.054)	8.510 (0.082)	log H/He=−4.80	···	−4.48	8.12
J0929+3310	701307621874580864	DQ	6643 (18)	0.509 (0.028)	7.887 (0.034)	H/He=0	log C/He=−5.11	−3.50	1.60
J0929+6649	1068317142866278016	DA	6029 (60)	0.696 (0.029)	8.173 (0.033)	He/H=0	···	−3.82	3.50
J0929−1732	5681903877596752640	DA	7396 (37)	0.632 (0.01)	8.064 (0.012)	He/H=0	···	−3.39	1.50
J0930+0628	586075122495366400	DC	6529 (50)	1.035 (0.02)	8.712 (0.026)	log H/He=−3.2	···	−4.04	4.59
J0930+3845	811435114533149056	DA	6105 (39)	0.550 (0.03)	7.935 (0.038)	He/H=0	···	−3.66	2.02
J0930+5941	1038689805623461376	DA	9201 (135)	0.841 (0.021)	8.381 (0.023)	He/H=0	···	−3.21	1.42
J0931+2100	634839219101579136	DC*	5942 (44)	0.632 (0.031)	8.098 (0.034)	H/He=0	···	−3.81	3.49
J0933+2911	696261653777188864	DA	8319 (36)	0.911 (0.006)	8.490 (0.006)	He/H=0	···	−3.46	2.62
J0933+3743	799278226781362048	DZA	5668 (35)	0.611 (0.019)	8.065 (0.021)	log H/He=−1.0	log Ca/He=−8.03	−3.87	4.15
J0934+1910	633295848373672320	DA	9188 (33)	0.620 (0.01)	8.037 (0.011)	He/H=0	···	−3.00	0.82
J0934+5637	1025040880593486720	DA	6754 (58)	0.846 (0.022)	8.395 (0.024)	He/H=0	···	−3.76	3.92
J0935+0024	3841045053027974912	DQ	5644 (25)	0.699 (0.029)	8.202 (0.032)	H/He=0	log C/He=−5.32	−3.96	5.27

Tableau A.2 *suite page suivante*

Tableau A.2 *(suite)*

Name	Gaia DR2/EDR3*	Sp Type	$T_{\rm eff}$ (K)	$M/M_{\odot}$	$\log g$	Composition	Métaux	$\log L/L_{\odot}$	τ (Gyr)
J0936+0428	3851443134492197888	DA	6202 (32)	0.713 (0.033)	8.197 (0.037)	He/H=0	···	−3.78	3.41
J0936+0747	587767202170593536	DA	8619 (58)	0.623 (0.015)	8.045 (0.018)	He/H=0	···	−3.12	0.98
J0936+8221	1145020139172129536	DA	9218 (72)	0.603 (0.012)	8.009 (0.013)	He/H=0	···	−2.98	0.79
J0938+0711	3854286918237953536	DC	6706 (60)	0.623 (0.051)	8.080 (0.058)	log H/He=−3.2	···	−3.59	2.03
J0938+5412	1021408850089922560	DA	8674 (95)	0.849 (0.019)	8.395 (0.021)	He/H=0	···	−3.32	1.82
J0939+1021	588813460499195264	DA	8317 (46)	0.612 (0.021)	8.027 (0.024)	He/H=0	···	−3.17	1.05
J0939+1341	617587538064096640	DA	6135 (31)	0.592 (0.016)	8.006 (0.02)	He/H=0	···	−3.69	2.23
J0939+4951	826275295988399232	DA	5978 (21)	0.803 (0.006)	8.334 (0.006)	He/H=0	···	−3.93	4.85
J0939+5201	1020158400426591872	DQ	8537 (41)	0.560 (0.01)	7.970 (0.012)	H/He=0	log C/He=−5.03	−3.10	0.95
J0939+5550	1022128244227188224	DZA	8888 (40)	0.583 (0.007)	8.008 (0.008)	log H/He=−4.0	log Ca/He=−8.48	−3.05	0.90
J0939+5911	1026514226174393344	DC	5935 (60)	0.631 (0.025)	8.096 (0.029)	log H/He=−3.0	···	−3.81	3.50
J0939+6018	1050825733935333376	DA	7079 (57)	0.562 (0.017)	7.950 (0.022)	He/H=0	···	−3.41	1.42
J0939−1458	5688717241916173568	DC	4325 (18)	0.542 (0.009)	7.942 (0.011)	He/H=0	···	−4.27	7.88
J0940+0210	3847322577227869952	DQ	7199 (27)	0.640 (0.008)	8.105 (0.009)	H/He=0	log C/He=−6.01	−3.48	1.75
J0940+0906	588349771535238912	DQ	6270 (37)	0.524 (0.035)	7.917 (0.043)	H/He=0	log C/He=−6.94	−3.62	1.94
J0940+0907	588349805894986624	DC	4691 (17)	0.325 (0.012)	7.524 (0.02)	H/He=0	···	−3.94	2.95
J0941+0901	588332900903805824	DQ	8634 (33)	0.280 (0.006)	7.354 (0.015)	H/He=0	log C/He=−5.17	−2.77	0.45
J0941+6511	1064978578888570496	DC	4368 (28)	0.415 (0.014)	7.709 (0.021)	He/H=0	···	−4.14	5.35
J0942+0117	3846462656056088448	DA	6158 (42)	0.754 (0.023)	8.260 (0.025)	He/H=0	···	−3.83	3.99
J0942+0347	3848159236857539584	DA	7939 (108)	0.875 (0.034)	8.436 (0.038)	He/H=0	···	−3.50	2.70
J0942+0942	588530847356236672	DA	5249 (18)	0.598 (0.012)	8.027 (0.013)	He/H=0	···	−3.98	4.66
J0942+4437	820899298308206208	DC	4625 (35)	0.218 (0.013)	7.126 (0.033)	He/H=0	···	−3.73	3.09
J0942+4654	824743882449610752	DA	9209 (37)	0.571 (0.007)	7.953 (0.008)	He/H=0	···	−2.95	0.74
J0942+6600	1065088220813167744	DC	7687 (65)	0.743 (0.021)	8.263 (0.022)	log H/He=−3.6	···	−3.46	2.00
J0943+5134	1020076452450631296	DC	4848 (22)	0.498 (0.012)	7.861 (0.014)	He/H=0	···	−4.03	5.03
J0943−0703	3820383996887145088	DA	5991 (18)	0.562 (0.004)	7.956 (0.006)	He/H=0	···	−3.70	2.19
J0944+4407	820169737983275904	DA	6863 (70)	0.814 (0.026)	8.348 (0.029)	He/H=0	···	−3.70	3.45
J0944+4807	825049851623687296	DC	6004 (46)	0.622 (0.014)	8.081 (0.016)	log H/He=−3.0	···	−3.78	3.15
J0944+6037	1050892563625773184	DA	9265 (62)	0.660 (0.013)	8.101 (0.014)	He/H=0	···	−3.02	0.88
J0945+0154	3846557660732848384	DA	6969 (25)	0.647 (0.009)	8.091 (0.011)	He/H=0	···	−3.51	1.82
J0945+2327	641625576666483584	DA	7197 (31)	0.583 (0.01)	7.985 (0.011)	He/H=0	···	−3.40	1.43
J0945+2327	641625576666484480	DA	6948 (34)	0.579 (0.011)	7.978 (0.014)	He/H=0	···	−3.46	1.55
J0945+4035	801512095107318144	DA	6772 (50)	0.582 (0.018)	7.984 (0.022)	He/H=0	···	−3.50	1.67
J0945+6850	1070129451562454400	DC	8732 (59)	0.809 (0.01)	8.359 (0.011)	log H/He=−4.0	···	−3.29	1.65

Tableau A.2 *suite page suivante*

Tableau A.2 *(suite)*

Name	Gaia DR2/EDR3*	Sp Type	$T_{\rm eff}$ (K)	$M/M_{\odot}$	$\log g$	Composition	Métaux	$\log L/L_{\odot}$	τ (Gyr)
J0946+2255	641362724667841536	DA	6630 (48)	0.632 (0.035)	8.067 (0.04)	He/H=0	···	−3.59	2.00
J0946+3251	793575201703625984	DA	6752 (30)	0.704 (0.008)	8.182 (0.008)	He/H=0	···	−3.62	2.40
J0946+6738	1069735341067492224	DA	6713 (44)	0.614 (0.016)	8.039 (0.019)	He/H=0	···	−3.55	1.85
J0947+4459	820969357814798080	DC	4616 (46)	0.830 (0.018)	8.399 (0.026)	log H/He=−2.61	···	−4.43	8.27
J0947+4500	820969357814799872	DA	4912 (56)	0.653 (0.027)	8.117 (0.03)	He/H=0	···	−4.14	7.84
J0948+1232	613553056239392768	DQ	7092 (42)	0.644 (0.019)	8.112 (0.02)	H/He=0	log C/He=−6.49	−3.51	1.83
J0948+1319	614379236149119360	DA	7059 (35)	0.662 (0.013)	8.114 (0.015)	He/H=0	···	−3.50	1.82
J0948+1519	616394263005286272	DA	7940 (68)	0.845 (0.025)	8.391 (0.027)	He/H=0	···	−3.47	2.44
J0948+2023	639665392247496576	DC	4773 (20)	0.538 (0.011)	7.932 (0.013)	He/H=0	···	−4.09	6.13
J0948+2441	643229626692471040	DA	9002 (41)	0.674 (0.013)	8.126 (0.014)	He/H=0	···	−3.09	0.99
J0948+5252	1020268248510254464	DA	7181 (58)	0.606 (0.024)	8.024 (0.027)	He/H=0	···	−3.42	1.52
J0950+1509	616396182856185728	DC	4999 (19)	0.420 (0.011)	7.733 (0.016)	H/He=0	···	−3.92	3.55
J0950+3238	793334404360693632	DQA	8178 (55)	0.417 (0.037)	7.702 (0.056)	log H/He=−4.0	log C/He=−5.36	−3.04	0.75
J0950+5315	1020653077580086784	DQ	8092 (11)	0.536 (0.003)	7.930 (0.003)	H/He=0	log C/He=−5.55	−3.18	1.03
J0951+1009	3879201783004024832	DA	6811 (32)	0.589 (0.014)	7.997 (0.017)	He/H=0	···	−3.50	1.67
J0951+1900	627240597321087488	DC	5659 (25)	0.531 (0.014)	7.933 (0.016)	H/He=0	···	−3.80	3.01
J0951+2045	628067498784238208	DC	6304 (54)	0.513 (0.036)	7.897 (0.046)	log H/He=−3.2	···	−3.60	1.86
J0951+4033	807280785942808320	DZA	8237 (53)	0.699 (0.011)	8.194 (0.013)	log H/He=−4.0	log Ca/He=−10.12	−3.29	1.42
J0951+8039	1132614349476009728	DC	6345 (66)	0.678 (0.027)	8.167 (0.03)	log H/He=−3.2	···	−3.73	3.02
J0952+0602	3850381865253059328	DC	7095 (46)	0.609 (0.028)	8.056 (0.031)	log H/He=−3.4	···	−3.47	1.70
J0952+4454	820542992117501952	DA+dM	10972 (111)	0.625 (0.013)	8.038 (0.015)	He/H=0	···	−2.69	0.52
J0952+4807	823393402996648960	DA	7855 (65)	0.592 (0.016)	7.997 (0.019)	He/H=0	···	−3.25	1.16
J0954+3046	744878171010647552	DC	5961 (56)	0.570 (0.05)	7.997 (0.059)	log H/He=−3.0	···	−3.75	2.64
J0954+3129	745127553991482368	DA	6793 (51)	0.544 (0.021)	7.918 (0.026)	He/H=0	···	−3.46	1.50
J0954+6022	1050272718241775488	DC	6041 (53)	0.572 (0.016)	8.001 (0.019)	log H/He=−3.0	···	−3.73	2.49
J0954+6702	1066726497434084864	DA	5786 (17)	0.740 (0.005)	8.242 (0.005)	He/H=0	···	−3.93	4.66
J0955+5056	826954824238274048	DA	7393 (49)	0.616 (0.015)	8.039 (0.018)	He/H=0	···	−3.38	1.44
J0956+2114	628141337862068864	DA	8726 (67)	0.957 (0.02)	8.562 (0.024)	He/H=0	···	−3.42	2.60
J0957+0515	3850056169293341824	DC	6936 (45)	0.495 (0.017)	7.862 (0.021)	log H/He=−3.4	···	−3.41	1.39
J0957+2432	642685200933153408	DA	8848 (21)	0.680 (0.004)	8.136 (0.004)	He/H=0	···	−3.12	1.05
J0957−0107	3832801498958855552	DA	7900 (49)	0.713 (0.013)	8.190 (0.014)	He/H=0	···	−3.35	1.53
J0958+0846	3877871477014130048	DA	6879 (26)	0.646 (0.009)	8.090 (0.01)	He/H=0	···	−3.54	1.88
J0958+4345	808268967721645696	DA	6448 (45)	0.570 (0.02)	7.967 (0.025)	He/H=0	···	−3.58	1.85
J0959+0257	3836456103811208064*	DA	7349 (30)	0.621 (0.016)	8.047 (0.018)	He/H=0	···	−3.40	1.48

Tableau A.2 *suite page suivante*

Tableau A.2 *(suite)*

Name	Gaia DR2/EDR3*	Sp Type	$T_{\rm eff}$ (K)	$M/M_{\odot}$	$\log g$	Composition	Métaux	$\log L/L_{\odot}$	τ (Gyr)
J0959+1445	615705144092773376	DC	7218 (48)	0.651 (0.016)	8.123 (0.019)	log H/He=−3.4	···	−3.48	1.78
J0959+1528	616587738397098240	DA	7612 (48)	0.566 (0.013)	7.953 (0.017)	He/H=0	···	−3.28	1.18
J0959+2513	642837135401004672	DA	6868 (41)	0.655 (0.017)	8.104 (0.019)	He/H=0	···	−3.55	1.93
J0959+2556	643650361688870656	DZ	8826 (41)	0.585 (0.01)	8.012 (0.011)	log H/He=−4.0	log Ca/He=−10.92	−3.07	0.92
J1000+1231	3881473820703514752	DA	8848 (66)	0.660 (0.024)	8.103 (0.028)	He/H=0	···	−3.10	1.00
J1000+4236	807222713688595200	DC	4733 (56)	0.556 (0.028)	7.963 (0.034)	He/H=0	···	−4.12	6.66
J1001+1441	615733593956317568	DC	6438 (13)	0.590 (0.004)	8.028 (0.004)	log H/He=−3.2	···	−3.63	2.08
J1001+2428	642463713764824192	DA	7122 (63)	0.920 (0.027)	8.508 (0.031)	He/H=0	···	−3.74	3.97
J1001+3903	803211596486728064	DC	4946 (28)	1.032 (0.028)	8.708 (0.045)	log H/He=−4.26	···	−4.53	7.30
J1001+4656	822352371643412352	DC	4191 (37)	0.409 (0.016)	7.700 (0.023)	He/H=0	···	−4.21	5.89
J1002+4326	808030648576069760	DC	4725 (18)	0.545 (0.01)	7.944 (0.012)	He/H=0	···	−4.12	6.47
J1002+6108	1050402662475992320	DC	4331 (43)	0.479 (0.016)	7.831 (0.022)	He/H=0	···	−4.21	6.85
J1003+3303	746736796632638976	DA	9563 (48)	0.586 (0.01)	7.978 (0.012)	He/H=0	···	−2.89	0.69
J1003+3543	795686191013196544	DA	8244 (112)	0.895 (0.037)	8.466 (0.042)	He/H=0	···	−3.46	2.57
J1003+5401	852604201427010816	DA	9732 (56)	0.604 (0.011)	8.007 (0.013)	He/H=0	···	−2.88	0.68
J1003−0337	3828424828500179584	DA	8564 (31)	0.627 (0.006)	8.051 (0.006)	He/H=0	···	−3.13	1.00
J1004+1052	3880219037418284160	DA	7051 (80)	0.922 (0.036)	8.511 (0.042)	He/H=0	···	−3.76	4.07
J1004+2003	626844326458669568	DA	8700 (65)	0.988 (0.013)	8.611 (0.017)	He/H=0	···	−3.46	2.82
J1004+3405	747348704918599552	DA	6440 (38)	0.715 (0.025)	8.199 (0.027)	He/H=0	···	−3.72	3.00
J1004−0506	3822028007288795264	DC	3527 (14)	0.385 (0.004)	7.604 (0.01)	log H/He=−0.36	···	−4.43	12.49
J1005+0308	3836605980989228928	DA	8071 (49)	0.600 (0.021)	8.009 (0.025)	He/H=0	···	−3.21	1.10
J1005+5354	852433880203843712	DA	6815 (31)	0.834 (0.01)	8.378 (0.01)	He/H=0	···	−3.73	3.72
J1006+0711	3874412413432643328	DC	4923 (24)	0.602 (0.021)	8.037 (0.024)	He/H=0	···	−4.09	6.88
J1006+0712	3874412413432647680	DA	9512 (33)	0.583 (0.007)	7.974 (0.008)	He/H=0	···	−2.90	0.69
J1006−1828	5672600772274345600	DC	4861 (31)	0.483 (0.015)	7.835 (0.019)	He/H=0	···	−4.01	4.59
J1007+1541	621824987157964544	DA	7327 (37)	0.582 (0.016)	7.983 (0.019)	He/H=0	···	−3.37	1.36
J1007+1623	621979502901486720	DAH	10671 (83)	1.022 (0.011)	8.662 (0.014)	He/H=0	···	−3.15	1.79
J1007+3229	745895322345421568	DA	9756 (90)	0.793 (0.017)	8.307 (0.018)	He/H=0	···	−3.06	1.06
J1009+3621	801684301820413952	DA	6469 (33)	0.523 (0.013)	7.883 (0.017)	He/H=0	···	−3.53	1.62
J1010+4028	803585018126670208	DA	6041 (26)	0.635 (0.015)	8.076 (0.017)	He/H=0	···	−3.76	2.67
J1010+6155	1051954485699665280	DA	6926 (66)	0.778 (0.023)	8.293 (0.024)	He/H=0	···	−3.65	2.99
J1011+0029	3831947801194371072	DAH	6209 (21)	0.623 (0.007)	8.056 (0.008)	He/H=0	···	−3.70	2.34
J1011+2647	739253825436690432	DA	5388 (15)	0.571 (0.011)	7.979 (0.013)	He/H=0	···	−3.90	3.31
J1011+2845	740483560857296768	DQ*	4595 (18)	0.740 (0.009)	8.266 (0.01)	H/He=0	log C/He=−6.69	−4.35	8.12

Tableau A.2 *suite page suivante*

Tableau A.2 *(suite)*

Name	Gaia DR2/EDR3*	Sp Type	$T_{\rm eff}$ (K)	$M/M_{\odot}$	$\log g$	Composition	Métaux	$\log L/L_{\odot}$	τ (Gyr)
J1011+3727	801851053926004608	DAH :	6363 (33)	0.669 (0.026)	8.128 (0.029)	He/H=0	···	−3.69	2.54
J1011+4958	823804585985883776	DAH	6183 (31)	0.743 (0.017)	8.244 (0.019)	He/H=0	···	−3.81	3.83
J1012+6116	1051676171819127040	DA	6022 (61)	0.566 (0.026)	7.963 (0.031)	He/H=0	···	−3.70	2.18
J1012−1843	5669427512997660800	DZ	5715 (23)	0.542 (0.006)	7.952 (0.006)	log H/He=−4.0	log Ca/He=−10.31	−3.80	2.96
J1013+0305	3835861439819152128	DA	5165 (19)	0.529 (0.018)	7.911 (0.022)	He/H=0	···	−3.94	3.68
J1013+1733	622536749138267904	DC	6717 (63)	0.741 (0.027)	8.262 (0.03)	log H/He=−3.2	···	−3.69	3.09
J1014+0305	3835866563715176192	DA	5210 (21)	0.578 (0.019)	7.994 (0.022)	He/H=0	···	−3.97	4.44
J1014+0401	3860751256335185408	DA	7488 (17)	0.569 (0.008)	7.959 (0.01)	He/H=0	···	−3.31	1.24
J1014+2027	625415030061614336	DA	9258 (49)	0.601 (0.013)	8.005 (0.016)	He/H=0	···	−2.97	0.78
J1014+4226	805470233890349440	DA	7758 (29)	0.883 (0.005)	8.449 (0.006)	He/H=0	···	−3.55	2.96
J1014+5027	847884509109410816	DA	7570 (52)	0.608 (0.015)	8.024 (0.018)	He/H=0	···	−3.33	1.33
J1015+0806	3875651975353757440	DC	4597 (14)	0.521 (0.011)	7.904 (0.013)	He/H=0	···	−4.14	6.62
J1015+0806	3875652014008894720	DA	6650 (15)	0.561 (0.004)	7.949 (0.005)	He/H=0	···	−3.52	1.66
J1015+0907	3876618892751168000	DAH	7250 (61)	0.808 (0.024)	8.338 (0.027)	He/H=0	···	−3.60	2.87
J1015+1850	624921521139276800	DC	4712 (24)	0.270 (0.014)	7.361 (0.028)	He/H=0	···	−3.84	2.42
J1016+1817	624090737025312000	DC*	6844 (69)	0.708 (0.034)	8.211 (0.037)	log H/He=−3.4	···	−3.63	2.60
J1016+1932	625075796364911360	DA	9163 (53)	0.601 (0.013)	8.005 (0.015)	He/H=0	···	−2.98	0.80
J1016−0119	3830623164560911872	DA	7779 (16)	0.239 (0.002)	7.162 (0.005)	He/H=0	···	−2.83	0.44
J1017+0838	3875789001991057536	DQ	7465 (25)	0.514 (0.006)	7.895 (0.007)	H/He=0	log C/He=−6.15	−3.30	1.21
J1017+2336	725478112972149504	DAH :	10703 (102)	1.028 (0.012)	8.674 (0.016)	He/H=0	···	−3.15	1.81
J1017+7619	1127701323501940224	DA	6511 (31)	0.467 (0.007)	7.778 (0.01)	He/H=0	···	−3.46	1.40
J1018+0111	3832329434808415744	DAH	10962 (58)	0.969 (0.007)	8.576 (0.008)	He/H=0	···	−3.04	1.32
J1018+0547	3861407596057614080	DA	6290 (55)	0.754 (0.066)	8.259 (0.073)	He/H=0	···	−3.79	3.75
J1018+3421	752524965144307584	DA	7190 (63)	1.215 (0.011)	9.046 (0.022)	He/H=0	···	−4.14	4.28
J1018−0442	3780210350269115776	DAZ	7927 (40)	0.654 (0.011)	8.098 (0.012)	He/H=0	···	−3.29	1.32
J1019+3138	742962753035089792	DA	7331 (81)	0.852 (0.021)	8.403 (0.023)	He/H=0	···	−3.62	3.18
J1019+5214	848290091460808448	DA	5360 (24)	0.571 (0.01)	7.980 (0.012)	He/H=0	···	−3.91	3.42
J1021+1905	624600566824086016	DA	6346 (42)	0.573 (0.021)	7.973 (0.026)	He/H=0	···	−3.61	1.94
J1021+2503	726057456815979904	DA	8422 (66)	0.629 (0.021)	8.055 (0.025)	He/H=0	···	−3.16	1.05
J1021+4257	805697489201014272	DA	6422 (51)	0.669 (0.017)	8.128 (0.019)	He/H=0	···	−3.68	2.47
J1021−1034	3767515389014753152	DAH*	10587 (50)	0.985 (0.006)	8.603 (0.007)	He/H=0	···	−3.12	1.61
J1022+0708	3863287692225892736	DA	6343 (43)	0.655 (0.023)	8.106 (0.026)	He/H=0	···	−3.69	2.42
J1022+1328	3886816622581111552	DA	6673 (32)	0.635 (0.032)	8.072 (0.037)	He/H=0	···	−3.58	1.98
J1022+1658	3890322415406225408	DA	6637 (35)	0.593 (0.017)	8.003 (0.02)	He/H=0	···	−3.55	1.81

Tableau A.2 *suite page suivante*

Tableau A.2 *(suite)*

Name	Gaia DR2/EDR3*	Sp Type	$T_{\rm eff}$ (K)	$M/M_{\odot}$	$\log g$	Composition	Métaux	$\log L/L_{\odot}$	τ (Gyr)
J1022+2523	726160806613850624	DA	8619 (66)	0.694 (0.016)	8.158 (0.019)	He/H=0	···	−3.18	1.16
J1022+3904	755877620910173696	DZ	5774 (19)	0.676 (0.008)	8.167 (0.009)	log H/He=−3.0	log Ca/He=−10.28	−3.90	4.58
J1022+4600	833452873535333760	DA	7819 (30)	0.350 (0.005)	7.507 (0.009)	He/H=0	···	−3.00	0.67
J1022+4612	833470465721350784	DA	7223 (23)	0.732 (0.006)	8.223 (0.006)	He/H=0	···	−3.53	2.14
J1022+5344	851806982481563264	DA	6908 (67)	0.598 (0.032)	8.010 (0.038)	He/H=0	···	−3.48	1.65
J1022+8243	1146403741412820864	DA	5669 (31)	0.839 (0.014)	8.390 (0.015)	He/H=0	···	−4.06	6.07
J1023+3319	749177746806827264	DC :	8064 (59)	0.635 (0.019)	8.095 (0.021)	log H/He=−3.8	···	−3.27	1.30
J1023+6327	1052520154368111872	DA	6781 (15)	0.616 (0.004)	8.041 (0.004)	He/H=0	···	−3.53	1.81
J1023+6348	1052563683861162880	DA	6153 (21)	0.587 (0.01)	7.996 (0.011)	He/H=0	···	−3.68	2.18
J1024+8019	1133810794221801856	DA	7662 (56)	0.604 (0.012)	8.017 (0.014)	He/H=0	···	−3.31	1.27
J1024−0023	3830990156631488128	DA	9473 (53)	0.669 (0.015)	8.146 (0.017)	log H/He=−4.0	···	−3.02	0.93
J1025+0521	3860625435268868864	DA	8874 (61)	0.607 (0.017)	8.016 (0.02)	He/H=0	···	−3.05	0.88
J1025+6142	1048769578471443072	DC	5760 (33)	0.621 (0.019)	8.081 (0.022)	H/He=0	···	−3.85	3.96
J1025+6407	1053321934567306752	DC	6443 (55)	0.634 (0.022)	8.099 (0.024)	log H/He=−3.2	···	−3.67	2.40
J1026+1439	3887433414244718464	DA	8743 (54)	0.545 (0.014)	7.910 (0.018)	He/H=0	···	−3.01	0.79
J1026+5807	1047132925349510784	DQ	8351 (34)	0.554 (0.008)	7.960 (0.01)	H/He=0	log C/He=−5.18	−3.14	0.99
J1027+1218	3883495444630204672	DQ	7209 (77)	0.645 (0.034)	8.113 (0.038)	H/He=0	log C/He=−6.42	−3.48	1.76
J1027+1644	3890141958060313984	DA	9400 (108)	0.978 (0.023)	8.593 (0.029)	He/H=0	···	−3.32	2.24
J1027+1928	624510170646474112	DA	7260 (38)	0.867 (0.01)	8.427 (0.011)	He/H=0	···	−3.65	3.40
J1027+5019	847272257226467840	DZ	5596 (39)	0.616 (0.03)	8.074 (0.035)	log H/He=−2.0	log Ca/He=−10.75	−3.90	4.48
J1028+0344	3857118439852847744	DA	8071 (70)	0.642 (0.015)	8.077 (0.016)	He/H=0	···	−3.25	1.22
J1028+1451	3888929097950924416	DAH	5856 (29)	0.575 (0.013)	7.980 (0.016)	He/H=0	···	−3.76	2.40
J1028+3512	752814274140797568	DQ	5943 (18)	0.671 (0.018)	8.159 (0.02)	H/He=0	log C/He=−5.65	−3.84	3.97
J1028+3750	754853769426521856	DA	6780 (54)	0.611 (0.025)	8.033 (0.029)	He/H=0	···	−3.53	1.79
J1028+5815	1047228922162323968	DC	6597 (26)	0.471 (0.01)	7.819 (0.014)	log H/He=−3.2	···	−3.48	1.49
J1029+1127	3882611201058534400	DAH	7041 (25)	0.806 (0.005)	8.335 (0.005)	He/H=0	···	−3.65	3.12
J1029+2300	722391440239688064	DA	6917 (68)	0.840 (0.028)	8.387 (0.031)	He/H=0	···	−3.71	3.62
J1029+7931	1132966468074614272	DA	6242 (39)	0.950 (0.013)	8.556 (0.016)	He/H=0	···	−4.00	5.40
J1029−2624	5469171261208778240	DA	5740 (16)	0.588 (0.006)	8.002 (0.007)	He/H=0	···	−3.80	2.63
J1030+0845	3863974783909961600	DA	6140 (20)	0.602 (0.019)	8.022 (0.022)	He/H=0	···	−3.70	2.29
J1030−1423	3750749378584132992	DA	6079 (24)	0.737 (0.007)	8.234 (0.006)	He/H=0	···	−3.84	3.95
J1031+1203	3883044266905679488	DZ	8403 (62)	0.630 (0.027)	8.087 (0.031)	log H/He=−4.0	log Ca/He=−8.81	−3.20	1.16
J1032+0218	3856005626711298560	DA	10362 (46)	0.606 (0.008)	8.008 (0.01)	He/H=0	···	−2.77	0.58
J1032+1516	3889004478921783296	DC	5428 (41)	0.529 (0.026)	7.932 (0.031)	H/He=0	···	−3.88	3.79

Tableau A.2 *suite page suivante*

Tableau A.2 *(suite)*

Name	Gaia DR2/EDR3*	Sp Type	$T_{\rm eff}$ (K)	$M/M_{\odot}$	$\log g$	Composition	Métaux	$\log L/L_{\odot}$	τ (Gyr)
J1032+4104	756515161560637952	DA	6814 (32)	0.640 (0.011)	8.080 (0.011)	He/H=0	···	−3.55	1.90
J1032−0205	3781742343628799232	DA	6374 (41)	0.671 (0.042)	8.131 (0.047)	He/H=0	···	−3.69	2.55
J1033+1446	3885878502939219712	DA	7266 (44)	0.593 (0.028)	8.001 (0.034)	He/H=0	···	−3.39	1.43
J1033+2839	729219716681441280	DA	9642 (44)	0.596 (0.013)	7.994 (0.015)	He/H=0	···	−2.89	0.69
J1034+2245	721648380828681984	DZ	7228 (22)	0.697 (0.006)	8.194 (0.006)	log H/He=−4.0	log Ca/He=−8.74	−3.52	2.05
J1034+3949	755466845943050368	DA	7063 (113)	1.285 (0.014)	9.245 (0.04)	He/H=0	···	−4.35	3.69
J1035+0430	3858586012997916160	DC	7035 (34)	0.699 (0.015)	8.197 (0.017)	log H/He=−3.4	···	−3.57	2.27
J1035+0727	3862830334039617408	DA	7173 (51)	0.637 (0.028)	8.073 (0.032)	He/H=0	···	−3.45	1.65
J1035+2126	721244821406496640	DAH	6797 (35)	0.605 (0.011)	8.024 (0.013)	He/H=0	···	−3.52	1.75
J1035+4041	780275504757613568	DA*	5254 (26)	0.523 (0.021)	7.900 (0.026)	He/H=0	···	−3.91	3.17
J1036+0732	3862858165427681536	DC	4151 (18)	0.361 (0.02)	7.597 (0.032)	He/H=0	···	−4.17	4.98
J1036+7110	1076941716370493696	DC	4751 (24)	0.702 (0.011)	8.193 (0.011)	He/H=0	···	−4.25	9.13
J1037+4227	780712285751716224	DA	6395 (41)	0.893 (0.025)	8.468 (0.028)	He/H=0	···	−3.90	4.84
J1037+6304	1049324629980448256	DA	7399 (32)	0.397 (0.01)	7.624 (0.016)	He/H=0	···	−3.16	0.87
J1038+0202	3855792630692650112	DA	7198 (44)	0.660 (0.027)	8.111 (0.03)	He/H=0	···	−3.47	1.73
J1038+3402	750160156150755328	DZ	5784 (39)	0.707 (0.038)	8.214 (0.041)	log H/He=−1.0	log Ca/He=−10.45	−3.92	4.88
J1038−2040	3553682127126319360	DQP*	5362 (9)	0.868 (0.003)	8.454 (0.003)	H/He=0	log C/He=−6.56	−4.21	7.03
J1039+1803	3986005971704112256	DQ	5583 (27)	0.535 (0.078)	7.940 (0.096)	H/He=0	log C/He=−6.86	−3.83	3.30
J1039+3800	752057981939651584	DA	7149 (47)	0.595 (0.014)	8.004 (0.016)	He/H=0	···	−3.42	1.49
J1039+4135	780429608184054912	DA	7631 (46)	0.607 (0.017)	8.023 (0.019)	He/H=0	···	−3.32	1.30
J1039+4614	830472368094495232	DC	5818 (68)	0.751 (0.079)	8.279 (0.085)	H/He=0	···	−3.95	5.18
J1040+1003	3870354528331257984	DC	5994 (21)	0.648 (0.008)	8.122 (0.009)	H/He=0	···	−3.81	3.53
J1040+2407	723361209490895744	DZ	5940 (32)	0.667 (0.027)	8.152 (0.03)	log H/He=−4.0	log Ca/He=−8.42	−3.84	3.92
J1040+3943	779223787525884928	DA	7976 (53)	0.577 (0.016)	7.970 (0.019)	He/H=0	···	−3.21	1.08
J1041+1415	3884899559633556224	DC*	7045 (25)	0.597 (0.006)	8.037 (0.007)	log H/He=−3.4	···	−3.48	1.69
J1042+1017	3870346934829606528	DC	6050 (30)	0.734 (0.015)	8.252 (0.016)	log H/He=−3.0	···	−3.87	4.31
J1042+2412	723319324969842304	DA	6395 (65)	0.861 (0.047)	8.420 (0.053)	He/H=0	···	−3.87	4.60
J1042+4448	829441717689202816	DC	6093 (54)	0.673 (0.041)	8.161 (0.045)	H/He=0	···	−3.80	3.54
J1042+4932	835731057331866880	DC	4824 (31)	0.339 (0.017)	7.558 (0.028)	H/He=0	···	−3.90	2.91
J1042−2108	3553408245652181760	DA :	10701 (277)	0.819 (0.026)	8.344 (0.03)	He/H=0	···	−2.92	0.89
J1043+3516	750713313579071232	DZ	5868 (40)	0.588 (0.028)	8.028 (0.032)	log H/He=−3.0	log Ca/He=−9.34	−3.79	3.11
J1044+0214	3809230860172408320	DA	7194 (23)	0.621 (0.014)	8.048 (0.016)	He/H=0	···	−3.43	1.57
J1044+2023	3987528623509801984	DZ	8261 (53)	0.600 (0.019)	8.039 (0.022)	log H/He=−4.0	log Ca/He=−10.34	−3.20	1.13
J1044+2645	730811362842136704	DA	8391 (67)	0.678 (0.021)	8.134 (0.025)	He/H=0	···	−3.21	1.20

Tableau A.2 *suite page suivante*

Tableau A.2 *(suite)*

Name	Gaia DR2/EDR3*	Sp Type	$T_{\rm eff}$ (K)	$M/M_{\odot}$	$\log g$	Composition	Métaux	$\log L/L_{\odot}$	τ (Gyr)
J1044+2921	734744453373358848	DA	6050 (50)	0.627 (0.046)	8.064 (0.053)	He/H=0	···	−3.75	2.58
J1044+5513	850713449448779008	DC	6761 (52)	0.672 (0.031)	8.157 (0.034)	log H/He=−3.4	···	−3.62	2.33
J1045+5904	855361055035055104	DQ	8367 (49)	0.956 (0.008)	8.582 (0.009)	H/He=0	log C/He=−4.26	−3.52	2.76
J1045−1906	3554395813252626048	DQ	5387 (17)	0.354 (0.006)	7.588 (0.009)	H/He=0	log C/He=−7.20	−3.72	2.25
J1046+2424	723524383888419840	DZ	6314 (41)	0.647 (0.014)	8.119 (0.016)	log H/He=−3.0	log Ca/He=−10.81	−3.71	2.74
J1047+0007	3806529291383459456	DC	6959 (27)	0.245 (0.009)	7.262 (0.021)	log H/He=−3.4	···	−3.11	0.69
J1047+3453	750469737393655936	DA	8270 (50)	0.286 (0.005)	7.319 (0.012)	He/H=0	···	−2.80	0.47
J1047+3736	775758092515293696	DA	5836 (50)	0.535 (0.062)	7.912 (0.077)	He/H=0	···	−3.73	2.20
J1047+4509	829430275896255232	DA	8100 (67)	0.525 (0.017)	7.878 (0.022)	He/H=0	···	−3.13	0.92
J1047+5912	855387061061127168	DQ	8512 (36)	0.525 (0.014)	7.909 (0.017)	H/He=0	log C/He=−5.17	−3.08	0.88
J1047−0924	3761499853524374784	DA	9664 (47)	0.798 (0.008)	8.315 (0.009)	He/H=0	···	−3.08	1.10
J1048+2113	3989101543613421184	DA	6775 (68)	0.876 (0.057)	8.441 (0.064)	He/H=0	···	−3.78	4.14
J1048+6334	1055313016981775488	DA	5147 (14)	0.551 (0.006)	7.949 (0.008)	He/H=0	···	−3.97	4.25
J1049+0958	3869429224872527744	DA	6987 (28)	0.784 (0.01)	8.302 (0.01)	He/H=0	···	−3.64	2.97
J1049+4543	830949079408842752	DC	4721 (46)	0.542 (0.033)	7.940 (0.04)	He/H=0	···	−4.12	6.44
J1049+4752	832162626703637888	DA	5246 (38)	0.546 (0.053)	7.938 (0.065)	He/H=0	···	−3.93	3.53
J1049+5154	836823151552466304	DZ	6847 (37)	0.547 (0.014)	7.955 (0.017)	log H/He=−4.0	log Ca/He=−9.65	−3.48	1.62
J1049−0008	3806277464565712256	DA	6812 (41)	0.548 (0.025)	7.927 (0.032)	He/H=0	···	−3.46	1.51
J1050+3225	737619062099922688	DA	5601 (18)	0.604 (0.009)	8.031 (0.01)	He/H=0	···	−3.86	3.11
J1050+3306	737721346745881728	DA	5643 (46)	0.567 (0.033)	7.968 (0.04)	He/H=0	···	−3.82	2.63
J1050+3426	738375899762150912	DA	6419 (33)	0.559 (0.018)	7.948 (0.022)	He/H=0	···	−3.58	1.81
J1052+4050	776762672481353984	DC	6116 (23)	0.563 (0.006)	7.985 (0.007)	log H/He=−3.0	···	−3.69	2.30
J1053+2425	3996172640334271872	DA	5872 (21)	0.731 (0.01)	8.227 (0.011)	He/H=0	···	−3.90	4.32
J1055+0403	3809758930696054784	DC	6512 (53)	0.685 (0.027)	8.177 (0.03)	log H/He=−3.2	···	−3.69	2.82
J1055+2111	3988212592756945152	DAH	6100 (22)	0.663 (0.009)	8.121 (0.01)	He/H=0	···	−3.77	2.89
J1055+2525	729726763340729600	DAH	7126 (35)	0.747 (0.028)	8.245 (0.031)	He/H=0	···	−3.57	2.38
J1055+4130	778305557877833088	DC	6195 (81)	0.603 (0.041)	8.050 (0.047)	log H/He=−3.0	···	−3.71	2.46
J1055+5241	837242890116333312	DA	9158 (65)	0.837 (0.016)	8.376 (0.018)	He/H=0	···	−3.21	1.43
J1056+0644	3864754303293985792	DC :	7446 (56)	0.604 (0.022)	8.048 (0.026)	log H/He=−3.6	···	−3.39	1.49
J1056+2336	3989883777417007232	DA	5202 (15)	0.550 (0.01)	7.947 (0.012)	He/H=0	···	−3.95	3.88
J1056+3852	775531009004593664	DA	5805 (28)	0.716 (0.015)	8.204 (0.016)	He/H=0	···	−3.90	4.28
J1056+5714	857165662854257792	DZ	7306 (56)	0.605 (0.016)	8.049 (0.018)	log H/He=−3.0	log Ca/He=−10.47	−3.42	1.56
J1056−2252	3549471753507182592	DA	7783 (35)	0.645 (0.007)	8.083 (0.007)	He/H=0	···	−3.32	1.35
J1057+0411	3815759279181364864	DAH	8085 (41)	0.671 (0.012)	8.124 (0.014)	He/H=0	···	−3.27	1.30

Tableau A.2 *suite page suivante*

Tableau A.2 *(suite)*

Name	Gaia DR2/EDR3*	Sp Type	$T_{\rm eff}$ (K)	$M/M_{\odot}$	$\log g$	Composition	Métaux	$\log L/L_{\odot}$	τ (Gyr)
J1057+1158	3871736820606012928	DA	8375 (71)	0.695 (0.017)	8.161 (0.019)	He/H=0	···	−3.23	1.26
J1057+3008	733294781652279680	DC	6231 (21)	0.539 (0.012)	7.942 (0.014)	log H/He=−3.0	···	−3.64	2.04
J1057+3208	736984742674902912	DC	6579 (45)	0.528 (0.016)	7.922 (0.019)	log H/He=−3.2	···	−3.53	1.71
J1057+4145	778326792196212352	DC	6975 (40)	0.626 (0.022)	8.084 (0.025)	log H/He=−3.4	···	−3.52	1.83
J1057−0413	3789156870225942656	DZ	6534 (41)	0.594 (0.009)	8.033 (0.01)	log H/He=−4.0	log Ca/He=−10.30	−3.61	2.02
J1057−0731	3763445409285757824	DC	7128 (10)	0.725 (0.002)	8.237 (0.002)	log H/He=−3.4	···	−3.57	2.41
J1058+3503	762295264123316864	DC	7729 (42)	0.705 (0.017)	8.206 (0.019)	log H/He=−3.6	···	−3.41	1.70
J1058+4748	831785498511369344	DC	4301 (39)	0.457 (0.041)	7.792 (0.054)	He/H=0	···	−4.20	6.49
J1059+2700	730264772419060608	DC	5759 (46)	0.660 (0.036)	8.142 (0.04)	H/He=0	···	−3.89	4.45
J1059−1748	3556190937783724928	DA	6631 (63)	0.609 (0.029)	8.031 (0.033)	He/H=0	···	−3.57	1.89
J1101+1942	3984813379545559424	DA	6427 (48)	0.685 (0.045)	8.152 (0.051)	He/H=0	···	−3.69	2.64
J1102+0214	3808536101967194368	DZ	5675 (46)	0.656 (0.05)	8.137 (0.056)	log H/He=−4.0	log Ca/He=−9.77	−3.91	4.71
J1102+2054	3985469616188225152	DS*	8810 (54)	0.753 (0.011)	8.276 (0.011)	H/He=0	···	−3.23	1.35
J1102+4030	777221198894621440	DA	5149 (24)	0.547 (0.015)	7.943 (0.018)	He/H=0	···	−3.96	4.16
J1102+4112	777395029106166272	DC	3794 (16)	0.598 (0.014)	8.036 (0.015)	He/H=0	···	−4.55	10.37
J1102+6707	1059423708705441152	DC	5147 (53)	0.652 (0.025)	8.113 (0.027)	He/H=0	···	−4.06	6.46
J1103+0902	3866845986727270400	DA	6073 (31)	0.783 (0.026)	8.304 (0.029)	He/H=0	···	−3.88	4.46
J1103+3935	776981269136616960	DAZ	5010 (17)	0.521 (0.009)	7.920 (0.011)	He/H=0	log Ca/H=−9.00	−4.01	5.18
J1103+4248	778845108849112704	DC	5780 (22)	0.489 (0.048)	7.857 (0.062)	H/He=0	···	−3.73	2.38
J1104+0436	3815105615223622144	DC	4386 (55)	0.499 (0.027)	7.868 (0.034)	He/H=0	···	−4.21	7.07
J1104−1837	3552845261339955200	DA	8188 (31)	0.612 (0.006)	8.028 (0.006)	He/H=0	···	−3.20	1.09
J1106+2539	3996544137821457664	DC	6809 (67)	0.661 (0.046)	8.140 (0.051)	log H/He=−3.4	···	−3.59	2.18
J1106+4518	782378320745502336	DA	7557 (31)	0.863 (0.008)	8.419 (0.008)	He/H=0	···	−3.58	3.01
J1106+6210	862260868456553856	DA	10063 (75)	0.824 (0.011)	8.353 (0.012)	He/H=0	···	−3.03	1.06
J1107+1446	3968635204109066880	DA	6689 (16)	0.591 (0.005)	8.000 (0.005)	He/H=0	···	−3.53	1.76
J1107+4059	777512951728187392	DQ	6853 (33)	0.503 (0.012)	7.877 (0.014)	H/He=0	log C/He=−6.67	−3.44	1.46
J1107+4855	831946229073235200	DC	4549 (49)	0.515 (0.024)	7.895 (0.03)	He/H=0	···	−4.16	6.73
J1107+5246	842498482680906496	DA	7166 (57)	0.616 (0.02)	8.040 (0.024)	He/H=0	···	−3.44	1.57
J1107+5246	842504358196167680	DA	6753 (48)	0.612 (0.021)	8.035 (0.024)	He/H=0	···	−3.54	1.81
J1107−0220	3791246075462610304	DA	10417 (83)	0.774 (0.015)	8.276 (0.016)	He/H=0	···	−2.92	0.85
J1108+0801	3818473629793533312	DA	7647 (16)	0.608 (0.004)	8.024 (0.005)	He/H=0	···	−3.31	1.29
J1108+1349	3968318334306923264	DQ	7488 (43)	0.576 (0.018)	8.000 (0.022)	H/He=0	log C/He=−6.24	−3.35	1.38
J1108+3021	732841233105592320	DA	6858 (88)	0.925 (0.038)	8.515 (0.046)	He/H=0	···	−3.81	4.34
J1109+1226	3964744479135122560	DC	6744 (56)	0.823 (0.019)	8.384 (0.021)	log H/He=−3.2	···	−3.76	3.63

Tableau A.2 *suite page suivante*

Tableau A.2 *(suite)*

Name	Gaia DR2/EDR3*	Sp Type	$T_{\rm eff}$ (K)	$M/M_{\odot}$	$\log g$	Composition	Métaux	$\log L/L_{\odot}$	τ (Gyr)
J1109+4249	778707154499553792	DQ	8878 (46)	0.537 (0.018)	7.929 (0.022)	H/He=0	log C/He=−5.22	−3.01	0.81
J1109+5512	843807902246527232	DA	7084 (24)	0.977 (0.005)	8.597 (0.006)	He/H=0	···	−3.81	4.35
J1109−0312	3790932787663209344	DC	8226 (50)	0.621 (0.015)	8.072 (0.017)	log H/He=−3.8	···	−3.23	1.20
J1109−2601	3532509621985958912	DC	5959 (38)	0.677 (0.011)	8.167 (0.013)	H/He=0	···	−3.84	3.98
J1110+0054	3810397128476695424	DA	8943 (65)	0.685 (0.013)	8.143 (0.015)	He/H=0	···	−3.11	1.03
J1110+0110	3810416820902223616	DC	6477 (28)	0.678 (0.009)	8.166 (0.01)	log H/He=−3.2	···	−3.70	2.79
J1110+2026	3990494251184010496	DC	4735 (16)	0.586 (0.009)	8.013 (0.01)	He/H=0	···	−4.15	7.37
J1111+0337	3812098863243533824	DA	5820 (28)	0.737 (0.012)	8.237 (0.013)	He/H=0	···	−3.92	4.54
J1111+2519	3995728953028752768	DC	5336 (35)	0.662 (0.043)	8.147 (0.047)	H/He=0	···	−4.02	5.87
J1111+3848	764725833360592640	DC	4862 (29)	0.259 (0.015)	7.347 (0.031)	H/He=0	···	−3.79	2.17
J1111+5604	855892153511070080	DA	8984 (52)	0.495 (0.009)	7.817 (0.012)	He/H=0	···	−2.92	0.66
J1112+0858	3819003074706435200	DC	4593 (46)	0.455 (0.033)	7.785 (0.044)	He/H=0	···	−4.09	5.29
J1112+1524	3970216984735025792	DC	7030 (60)	0.686 (0.048)	8.178 (0.053)	log H/He=−3.4	···	−3.56	2.17
J1113+0032	3810134246413902848	DC	6584 (54)	0.636 (0.017)	8.100 (0.019)	log H/He=−3.2	···	−3.63	2.23
J1113+0146	3810552434493888768	DQH*	4988 (13)	0.744 (0.012)	8.271 (0.013)	H/He=0	log C/He=−6.79	−4.21	7.41
J1113+0324	3812052855548962816*	DA	6421 (39)	0.547 (0.025)	7.927 (0.032)	He/H=0	···	−3.57	1.75
J1113+2859	3999033225988190720	DA	4816 (13)	0.266 (0.016)	7.344 (0.034)	He/H=0	···	−3.80	2.18
J1113+2922	3999150942451828480	DA	6891 (31)	0.374 (0.018)	7.578 (0.03)	He/H=0	···	−3.26	0.99
J1113−1903	3557916273390162560	DC	5093 (16)	0.565 (0.011)	7.974 (0.014)	He/H=0	···	−4.00	4.97
J1114+3638	763471702912929024	DC	6180 (56)	0.640 (0.043)	8.109 (0.048)	log H/He=−3.0	···	−3.75	2.92
J1114+6546	1056003918305358592	DZ	5864 (40)	0.682 (0.016)	8.175 (0.018)	log H/He=−4.0	log Ca/He=−10.44	−3.88	4.33
J1115+0033	3810099989754827136	DA	4983 (6)	0.332 (0.005)	7.516 (0.009)	He/H=0	···	−3.81	2.30
J1115+2315	3992108467396622464	DA	6560 (31)	0.224 (0.016)	7.131 (0.046)	He/H=0	···	−3.12	0.67
J1116+0627	3817262208497857024	DA	6418 (9)	0.590 (0.004)	8.000 (0.004)	He/H=0	···	−3.61	1.97
J1116+0925	3915111042492943360	DA	5402 (25)	0.617 (0.015)	8.054 (0.017)	He/H=0	···	−3.94	4.11
J1116−0032	3791951961927535616	DA*	5950 (29)	0.613 (0.013)	8.041 (0.015)	He/H=0	···	−3.76	2.59
J1116−1035	3566532561902107648	DA	5754 (43)	0.645 (0.031)	8.094 (0.035)	He/H=0	···	−3.85	3.37
J1116−1035	3566532561902107904	DA	6493 (40)	0.548 (0.018)	7.928 (0.022)	He/H=0	···	−3.55	1.71
J1116−1252	3565057738851555840	DA	8249 (59)	0.633 (0.02)	8.062 (0.023)	He/H=0	···	−3.20	1.12
J1117+1821	3971863297233655040	DA	9695 (86)	1.034 (0.032)	8.685 (0.042)	He/H=0	···	−3.33	2.39
J1117+3029	4023258765683278720	DA	8193 (60)	0.822 (0.021)	8.356 (0.025)	He/H=0	···	−3.39	1.98
J1117+4851	789712823515276416	DA	6585 (39)	0.529 (0.017)	7.894 (0.021)	He/H=0	···	−3.50	1.57
J1117+5010	837941213142775680	DC	4901 (23)	0.578 (0.017)	7.998 (0.02)	He/H=0	···	−4.08	6.51
J1118+2836	3998830061150314368	DA	8806 (43)	0.687 (0.008)	8.146 (0.009)	He/H=0	···	−3.14	1.08

Tableau A.2 *suite page suivante*

Tableau A.2 *(suite)*

Name	Gaia DR2/EDR3*	Sp Type	$T_{\rm eff}$ (K)	$M/M_{\odot}$	$\log g$	Composition	Métaux	$\log L/L_{\odot}$	τ (Gyr)
J1118−0314	3790040465258127616	DQ	9326 (27)	0.533 (0.004)	7.920 (0.005)	H/He=0	log C/He=−4.73	−2.92	0.71
J1119+3224	757272896870658176	DA	6048 (36)	0.731 (0.024)	8.227 (0.026)	He/H=0	···	−3.84	3.95
J1119+4708	788592386816314752	DA	8054 (44)	0.487 (0.012)	7.807 (0.015)	He/H=0	···	−3.10	0.86
J1119−0107	3791660630001113344	DC	4748 (47)	0.615 (0.034)	8.059 (0.037)	He/H=0	···	−4.17	7.92
J1119−0831	3783206210217512320	DA	5608 (19)	0.629 (0.007)	8.072 (0.008)	He/H=0	···	−3.88	3.50
J1119−1038	3566494186369726720	DA	7332 (25)	0.211 (0.004)	7.052 (0.011)	He/H=0	···	−2.87	0.42
J1120+3745	763955591105229056	DA	7855 (31)	0.582 (0.015)	7.979 (0.018)	He/H=0	···	−3.24	1.13
J1120+4734	788619668448368512	DC	6232 (32)	0.658 (0.015)	8.136 (0.016)	H/He=0	···	−3.75	3.02
J1121+1553	3967492742808436864	DA	7550 (48)	0.601 (0.023)	8.012 (0.026)	He/H=0	···	−3.33	1.31
J1121+3756	763981296484951936	DA	9449 (36)	0.636 (0.005)	8.062 (0.007)	He/H=0	···	−2.96	0.79
J1122+2839	4022081429247669632	DA	5649 (26)	0.689 (0.011)	8.165 (0.013)	He/H=0	···	−3.93	4.35
J1122+4708	788768476168350976	DA	6301 (16)	0.725 (0.017)	8.215 (0.019)	He/H=0	···	−3.76	3.38
J1123+0956	3915026861134449664	DAH	9417 (78)	0.769 (0.019)	8.271 (0.021)	He/H=0	···	−3.10	1.10
J1123+1446	3966812278254805248	DA	7563 (42)	0.613 (0.015)	8.033 (0.018)	He/H=0	···	−3.34	1.35
J1123+5844	857552239974460160	DA	6399 (46)	0.574 (0.022)	7.973 (0.026)	He/H=0	···	−3.60	1.90
J1124+1705	3970693313784409344	DA	7812 (83)	0.801 (0.032)	8.326 (0.035)	He/H=0	···	−3.46	2.16
J1125+2111	3978862277154958592	DC	5968 (24)	0.515 (0.005)	7.903 (0.007)	log H/He=−3.0	···	−3.69	2.23
J1125+4223	771517005584473600	DA	9510 (38)	0.713 (0.007)	8.185 (0.008)	He/H=0	···	−3.03	0.93
J1126+0906	3914160793864337280	DAH	10582 (103)	1.086 (0.013)	8.774 (0.018)	He/H=0	···	−3.25	2.17
J1126+1433	3967110520783248640	DA	6276 (36)	0.581 (0.016)	7.987 (0.019)	He/H=0	···	−3.64	2.04
J1126+5919	859082970614616448	DA	10419 (21)	1.008 (0.003)	8.639 (0.004)	He/H=0	···	−3.17	1.83
J1126−0653	3785295862130129792	DC	4517 (36)	0.707 (0.026)	8.201 (0.027)	He/H=0	···	−4.34	9.91
J1127+0623	3814445324131846272	DA	8477 (48)	0.584 (0.011)	7.979 (0.013)	He/H=0	···	−3.11	0.94
J1127+7531	1080303919849120128	DC	8311 (45)	0.576 (0.007)	7.998 (0.008)	log H/He=−4.0	···	−3.17	1.05
J1127−0138	3796601418644353536	DZ	7393 (45)	0.582 (0.021)	8.012 (0.026)	log H/He=−4.0	log Ca/He=−9.22	−3.38	1.44
J1127−2940	3482983495102507904	DA	9284 (23)	0.577 (0.004)	7.964 (0.005)	He/H=0	···	−2.94	0.73
J1128+0736	3913666009336762624	DA	6507 (53)	0.763 (0.033)	8.272 (0.035)	He/H=0	···	−3.74	3.47
J1128+1825	3976920329166692736	DA	7205 (43)	0.708 (0.019)	8.185 (0.021)	He/H=0	···	−3.51	1.96
J1128+4150	771045212017101952	DA	9051 (56)	0.640 (0.014)	8.070 (0.016)	He/H=0	···	−3.04	0.90
J1130+1002	3914686699729551744	DA	5160 (48)	0.585 (0.023)	8.007 (0.028)	He/H=0	···	−4.00	4.96
J1130+6647	1057653804222121600	DC :*	6860 (41)	0.568 (0.012)	7.990 (0.015)	log H/He=−3.4	···	−3.50	1.69
J1131+0643	3910338303034941824	DA	7591 (30)	0.543 (0.011)	7.913 (0.013)	He/H=0	···	−3.26	1.13
J1131+4920	789242022082351616	DA	6037 (29)	0.691 (0.017)	8.164 (0.019)	He/H=0	···	−3.81	3.41
J1131+4938	790014605097236224	DA	10016 (31)	0.333 (0.005)	7.435 (0.01)	He/H=0	···	−2.52	0.32

Tableau A.2 *suite page suivante*

Tableau A.2 *(suite)*

Name	Gaia DR2/EDR3*	Sp Type	$T_{\rm eff}$ (K)	$M/M_{\odot}$	$\log g$	Composition	Métaux	$\log L/L_{\odot}$	τ (Gyr)
J1132+2328	3993006940195159552	DA	7488 (55)	0.546 (0.017)	7.918 (0.022)	He/H=0	···	−3.29	1.18
J1132+2809	4018868591847502208	DAH	7523 (36)	0.671 (0.008)	8.127 (0.009)	He/H=0	···	−3.40	1.58
J1132+3634	759949799663166464	DA	8861 (59)	0.558 (0.01)	7.933 (0.013)	He/H=0	···	−3.00	0.79
J1132−0532	3785855994584716288	DA	6813 (59)	0.803 (0.031)	8.331 (0.034)	He/H=0	···	−3.70	3.41
J1133+3301	4025333681563592960	DA	9053 (50)	0.950 (0.008)	8.549 (0.009)	He/H=0	···	−3.35	2.30
J1133+6243	862946654474456832	DA+DC	7017 (26)	0.415 (0.005)	7.668 (0.008)	He/H=0	···	−3.27	1.03
J1134+6108	859567752163281792	DA	7731 (21)	0.618 (0.004)	8.040 (0.005)	He/H=0	···	−3.30	1.29
J1135+1240	3917662149987657472	DC	4682 (25)	0.453 (0.035)	7.781 (0.047)	He/H=0	···	−4.05	4.84
J1135+2717	4018536882933053056*	DC	4609 (24)	0.523 (0.015)	7.908 (0.018)	He/H=0	···	−4.14	6.60
J1135+5724	845973046799769984	DQ	7487 (30)	0.292 (0.005)	7.403 (0.01)	H/He=0	log C/He=−6.23	−3.05	0.68
J1135+6429	864111582748403968	DA	9001 (86)	0.969 (0.014)	8.580 (0.017)	He/H=0	···	−3.38	2.47
J1136+0802	3910941183300119808	DA	5415 (19)	0.505 (0.011)	7.863 (0.014)	He/H=0	···	−3.83	2.55
J1136+0838	3911257636490384512	DA	6544 (25)	0.631 (0.011)	8.067 (0.013)	He/H=0	···	−3.61	2.06
J1136+1530	3972493871447452032	DA	7439 (40)	0.571 (0.015)	7.962 (0.019)	He/H=0	···	−3.33	1.27
J1137+0343	3800902265750001664	DZ	6837 (44)	0.641 (0.016)	8.108 (0.018)	log H/He=−4.0	log Ca/He=−10.95	−3.57	2.00
J1137+1347	3918024679587352960	DC	5994 (54)	0.528 (0.049)	7.926 (0.06)	log H/He=−3.0	···	−3.70	2.26
J1137+2005	3978988652273088128	DZ	6231 (44)	0.711 (0.038)	8.218 (0.042)	log H/He=−2.0	log Ca/He=−10.98	−3.79	3.61
J1137+2041	3979070527235441792	DA	7431 (47)	0.479 (0.013)	7.795 (0.018)	He/H=0	···	−3.24	1.03
J1137+2451	4017215231301573376	DA	7677 (92)	0.474 (0.025)	7.784 (0.036)	He/H=0	···	−3.17	0.94
J1137+3117	4024105492715825152	DA	6002 (48)	0.645 (0.03)	8.093 (0.035)	He/H=0	···	−3.78	2.85
J1137+4019	767724270288678784	DC	7289 (48)	0.528 (0.019)	7.920 (0.023)	log H/He=−3.6	···	−3.35	1.32
J1137+5740	845982667526493440	DAH	7621 (32)	0.703 (0.007)	8.176 (0.007)	He/H=0	···	−3.41	1.65
J1138+1323	3917811443050820736	DA	6677 (50)	0.728 (0.041)	8.218 (0.045)	He/H=0	···	−3.67	2.78
J1138+3610	765628876004078464	DA	6919 (129)	1.166 (0.041)	8.936 (0.074)	He/H=0	···	−4.12	4.75
J1138+6438	864108971408318848	DC	6423 (52)	0.859 (0.016)	8.438 (0.018)	log H/He=−3.2	···	−3.88	4.31
J1138−1313	3585097235918075776	DC	5986 (30)	0.670 (0.009)	8.156 (0.01)	H/He=0	···	−3.83	3.82
J1139+2613	4017476365313408512	DA	6595 (29)	0.760 (0.014)	8.268 (0.015)	He/H=0	···	−3.72	3.30
J1139−2852	3483746453090944896	DC	4421 (73)	0.388 (0.07)	7.653 (0.107)	He/H=0	···	−4.09	4.54
J1140+0112	3799009353404271488	DA	9466 (39)	0.604 (0.006)	8.009 (0.006)	He/H=0	···	−2.93	0.74
J1140+1245	3917712246486088064	DC :	6231 (25)	0.566 (0.01)	7.990 (0.013)	log H/He=−3.0	···	−3.67	2.17
J1140+5938	858407492517973888	DA	6969 (41)	0.612 (0.015)	8.033 (0.018)	He/H=0	···	−3.48	1.67
J1141+3836	766499483055284864	DQ	5940 (18)	0.720 (0.032)	8.233 (0.036)	H/He=0	log C/He=−5.10	−3.89	4.50
J1141−0132	3793871056394569600	DA	7409 (65)	0.852 (0.022)	8.404 (0.024)	He/H=0	···	−3.60	3.09
J1142+1538	3972360517007764096	DA	5699 (42)	0.699 (0.031)	8.180 (0.035)	He/H=0	···	−3.92	4.33

Tableau A.2 *suite page suivante*

Tableau A.2 *(suite)*

Name	Gaia DR2/EDR3*	Sp Type	$T_{\rm eff}$ (K)	$M/M_{\odot}$	$\log g$	Composition	Métaux	$\log L/L_{\odot}$	τ (Gyr)
J1142−0208	3793038176336413568	DA	7270 (77)	0.876 (0.028)	8.440 (0.032)	He/H=0	···	−3.66	3.47
J1143+1448	3924198849694079488	DC	6402 (55)	0.539 (0.039)	7.941 (0.048)	log H/He=−3.2	···	−3.59	1.89
J1143+4053	769043546803129216	DA	6715 (56)	0.667 (0.027)	8.123 (0.031)	He/H=0	···	−3.60	2.13
J1143+7036	1062419637373273728	DA	6132 (38)	0.612 (0.023)	8.039 (0.026)	He/H=0	···	−3.71	2.36
J1143−0131	3793132257595347200	DA	6598 (25)	0.820 (0.007)	8.357 (0.007)	He/H=0	···	−3.77	3.90
J1144+0621	3909703579883878528	DC	5295 (67)	0.511 (0.031)	7.901 (0.038)	H/He=0	···	−3.90	4.05
J1144+1132	3916509896161613056	DA	6184 (17)	0.531 (0.008)	7.901 (0.009)	He/H=0	···	−3.62	1.86
J1144+1218	3916712206301454720	DZ	5345 (16)	0.576 (0.013)	8.011 (0.014)	log H/He=−4.0	log Ca/He=−9.30	−3.95	4.82
J1144+6629	1056998259069523584	DAH	6728 (28)	0.474 (0.007)	7.791 (0.01)	He/H=0	···	−3.41	1.31
J1145+1523	3924625975601987968	DA	5115 (30)	0.545 (0.043)	7.940 (0.053)	He/H=0	···	−3.98	4.33
J1145+6305	863131372427958912	DA	5545 (11)	0.551 (0.004)	7.942 (0.005)	He/H=0	···	−3.83	2.66
J1146+0514	3897015868534544000	DA	6659 (24)	0.295 (0.005)	7.371 (0.01)	He/H=0	···	−3.21	0.87
J1146−0136	3794567429507510528	DA	6598 (13)	0.602 (0.004)	8.019 (0.005)	He/H=0	···	−3.57	1.88
J1147+0747	3911460633824772224	DQA*	8728 (22)	0.541 (0.005)	7.936 (0.005)	log H/He=−4.0	log C/He=−4.90	−3.05	0.86
J1147+2001	3976193895578807296	DC	7780 (49)	0.588 (0.019)	8.021 (0.022)	log H/He=−3.8	···	−3.29	1.28
J1147+2218	3979704120809463808	DC	6113 (46)	0.738 (0.045)	8.259 (0.048)	H/He=0	···	−3.85	4.17
J1147+2220	3979751266665795456	DC	4661 (44)	0.613 (0.035)	8.072 (0.054)	log H/He=−3.05	···	−4.22	7.05
J1147+3009	4020794214664565120	DC	6679 (27)	0.588 (0.01)	8.024 (0.012)	log H/He=−3.2	···	−3.56	1.89
J1147+4303	769543893313272576	DC	4941 (12)	0.530 (0.011)	7.917 (0.013)	He/H=0	···	−4.02	5.18
J1148+3541	4032410520652747648	DA	6649 (35)	0.611 (0.014)	8.033 (0.017)	He/H=0	···	−3.56	1.88
J1148−0126	3794415245931016320	DQ	10632 (61)	0.972 (0.01)	8.605 (0.011)	H/He=0	log C/He=−2.72	−3.12	1.58
J1149+2353	4004175916749342592	DC	5054 (24)	0.572 (0.014)	7.986 (0.016)	He/H=0	···	−4.02	5.41
J1149−0221	3602129564384942848	DC	6485 (38)	0.597 (0.029)	8.039 (0.033)	log H/He=−3.2	···	−3.62	2.08
J1149−2921	3480776843983381632	DA	5821 (30)	0.841 (0.008)	8.392 (0.008)	He/H=0	···	−4.01	5.59
J1150+0342	3895853993981558400	DA	5906 (12)	0.637 (0.011)	8.081 (0.013)	He/H=0	···	−3.80	2.93
J1150+2518	4005438916307756928	DA	10135 (53)	0.602 (0.006)	8.002 (0.007)	He/H=0	···	−2.81	0.61
J1150+6831	1058284412796260480	DA	6783 (11)	0.781 (0.003)	8.299 (0.003)	He/H=0	···	−3.69	3.23
J1150−0636	3598424931753893888	DA	8835 (56)	0.912 (0.007)	8.491 (0.008)	He/H=0	···	−3.35	2.19
J1151+1253	3922795941576557184	DC	4807 (38)	0.389 (0.029)	7.671 (0.044)	H/He=0	···	−3.96	3.49
J1151+5411	840622479622035712	DA	9755 (41)	0.604 (0.007)	8.008 (0.009)	He/H=0	···	−2.88	0.68
J1151−2732	3487220772397809536	DQ	6341 (15)	0.535 (0.004)	7.935 (0.004)	H/He=0	log C/He=−6.98	−3.60	1.92
J1152+1803	3974607884414675584	DA	6988 (47)	0.610 (0.023)	8.031 (0.027)	He/H=0	···	−3.48	1.65
J1153−0312	3601778888894719616	DA	7344 (43)	0.552 (0.016)	7.930 (0.02)	He/H=0	···	−3.33	1.26
J1154+0441	3896315612771069184	DC*	6291 (47)	0.559 (0.02)	7.976 (0.023)	log H/He=−3.2	···	−3.64	2.07

Tableau A.2 *suite page suivante*

Tableau A.2 *(suite)*

Name	Gaia DR2/EDR3*	Sp Type	$T_{\rm eff}$ (K)	$M/M_{\odot}$	$\log g$	Composition	Métaux	$\log L/L_{\odot}$	τ (Gyr)
J1154+2422	4004395720290994048	DA	8864 (32)	0.932 (0.004)	8.522 (0.005)	He/H=0	···	−3.37	2.32
J1154+3749	4034132866962718848	DA	8105 (59)	0.634 (0.016)	8.065 (0.018)	He/H=0	···	−3.23	1.18
J1154+7914	1129251428738666880	DA	10155 (64)	0.539 (0.008)	7.892 (0.01)	He/H=0	···	−2.74	0.53
J1156+0503	3896442675083660288	DA	8382 (59)	0.648 (0.017)	8.086 (0.019)	He/H=0	···	−3.19	1.12
J1156+1822	3926968661219149184	DC	7356 (19)	0.607 (0.004)	8.053 (0.005)	log H/He=−3.6	···	−3.41	1.55
J1156+3233	4027510375284724608	DC*	7635 (45)	0.677 (0.017)	8.162 (0.019)	log H/He=−3.6	···	−3.41	1.63
J1157+0631	3898377201369256576	DA	8051 (26)	0.556 (0.011)	7.934 (0.015)	He/H=0	···	−3.17	1.00
J1157+0854	3899975238440888064	DA	6245 (25)	0.343 (0.008)	7.508 (0.014)	He/H=0	···	−3.40	1.16
J1157+2308	4001198168679083648	DC	6554 (35)	0.611 (0.018)	8.061 (0.021)	log H/He=−3.2	···	−3.62	2.10
J1158+0005	3795052348495488896	DC	4437 (22)	0.489 (0.011)	7.849 (0.014)	He/H=0	···	−4.18	6.69
J1158+0739	3899642425719062400	DA	5861 (41)	0.551 (0.017)	7.938 (0.022)	He/H=0	···	−3.73	2.26
J1158+2853	4007991157673846144	DA	8778 (52)	0.557 (0.008)	7.932 (0.011)	He/H=0	···	−3.02	0.81
J1159+0007	3891115064506627840	DA	8715 (30)	0.880 (0.004)	8.466 (0.005)	log H/He=−2.0	···	−3.37	2.13
J1159+1300	3919950955240152832	DQ	6890 (14)	0.686 (0.014)	8.177 (0.015)	H/He=0	log C/He=−5.18	−3.60	2.31
J1159+3538	4031471636506212352	DA	7268 (38)	0.887 (0.008)	8.457 (0.009)	He/H=0	···	−3.67	3.56
J1159+4842	786717135370412800	DA	5904 (14)	0.618 (0.006)	8.051 (0.007)	He/H=0	···	−3.78	2.71
J1200+4237	1537367257087358592	DQ	6292 (47)	0.690 (0.027)	8.185 (0.03)	H/He=0	log C/He=−6.50	−3.76	3.25
J1200+4335	1537794524729363712	DA	7900 (28)	0.538 (0.006)	7.903 (0.006)	He/H=0	···	−3.19	1.01
J1200+4833	1546270625514967168	DA	8510 (50)	0.623 (0.015)	8.045 (0.016)	He/H=0	···	−3.14	1.01
J1200−1032	3575728709655386752	DA	7876 (24)	0.867 (0.005)	8.425 (0.005)	He/H=0	···	−3.51	2.70
J1201+0847	3900013579612540672	DAH	7395 (68)	0.794 (0.035)	8.316 (0.04)	He/H=0	···	−3.55	2.55
J1201+3400	4028120776036373760	DQ	6101 (14)	0.694 (0.006)	8.192 (0.006)	H/He=0	log C/He=−5.98	−3.82	3.74
J1202+4929	1546780420950246912	DA :	4847 (42)	0.528 (0.036)	7.915 (0.044)	He/H=0	···	−4.06	5.67
J1202+5344	1549208138324951936	DA	8397 (70)	0.905 (0.015)	8.481 (0.016)	He/H=0	···	−3.44	2.50
J1202−0313	3600899515814587904	DC	4617 (33)	0.541 (0.024)	7.938 (0.029)	He/H=0	···	−4.16	6.85
J1202−1004	3575770010060921728	DA	9359 (53)	0.960 (0.006)	8.565 (0.007)	He/H=0	···	−3.31	2.15
J1203+0426	3894780007343533184	DC	4979 (20)	0.349 (0.006)	7.498 (0.016)	log H/He=−1.12	···	−3.77	4.11
J1203+0834	3899809757644549632	DZ	6066 (27)	0.574 (0.019)	8.003 (0.022)	log H/He=−4.0	log Ca/He=−10.20	−3.72	2.46
J1203+1330	3920078086272085888	DC	7274 (53)	0.600 (0.027)	8.042 (0.03)	log H/He=−3.6	···	−3.42	1.57
J1203+1422	3921843867586039808	DC	6741 (37)	0.572 (0.018)	7.997 (0.022)	log H/He=−3.2	···	−3.53	1.78
J1203+5910	1576088036528753408	DC :	8867 (63)	0.753 (0.015)	8.276 (0.016)	log H/He=−4.2	···	−3.21	1.32
J1204+2316	4001074538044978816	DC	4972 (26)	0.567 (0.017)	7.979 (0.02)	He/H=0	···	−4.05	5.84
J1204+6222	1582945145090883200	DC	4861 (24)	0.549 (0.013)	7.950 (0.015)	He/H=0	···	−4.07	6.04
J1204+6259	1582991152779542400	DA	6148 (36)	0.648 (0.018)	8.096 (0.02)	He/H=0	···	−3.74	2.63

Tableau A.2 *suite page suivante*

Tableau A.2 *(suite)*

Name	Gaia DR2/EDR3*	Sp Type	$T_{\rm eff}$ (K)	$M/M_{\odot}$	$\log g$	Composition	Métaux	$\log L/L_{\odot}$	τ (Gyr)
J1205+0449	3894911089745430656	DC	5394 (29)	0.247 (0.013)	7.302 (0.029)	H/He=0	···	−3.59	1.54
J1205+1607	3925475283910531328	DA	9981 (83)	0.764 (0.013)	8.262 (0.015)	He/H=0	···	−2.99	0.93
J1205−0042	3698611842864771328	DC	6448 (56)	0.519 (0.045)	7.907 (0.056)	log H/He=−3.2	···	−3.56	1.77
J1205−2333	3489719481290397696	DAZ	8712 (45)	0.622 (0.004)	8.042 (0.004)	He/H=0	···	−3.10	0.95
J1206+0823	3904993787466857472	DA	8161 (52)	0.611 (0.01)	8.027 (0.011)	He/H=0	···	−3.20	1.10
J1206+2353	4002617427736191872	DC	5184 (30)	0.636 (0.026)	8.089 (0.029)	He/H=0	···	−4.03	5.91
J1207+2916	4013877015215909632	DC	6027 (44)	0.626 (0.025)	8.088 (0.028)	H/He=0	···	−3.78	3.14
J1207+3953	1536034236678159232	DA	8690 (54)	0.630 (0.013)	8.056 (0.015)	He/H=0	···	−3.11	0.98
J1208+0312	3893651289938122496	DA	6086 (33)	0.614 (0.024)	8.042 (0.027)	He/H=0	···	−3.72	2.42
J1208+0845	3905035495893288448	DA	4985 (18)	0.540 (0.012)	7.933 (0.014)	He/H=0	···	−4.02	5.10
J1208+2343	4001862578644425344	DA	8413 (70)	0.714 (0.021)	8.191 (0.023)	He/H=0	···	−3.24	1.30
J1208+5429	1573121554156399872	DA	8018 (62)	0.652 (0.012)	8.094 (0.013)	He/H=0	···	−3.27	1.27
J1209+0939	3905948159264050432	DA	6207 (41)	0.930 (0.018)	8.525 (0.022)	He/H=0	···	−3.99	5.36
J1211+0724	3904628406009296896	DA	5213 (9)	0.543 (0.004)	7.935 (0.005)	He/H=0	···	−3.94	3.67
J1211+1046	3906450326840122368	DA	7356 (56)	0.585 (0.017)	7.988 (0.02)	He/H=0	···	−3.36	1.35
J1211+2053	3951770649948609920	DA	6733 (29)	0.239 (0.007)	7.186 (0.021)	He/H=0	···	−3.10	0.68
J1211+2815	4012821445398156416	DC	7062 (60)	0.711 (0.032)	8.215 (0.035)	log H/He=−3.4	···	−3.58	2.35
J1211+3653	4030292070983358208	DA	9883 (62)	0.621 (0.012)	8.036 (0.014)	He/H=0	···	−2.87	0.68
J1211+4953	1548117972546002560	DA	5562 (27)	0.612 (0.017)	8.043 (0.02)	He/H=0	···	−3.88	3.34
J1211+5724	1575357587146077056	DAZ	5887 (11)	0.600 (0.003)	8.020 (0.003)	He/H=0	···	−3.77	2.54
J1211−0242	3598349645270793984	DA	8165 (58)	1.001 (0.019)	8.632 (0.024)	He/H=0	···	−3.59	3.34
J1212+0440	3894294439815819904	DC	4487 (54)	0.534 (0.03)	7.928 (0.037)	He/H=0	···	−4.20	7.23
J1212+3834	1532708866839099648	DC	7626 (55)	0.790 (0.022)	8.334 (0.025)	log H/He=−3.6	···	−3.51	2.42
J1212+4345	1538365922883198336	DA	5426 (35)	0.638 (0.027)	8.088 (0.03)	He/H=0	···	−3.95	4.41
J1212+5452	1573476112296657408	DQ	8138 (48)	0.546 (0.012)	7.948 (0.014)	H/He=0	log C/He=−5.36	−3.17	1.04
J1212−0622	3596192953212776704	DA	6380 (22)	0.568 (0.008)	7.964 (0.01)	He/H=0	···	−3.60	1.89
J1214+6216	1582663189077609088	DA*	5276 (17)	0.530 (0.009)	7.910 (0.011)	He/H=0	···	−3.90	3.15
J1214+7822	1717341818608187648	DZ	4895 (31)	0.514 (0.011)	7.908 (0.014)	He/H=0	log Ca/H=−9.40	−4.04	5.35
J1214−0142	3694595296825212288	DA	5179 (36)	0.610 (0.026)	8.047 (0.029)	He/H=0	···	−4.01	5.41
J1214−0234	3694399755554510720	DZH*	5115 (16)	0.679 (0.009)	8.173 (0.01)	log H/He=−3.0	log Ca/He=−9.40	−4.11	6.65
J1215+0948	3905534918987016576	DA	9657 (80)	0.871 (0.018)	8.426 (0.02)	He/H=0	···	−3.15	1.36
J1215+0948	3905533368502667520	DA	8428 (69)	0.634 (0.019)	8.064 (0.022)	He/H=0	···	−3.17	1.07
J1215+4630	1545050717357814272	DA	6595 (21)	0.618 (0.007)	8.046 (0.007)	He/H=0	···	−3.58	1.96
J1215−0056	3698040337339931776	DAH	6643 (57)	0.781 (0.032)	8.298 (0.035)	He/H=0	···	−3.72	3.44

Tableau A.2 *suite page suivante*

Tableau A.2 *(suite)*

Name	Gaia DR2/EDR3*	Sp Type	$T_{\rm eff}$ (K)	$M/M_{\odot}$	$\log g$	Composition	Métaux	$\log L/L_{\odot}$	τ (Gyr)
J1216+0338	3893925965982400384	DA	6010 (35)	0.602 (0.027)	8.023 (0.032)	He/H=0	···	−3.73	2.42
J1216+3023	4013717723468865152	DC*	7428 (66)	0.685 (0.029)	8.174 (0.033)	log H/He=−3.6	···	−3.46	1.79
J1217+0403	3893966162580541184	DA	5435 (37)	0.371 (0.034)	7.593 (0.056)	He/H=0	···	−3.69	1.77
J1217+3044	4013798537573517568	DA	7166 (56)	0.573 (0.025)	7.967 (0.03)	He/H=0	···	−3.40	1.41
J1217+3205	4016142868162408576	DC	6818 (37)	0.589 (0.01)	8.024 (0.011)	log H/He=−3.4	···	−3.53	1.80
J1217+3226	4016204440813547520	DA	7311 (52)	0.543 (0.015)	7.915 (0.018)	He/H=0	···	−3.33	1.24
J1217+3656	1531580424311162880	DC	5734 (41)	0.578 (0.02)	8.011 (0.023)	H/He=0	···	−3.82	3.39
J1217+6404	1584734595969095424	DA	7425 (43)	0.281 (0.006)	7.318 (0.014)	He/H=0	···	−2.99	0.63
J1217+6848	1683330453627242752	DA	6562 (28)	0.862 (0.006)	8.421 (0.006)	He/H=0	···	−3.82	4.34
J1219+4015	1533299819978845312	DA	6435 (40)	0.594 (0.021)	8.006 (0.024)	He/H=0	···	−3.60	1.97
J1219+4715	1545014807135001088	DC*	7277 (54)	0.537 (0.013)	7.936 (0.015)	log H/He=−3.6	···	−3.37	1.36
J1219+5827	1575107070293783296	DA	9340 (54)	0.610 (0.009)	8.020 (0.01)	He/H=0	···	−2.96	0.77
J1220+4414	1538625407627245056	DA	7072 (25)	0.877 (0.007)	8.442 (0.008)	He/H=0	···	−3.71	3.73
J1221+3306	4016670251491467520	DA	7783 (74)	0.587 (0.017)	7.989 (0.021)	He/H=0	···	−3.26	1.18
J1221+5320	1572216243769902336	DA	7657 (80)	0.854 (0.019)	8.406 (0.022)	He/H=0	···	−3.54	2.82
J1221+6520	1680980518105612672	DC	6127 (60)	0.568 (0.018)	7.993 (0.021)	log H/He=−3.0	···	−3.70	2.31
J1223+5410	1572454940873010176	DZ	5651 (55)	0.628 (0.028)	8.093 (0.031)	log H/He=−1.0	log Ca/He=−8.90	−3.89	4.45
J1223+5645	1574853491129437440	DC	6536 (57)	0.594 (0.023)	8.034 (0.027)	log H/He=−3.2	···	−3.60	2.02
J1223−1852	3519617951228451328	DC	8674 (30)	0.679 (0.006)	8.163 (0.006)	log H/He=−4.0	···	−3.19	1.19
J1224+2838	4010119017615780608	DZ	5006 (33)	0.570 (0.032)	8.002 (0.037)	log H/He=−3.0	log Ca/He=−9.75	−4.05	5.84
J1224−0018	3696633688303809664	DA	6556 (28)	0.653 (0.008)	8.102 (0.009)	He/H=0	···	−3.63	2.19
J1225+1522	3945304834382891008	DA	6575 (70)	0.942 (0.03)	8.542 (0.036)	He/H=0	···	−3.90	4.84
J1225+2836	4010090670831602432	DC	5881 (40)	0.535 (0.024)	7.939 (0.029)	log H/He=−3.0	···	−3.74	2.48
J1226+1836	3947104533054775168	DC	7392 (27)	0.636 (0.006)	8.098 (0.007)	log H/He=−3.6	···	−3.43	1.62
J1226+1949	3949023868038967808	DA	6798 (64)	0.805 (0.038)	8.335 (0.042)	He/H=0	···	−3.71	3.46
J1226+2936	4011709259321463808	DZ	4565 (33)	0.553 (0.062)	7.975 (0.074)	log H/He=−4.0	log Ca/He=−10.51	−4.20	6.54
J1226+3513	1518943638389520384	DA	5094 (18)	0.477 (0.008)	7.819 (0.01)	He/H=0	···	−3.92	3.20
J1226+3632	1519362376225775744	DA	5733 (40)	0.634 (0.032)	8.078 (0.037)	He/H=0	···	−3.85	3.25
J1227+0407	3707668520142907392	DA	7735 (53)	0.714 (0.018)	8.193 (0.02)	He/H=0	···	−3.39	1.63
J1227+3150	4015547856277853824	DA	6523 (18)	0.563 (0.005)	7.955 (0.006)	He/H=0	···	−3.55	1.76
J1227+6330	1583921850718408960	DZ	7803 (101)	0.678 (0.019)	8.164 (0.022)	log H/He=−3.0	log Ca/He=−8.36	−3.37	1.54
J1228+0022	3696778892558087552	DA	9346 (25)	0.595 (0.004)	7.995 (0.004)	He/H=0	···	−2.94	0.75
J1228+1256	3907977484067188096	DA	7339 (23)	0.597 (0.007)	8.007 (0.008)	He/H=0	···	−3.38	1.40
J1228+2056	3952478391839564928	DAZ	6046 (17)	0.588 (0.008)	8.026 (0.009)	He/H=0	log Ca/H=−9.11	−3.74	2.62

Tableau A.2 *suite page suivante*

Tableau A.2 *(suite)*

Name	Gaia DR2/EDR3*	Sp Type	$T_{\rm eff}$ (K)	$M/M_{\odot}$	$\log g$	Composition	Métaux	$\log L/L_{\odot}$	τ (Gyr)
J1228+3300	4015951102167164032	DC	4600 (22)	0.247 (0.009)	7.294 (0.019)	He/H=0	···	−3.86	2.41
J1228+4150	1534836250044023168	DC	5580 (37)	0.534 (0.021)	7.939 (0.026)	H/He=0	···	−3.83	3.30
J1228−0247	3693624423762089216	DA	7383 (47)	0.599 (0.014)	8.010 (0.016)	He/H=0	···	−3.37	1.39
J1229+4126	1534719152051775616	DAH	6345 (47)	0.573 (0.03)	7.972 (0.036)	He/H=0	···	−3.61	1.94
J1229+5047	1544707665434144640	DC	6814 (53)	0.578 (0.021)	8.007 (0.025)	log H/He=−3.4	···	−3.52	1.76
J1229−0432	3681000076065709312	DC	8102 (32)	0.635 (0.007)	8.095 (0.008)	log H/He=−3.8	···	−3.27	1.29
J1229−0707	3583402849843287680	DA	5001 (14)	0.477 (0.007)	7.820 (0.009)	He/H=0	···	−3.95	3.65
J1231+0531	3708253980021111168	DA	8474 (53)	0.607 (0.012)	8.019 (0.013)	He/H=0	···	−3.13	0.99
J1231+1452	3933031020441648384	DA	5792 (25)	0.832 (0.012)	8.380 (0.012)	He/H=0	···	−4.01	5.59
J1231+3924	1533568375694548480	DA	5614 (32)	0.674 (0.016)	8.141 (0.019)	He/H=0	···	−3.92	4.24
J1233+0607	3708578473389974528	DA	5394 (17)	0.746 (0.009)	8.254 (0.009)	He/H=0	···	−4.06	6.41
J1233+0824	3902698243410506112	DQ	6358 (28)	0.556 (0.023)	7.972 (0.029)	H/He=0	log C/He=−6.48	−3.62	2.00
J1233+1253	3931756484602030848	DQ	6698 (15)	0.556 (0.007)	7.970 (0.008)	H/He=0	log C/He=−6.65	−3.53	1.74
J1233+2825	4010592357371458944	DA	5881 (31)	0.743 (0.023)	8.245 (0.025)	He/H=0	···	−3.90	4.46
J1233+6008	1581483997215646208	DA	8354 (68)	0.420 (0.019)	7.669 (0.03)	He/H=0	···	−2.96	0.67
J1233+6745	1682417167486191360	DA	9603 (60)	0.484 (0.01)	7.792 (0.014)	He/H=0	···	−2.78	0.54
J1234+0109	3697125646741428224	DA	5341 (37)	0.660 (0.03)	8.123 (0.034)	He/H=0	···	−4.00	5.32
J1234+0547	3708366954839619328	DA	7695 (40)	0.887 (0.008)	8.456 (0.009)	He/H=0	···	−3.57	3.06
J1234+1248	3931751257626586880	DA	8260 (53)	0.472 (0.012)	7.777 (0.017)	He/H=0	···	−3.04	0.78
J1234+1503	3933386712453327360	DA+DC*	6227 (22)	0.723 (0.018)	8.213 (0.019)	He/H=0	···	−3.78	3.49
J1234+4911	1544285079309656064	DA	7614 (37)	0.563 (0.013)	7.947 (0.017)	He/H=0	···	−3.28	1.17
J1234+6045	1583023618437189504	DA	7094 (45)	0.574 (0.012)	7.970 (0.014)	He/H=0	···	−3.41	1.45
J1234+6605	1680532535836237440	DA	5359 (35)	0.609 (0.019)	8.042 (0.021)	He/H=0	···	−3.95	4.21
J1235+2107	3949551801124462976	DC	6178 (46)	0.627 (0.019)	8.089 (0.021)	H/He=0	···	−3.73	2.76
J1235+2318	3958889751516035200	DA	7775 (42)	0.585 (0.012)	7.984 (0.014)	He/H=0	···	−3.26	1.17
J1235+3918	1533514911941019008	DQ	9263 (39)	0.585 (0.01)	8.010 (0.012)	H/He=0	log C/He=−4.48	−2.98	0.81
J1235+5503	1571109898850692608	DA	8278 (49)	0.298 (0.006)	7.356 (0.014)	He/H=0	···	−2.82	0.49
J1236+3307	1514736047908364928	DC	9163 (67)	0.664 (0.015)	8.139 (0.016)	log H/He=−4.2	···	−3.08	1.00
J1237+1814	3947604806549970560	DC	9520 (62)	0.575 (0.012)	7.993 (0.014)	log H/He=−4.4	···	−2.93	0.74
J1237+3448	1518352719609121280	DA	9066 (71)	0.785 (0.013)	8.298 (0.014)	He/H=0	···	−3.18	1.27
J1237+4156	1534384148897669248	DQP	6178 (16)	0.715 (0.005)	8.223 (0.005)	H/He=0	log C/He=−5.24	−3.81	3.76
J1237+6023	1580009552123749888	DA	5091 (20)	0.510 (0.01)	7.878 (0.013)	He/H=0	···	−3.95	3.70
J1238+3502	1518373537314807552	DC	3479 (152)	0.585 (0.054)	8.028 (0.088)	log H/He=−0.87	···	−4.70	8.94
J1238+3933	1521599470071180672	DA	6581 (42)	0.747 (0.018)	8.247 (0.019)	He/H=0	···	−3.71	3.16

Tableau A.2 *suite page suivante*

Tableau A.2 *(suite)*

Name	Gaia DR2/EDR3*	Sp Type	$T_{\rm eff}$ (K)	$M/M_{\odot}$	$\log g$	Composition	Métaux	$\log L/L_{\odot}$	τ (Gyr)
J1238+4931	1544353553970169728	DA	6481 (54)	0.809 (0.028)	8.341 (0.032)	He/H=0	···	−3.79	3.98
J1238+5122	1568579647717853184	DA	7466 (38)	0.582 (0.01)	7.982 (0.012)	He/H=0	···	−3.33	1.29
J1238+5840	1578256136019422080	DC	5910 (80)	0.571 (0.034)	7.999 (0.041)	log H/He=−3.0	···	−3.76	2.76
J1238−0045	3695839596094423296	DA	6574 (37)	0.653 (0.02)	8.102 (0.022)	He/H=0	···	−3.62	2.17
J1239+4525	1541286711100812160	DA	6427 (15)	0.797 (0.004)	8.324 (0.005)	He/H=0	···	−3.80	3.96
J1240+0932	3903151246497510784	DC	5989 (30)	0.627 (0.016)	8.090 (0.018)	log H/He=−3.0	···	−3.79	3.27
J1240+1807	3935942939548822272	DA	5455 (20)	0.598 (0.008)	8.023 (0.01)	He/H=0	···	−3.91	3.51
J1240−0310	3682835848166848896	DA	10003 (30)	0.854 (0.005)	8.400 (0.005)	He/H=0	···	−3.08	1.16
J1240−2317	3501922067493606272	DA	5509 (19)	0.200 (0.001)	7.070 (0.007)	He/H=0	···	−3.41	0.97
J1241+2614	3961323069532233984	DQ	5839 (16)	0.556 (0.022)	7.974 (0.026)	H/He=0	log C/He=−6.90	−3.77	2.76
J1241+4706	1542933401563275136	DA	9405 (46)	0.575 (0.009)	7.959 (0.011)	He/H=0	···	−2.91	0.70
J1241+5407	1570797397030134912	DA	9777 (54)	0.626 (0.011)	8.045 (0.013)	He/H=0	···	−2.89	0.71
J1241−0733	3676222491884053376	DA	9930 (45)	0.605 (0.013)	8.009 (0.015)	He/H=0	···	−2.85	0.65
J1241−1506	3526928874624208128	DAH	8141 (106)	0.970 (0.021)	8.583 (0.026)	He/H=0	···	−3.56	3.18
J1242+1123	3927653893186082176	DA	6404 (37)	0.757 (0.022)	8.264 (0.024)	He/H=0	···	−3.77	3.58
J1242+1311	3929166408868873344	DC	5035 (24)	0.580 (0.013)	7.999 (0.014)	He/H=0	···	−4.04	5.72
J1242+2733	3962296416495937152	DA	5734 (25)	0.720 (0.011)	8.212 (0.012)	He/H=0	···	−3.93	4.53
J1242+2957	4011194202932877696	DA	4924 (30)	0.612 (0.018)	8.053 (0.02)	He/H=0	···	−4.10	7.06
J1242+6542	1680452683804651520	DA	6622 (26)	0.595 (0.008)	8.008 (0.009)	He/H=0	···	−3.56	1.83
J1242−0211	3683074094297008128	DA	6111 (31)	0.621 (0.018)	8.054 (0.021)	He/H=0	···	−3.72	2.45
J1243+6712	1682144424177509888	DA :	7031 (64)	0.817 (0.022)	8.352 (0.025)	He/H=0	···	−3.66	3.25
J1244−1051	3530399693530713344	DA	8041 (11)	0.209 (0.001)	7.022 (0.003)	He/H=0	···	−2.69	0.28
J1244−1947	3503786766199868416	DA	6778 (52)	0.839 (0.024)	8.386 (0.027)	He/H=0	···	−3.75	3.82
J1245+1205	3928077827935031168	DA	6633 (36)	0.630 (0.021)	8.065 (0.025)	He/H=0	···	−3.58	1.99
J1245+4238	1540371883066128768	DA*	8944 (51)	0.625 (0.01)	8.077 (0.011)	log H/He=−4.0	···	−3.08	0.98
J1245−1837	3521882906526249088	DA	7126 (48)	0.813 (0.025)	8.345 (0.027)	He/H=0	···	−3.63	3.07
J1245−1946	3503777905682327552	DA	10560 (51)	0.880 (0.006)	8.437 (0.008)	He/H=0	···	−3.00	1.06
J1246+1155	3928060510626899200	DZ	8129 (41)	0.607 (0.012)	8.050 (0.014)	log H/He=−4.0	log Ca/He=−9.13	−3.23	1.20
J1247+0646	3709565658737443200	DQ	4772 (20)	0.657 (0.017)	8.141 (0.018)	H/He=0	log C/He=−7.11	−4.21	7.25
J1247+3030	1465214177336901376	DA	7644 (50)	0.697 (0.014)	8.166 (0.016)	He/H=0	···	−3.40	1.61
J1247−0111	3683627840135415808	DA	7064 (18)	0.602 (0.005)	8.017 (0.006)	He/H=0	···	−3.45	1.57
J1248+1222	3928101738016062336	DA	7304 (43)	0.570 (0.018)	7.962 (0.022)	He/H=0	···	−3.36	1.33
J1248+1230	3928119295842399360	DA	6583 (49)	0.846 (0.018)	8.396 (0.02)	He/H=0	···	−3.80	4.17
J1248+2942	1465092887460185600	DA	6899 (28)	0.630 (0.01)	8.063 (0.011)	He/H=0	···	−3.52	1.79

Tableau A.2 *suite page suivante*

Tableau A.2 *(suite)*

Name	Gaia DR2/EDR3*	Sp Type	$T_{\rm eff}$ (K)	$M/M_{\odot}$	$\log g$	Composition	Métaux	$\log L/L_{\odot}$	τ (Gyr)
J1248+4104	1527940564084210816	DAH*	7399 (49)	0.774 (0.012)	8.286 (0.013)	He/H=0	···	−3.53	2.34
J1248−1028	3530520910392199680	DC	7062 (23)	0.724 (0.006)	8.236 (0.007)	log H/He=−3.4	···	−3.59	2.48
J1249+2742	3961972747760766720	DA	7063 (69)	0.639 (0.025)	8.078 (0.028)	He/H=0	···	−3.48	1.73
J1249+2800	3961998375830065152	DQ	7468 (65)	0.713 (0.029)	8.217 (0.032)	H/He=0	log C/He=−6.40	−3.48	1.94
J1249+3407	1515081328918440064	DQ	8402 (45)	0.538 (0.009)	7.933 (0.011)	H/He=0	log C/He=−5.21	−3.11	0.94
J1250+1955	3942229672158400640	DA	8097 (52)	0.855 (0.018)	8.406 (0.021)	He/H=0	···	−3.45	2.38
J1250+5446	1570514066627694336	DC	4019 (17)	0.398 (0.007)	7.678 (0.009)	He/H=0	···	−4.27	6.14
J1251+0753	3709760890770697856	DA	9902 (104)	1.004 (0.019)	8.635 (0.025)	He/H=0	···	−3.26	2.10
J1251+2912	1464837457164974976	DC	4699 (51)	0.519 (0.07)	7.901 (0.087)	He/H=0	···	−4.10	6.17
J1251+4403	1528861748669458432	DC	4787 (42)	1.289 (0.011)	9.282 (0.038)	log H/He=−3.48	···	−5.06	4.10
J1252+1943	3942041105914664832	DQ	6774 (23)	0.319 (0.022)	7.485 (0.039)	H/He=0	log C/He=−6.57	−3.26	0.95
J1252+2153	3954943428189717504	DAZ	6150 (34)	0.571 (0.025)	7.998 (0.03)	He/H=0	log Ca/H=−7.43	−3.69	2.30
J1252−0234	3682469122383597056	DC	7278 (48)	0.424 (0.012)	7.723 (0.017)	log H/He=−3.6	···	−3.25	1.03
J1253+0355	3704624487842182656	DA	6409 (29)	0.639 (0.018)	8.081 (0.02)	He/H=0	···	−3.65	2.23
J1253+2203	3954947379559880064	DC	4995 (18)	0.555 (0.013)	7.959 (0.016)	He/H=0	···	−4.03	5.41
J1253+3437	1515869884914637824	DC	4824 (32)	0.547 (0.021)	7.947 (0.025)	He/H=0	···	−4.08	6.09
J1254+1432	3930720057454344960	DC	9776 (49)	0.640 (0.011)	8.099 (0.013)	log H/He=−4.6	···	−2.94	0.80
J1254+2054	3942685179209931008	DA	6941 (53)	0.768 (0.022)	8.277 (0.024)	He/H=0	···	−3.63	2.86
J1254+3620	1517239773324267904	DC	4752 (14)	0.486 (0.006)	7.842 (0.008)	He/H=0	···	−4.05	5.29
J1254+4918	1555410036744248832	DAH	6490 (69)	0.760 (0.027)	8.267 (0.029)	He/H=0	···	−3.74	3.46
J1254−0236	3682412703692940032	DZ	6989 (51)	0.740 (0.017)	8.260 (0.019)	log H/He=−4.0	log Ca/He=−10.28	−3.62	2.72
J1255+4655	1531097433767946240	DC	4697 (28)	0.748 (0.014)	8.261 (0.015)	He/H=0	···	−4.31	9.75
J1256+1355	3929872707650824320	DA	6108 (38)	0.597 (0.028)	8.015 (0.033)	He/H=0	···	−3.70	2.29
J1256+1551	3931506719368273792	DA	8924 (90)	0.882 (0.017)	8.446 (0.019)	He/H=0	···	−3.31	1.89
J1256+1839	3941103359935056640	DA	6630 (53)	0.738 (0.034)	8.233 (0.037)	He/H=0	···	−3.69	2.97
J1257+2312	3956630388264212992	DA	5920 (59)	0.649 (0.044)	8.100 (0.05)	He/H=0	···	−3.81	3.07
J1257+2911	1464134289414972288	DA	6759 (34)	0.569 (0.012)	7.963 (0.014)	He/H=0	···	−3.50	1.62
J1257+3414	1515693894335906688	DAH	9603 (38)	0.891 (0.007)	8.457 (0.008)	He/H=0	···	−3.19	1.51
J1257+5127	1557524191442926336	DA	7535 (53)	0.893 (0.021)	8.464 (0.023)	He/H=0	···	−3.61	3.29
J1258+1946	3941619958601686016	DC	4616 (20)	0.496 (0.02)	7.860 (0.025)	He/H=0	···	−4.12	6.12
J1258+5014	1555883930548870400	DA	8324 (29)	0.683 (0.005)	8.142 (0.006)	He/H=0	···	−3.23	1.24
J1259+0442	3705109338109763712	DC	4807 (23)	0.597 (0.019)	8.030 (0.022)	He/H=0	···	−4.13	7.32
J1259+2734	1460689760003983232	DAZ	8690 (20)	0.619 (0.004)	8.068 (0.005)	He/H=0	log Ca/H=−8.00	−3.13	1.04
J1259+2754	1460807304669403136	DQ	9279 (67)	0.529 (0.014)	7.913 (0.017)	H/He=0	log C/He=−4.86	−2.93	0.71

Tableau A.2 *suite page suivante*

Tableau A.2 *(suite)*

Name	Gaia DR2/EDR3*	Sp Type	$T_{\rm eff}$ (K)	$M/M_{\odot}$	$\log g$	Composition	Métaux	$\log L/L_{\odot}$	τ (Gyr)
J1259+6234	1675850407304241536	DC	6285 (36)	0.694 (0.009)	8.191 (0.011)	log H/He=−3.2	···	−3.76	3.31
J1300+0130	3690395231125833600	DA	5421 (19)	0.601 (0.007)	8.028 (0.008)	He/H=0	···	−3.92	3.71
J1300+0328	3704392873140270336	DA	5679 (8)	0.723 (0.004)	8.217 (0.004)	He/H=0	···	−3.95	4.73
J1300+0836	3733693754214402816	DA	6223 (48)	0.719 (0.024)	8.207 (0.027)	He/H=0	···	−3.78	3.45
J1300+1817	3940853397134158848	DA	9349 (55)	0.382 (0.007)	7.572 (0.012)	He/H=0	···	−2.71	0.45
J1300+3931	1523861990123367808	DQ	5870 (21)	0.849 (0.032)	8.425 (0.034)	H/He=0	log C/He=−5.31	−4.03	5.61
J1300+5904	1578748824604827648	DAH	6162 (34)	0.578 (0.013)	7.983 (0.014)	He/H=0	···	−3.67	2.12
J1301+1520	3930500666228897536	DC	6434 (51)	0.600 (0.023)	8.044 (0.026)	log H/He=−3.2	···	−3.64	2.14
J1301+2600	1460293317343353344	DA	6976 (26)	0.607 (0.009)	8.025 (0.011)	He/H=0	···	−3.48	1.64
J1301+6713	1679365202380970880	DA	6645 (20)	0.747 (0.005)	8.247 (0.006)	He/H=0	···	−3.69	3.06
J1301−0235	3685203985758805120	DA	7130 (93)	1.091 (0.028)	8.789 (0.04)	He/H=0	···	−3.95	4.63
J1302+2120	3944082692848953088	DC	6017 (40)	0.524 (0.018)	7.918 (0.022)	log H/He=−3.0	···	−3.69	2.20
J1303+1949	3941482519648231296	DA	6732 (46)	0.572 (0.018)	7.968 (0.022)	He/H=0	···	−3.50	1.65
J1303+2603	1459546263999675264	DC	4344 (28)	0.569 (0.014)	7.987 (0.016)	He/H=0	···	−4.29	8.33
J1303+3854	1523586253222618112	DC	6114 (78)	0.700 (0.033)	8.201 (0.037)	H/He=0	···	−3.82	3.77
J1303+7510	1691837787408390400	DC	7407 (27)	0.581 (0.006)	8.010 (0.006)	log H/He=−3.6	···	−3.37	1.43
J1303−0323	3684329706511747840	DA	7285 (25)	0.358 (0.006)	7.534 (0.009)	He/H=0	···	−3.14	0.82
J1304+0126	3691095100341397632	DC*	4288 (52)	0.635 (0.037)	8.107 (0.057)	log H/He=−2.37	···	−4.38	7.92
J1304−0528	3629758603668233728	DA	5253 (13)	0.610 (0.007)	8.046 (0.007)	He/H=0	···	−3.99	4.90
J1305+1525	3936440262402010368	DA	9882 (51)	0.666 (0.012)	8.109 (0.014)	He/H=0	···	−2.91	0.76
J1305+6034	1579314622119638400	DC :	8516 (83)	0.647 (0.016)	8.114 (0.018)	log H/He=−4.0	···	−3.19	1.16
J1305+7022	1686322048672412288	DC	5042 (47)	1.216 (0.009)	9.052 (0.019)	He/H=0	···	−4.76	6.91
J1306+1811	3938160280840704000	DA	8649 (87)	0.939 (0.014)	8.533 (0.017)	He/H=0	···	−3.42	2.54
J1306+4355	1529609897612606592	DA	6576 (44)	0.559 (0.014)	7.946 (0.018)	He/H=0	···	−3.53	1.70
J1307+4910	1554850591480752384	DA	5685 (30)	0.621 (0.019)	8.058 (0.022)	He/H=0	···	−3.85	3.16
J1308+8502	1726678630833373824	DAP	5375 (17)	0.681 (0.006)	8.156 (0.007)	He/H=0	···	−4.01	5.50
J1309+3715	1522443933657255936	DA	9375 (85)	0.574 (0.015)	7.958 (0.018)	He/H=0	···	−2.92	0.71
J1309+4913	1554843655110340992	DZ	8422 (43)	0.582 (0.009)	8.007 (0.011)	log H/He=−4.0	log Ca/He=−9.96	−3.15	1.03
J1310+1214	3736695803210593664	DA	8454 (47)	0.615 (0.014)	8.032 (0.016)	He/H=0	···	−3.14	1.01
J1310+1404	3743905507112335616	DA	8609 (24)	0.549 (0.005)	7.917 (0.007)	He/H=0	···	−3.04	0.83
J1310+6117	1675399401377503360	DC	4387 (70)	0.426 (0.059)	7.732 (0.083)	He/H=0	···	−4.14	5.51
J1310+6118	1675399225287958272	DC	5220 (32)	0.405 (0.026)	7.702 (0.038)	H/He=0	···	−3.83	2.92
J1310+6746	1679458897091659008	DC	6002 (60)	0.689 (0.017)	8.186 (0.019)	log H/He=−3.0	···	−3.84	3.98
J1310+7236	1688070959355309312	DA	7811 (50)	0.587 (0.009)	7.988 (0.011)	He/H=0	···	−3.25	1.16

Tableau A.2 *suite page suivante*

Tableau A.2 *(suite)*

Name	Gaia DR2/EDR3*	Sp Type	$T_{\rm eff}$ (K)	$M/M_{\odot}$	$\log g$	Composition	Métaux	$\log L/L_{\odot}$	τ (Gyr)
J1310−0202	3684909561456453248	DA :	6552 (39)	0.781 (0.02)	8.299 (0.021)	He/H=0	···	−3.75	3.59
J1311+2923	1462641629366243712	DQ	5618 (14)	0.714 (0.012)	8.225 (0.013)	H/He=0	log C/He=−5.18	−3.98	5.51
J1311+3837	1523116177642231808	DC	6304 (48)	0.612 (0.019)	8.063 (0.022)	log H/He=−3.2	···	−3.69	2.37
J1311−0034	3687414210289577344	DA	6517 (36)	0.824 (0.021)	8.364 (0.024)	He/H=0	···	−3.80	4.07
J1312+5805	1566603962760532736	DA	10211 (31)	0.401 (0.006)	7.608 (0.01)	He/H=0	···	−2.58	0.37
J1313+0226	3691685882071367936	DC	4289 (41)	0.499 (0.015)	7.868 (0.018)	He/H=0	···	−4.25	7.38
J1313+1057	3733305179932909312	DA :	5810 (27)	0.734 (0.019)	8.231 (0.02)	He/H=0	···	−3.92	4.51
J1313+1341	3743646365965636352	DC	8961 (52)	0.719 (0.01)	8.224 (0.011)	log H/He=−4.2	···	−3.17	1.20
J1313+5738	1566553007268519168	DZA	8774 (48)	0.571 (0.007)	7.988 (0.008)	log H/He=−4.0	log Ca/He=−9.10	−3.07	0.91
J1313−0223	3684741301817503872	DA*	6548 (15)	0.654 (0.007)	8.103 (0.007)	He/H=0	···	−3.63	2.20
J1314+0700	3729759568466399488	DA	9596 (51)	0.603 (0.013)	8.007 (0.015)	He/H=0	···	−2.90	0.71
J1314+1456	3744078023062858624	DA	6284 (34)	0.777 (0.011)	8.295 (0.012)	He/H=0	···	−3.82	4.01
J1314+1732	3937174942327932544	DAH	7230 (55)	0.837 (0.019)	8.381 (0.021)	He/H=0	···	−3.63	3.17
J1314+5327	1563260687202320256	DC	9836 (52)	0.586 (0.009)	8.010 (0.011)	log H/He=−4.6	···	−2.88	0.69
J1315+4711	1551346520939849728	DQ	7747 (47)	0.528 (0.011)	7.918 (0.014)	H/He=0	log C/He=−5.82	−3.25	1.13
J1315+6046	1663349849153677952	DA	6933 (44)	0.661 (0.014)	8.113 (0.015)	He/H=0	···	−3.54	1.91
J1316+0149	3688402091422432128	DA :*	6615 (34)	0.638 (0.021)	8.077 (0.023)	He/H=0	···	−3.60	2.04
J1316+0810	3731530843043705216	DQ	6804 (31)	0.603 (0.024)	8.047 (0.027)	H/He=0	log C/He=−6.77	−3.54	1.86
J1316−2007	3506567328028533120	DZ	4629 (12)	0.570 (0.007)	8.003 (0.008)	log H/He=−5.0	log Ca/He=−10.50	−4.19	6.62
J1317+0621	3717651845204820864	DA	5306 (23)	0.665 (0.014)	8.132 (0.014)	He/H=0	···	−4.02	5.64
J1317+2157	3943650619138622848	DC	6159 (25)	0.655 (0.007)	8.132 (0.008)	log H/He=−3.0	···	−3.77	3.15
J1317+4434	1550492952021749248	DC :	6286 (41)	0.638 (0.015)	8.106 (0.016)	log H/He=−3.2	···	−3.71	2.69
J1317+4833	1556005701461744640	DA	5885 (19)	0.608 (0.007)	8.034 (0.008)	He/H=0	···	−3.78	2.63
J1317+6005	1663262163101591936	DC	7057 (29)	0.568 (0.008)	7.990 (0.01)	log H/He=−3.4	···	−3.45	1.58
J1317−1121	3623233040812235904	DA	8995 (27)	0.612 (0.005)	8.025 (0.005)	He/H=0	···	−3.03	0.86
J1318+1241	3742597358857731712	DA	6268 (42)	0.621 (0.023)	8.053 (0.026)	He/H=0	···	−3.68	2.26
J1318+5003	1556577584947193856	DC	10256 (80)	0.624 (0.013)	8.071 (0.015)	log H/He=−4.8	···	−2.84	0.68
J1319−2148	3506061587037686144	DA	5873 (14)	0.985 (0.005)	8.612 (0.005)	He/H=0	···	−4.15	6.34
J1320+2801	1461469893567499904	DC	3509 (34)	0.199 (0.03)	7.085 (0.084)	He/H=0	···	−4.21	5.57
J1320+3942	1524536884104266368	DA	7170 (68)	1.135 (0.042)	8.872 (0.069)	He/H=0	···	−4.00	4.59
J1320+4712	1551402252435630592	DA	7974 (39)	0.593 (0.01)	7.998 (0.012)	He/H=0	···	−3.23	1.12
J1320+5530	1563853976804546688	DC	5770 (74)	0.618 (0.036)	8.077 (0.041)	H/He=0	···	−3.85	3.89
J1320−0224	3638148805100101888	DA	4982 (28)	0.558 (0.03)	7.964 (0.037)	He/H=0	···	−4.04	5.57
J1321+1645	3746179365877952256	DAH*	7618 (51)	0.694 (0.014)	8.162 (0.016)	He/H=0	···	−3.40	1.62

Tableau A.2 *suite page suivante*

Tableau A.2 *(suite)*

Name	Gaia DR2/EDR3*	Sp Type	$T_{\rm eff}$ (K)	$M/M_{\odot}$	$\log g$	Composition	Métaux	$\log L/L_{\odot}$	τ (Gyr)
J1321+3345	1472821908743764096	DA	8930 (62)	0.971 (0.012)	8.583 (0.014)	He/H=0	···	−3.40	2.53
J1323+1756	3746422113133965696	DC :	6336 (84)	0.710 (0.038)	8.216 (0.042)	log H/He=−3.2	···	−3.76	3.38
J1324+0857	3731853549706103680	DA	8171 (24)	0.536 (0.006)	7.897 (0.008)	He/H=0	···	−3.13	0.92
J1324+4149	1525359868557998336	DA	5334 (52)	0.520 (0.024)	7.892 (0.03)	He/H=0	···	−3.88	2.84
J1324+6226	1663956268471724288	DA	9999 (39)	0.609 (0.006)	8.015 (0.008)	He/H=0	···	−2.84	0.65
J1325+0852	3731848189586855040	DA	9782 (52)	0.775 (0.011)	8.280 (0.012)	He/H=0	···	−3.04	1.01
J1325+4523	1550208900064886656	DC	5570 (72)	0.368 (0.02)	7.618 (0.03)	log H/He=−5.0	···	−3.67	2.04
J1326+0504	3716300103033172608	DA	6636 (37)	0.277 (0.011)	7.318 (0.024)	He/H=0	···	−3.19	0.83
J1326+5025	1553656418774428032	DA	6808 (48)	0.646 (0.02)	8.090 (0.023)	He/H=0	···	−3.55	1.94
J1327+5755	1566012013187728768	DA	6714 (23)	0.574 (0.006)	7.972 (0.006)	He/H=0	···	−3.51	1.67
J1327+5805	1566020598826667904	DC	5713 (62)	0.678 (0.028)	8.170 (0.031)	H/He=0	···	−3.92	4.82
J1328+4450	1550124654283201920	DC	7003 (100)	0.492 (0.024)	7.855 (0.031)	log H/He=−3.4	···	−3.39	1.34
J1329+0746	3719493011785709056	DQ	8014 (41)	0.562 (0.01)	7.976 (0.012)	H/He=0	log C/He=−5.54	−3.22	1.12
J1329+2450	1447925976193082368	DC	4132 (21)	0.526 (0.013)	7.915 (0.016)	He/H=0	···	−4.34	8.21
J1329+3109	1468305213760240384	DC	4616 (83)	0.494 (0.061)	7.857 (0.077)	He/H=0	···	−4.11	6.09
J1329+3927	1476702321500114432	DA	7949 (61)	0.531 (0.015)	7.889 (0.018)	He/H=0	···	−3.17	0.98
J1329−0134	3638457669084084224	DA	7278 (29)	0.631 (0.009)	8.064 (0.01)	He/H=0	···	−3.42	1.56
J1329−0238	3637209066255998592	DA	8955 (75)	0.769 (0.028)	8.273 (0.031)	He/H=0	···	−3.19	1.26
J1330+2329	1443266623871074816	DA	6170 (47)	0.867 (0.019)	8.430 (0.022)	He/H=0	···	−3.94	5.03
J1330+3029	1468213546275054208	DZH	6274 (12)	0.703 (0.004)	8.205 (0.003)	log H/He=−3.0	log Ca/He=−8.16	−3.77	3.43
J1330+5445	1565012935076040832	DA	7583 (20)	0.665 (0.005)	8.116 (0.006)	He/H=0	···	−3.38	1.52
J1330+6435	1666074615061406336	DC*	3914 (250)	0.589 (0.12)	8.021 (0.138)	He/H=0	···	−4.49	9.89
J1331+6809	1684555515739151360	DA	9659 (60)	0.615 (0.008)	8.026 (0.01)	He/H=0	···	−2.90	0.72
J1332+0117	3711214067185666560	DAH	7204 (24)	0.829 (0.006)	8.370 (0.006)	He/H=0	···	−3.63	3.13
J1332+1043	3738162616145822208	DC	6600 (46)	0.574 (0.034)	8.000 (0.041)	log H/He=−3.2	···	−3.57	1.88
J1332+2740	1448881864114808448	DQZ	8303 (39)	0.552 (0.009)	7.957 (0.011)	H/He=0	log C/He=−5.52	−3.15	1.00
J1333+0016	3662951038644235776	DQ	5156 (13)	0.894 (0.013)	8.493 (0.015)	H/He=0	log C/He=−6.28	−4.30	7.45
J1333+0649	3718579386342034816	DA	7648 (46)	0.830 (0.016)	8.369 (0.018)	He/H=0	···	−3.52	2.61
J1333+1550	3744991824600484864	DA	8516 (68)	0.966 (0.013)	8.576 (0.016)	He/H=0	···	−3.48	2.83
J1333+2450	1444926572896853376	DC	4611 (28)	0.540 (0.016)	7.937 (0.019)	He/H=0	···	−4.16	6.86
J1333+4225	1501320872177341952	DAZ	6792 (71)	0.906 (0.029)	8.487 (0.033)	He/H=0	···	−3.81	4.33
J1334+0647	3718388689794769664	DA	7797 (53)	0.706 (0.022)	8.180 (0.025)	He/H=0	···	−3.37	1.56
J1334+4704	1551761857160285312	DC	6024 (62)	0.609 (0.027)	8.060 (0.03)	log H/He=−3.0	···	−3.76	2.92
J1334+6601	1666261218505739008	DA	6017 (18)	0.742 (0.008)	8.243 (0.008)	He/H=0	···	−3.86	4.14

Tableau A.2 *suite page suivante*

Tableau A.2 *(suite)*

Name	Gaia DR2/EDR3*	Sp Type	$T_{\rm eff}$ (K)	$M/M_{\odot}$	$\log g$	Composition	Métaux	$\log L/L_{\odot}$	τ (Gyr)
J1335+3322	1469189191046042112	DA	8731 (69)	0.412 (0.01)	7.648 (0.017)	He/H=0	···	−2.88	0.59
J1335+3610	1471998511973713152	DA	10050 (57)	0.593 (0.009)	7.988 (0.01)	He/H=0	···	−2.81	0.62
J1335−0542	3633287421812873600	DA	7701 (23)	0.552 (0.006)	7.927 (0.006)	He/H=0	···	−3.25	1.11
J1336+3034	1456253707325896960	DA	6206 (42)	0.606 (0.035)	8.029 (0.041)	He/H=0	···	−3.68	2.24
J1336+3547	1471788161655374080	DZH*	6395 (22)	0.671 (0.009)	8.157 (0.01)	log H/He=−4.0	log Ca/He=−8.66	−3.71	2.86
J1336+3623	1472029470098019072	DA	6851 (20)	0.592 (0.004)	8.001 (0.005)	He/H=0	···	−3.49	1.66
J1336+3648	1472094341284011904	DA	6052 (20)	0.607 (0.009)	8.031 (0.009)	He/H=0	···	−3.73	2.41
J1336+3727	1472500473391093120	DA	7856 (35)	0.904 (0.006)	8.480 (0.006)	He/H=0	···	−3.55	3.02
J1336+5403	1561941170170300288	DA	6011 (38)	0.638 (0.018)	8.082 (0.021)	He/H=0	···	−3.77	2.76
J1337+0001	3662779171232754688	DC	4944 (25)	1.058 (0.023)	8.753 (0.04)	log H/He=−3.00	···	−4.56	7.10
J1337+6110	1662871286717909632	DA	5473 (17)	0.601 (0.008)	8.027 (0.008)	He/H=0	···	−3.90	3.49
J1337−1203	3610422798340344704	DC	6535 (34)	0.595 (0.014)	8.035 (0.016)	log H/He=−3.2	···	−3.61	2.03
J1338+3213	1468882118064381696	DA	6089 (40)	0.606 (0.026)	8.030 (0.029)	He/H=0	···	−3.72	2.37
J1338−0045	3661843349398271232	DA	6134 (30)	0.671 (0.026)	8.133 (0.029)	He/H=0	···	−3.76	2.94
J1339+6010	1662524184641472640	DA	8032 (64)	0.659 (0.014)	8.105 (0.016)	He/H=0	···	−3.27	1.29
J1339−0020	3661954022115425536	DA	7817 (56)	0.629 (0.027)	8.057 (0.03)	He/H=0	···	−3.29	1.28
J1340+0203	3663664003222454528	DA	5613 (23)	0.722 (0.009)	8.215 (0.011)	He/H=0	···	−3.97	4.95
J1340+3228	1456903763514134272	DA	8734 (49)	0.581 (0.009)	7.973 (0.01)	He/H=0	···	−3.05	0.86
J1340+4033	1500140065408640512	DC	4800 (28)	0.445 (0.023)	7.764 (0.031)	He/H=0	···	−4.00	4.08
J1341+0227	3713218786120541824	DQ	5843 (9)	0.640 (0.006)	8.110 (0.007)	H/He=0	log C/He=−5.97	−3.85	3.92
J1341+0500	3714914271705535360	DC	4223 (11)	0.503 (0.005)	7.876 (0.005)	He/H=0	···	−4.28	7.65
J1341+0721	3724485756648081920	DA	5994 (31)	0.501 (0.025)	7.849 (0.031)	He/H=0	···	−3.65	1.87
J1341+2156	1249747212968218496	DC	4778 (18)	0.513 (0.013)	7.889 (0.016)	He/H=0	···	−4.07	5.71
J1341+4150	1501012287368950528	DA	7973 (60)	0.900 (0.01)	8.475 (0.012)	He/H=0	···	−3.52	2.87
J1342+4436	1503203059990907648	DC	6012 (69)	0.560 (0.02)	7.980 (0.023)	log H/He=−3.0	···	−3.72	2.44
J1343+1157	3728216571400055040	DA	7590 (50)	0.913 (0.019)	8.496 (0.022)	He/H=0	···	−3.62	3.37
J1344+4349	1503091085900019712	DA	6259 (35)	0.813 (0.012)	8.348 (0.013)	He/H=0	···	−3.86	4.41
J1345+1514	3741324506644465280	DC	3966 (60)	0.431 (0.037)	7.744 (0.05)	He/H=0	···	−4.32	6.95
J1345+4200	1500607765872799616	DC	4616 (17)	0.223 (0.005)	7.145 (0.011)	He/H=0	···	−3.75	3.21
J1346+0918	3725166869742133248	DA	5363 (32)	0.554 (0.016)	7.950 (0.019)	He/H=0	···	−3.90	3.12
J1346−1350	3606199608537728768	DA	9102 (39)	0.216 (0.003)	7.023 (0.009)	He/H=0	···	−2.46	0.16
J1347+1021	3725570772761744384	DAZ*	7030 (13)	0.606 (0.003)	8.023 (0.004)	He/H=0	···	−3.46	1.61
J1347+2552	1444528416543875456	DA	7192 (28)	0.606 (0.008)	8.023 (0.01)	He/H=0	···	−3.42	1.51
J1347+5036	1558872261424381184	DA	5135 (22)	0.540 (0.012)	7.930 (0.014)	He/H=0	···	−3.96	4.08

Tableau A.2 *suite page suivante*

Tableau A.2 *(suite)*

Name	Gaia DR2/EDR3*	Sp Type	$T_{\rm eff}$ (K)	$M/M_{\odot}$	$\log g$	Composition	Métaux	$\log L/L_{\odot}$	τ (Gyr)
J1348+2334	1251824057289839744	DC	4618 (9)	0.462 (0.004)	7.798 (0.006)	He/H=0	···	−4.08	5.36
J1348+4618	1503808066264043136	DA	8616 (59)	0.601 (0.013)	8.007 (0.015)	He/H=0	···	−3.09	0.93
J1348−0152	3658513620167922816	DC	5938 (44)	0.660 (0.035)	8.141 (0.039)	H/He=0	···	−3.83	3.85
J1349+1155	3728074738695246336	DC	4494 (26)	0.691 (0.011)	8.177 (0.013)	He/H=0	···	−4.33	9.80
J1349+2755	1451566149955227520	DA	7308 (17)	0.862 (0.004)	8.418 (0.004)	He/H=0	···	−3.63	3.30
J1349+4332	1502284452385828864	DA	8473 (102)	0.891 (0.018)	8.460 (0.021)	He/H=0	···	−3.40	2.33
J1351+1214	3728063945441922176	DC	4960 (94)	0.741 (0.474)	8.250 (0.622)	He/H=0	···	−4.21	8.79
J1351+1719	1244753299874351488	DAH	9274 (82)	0.958 (0.012)	8.562 (0.014)	He/H=0	···	−3.32	2.20
J1351+3654	1495325853747745536	DA	7041 (59)	0.569 (0.017)	7.960 (0.022)	He/H=0	···	−3.42	1.46
J1351+4141	1500444625834675200	DA	8149 (69)	0.886 (0.017)	8.452 (0.019)	He/H=0	···	−3.47	2.59
J1351+4253	1502063317405058304	DZ	6655 (27)	0.694 (0.007)	8.191 (0.008)	log H/He=−2.0	log Ca/He=−10.90	−3.66	2.71
J1351+4653	1509842495314395264	DA	6020 (58)	0.954 (0.027)	8.563 (0.033)	He/H=0	···	−4.07	5.83
J1351+6623	1672147149062665472	DQ	8840 (64)	0.544 (0.012)	7.941 (0.015)	H/He=0	log C/He=−4.92	−3.03	0.83
J1351−2734	6177238676273826304	DA	9147 (34)	0.512 (0.005)	7.848 (0.007)	He/H=0	···	−2.90	0.66
J1352+0818	3721801956139414400	DA	7047 (53)	0.549 (0.02)	7.927 (0.026)	He/H=0	···	−3.40	1.39
J1352+0907	3722192007889372800	DC	5198 (48)	0.862 (0.02)	8.428 (0.022)	He/H=0	···	−4.24	8.73
J1352+1053	3727155340815968256	DA	6030 (14)	0.589 (0.005)	8.001 (0.005)	He/H=0	···	−3.72	2.31
J1352−0054	3659054987910568320	DA	7111 (34)	0.592 (0.011)	8.000 (0.013)	He/H=0	···	−3.43	1.50
J1353+2928	1452337006389928960	DA	7630 (51)	0.761 (0.01)	8.264 (0.011)	He/H=0	···	−3.46	1.96
J1353−0916	3618657732410663808	DAP	8481 (21)	0.747 (0.004)	8.241 (0.004)	He/H=0	···	−3.26	1.39
J1353−2738	6177179298350278016	DA	7469 (70)	0.556 (0.013)	7.937 (0.017)	He/H=0	···	−3.31	1.22
J1354+6009	1661023419988816256	DA	8683 (95)	0.940 (0.016)	8.535 (0.019)	He/H=0	···	−3.41	2.52
J1354−0051	3658879826259633664	DA	7606 (31)	0.799 (0.008)	8.322 (0.008)	He/H=0	···	−3.50	2.35
J1355+3636	1495340933377121792	DQ	8059 (38)	0.532 (0.01)	7.923 (0.013)	H/He=0	log C/He=−4.77	−3.18	1.03
J1355+4553	1508988758895110656	DC	8290 (76)	0.575 (0.014)	7.997 (0.018)	log H/He=−4.0	···	−3.17	1.06
J1355−2622	6178524211524592640	DA	6116 (23)	0.635 (0.007)	8.076 (0.007)	He/H=0	···	−3.73	2.56
J1356+1336	1230679413599906176	DC	5783 (37)	0.574 (0.03)	8.005 (0.036)	H/He=0	···	−3.81	3.17
J1356+2416	1257923215792065152	DZ	6307 (42)	0.615 (0.026)	8.069 (0.03)	log H/He=−3.0	log Ca/He=−8.85	−3.69	2.40
J1356+5853	1659211974581862912	DA	7254 (56)	0.855 (0.013)	8.409 (0.014)	He/H=0	···	−3.64	3.31
J1356−0009	3660622479174640640	DQ	6503 (18)	0.611 (0.017)	8.062 (0.019)	H/He=0	log C/He=−5.84	−3.63	2.15
J1356−0920	3615616169715231104	DA	8505 (51)	0.564 (0.012)	7.945 (0.014)	He/H=0	···	−3.08	0.89
J1357+2954	1453676525085505408	DC	7204 (47)	0.600 (0.014)	8.042 (0.016)	log H/He=−3.4	···	−3.44	1.60
J1357+6028	1660937971614743808	DC	6018 (35)	0.665 (0.012)	8.148 (0.013)	H/He=0	···	−3.81	3.66
J1358+1442	1231038060549269120	DC	7995 (62)	0.688 (0.018)	8.178 (0.02)	log H/He=−3.8	···	−3.34	1.49

Tableau A.2 *suite page suivante*

Tableau A.2 *(suite)*

Name	Gaia DR2/EDR3*	Sp Type	$T_{\rm eff}$ (K)	$M/M_{\odot}$	$\log g$	Composition	Métaux	$\log L/L_{\odot}$	τ (Gyr)
J1358+3704	1483371791532150784	DAZ	5532 (42)	0.585 (0.021)	8.000 (0.025)	He/H=0	···	−3.87	3.05
J1359−2333	6275184065428686464	DA	9335 (18)	0.589 (0.003)	7.985 (0.004)	He/H=0	···	−2.94	0.74
J1401+3659	1483683911099065088	DZ	6033 (36)	0.586 (0.019)	8.024 (0.021)	log H/He=−3.0	log Ca/He=−9.87	−3.74	2.64
J1402−0254	3645620879964502016	DA	7011 (51)	0.796 (0.043)	8.320 (0.047)	He/H=0	···	−3.64	3.06
J1402−0736	3616350265525122816	DA	8483 (22)	0.924 (0.005)	8.510 (0.006)	He/H=0	···	−3.44	2.57
J1402−0902	3615906062827657344	DC	7530 (38)	0.782 (0.012)	8.321 (0.014)	log H/He=−3.6	···	−3.53	2.46
J1403+0452	3671751946324947584	DA	8900 (21)	0.617 (0.005)	8.033 (0.005)	He/H=0	···	−3.05	0.89
J1403+0644	3672656947473710592	DC	6602 (23)	0.611 (0.009)	8.060 (0.01)	log H/He=−3.2	···	−3.60	2.06
J1403+4052	1497899703093177728	DA	7758 (41)	0.582 (0.013)	7.980 (0.015)	He/H=0	···	−3.26	1.17
J1403+4533	1505825635741455872	DC	4823 (17)	1.183 (0.004)	8.995 (0.006)	log H/He=−3.47	···	−4.80	5.76
J1403+5206	1512752769450543488	DA	7347 (27)	0.588 (0.006)	7.992 (0.007)	He/H=0	···	−3.37	1.37
J1403+6439	1670992421335403904	DA*	9604 (54)	0.659 (0.009)	8.129 (0.01)	log H/He=−5.0	···	−2.99	0.87
J1403−0914	3615854321357005824	DA	9568 (57)	0.562 (0.01)	7.936 (0.014)	He/H=0	···	−2.87	0.65
J1403−1514	6300991145225638272	DC	4790 (46)	0.536 (0.009)	7.947 (0.014)	log H/He=−1.84	···	−4.10	5.88
J1404+0936	3723164143671997952	DA	9946 (44)	0.534 (0.008)	7.884 (0.01)	He/H=0	···	−2.77	0.55
J1404+1330	1229916112012470528	DC	4637 (33)	0.508 (0.032)	7.898 (0.055)	log H/He=−2.62	···	−4.13	5.82
J1404+1349	1229959542721326080	DAZ	5730 (38)	0.632 (0.041)	8.075 (0.046)	He/H=0	···	−3.85	3.23
J1404+3620	1483427385588999936	DZ	6310 (44)	0.700 (0.017)	8.201 (0.019)	log H/He=−3.0	log Ca/He=−9.14	−3.76	3.33
J1404+5020	1511457265578685440	DC	4919 (41)	0.341 (0.016)	7.561 (0.028)	H/He=0	···	−3.87	2.81
J1404+5243	1512865022715710464	DA	8138 (61)	0.645 (0.013)	8.082 (0.015)	He/H=0	···	−3.24	1.20
J1405+4300	1499290379143445760	DC	6361 (49)	0.585 (0.017)	8.019 (0.019)	log H/He=−3.2	···	−3.65	2.12
J1405+6648	1671668067321674368	DC	3852 (46)	0.395 (0.016)	7.672 (0.025)	He/H=0	···	−4.34	6.59
J1406+0849	3722502856146928256	DA	6463 (47)	0.796 (0.033)	8.323 (0.037)	He/H=0	···	−3.79	3.89
J1406+1608	1231446224176456064	DA	6694 (32)	0.605 (0.009)	8.023 (0.011)	He/H=0	···	−3.55	1.82
J1406+1812	1245468295966061952	DA	7243 (40)	0.848 (0.008)	8.397 (0.01)	He/H=0	···	−3.64	3.25
J1406+2003	1246230047071154944	DC	7368 (55)	0.547 (0.018)	7.953 (0.023)	log H/He=−3.6	···	−3.35	1.34
J1406+3130	1454347089739329152	DC	4798 (29)	0.540 (0.014)	7.936 (0.017)	He/H=0	···	−4.09	6.05
J1406+3401	1481854770426696704	DQ+DA	6849 (36)	0.272 (0.009)	7.353 (0.019)	H/He=0	log C/He=−6.68	−3.18	0.81
J1407+1133	1226206806457202432	DA	5381 (21)	0.627 (0.013)	8.071 (0.015)	He/H=0	···	−3.96	4.44
J1407+5509	1609392862209121664	DA	6747 (64)	1.261 (0.008)	9.169 (0.019)	He/H=0	···	−4.36	4.18
J1407−0626	3643555726544985088	DA	8531 (37)	0.738 (0.006)	8.227 (0.006)	He/H=0	···	−3.24	1.33
J1408−2649	6270584739570554880	DC	6608 (39)	0.663 (0.01)	8.142 (0.011)	log H/He=−3.2	···	−3.65	2.43
J1409+1511	1230575131794474752	DZ	6630 (36)	0.688 (0.021)	8.181 (0.023)	log H/He=−2.0	log Ca/He=−10.49	−3.67	2.67
J1409+3828	1485197354494658176	DA	7343 (56)	0.580 (0.018)	7.979 (0.021)	He/H=0	···	−3.36	1.34

Tableau A.2 *suite page suivante*

Tableau A.2 *(suite)*

Name	Gaia DR2/EDR3*	Sp Type	$T_{\rm eff}$ (K)	$M/M_{\odot}$	$\log g$	Composition	Métaux	$\log L/L_{\odot}$	τ (Gyr)
J1409+4216	1498447607777405312	DA	9862 (39)	0.623 (0.005)	8.040 (0.005)	He/H=0	···	−2.88	0.69
J1410+0245	3667514634669861120	DAZ	5636 (10)	0.568 (0.004)	7.995 (0.005)	He/H=0	log Ca/H=−9.29	−3.84	3.61
J1411+1630	1232925891949581824	DA	8773 (48)	0.505 (0.012)	7.837 (0.016)	He/H=0	···	−2.97	0.72
J1411+2206	1253353890280943104	DC	6608 (34)	0.607 (0.01)	8.055 (0.011)	log H/He=−3.2	···	−3.60	2.03
J1412+1129	1226246251436497152	DA	7222 (57)	0.711 (0.022)	8.215 (0.024)	log H/He=−2.0	···	−3.54	2.17
J1412+1532	1232045934759720192	DA*	4982 (24)	0.664 (0.012)	8.134 (0.013)	He/H=0	···	−4.13	7.67
J1412+1815	1233764059112037632	DA	6215 (61)	0.742 (0.035)	8.241 (0.038)	He/H=0	···	−3.80	3.75
J1412+4216	1498271406743008640	DAH :*	7180 (40)	0.620 (0.017)	8.046 (0.019)	He/H=0	···	−3.44	1.57
J1412−1842	6296317052576778240	DC	5428 (19)	0.513 (0.007)	7.903 (0.008)	H/He=0	···	−3.86	3.52
J1413+1205	1226307755368045824	DA	6771 (38)	0.727 (0.021)	8.217 (0.023)	He/H=0	···	−3.64	2.63
J1413+3256	1478514389681253248	DA	10135 (41)	0.586 (0.008)	7.975 (0.01)	He/H=0	···	−2.79	0.59
J1413−0014	3659914737283635840	DA	10060 (59)	1.025 (0.012)	8.669 (0.017)	He/H=0	···	−3.25	2.13
J1413−0026	3647875570291353344	DA	9513 (47)	0.754 (0.011)	8.248 (0.011)	He/H=0	···	−3.06	1.03
J1414+2237	1253770497813126144	DA*	8102 (51)	0.577 (0.011)	8.001 (0.012)	log H/He=−3.5	···	−3.21	1.13
J1414+2906	1260898494256935040	DA	7287 (40)	0.687 (0.011)	8.152 (0.012)	He/H=0	···	−3.47	1.78
J1414+4336	1504443450842002176	DA	6398 (26)	0.600 (0.008)	8.016 (0.009)	He/H=0	···	−3.62	2.03
J1415+4337	1504453896202493568	DA	6885 (33)	0.646 (0.01)	8.089 (0.011)	He/H=0	···	−3.53	1.88
J1416+2822	1260609838099260928	DC	6453 (74)	0.596 (0.032)	8.038 (0.037)	log H/He=−3.2	···	−3.63	2.10
J1416−0902	3638957019161984640	DA+DA	9370 (31)	0.267 (0.003)	7.235 (0.007)	He/H=0	···	−2.53	0.30
J1417+0346	3667872216467035776	DA	6176 (31)	0.622 (0.017)	8.055 (0.019)	He/H=0	···	−3.71	2.38
J1417+1805	1233598174590839296	DAH	9090 (76)	0.928 (0.012)	8.515 (0.014)	He/H=0	···	−3.32	2.12
J1417+4941	1508482266288333952	DC	9616 (76)	0.582 (0.012)	8.003 (0.015)	log H/He=−4.4	···	−2.91	0.73
J1417+5735	1611509353373118336	DAH	5697 (88)	0.758 (0.047)	8.269 (0.051)	He/H=0	···	−3.97	5.14
J1417−0012	3653854572788715520	DC	7196 (42)	0.585 (0.013)	8.017 (0.016)	log H/He=−3.4	···	−3.43	1.56
J1418+0408	3669400430255790336	DA	7940 (44)	0.897 (0.013)	8.470 (0.015)	He/H=0	···	−3.52	2.88
J1418+1452	1228760220348642304	DA	7480 (52)	0.331 (0.032)	7.462 (0.062)	He/H=0	···	−3.05	0.71
J1419+1103	1225189552042779904	DC	7935 (49)	0.615 (0.012)	8.063 (0.014)	log H/He=−3.8	···	−3.28	1.30
J1419+2543	1258934014870979712	DAH	9040 (49)	0.805 (0.011)	8.327 (0.013)	He/H=0	···	−3.20	1.35
J1420+0351	3669328034286134016	DC	5921 (48)	0.661 (0.03)	8.143 (0.034)	H/He=0	···	−3.84	3.92
J1420+4656	1506805751574450048	DA	9860 (44)	0.335 (0.005)	7.442 (0.009)	He/H=0	···	−2.55	0.33
J1420+5322	1608061254844374784	DA	7606 (39)	0.464 (0.007)	7.765 (0.01)	He/H=0	···	−3.18	0.94
J1420−0905	6329136310728635776	DA	7726 (16)	0.371 (0.005)	7.562 (0.007)	He/H=0	···	−3.05	0.73
J1421+0709	3673479966286848640	DC	5980 (53)	0.551 (0.038)	7.966 (0.046)	log H/He=−3.0	···	−3.73	2.43
J1421+0930	1176784239825009280	DA	9525 (51)	0.704 (0.013)	8.170 (0.014)	He/H=0	···	−3.01	0.91

Tableau A.2 *suite page suivante*

Tableau A.2 *(suite)*

Name	Gaia DR2/EDR3*	Sp Type	$T_{\rm eff}$ (K)	$M/M_{\odot}$	$\log g$	Composition	Métaux	$\log L/L_{\odot}$	τ (Gyr)
J1421+1436	1228599279334490496	DA	5852 (45)	0.480 (0.039)	7.810 (0.052)	He/H=0	···	−3.67	1.89
J1421+2147	1252685559010039424	DA	8712 (58)	0.637 (0.01)	8.067 (0.012)	He/H=0	···	−3.11	0.98
J1421+4226	1492278518615941504	DA	9305 (95)	1.161 (0.007)	8.922 (0.012)	He/H=0	···	−3.59	3.06
J1421−0046	3653562656746977792	DA	8619 (50)	0.554 (0.013)	7.927 (0.016)	He/H=0	···	−3.05	0.84
J1422+0459	3669573053580577536	DC	4753 (27)	0.516 (0.02)	7.895 (0.024)	He/H=0	···	−4.08	5.88
J1422+3056	1285142833024133760	DA	9097 (35)	0.838 (0.007)	8.378 (0.008)	He/H=0	···	−3.23	1.46
J1423+3037	1284932139108595712	DA	5264 (16)	0.200 (0.0)	7.057 (0.009)	He/H=0	···	−3.48	1.08
J1423−1820	6284524274971664000	DA	7355 (63)	0.856 (0.024)	8.409 (0.027)	He/H=0	···	−3.62	3.19
J1424+0319	3668476222012308480	DA	7157 (40)	0.747 (0.015)	8.246 (0.017)	He/H=0	···	−3.56	2.35
J1424+1743	1238591671072637184	DC	5974 (75)	0.669 (0.046)	8.155 (0.051)	H/He=0	···	−3.83	3.85
J1424+2028	1240475993483896832	DA	8139 (72)	0.630 (0.022)	8.058 (0.025)	He/H=0	···	−3.22	1.16
J1424+2546	1256240383181740928	DA	6610 (36)	0.295 (0.007)	7.371 (0.014)	He/H=0	···	−3.23	0.88
J1424+4405	1492836834300292992	DC	6761 (41)	0.471 (0.009)	7.817 (0.013)	log H/He=−3.4	···	−3.43	1.40
J1424+6246	1666805889078252928	DA	5010 (20)	0.521 (0.009)	7.900 (0.011)	He/H=0	···	−3.99	4.48
J1425−0050	3652865390281317120	DZ	7054 (34)	0.679 (0.015)	8.166 (0.017)	log H/He=−4.0	log Ca/He=−10.93	−3.55	2.08
J1426+0937	1176378520034381952	DC	4731 (29)	0.305 (0.025)	7.475 (0.047)	H/He=0	···	−3.90	2.72
J1426+4455	1494432053873688448	DC :	6215 (51)	0.561 (0.019)	7.980 (0.022)	log H/He=−3.0	···	−3.67	2.16
J1426+4921	1507571286545131648	DC	6392 (16)	0.680 (0.004)	8.170 (0.005)	log H/He=−3.2	···	−3.72	2.96
J1427+0532	3669936102871625600	DC	6500 (22)	0.546 (0.006)	7.954 (0.008)	log H/He=−3.2	···	−3.57	1.84
J1427+4126	1491559506730816384	DC	6216 (61)	0.770 (0.032)	8.306 (0.034)	log H/He=−3.0	···	−3.85	4.16
J1427+4536	1494485758144731520	DC	7193 (30)	0.623 (0.007)	8.079 (0.007)	log H/He=−3.4	···	−3.46	1.69
J1427+6110	1666378698746614528	DQ	6441 (15)	0.556 (0.005)	7.971 (0.006)	H/He=0	log C/He=−6.62	−3.60	1.93
J1428+4403	1494157691363079168	DZ	6622 (17)	0.625 (0.005)	8.083 (0.005)	log H/He=−4.0	log Ca/He=−9.40	−3.61	2.12
J1428+4531	1494564162771398016	DC	5685 (77)	0.572 (0.029)	8.003 (0.034)	H/He=0	···	−3.83	3.49
J1429+0925	1176312965948448512	DC	6420 (42)	0.599 (0.018)	8.042 (0.021)	log H/He=−3.2	···	−3.64	2.15
J1430+0438	3669065354086975872	DA	7980 (37)	0.644 (0.01)	8.081 (0.011)	He/H=0	···	−3.27	1.26
J1430+2811	1280674894509973760	DAH	9050 (73)	0.939 (0.012)	8.533 (0.014)	He/H=0	···	−3.34	2.23
J1430−2403	6272326022391660928	DC	4857 (13)	0.519 (0.008)	7.899 (0.009)	He/H=0	···	−4.04	5.45
J1431+2921	1284194603029215104	DA	6813 (38)	0.815 (0.012)	8.349 (0.013)	He/H=0	···	−3.71	3.53
J1431+4848	1603370081109395200	DC	5915 (38)	0.522 (0.026)	7.916 (0.031)	H/He=0	···	−3.72	2.35
J1433+1026	1176494381072110848	DAH	6904 (33)	0.829 (0.012)	8.371 (0.014)	He/H=0	···	−3.70	3.54
J1433+1326	1179764607826002688	DA	10167 (50)	0.810 (0.006)	8.332 (0.008)	He/H=0	···	−3.00	0.99
J1433+1907	1239213243034520192	DA	5049 (29)	0.521 (0.016)	7.899 (0.019)	He/H=0	···	−3.98	4.21
J1433+3751	1487362258530962944	DA	10320 (69)	0.741 (0.012)	8.225 (0.014)	He/H=0	···	−2.91	0.80

Tableau A.2 *suite page suivante*

Tableau A.2 *(suite)*

Name	Gaia DR2/EDR3*	Sp Type	$T_{\rm eff}$ (K)	$M/M_{\odot}$	$\log g$	Composition	Métaux	$\log L/L_{\odot}$	τ (Gyr)
J1435+5052	1604147165248626048	DA	9325 (43)	0.610 (0.009)	8.020 (0.01)	He/H=0	···	−2.96	0.78
J1436+0537	1171041215714699904	DC	4235 (32)	0.501 (0.028)	7.872 (0.034)	He/H=0	···	−4.27	7.58
J1436+2107	1241188721832696704	DC	8197 (50)	0.689 (0.01)	8.179 (0.012)	log H/He=−3.8	···	−3.29	1.41
J1436+4332	1493367245581725184	DC	4703 (17)	0.538 (0.008)	7.933 (0.01)	He/H=0	···	−4.12	6.45
J1436+4753	1591250718488330112	DA	8208 (64)	0.838 (0.011)	8.380 (0.013)	He/H=0	···	−3.41	2.12
J1436+5635	1610657197502002048	DA	6768 (53)	0.558 (0.017)	7.943 (0.022)	He/H=0	···	−3.48	1.57
J1437+2003	1240776435036602368	DC	7365 (39)	0.602 (0.015)	8.045 (0.018)	log H/He=−3.6	···	−3.40	1.52
J1437+4151	1492944375984949504	DC	5123 (45)	0.617 (0.009)	8.077 (0.014)	log H/He=−1.69	···	−4.06	6.04
J1440+0112	3654870693331906304	DC*	4234 (23)	0.577 (0.022)	8.000 (0.025)	He/H=0	···	−4.34	8.81
J1440+0310	3656509794586217984	DA*	6036 (17)	0.246 (0.006)	7.225 (0.014)	He/H=0	···	−3.32	0.94
J1440+0626	1171211743096194560	DA	6962 (64)	1.132 (0.011)	8.866 (0.018)	He/H=0	···	−4.05	4.80
J1440+0807	1172780578685760512	DA	5599 (18)	0.630 (0.01)	8.072 (0.011)	He/H=0	···	−3.89	3.54
J1440+0958	1174728432253334784	DQ	8209 (26)	0.569 (0.011)	7.987 (0.014)	H/He=0	log C/He=−5.43	−3.18	1.07
J1440+1318	1179626958418884864	DC	4869 (25)	0.411 (0.014)	7.715 (0.02)	H/He=0	···	−3.96	3.67
J1440−0232	3648790157806712448	DZ	6704 (55)	0.530 (0.024)	7.925 (0.029)	log H/He=−3.0	log Ca/He=−10.49	−3.50	1.64
J1441+0518	1159061967810978432	DA	6565 (43)	0.707 (0.027)	8.186 (0.03)	He/H=0	···	−3.67	2.70
J1441+0831	1172831907840206848	DZ	7126 (51)	0.591 (0.035)	8.027 (0.042)	log H/He=−4.0	log Ca/He=−10.79	−3.45	1.62
J1441+4511	1493934284343845504	DA	9309 (68)	0.556 (0.01)	7.927 (0.014)	He/H=0	···	−2.91	0.69
J1441+5322	1605951944865784960	DC	6413 (69)	0.654 (0.025)	8.129 (0.027)	log H/He=−3.2	···	−3.69	2.64
J1441+5639	1607738921843325440	DA	7347 (69)	0.807 (0.017)	8.335 (0.019)	He/H=0	···	−3.57	2.73
J1441+5816	1616879612977156352	DA	6586 (33)	0.618 (0.01)	8.045 (0.011)	He/H=0	···	−3.59	1.96
J1441+6228	1618920714579089280	DA	7149 (39)	0.588 (0.013)	7.993 (0.015)	He/H=0	···	−3.41	1.47
J1442+0027	3651747667992161920	DAH :*	8266 (75)	0.812 (0.02)	8.341 (0.022)	He/H=0	···	−3.37	1.83
J1442+0635	1171581179003421312	DZ :	6474 (47)	0.659 (0.015)	8.112 (0.017)	He/H=0	···	−3.65	2.31
J1442+4013	1488064949540111104	DQP	5704 (23)	0.653 (0.017)	8.132 (0.019)	H/He=0	log C/He=−6.60	−3.90	4.57
J1442+5546	1607546129351189888	DA	5348 (43)	0.703 (0.019)	8.190 (0.021)	He/H=0	···	−4.04	6.04
J1442−1947	6281523986913711872	DC :	4919 (21)	0.555 (0.011)	7.978 (0.014)	H/He=0	···	−4.07	5.86
J1443−1437	6310804634396281984	DA	6791 (42)	0.758 (0.008)	8.263 (0.009)	He/H=0	···	−3.66	2.97
J1444+1048	1175242896321238400	DC	5995 (39)	0.530 (0.018)	7.929 (0.022)	log H/He=−3.0	···	−3.70	2.27
J1444+1848	1237419351158798336	DA	7062 (39)	0.589 (0.019)	7.995 (0.022)	He/H=0	···	−3.44	1.52
J1444+3759	1486801267085903488	DC	5774 (65)	0.616 (0.032)	8.073 (0.036)	H/He=0	···	−3.85	3.84
J1444+4717	1590192369827025152	DA	9221 (43)	0.476 (0.007)	7.778 (0.009)	He/H=0	···	−2.85	0.59
J1444−0052	3651305423799211008	DA	6961 (43)	0.658 (0.034)	8.109 (0.038)	He/H=0	···	−3.53	1.88
J1445+2921	1282448170543051520	DA	5369 (15)	0.553 (0.007)	7.950 (0.007)	He/H=0	···	−3.89	3.10

Tableau A.2 *suite page suivante*

Tableau A.2 *(suite)*

Name	Gaia DR2/EDR3*	Sp Type	$T_{\rm eff}$ (K)	$M/M_{\odot}$	$\log g$	Composition	Métaux	$\log L/L_{\odot}$	τ (Gyr)
J1445−0208	3648744214542134912	DZ	6476 (57)	0.660 (0.022)	8.140 (0.024)	log H/He=−3.0	log Ca/He=−10.27	−3.68	2.61
J1446+2130	1238445745263425536	DA	5816 (28)	0.588 (0.018)	8.002 (0.021)	He/H=0	···	−3.78	2.53
J1446+2512	1267289165075531008	DC	6052 (53)	0.575 (0.027)	8.005 (0.032)	H/He=0	···	−3.73	2.50
J1446+2825	1281584774741482880	DC	7758 (57)	0.682 (0.019)	8.170 (0.021)	log H/He=−3.8	···	−3.38	1.58
J1447+2014	1238026522095817728	DA	6070 (52)	0.711 (0.033)	8.196 (0.037)	He/H=0	···	−3.82	3.64
J1447+5427	1606475479904001792	DC	4839 (37)	0.265 (0.015)	7.340 (0.031)	He/H=0	···	−3.79	2.13
J1447−1742	6282457918962299776	DC	4794 (17)	0.796 (0.007)	8.348 (0.007)	H/He=0	···	−4.33	7.91
J1447−3035	6217739938701063808	DA	6944 (45)	0.602 (0.01)	8.017 (0.011)	He/H=0	···	−3.48	1.64
J1448+0157	3652390092020688128	DA	6984 (35)	0.608 (0.014)	8.027 (0.017)	He/H=0	···	−3.47	1.64
J1448+1047	1175204104176381696	DZ	6165 (35)	0.641 (0.025)	8.110 (0.027)	log H/He=−4.0	log Ca/He=−9.53	−3.75	2.96
J1448+1456	1186165582270482688	DA	6760 (62)	0.550 (0.022)	7.929 (0.028)	He/H=0	···	−3.48	1.54
J1448−0047	3650615686411758080	DQ	6936 (40)	0.561 (0.023)	7.977 (0.027)	H/He=0	log C/He=−6.38	−3.47	1.62
J1448−0232	6338811188419479040	DA	9340 (37)	0.609 (0.01)	8.019 (0.011)	He/H=0	···	−2.96	0.77
J1449+1030	1174996090320432000	DA	7501 (51)	0.879 (0.022)	8.444 (0.025)	He/H=0	···	−3.61	3.22
J1449+2054	1238352149340737536	DAH :	5717 (48)	0.758 (0.027)	8.270 (0.029)	He/H=0	···	−3.97	5.08
J1450+0742	1173230210222240640	DA	8090 (71)	0.767 (0.019)	8.272 (0.02)	He/H=0	···	−3.36	1.67
J1450+2403	1265985590961480192	DC*	6822 (47)	0.690 (0.016)	8.184 (0.018)	log H/He=−3.4	···	−3.62	2.44
J1450+5753	1613862480054872320	DA	7047 (50)	0.686 (0.012)	8.151 (0.014)	He/H=0	···	−3.53	1.94
J1450−1454	6310405202436481024	DA :*	7219 (20)	0.520 (0.005)	7.874 (0.006)	He/H=0	···	−3.33	1.22
J1450−1914	6281218357040987136	DA	7219 (17)	0.245 (0.002)	7.196 (0.005)	He/H=0	···	−2.98	0.57
J1451+0243	1154456216681249536	DA	8302 (52)	0.933 (0.017)	8.525 (0.021)	He/H=0	···	−3.48	2.79
J1451+4221	1489418418289775616	DA	9413 (31)	0.557 (0.005)	7.929 (0.006)	He/H=0	···	−2.90	0.67
J1452+4049	1488715482466110080	DC	4811 (56)	0.541 (0.032)	7.937 (0.038)	He/H=0	···	−4.08	6.01
J1452+4522	1586838374030594048	DC	5521 (47)	0.685 (0.031)	8.181 (0.034)	H/He=0	···	−3.98	5.53
J1452+4746	1590462948470580480	DA	6191 (62)	0.749 (0.03)	8.252 (0.033)	He/H=0	···	−3.82	3.87
J1452−0011	3651028381228835456	DA	5240 (19)	0.591 (0.012)	8.014 (0.014)	He/H=0	···	−3.97	4.53
J1452−0051	3650426742210702976	DC :	5023 (43)	0.468 (0.025)	7.826 (0.032)	H/He=0	···	−3.96	4.31
J1453+0925	1174070610767977728	DA	10330 (66)	1.035 (0.014)	8.686 (0.019)	He/H=0	···	−3.22	2.04
J1453+3244	1289485349902909440	DC	5091 (23)	0.616 (0.015)	8.058 (0.017)	He/H=0	···	−4.05	6.14
J1453+4225	1489504004102020864	DA	5832 (35)	0.717 (0.016)	8.206 (0.017)	He/H=0	···	−3.89	4.23
J1454+0603	1160054281350128384	DA	6668 (34)	0.930 (0.011)	8.524 (0.014)	He/H=0	···	−3.87	4.64
J1454+1253	1181607110141081984	DA	5677 (36)	0.621 (0.037)	8.057 (0.042)	He/H=0	···	−3.85	3.17
J1454+4406	1586427298416103296	DA	7690 (44)	0.584 (0.012)	7.983 (0.014)	He/H=0	···	−3.28	1.20
J1454−0110	3650730589671206528	DC	4606 (40)	0.613 (0.042)	8.056 (0.048)	He/H=0	···	−4.22	8.39

Tableau A.2 *suite page suivante*

Tableau A.2 *(suite)*

Name	Gaia DR2/EDR3*	Sp Type	$T_{\rm eff}$ (K)	$M/M_{\odot}$	$\log g$	Composition	Métaux	$\log L/L_{\odot}$	τ (Gyr)
J1455+0141	1154089117236952960	DC	6300 (32)	0.555 (0.017)	7.970 (0.021)	log H/He=−3.2	···	−3.64	2.05
J1455+3725	1295170344710806400	DA	7915 (50)	0.630 (0.011)	8.060 (0.012)	He/H=0	···	−3.27	1.25
J1457+2107	1261421999231535616	DQ	5909 (22)	0.557 (0.023)	7.975 (0.028)	H/He=0	log C/He=−6.67	−3.75	2.61
J1457+2827	1269774649765271552	DA	9281 (60)	0.640 (0.013)	8.070 (0.015)	He/H=0	···	−3.00	0.84
J1457+2952	1282030970304135296	DA	5149 (35)	0.481 (0.016)	7.826 (0.022)	He/H=0	···	−3.90	3.04
J1457+3331	1289812355829447040	DC	8995 (62)	0.572 (0.012)	7.989 (0.015)	log H/He=−4.2	···	−3.02	0.85
J1458+0605	1160021841461912448	DA	6777 (44)	0.789 (0.049)	8.310 (0.054)	He/H=0	···	−3.70	3.32
J1458+1146	1181245508254835584	DC	4742 (16)	0.199 (0.011)	7.041 (0.033)	He/H=0	···	−3.65	2.44
J1458+2937	1281989124439286912	DAZ	7381 (19)	0.562 (0.004)	7.978 (0.005)	He/H=0	log Ca/H=−9.31	−3.36	1.38
J1458+3416	1290050262657404544	DC*	6618 (55)	0.651 (0.018)	8.124 (0.02)	log H/He=−3.2	···	−3.63	2.31
J1459+0851	1161820298887863424	DA	5433 (34)	0.695 (0.027)	8.176 (0.029)	He/H=0	···	−4.00	5.38
J1500+0512	1159705388271330176	DA	5969 (53)	0.649 (0.052)	8.099 (0.059)	He/H=0	···	−3.79	2.96
J1500+3600	1294793345366747776	DC :	4864 (62)	0.415 (0.031)	7.704 (0.045)	He/H=0	···	−3.94	3.37
J1501+0719	1160623343042019968	DA	6844 (66)	0.800 (0.045)	8.326 (0.051)	He/H=0	···	−3.69	3.33
J1501+2100	1261253842671908096	DQ	5794 (12)	0.248 (0.012)	7.294 (0.028)	H/He=0	log C/He=−6.42	−3.46	1.19
J1501+6138	1619166249269416832	DA	5692 (22)	0.218 (0.004)	7.136 (0.011)	He/H=0	···	−3.38	0.97
J1502+0920	1167866620703225984	DA	6826 (53)	0.839 (0.027)	8.385 (0.03)	He/H=0	···	−3.73	3.74
J1502+4933	1592242645479324288	DZ	6517 (43)	0.637 (0.018)	8.103 (0.02)	log H/He=−4.0	log Ca/He=−9.81	−3.65	2.33
J1503+2956	1275981324189764608	DC	6981 (37)	0.384 (0.01)	7.640 (0.015)	log H/He=−3.4	···	−3.29	1.04
J1504+0750	1160759923002231936	DA	6633 (42)	0.679 (0.028)	8.143 (0.031)	He/H=0	···	−3.63	2.32
J1504+2302	1262123144052263040	DC	6105 (40)	0.602 (0.021)	8.048 (0.024)	log H/He=−3.0	···	−3.73	2.63
J1505+3259	1289020673097509760	DA	8960 (41)	0.453 (0.007)	7.733 (0.01)	He/H=0	···	−2.88	0.61
J1505−0714	6332763530870415488	DAH	6889 (14)	0.647 (0.004)	8.090 (0.003)	He/H=0	···	−3.53	1.88
J1506+0151	1153544794556784384	DC	5977 (52)	0.596 (0.028)	8.040 (0.032)	H/He=0	···	−3.77	2.90
J1506+0638	1160300056558791168	DA	9500 (54)	0.335 (0.007)	7.447 (0.014)	He/H=0	···	−2.62	0.37
J1506+2934	1275760219272654080	DA	8394 (52)	0.536 (0.012)	7.896 (0.015)	He/H=0	···	−3.08	0.86
J1506+4152	1392973720770987392	DZ	9162 (76)	0.620 (0.014)	8.069 (0.015)	log H/He=−5.0	log Ca/He=−10.76	−3.04	0.91
J1507+3218	1288658006059681408	DA	8207 (106)	1.096 (0.02)	8.797 (0.03)	He/H=0	···	−3.71	3.67
J1508+0135	4420124124769394176	DA*	8093 (61)	0.808 (0.018)	8.359 (0.02)	log H/He=−3.0	···	−3.43	2.13
J1508+1826	1211862818279517824	DC	5138 (32)	0.598 (0.027)	8.028 (0.031)	He/H=0	···	−4.01	5.41
J1509+5020	1592629707931918720	DC	6230 (47)	0.534 (0.018)	7.934 (0.022)	log H/He=−3.0	···	−3.63	2.02
J1509+6332	1620030637207462912	DA	10495 (44)	0.597 (0.005)	7.993 (0.006)	He/H=0	···	−2.74	0.55
J1510+0627	1157317008497672320	DC	5842 (63)	0.588 (0.033)	8.027 (0.04)	log H/He=−3.0	···	−3.80	3.19
J1510+1248	1182318120502368256	DA	6168 (45)	0.682 (0.045)	8.150 (0.051)	He/H=0	···	−3.76	3.04

Tableau A.2 *suite page suivante*

Tableau A.2 *(suite)*

Name	Gaia DR2/EDR3*	Sp Type	$T_{\rm eff}$ (K)	$M/M_{\odot}$	$\log g$	Composition	Métaux	$\log L/L_{\odot}$	τ (Gyr)
J1510+1453	1183956427187401344	DA	7825 (35)	0.891 (0.008)	8.462 (0.009)	He/H=0	···	−3.54	2.96
J1510−1045	6318882711964895872	DA	10023 (41)	0.371 (0.004)	7.538 (0.007)	He/H=0	···	−2.57	0.36
J1511+4048	1392065975139109504	DA	8300 (17)	0.294 (0.002)	7.344 (0.005)	He/H=0	···	−2.81	0.48
J1511+5624	1600882264252963072	DA	9100 (40)	0.587 (0.007)	7.982 (0.008)	He/H=0	···	−2.98	0.79
J1512−0946	6319467136754514176	DA	9647 (36)	0.542 (0.006)	7.899 (0.007)	He/H=0	···	−2.83	0.61
J1513+2359	1263732043096088320	DC	4388 (57)	0.494 (0.071)	7.859 (0.091)	He/H=0	···	−4.20	6.98
J1513+3022	1275492999287723392	DA	6535 (34)	0.926 (0.01)	8.518 (0.011)	He/H=0	···	−3.90	4.82
J1514+0157	4421694158655153664	DA	9429 (52)	0.767 (0.01)	8.269 (0.011)	He/H=0	···	−3.09	1.10
J1514+1941	1212425463290645504	DA	9291 (61)	0.638 (0.013)	8.067 (0.014)	He/H=0	···	−3.00	0.83
J1515+3707	1292166062330701056	DC	6045 (62)	0.628 (0.027)	8.090 (0.03)	H/He=0	···	−3.77	3.11
J1515+6642	1645204475617697536	DA	9983 (46)	0.740 (0.006)	8.225 (0.006)	He/H=0	···	−2.97	0.88
J1515+8230	1722236328978172928	DZH	4532 (26)	0.512 (0.014)	7.905 (0.018)	He/H=0	log Ca/H=−8.50	−4.18	6.07
J1516+0647	1163166719594895872	DA	6645 (53)	0.885 (0.02)	8.455 (0.022)	He/H=0	···	−3.83	4.39
J1516+2316	1215408610135114112	DA	6900 (35)	0.350 (0.009)	7.519 (0.018)	He/H=0	···	−3.23	0.93
J1516+2803	1271649969930799872	DAH	8073 (40)	0.682 (0.007)	8.141 (0.009)	He/H=0	···	−3.29	1.34
J1517+2256	1215384313505335424	DQ	7426 (25)	0.557 (0.01)	7.969 (0.013)	H/He=0	log C/He=−6.08	−3.35	1.35
J1518+0506	1156006287558141056	DZ	5192 (30)	0.678 (0.033)	8.171 (0.037)	log H/He=−3.0	log Ca/He=−9.29	−4.09	6.43
J1519+1239	1170279945646967424	DA	9147 (44)	0.570 (0.014)	7.952 (0.018)	He/H=0	···	−2.96	0.75
J1519+3214	1278042010837800192	DA	9107 (89)	0.982 (0.016)	8.600 (0.019)	He/H=0	···	−3.38	2.47
J1520+3355	1278756555956826624	DA	6311 (51)	0.845 (0.02)	8.396 (0.021)	He/H=0	···	−3.88	4.60
J1520+3903	1388493176528426752	DA	8046 (35)	0.284 (0.004)	7.316 (0.01)	He/H=0	···	−2.85	0.51
J1520−0238	4414809875835433216	DA	10305 (59)	0.639 (0.013)	8.063 (0.014)	He/H=0	···	−2.81	0.64
J1521+0748	1163714413825307776	DC	4722 (59)	0.443 (0.06)	7.761 (0.083)	He/H=0	···	−4.03	4.42
J1521+1358	1170894503927889024	DC	9287 (51)	0.457 (0.01)	7.778 (0.014)	log H/He=−4.4	···	−2.85	0.59
J1522+2535	1270140821499608832	DC	9142 (64)	0.568 (0.013)	7.981 (0.015)	log H/He=−4.2	···	−2.99	0.81
J1522−0206	4415230812694612864	DA	7359 (65)	0.753 (0.029)	8.254 (0.032)	He/H=0	···	−3.52	2.18
J1523+1607	1207403993686544256	DA	6305 (24)	0.579 (0.014)	7.983 (0.016)	He/H=0	···	−3.63	2.01
J1525+5629	1602197696772907648	DA*	5532 (14)	0.506 (0.005)	7.863 (0.006)	He/H=0	···	−3.79	2.37
J1525−0421	4401558183740868480	DA	9977 (63)	0.579 (0.01)	7.963 (0.012)	He/H=0	···	−2.81	0.61
J1526+2936	1273685372108354176	DA	5144 (8)	0.568 (0.004)	7.977 (0.004)	He/H=0	···	−3.98	4.66
J1527+2442	1222024990079978368	DA	8932 (58)	0.922 (0.01)	8.507 (0.012)	He/H=0	···	−3.35	2.20
J1528+3254	1277756687570196096	DC	4744 (36)	0.428 (0.017)	7.749 (0.024)	H/He=0	···	−4.02	4.30
J1529+1304	1193808772927091712	DA	9186 (45)	0.644 (0.009)	8.107 (0.01)	log H/He=−4.0	···	−3.05	0.95
J1529−0038	4416948833973175168	DA	7039 (52)	0.991 (0.02)	8.620 (0.024)	He/H=0	···	−3.84	4.48

Tableau A.2 *suite page suivante*

Tableau A.2 *(suite)*

Name	Gaia DR2/EDR3*	Sp Type	$T_{\rm eff}$ (K)	$M/M_{\odot}$	$\log g$	Composition	Métaux	$\log L/L_{\odot}$	τ (Gyr)
J1530+0235	4421098773108860928	DA	7716 (35)	0.581 (0.008)	7.979 (0.009)	He/H=0	···	−3.27	1.19
J1530+0630	1162536355835288320	DC	7195 (53)	0.897 (0.02)	8.494 (0.022)	log H/He=−3.4	···	−3.72	3.50
J1530+4650	1395759333479862016	DA	6668 (49)	0.541 (0.017)	7.915 (0.021)	He/H=0	···	−3.49	1.57
J1531+2514	1222254066452610176	DC	6132 (59)	0.713 (0.018)	8.222 (0.019)	log H/He=−3.0	···	−3.83	3.87
J1531+4240	1391331222197901696	DZ	7054 (49)	0.589 (0.014)	8.024 (0.016)	log H/He=−3.0	log Ca/He=−9.66	−3.47	1.65
J1531+4421	1394479501945576064	DC*	4526 (86)	0.695 (0.035)	8.199 (0.053)	log H/He=−2.46	···	−4.34	7.97
J1532+1356	1193974077628437760	DA+DQ	7761 (16)	0.263 (0.006)	7.311 (0.014)	H/He=0	log C/He=−5.92	−2.94	0.56
J1533+0717	1164185283975493120	DA	10287 (63)	0.558 (0.009)	7.925 (0.013)	He/H=0	···	−2.74	0.53
J1533+2109	1211355290583415168	DA	6034 (56)	0.515 (0.024)	7.873 (0.031)	He/H=0	···	−3.65	1.91
J1534+0037	4417527967363383680	DA	8418 (62)	0.654 (0.021)	8.096 (0.024)	He/H=0	···	−3.19	1.12
J1534+0218	4424031479858305408	DA	8449 (32)	0.927 (0.005)	8.515 (0.005)	He/H=0	···	−3.45	2.62
J1534+0711	4430709068108076544	DA	5246 (20)	0.618 (0.016)	8.058 (0.018)	He/H=0	···	−4.00	5.10
J1534+1010	1165926910393567872	DA	7130 (38)	0.556 (0.013)	7.938 (0.016)	He/H=0	···	−3.39	1.37
J1534+1010	1165926910393568384	DA	6503 (38)	0.556 (0.018)	7.942 (0.022)	He/H=0	···	−3.55	1.74
J1534+4146	1390295486540598656	DQZ	7871 (38)	0.560 (0.007)	7.972 (0.009)	H/He=0	log C/He=−5.89	−3.25	1.17
J1534+4649	1401010605309570816	DC	4335 (18)	0.489 (0.008)	7.850 (0.01)	He/H=0	···	−4.22	7.06
J1534+5624	1601489813146914176	DC	5093 (34)	0.587 (0.046)	8.011 (0.054)	He/H=0	···	−4.02	5.49
J1535+1115	1166330259362301440	DC	10058 (28)	0.598 (0.005)	8.028 (0.006)	log H/He=−4.6	···	−2.85	0.67
J1535+1247	1193520666521113344	DZP	5969 (10)	0.677 (0.003)	8.167 (0.003)	log H/He=−3.0	log Ca/He=−8.48	−3.84	3.94
J1535+1645	1197139189352207232	DC	5114 (33)	0.593 (0.024)	8.020 (0.028)	He/H=0	···	−4.02	5.46
J1535+2125	1211378350265079808	DA	6341 (11)	0.621 (0.006)	8.052 (0.006)	He/H=0	···	−3.66	2.19
J1536+1717	1197240000824171648	DA	5740 (29)	0.591 (0.026)	8.007 (0.03)	He/H=0	···	−3.81	2.66
J1536+3626	1374676889508967680	DC	6358 (48)	0.551 (0.015)	7.963 (0.018)	log H/He=−3.2	···	−3.62	1.98
J1536+5013	1402721307964211072	DA	8774 (30)	0.266 (0.003)	7.243 (0.006)	He/H=0	···	−2.65	0.36
J1537+1041	1166063073741131520	DA	5717 (40)	0.704 (0.057)	8.188 (0.064)	He/H=0	···	−3.92	4.35
J1537+6501	1641386833807056640	DA	9176 (19)	0.563 (0.003)	7.940 (0.003)	He/H=0	···	−2.95	0.73
J1537−0030	4416438420059253248	DC	6316 (54)	0.590 (0.032)	8.028 (0.037)	log H/He=−3.2	···	−3.66	2.19
J1538+0206	4423790579436883072	DA	5982 (52)	0.746 (0.04)	8.250 (0.043)	He/H=0	···	−3.88	4.27
J1538+0842	1164767677244452096	DAH	9004 (77)	0.896 (0.018)	8.466 (0.021)	He/H=0	···	−3.30	1.94
J1538+5211	1596812426258489600	DA	8269 (28)	0.544 (0.007)	7.912 (0.008)	He/H=0	···	−3.11	0.91
J1539+0153	4423768662219609088	DA	8600 (56)	0.577 (0.015)	7.967 (0.018)	He/H=0	···	−3.08	0.89
J1539+5241	1596840493868996864	DA	6191 (34)	0.750 (0.019)	8.253 (0.02)	He/H=0	···	−3.82	3.88
J1539+5811	1602106536090424832	DA	7095 (47)	0.613 (0.012)	8.035 (0.013)	He/H=0	···	−3.45	1.60
J1540+3308	1370654257498865536	DA	8702 (34)	0.620 (0.005)	8.040 (0.005)	He/H=0	···	−3.10	0.95

Tableau A.2 *suite page suivante*

Tableau A.2 *(suite)*

Name	Gaia DR2/EDR3*	Sp Type	$T_{\rm eff}$ (K)	$M/M_{\odot}$	$\log g$	Composition	Métaux	$\log L/L_{\odot}$	τ (Gyr)
J1541+2053	1216353051968362112	DA	6236 (42)	0.779 (0.021)	8.297 (0.023)	He/H=0	···	−3.83	4.11
J1541+2557	1223091649497003264	DA	7075 (48)	0.888 (0.023)	8.458 (0.027)	He/H=0	···	−3.72	3.81
J1542+0153	4423803223819720704	DA	6781 (43)	0.730 (0.019)	8.221 (0.021)	He/H=0	···	−3.64	2.65
J1542+2329	1218051664291152000	DA	5951 (17)	0.730 (0.005)	8.225 (0.006)	He/H=0	···	−3.87	4.13
J1542+4614	1397791368407211264	DA	6939 (47)	0.634 (0.016)	8.070 (0.017)	He/H=0	···	−3.51	1.79
J1542+7247	1696660893947352704	DC	5642 (79)	0.314 (0.018)	7.488 (0.032)	log H/He=−5.0	···	−3.59	1.65
J1542−0341	4402583302239225600	DA	9651 (33)	0.340 (0.017)	7.461 (0.034)	He/H=0	···	−2.60	0.36
J1542−1356	6265350823707860480	DC	5018 (58)	0.413 (0.022)	7.718 (0.032)	H/He=0	···	−3.91	3.40
J1544+2548	1222865601075380480	DC	6267 (50)	0.567 (0.019)	7.991 (0.022)	log H/He=−3.2	···	−3.66	2.13
J1545+6021	1627064973301021056	DA	6285 (31)	0.537 (0.01)	7.911 (0.012)	He/H=0	···	−3.59	1.81
J1546+0458	4426297740826647680	DA	6122 (67)	0.744 (0.039)	8.246 (0.042)	He/H=0	···	−3.83	3.96
J1546+2437	1219722127394433920	DAH	6454 (45)	0.770 (0.017)	8.283 (0.019)	He/H=0	···	−3.76	3.63
J1546+4548	1397898124114691456	DA	6177 (30)	0.645 (0.021)	8.092 (0.023)	He/H=0	···	−3.73	2.56
J1546+4911	1401717243394126464	DA	6604 (34)	0.612 (0.012)	8.035 (0.013)	He/H=0	···	−3.58	1.92
J1547+0659	4430165650933432576	DZ	8690 (67)	0.593 (0.013)	8.025 (0.015)	log H/He=−5.0	log Ca/He=−9.74	−3.10	0.98
J1547+5426	1597468108851256192	DC	5862 (60)	0.681 (0.031)	8.174 (0.034)	H/He=0	···	−3.88	4.33
J1548+5708	1598771000065137536	DC	5760 (23)	0.667 (0.008)	8.153 (0.008)	H/He=0	···	−3.89	4.53
J1549+2009	1204095391402194944	DA	8924 (63)	0.579 (0.013)	7.970 (0.015)	He/H=0	···	−3.01	0.81
J1549+4802	1401366366041668224	DC	6253 (28)	0.613 (0.008)	8.065 (0.008)	log H/He=−3.2	···	−3.70	2.46
J1549−0149	4403335028894782464	DC	6616 (31)	0.560 (0.021)	7.978 (0.026)	log H/He=−3.2	···	−3.55	1.82
J1550+0838	4455205894384768256	DA	6455 (48)	0.804 (0.02)	8.334 (0.022)	He/H=0	···	−3.80	3.98
J1550+2200	1216863676336891520	DA	10354 (53)	0.761 (0.008)	8.256 (0.009)	He/H=0	···	−2.92	0.84
J1551+0824	4454432667131057792	DQ	6765 (36)	0.557 (0.012)	7.971 (0.014)	H/He=0	log C/He=−6.30	−3.51	1.71
J1551+1439	1192571822348252160	DZA	9611 (75)	0.650 (0.019)	8.114 (0.021)	log H/He=−4.4	···	−2.98	0.86
J1551+3222	1369772925913456768	DA	8432 (42)	0.596 (0.01)	7.999 (0.011)	He/H=0	···	−3.13	0.97
J1551+6227	1639910911246160896	DQ	7753 (33)	0.528 (0.006)	7.917 (0.007)	H/He=0	log C/He=−5.70	−3.24	1.13
J1551−1638	6261001052630781312	DA	7932 (43)	0.371 (0.01)	7.559 (0.018)	He/H=0	···	−3.00	0.68
J1552+1852	1203637376090060928	DA	7797 (35)	0.307 (0.005)	7.390 (0.009)	He/H=0	···	−2.94	0.60
J1552+3419	1371714251131163264	DC	7332 (70)	0.610 (0.017)	8.057 (0.02)	log H/He=−3.6	···	−3.42	1.57
J1552+4638	1398051402907424512	DA	5179 (49)	0.590 (0.034)	8.014 (0.04)	He/H=0	···	−3.99	4.93
J1552−0219	4403059253334693248	DZ	7701 (49)	0.597 (0.017)	8.035 (0.02)	log H/He=−4.0	log Ca/He=−9.46	−3.32	1.34
J1553−0114	4409340076070042496	DA	7488 (49)	0.587 (0.023)	7.990 (0.027)	He/H=0	···	−3.33	1.30
J1554+0336	4425127624234553984	DQ	6559 (40)	0.529 (0.027)	7.925 (0.032)	H/He=0	log C/He=−6.88	−3.54	1.73
J1554+0401	4425202936481819520	DA	7264 (78)	0.850 (0.028)	8.401 (0.031)	He/H=0	···	−3.63	3.25

Tableau A.2 *suite page suivante*

Tableau A.2 *(suite)*

Name	Gaia DR2/EDR3*	Sp Type	$T_{\rm eff}$ (K)	$M/M_{\odot}$	$\log g$	Composition	Métaux	$\log L/L_{\odot}$	τ (Gyr)
J1554+1408	1192479390353665280	DA	8386 (54)	0.556 (0.012)	7.932 (0.016)	He/H=0	···	−3.10	0.90
J1554+1735	1202552914026910976	DZ	6794 (25)	0.707 (0.009)	8.210 (0.01)	log H/He=−4.0	log Ca/He=−8.59	−3.64	2.65
J1554+2657	1223443630657641728	DA	5226 (60)	0.610 (0.038)	8.046 (0.043)	He/H=0	···	−4.00	5.07
J1554+5730	1622769245794819968	DA	6714 (47)	0.596 (0.017)	8.008 (0.02)	He/H=0	···	−3.53	1.77
J1554+6145	1627811571760152960	DA	6123 (98)	0.894 (0.035)	8.471 (0.04)	He/H=0	···	−3.98	5.31
J1555+0647	4427021425634792832	DA	5748 (26)	0.763 (0.017)	8.277 (0.018)	He/H=0	···	−3.96	5.05
J1555+3153	1321738565727229184	DA	6651 (28)	0.577 (0.008)	7.977 (0.01)	He/H=0	···	−3.53	1.73
J1555+5025	1403348682426861568	DA	6161 (11)	0.620 (0.004)	8.052 (0.004)	He/H=0	···	−3.71	2.38
J1556+1153	4456309700985355264	DC	4847 (32)	0.544 (0.042)	7.942 (0.05)	He/H=0	···	−4.07	5.98
J1556+3810	1373569711363357056	DC	5897 (30)	0.514 (0.01)	7.903 (0.012)	log H/He=−3.0	···	−3.72	2.33
J1557+0746	4454109681291473536	DA	6835 (36)	0.601 (0.019)	8.016 (0.022)	He/H=0	···	−3.50	1.71
J1557+0953	4455760769799431040	DC	6082 (73)	0.632 (0.035)	8.097 (0.038)	H/He=0	···	−3.77	3.06
J1557+1108	4456018914514270592	DC	6891 (40)	0.646 (0.02)	8.115 (0.022)	log H/He=−3.4	···	−3.56	1.99
J1557+1412	1191742717564070528	DC	4689 (19)	0.524 (0.012)	7.910 (0.014)	He/H=0	···	−4.11	6.30
J1558+0417	4425632987265111680	DC	6538 (15)	0.799 (0.005)	8.349 (0.005)	log H/He=−3.2	···	−3.79	3.76
J1558+0736	4451097882722882432	DA	6195 (45)	0.663 (0.022)	8.119 (0.024)	He/H=0	···	−3.74	2.72
J1558+0840	4454328930782860800	DA	7024 (58)	0.562 (0.017)	7.949 (0.022)	He/H=0	···	−3.42	1.44
J1558+2512	1219957873855946240	DZ	7202 (33)	0.622 (0.007)	8.076 (0.008)	log H/He=−4.0	log Ca/He=−10.87	−3.46	1.68
J1559+2529	1220062430539961344	DA	8308 (36)	0.596 (0.006)	8.001 (0.007)	He/H=0	···	−3.15	1.01
J1600+5038	1403545284553914880	DA	6142 (49)	0.767 (0.019)	8.279 (0.021)	He/H=0	···	−3.85	4.17
J1600−1654	6250213984568447872	DC	3766 (29)	0.377 (0.011)	7.634 (0.017)	He/H=0	···	−4.36	6.56
J1601+1334	1191779830379112192	DA	9641 (107)	1.014 (0.02)	8.651 (0.026)	He/H=0	···	−3.32	2.31
J1601+2735	1316607896578157824	DA	7081 (43)	0.608 (0.011)	8.027 (0.013)	He/H=0	···	−3.45	1.58
J1601+4120	1383292181587562496	DC	4624 (24)	0.393 (0.012)	7.660 (0.018)	He/H=0	···	−4.01	3.86
J1601+5317	1404831472640252928	DA	6789 (11)	0.608 (0.003)	8.028 (0.004)	He/H=0	···	−3.52	1.77
J1602+1630	1199192840852373376	DA	5700 (15)	0.404 (0.004)	7.661 (0.007)	He/H=0	···	−3.64	1.69
J1602+1858	1203132627235232256	DA	5723 (63)	0.582 (0.038)	7.993 (0.045)	He/H=0	···	−3.80	2.61
J1602+2336	1218800393053400576	DA	6266 (51)	0.927 (0.017)	8.520 (0.021)	He/H=0	···	−3.97	5.24
J1602+2644	1316238426312036096	DA	7081 (42)	0.607 (0.015)	8.025 (0.018)	He/H=0	···	−3.45	1.58
J1602+3323	1323407624377828224	DA	7364 (63)	0.569 (0.017)	7.960 (0.022)	He/H=0	···	−3.34	1.30
J1603+0808	4451552182885460480	DA	7349 (40)	0.566 (0.011)	7.955 (0.014)	He/H=0	···	−3.34	1.30
J1604+0055	4411572123331402880	DC	4850 (23)	0.517 (0.009)	7.896 (0.011)	He/H=0	···	−4.05	5.44
J1604+4908	1400157173832960384	DAH	9146 (71)	0.882 (0.011)	8.445 (0.013)	He/H=0	···	−3.26	1.73
J1604−0727	4349513797276615680	DC	4685 (15)	0.839 (0.008)	8.396 (0.008)	He/H=0	···	−4.40	10.28

Tableau A.2 *suite page suivante*

Tableau A.2 *(suite)*

Name	Gaia DR2/EDR3*	Sp Type	$T_{\rm eff}$ (K)	$M/M_{\odot}$	$\log g$	Composition	Métaux	$\log L/L_{\odot}$	τ (Gyr)
J1604−1331	4341773063622911872	DA	5040 (14)	0.465 (0.007)	7.798 (0.01)	He/H=0	···	−3.93	3.30
J1605+5311	1428781653392160128	DA	6550 (57)	0.579 (0.02)	7.981 (0.025)	He/H=0	···	−3.56	1.81
J1605+5556	1621523537776065280	DA	6886 (26)	0.318 (0.006)	7.434 (0.01)	He/H=0	···	−3.19	0.85
J1605−0028	4406733207018066944	DA	9327 (44)	0.595 (0.009)	7.994 (0.01)	He/H=0	···	−2.95	0.75
J1606+0518	4449634256649531776	DC	6380 (61)	0.585 (0.03)	8.019 (0.036)	log H/He=−3.2	···	−3.64	2.10
J1606+2547	1315371255234720896	DA*	4795 (24)	0.501 (0.014)	7.868 (0.017)	He/H=0	···	−4.05	5.39
J1606+6733	1643544689800386176	DC*	9355 (105)	0.690 (0.015)	8.178 (0.016)	log H/He=−4.4	···	−3.06	1.00
J1606+7022	1647162396588999552	DA	6525 (39)	0.641 (0.009)	8.083 (0.01)	He/H=0	···	−3.62	2.13
J1607+1343	4458454611944673408	DA	9307 (77)	0.942 (0.011)	8.537 (0.014)	He/H=0	···	−3.29	2.06
J1607+3423	1323922779935068160	DA	5572 (16)	0.569 (0.006)	7.972 (0.006)	He/H=0	···	−3.84	2.77
J1607−0230	4405080812841630592	DA	7499 (47)	0.615 (0.014)	8.036 (0.016)	He/H=0	···	−3.35	1.39
J1607−1404	4341495230772911616	DAH	5775 (31)	0.614 (0.01)	8.046 (0.011)	He/H=0	···	−3.82	2.87
J1608+1723	1199686173677816576	DA	7964 (28)	0.933 (0.01)	8.525 (0.012)	He/H=0	···	−3.56	3.10
J1608+4235	1384938730313376512	DC	5028 (23)	0.585 (0.015)	8.008 (0.018)	He/H=0	···	−4.04	5.89
J1608+4256	1384982332821602560	DA	8493 (46)	0.558 (0.009)	7.934 (0.012)	He/H=0	···	−3.08	0.88
J1609+0655	4450425359563998720	DQ	7808 (59)	0.525 (0.014)	7.911 (0.018)	H/He=0	log C/He=−5.79	−3.23	1.10
J1609+1619	1198427031003111552	DA	7222 (37)	0.622 (0.011)	8.050 (0.012)	He/H=0	···	−3.43	1.56
J1609+2441	1303034120592956160	DA	7120 (32)	0.998 (0.008)	8.630 (0.011)	He/H=0	···	−3.83	4.41
J1609+5222	1427746463194276736	DAM	6609 (39)	0.986 (0.008)	8.613 (0.01)	He/H=0	···	−3.94	5.02
J1609−0031	4406683522836435968	DA	6833 (54)	0.608 (0.025)	8.028 (0.03)	He/H=0	···	−3.51	1.74
J1610+0619	4449818459207085696	DC*	4955 (258)	1.042 (0.053)	8.726 (0.089)	log H/He=−4.19	···	−4.54	7.21
J1610+1327	4458251064854338176	DAH	6646 (16)	0.608 (0.006)	8.028 (0.007)	He/H=0	···	−3.56	1.87
J1610−2513	6049555929998115072	DA	9722 (34)	0.488 (0.005)	7.798 (0.006)	He/H=0	···	−2.77	0.53
J1611+0451	4437515851806126208	DQ	5833 (23)	0.559 (0.013)	7.980 (0.016)	H/He=0	log C/He=−6.90	−3.78	2.82
J1611+1322	4458207634145130368	DA	9051 (29)	0.892 (0.004)	8.483 (0.004)	log H/He=−1.0	···	−3.31	1.97
J1611+6141	1628349890076998912	DA	10305 (52)	0.606 (0.006)	8.008 (0.008)	He/H=0	···	−2.78	0.59
J1613+4428	1385719147346936064	DA	5135 (48)	0.467 (0.019)	7.799 (0.026)	He/H=0	···	−3.90	2.95
J1614+0905	4452997701376633728	DC	4807 (12)	0.534 (0.007)	7.925 (0.008)	He/H=0	···	−4.08	5.91
J1614+1728	1198984345958836864	DQ	5791 (15)	0.663 (0.008)	8.146 (0.009)	H/He=0	log C/He=−6.36	−3.88	4.37
J1615+1503	4464661728744046848	DC	7224 (59)	0.604 (0.026)	8.047 (0.03)	log H/He=−3.4	···	−3.44	1.60
J1615+1819	1200578152485877376	DC	6454 (37)	0.666 (0.018)	8.148 (0.02)	log H/He=−3.2	···	−3.69	2.70
J1615+4449	1385742821206707456	DC	4920 (23)	0.557 (0.019)	7.963 (0.022)	He/H=0	···	−4.06	5.94
J1615+4602	1386704545987569280	DA :	4881 (52)	0.469 (0.031)	7.809 (0.041)	He/H=0	···	−3.99	4.15
J1616+3924	1380443823700583552	DQ	7287 (46)	0.566 (0.013)	7.985 (0.015)	H/He=0	log C/He=−6.02	−3.39	1.44

Tableau A.2 *suite page suivante*

Tableau A.2 *(suite)*

Name	Gaia DR2/EDR3*	Sp Type	$T_{\rm eff}$ (K)	$M/M_{\odot}$	$\log g$	Composition	Métaux	$\log L/L_{\odot}$	τ (Gyr)
J1616+4600	1386691867244096000	DZ	6414 (42)	0.656 (0.016)	8.133 (0.017)	log H/He=−2.0	log Ca/He=−9.82	−3.69	2.66
J1616+6310	1629354495811136384	DA	7547 (60)	0.850 (0.015)	8.399 (0.017)	He/H=0	···	−3.57	2.90
J1618+0611	4438164190006954880	DQ	8259 (46)	0.917 (0.014)	8.523 (0.016)	H/He=0	log C/He=−5.08	−3.50	2.65
J1619−1831	6246049446837287680	DAH :*	5578 (22)	0.897 (0.01)	8.479 (0.011)	He/H=0	···	−4.15	6.99
J1620+0756	4451874958268328960	DA	6278 (35)	0.614 (0.02)	8.040 (0.022)	He/H=0	···	−3.67	2.21
J1620+1256	4463278336956814208	DA	8001 (80)	0.892 (0.016)	8.462 (0.018)	He/H=0	···	−3.51	2.78
J1620+1436	4464010508621809664	DA	4973 (40)	0.489 (0.028)	7.844 (0.037)	He/H=0	···	−3.98	4.05
J1620+1809	1200428928142394496	DQ	7737 (47)	0.508 (0.017)	7.883 (0.021)	H/He=0	log C/He=−5.79	−3.23	1.08
J1620+2044	1202123726533582848	DA	8255 (34)	0.474 (0.01)	7.780 (0.014)	He/H=0	···	−3.04	0.79
J1621+0552	4437908587914479360	DA	8311 (45)	0.918 (0.011)	8.501 (0.013)	He/H=0	···	−3.47	2.67
J1621−0552	4355229123137665792	DC	4687 (18)	0.467 (0.01)	7.806 (0.014)	He/H=0	···	−4.06	5.14
J1622+0532	4437884055061048064	DA	7261 (115)	0.295 (0.013)	7.362 (0.027)	He/H=0	···	−3.06	0.69
J1622+0713	4439766762564880512	DA	8398 (109)	0.651 (0.022)	8.090 (0.024)	He/H=0	···	−3.19	1.12
J1622+1309	4463261431966304768	DC*	5226 (54)	0.517 (0.033)	7.912 (0.04)	H/He=0	···	−3.93	4.42
J1622+1822	1200416902234462464	DA	6407 (37)	0.741 (0.026)	8.240 (0.029)	He/H=0	···	−3.75	3.39
J1622+2651	1305209190813293440	DC	5955 (62)	0.490 (0.021)	7.858 (0.027)	log H/He=−3.0	···	−3.68	2.12
J1622+2919	1317956898562626176	DC	4399 (56)	0.617 (0.023)	8.064 (0.026)	He/H=0	···	−4.31	9.14
J1622+6701	1642588149044082688	DA	7764 (100)	0.903 (0.018)	8.479 (0.021)	He/H=0	···	−3.57	3.11
J1623+1336	4463651999111841024	DC	4767 (23)	0.594 (0.016)	8.026 (0.019)	He/H=0	···	−4.14	7.42
J1623+3340	1325705942981586176	DA	6886 (71)	0.653 (0.023)	8.100 (0.026)	He/H=0	···	−3.54	1.91
J1623+4650	1410031887762012800	DA	9307 (66)	0.699 (0.009)	8.193 (0.01)	log H/He=−3.5	···	−3.08	1.04
J1623+5642	1429800419634352000	DC	5991 (60)	0.655 (0.032)	8.133 (0.035)	H/He=0	···	−3.81	3.63
J1624+1347	4463664815294536192	DA	6828 (45)	0.587 (0.02)	7.993 (0.024)	He/H=0	···	−3.49	1.65
J1624+1448	4464073180784561408	DQ	5899 (31)	0.574 (0.025)	8.004 (0.029)	H/He=0	log C/He=−7.22	−3.77	2.83
J1624+2013	1201304517354978688	DC	5127 (37)	0.591 (0.025)	8.036 (0.029)	H/He=0	···	−4.03	5.74
J1625+1752	4466984859374027904	DC	6258 (56)	0.668 (0.023)	8.152 (0.026)	H/He=0	···	−3.75	3.08
J1625+2835	1305852233317101184	DA	7238 (55)	0.387 (0.011)	7.603 (0.018)	He/H=0	···	−3.18	0.90
J1625+3759	1332001785217988992	DA	7166 (84)	0.864 (0.019)	8.423 (0.022)	He/H=0	···	−3.67	3.50
J1626+0210	4432834444826809088	DC	4854 (52)	0.211 (0.016)	7.162 (0.040)	He/H=0	···	−3.70	1.68
J1626+0552	4438653541403499776	DAH	9070 (77)	0.767 (0.015)	8.270 (0.017)	He/H=0	···	−3.16	1.22
J1626+1355	4463681655863346816	DA	6576 (30)	0.508 (0.008)	7.856 (0.01)	He/H=0	···	−3.48	1.50
J1626+1938	1201036206454896000	DA	6158 (13)	0.753 (0.004)	8.259 (0.004)	He/H=0	···	−3.83	3.99
J1626+4738	1410897688745546752	DA	8646 (38)	0.341 (0.004)	7.474 (0.009)	He/H=0	···	−2.80	0.50
J1626+4918	1411292580922301312	DA	9357 (46)	0.609 (0.007)	8.017 (0.008)	He/H=0	···	−2.96	0.77

Tableau A.2 *suite page suivante*

Tableau A.2 *(suite)*

Name	Gaia DR2/EDR3*	Sp Type	$T_{\rm eff}$ (K)	$M/M_{\odot}$	$\log g$	Composition	Métaux	$\log L/L_{\odot}$	τ (Gyr)
J1627+0028	4407614499946419200	DA	5929 (13)	0.594 (0.007)	8.010 (0.008)	He/H=0	···	−3.75	2.45
J1627+0912	4452521234885949184	DA	6865 (12)	0.826 (0.003)	8.365 (0.003)	He/H=0	···	−3.71	3.56
J1627+3726	1331208070965684224	DC	4629 (25)	0.600 (0.016)	8.036 (0.018)	He/H=0	···	−4.20	8.07
J1627+4859	1411226507145210624	DZA	5228 (26)	0.616 (0.016)	8.076 (0.017)	He/H=0	log Ca/H=−9.17	−4.02	5.72
J1628+2332	1299122058220640512	DAH	7467 (62)	0.821 (0.014)	8.357 (0.016)	He/H=0	···	−3.56	2.73
J1628+3646	1331106782752978688	DZA	8177 (21)	0.559 (0.003)	7.970 (0.004)	log H/He=−3.0	log Ca/He=−8.86	−3.18	1.06
J1628+7053	1653044367185115264	DA	4894 (36)	0.555 (0.014)	7.960 (0.017)	He/H=0	···	−4.06	6.05
J1628−1739	4323956302321933952	DA	4930 (21)	0.501 (0.01)	7.866 (0.012)	He/H=0	···	−4.00	4.58
J1629+0045	4431665212995124608	DA	9793 (65)	0.845 (0.014)	8.385 (0.016)	He/H=0	···	−3.10	1.20
J1629+2022	1297161594628972672	DA	10015 (71)	0.606 (0.011)	8.010 (0.013)	He/H=0	···	−2.83	0.64
J1629+5357	1425374610454574464	DA	9030 (61)	0.950 (0.01)	8.549 (0.011)	He/H=0	···	−3.36	2.31
J1631−0516	4352651700380171392	DA	6533 (41)	0.604 (0.02)	8.023 (0.024)	He/H=0	···	−3.59	1.94
J1632+0851	4440264291578812928	DA	5642 (11)	0.616 (0.004)	8.049 (0.004)	He/H=0	···	−3.86	3.17
J1632+2426	1300727345195414272	DC	4733 (38)	0.902 (0.009)	8.506 (0.013)	log H/He=−0.53	···	−4.46	8.04
J1633+5231	1424245175791207936	DA	6561 (23)	0.572 (0.006)	7.969 (0.007)	He/H=0	···	−3.55	1.77
J1633+5521	1430007784951049216	DC	7500 (47)	0.585 (0.012)	8.016 (0.014)	log H/He=−3.6	···	−3.36	1.40
J1634+0934	4446506356529203968	DA	6668 (36)	0.462 (0.012)	7.767 (0.018)	He/H=0	···	−3.41	1.30
J1634+1736	4466388790929771904	DAZ	9669 (145)	0.253 (0.007)	7.173 (0.021)	He/H=0	···	−2.44	0.23
J1634+3350	1325899461324069376	DC	7445 (29)	0.557 (0.007)	7.969 (0.008)	log H/He=−3.6	···	−3.34	1.34
J1634+5710	1431176943768691328	DQ	6059 (10)	0.567 (0.003)	7.991 (0.003)	H/He=0	log C/He=−7.18	−3.71	2.42
J1634+7558	1703379704562897280	DA	8063 (25)	0.245 (0.002)	7.180 (0.006)	He/H=0	···	−2.77	0.41
J1634−0901	4338593516506343424	DA	8404 (52)	0.621 (0.015)	8.042 (0.018)	He/H=0	···	−3.16	1.04
J1635+4317	1405343643196929536	DAZ	6543 (10)	0.671 (0.003)	8.155 (0.002)	He/H=0	log Ca/H=−9.20	−3.67	2.61
J1636+1255	4459666716138776576	DC	5432 (43)	0.658 (0.025)	8.141 (0.027)	H/He=0	···	−3.99	5.53
J1636+1619	4465939601772584448	DZ	4375 (23)	0.555 (0.038)	7.979 (0.044)	log H/He=−5.0	log Ca/He=−9.84	−4.28	6.93
J1636+2049	4564212061278453248	DA	7439 (75)	0.855 (0.026)	8.408 (0.029)	He/H=0	···	−3.60	3.08
J1637+0110	4384056565671592576	DA	7104 (30)	0.587 (0.01)	7.992 (0.012)	He/H=0	···	−3.42	1.49
J1637+1110	4447152865064276736	DA	5484 (25)	0.557 (0.014)	7.953 (0.016)	He/H=0	···	−3.86	2.84
J1637+1340	4461228611063376128	DAZ	6878 (29)	0.568 (0.006)	7.990 (0.008)	He/H=0	log Ca/H=−9.72	−3.49	1.68
J1637+5133	1425397189098547200	DA	7166 (36)	0.674 (0.008)	8.132 (0.009)	He/H=0	···	−3.49	1.80
J1637−0204	4358066107952246784	DA	8080 (32)	0.590 (0.008)	7.992 (0.009)	He/H=0	···	−3.20	1.07
J1638+0540	4435778215414219520	DA	8366 (8)	0.915 (0.002)	8.497 (0.002)	He/H=0	···	−3.45	2.61
J1638−2035	4130191322368475392	DA	8687 (36)	0.611 (0.006)	8.024 (0.007)	He/H=0	···	−3.09	0.93
J1639+1036	4447039585308297088	DAH	6425 (44)	0.755 (0.02)	8.260 (0.022)	He/H=0	···	−3.76	3.52

Tableau A.2 *suite page suivante*

Tableau A.2 *(suite)*

Name	Gaia DR2/EDR3*	Sp Type	$T_{\rm eff}$ (K)	$M/M_{\odot}$	$\log g$	Composition	Métaux	$\log L/L_{\odot}$	τ (Gyr)
J1639+3325	1326398777041821568	DA	9919 (30)	0.603 (0.004)	8.005 (0.005)	He/H=0	···	−2.85	0.65
J1639+4030	1355979969155873792	DA	8275 (48)	0.668 (0.009)	8.119 (0.01)	He/H=0	···	−3.23	1.22
J1639+8038	1710386067532886272	DC	5504 (73)	0.617 (0.025)	8.077 (0.028)	H/He=0	···	−3.93	4.81
J1640+2229	1299314816353108992	DAZ	7502 (49)	0.615 (0.011)	8.065 (0.013)	He/H=0	log Ca/H=−8.47	−3.38	1.50
J1640+5341	1425909733315616000	DAH	7923 (23)	0.800 (0.004)	8.323 (0.004)	He/H=0	···	−3.43	2.04
J1640+7310	1654560662439820416	DQ	8485 (37)	0.556 (0.005)	7.963 (0.006)	H/He=0	log C/He=−4.87	−3.11	0.95
J1641+1512	4462612140287443840	DA	7422 (20)	0.552 (0.005)	7.929 (0.006)	He/H=0	···	−3.31	1.22
J1641+2543	1301111585855899136	DA	7216 (68)	0.645 (0.022)	8.087 (0.025)	He/H=0	···	−3.45	1.66
J1641+4833	1410448259071414528	DQ	7641 (56)	0.581 (0.014)	8.009 (0.016)	H/He=0	log C/He=−5.80	−3.32	1.32
J1643+1422	4461739604794187520	DZ	6495 (44)	0.632 (0.017)	8.095 (0.019)	log H/He=−3.0	log Ca/He=−11.18	−3.65	2.31
J1643+4438	1405848383457312512	DC	5019 (31)	0.574 (0.024)	7.990 (0.029)	He/H=0	···	−4.04	5.69
J1644+2253	1299436415467829888	DC	7641 (49)	0.663 (0.014)	8.140 (0.016)	log H/He=−3.6	···	−3.39	1.58
J1644+7628	1704918191912744192	DA	6765 (29)	0.630 (0.008)	8.064 (0.009)	He/H=0	···	−3.55	1.89
J1645+3059	1311660540930405632	DAZ	7193 (44)	0.698 (0.015)	8.196 (0.017)	He/H=0	log Ca/H=−7.66	−3.53	2.10
J1645+4958	1412228093519039744	DA	6670 (27)	0.524 (0.009)	7.884 (0.012)	He/H=0	···	−3.48	1.50
J1646+0303	4385909109622569088	DA	8427 (50)	0.598 (0.013)	8.004 (0.015)	He/H=0	···	−3.13	0.98
J1646+3246	1314253292427950720	DA	5700 (34)	0.568 (0.021)	7.970 (0.026)	He/H=0	···	−3.80	2.55
J1647+2636	1307226283551364224	DZ	7126 (30)	0.601 (0.006)	8.043 (0.007)	log H/He=−4.0	log Ca/He=−9.94	−3.46	1.65
J1647+3946	1352743419240352384	DC	4004 (98)	0.479 (0.056)	7.833 (0.072)	He/H=0	···	−4.35	7.85
J1648+3939	1352692734330406912	DC	4999 (23)	0.167 (0.005)	6.942 (0.019)	H/He=0	···	−3.53	1.83
J1649−2155	4126670518631322880	DA	5586 (28)	0.796 (0.012)	8.326 (0.013)	He/H=0	···	−4.04	5.98
J1650−1004	4334670557801027840	DA	7442 (58)	0.531 (0.017)	7.892 (0.021)	He/H=0	···	−3.29	1.16
J1651+4249	1356633384004567168	DZH*	5512 (25)	0.709 (0.028)	8.218 (0.031)	log H/He=−5.0	log Ca/He=−8.16	−4.01	5.79
J1651+6635	1636125872530936192	DZ	8965 (94)	0.554 (0.012)	7.958 (0.015)	log H/He=−4.0	log Ca/He=−9.76	−3.01	0.82
J1652+1324	4449419409503701376	DA	5283 (31)	0.457 (0.041)	7.777 (0.056)	He/H=0	···	−3.83	2.46
J1652+1346	4449495546386664832	DA	6003 (31)	0.586 (0.022)	7.997 (0.026)	He/H=0	···	−3.72	2.32
J1652−0114	4379328051494006784	DA	5588 (15)	0.771 (0.006)	8.290 (0.006)	He/H=0	···	−4.02	5.70
J1653+6253	1631578537252535040	DC	5036 (30)	1.058 (0.003)	8.753 (0.005)	log H/He=−2.78	···	−4.53	7.02
J1654+1243	4449057326579614592	DA	5361 (28)	0.595 (0.015)	8.019 (0.016)	He/H=0	···	−3.93	3.89
J1654+3157	1313265900922425856	DQ	7150 (28)	0.555 (0.007)	7.966 (0.008)	H/He=0	log C/He=−6.01	−3.41	1.48
J1654+3829	1351956512512484480	DAZ	5907 (14)	0.701 (0.004)	8.204 (0.005)	He/H=0	log Ca/H=−8.00	−3.88	4.40
J1654+5742	1436666805326235648	DA	8884 (34)	0.463 (0.005)	7.755 (0.007)	He/H=0	···	−2.90	0.64
J1655+1850	4559800992425812096	DA	6332 (50)	0.571 (0.019)	7.969 (0.024)	He/H=0	···	−3.61	1.94
J1656+4911	1409166984427845632	DC	5549 (75)	0.592 (0.023)	8.035 (0.026)	log H/He=−5.0	···	−3.89	4.30

Tableau A.2 *suite page suivante*

Tableau A.2 *(suite)*

Name	Gaia DR2/EDR3*	Sp Type	$T_{\rm eff}$ (K)	$M/M_{\odot}$	$\log g$	Composition	Métaux	$\log L/L_{\odot}$	τ (Gyr)
J1657+2126	4565048312887877888	DA	9233 (26)	0.613 (0.003)	8.025 (0.004)	He/H=0	···	−2.98	0.80
J1657+2414	4572405140891735296	DC	4703 (60)	0.561 (0.055)	7.972 (0.065)	He/H=0	···	−4.14	6.90
J1658+2210	4565386996828484224	DA	6587 (39)	0.576 (0.016)	7.976 (0.02)	He/H=0	···	−3.55	1.77
J1658−0617	4340322876499078400	DA	5582 (13)	0.643 (0.006)	8.093 (0.007)	He/H=0	···	−3.90	3.83
J1659+1705	4558448219470271616	DA	9256 (54)	0.652 (0.012)	8.089 (0.013)	He/H=0	···	−3.02	0.87
J1659+3203	1313405848136604672	DA	6408 (22)	0.896 (0.005)	8.473 (0.006)	He/H=0	···	−3.90	4.84
J1659+4425	1358325021299899136	DA	5491 (10)	0.536 (0.004)	7.918 (0.004)	He/H=0	···	−3.84	2.64
J1701+4124	1354610798005917312	DA	10099 (73)	0.830 (0.011)	8.362 (0.013)	He/H=0	···	−3.03	1.06
J1702+1022	4444590625015876864	DA	5162 (21)	0.856 (0.008)	8.420 (0.009)	He/H=0	···	−4.24	8.86
J1704+1852	4560373769265200640	DC	5541 (78)	0.718 (0.053)	8.231 (0.057)	H/He=0	···	−4.01	5.79
J1704+2007	4561641991506408448	DA	6361 (24)	0.616 (0.008)	8.044 (0.008)	He/H=0	···	−3.65	2.14
J1704+3608	1339274053906752896	DC	4746 (23)	0.455 (0.01)	7.785 (0.013)	He/H=0	···	−4.03	4.57
J1704−1446	4139348334376604928	DA	7163 (31)	0.814 (0.006)	8.347 (0.008)	He/H=0	···	−3.62	3.04
J1705+0423	4391500847801807104	DA	8261 (33)	0.574 (0.006)	7.963 (0.007)	He/H=0	···	−3.14	0.98
J1705+2605	4573071139998034048	DA	6064 (20)	0.746 (0.006)	8.249 (0.006)	He/H=0	···	−3.85	4.10
J1705+4803	1408135749896104192	DA	9041 (21)	0.249 (0.002)	7.172 (0.004)	He/H=0	···	−2.56	0.29
J1705−0145	4379812558164849408	DC	4760 (11)	0.579 (0.006)	8.001 (0.007)	He/H=0	···	−4.13	7.08
J1706+6316	1631186458277453440	DAH	10501 (79)	0.897 (0.012)	8.464 (0.014)	He/H=0	···	−3.03	1.14
J1706−1238	4140966708116861440	DQ	6122 (41)	0.541 (0.036)	7.946 (0.044)	H/He=0	log C/He=−6.82	−3.67	2.16
J1707+6413	1632041328568823424	DA	7637 (45)	0.577 (0.012)	7.972 (0.014)	He/H=0	···	−3.29	1.21
J1708+0257	4388138816124225792	DZ	6259 (16)	0.616 (0.005)	8.070 (0.005)	log H/He=−4.0	log Ca/He=−10.01	−3.70	2.48
J1709+2332	4571723134445705856	DC	6377 (44)	0.599 (0.02)	8.043 (0.023)	log H/He=−3.2	···	−3.65	2.19
J1709+6820	1636757232723867264	DA	6526 (16)	0.547 (0.007)	7.926 (0.008)	He/H=0	···	−3.54	1.68
J1711+0932	4443586358581794176	DA	7517 (41)	0.572 (0.012)	7.964 (0.015)	He/H=0	···	−3.31	1.24
J1711−1447	4139531467491239680	DQ	9004 (54)	0.491 (0.006)	7.845 (0.007)	H/He=0	log C/He=−4.67	−2.94	0.70
J1712+3559	1338388813904333952	DC	8518 (45)	0.558 (0.008)	7.966 (0.01)	log H/He=−4.0	···	−3.11	0.95
J1712+3921	1341599143042727680	DAH	6103 (30)	0.661 (0.015)	8.117 (0.016)	He/H=0	···	−3.76	2.86
J1712+5629	1432420624562923520	DA	7203 (38)	0.569 (0.01)	7.961 (0.012)	He/H=0	···	−3.38	1.38
J1713+3240	1334374153353733888	DQ	7879 (29)	0.549 (0.007)	7.954 (0.009)	H/He=0	log C/He=−5.43	−3.24	1.14
J1713+4053	1342008814203085440	DA	8958 (61)	0.963 (0.008)	8.570 (0.01)	He/H=0	···	−3.38	2.46
J1713−0032	4368448074699014528	DA	8422 (38)	0.568 (0.01)	7.952 (0.013)	He/H=0	···	−3.10	0.92
J1714+2127	4567158653660872064	DC	7044 (20)	0.601 (0.005)	8.043 (0.005)	log H/He=−3.4	···	−3.48	1.70
J1714+3918	1341543072245722752	DAH	6743 (16)	0.485 (0.004)	7.811 (0.005)	He/H=0	···	−3.42	1.33
J1714−0534	4361621688038664064	DA*	9556 (20)	0.693 (0.003)	8.152 (0.004)	He/H=0	···	−3.00	0.88

Tableau A.2 *suite page suivante*

Tableau A.2 *(suite)*

Name	Gaia DR2/EDR3*	Sp Type	$T_{\rm eff}$ (K)	$M/M_{\odot}$	$\log g$	Composition	Métaux	$\log L/L_{\odot}$	τ (Gyr)
J1716+2612	4573650303451549952	DA	8192 (47)	0.506 (0.01)	7.842 (0.014)	He/H=0	···	−3.09	0.86
J1716+4129	1348007784003797376	DC	7198 (60)	0.622 (0.02)	8.076 (0.022)	log H/He=−3.4	···	−3.46	1.68
J1716−0821	4359722208685335552	DQ	5956 (15)	0.478 (0.006)	7.835 (0.007)	H/He=0	log C/He=−7.01	−3.66	2.05
J1717+6136	1438490650303065984	DA	6481 (81)	0.945 (0.027)	8.548 (0.032)	He/H=0	···	−3.93	5.00
J1719−0130	4367353266060378624	DC :	4668 (37)	0.574 (0.017)	7.994 (0.02)	He/H=0	···	−4.17	7.33
J1720+1022	4491748511228743808	DC	4938 (14)	0.525 (0.008)	7.908 (0.009)	He/H=0	···	−4.02	5.08
J1720+4253	1360235560190381440	DC	5157 (25)	0.613 (0.012)	8.072 (0.013)	H/He=0	···	−4.04	5.91
J1722+2848	4598568230530318592	DA	5231 (39)	0.674 (0.017)	8.147 (0.019)	He/H=0	···	−4.05	6.30
J1722+3221	1333697880686680960	DA	6706 (41)	0.590 (0.019)	7.998 (0.022)	He/H=0	···	−3.53	1.75
J1722+5752	1433166540130924544	DC	5249 (49)	0.698 (0.012)	8.201 (0.019)	log H/He=−1.50	···	−4.08	6.44
J1723+0458	4390134326651497728	DA	8299 (52)	0.567 (0.01)	7.951 (0.012)	He/H=0	···	−3.13	0.95
J1723+0905	4490607183799536896	DA	6900 (25)	0.346 (0.009)	7.508 (0.015)	He/H=0	···	−3.22	0.92
J1724+2756	4598266758185956864	DA	6067 (18)	0.772 (0.006)	8.288 (0.006)	He/H=0	···	−3.88	4.37
J1725+6209	1439283711720415872	DA	7716 (54)	0.564 (0.01)	7.949 (0.013)	He/H=0	···	−3.25	1.14
J1726+3112	4599998179762051200	DA	7788 (32)	0.524 (0.007)	7.877 (0.009)	He/H=0	···	−3.20	1.01
J1726+3245	4600426645699105664	DA*	6978 (64)	0.553 (0.019)	7.933 (0.023)	He/H=0	···	−3.42	1.43
J1727+0808	4490300553197280256	DC	4414 (74)	0.507 (0.052)	7.896 (0.091)	log H/He=−2.43	···	−4.22	6.25
J1728+0211	4376680324417193472	DA	8165 (41)	0.657 (0.007)	8.101 (0.008)	He/H=0	···	−3.24	1.22
J1729+1435	4542785981266940416	DC	4840 (22)	0.784 (0.01)	8.314 (0.01)	He/H=0	···	−4.29	9.57
J1729+2916	4598830738931385984	DA	7041 (30)	0.815 (0.006)	8.348 (0.007)	He/H=0	···	−3.65	3.21
J1730+1346	4542521278141244288	DA	10711 (55)	0.633 (0.005)	8.052 (0.006)	He/H=0	···	−2.74	0.57
J1731+3705	1336442472164656000	DAZB	9825 (59)	0.574 (0.007)	7.990 (0.009)	log H/He=−1.5	log Ca/He=−7.00	−2.87	0.68
J1732+0213	4376589580346060928	DA	7376 (39)	0.465 (0.009)	7.769 (0.012)	He/H=0	···	−3.24	1.02
J1733+2705	4595011409196652544	DA	6263 (43)	0.617 (0.021)	8.046 (0.024)	He/H=0	···	−3.67	2.24
J1733+2903	4598775557191664384	DC	6318 (19)	0.660 (0.006)	8.140 (0.007)	H/He=0	···	−3.73	2.88
J1733+3013	4598979924619296384	DZ	7937 (23)	0.674 (0.006)	8.157 (0.006)	log H/He=−4.0	log Ca/He=−7.80	−3.34	1.47
J1733+7949	1706631093589103872	DC	5326 (25)	0.668 (0.009)	8.156 (0.01)	H/He=0	···	−4.03	5.96
J1734+4236	1347620038652968192	DA	7218 (26)	0.268 (0.004)	7.277 (0.008)	He/H=0	···	−3.02	0.64
J1734+4423	1348795004265872000	DA	5089 (17)	0.608 (0.008)	8.044 (0.009)	He/H=0	···	−4.04	5.97
J1737+0138	4375699353885688448	DA	7282 (20)	0.667 (0.006)	8.121 (0.006)	He/H=0	···	−3.46	1.70
J1738+0516	4485626636646013696	DA	8816 (28)	0.590 (0.005)	7.988 (0.006)	He/H=0	···	−3.04	0.86
J1738−0826	4168312459956062208	DAZ	7084 (13)	0.598 (0.004)	8.038 (0.004)	He/H=0	log Ca/H=−8.73	−3.47	1.67
J1739+4404	1350007967453813632	DA	8116 (54)	0.681 (0.011)	8.140 (0.013)	He/H=0	···	−3.28	1.32
J1739+6043	1435776922462177408	DA	6664 (35)	0.572 (0.009)	7.968 (0.01)	He/H=0	···	−3.52	1.70

Tableau A.2 *suite page suivante*

Tableau A.2 *(suite)*

Name	Gaia DR2/EDR3*	Sp Type	$T_{\rm eff}$ (K)	$M/M_{\odot}$	$\log g$	Composition	Métaux	$\log L/L_{\odot}$	τ (Gyr)
J1741+2401	4581383928942599296	DA	6949 (22)	0.816 (0.004)	8.350 (0.005)	He/H=0	···	−3.68	3.34
J1742+4338	1349256249394224128	DA	5449 (10)	0.580 (0.004)	7.993 (0.004)	He/H=0	···	−3.89	3.23
J1742+5136	1368236912466084352	DA	8649 (31)	0.605 (0.005)	8.014 (0.005)	He/H=0	···	−3.09	0.93
J1743+0502	4473632403597115776	DA	6802 (114)	1.109 (0.313)	8.822 (0.825)	He/H=0	···	−4.05	4.98
J1743+1434	4500646618315862144	DC	10526 (46)	0.581 (0.006)	7.998 (0.007)	log H/He=−4.8	···	−2.75	0.57
J1743+1701	4549622027311531904	DC	4339 (26)	0.548 (0.012)	7.953 (0.014)	He/H=0	···	−4.27	7.94
J1745+4825	1363721110836082176	DA	7890 (41)	0.625 (0.011)	8.051 (0.013)	He/H=0	···	−3.27	1.24
J1746−1234	4150020774057837440	DA	6197 (31)	0.808 (0.008)	8.341 (0.009)	He/H=0	···	−3.87	4.47
J1747+2859	4596322473734130304	DC	4600 (18)	0.348 (0.007)	7.581 (0.013)	H/He=0	···	−4.00	3.32
J1748+0052	4372558083524803072	DAH	9043 (48)	0.884 (0.008)	8.447 (0.009)	He/H=0	···	−3.28	1.81
J1748+4503	1350517492310172416	DC	8486 (25)	0.696 (0.004)	8.190 (0.005)	log H/He=−4.0	···	−3.24	1.31
J1748+7052	1638979384378696704	DXP	5058 (5)	0.586 (0.002)	8.028 (0.003)	H/He=0	···	−4.05	5.89
J1749+8247	1711005951573009792	DA	7260 (0)	0.535 (0.0)	7.901 (0.0)	He/H=0	···	−3.33	1.24
J1749−2355	4068499305485306240	DAZ	7505 (37)	0.623 (0.007)	8.077 (0.008)	He/H=0	log Ca/H=−8.50	−3.39	1.52
J1751+4455	1349726324974648192	DC	7163 (40)	0.580 (0.01)	8.009 (0.011)	log H/He=−3.4	···	−3.43	1.56
J1752+0947	4488750108662714624	DA	9706 (82)	0.576 (0.011)	7.993 (0.013)	log H/He=−5.0	···	−2.89	0.70
J1752+5037	1367469041032593024	DA	9193 (31)	0.658 (0.005)	8.099 (0.006)	He/H=0	···	−3.03	0.90
J1753+5039	1367551813642685952	DA	8754 (50)	0.837 (0.009)	8.376 (0.01)	He/H=0	···	−3.29	1.67
J1754+3846	4610983121260366336	DAH	6423 (27)	0.695 (0.007)	8.168 (0.008)	He/H=0	···	−3.70	2.78
J1754+5938	1423078520938173056	DA	6322 (49)	0.589 (0.022)	7.999 (0.026)	He/H=0	···	−3.63	2.04
J1757+1021	4494877446445481472	DZ	8075 (24)	0.571 (0.005)	7.991 (0.005)	log H/He=−3.0	log Ca/He=−8.42	−3.21	1.12
J1757+3900	4610819951159775616	DA	6903 (87)	0.823 (0.029)	8.361 (0.032)	He/H=0	···	−3.70	3.48
J1757+4052	4611543459874840832	DC	5258 (16)	0.537 (0.007)	7.946 (0.008)	H/He=0	···	−3.94	4.59
J1757+5441	1417200020676904704	DA	7624 (31)	0.567 (0.006)	7.955 (0.007)	He/H=0	···	−3.28	1.18
J1758+1417	4499839473701254400	DA	5424 (15)	0.575 (0.005)	7.985 (0.006)	He/H=0	···	−3.90	3.24
J1758+2310	4577666681988285696	DC	5819 (70)	0.610 (0.033)	8.063 (0.037)	H/He=0	···	−3.83	3.59
J1758+5201	1367876852471768320	DA	8364 (66)	0.845 (0.013)	8.390 (0.014)	He/H=0	···	−3.38	2.04
J1759+3924	4611204329256349312	DC	4603 (40)	0.500 (0.017)	7.868 (0.021)	He/H=0	···	−4.12	6.26
J1801+0846	4476287041283507840	DA	5624 (15)	0.419 (0.008)	7.694 (0.01)	He/H=0	···	−3.68	1.81
J1801+5050	2123432247756223488	DC	4763 (19)	0.507 (0.002)	7.896 (0.004)	log H/He=−0.06	···	−4.09	5.54
J1802+1354	4496751667093478016	DAZ	8055 (36)	0.588 (0.007)	8.019 (0.007)	He/H=0	log Ca/H=−8.10	−3.23	1.18
J1803+2320	4577545533852426624	DQ	4230 (15)	0.237 (0.015)	7.282 (0.035)	H/He=0	log C/He=−8.21	−4.01	2.73
J1806+2312	4578278903808759040	DA	8865 (90)	0.960 (0.013)	8.566 (0.016)	He/H=0	···	−3.40	2.51
J1807+0356	4470233817461336704	DA	10176 (33)	0.640 (0.004)	8.066 (0.005)	He/H=0	···	−2.84	0.66

Tableau A.2 *suite page suivante*

Tableau A.2 *(suite)*

Name	Gaia DR2/EDR3*	Sp Type	$T_{\rm eff}$ (K)	$M/M_{\odot}$	$\log g$	Composition	Métaux	$\log L/L_{\odot}$	τ (Gyr)
J1807−1955	4095056359580563328	DC	8750 (49)	0.841 (0.013)	8.408 (0.014)	log H/He=−4.2	···	−3.32	1.86
J1811+2213	4577915996250307968	DA	7657 (56)	0.632 (0.018)	8.063 (0.021)	He/H=0	···	−3.33	1.37
J1811+2423	4578464515115212672	DA	8200 (49)	0.617 (0.01)	8.036 (0.011)	He/H=0	···	−3.20	1.10
J1813+3248	4592910074976281472	DA	7613 (20)	0.577 (0.005)	7.972 (0.006)	He/H=0	···	−3.29	1.22
J1813+3248	4592910105037219072	DA	6510 (28)	0.586 (0.007)	7.992 (0.007)	He/H=0	···	−3.58	1.87
J1814+1301	4497001870409825280	DC	8858 (67)	0.586 (0.013)	8.013 (0.015)	log H/He=−4.2	···	−3.06	0.92
J1815+3158	4592623171160970112	DA	4998 (11)	0.474 (0.006)	7.815 (0.008)	He/H=0	···	−3.95	3.62
J1815−1140	4153937891610652928	DC	4789 (15)	0.467 (0.008)	7.805 (0.012)	He/H=0	···	−4.02	4.61
J1816+2454	4578913738632417920	DAP	6880 (19)	0.794 (0.005)	8.318 (0.005)	He/H=0	···	−3.67	3.22
J1817+1328	4497414466452138496	DA	4890 (3)	0.474 (0.002)	7.817 (0.003)	He/H=0	···	−3.99	4.19
J1817−1335	4146666271458052352	DA	5910 (35)	0.794 (0.009)	8.321 (0.01)	He/H=0	···	−3.94	4.92
J1819+1739	4523585076572785408	DC	4891 (20)	0.598 (0.009)	8.031 (0.011)	He/H=0	···	−4.10	6.96
J1819−1934	4094555467661923328	DC	4444 (37)	0.459 (0.016)	7.794 (0.022)	He/H=0	···	−4.15	6.00
J1820+2619	4585067258532443776	DA	5002 (17)	0.733 (0.01)	8.239 (0.011)	He/H=0	···	−4.18	8.53
J1820+7454	2268813145513879808	DA	9543 (61)	0.633 (0.01)	8.057 (0.011)	He/H=0	···	−2.94	0.77
J1821+5509	2149253075743572224	DA	5045 (29)	0.560 (0.01)	7.966 (0.013)	He/H=0	···	−4.01	5.19
J1821+6100	2158285185808357504	DA	4945 (6)	0.495 (0.003)	7.854 (0.003)	He/H=0	···	−3.99	4.34
J1822+2257	4530172280800983808	DA	6366 (61)	0.806 (0.026)	8.338 (0.029)	He/H=0	···	−3.82	4.15
J1823+2022	4528439381757452928	DC	4936 (17)	0.577 (0.009)	7.995 (0.01)	He/H=0	···	−4.07	6.28
J1823−1123	4154063678315488640	DA	5872 (23)	0.710 (0.009)	8.195 (0.01)	He/H=0	···	−3.88	4.03
J1824+1209	4484277256704949376	DA	5164 (15)	0.617 (0.006)	8.058 (0.007)	He/H=0	···	−4.02	5.64
J1824+1212	4484289866726156160	DZ	3381 (42)	0.346 (0.008)	7.517 (0.018)	log H/He=−0.06	···	−4.47	11.74
J1824−1308	4152557420406043264	DAZ	6124 (29)	0.616 (0.007)	8.045 (0.008)	He/H=0	···	−3.71	2.39
J1825+1135	4484184592790777728	DA	4926 (16)	0.534 (0.007)	7.925 (0.008)	He/H=0	···	−4.03	5.39
J1826+1120	4483974792231866624	DA	4913 (6)	0.493 (0.004)	7.852 (0.006)	He/H=0	···	−4.00	4.51
J1827+0621	4477166581862730752	DC*	9562 (87)	0.417 (0.013)	7.693 (0.021)	log H/He=−4.4	···	−2.76	0.50
J1828+4149	2111294734600515072	DA	6607 (39)	0.748 (0.02)	8.249 (0.022)	He/H=0	···	−3.70	3.13
J1829−0429	4257461275049675008	DA	9059 (21)	0.599 (0.015)	8.003 (0.017)	He/H=0	···	−3.00	0.82
J1829−0536	4257063458004688896	DA	5489 (24)	0.586 (0.009)	8.003 (0.01)	He/H=0	···	−3.88	3.19
J1829−0536	4257063453704172416	DC	6149 (32)	0.499 (0.008)	7.874 (0.009)	log H/He=−3.0	···	−3.63	1.93
J1830+2529	4537112917885892608	DC	4626 (25)	0.982 (0.037)	8.627 (0.059)	log H/He=−2.56	···	−4.58	7.91
J1830+5447	2150504594853811456	DXP	6482 (16)	0.831 (0.004)	8.396 (0.004)	H/He=0	···	−3.84	4.05
J1831+4658	2118649750133781376	DA	7451 (30)	0.619 (0.006)	8.042 (0.006)	He/H=0	···	−3.37	1.42
J1833+1945	4525569007873380736	DQ	7110 (17)	0.553 (0.004)	7.964 (0.005)	H/He=0	log C/He=−6.20	−3.42	1.49

Tableau A.2 *suite page suivante*

Tableau A.2 *(suite)*

Name	Gaia DR2/EDR3*	Sp Type	$T_{\rm eff}$ (K)	$M/M_{\odot}$	$\log g$	Composition	Métaux	$\log L/L_{\odot}$	τ (Gyr)
J1833+3217	4589139574728058880	DZA	7610 (52)	0.590 (0.009)	8.024 (0.011)	log H/He=−3.0	log Ca/He=−8.46	−3.33	1.36
J1834+1215	4508113436149576960	DQ*	7788 (50)	0.525 (0.015)	7.912 (0.018)	H/He=0	log C/He=−5.65	−3.23	1.11
J1835+6421	2256410856215182464	DC	4841 (18)	0.562 (0.008)	7.972 (0.01)	He/H=0	···	−4.09	6.38
J1835+6429	2256422164865057536	DQ	6755 (13)	0.549 (0.004)	7.958 (0.006)	H/He=0	log C/He=−5.27	−3.51	1.68
J1838+6251	2160181598552871040	DC	5633 (72)	0.508 (0.018)	7.894 (0.022)	log H/He=−5.0	···	−3.79	2.82
J1841+4107	2110551602180192256	DA	5789 (42)	0.587 (0.029)	8.001 (0.035)	He/H=0	···	−3.79	2.56
J1842−1108	4107012041007171456	DA	9937 (19)	0.644 (0.003)	8.073 (0.003)	He/H=0	···	−2.88	0.71
J1843+0420	4280632829779587072	DA	8901 (40)	0.690 (0.006)	8.150 (0.006)	He/H=0	···	−3.12	1.05
J1847+2820	4539227892919675648	DC	4799 (30)	0.743 (0.015)	8.255 (0.015)	He/H=0	···	−4.27	9.40
J1848+6852	2259262581356603136	DA	6994 (22)	0.305 (0.006)	7.396 (0.012)	He/H=0	···	−3.14	0.79
J1849−0736	4252064631569619712	DC	6341 (19)	0.689 (0.006)	8.184 (0.007)	log H/He=−3.2	···	−3.74	3.15
J1851+7738	2292861388958880640	DC	5158 (19)	0.548 (0.008)	7.943 (0.009)	He/H=0	···	−3.96	4.10
J1852+1833	4517521407404432512	DAH	8664 (54)	0.907 (0.009)	8.483 (0.01)	He/H=0	···	−3.38	2.29
J1855+5359	2146645790077864704	DC	4690 (12)	0.547 (0.006)	7.949 (0.007)	He/H=0	···	−4.13	6.67
J1857+2026	4518917168694695168	DA+DC :*	6598 (29)	0.776 (0.007)	8.292 (0.007)	He/H=0	···	−3.73	3.47
J1857+5330	2146576589564898688	DC	4833 (12)	0.560 (0.005)	7.969 (0.006)	He/H=0	···	−4.09	6.34
J1857−2651	4073522222505044224	DA*	6915 (28)	0.565 (0.006)	7.954 (0.007)	He/H=0	···	−3.45	1.51
J1859+1158	4313658585693385984	DA	9633 (16)	0.530 (0.004)	7.878 (0.004)	He/H=0	···	−2.83	0.60
J1900+3922	2100304020669107328	DA	9434 (28)	0.606 (0.004)	8.012 (0.005)	He/H=0	···	−2.94	0.75
J1906+4446	2106132596228948480	DA	7522 (33)	0.576 (0.008)	7.971 (0.009)	He/H=0	···	−3.31	1.25
J1912+0242	4268167357267580160	DZ	5867 (36)	0.614 (0.01)	8.070 (0.011)	H/He=0	log Ca/He=−9.52	−3.81	3.49
J1913+2949	2039140284770609152	DA	5881 (15)	0.593 (0.006)	8.009 (0.006)	He/H=0	···	−3.77	2.49
J1914+1428	4320303621677848832	DA	6952 (41)	0.727 (0.008)	8.216 (0.009)	He/H=0	···	−3.59	2.38
J1914+4936	2132684535027576448	DA	8751 (29)	0.581 (0.006)	7.973 (0.007)	He/H=0	···	−3.05	0.86
J1916+8044	2295446546953958272	DA	5346 (22)	0.642 (0.009)	8.095 (0.01)	He/H=0	···	−3.98	4.94
J1918+3843	2052891361294411520	DC	6070 (11)	0.597 (0.003)	8.041 (0.003)	log H/He=−3.0	···	−3.74	2.66
J1918+3851	2100934448852549760	DA	8409 (108)	0.906 (0.024)	8.484 (0.027)	He/H=0	···	−3.43	2.51
J1918+6258	2252512954353689344	DA	7791 (43)	0.628 (0.011)	8.056 (0.013)	He/H=0	···	−3.30	1.29
J1921+0613	4293873732939569920	DA	5919 (12)	0.693 (0.004)	8.169 (0.004)	He/H=0	···	−3.85	3.69
J1922+0233	4288942973032203904	DZ	4436 (60)	1.065 (0.007)	8.765 (0.011)	log H/He=−1.73	···	−4.76	7.40
J1922+7137	2264228628701507200	DA	7542 (28)	0.514 (0.014)	7.860 (0.018)	He/H=0	···	−3.25	1.08
J1923+2141	2018864362679341824	DA	8659 (40)	0.330 (0.007)	7.446 (0.013)	He/H=0	···	−2.78	0.48
J1924+3751	2052569921645067008	DC	6212 (48)	0.699 (0.021)	8.200 (0.023)	H/He=0	···	−3.79	3.52
J1924+5506	2140241890760529408	DA	9534 (52)	0.598 (0.01)	7.999 (0.011)	He/H=0	···	−2.91	0.71

Tableau A.2 *suite page suivante*

Tableau A.2 *(suite)*

Name	Gaia DR2/EDR3*	Sp Type	$T_{\rm eff}$ (K)	$M/M_{\odot}$	$\log g$	Composition	Métaux	$\log L/L_{\odot}$	τ (Gyr)
J1926+4620	2127566548919332608	DA	8095 (27)	0.726 (0.005)	8.209 (0.005)	He/H=0	···	−3.32	1.48
J1927+5644	2142307563871222912	DA	6561 (21)	0.825 (0.006)	8.366 (0.006)	He/H=0	···	−3.79	4.02
J1930−0057	4215241712185612544	DC	7478 (29)	0.647 (0.006)	8.115 (0.006)	log H/He=−3.6	···	−3.42	1.62
J1935−1724	4180014832789446400	DC	4587 (64)	0.738 (0.026)	8.248 (0.027)	He/H=0	···	−4.34	10.00
J1939+6619	2248748668919802496	DC	4899 (20)	0.580 (0.009)	8.019 (0.011)	H/He=0	···	−4.10	6.21
J1940+4240	2077905319548753664	DA+DA	9204 (32)	0.587 (0.006)	7.981 (0.007)	He/H=0	···	−2.96	0.76
J1940+8348	2301882675705225472	DC	4774 (21)	0.770 (0.01)	8.294 (0.011)	He/H=0	···	−4.30	9.68
J1943+5011	2134968663059016832	DA	10351 (58)	0.629 (0.011)	8.046 (0.012)	He/H=0	···	−2.79	0.62
J1944−0425	4209580395521652352	DC	4925 (95)	0.680 (0.066)	8.159 (0.072)	He/H=0	···	−4.16	8.19
J1945+4650	2080526555267050496	DA	5380 (15)	0.664 (0.006)	8.129 (0.006)	He/H=0	···	−3.99	5.16
J1945+4650	2080526555267049984	DA	4902 (17)	0.552 (0.006)	7.955 (0.007)	He/H=0	···	−4.06	5.94
J1945−1719	6871494782188972672	DC	5151 (23)	0.455 (0.013)	7.801 (0.017)	H/He=0	···	−3.90	3.68
J1946+0937	4301829970867752704	DA	6168 (17)	0.583 (0.005)	7.991 (0.006)	He/H=0	···	−3.67	2.15
J1948+6122	2240605346504273280	DA	6063 (36)	0.584 (0.022)	7.993 (0.026)	He/H=0	···	−3.70	2.25
J1949+0747	4298029268399256704	DA	9219 (32)	0.646 (0.005)	8.080 (0.005)	He/H=0	···	−3.02	0.87
J1949−0855	4195385769125206144	DC	6716 (61)	0.674 (0.04)	8.160 (0.045)	log H/He=−3.2	···	−3.63	2.41
J1950+0033	4240231824768647040	DA	5806 (16)	0.548 (0.006)	7.935 (0.007)	He/H=0	···	−3.75	2.31
J1951+4026	2073772770741915264	DC	4196 (37)	0.500 (0.005)	7.884 (0.008)	log H/He=−1.41	···	−4.30	6.62
J1951+4209	2078430778727685632	DA	4992 (27)	0.570 (0.012)	7.984 (0.014)	He/H=0	···	−4.04	5.78
J1954+0115	4240366136980012416	DA	6240 (64)	0.782 (0.027)	8.302 (0.03)	He/H=0	···	−3.83	4.14
J1955−0030	4237044301894347392	DA	9026 (81)	0.862 (0.021)	8.415 (0.023)	He/H=0	···	−3.26	1.66
J1956−0102	4235280071072332672	DA	7776 (13)	0.710 (0.002)	8.187 (0.002)	He/H=0	···	−3.38	1.59
J2004+0109	4237555506083389568	DA	6214 (64)	0.677 (0.017)	8.141 (0.019)	He/H=0	···	−3.74	2.87
J2004−1058	4190734280885088128	DA	7842 (103)	0.773 (0.028)	8.282 (0.03)	He/H=0	···	−3.42	1.88
J2005−1056	4190813690536580608	DC	4670 (11)	0.732 (0.004)	8.239 (0.004)	He/H=0	···	−4.30	9.71
J2006+6143	2237893023118101504	DA	5297 (7)	0.264 (0.003)	7.316 (0.006)	He/H=0	···	−3.60	1.44
J2006−2101	6865904860773722496	DA	5118 (15)	0.541 (0.008)	7.932 (0.01)	He/H=0	···	−3.97	4.21
J2007+3222	2055059112897283712	DA	6330 (31)	0.885 (0.02)	8.457 (0.022)	He/H=0	···	−3.91	4.89
J2008−1619	6874124023727679104	DC	5414 (19)	0.733 (0.009)	8.254 (0.008)	H/He=0	···	−4.06	6.30
J2009+5955	2236900335916533248	DC	9278 (71)	0.744 (0.015)	8.261 (0.016)	log H/He=−4.4	···	−3.13	1.16
J2009−0059	4236208432541189376	DA	7066 (63)	0.813 (0.024)	8.345 (0.026)	He/H=0	···	−3.65	3.16
J2010−1126	6880851931079280512	DA	6238 (34)	0.572 (0.021)	7.972 (0.026)	He/H=0	···	−3.64	2.02
J2010−2146	6853784501721502720	DA	9608 (6)	0.575 (0.001)	7.958 (0.002)	He/H=0	···	−2.88	0.66
J2011+0913	4299397713684601088	DA	6815 (28)	0.414 (0.009)	7.667 (0.015)	He/H=0	···	−3.32	1.11

Tableau A.2 *suite page suivante*

Tableau A.2 *(suite)*

Name	Gaia DR2/EDR3*	Sp Type	$T_{\rm eff}$ (K)	$M/M_{\odot}$	$\log g$	Composition	Métaux	$\log L/L_{\odot}$	τ (Gyr)
J2012−1307	6879638761736608768	DC	9734 (58)	0.630 (0.012)	8.083 (0.013)	log H/He=−4.4	···	−2.94	0.79
J2012−2210	6853523539508720000	DC	5388 (14)	0.606 (0.007)	8.058 (0.008)	H/He=0	···	−3.96	5.06
J2013+0642	4249667902270614272	DC	6277 (14)	0.543 (0.004)	7.949 (0.005)	log H/He=−3.2	···	−3.63	2.02
J2015+0001	4230380819051252736	DC	4895 (14)	0.601 (0.007)	8.036 (0.007)	He/H=0	···	−4.11	7.01
J2015−1222	6879784584465884544	DC	9692 (59)	0.570 (0.011)	7.983 (0.014)	log H/He=−4.4	···	−2.89	0.69
J2020−0005	4230332092645516672	DA	6976 (36)	0.571 (0.01)	7.965 (0.013)	He/H=0	···	−3.44	1.50
J2021+5454	2185261016407220224	DC	5821 (25)	0.649 (0.008)	8.125 (0.009)	H/He=0	···	−3.86	4.11
J2022+8333	2302010356492847744	DC	5553 (49)	0.518 (0.015)	7.912 (0.018)	H/He=0	···	−3.83	3.16
J2023+0759	1752188773770447872	DC	6290 (49)	0.595 (0.025)	8.037 (0.029)	log H/He=−3.2	···	−3.67	2.26
J2027+0523	4246381595156273792	DA	7065 (27)	0.559 (0.009)	7.944 (0.01)	He/H=0	···	−3.41	1.41
J2030+0655	1748816983925915776	DA	5942 (20)	0.669 (0.007)	8.131 (0.008)	He/H=0	···	−3.82	3.29
J2030+0729	1748922296525519872	DC	8631 (33)	0.629 (0.006)	8.084 (0.006)	log H/He=−4.0	···	−3.15	1.08
J2030+4015	2067343097310013056	DC	5949 (41)	0.620 (0.021)	8.078 (0.024)	log H/He=−3.0	···	−3.79	3.30
J2031+3934	2064284054100290048	DC	4676 (24)	0.555 (0.012)	7.962 (0.014)	He/H=0	···	−4.14	6.88
J2031−1450	6875432476922523520	DC	4549 (21)	0.617 (0.012)	8.063 (0.013)	He/H=0	···	−4.25	8.65
J2031−1658	6862687522250677376	DAZ	5611 (11)	0.555 (0.004)	7.974 (0.005)	He/H=0	log Ca/H=−10.15	−3.84	3.51
J2033+3954	2064689567732385792	DA	6017 (12)	0.864 (0.004)	8.426 (0.004)	He/H=0	···	−3.98	5.31
J2034+1345	1756261467922806784	DA	7194 (79)	0.884 (0.021)	8.452 (0.024)	He/H=0	···	−3.68	3.63
J2038+0037	4231193525645520768	DA	7231 (68)	0.665 (0.03)	8.117 (0.034)	He/H=0	···	−3.46	1.72
J2041+4320	2069588300054515200	DA	7023 (27)	0.651 (0.009)	8.097 (0.01)	He/H=0	···	−3.50	1.80
J2041−0520	6914243308941804288	DC	4936 (30)	0.601 (0.017)	8.035 (0.019)	He/H=0	···	−4.09	6.78
J2042+0031	4228210894197669760	DC	4583 (38)	0.505 (0.025)	7.877 (0.03)	He/H=0	···	−4.14	6.43
J2042+3752	2063293355469201152	DA	6070 (47)	0.910 (0.024)	8.494 (0.027)	He/H=0	···	−4.01	5.50
J2044+4030	2066035777984385792	DAH	7508 (40)	0.876 (0.009)	8.440 (0.01)	He/H=0	···	−3.60	3.18
J2045+0227	4231922059473951616	DA	10596 (61)	1.023 (0.006)	8.665 (0.008)	He/H=0	···	−3.16	1.83
J2045+0424	1735171735387308160	DA	6355 (41)	0.936 (0.026)	8.534 (0.031)	He/H=0	···	−3.96	5.14
J2045+4146	2066251179185657856	DC	9597 (76)	0.655 (0.012)	8.124 (0.014)	log H/He=−4.4	···	−2.99	0.87
J2045+8105	2298135638862051968	DA	8019 (81)	0.352 (0.01)	7.511 (0.018)	He/H=0	···	−2.96	0.63
J2045−0016	4227915744043939584	DA*	7284 (44)	0.545 (0.023)	7.918 (0.028)	He/H=0	···	−3.34	1.26
J2045−0710	6907079269131974912	DA*	4966 (15)	0.243 (0.012)	7.269 (0.028)	He/H=0	···	−3.71	1.75
J2045−1612	6886287332455279104	DA	7461 (46)	0.594 (0.022)	8.001 (0.026)	He/H=0	···	−3.34	1.33
J2046−0644	6907108371830928768	DA	9175 (52)	0.547 (0.012)	7.912 (0.015)	He/H=0	···	−2.93	0.70
J2046−0710	6907031749613795968	DAH	8835 (102)	0.836 (0.018)	8.375 (0.021)	He/H=0	···	−3.27	1.61
J2046−1413	6887386745296346624	DA	8544 (41)	0.567 (0.008)	7.950 (0.01)	He/H=0	···	−3.08	0.88

Tableau A.2 *suite page suivante*

Tableau A.2 *(suite)*

Name	Gaia DR2/EDR3*	Sp Type	$T_{\rm eff}$ (K)	$M/M_{\odot}$	$\log g$	Composition	Métaux	$\log L/L_{\odot}$	τ (Gyr)
J2048+5110	2169971345155578752	DC	4986 (17)	0.612 (0.008)	8.053 (0.009)	He/H=0	···	−4.08	6.72
J2050+2630	1844125748497557632	DA	4958 (7)	0.245 (0.002)	7.275 (0.003)	He/H=0	···	−3.71	1.77
J2050+7740	2290785163113859712	DC	5030 (31)	0.557 (0.012)	7.961 (0.015)	He/H=0	···	−4.02	5.22
J2051+5636	2189957816542364800	DA	7075 (43)	0.607 (0.012)	8.025 (0.014)	He/H=0	···	−3.45	1.58
J2051−2452	6805808514433280000	DA	7540 (24)	0.647 (0.004)	8.088 (0.005)	He/H=0	···	−3.38	1.48
J2052+0133	4228576550540445184	DC*	5499 (22)	0.526 (0.01)	7.925 (0.012)	H/He=0	···	−3.85	3.45
J2052−2206	6808651507904773888	DC	7665 (27)	0.664 (0.004)	8.142 (0.005)	log H/He=−3.6	···	−3.39	1.57
J2053−0702	6909994246262080000	DQ	6741 (25)	0.634 (0.03)	8.097 (0.033)	H/He=0	log C/He=−5.10	−3.59	2.05
J2056+0621	1736555475066523008	DA	9249 (34)	0.377 (0.009)	7.561 (0.014)	He/H=0	···	−2.73	0.46
J2056+4313	2162041628635165824	DZ	9069 (70)	0.620 (0.012)	8.068 (0.014)	log H/He=−5.0	log Ca/He=−10.75	−3.05	0.93
J2056−0450	6913810483611035776	DC	4383 (21)	0.494 (0.007)	7.859 (0.009)	He/H=0	···	−4.21	6.99
J2056−2717	6801786157301360896	DA	9011 (57)	0.610 (0.018)	8.021 (0.021)	He/H=0	···	−3.02	0.85
J2057+0944	1750460792464604672	DA	7308 (60)	0.857 (0.023)	8.410 (0.025)	He/H=0	···	−3.63	3.25
J2057+2316	1839493604790492032	DC	5393 (26)	0.388 (0.015)	7.664 (0.022)	log H/He=−5.0	···	−3.75	2.48
J2058+1657	1764481588648685440	DZA*	5770 (27)	0.648 (0.023)	8.124 (0.025)	log H/He=−1.0	log Ca/He=−8.07	−3.87	4.28
J2059+5517	2188860027203347968	DC	4533 (14)	0.566 (0.006)	7.981 (0.007)	He/H=0	···	−4.21	7.65
J2059−0033	6917473674103954560	DA	7688 (30)	0.607 (0.011)	8.022 (0.013)	He/H=0	···	−3.30	1.27
J2100+5051	2169025009235266816	DA	9374 (28)	0.611 (0.004)	8.021 (0.005)	He/H=0	···	−2.95	0.77
J2101+3148	1864760695541016832	DQ	9206 (32)	0.508 (0.004)	7.876 (0.004)	H/He=0	log C/He=−4.73	−2.92	0.69
J2102+1912	1789361097242243584	DA	6720 (18)	0.625 (0.005)	8.057 (0.005)	He/H=0	···	−3.56	1.90
J2102+2457	1841254644460354688	DA	6119 (13)	0.702 (0.004)	8.181 (0.003)	He/H=0	···	−3.79	3.42
J2103−0024	2690065251596080384	DC	6099 (29)	0.675 (0.023)	8.164 (0.026)	H/He=0	···	−3.80	3.55
J2103−0055	6917223054171248256	DC	4903 (30)	0.561 (0.03)	7.970 (0.036)	He/H=0	···	−4.07	6.13
J2105+0602	1736329589850340736	DA	6171 (41)	0.637 (0.031)	8.078 (0.035)	He/H=0	···	−3.72	2.49
J2106+0106	2690697646876721152	DA	6154 (14)	0.585 (0.006)	7.993 (0.007)	He/H=0	···	−3.68	2.17
J2107+0740	1737167215848315264	DA	6922 (21)	0.571 (0.006)	7.965 (0.006)	He/H=0	···	−3.45	1.53
J2108−0033	2689915958535673472	DA	6271 (39)	0.677 (0.024)	8.141 (0.028)	He/H=0	···	−3.73	2.78
J2108−0312	6912866381081015552	DC	4986 (20)	0.438 (0.009)	7.768 (0.012)	H/He=0	···	−3.94	3.88
J2109+0131	2690830511689102336	DA	6119 (51)	0.845 (0.022)	8.397 (0.024)	He/H=0	···	−3.93	4.96
J2109+0628	1733833492297878656	DA	6884 (49)	0.903 (0.027)	8.482 (0.03)	He/H=0	···	−3.78	4.18
J2109−0111	2688986325747403264	DA	7656 (55)	0.693 (0.022)	8.160 (0.025)	He/H=0	···	−3.39	1.59
J2110−2129	6831993452567326592	DA	6073 (12)	0.660 (0.005)	8.116 (0.005)	He/H=0	···	−3.77	2.90
J2111−0036	2689129601561746560	DQ	7159 (48)	0.510 (0.021)	7.888 (0.027)	H/He=0	log C/He=−6.19	−3.37	1.33
J2112+0622	1733782571164433408	DC	9898 (50)	0.589 (0.008)	8.015 (0.01)	log H/He=−4.6	···	−2.87	0.69

Tableau A.2 *suite page suivante*

Tableau A.2 *(suite)*

Name	Gaia DR2/EDR3*	Sp Type	$T_{\rm eff}$ (K)	$M/M_{\odot}$	$\log g$	Composition	Métaux	$\log L/L_{\odot}$	τ (Gyr)
J2112−2922	6788656957673130112	DC	9524 (37)	0.599 (0.006)	8.032 (0.007)	log H/He=−4.4	···	−2.95	0.78
J2113+0727	1739921801713625600	DA	6390 (16)	0.562 (0.004)	7.952 (0.006)	He/H=0	···	−3.59	1.85
J2113+2621	1841683423932168832	DA	8073 (28)	0.332 (0.007)	7.457 (0.013)	He/H=0	···	−2.92	0.59
J2115+0400	1732272185785761408	DAH	6460 (45)	0.638 (0.029)	8.078 (0.032)	He/H=0	···	−3.64	2.17
J2115−0741	6898489884295407488	DA	8230 (35)	0.725 (0.01)	8.208 (0.011)	He/H=0	···	−3.29	1.42
J2116−0724	6898521877506794880	DC	4665 (12)	0.326 (0.006)	7.509 (0.01)	He/H=0	···	−3.93	3.04
J2118+1120	1746315255670491904	DA	5996 (29)	0.738 (0.012)	8.237 (0.013)	He/H=0	···	−3.86	4.14
J2118−0737	6898455661995166336	DC	4144 (37)	0.498 (0.032)	7.866 (0.04)	He/H=0	···	−4.31	7.78
J2118−0737	6898453913943607040	DC	6352 (49)	0.645 (0.053)	8.116 (0.06)	log H/He=−3.2	···	−3.70	2.65
J2119−0300	2685318075783946368	DA	8939 (43)	0.380 (0.011)	7.570 (0.018)	He/H=0	···	−2.79	0.51
J2120+1303	1747132467687929600	DA	8957 (44)	0.606 (0.01)	8.015 (0.011)	He/H=0	···	−3.03	0.85
J2120+2320	1792207664128299776	DA	6130 (41)	0.652 (0.027)	8.104 (0.03)	He/H=0	···	−3.75	2.71
J2120+5819	2191146977029443584	DA	7921 (58)	0.584 (0.01)	7.982 (0.012)	He/H=0	···	−3.23	1.11
J2121−0130	2685959542034846464	DA	6573 (14)	0.638 (0.005)	8.077 (0.005)	He/H=0	···	−3.61	2.07
J2122+0413	2693095097621419648	DA	4975 (10)	0.471 (0.004)	7.811 (0.006)	He/H=0	···	−3.96	3.69
J2123+1917	1785659488269249408	DA	9731 (40)	0.631 (0.009)	8.053 (0.011)	He/H=0	···	−2.91	0.73
J2124+0638	1738863620555712512	DC	6048 (43)	0.630 (0.022)	8.094 (0.024)	log H/He=−3.0	···	−3.77	3.13
J2125+2752	1847460116290325888	DA	6058 (59)	0.609 (0.029)	8.034 (0.034)	He/H=0	···	−3.73	2.42
J2126+0729	1739397914486670208	DA	6652 (41)	0.845 (0.018)	8.395 (0.02)	He/H=0	···	−3.78	4.06
J2127+0229	2691890685712023552	DA	7014 (65)	0.816 (0.035)	8.349 (0.04)	He/H=0	···	−3.66	3.25
J2127+2632	1847118992806013568	DA	6464 (41)	0.589 (0.018)	7.999 (0.021)	He/H=0	···	−3.59	1.93
J2129+0013	2687768066863960576	DA	8860 (30)	0.244 (0.002)	7.158 (0.006)	He/H=0	···	−2.59	0.29
J2130+1817	1786065654735928064	DC	8268 (52)	0.605 (0.021)	8.046 (0.025)	log H/He=−4.0	···	−3.20	1.14
J2130+2537	1798927947915336448	DC	5830 (30)	0.458 (0.012)	7.799 (0.016)	log H/He=−3.0	···	−3.68	2.12
J2131+0659	1739109601921701120	DAH :	6718 (55)	0.711 (0.05)	8.192 (0.056)	He/H=0	···	−3.64	2.52
J2132+2654	1847190701579945856	DC	6185 (36)	0.641 (0.014)	8.110 (0.015)	H/He=0	···	−3.75	2.91
J2133+2414	1797472370615364992	DA	6381 (22)	0.845 (0.006)	8.397 (0.006)	He/H=0	···	−3.86	4.49
J2133−0611	2670770991487735424	DC	6013 (24)	0.595 (0.019)	8.038 (0.021)	H/He=0	···	−3.75	2.79
J2134+3655	1951870157081161216	DA	7791 (27)	0.734 (0.005)	8.223 (0.005)	He/H=0	···	−3.40	1.67
J2135+0106	2688307166863547264	DA	6071 (28)	0.496 (0.042)	7.837 (0.055)	He/H=0	···	−3.62	1.79
J2135+4633	1977417206669775744	DA	4865 (21)	0.500 (0.01)	7.865 (0.013)	He/H=0	···	−4.03	4.98
J2136−1318	6842831888437047680	DA	9883 (12)	0.452 (0.002)	7.724 (0.002)	He/H=0	···	−2.70	0.46
J2138+1123	1766620929036759808	DAH	9910 (46)	0.641 (0.013)	8.068 (0.015)	He/H=0	···	−2.88	0.71
J2138+2309	1794118516552814336	DA	10179 (56)	0.528 (0.007)	7.908 (0.009)	log H/He=−1.0	···	−2.76	0.55

Tableau A.2 *suite page suivante*

Tableau A.2 *(suite)*

Name	Gaia DR2/EDR3*	Sp Type	$T_{\rm eff}$ (K)	$M/M_{\odot}$	$\log g$	Composition	Métaux	$\log L/L_{\odot}$	τ (Gyr)
J2138−0056	2686607906002083328	DC	4632 (59)	0.442 (0.022)	7.778 (0.042)	log H/He=−1.74	···	−4.08	4.85
J2139−1245	6844375121726139520	DA	8084 (73)	0.872 (0.01)	8.431 (0.011)	He/H=0	···	−3.47	2.54
J2140+2140	1793628851625008512	DA	10280 (56)	0.600 (0.014)	7.998 (0.017)	He/H=0	···	−2.78	0.59
J2141+0923	1741417790361772160	DA	9199 (39)	0.503 (0.007)	7.831 (0.008)	He/H=0	···	−2.88	0.64
J2142+0805	2701893698904233216	DA	4825 (13)	0.420 (0.006)	7.714 (0.008)	He/H=0	···	−3.96	3.58
J2142+1328	1767494804558717824	DA	7616 (33)	0.599 (0.007)	8.010 (0.007)	He/H=0	···	−3.31	1.28
J2142+1329	1767494868982336000	DC :	5057 (31)	0.541 (0.014)	7.955 (0.017)	H/He=0	···	−4.01	5.33
J2142+2059	1792830060723673472	DQ	8239 (129)	0.578 (0.012)	8.001 (0.014)	H/He=0	log C/He=−5.72	−3.18	1.08
J2142+2252	1794409921493969792	DZ	8839 (38)	0.504 (0.006)	7.870 (0.007)	log H/He=−4.0	log Ca/He=−10.46	−2.99	0.76
J2142−0036	2675091174536113792	DC*	6689 (38)	0.687 (0.022)	8.180 (0.024)	log H/He=−3.2	···	−3.65	2.58
J2143+1934	1786444230333492480	DA	6089 (45)	0.598 (0.034)	8.016 (0.039)	He/H=0	···	−3.71	2.31
J2143+2829	1801199745097109632	DA	5953 (33)	0.571 (0.025)	7.972 (0.031)	He/H=0	···	−3.72	2.27
J2143−0659	2667464656943675392	DA	8922 (26)	0.873 (0.004)	8.431 (0.004)	He/H=0	···	−3.29	1.82
J2144+4753	1977776953135753856	DA	7819 (50)	0.631 (0.01)	8.061 (0.012)	He/H=0	···	−3.29	1.29
J2145+1106	1765847182089067008	DC	3964 (92)	0.603 (0.06)	8.043 (0.067)	He/H=0	···	−4.48	10.03
J2145+1106	1765847186383576832	DC	3566 (151)	0.560 (0.11)	7.975 (0.129)	He/H=0	···	−4.62	10.16
J2146+1550	1772407315138035584	DA	7416 (41)	0.240 (0.009)	7.175 (0.026)	He/H=0	···	−2.92	0.52
J2146+4626	1974579637737581568	DC	6017 (71)	0.687 (0.032)	8.183 (0.035)	H/He=0	···	−3.83	3.91
J2147+1127	1765881576187554432	DA :	4927 (19)	0.550 (0.018)	7.952 (0.022)	He/H=0	···	−4.05	5.74
J2147−0647	2667108891917960960	DA	7632 (37)	0.634 (0.017)	8.066 (0.02)	He/H=0	···	−3.34	1.38
J2147−0824	2666306798185155200	DA	6022 (17)	0.554 (0.008)	7.943 (0.01)	He/H=0	···	−3.69	2.12
J2147−2910	6809585263858474240	DZ	8301 (90)	0.744 (0.022)	8.262 (0.023)	H/He=0	···	−3.32	1.54
J2148−2821	6809702159983236992	DC	4600 (94)	0.954 (0.061)	8.584 (0.095)	log H/He=−2.55	···	−4.56	8.07
J2149+0415	2696628687474414208	DA	5137 (8)	0.273 (0.003)	7.352 (0.006)	He/H=0	···	−3.68	1.66
J2150+1953	1780497934010525312	DA	8584 (57)	0.670 (0.019)	8.121 (0.021)	He/H=0	···	−3.17	1.11
J2150−0113	2674012072593383168	DQ	8652 (38)	0.532 (0.016)	7.921 (0.021)	H/He=0	log C/He=−5.22	−3.05	0.86
J2150−0439	2669936427801840256	DC	4564 (28)	0.610 (0.005)	8.067 (0.007)	log H/He=−2.49	···	−4.25	7.19
J2151+0031	2681243457490130304	DC*	8041 (45)	0.672 (0.021)	8.154 (0.023)	log H/He=−3.8	···	−3.31	1.42
J2151+2305	1795037875776233984	DA	9311 (72)	0.860 (0.014)	8.411 (0.015)	He/H=0	···	−3.21	1.47
J2151+5917	2202703050401536000	DAH	5075 (7)	0.564 (0.003)	7.973 (0.004)	He/H=0	···	−4.01	5.08
J2153+0726	2700725635303873024	DA	8796 (58)	0.615 (0.014)	8.031 (0.017)	He/H=0	···	−3.07	0.91
J2153+2948	1897310564741680512	DA	6194 (39)	0.747 (0.023)	8.249 (0.026)	He/H=0	···	−3.81	3.85
J2154+1300	1767957488499891968	DAZ*	5187 (20)	0.576 (0.013)	8.011 (0.015)	He/H=0	log Ca/H=−9.49	−4.00	5.37
J2154+2657	1799905929149972352	DA	6437 (32)	0.565 (0.018)	7.958 (0.022)	He/H=0	···	−3.58	1.83

Tableau A.2 *suite page suivante*

Tableau A.2 *(suite)*

Name	Gaia DR2/EDR3*	Sp Type	$T_{\rm eff}$ (K)	$M/M_{\odot}$	$\log g$	Composition	Métaux	$\log L/L_{\odot}$	τ (Gyr)
J2155+1201	1766164322474245376	DA	6051 (25)	0.610 (0.052)	8.035 (0.062)	He/H=0	···	−3.73	2.43
J2155+4103	1959573541696236032	DZ	6525 (53)	0.775 (0.014)	8.313 (0.014)	log H/He=−2.0	log Ca/He=−10.90	−3.77	3.62
J2155−2750	6617996741403360128	DC	5139 (13)	0.437 (0.006)	7.767 (0.007)	H/He=0	···	−3.89	3.46
J2156+0559	2697327113581223936	DQ	6730 (41)	0.561 (0.024)	7.978 (0.029)	H/He=0	log C/He=−6.57	−3.52	1.74
J2157+2705	1892992267183979776	DC	4548 (14)	0.428 (0.009)	7.735 (0.012)	He/H=0	···	−4.08	4.86
J2158+1814	1779145878305570944	DA	9544 (72)	1.007 (0.019)	8.641 (0.024)	He/H=0	···	−3.33	2.34
J2158+5804	2199338643594260352	DA	6617 (40)	0.449 (0.009)	7.741 (0.012)	He/H=0	···	−3.41	1.29
J2158−0239	2676567307551465088	DC	4852 (10)	0.517 (0.005)	7.895 (0.006)	He/H=0	···	−4.04	5.42
J2158−0240	2676566272464334720	DC	4789 (7)	0.506 (0.008)	7.876 (0.01)	He/H=0	···	−4.06	5.52
J2200+5822	2199371701965748992	DA	5538 (21)	0.608 (0.008)	8.037 (0.008)	He/H=0	···	−3.89	3.36
J2201+0219	2683345934175922176	DZ	4580 (20)	0.521 (0.026)	7.921 (0.031)	log H/He=−5.0	log Ca/He=−10.80	−4.17	6.10
J2202+0237	2683452758602312192	DA	5825 (13)	0.727 (0.007)	8.222 (0.007)	He/H=0	···	−3.91	4.39
J2202+3848	1956112657053495296	DA	9324 (32)	0.570 (0.005)	7.951 (0.006)	He/H=0	···	−2.92	0.71
J2203+2434	1795467063268699264	DC	6274 (63)	0.541 (0.024)	7.947 (0.03)	log H/He=−3.2	···	−3.63	2.01
J2204−0109	2677191860220980480	DC	4732 (48)	0.524 (0.046)	7.908 (0.056)	He/H=0	···	−4.10	6.10
J2204−0331	2675503117734361344	DC	6248 (93)	0.912 (0.048)	8.517 (0.055)	log H/He=−3.0	···	−3.98	4.83
J2206+0825	2722195455261832448	DA	6089 (62)	0.836 (0.051)	8.383 (0.057)	He/H=0	···	−3.93	4.93
J2206−0103	2677172996724050048	DAP*	6467 (57)	0.653 (0.041)	8.103 (0.047)	He/H=0	···	−3.65	2.27
J2206−0112	2677157569201482624	DC	6090 (67)	0.937 (0.074)	8.557 (0.087)	H/He=0	···	−4.05	5.29
J2207+3428	1900382604528495744	DA	10076 (22)	0.613 (0.003)	8.021 (0.003)	He/H=0	···	−2.83	0.64
J2208+2221	1782874287875828864	DA	9143 (48)	0.975 (0.013)	8.589 (0.016)	He/H=0	···	−3.36	2.40
J2209+1429	2735175263041913088	DA	7591 (18)	0.686 (0.003)	8.149 (0.004)	He/H=0	···	−3.40	1.60
J2211+1136	2727596187657230592	DAH	9122 (168)	1.316 (0.011)	9.362 (0.04)	He/H=0	···	−4.01	2.50
J2212+1916	1777927516344108416	DA	6918 (74)	0.878 (0.038)	8.444 (0.042)	He/H=0	···	−3.75	3.95
J2212−1429	2600033326799287296	DA	7758 (20)	0.272 (0.002)	7.282 (0.005)	He/H=0	···	−2.90	0.54
J2213+0349	2707796667595813248	DC	5043 (13)	0.514 (0.014)	7.888 (0.018)	He/H=0	···	−3.97	4.10
J2213+2925	1894996161487458048	DA	6923 (43)	0.972 (0.011)	8.589 (0.013)	He/H=0	···	−3.85	4.53
J2214+0650	2720807150033137024	DC	5863 (36)	0.649 (0.025)	8.124 (0.027)	H/He=0	···	−3.85	3.96
J2214+3727	1955134710179436672	DC	6266 (32)	0.828 (0.007)	8.392 (0.008)	log H/He=−3.2	···	−3.89	4.42
J2215+3158	1898875311527105152	DA	7221 (30)	0.646 (0.008)	8.089 (0.01)	He/H=0	···	−3.45	1.66
J2215−0728	2619561508006403712	DA	5818 (61)	0.739 (0.055)	8.240 (0.061)	He/H=0	···	−3.92	4.56
J2217+3707	1907041590544054656	DC	4546 (17)	0.558 (0.007)	7.968 (0.009)	He/H=0	···	−4.20	7.43
J2218+0319	2706795626682842752	DA	8781 (42)	0.619 (0.01)	8.037 (0.011)	He/H=0	···	−3.08	0.93
J2218+2123	1778839767397091200	DQ	8075 (42)	0.543 (0.016)	7.943 (0.019)	H/He=0	log C/He=−5.37	−3.19	1.05

Tableau A.2 *suite page suivante*

Tableau A.2 *(suite)*

Name	Gaia DR2/EDR3*	Sp Type	$T_{\rm eff}$ (K)	$M/M_{\odot}$	$\log g$	Composition	Métaux	$\log L/L_{\odot}$	τ (Gyr)
J2218+3908	1956838712683591296	DZ	8354 (24)	0.576 (0.004)	7.999 (0.005)	log H/He=−4.0	log Ca/He=−8.72	−3.16	1.04
J2218+4839	1999615350008375552	DA+DC*	7269 (22)	0.479 (0.005)	7.797 (0.006)	He/H=0	···	−3.28	1.09
J2218+5602	2006217676803960960	DC	4335 (19)	0.391 (0.009)	7.660 (0.013)	He/H=0	···	−4.13	4.95
J2219+1353	2734163982926890624	DC	6876 (59)	0.637 (0.039)	8.101 (0.044)	log H/He=−3.4	···	−3.56	1.95
J2219+2122	1778836056545324160	DC	4764 (19)	0.210 (0.007)	7.162 (0.018)	He/H=0	···	−3.74	1.81
J2219+4805	1987576380575220352	DA	6274 (37)	0.633 (0.011)	8.072 (0.013)	He/H=0	···	−3.69	2.33
J2219−0930	2615280147167407104	DA	6968 (70)	0.912 (0.032)	8.495 (0.037)	He/H=0	···	−3.77	4.12
J2220−0041	2677851743291189888	DA	7600 (41)	0.543 (0.017)	7.913 (0.021)	He/H=0	···	−3.26	1.13
J2220−0600	2625820512307604352	DA	6071 (46)	0.826 (0.033)	8.369 (0.037)	He/H=0	···	−3.93	4.88
J2221−0408	2626677723354947968	DA	8195 (39)	0.444 (0.018)	7.719 (0.026)	He/H=0	···	−3.02	0.75
J2223+2319	1878189370339859328	DAH	8927 (85)	0.958 (0.014)	8.563 (0.017)	He/H=0	···	−3.39	2.45
J2224+2158	1874951106733026048	DA	8234 (30)	0.619 (0.007)	8.039 (0.008)	He/H=0	···	−3.19	1.09
J2224+2716	1881612734154248320	DAM	9609 (109)	0.712 (0.019)	8.183 (0.021)	He/H=0	···	−3.01	0.91
J2224−1615	2595728287804350720	DAZ	9725 (51)	0.648 (0.008)	8.081 (0.008)	He/H=0	···	−2.92	0.76
J2225+1835	1777269424274555776	DC	7394 (32)	0.652 (0.007)	8.125 (0.007)	log H/He=−3.6	···	−3.44	1.69
J2225+3005	1894563160062140416	DA	7848 (63)	0.853 (0.014)	8.403 (0.016)	He/H=0	···	−3.50	2.60
J2225+6357	2205493129867600256	DC	5105 (30)	0.504 (0.012)	7.868 (0.014)	He/H=0	···	−3.94	3.52
J2225−0113	2629899631727265920	DA	5032 (33)	0.537 (0.07)	7.928 (0.086)	He/H=0	···	−4.00	4.72
J2225−0114	2629899631727265280	DA	5677 (24)	0.416 (0.022)	7.687 (0.033)	He/H=0	···	−3.66	1.75
J2226+0112	2702527013306504064	DC*	6937 (39)	0.716 (0.018)	8.224 (0.019)	log H/He=−3.4	···	−3.61	2.56
J2227+1753	2737921155893258496	DAZ	6739 (26)	0.555 (0.007)	7.968 (0.009)	He/H=0	log Ca/H=−8.89	−3.52	1.71
J2228+1207	2730508416002618752	DZ	6885 (18)	0.634 (0.005)	8.096 (0.005)	log H/He=−4.0	log Ca/He=−9.73	−3.55	1.93
J2229+2327	1875613386395668864	DA	5052 (19)	0.672 (0.011)	8.145 (0.012)	He/H=0	···	−4.11	7.40
J2229+3024	1900545847646195840	DA	9860 (66)	0.323 (0.006)	7.409 (0.013)	He/H=0	···	−2.53	0.32
J2229+3927	1909045549271308928	DA	7038 (36)	0.880 (0.009)	8.447 (0.01)	He/H=0	···	−3.72	3.80
J2230+1256	2730989658498251776	DA	7522 (32)	0.893 (0.007)	8.465 (0.008)	He/H=0	···	−3.62	3.31
J2230+1523	2736054627915080448	DA	5308 (9)	0.670 (0.007)	8.139 (0.008)	He/H=0	···	−4.02	5.71
J2230+2254	1875301369907249024	DC	5734 (20)	0.685 (0.007)	8.181 (0.008)	H/He=0	···	−3.92	4.82
J2230−0023	2630076966632012160	DA	9432 (22)	0.523 (0.004)	7.867 (0.005)	He/H=0	···	−2.86	0.62
J2230−0945	2609067704606647680	DA	7279 (32)	0.546 (0.01)	7.919 (0.013)	He/H=0	···	−3.34	1.27
J2231+0137	2702619273499003776	DA	6718 (43)	0.729 (0.02)	8.220 (0.023)	He/H=0	···	−3.65	2.73
J2231+0906	2711092621203766912	DZ	5626 (52)	0.571 (0.045)	8.001 (0.052)	log H/He=−2.0	log Ca/He=−9.96	−3.85	3.70
J2231−0204	2628823381642484864	DC	6069 (91)	0.651 (0.044)	8.127 (0.049)	log H/He=−3.0	···	−3.79	3.35
J2231−0902	2621138310760174592	DA	6097 (30)	0.634 (0.023)	8.075 (0.026)	He/H=0	···	−3.74	2.58

Tableau A.2 *suite page suivante*

Tableau A.2 *(suite)*

Name	Gaia DR2/EDR3*	Sp Type	$T_{\rm eff}$ (K)	$M/M_{\odot}$	$\log g$	Composition	Métaux	$\log L/L_{\odot}$	τ (Gyr)
J2232+2155	1874375473741569664	DA	7233 (60)	0.758 (0.023)	8.261 (0.025)	He/H=0	···	−3.55	2.37
J2232+3205	1901175799087508608	DA	6348 (24)	0.508 (0.011)	7.858 (0.014)	He/H=0	···	−3.55	1.64
J2232−0744	2621565333592122496	DQ	6377 (11)	0.725 (0.01)	8.239 (0.011)	H/He=0	log C/He=−5.47	−3.77	3.48
J2234+1456	2733055335904034432	DA	6320 (16)	0.607 (0.005)	8.029 (0.006)	He/H=0	···	−3.65	2.13
J2234+5543	2006489634151514112	DA	6962 (24)	0.632 (0.006)	8.066 (0.007)	He/H=0	···	−3.50	1.76
J2235+6439	2205619397609830656	DC	4809 (37)	0.437 (0.018)	7.767 (0.025)	H/He=0	···	−4.00	4.30
J2236+5303	2002232359484482304	DC	10998 (80)	0.647 (0.011)	8.106 (0.012)	log H/He=−5.0	···	−2.74	0.59
J2237+3206	1901132845117712256	DA	6536 (56)	0.796 (0.021)	8.321 (0.024)	He/H=0	···	−3.77	3.77
J2238+1313	2731772377633104128	DAZ	8147 (41)	0.591 (0.01)	8.023 (0.011)	He/H=0	log Ca/H=−7.50	−3.21	1.15
J2239+0018	2654379433485461632	DC	4582 (73)	0.773 (0.095)	8.315 (0.141)	log H/He=−2.33	···	−4.39	8.24
J2239+1904	2833291244003645440	DC	6090 (90)	0.908 (0.081)	8.512 (0.093)	H/He=0	···	−4.02	5.18
J2239−0011	2653903963426062208	DA	7482 (72)	0.913 (0.027)	8.496 (0.031)	He/H=0	···	−3.65	3.50
J2240−0303	2625541412447911424	DC	5060 (29)	0.581 (0.016)	8.001 (0.018)	He/H=0	···	−4.03	5.57
J2241+0432	2704955971931335168	DQ	5962 (15)	0.533 (0.014)	7.934 (0.018)	H/He=0	log C/He=−6.84	−3.71	2.33
J2241+0801	2715786505062211840	DA	5821 (32)	0.639 (0.016)	8.084 (0.018)	He/H=0	···	−3.83	3.12
J2241+1332	2731866347221858432	DA	5989 (17)	0.751 (0.007)	8.257 (0.008)	He/H=0	···	−3.88	4.31
J2241+3646	1904585689586580736	DA	7261 (22)	0.661 (0.006)	8.112 (0.008)	He/H=0	···	−3.45	1.69
J2241−1940	2400975126071250944	DC	5215 (69)	0.493 (0.049)	7.869 (0.061)	H/He=0	···	−3.91	4.07
J2242+0048	2654423998066862464	DC	3859 (35)	0.368 (0.011)	7.564 (0.025)	log H/He=−0.71	···	−4.26	9.95
J2242+1403	2731922422315395968	DA	7943 (55)	0.605 (0.016)	8.018 (0.019)	He/H=0	···	−3.24	1.16
J2243−0127	2652784694950778624	DA	9126 (47)	0.597 (0.007)	7.999 (0.008)	He/H=0	···	−2.99	0.80
J2244+1305	2731591469315403520	DA	6716 (46)	0.433 (0.028)	7.708 (0.041)	He/H=0	···	−3.37	1.20
J2244+1513	2732515029018125312	DA	5724 (33)	0.555 (0.014)	7.948 (0.018)	He/H=0	···	−3.78	2.44
J2244+3835	1929002200706278144	DC	4994 (34)	0.550 (0.022)	7.951 (0.027)	He/H=0	···	−4.02	5.31
J2245−1002	2608247533357159424	DA	8773 (45)	0.827 (0.01)	8.362 (0.011)	He/H=0	···	−3.28	1.59
J2248+0436	2705188999676567936	DA	9824 (32)	0.627 (0.011)	8.046 (0.012)	He/H=0	···	−2.89	0.70
J2249+2236	2836609093355562496	DA	10304 (30)	1.007 (0.003)	8.638 (0.004)	He/H=0	···	−3.19	1.89
J2249+3623	1903614958258305536	DA	5059 (20)	0.595 (0.01)	8.023 (0.011)	He/H=0	···	−4.04	5.89
J2249−0608	2611836167511100800	DC	6837 (106)	0.881 (0.079)	8.470 (0.09)	log H/He=−3.4	···	−3.79	3.83
J2250+0351	2656959231361709056	DA	6448 (52)	0.783 (0.027)	8.302 (0.029)	He/H=0	···	−3.78	3.78
J2251+2939	1884744525522874880	DA	5516 (12)	0.386 (0.004)	7.624 (0.006)	He/H=0	···	−3.68	1.76
J2251−1015	2605271846869877632	DA	5978 (22)	0.651 (0.013)	8.102 (0.014)	He/H=0	···	−3.79	2.97
J2252+3928	1929287700069881856	DC	4872 (22)	0.556 (0.01)	7.963 (0.012)	He/H=0	···	−4.07	6.17
J2253+8130	2286958798223194624	DC	5044 (74)	0.491 (0.023)	7.846 (0.029)	He/H=0	···	−3.95	3.64

Tableau A.2 *suite page suivante*

Tableau A.2 *(suite)*

Name	Gaia DR2/EDR3*	Sp Type	$T_{\rm eff}$ (K)	$M/M_{\odot}$	$\log g$	Composition	Métaux	$\log L/L_{\odot}$	τ (Gyr)
J2253−0647	2611561706216413696	DZ	4323 (2)	0.657 (0.002)	8.141 (0.002)	log H/He=−5.0	log Ca/He=−9.25	−4.39	8.03
J2253−1438	2410908771246898176	DC :	4989 (19)	0.496 (0.01)	7.877 (0.011)	H/He=0	···	−4.00	4.86
J2254+1323	2719852224183359360	DC	4338 (15)	0.449 (0.012)	7.776 (0.016)	He/H=0	···	−4.18	6.17
J2255+0545	2711324446359728384	DA	5912 (10)	0.582 (0.004)	7.991 (0.005)	He/H=0	···	−3.75	2.38
J2255−0750	2610488514148351360	DA	6693 (18)	0.581 (0.006)	7.983 (0.006)	He/H=0	···	−3.52	1.72
J2256+3735	1928174375826595072	DA :*	10379 (43)	0.799 (0.006)	8.314 (0.006)	He/H=0	···	−2.95	0.91
J2257+1205	2718818202217242240	DC	5685 (57)	0.675 (0.038)	8.166 (0.043)	H/He=0	···	−3.92	4.88
J2257+1921	2831963931606829312	DA	8711 (47)	0.615 (0.009)	8.031 (0.01)	He/H=0	···	−3.09	0.94
J2257+5130	1989342372349280384	DA	7236 (57)	0.850 (0.01)	8.401 (0.01)	He/H=0	···	−3.64	3.28
J2258+6430	2208752769527485568	DA	7821 (41)	0.641 (0.009)	8.077 (0.01)	He/H=0	···	−3.30	1.32
J2258−0054	2651505207011569152	DC	4813 (40)	0.523 (0.045)	7.923 (0.056)	H/He=0	···	−4.08	5.65
J2259+5717	2010066242392545792	DA	5247 (56)	0.544 (0.02)	7.936 (0.025)	He/H=0	···	−3.93	3.50
J2259−0828	2607380156121387648	DAH	6101 (23)	0.761 (0.016)	8.270 (0.017)	He/H=0	···	−3.85	4.18
J2300+2204	2835805586577740288	DZ	7060 (42)	0.614 (0.009)	8.064 (0.01)	log H/He=−4.0	log Ca/He=−10.14	−3.49	1.73
J2300+6408	2208530698238308736	DC	4622 (21)	0.535 (0.01)	7.929 (0.012)	He/H=0	···	−4.15	6.74
J2301+2323	2842112183412398336	DA	9918 (42)	0.635 (0.007)	8.090 (0.008)	log H/He=−5.0	···	−2.91	0.76
J2301+4056	1930213488860610176	DA	9555 (34)	0.643 (0.006)	8.073 (0.007)	He/H=0	···	−2.95	0.78
J2302+2430	2843077206728009472	DQ	6756 (33)	0.595 (0.014)	8.034 (0.016)	H/He=0	log C/He=−6.48	−3.55	1.86
J2302+4312	1931838292168404480	DA	8033 (28)	0.573 (0.006)	7.963 (0.007)	He/H=0	···	−3.19	1.05
J2303+4632	1936315366080098432	DC	4721 (29)	0.679 (0.013)	8.159 (0.014)	He/H=0	···	−4.24	8.94
J2304+2415	2842312874347797632	DZ	4969 (39)	0.510 (0.031)	7.900 (0.038)	log H/He=−3.0	log Ca/He=−9.58	−4.01	5.11
J2304−0701	2634608741244388096	DC	4491 (71)	0.532 (0.038)	7.925 (0.046)	He/H=0	···	−4.20	7.19
J2304−0701	2634608741244966016	DC	7404 (41)	0.597 (0.01)	8.036 (0.012)	log H/He=−3.6	···	−3.39	1.49
J2305+3922	1929838143078434432	DC	4553 (32)	0.707 (0.005)	8.217 (0.007)	log H/He=−2.71	···	−4.34	8.00
J2305+4334	1931870929622075008	DC	4797 (17)	0.454 (0.009)	7.781 (0.012)	He/H=0	···	−4.01	4.28
J2307+0821	2713617271700011008	DC	6047 (82)	0.682 (0.045)	8.175 (0.05)	log H/He=−3.0	···	−3.82	3.77
J2307+1400	2815415285174565248	DC*	5484 (40)	0.462 (0.029)	7.810 (0.038)	H/He=0	···	−3.80	2.80
J2308+0553	2663502184540697856	DA	6065 (35)	0.766 (0.029)	8.279 (0.032)	He/H=0	···	−3.87	4.31
J2308+2414	2842462137347560320	DC	4798 (19)	0.493 (0.01)	7.854 (0.012)	He/H=0	···	−4.04	5.21
J2309+5506	1996725077535283200	DA	5352 (12)	0.585 (0.005)	8.002 (0.005)	He/H=0	···	−3.93	3.73
J2309−0705	2631652528139944832	DA	7850 (74)	0.524 (0.019)	7.878 (0.024)	He/H=0	···	−3.19	1.00
J2310−0243	2638053472519840256	DC	6392 (62)	0.637 (0.032)	8.103 (0.036)	log H/He=−3.2	···	−3.68	2.50
J2310−2948	6605335899369392128	DA	7940 (60)	0.553 (0.013)	7.930 (0.017)	He/H=0	···	−3.19	1.03
J2312+1310	2812250821990695936	DA :	5171 (16)	0.546 (0.007)	7.940 (0.008)	He/H=0	···	−3.96	3.99

Tableau A.2 *suite page suivante*

Tableau A.2 *(suite)*

Name	Gaia DR2/EDR3*	Sp Type	$T_{\rm eff}$ (K)	$M/M_{\odot}$	$\log g$	Composition	Métaux	$\log L/L_{\odot}$	τ (Gyr)
J2312+2133	2838537563735201664	DA	5991 (52)	0.633 (0.023)	8.073 (0.026)	He/H=0	···	−3.77	2.73
J2312−0030	2651072927142789632	DA	5946 (62)	1.050 (0.025)	8.719 (0.034)	He/H=0	···	−4.21	6.32
J2312−2722	2379201119352265472	DA :	10087 (58)	0.800 (0.01)	8.317 (0.011)	He/H=0	···	−3.01	0.99
J2314+0109	2657451056656635648	DA	7976 (52)	0.589 (0.017)	7.991 (0.02)	He/H=0	···	−3.22	1.11
J2314+2333	2839397832801325952	DA :*	7085 (18)	0.293 (0.004)	7.359 (0.009)	He/H=0	···	−3.10	0.74
J2314−0632	2631876970245863552	DQ	7432 (18)	0.570 (0.003)	7.991 (0.004)	H/He=0	log C/He=−6.01	−3.36	1.39
J2315+6831	2214678175128464256	DA	8922 (34)	0.687 (0.005)	8.146 (0.006)	He/H=0	···	−3.11	1.04
J2315−0209	2638553754605793408	DZ	6337 (34)	0.621 (0.007)	8.078 (0.008)	log H/He=−3.0	log Ca/He=−9.88	−3.68	2.42
J2315−1440	2407167579853954688	DA	8800 (69)	0.839 (0.009)	8.380 (0.01)	He/H=0	···	−3.29	1.66
J2316+1720	2818727009902345600	DC	4780 (16)	0.177 (0.004)	6.937 (0.015)	He/H=0	···	−3.58	2.02
J2316−0938	2437933525811466112	DC	7188 (88)	0.713 (0.033)	8.218 (0.037)	log H/He=−3.4	···	−3.54	2.22
J2317+1830	2818957013992481280	DZ	4557 (62)	1.077 (0.012)	8.785 (0.021)	log H/He=−0.01	···	−4.72	7.21
J2317−0840	2630264429069509888	DA	6823 (58)	0.442 (0.021)	7.727 (0.03)	He/H=0	···	−3.35	1.18
J2318+2117	2837909055400871424	DC	5908 (53)	0.619 (0.02)	8.076 (0.022)	log H/He=−3.0	···	−3.81	3.42
J2318+2345	2839231634746334976	DC	5828 (86)	0.505 (0.035)	7.887 (0.044)	log H/He=−3.0	···	−3.73	2.40
J2318+2345	2839231634746334848	DA	5227 (21)	0.520 (0.042)	7.895 (0.052)	He/H=0	···	−3.91	3.24
J2319−0229	2637741490390750080	DA	5088 (14)	0.233 (0.003)	7.225 (0.01)	He/H=0	···	−3.64	1.49
J2319−0613	2631967439437024384	DC	4585 (22)	0.468 (0.013)	7.810 (0.017)	He/H=0	···	−4.10	5.64
J2320+1945	2825325213544431360	DA	6150 (37)	0.992 (0.014)	8.623 (0.018)	He/H=0	···	−4.08	5.75
J2321+0102	2645295921252503424	DA	5650 (46)	0.857 (0.021)	8.417 (0.023)	He/H=0	···	−4.08	6.32
J2321+0102	2645295955612242688	DC	4754 (41)	0.543 (0.026)	7.941 (0.031)	He/H=0	···	−4.11	6.31
J2321+5511	1996831828951826176	DA	7228 (40)	0.579 (0.011)	7.978 (0.013)	He/H=0	···	−3.38	1.40
J2321+6925	2214973561500636544	DC	7511 (38)	0.668 (0.009)	8.149 (0.01)	log H/He=−3.6	···	−3.43	1.67
J2321−1327	2408844399510334464	DC	5760 (53)	0.547 (0.038)	7.960 (0.046)	H/He=0	···	−3.79	2.88
J2322+0946	2762076666146759040	DC :	5409 (35)	0.447 (0.021)	7.784 (0.03)	H/He=0	···	−3.81	2.87
J2323+1135	2810953668852136064	DA	6919 (38)	0.847 (0.021)	8.397 (0.023)	He/H=0	···	−3.72	3.69
J2323+7255	2228616684031896192	DA	7522 (29)	0.491 (0.006)	7.817 (0.007)	He/H=0	···	−3.23	1.03
J2324+2835	2869130517001766400	DA	7195 (27)	0.590 (0.006)	7.997 (0.007)	He/H=0	···	−3.40	1.45
J2324+3014	2870129010998688512	DA	8090 (50)	0.562 (0.011)	7.944 (0.014)	He/H=0	···	−3.17	1.00
J2324−0216	2637627549202579328	DAZ	6476 (35)	0.562 (0.018)	7.981 (0.022)	He/H=0	log Ca/H=−8.25	−3.59	1.93
J2325+0949	2762042070184969216	DC :	7012 (53)	0.571 (0.029)	7.995 (0.035)	log H/He=−3.4	···	−3.46	1.61
J2325+1403	2813020961166816512	DA	5007 (10)	0.246 (0.003)	7.274 (0.006)	He/H=0	···	−3.69	1.70
J2325+2511	2841283151645302272	DA	9164 (107)	0.462 (0.016)	7.751 (0.023)	He/H=0	···	−2.84	0.58
J2325+2552	2841348430852439680	DA	5880 (19)	0.351 (0.005)	7.535 (0.009)	He/H=0	···	−3.52	1.38

Tableau A.2 *suite page suivante*

Tableau A.2 *(suite)*

Name	Gaia DR2/EDR3*	Sp Type	$T_{\rm eff}$ (K)	$M/M_{\odot}$	$\log g$	Composition	Métaux	$\log L/L_{\odot}$	τ (Gyr)
J2325−0936	2437760730687096192	DA	8072 (66)	0.542 (0.02)	7.908 (0.025)	He/H=0	···	−3.15	0.96
J2326+1600	2814629409239942272	DC	9688 (39)	0.559 (0.005)	7.965 (0.007)	log H/He=−4.4	···	−2.88	0.68
J2327+0415	2659860636389069312	DA	7190 (31)	0.610 (0.016)	8.029 (0.018)	He/H=0	···	−3.42	1.53
J2327+1444	2813447365520332672	DA	8619 (62)	0.616 (0.019)	8.033 (0.022)	He/H=0	···	−3.11	0.96
J2327+2638	2841680934336159104	DC	4951 (19)	0.615 (0.014)	8.058 (0.015)	He/H=0	···	−4.10	6.99
J2327+2638	2841680934336158976	DA	6631 (37)	0.867 (0.01)	8.428 (0.011)	He/H=0	···	−3.81	4.28
J2328+7059	2227233773282607488	DA	8364 (72)	0.478 (0.013)	7.788 (0.018)	He/H=0	···	−3.02	0.77
J2329+0047	2645449715440904960	DA	6302 (34)	0.686 (0.015)	8.155 (0.018)	He/H=0	···	−3.73	2.85
J2329+6159	2015698348961991552	DC	6146 (58)	0.634 (0.014)	8.099 (0.015)	log H/He=−3.0	···	−3.75	2.91
J2330+0028	2644672498158933248	DC	4485 (22)	0.484 (0.022)	7.839 (0.029)	He/H=0	···	−4.16	6.41
J2330+0100	2645480299903701504	DA	6632 (16)	0.740 (0.008)	8.237 (0.009)	He/H=0	···	−3.69	3.00
J2330+0120	2645509810623287552	DC	6158 (26)	0.529 (0.011)	7.926 (0.013)	log H/He=−3.0	···	−3.65	2.07
J2331+3001	2869685285040721536	DA	6612 (84)	0.834 (0.036)	8.378 (0.041)	He/H=0	···	−3.78	4.02
J2332+2658	2865535629374939520	DAH	9570 (25)	0.876 (0.004)	8.435 (0.004)	He/H=0	···	−3.17	1.43
J2332+3353	2872712618509070080	DA	8532 (53)	0.589 (0.013)	7.988 (0.016)	He/H=0	···	−3.10	0.93
J2335+1230	2764723912188128896	DC	6490 (63)	0.660 (0.025)	8.138 (0.027)	log H/He=−3.2	···	−3.68	2.58
J2336+3252	2872373629627611520	DA	7018 (47)	0.869 (0.012)	8.430 (0.014)	He/H=0	···	−3.71	3.74
J2337+0032	2645946252315491200	DA	5749 (18)	0.598 (0.011)	8.019 (0.013)	He/H=0	···	−3.81	2.72
J2338+0627	2756665763266917888	DA	6365 (39)	0.700 (0.05)	8.177 (0.056)	He/H=0	···	−3.72	2.95
J2338+2101	2826254713186397440	DA	5283 (21)	0.625 (0.009)	8.069 (0.011)	He/H=0	···	−3.99	5.01
J2338+3101	2871162547632415744	DA	6520 (49)	0.662 (0.032)	8.117 (0.037)	He/H=0	···	−3.65	2.29
J2338−1826	2393875961742886656	DA	7852 (30)	0.444 (0.005)	7.723 (0.007)	He/H=0	···	−3.10	0.84
J2339+2843	2866228901519900544	DA	5932 (33)	0.735 (0.025)	8.232 (0.027)	He/H=0	···	−3.88	4.24
J2339+4919	1943422948539962240	DC	5981 (44)	0.651 (0.032)	8.126 (0.035)	H/He=0	···	−3.81	3.61
J2339+5316	1993289138054372480	DA	6359 (30)	0.605 (0.008)	8.026 (0.01)	He/H=0	···	−3.64	2.09
J2340+4357	1925701917774697344	DA	8771 (31)	0.695 (0.008)	8.160 (0.01)	He/H=0	···	−3.15	1.11
J2342+0950	2760011096114471040	DA	6607 (48)	0.757 (0.033)	8.262 (0.037)	He/H=0	···	−3.71	3.23
J2342−1001	2435433202010203264	DA	4925 (28)	0.515 (0.015)	7.890 (0.018)	He/H=0	···	−4.02	4.93
J2343+0837	2759588063311504768	DA	6836 (39)	0.579 (0.011)	7.980 (0.013)	He/H=0	···	−3.48	1.61
J2343+1309	2764079838893099136	DC :	6716 (112)	0.707 (0.04)	8.210 (0.045)	log H/He=−3.2	···	−3.66	2.76
J2343+4725	1939308236730745472	DC	5287 (31)	0.468 (0.012)	7.823 (0.016)	H/He=0	···	−3.87	3.41
J2343−1659	2394366515727615104	DZ	4528 (12)	0.519 (0.008)	7.918 (0.009)	H/He=0	log Ca/He=−10.52	−4.19	6.18
J2344+1429	2771071908211662464	DA	5147 (49)	0.533 (0.032)	7.919 (0.04)	He/H=0	···	−3.95	3.87
J2346+1158	2763719512612656000	DC	6001 (18)	0.697 (0.006)	8.197 (0.006)	H/He=0	···	−3.85	4.06

Tableau A.2 *suite page suivante*

Tableau A.2 *(suite)*

Name	Gaia DR2/EDR3*	Sp Type	$T_{\rm eff}$ (K)	$M/M_{\odot}$	$\log g$	Composition	Métaux	$\log L/L_{\odot}$	τ (Gyr)
J2346+2728	2865060636057386112	DA	6211 (37)	0.536 (0.024)	7.909 (0.03)	He/H=0	···	−3.61	1.86
J2347+0223	2646617809106367360	DA	5134 (25)	0.226 (0.011)	7.198 (0.029)	He/H=0	···	−3.61	1.40
J2347+0304	2742789930821144320	DC	4641 (13)	0.438 (0.002)	7.705 (0.003)	log H/He=−1.02	···	−4.00	7.58
J2347+0656	2744932943406490112	DA	6590 (61)	0.899 (0.042)	8.477 (0.048)	He/H=0	···	−3.85	4.58
J2348+4300	1922778419431649280	DC	4788 (17)	0.249 (0.007)	7.295 (0.015)	He/H=0	···	−3.79	2.10
J2349+1423	2770647462363429376	DC	5679 (30)	0.599 (0.018)	8.046 (0.021)	H/He=0	···	−3.86	3.94
J2349+2933	2867032958053059200	DA	5898 (23)	0.539 (0.006)	7.918 (0.006)	He/H=0	···	−3.71	2.16
J2350−0846	2436043980719301504	DA	5538 (22)	0.719 (0.018)	8.212 (0.02)	He/H=0	···	−3.99	5.21
J2351+4103	1921255247935490944	DC	7108 (92)	0.758 (0.042)	8.286 (0.046)	log H/He=−3.4	···	−3.61	2.73
J2351+5839	1999250788878655360	DA	6145 (31)	0.645 (0.015)	8.092 (0.016)	He/H=0	···	−3.73	2.61
J2352+0212	2739624711723101312	DA	5373 (59)	0.659 (0.046)	8.121 (0.052)	He/H=0	···	−3.99	5.10
J2352+2531	2851868317587963136	DA	8193 (102)	0.996 (0.033)	8.624 (0.041)	He/H=0	···	−3.58	3.29
J2352−0253	2448933731627261824	DA	10743 (94)	1.319 (0.002)	9.374 (0.009)	He/H=0	···	−3.74	2.08
J2353+2051	2823398800448735104	DA	7228 (27)	0.367 (0.005)	7.556 (0.009)	He/H=0	···	−3.16	0.86
J2354+0548	2743812644136889600	DA	6300 (40)	0.523 (0.03)	7.884 (0.038)	He/H=0	···	−3.58	1.73
J2354+4027	1921351390779081600	DQ	7609 (26)	0.542 (0.004)	7.942 (0.005)	H/He=0	log C/He=−5.69	−3.29	1.22
J2354+6522	2017484922210746368	DC	4785 (66)	0.594 (0.03)	8.025 (0.034)	He/H=0	···	−4.14	7.33
J2354+6522	2017484922214792576	DQ	5753 (10)	0.470 (0.008)	7.823 (0.01)	H/He=0	log C/He=−7.02	−3.72	2.31
J2355+2314	2848334010475644288	DC	9846 (46)	0.632 (0.009)	8.085 (0.01)	log H/He=−4.6	···	−2.92	0.77
J2355−1916	2389966854309408512	DA	8766 (46)	0.570 (0.009)	7.955 (0.012)	He/H=0	···	−3.03	0.83
J2356+0537	2745244002118134400	DA	6547 (37)	0.565 (0.017)	7.958 (0.022)	He/H=0	···	−3.55	1.75
J2356−2054	2341622358827194880	DZ	4301 (23)	0.667 (0.04)	8.157 (0.043)	log H/He=−5.0	log Ca/He=−7.74	−4.41	8.14
J2357+1949	2822330113802737408	DZ	6078 (15)	0.674 (0.006)	8.162 (0.007)	log H/He=−2.0	log Ca/He=−8.00	−3.81	3.59
J2357+2602	2853372247632375040	DA	8135 (39)	0.589 (0.01)	7.989 (0.012)	He/H=0	···	−3.19	1.05
J2357+5057	1944042802521121024	DA	5590 (31)	0.662 (0.017)	8.124 (0.02)	He/H=0	···	−3.92	4.14
J2359+2733	2854727528856212992	DC	4825 (47)	0.511 (0.044)	7.885 (0.055)	He/H=0	···	−4.05	5.43